

**Geophysical Monograph Series**

**Number 8**

**American Geophysical Union**

**TERRESTRIAL HEAT FLOW**

**William H. K. Lee, *Editor***

**Geophysical Monograph Series**  
**American Geophysical Union**

WALDO E. SMITH, *Managing Editor*

**1. Antarctica in the International Geophysical Year**

*A. P. Crary, L. M. Gould, E. O. Hulburt, Hugh Odishaw, and  
Waldo E. Smith, Eds.*

**2. Geophysics and the IGY**

*Hugh Odishaw and Stanley Ruttenberg, Eds.*

**3. Atmospheric Chemistry of Chlorine and Sulfur Compounds**

*James P. Lodge, Jr., Ed.*

**4. Contemporary Geodesy**

*Charles A. Whitten and Kenneth H. Drummond, Eds.*

**5. Physics of Precipitation**

*Helmut Weickmann, Ed.*

**6. The Crust of the Pacific Basin**

*Gordon A. Macdonald and Hisashi Kuno, Eds.*

**7. Antarctic Research**

*H. Wexler, M. J. Rubin, and J. E. Caskey, Jr., Eds.*

**8. Terrestrial Heat Flow**

*William H. K. Lee, Ed.*

## **Terrestrial Heat Flow**

**Geophysical Monograph Series**

**Number 8**

**TERRESTRIAL HEAT FLOW**

**William H. K. Lee, *Editor***

*Published with the aid of a grant from the Charles F. Kettering Foundation*

PUBLISHER

**AMERICAN GEOPHYSICAL UNION**

of the

**NATIONAL ACADEMY OF SCIENCES—NATIONAL RESEARCH COUNCIL**

**Publication No. 1288**

**1965**

Geophysical Monograph Series Number 8

TERRESTRIAL HEAT FLOW

WILLIAM H. K. LEE, *Editor*

Copyright © 1965 by the American Geophysical Union  
Suite 506, 1145 Nineteenth Street, N. W.  
Washington, D. C., 20036

Library of Congress Catalog No. 65-60080

List Price, \$10.00

Printed by  
Port City Press, Inc.  
Baltimore, Maryland

## Preface

Geothermal processes play an important role in all theories about the origin, development, and surface features of the Earth. There are several theories as to the source of the distortion of the Earth's crust, which is directly or indirectly thermal in origin: for example, the energy is derived (1) from the contraction of a cooling Earth; (2) from the expansion of a heated Earth; or (3) from convection currents driven by the force of gravity acting on density differences caused by nonuniform temperature distributions. In all these theories, heat flow at the Earth's surface appears as an essential boundary condition.

*Terrestrial heat flow* is the study of the outflow of heat from the Earth's interior, but in a broader sense it embraces all geothermal problems. This Monograph is the first attempt to present an up-to-date review of the fundamentals of terrestrial heat flow: theories and techniques of measuring heat flow, results of heat flow observations, and geophysical deductions. It also includes reviews of physical processes in geothermal areas and of geothermal resources, together with an historical introduction to terrestrial heat flow by Sir Edward C. Bullard.

A fair amount of the materials in this Monograph have not been published before. Each chapter has been written to be as self-sufficient as possible; all chapters have an abstract and most of them also have a summary. This Monograph is intended for Earth scientists in general,

although there are sections containing technical details, and certain parts may require some knowledge of advanced mathematics. We hope that this volume will provide guidance for geophysicists beginning this field of research and serve as a reference for both specialists and nonspecialists.

I thank the following colleagues for reviewing one or more chapters of this Monograph: Drs. L. H. Adams, C. J. Banwell, G. Bodvarsson, C. S. Cox, W. M. Elsasser, G. D. Garland, J. Healy, R. Hide, J. A. Jacobs, W. M. Kaula, T. S. Lovering, P. Penta, J. Reitzel, A. E. Scheidegger, L. B. Slichter, D. E. White, and R. A. Wooding. Their comments were extremely useful to the contributors and have also greatly facilitated the editing.

This Monograph was a project of the Heat Flow Committee of the International Union of Geodesy and Geophysics. We are indebted to its chairman, Professor Francis Birch, and other Committee members for their suggestions. We are also grateful to Professors G. D. Garland and J. A. Jacobs for encouraging the publication of this work.

Editing of this volume was carried out while I was supported by grants from the National Aeronautics and Space Administration (NsG 216-62).

W. H. K. Lee

Los Angeles, California  
April 1965

## Contents

<b>Preface</b> . . . . .	vii
<i>by W. H. K. Lee</i>	
 <b>Chapter 1. Historical Introduction to Terrestrial Heat Flow</b> . . . . .	 1
<i>by Edward C. Bullard</i>	
References . . . . .	5
 <b>Chapter 2. Application of the Theory of Heat Conduction to Geothermal Measurements</b> . . . . .	 7
<i>by John C. Jaeger</i>	
1. Introduction . . . . .	7
2. Diurnal and annual temperature variation . . . . .	8
3. Reduction of observations in drill holes: horizontal layering . . . . .	8
4. Heat production and extrapolation of temperature . . . . .	9
5. The topographic correction . . . . .	10
6. The effect of past climatic changes . . . . .	12
7. The effect of intrusions . . . . .	13
8. Erosion, sedimentation, and uplift . . . . .	13
9. Underground water movement . . . . .	14
10. The effect of local variations in thermal conductivity on the geothermal gradient . . . . .	15
11. Temperatures around drill holes . . . . .	16
12. The disturbance in temperature caused by the sudden introduction of a cylindrical conductor at a different temperature . . . . .	18
13. Transient methods for measuring thermal conductivity . . . . .	18
14. Anisotropic thermal conductivity . . . . .	20
15. Summary . . . . .	20
References . . . . .	21
 <b>Chapter 3. Techniques of Measuring Heat Flow on Land</b> . . . . .	 24
<i>by Alan E. Beck</i>	
1. Introduction . . . . .	24
2. Measurement of thermal conductivity . . . . .	26
3. Measurement of temperature gradient . . . . .	40
4. Calculation of heat flow . . . . .	45
5. Summary . . . . .	46
References . . . . .	48
Appendix: Theoretical temperature-time curves for the cylindrical thermal conductivity probe (prepared by J. H. Sass) . . . . .	50
 <b>Chapter 4. Techniques of Measuring Heat Flow through the Ocean Floor</b> . . . . .	 58
<i>by Marcus G. Langseth</i>	
1. Introduction . . . . .	58
2. Techniques of temperature gradient measurement in the sediment . . . . .	58
3. Techniques of measuring thermal conductivity of the sediment . . . . .	68
4. Some notes on procedure . . . . .	71
5. Constant thermal conditions of the ocean bottom . . . . .	74
References . . . . .	76

<b>Chapter 5. On Heat Transfer through the Ocean Floor</b> . . . . .	78
<i>by Elena A. Lubimova, Richard P. Von Herzen, and Gleb B. Udintsev</i>	
1. Introduction . . . . .	78
2. Thermal stability of deep ocean water . . . . .	79
3. Measurements of temperature gradients in near bottom waters . . . . .	79
4. Heat exchange between ocean floor and near bottom water . . . . .	81
5. The influence of heat transfer by migration of interstitial water in sediments . . . . .	84
6. Summary . . . . .	85
References . . . . .	86
<b>Chapter 6. Review of Heat Flow Data</b> . . . . .	87
<i>by William H. K. Lee and Seiya Uyeda</i>	
1. Introduction . . . . .	87
2. Heat flow data . . . . .	88
3. Review of heat flow data on land . . . . .	92
4. Review of heat flow data at sea . . . . .	114
5. Global review of heat flow data . . . . .	134
6. Global analysis of heat flow observations . . . . .	148
7. Summary . . . . .	154
Appendix: A listing of heat flow data . . . . .	157
References . . . . .	186
<b>Chapter 7. Geophysical Deductions from Observations of Heat Flow</b> . . . . .	191
<i>by Gordon J. F. MacDonald</i>	
1. Introduction . . . . .	191
2. Observational evidence on radioactivity . . . . .	192
3. Thermal conditions of the Earth's interior . . . . .	197
4. Summary . . . . .	205
References . . . . .	209
<b>Chapter 8. Physical Processes in Geothermal Areas</b> . . . . .	211
<i>by John W. Elder</i>	
1. Introduction . . . . .	211
2. Surface mechanisms . . . . .	212
3. Convection of water in the crust . . . . .	220
4. Inferences about convection in the mantle . . . . .	230
5. A speculation on the development of the Earth . . . . .	236
6. Summary . . . . .	237
References . . . . .	237
<b>Chapter 9. Review of Geothermal Resources</b> . . . . .	240
<i>by James R. McNitt</i>	
1. Introduction . . . . .	240
2. History and status of projects . . . . .	241
3. Geologic environment . . . . .	247
4. Thermal fluid reservoir . . . . .	250
5. Physical characteristics of thermal systems . . . . .	252
6. Chemical investigations . . . . .	257
7. Problems of exploration, development, and management . . . . .	259
8. Summary and conclusions . . . . .	262
References . . . . .	262
<b>Name Index</b> . . . . .	267
<b>Subject Index</b> . . . . .	272

## Chapter 1. Historical Introduction to Terrestrial Heat Flow

EDWARD C. BULLARD

*Department of Geodesy and Geophysics  
Cambridge University, Cambridge, England*

*Abstract.* The first reference to high temperatures within the Earth known to the writer is by J. B. Morin in 1619; there is no known reference to the matter in the works of Agricola. Boyle, in 1671, raised many of the questions discussed in recent work. Little interest was taken in underground temperatures during the 18th century. The subject was energetically pursued by Committees of the British Association in 1868-1883 and 1935-1939. Measurements were first made at sea in 1950. In spite of the existence of about 2000 measurements of heat flow, the temperatures deep within the Earth are still very uncertain. Observations of magnetic variations combined with the study of samples from Moholes may give better estimates.

The study of temperatures within the Earth has a long history. The occurrence of volcanoes must have made it evident from the earliest times that some parts of the interior of the Earth are hot. That there is a general increase of temperature with depth could only have been discovered when mines were dug to depths of five hundred feet or more. An early work by Agricola [1530] (see also Singer *et al.* [1956]) states that a mine at Schneeberg 20 km from his home had a depth of 1200 feet and that there was a mine 3000 feet deep at Kuttenberg. President Hoover and his wife, the translators of Agricola's later work [Agricola, 1556], express disbelief in the existence of such deep mines at that time, though there is no doubt as to what Agricola says (he uses the word *passus* which, from other occurrences in his text, clearly has its usual meaning of the Roman double pace of 58 inches). If such depths had been reached, the downward increase in temperature would have been very conspicuous; that it is nowhere mentioned by Agricola tends to confirm the doubts of the Hoovers. Boyle [1671] gives a summary of an account by Morinus 'who above forty five years agoe, visited the deep Hungarian-mines in the month of July, and takes notice . . . that when they had descended about 80 fathoms beneath the surface of the Earth, he began to feel a breath of an almost luke-warm air; which warmth increased upon him, as he descended lower.' Boyle's Morinus is probably the French anti-Copernican astronomer J. B. Morin; I have not been able to find the passage summarized

by Boyle, but have found statements by Morin about high temperatures within the Earth [Morin, 1619]. No doubt a search of the German mining literature of the 16th and 17th centuries would yield other and perhaps earlier references to high temperatures underground.

The first systematic discussion of underground temperatures is in a remarkable and little known work by Boyle [1671]. Robert Boyle starts by saying 'because of my being particularly subject to be offended by any thing that hinders a full freedom of Respiration, I was not solicitous to goe down into the deep mines'; he therefore collected information '(by diligent enquiry purposely made) from the credible Relations of severall Eye-witnesses differing in nation, and for the most part unacquainted with each other.' One of his informants, 'an ingenious Physitian,' was probably Edward Browne or Brown (the son of Sir Thomas Browne the essayist), who visited the Hungarian mines in 1669 and described them in a book published two years after Boyle's [Browne, 1673].

Boyle considers three regions, of which the first extends a few tens of feet below the surface. Here he correctly points out that the annual range of temperature is reduced below that found at the surface of the Earth; in support of this he notes, among much else, that beer does not freeze in Moscow 'in Cellars that were not above 12 or 14 foot deep.'

Boyle's second region is a cold region lying below the first. He quotes discrepant accounts by Morinus and others saying that the upper parts of mines in Hungary are cold, whereas

English miners say that there is no cold region. He remarks, what is probably the true explanation, that Morinus visited the mines in the summer and 'felt it much the Colder, because he had left of his own Clothes, and put on the slight Garments used there by the Diggers.' In spite of this, Boyle is inclined to believe in a moderately cold region which we now know to be nonexistent.

Boyle describes his third region as being 'constantly and sensibly warm, but not uniformly so; being in some places considerably hot.' He discusses the possibility that 'the narrowness of the Cavities wherein the Diggers were in divers places reduc'd to worke, might make the warmth they felt, proceed in great part from the Steams of their own Bodies'; he concludes, however, that the high temperatures are not due to such causes and are a genuine property of the interior of the Earth. Boyle had to judge underground temperatures by the accounts his informants gave him of their subjective impressions; he had no measurements made with thermometers, though he 'did indeed send fitt Instruments to some daies journey from this place (Oxford), to examine the Air at the bottom of some of our deep mines: but through some unlucky casualties upon the place, the attempt miscarried.' Boyle was not the last man to have his thermometers broken while measuring underground temperatures, but it is remarkable that I can find no measurements by him or anyone else till those said by *Arago* [1856] to have been made by Gensanne in a mine near Belfort, France, in 1740. There is no mention of underground temperatures in the index to the *Philosophical Transactions* for 1665-1780.

Boyle discusses the origin of terrestrial heat in a passage that is truly remarkable when it is considered that it was written a hundred years before there was any clear distinction between temperature and quantity of heat and when most men believed that certain bodies had an innate tendency to be hot or cold. He says:

I shall add as a Conjecture, that the positive cause of the actuall warmth may proceed from those deeper parts of the Subterranean Region, which ly beneath those places which men have yet had occasion and ability to dig. For it seems probable to me, that in these yet unpenetrated Bowells of the Earth, there are

great store-houses of either actual Fires, or places considerably Hot, or, (in some Regions) of both; from which *Reconditories* (if I may so call them) or magazines of hypogeall heat, that quality is communicated, especially by Subterranean Channells, Clefts, Fibres or other Conveyances, to the less deep parts of the Earth, either by a propagation of heat through the substance of the interposed part of the Soil. (as when the upper part of an Oven is remisly heated by the same Agents that produce an intense heat in the Cavity,) or by a more easy diffusion of the Fire or heat through the above mentioned Conveyances as may be exemplified by the pipes that convey heat in some Chymicall structures:) Or else, (which is perhaps the most usuall way,) by sending upwards hot minerall Exhalations and Steams.

It is easy to read modern ideas into seventeenth century writings whose authors were, in fact, using words in quite other senses than those we ascribe to them. In this passage by Boyle, however, I believe we really can see the germ of many of the ideas of this book. He interprets the observed increase of temperature with depth as being due to sources of heat within the Earth and discusses its transport by conduction and by the motion of matter quite in the modern manner. As to the source of the heat, he tends to the belief that at any rate part of it has a chemical origin and mentions the generation of heat by 'the incalescence there is produced in many mines, and other Places, by the mutuall action of the component parts promoted by water of immature and more loosely contexted minerals, especially such as are of a Marchasiticall nature.' He says that he has written a 'Discourse of Subterranean Fires and Heats' which discusses these matters; this was, in fact, never published, but might perhaps be found among the great mass of the Boyle papers at the Royal Society and elsewhere.

In the 18th century very little interest was taken in underground temperatures; there are a few published measurements which have been collected by *Prestwich* [1895]. In the first half of the 19th century there are discussions by *Arago* [1856] and *Humbolt* [1846]; the latter gives an interesting discussion of gradients in permanently frozen ground in Siberia.

The weakness of the investigations up to the middle of the 19th century was that they gave only the temperature gradient and not the thermal conductivity; this made it impossible

to say whether variations in gradient were due to variations in heat flow or to variations in conductivity. In 1868 a committee was set up by the British Association 'to consider the rate of increase of underground temperature in various locations of dry land and under water.' This committee, whose secretary was J. D. Everett and of which Lord Kelvin was a member, produced sixteen reports between 1868 and 1883; the fifteenth of these [Everett, 1883] summarized the preceding reports. As well as collecting numerous measurements of temperature, the committee determined the conductivity of many types of rock and estimated the heat flow. They obtained a mean of  $1.3 \mu\text{cal}/\text{cm}^2 \text{ sec}$ , which is surprisingly near the continental mean of 1.41 given by Lee and Uyeda in chapter 6 of this book. The work of the committee was doubtless stimulated by the importance of its results for the calculations of Lord Kelvin on the age and past history of the Earth, and also by its practical importance in deep mining; the latter led to an enquiry by the British 'Coal Commission' of 1866-1870, which gathered much further data [Anonymous, 1871]. All the 19th century material is collected and discussed by Prestwich [1895]. Another discussion from this period is that of Fisher [1889].

The main weakness of the work of the British Association committee was that the conductivities used were not the actual conductivities of the strata penetrated by particular mines and borings in which temperatures had been measured, but estimates based on measurements made on 'typical' samples of the types of rocks concerned. It was difficult, also, to estimate the accuracy of either the temperature or the conductivity measurements; in view of these uncertainties, Sir Harold Jeffreys suggested that the British Association should appoint another committee to 'consider the direct determination of the thermal conductivities of rocks in mines or borings where the temperature gradient has been, or is likely to be, measured.' This committee was appointed in 1935 with E. Griffiths as chairman and D. W. Phillips as secretary; it produced five reports during the period 1935 to 1939 [Anonymous, 1935-1940]. The experimental work of the committee was carried out by Benfield [1939] and Bullard [1939]. The outbreak of war brought the

activities of the committee to an end, and it was not re-established after the war; its work was continued, however, by Bullard and his collaborators at Cambridge. The aim of the committee was to find boreholes where a detailed series of temperatures could be measured and from which an adequate set of samples could be obtained for the determination of thermal conductivity. Great difficulty was experienced in finding suitable holes, but very satisfactory results were obtained from those that were found. The detail available enabled plots to be made of temperature versus integrated thermal resistance; for a constant heat flow these should be straight lines. Any departure from a straight line shows some source of error and enables a much more satisfactory evaluation to be made of the reliability of the results than is possible with the earlier measurements. For example, the transport of heat by the movement of groundwater in a porous surface layer, the entrance of water into a borehole from an aquifer, and the use of inadequate samples for thermal conductivity can all be detected from such plots. The methods are now the standard practice and, as is shown in Lee and Uyeda's tables in chapter 6 of this volume, have been widely used. The committee also investigated the effects of topography and geological structure on heat flow.

The British Association Committee of 1868 was charged with collecting data on 'dry land and under the sea,' but in fact their only submarine measurements were in an English colliery whose workings extended about 1 km under the Irish Sea. It was clearly desirable to make measurements in the floor of the deep ocean; about 1939 the present writer considered two schemes for doing this; in one a slab of poorly conducting material was to be put on the sea floor and the temperature difference across it measured, and in the other the temperature gradient in the sediment was to be measured with a probe driven into the bottom. The second scheme appeared the more practicable, but facilities for trying it could not be found until ten years later, in 1949. In the meantime a similar scheme had been devised by Pettersson [1949], who attempted a measurement in the Indian Ocean in 1948 during the *Albatross* expedition. No details of this measurement have been published, but it seems likely

that what was measured was not the geothermal gradient but the heat produced by friction while running the probe into the bottom. In the summer of 1949, Maxwell and Bullard constructed a probe that contained thermocouples and was attached to a pressure-tight vessel containing a recording galvanometer. A few months later this equipment was modified by Maxwell, thermistors being substituted for the thermocouples, and a potentiometer recorder for the galvanometer. The first measurements were made in 1950 in the Pacific by *Revelle and Maxwell* [1952] on the expedition *Capricorn* of the Scripps Institution of Oceanography. Equipment similar to the original was used in the Atlantic in 1952 by *Bullard* [1954]; the high heat flow in the central valley of the Mid-Atlantic Ridge was found in 1956.

The measurement of heat flow with the probe was tedious, since it was necessary to make a separate lowering of a corer at each station to get a sample for the determination of conductivity. A more convenient instrument combining a corer and a temperature probe was introduced by *Gerard et al.* [1962]; it is described by Langseth in chapter 4 of this volume.

Both types of instrument have been very extensively used, and today we have about 2000 measurements of the heat flow from the Earth, of which 89% have been made at sea; clearly this is a tremendous advance over the 15 or so measurements, all on land, that existed 20 years ago. However, the distribution of the measurements is still far from what we would wish to have, and some aspects of the results are difficult to understand. Only about a tenth of the measurements are on the continents, and there are immense regions with none at all. There are no measurements in South America or Antarctica, and the whole of Asia is very badly represented. Perhaps an even more serious fault is that the measurements are usually situated in special places, where borings have been made for other purposes; that is, they are predominantly in oil fields and in mineralized areas; we therefore get a rather poor idea of the variation of heat flow from one tectonic region to another. As *Boyle* [1671] said:

For almost all the deep Grooves that mineralists have given us accounts of, and wherein men have wrought long enough to take sufficient notice of the Temperature of the Air,

have been made in Soils furnished with metalline Oars, or other mineralls, without which, men would not be invited to be at so great a charge, as that of sinking so very deep pits, and maintaining workmen in them. So that experience has yet but slenderly, or at least not sufficiently, informed us of the Temperature of those parts of the third Region of the Earth, that are not furnished with ponderous mineralls, and consequently has not informed us of the Temperature of the Lowermost Region in generall.

Investigations now in progress in the United States and in Russia, where special holes are drilled in places where measurements are needed, should do much to remedy this. The main result that can be deduced from the existing measurements on land is that the heat flow in shield areas is less than that in sedimentary basins and mountain ranges.

At sea the distribution of measurements is much better than it is on land, but the measurements are subject to a puzzling variation over short distances. Much of this may be due to steep topography and to rapid variations in the thickness of sediments, but some may also be due to the unexpected complications in heat transfer from sediment to ocean water described by *Lubimova et al.* in chapter 5 of this volume. The most remarkable result is the close equality of the oceanic and continental means. The smallness of the low order harmonics is also noteworthy.

Surprisingly little attention has been given to volcanic areas in the study of heat flow. It is generally, and probably correctly, supposed that, although the heat emerging per unit area in such regions is large, their contribution to the total heat flow is negligible. Even if this is so, it would be interesting to see a line of closely spaced measurements running from a geothermally 'normal' area across a volcanic district. We have something of this kind in the lines across the East Pacific Rise and the Mid-Atlantic Ridge; these show surprisingly sharp peaks only 20 km or so across, which are presumably associated with the intrusion of dykes at no great depth. To be able to map concealed masses of hot rock and to determine whether they are dykes, sills, or batholiths is presumably possible and should be of interest in elucidating the tectonics of an active area.

When we turn to the sources of heat within the Earth, we are faced with a formally insoluble

ble problem. We have only the boundary conditions, the temperature and the heat flow at the Earth's surface, from which to deduce the thermal state of the interior. As Boyle [1671] said:

And much less have we any certain knowledge of the Temperature of the more inward, and (if I may so speak) the more Centrall parts of the Earth; in which, whether there be not a continued solidity or great Tracts of Fluid matter . . . we are as yet ignorant, and shall I fear long continue so, For it is to be noted. . . that what has been hitherto discoursed, belongs only to the Temper of those Subterranean parts, to which men have been enabled to reach by diging. 'Tis true indeed that some Mines especially in Germany, and Hungary are of a Stupendous depth, . . . yet this prodigious depth does not much exceed half a mile and fals short of three quarters, and how small a part is that of the whole depth of the Terrestriall Globe?

In fact even today we have no direct knowledge of the radial distribution of temperature or of heat sources within the Earth or of what proportions of the heat are carried by conduction, radiation, and convection; we are also largely ignorant of the initial temperature and physical state of the Earth. In these circumstances there is a wide field for speculation; the position has, however, been greatly clarified by discussions by Birch and others based on thermodynamics and the theory of the solid state and by detailed calculations of the thermal history of the Earth on a number of hypotheses about the quantities that are in doubt. These discussions have set some limits to the present internal temperatures and suggest that they are lower than was usually supposed 10 years ago.

The subject would be transformed if we could estimate temperature as a function of radius. For the upper parts of the mantle this may be possible; the electrical conductivity can be found from the study of magnetic variations and Earth currents and, if samples of the material are available from Moholes, the temperature can be found at which the samples reach the conductivity that is observed in the mantle. There may be difficulties due to phase changes at depth, but it should be possible to reproduce these by working at high pressure.

It would also be of great interest to determine whether the high heat flows observed in

Tasmania and Hungary, for example, are associated with near-surface igneous activity or whether the upper mantle is anomalously hot under these places. This problem should be capable of fairly easy solution through the study of magnetic variations.

It may be that in the next ten years the greatest advances in the study of the Earth's heat will come from an increase of knowledge of the material of the mantle and from laboratory experiments on its chemistry and radioactivity and on its thermal, electrical, and mechanical properties. Such work could give a new reality to discussions of heat flow, magnetic variations, and mantle convection.

## REFERENCES

- Agricola, G., *Bermanus*, Froben, Basel, 1530.  
 Agricola, G., *De Re Metallica*, Froben, Basel (translated into English by H. C. Hoover and L. H. Hoover and published in 1912 by the Mining Magazine and in 1950 by Dover Publications).  
 Anonymous, *Report of the Commissioners Appointed To Enquire into the Several Matters Relating to Coal in the United Kingdom* (c.435-1) 2, 81-212, 1871.  
 Anonymous, *Rept. Brit. Assoc. for 1935-1939*, 1935-1940.  
 Arago, D. F. J., *Oeuvres Complètes de Francois Arago*, 6, (*Notices Scientifiques*, 3), 317, Gide, Paris, 1856.  
 Benfield, A. E., Terrestrial heat flow in Great Britain, *Proc. Roy. Soc. London, A*, 173, 428-450, 1939.  
 Boyle, R., Of the temperature of the subterranean regions as to heat and cold, in *Tracts Written by the Honourable Robert Boyle etc.* (usually called *Cosmical Qualities*), Davis, Oxford, 1671.  
 Browne, E., *A Brief Account of Some Travels in Hungaria etc.*, Tooke, London, 1673.  
 Bullard, E. C., Heat flow in South Africa, *Proc. Roy. Soc. London, A*, 173, 474-502, 1939.  
 Bullard, E. C., The flow of heat through the floor of the Atlantic Ocean, *Proc. Roy. Soc. London, A*, 222, 408-429, 1954.  
 Everett, J. D., *Rept. Brit. Assoc. for 1882*, 72-90, 1883.  
 Gerard, R., M. G. Langseth, and M. Ewing, Thermal gradient measurements in the water and bottom sediment of the western Atlantic, *J. Geophys. Res.*, 67, 785-803, 1962.  
 Fisher, O., *Physics of the Earth's Crust*, Macmillan, London, 1889.  
 Humbolt, A. von, *Cosmos*, vols. 1 and 4 (translated into English by Mrs. E. Sabine), Longman and Murray, London, 1846-1858.

- Morin, J. B., *Nova Mundi Sublunaris Anatomia* etc., Du Fossé, Paris, 1619.
- Pettersson, H., Exploring the bed of the ocean, *Nature*, 164, 468-470, 1949.
- Prestwich, J., *Controverted Questions in Geology*, Macmillan, London, 1895.
- Revelle, R., and A. Maxwell, Heat flow through the ocean floor, *Nature*, 170, 199-200, 1952.
- Singer, C., E. J. Holmyard, A. R. Hall, and T. I. Williams, *A History of Technology*, vol. 2, Clarendon Press, Oxford, 1956.

(Manuscript received April 6, 1965.)

## Chapter 2. Application of the Theory of Heat Conduction to Geothermal Measurements

JOHN C. JAEGER

*Department of Geophysics, Australian National University, Canberra*

*Abstract.* Mathematical problems encountered in the measurement of heat flow at the Earth's surface are reviewed. Most of these problems can be solved by simple solutions of the equation of heat conduction. Reduction of observations in drill holes for horizontal layering are given by the methods of Bullard and Gough. Described briefly are: heat production; the methods of Jeffreys and Bullard, Lees, and Birch for topographic correction; perturbations of the temperature gradient caused by the oscillations of surface temperature; past climatic changes; uplift and erosion; igneous intrusion; groundwater circulation; mine ventilation; the process of drilling and circulation of drilling fluid; and the sudden insertion of temperature probes. The theory of transient methods for determining thermal conductivity and the effect of anisotropic thermal conductivity are also discussed.

### 1. INTRODUCTION

The object of this review is to discuss the mathematical problems encountered in the measurement of the heat flow at the Earth's surface. Most of these can be illustrated in principle by very simple solutions of the equation of heat conduction, and refinements can be taken care of by more sophisticated mathematics. The simple solutions will be given here, together with references to the refinements. Most of the theory is given by *Carslaw and Jaeger* [1959] and by *Ingersoll et al.* [1954], and references will be given to the former work as well as to published papers.

The notation used will be similar to that of *Carslaw and Jaeger* [1959]: temperature  $T$ , thermal conductivity  $K$ , specific heat  $c$ , density  $\rho$ , rate of heat production  $A$ , and diffusivity  $\kappa$  defined by

$$\kappa = K/\rho c \quad (1)$$

The dimensions of  $\kappa$  are  $L^2t^{-1}$ .  $K$ ,  $\rho$ , and  $c$  will be assumed to be independent of temperature, but variation with position will be taken into account in some cases. When numerical values are given, units will always be centimeters, grams, seconds, calories, and degrees centigrade. Except in section 14, the material will be assumed to be isotropic. The range in values of  $K$  and  $\kappa$  in rocks commonly met with is 3 to 15 mcal/cm sec °C for  $K$  and 0.005 to 0.025 cm<sup>2</sup>/sec for  $\kappa$ . In calculating rough orders of

magnitude, it is often convenient to take 5 mcal/cm sec °C for  $K$  and 0.01 cm<sup>2</sup>/sec for  $\kappa$ .

The heat flux by conduction at any point is defined as the vector  $K \nabla T$ . The *geothermal flux*  $q$ , which is the heat flow toward the earth's surface, is  $K(\partial T/\partial z)$ , where the  $z$  axis is taken vertically downward. The *geothermal gradient*  $g$  is  $\partial T/\partial z$ , the rate of increase of temperature with depth. The central problems of this book are the measurement of  $q$  and the study and interpretation of its global variation.

The differential equation of heat conduction is the mathematical expression of the fact that the rate of increase of the heat content of a small volume is equal to the sum of the rate of heat generation in it and the rate of flow of heat into it across its surface. For a material of constant conductivity with heat generated at the rate  $A$  per unit time per unit volume, the equation is [*Carslaw and Jaeger*, 1959, section 1.6(7)]

$$\nabla^2 T - (1/\kappa) \partial T/\partial t = -A/K \quad (2)$$

For the cases of variable conductivity, moving material, or water movement, modifications to (2) are needed which will be indicated as they arise.

In an ideal uniform medium, two measurements of temperature and a measurement of conductivity would suffice to determine  $q$ . In practice, there are many material effects which affect underground temperatures and which have to be allowed for in determining  $q$  from them. Examples of these effects are vertical and

lateral variation of thermal conductivity, irregularity of terrain, underground water movement, uplift and erosion, and recent glaciation. The fundamental theory for these is given in sections 2 to 10.

In addition to these natural effects, man-made disturbances of temperature, such as those produced by drilling or by ventilation cooling in mines, have to be assessed and perhaps corrected for. These are discussed in sections 11 and 12.

## 2. DIURNAL AND ANNUAL TEMPERATURE VARIATION

In a uniform Earth, the temperature due to a sinusoidal oscillation,  $T_0 \cos(\omega t)$ , at the surface  $z = 0$  is propagated in accordance with the damped wave equation [*Carslaw and Jaeger*, 1959, section 2.6(8)]

$$T = T_0 \exp(-kz) \cos(\omega t - kz) \quad (3)$$

Here  $\omega = 2\pi/P$ , where  $P$  is the period,  $k = (\omega/2\kappa)^{1/2}$ , and the wavelength  $\lambda$  is

$$\lambda = 2\pi/k = (8\pi^2\kappa/\omega)^{1/2} = (4\pi\kappa P)^{1/2}$$

Taking  $\kappa = 0.01 \text{ cm}^2/\text{sec}$ , the wavelength of the diurnal oscillation is about 1 meter and that of the annual oscillation is about 20 meters. At a depth of 1 wavelength, the amplitude of the oscillations is reduced by a factor of  $\exp(-2\pi) = 0.0019$  and so is negligible for most purposes. Formulas for a two-layer system, such as rock with a weathered cover, are readily written but are rather complicated.

In general, the oscillation of the surface temperature, whether diurnal or annual, can be represented by a Fourier series in which the higher harmonics die out much more rapidly with depth than the fundamental, so that the use of (3) is adequate. Measurements of the amplitude or the phase at depth  $z$ , or of the velocity of propagation of the temperature wave, can be used to determine  $\kappa$ . The general theory was given by *Kelvin* [1861]. A very complete study, with a discussion of the reduction of experimental results, is given by *Lovering and Goode* [1963]

The annual oscillation described above becomes increasingly important toward the surface but can usually be neglected at depths greater than 20 meters. *Lovering and Goode* [1963] have shown that careful measurements in holes

of this depth, combined with a correction for the annual oscillation, can sometimes be used to determine the geothermal gradient.

Often, however, temperatures measured in the topmost 50 or 100 meters of deeper drill holes depart considerably from the (usually approximately linear) variation measured at greater depths. Such effects may be caused by weathering (which will usually increase the gradient and may persist to considerable depths) or the presence of moving water vapor or groundwater, even if this movement is very slow. Because of these uncertainties (to which may be added the fact that such holes are often partially cased, and the difficulty of measuring the thermal conductivity of weathered rock), the use of shallow holes (say less than 150 meters) for measuring  $q$  is rare, despite the fact that such holes are drilled in great numbers for engineering purposes and for exploration of shallow deposits.

When experimental temperature-depth curves are extrapolated to the surface, the extrapolated surface temperatures so obtained usually differ from the mean annual air temperature at the surface, the excess being denoted by  $e$ . *Van Orstrand* [1941] has collected 125 early measurements of  $e$ ; these range from  $-6.9^\circ\text{C}$  to  $5^\circ\text{C}$ , the mean value being  $-1.6^\circ\text{C}$  and 82% being negative. The value of  $e$  depends on the micro-meteorology at the surface. It is usually found that regions with comparable surface conditions give similar values of  $e$ .

## 3. REDUCTION OF OBSERVATIONS IN DRILL HOLES: HORIZONTAL LAYERING

The equation of steady flow of heat in one dimension can be written

$$q = K(\partial T/\partial z) \quad (4)$$

where  $z$  is measured vertically downward, and  $q$  is the constant geothermal flux. If  $K$  varies with depth, (4) can be simplified by introducing the thermal resistance from the surface defined by

$$\xi = \int_0^z (1/K) dz \quad (5)$$

With this change of variable, (4) becomes

$$q = dT/d\xi \quad (6)$$

so that when  $T$  is plotted against  $\xi$  the result is a straight line whose slope is the geothermal flux. Such plots, which were introduced by *Bullard*

[1939], are in principle the most satisfactory way of presenting observations.  $K$  as a function of  $z$  can be estimated from the lithology in the driller's log, together with measurements on representative core samples.

If there are  $n$  discrete layers of thicknesses  $L_1, \dots, L_n$  and conductivities  $K_1, \dots, K_n$ , (5) gives a weighted mean thermal conductivity of

$$(L_1 + \dots + L_n) [(L_1/K_1) + \dots + (L_n/K_n)]^{-1} \quad (7)$$

In this case Bullard's method is equivalent to using a weighted mean thermal gradient, with the weighted mean thermal conductivity given by (7). It is sometimes objected that this method is suitable only when no more than two or three well defined layers are present and is unsuitable for regions in which there are many rapid changes in lithology. This is not so; all that is required in such cases is an estimate of the weighted mean thermal conductivity. *Lovering* [1965] remarks that it may be almost impossible to sample some formations adequately, but a mean conductivity for them can be determined by comparing the observed temperature gradient in them with that in a uniform formation for which meaningful laboratory measurements can be made.

If the plot of  $T$  against  $\xi$  is not linear, the cause may be three-dimensional variation of conductivity, water movement, recent glaciation, or others.

An alternative method of reduction which may be useful in such cases has been developed by *Gough* [1963]. He divides the length of the hole into a number of short intervals (60 meters), determines a heat flow value for each of these, and then examines the regression of these values on depth. Calculation of heat flow from experimental data on land is discussed by *Beck* in chapter 3, section 4, of this volume.

The theory described here holds strictly for horizontal beds only. No complete theory for the case of dipping beds exists as yet, and in practice observations are reduced on the tacit assumption that the structures are horizontal. Some approximations are given in section 10.

#### 4. HEAT PRODUCTION AND EXTRAPOLATION OF TEMPERATURE

##### 4.1 Heat Production

Heat may be produced at an approximately constant rate by radioactivity or a chemical reaction such as oxidation. Sometimes the effects of water movement also may be simulated by a source of heat. If conductivity varies with depth, the equation of steady flow of heat in one dimension becomes

$$\frac{d}{dz} \left( K \frac{dT}{dz} \right) = -A \quad (8)$$

where  $A$  is the rate of production of heat per unit time per unit volume. Making the substitution (5), this becomes

$$d^2T/d\xi^2 = -AK \quad (9)$$

It follows from (9) that the graph of  $T$  against  $\xi$  is concave downward in a region where heat is being produced.

If both  $A$  and  $K$  are independent of position and time, (8) gives

$$T = T_0 + (q/K)z - Az^2/2K \quad (10)$$

where  $T_0$  is the surface temperature, and  $q$  is the surface heat flux.

If  $A = 0$ , but there is heat supplied at the rate  $Q$  per unit time per unit area in the plane  $\xi = \xi_1$ , (9) gives

$$\begin{aligned} T &= T_0 + q\xi & 0 \leq \xi \leq \xi_1 \\ T &= T_0 + q\xi - Q(\xi - \xi_1) & \xi \geq \xi_1 \end{aligned} \quad (11)$$

Thus supply of heat in a plane (e.g., by flowing water) causes a change in slope of the curve of  $T$  against  $\xi$ .

##### 4.2 Extrapolation of Temperature to Greater Depths in the Crust

Calculations of temperature in the crust and upper mantle involve extrapolating the surface heat flux downward with various assumptions about the distribution of radioactivity and conductivity. For example, (10) is the result for uniform conductivity and heat production. If these values changed abruptly to  $K_1$  and  $A_1$  at depth  $z_1$ , the temperature for  $z > z_1$  would be

$$\begin{aligned} T &= T_0 + qz_1/K - Az_1^2/2K \\ &\quad + (q - Az_1)(z - z_1)/K_1 \\ &\quad - A_1(z - z_1)^2/2K_1 \end{aligned}$$

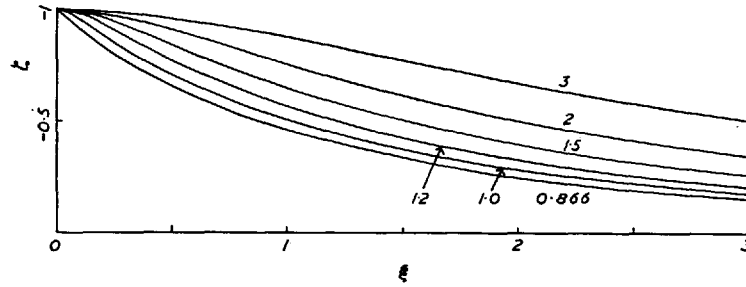


Fig. 1. Lees-type hills. The coordinates are dimensionless,  $\xi = x/H$ ,  $\zeta = z/H$ , and the numbers on the curves are values of the parameter  $b/H$ .

Calculations of this type have been made by *Birch* [1955], *Clark and Ringwood* [1964], *Schössler and Schwarzlose* [1959], and many others. They are reviewed by MacDonal in chapter 7 of this volume.

#### 5. THE TOPOGRAPHIC CORRECTION

Taking  $x$  and  $y$  axes in the sea level surface and the  $z$  axis vertically downward, the height  $h(x, y)$  above sea level and the mean annual surface temperature  $T_s(x, y)$  at all points  $(x, y)$  can be assumed to be known. If the thermal conductivity of the material is independent of position and the geothermal gradient is  $g$  at great depths, and there are no sources of heat, the temperature  $T$  is a solution of Laplace's equation,  $\nabla^2 T = 0$ , which satisfies the conditions

$$\begin{aligned} T &\rightarrow gz \text{ as } z \rightarrow \infty \\ T &= T_s(x, y) \text{ at the surface,} \\ &\text{where } z = -h(x, y) \end{aligned} \quad (12)$$

This problem can be treated by standard numerical methods, such as relaxation methods [Southwell, 1940; Emmons, 1943, 1944]. *Howard* [1964] shows that its solution can be expressed as an integral equation of Fredholm type, which can then be solved numerically.

In practice,  $T_s(x, y)$  is usually not known, and most authors have assumed a linear variation of  $T_s$  with height, that is,

$$T_s(x, y) = T_0 - g'h(x, y) \quad (13)$$

where  $T_0$  and  $g'$  are constants. Jaeger and Moyer (unpublished) have found that in the Snowy Mountains, Australia, extrapolated surface temperatures obtained from short (50-meter) drill holes are consistent with (13). In the absence of information of this sort, or from meteorologi-

cal stations, it is usual to take the value  $0.98^\circ\text{C}$  per 100 meters for  $g'$ , which is the adiabatic lapse rate of atmospheric temperature [Berry *et al.*, 1945].

Two specific problems arise in the calculation of the geothermal gradient: (1) to determine  $g$  from observations in a hole drilled from the surface, and (2) to determine  $g$  from temperatures measured in a horizontal tunnel. Three different methods are discussed in sections 5.1, 5.2, and 8.2, and more fully by *Birch* [1950], who includes a historical survey. Of these, section 8.2 is in most general use for dealing with complicated topography; the simple results of section 5.1 are useful for estimating orders of magnitude.

#### 5.1 Simple Model Solutions

Several explicit solutions of (12) and (13) are known. The simplest is that of *Lees* [1910], who noticed that in two dimensions

$$T = T_0 + gz + B(z + a)/[x^2 + (z + a)^2] \quad (14)$$

where  $T_0$ ,  $g$ ,  $B$ , and  $a$  are constants, satisfies  $\nabla^2 T = 0$ , and  $T$  tends to  $gz$  as  $z \rightarrow \infty$ . Also, it takes the surface value ( $T_0 + g'z$ ) required by (13) on the surface

$$(g' - g)z = B(z + a)/[x^2 + (z + a)^2] \quad (15)$$

The surface (15) provides a reasonable representation of a single mountain range. If  $H$  is its height and  $2b$  its width at half its height, the parameters  $B$  and  $a$  are given by

$$\begin{aligned} a &= H + (\frac{1}{4}H^2 + b^2)^{1/2} \\ B &= (g - g')H(\frac{1}{4}H^2 + b^2)^{1/2} \end{aligned} \quad (16)$$

The shape of the surface is shown in Figure 1.

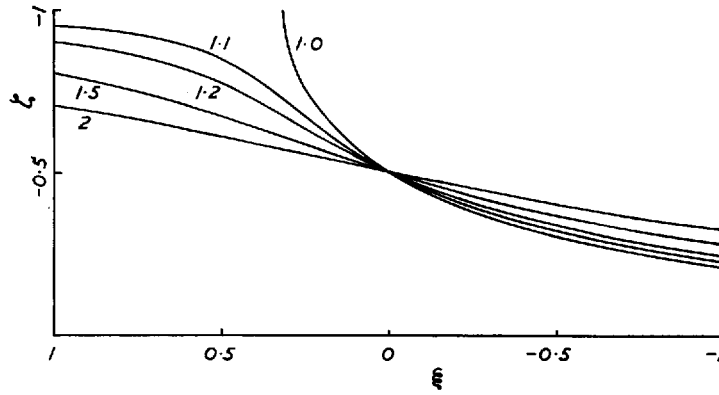


Fig. 2. Lees-type monoclines. The coordinates are dimensionless,  $\xi = x/H$ ,  $\zeta = z/H$ , and the numbers on the curves are values of the parameter  $b/H$ .

*Jaeger and Sass* [1963] have used this solution to estimate topographic corrections. Parallel ranges of hills can be simulated by superimposing solutions of this type [*Van Orstrand*, 1934]. The method as originally given by *Lees* [1910] allowed for radioactive heating, and the model is readily extended to three dimensions. The case of a monocline has been treated in the same way by *Jaeger and Sass* [1963]: the temperature given by

$$T = T_0 + gz + \frac{1}{2}(g - g')H \{1 + (2/\pi) \tan^{-1} [x/(z + a)]\} \quad (17)$$

has the required value ( $T_0 + g'z$ ) on the surface

$$x = (z + a) \cot(\pi z/H) \quad (18)$$

where  $a$  is defined in (16). The surface (18) is a typical monocline passing through the points  $(\infty, -H)$ ,  $(0, -\frac{1}{2}H)$ ,  $(\infty, 0)$ . Its shape is shown in Figure 2.

The geothermal gradient ( $\partial T/\partial z$ ) at any point near hills or monoclines of the described shapes is obtained by differentiating (14) or (17). These results are useful for estimating the order of magnitude of the corrections to be expected in simple situations. For example, for a hill with  $b = 2H$  the vertical gradient ( $\partial T/\partial z$ ) at the surface is  $[g - \frac{1}{2}(g - g')]$  at the top of the hill and  $[g - (g - g')/20]$  at the half-way point  $x = 2H$  approximately.

A different type of explicit solution, which is periodic in  $x$  and so represents a periodic hill and valley system, has been used by *Andreae* [1958].

## 5.2 The Jeffreys-Bullard Reduction

*Jeffreys* [1940] devised a method of correction which in practice is similar to the topographic correction for other geophysical quantities. Since the temperature can be assumed to increase downward at approximately the rate  $g$ , its value at depth  $h$  below the surface will be approximately  $(T_s - gh)$ . If  $T_s$  is given by (13), the temperature  $T(x, y)$  in the plane  $z = 0$  will be approximately

$$T(x, y) = T_0 + (g - g')h(x, y) \quad (19)$$

*Jeffreys* replaces the actual problem by that of the semi-infinite solid  $z > 0$  with its surface temperature given by (19). The temperature  $T_z$  at the point  $(0, 0, z)$  is in this case [*Carslaw and Jaeger*, 1959, sections 14.9(3), 16.3(7)]

$$T_z = (1/2\pi) \int_{-\infty}^{\infty} \int_{-\infty}^{\infty} z T(x', y') R^{-3} dx' dy' \quad (20)$$

where

$$R^2 = r'^2 + z^2 \quad \text{and} \quad r'^2 = x'^2 + y'^2 \quad (21)$$

The temperature  $T_z$  given by (20) is the perturbation imposed by the surface conditions, and its derivative ( $\partial T_z/\partial z$ ) at  $z = 0$  is the perturbation of the geothermal gradient. This is found to be

$$[\partial T_z/\partial z]_{z=0} = \int_0^{\infty} (d\bar{T}/dr') (dr'/r') \quad (22)$$

where

$$\bar{T} = (1/2\pi) \int_0^{2\pi} T(r' \cos \theta, r' \sin \theta) d\theta \quad (23)$$

is the mean value of  $T(x', y')$  over a circle of

radius  $r'$  around the origin. Equations 22 and 23 are readily evaluated numerically by using a grid of polar coordinates. *Bullard* [1940] has extended the theory slightly to give the mean disturbance of gradient from the surface to any depth.

### 5.3 The Effect of Changes in Surface Conditions

At the boundaries of the sea or of lakes, it may be expected that there will be a change of surface conditions. Suppose that steady conditions prevail and that the temperature in the surface  $z = 0$  is  $T_0$ , constant, for  $y > 0$  and zero for  $y < 0$ ; then, as in (20), the temperature at  $(x, y, z)$  is

$$T(x, y, z) = (zT_0/2\pi) \int_{-\infty}^{\infty} dx' \int_0^{\infty} [z^2 + (x - x')^2 + (y - y')^2]^{-3/2} dy' \quad (24)$$

$$= T_0 \left[ \frac{1}{2} + (1/\pi) \tan^{-1}(y/z) \right] \quad (25)$$

$$\partial T / \partial z = -yT_0 / [\pi(y^2 + z^2)] \quad (26)$$

*Lachenbruch* [1957] has considered the time-dependent case which occurs during changes of sea level or the drying up of lakes.

### 5.4 The Effect of Variations in Thermal Conductivity

The topographic correction as discussed above for uniform thermal conductivity is slightly unrealistic, since this condition is rarely encountered. If the geological structure of the region is reasonably well known, any of the standard numerical or analog methods for the solution of Laplace's equation can be used. *Bullard* [1939] and *Coster* [1947] used the electrolytic tank; conducting paper is also useful. The effects of simple model systems can be studied as in section 10.

## 6. THE EFFECT OF PAST CLIMATIC CHANGES

The surface temperature of the Earth has not remained constant and, in particular, many regions have been subjected to Pleistocene and recent glaciations whose effects may be preserved at depths of the order of those penetrated by boreholes.

An early classical study of the influence of the

ice age is that of *Hotchkiss and Ingersoll* [1934] in a deep copper mine at Calumet, Michigan. The theory has been set out very completely by *Birch* [1948].

The effect may be considered by assuming that in the time intervals  $(0, t_1)$ ,  $(t_1, t_2)$ ,  $(t_2, t_3)$ ,  $\dots$ , measured backward from the present, the surface temperature differed from its present value by fixed amounts,  $0, T_1, T_2, \dots$ , respectively. It is known [*Carlaw and Jaeger*, 1959, section 2.4] that

$$T = 1 - (2/\pi^{1/2}) \int_0^{z/2(\kappa t)^{1/2}} \exp(-\xi^2) d\xi \quad (27)$$

$$= 1 - \operatorname{erf} [z/2(\kappa t)^{1/2}]$$

satisfies the equation of conduction of heat in one dimension and the conditions  $T = 1$  when  $z = 0$ ,  $t > 0$  and  $T = 0$  when  $t = 0$ ,  $z > 0$ . It is therefore the solution appropriate to a sudden change of surface temperature for the semi-infinite region  $z > 0$ . The error function  $\operatorname{erf}(u)$  defined in (27) is tabulated in most books of tables. It is worth noting that  $\operatorname{erf}(\frac{1}{2}) = 0.520$ ,  $\operatorname{erf}(1) = 0.843$ ,  $\operatorname{erf}(2) = 0.995$  and, for small  $u$ ,  $\operatorname{erf}(u) = 2u/\pi^{1/2}$ .

The result for the step-function surface temperature assumed above can be written by combining solutions of type (27). Adding the effect of a geothermal gradient  $g$ , the temperature  $T$  at depth  $z$  is

$$T = T_0 + gz + T_1 R_1 + T_2 R_2 + \dots \quad (28)$$

where  $T_0$  is the present surface temperature and

$$R_n = \operatorname{erf} [z/2(\kappa t_n)^{1/2}] - \operatorname{erf} [z/2(\kappa t_{n+1})^{1/2}] \quad (29)$$

As a simple example, for a single ice age with  $T_1 = -V_1$  lasting from  $t_2$  to  $t_1$ , the temperature is

$$T = T_0 + gz - V_1 \{ \operatorname{erf} [z/2(\kappa t_1)^{1/2}] - \operatorname{erf} [z/2(\kappa t_2)^{1/2}] \} \quad (30)$$

The geothermal gradient at the surface  $z = 0$  is

$$g_0 = g - V_1 \{ (\pi \kappa t_1)^{-1/2} - (\pi \kappa t_2)^{-1/2} \} \quad (31)$$

For  $V_1 = 15^\circ\text{C}$ ,  $\kappa = 0.01 \text{ cm}^2/\text{sec}$ ,  $t_1 = 10^4$  years,  $t_2 = \infty$ , the disturbance of the geothermal gradient amounts to  $15^\circ\text{C}/\text{km}$ , and so the effect can be serious by comparison with the undisturbed gradient, which may be of the order of  $30^\circ\text{C}/\text{km}$ .

It follows from (30) that  $(\partial^2 T / \partial z^2)$  is positive, so that in this case the curve of  $T$  against  $z$  is concave upward.

Recently *Gough* [1963] has studied a number of relatively deep holes in which times of up to a million years may be of importance. In such cases it is necessary to hypothesize climatic changes and to compare temperatures calculated from them with observed temperature-depth curves.

### 7. THE EFFECT OF INTRUSIONS

Many calculations of temperatures in and around cooling igneous bodies of various shapes have been made. These have been reviewed by *Lovering* [1955] and more recently by *Jaeger* [1964]. *Lovering* [1935] gave full information in graphical form for cooling of plane intrusive or extrusive sheets and also of a laccolith of spherical or rectangular shape. His calculations ignored the effect of latent heat of solidification, but this has been taken into account by *Jaeger* [1959a] for the plane sheet and by *Pekeris and Slichter* [1939] for cylindrical geometry.

The cooling of an igneous intrusion is relatively rapid on the geological time scale. For example, if a plane sheet of thickness  $2d$  and infinite lateral extent is intruded at a temperature which exceeds that of the country rock by  $T_0$ , the excess temperature  $T_m$  on its mid-plane a relatively long time  $t$  after intrusion is approximately

$$T_m = dT_0(\pi\kappa t)^{-1/2} \quad (32)$$

If  $d = 500$  meters and  $\kappa = 0.01$  cm<sup>2</sup>/sec, it will have fallen to  $T_0/10$  after 250,000 years. The effect of latent heat may be included approximately by replacing  $T_0$  in (32) by  $(T_0 + L/c)$ , where  $L$  is the latent heat of solidification, and  $c$  the specific heat of magma.

If the geothermal gradient is  $g$ , its value at the surface a long time  $t$  after the intrusion is

$$g[1 - 2d(\pi\kappa t)^{-1/2}] \quad (33)$$

independent of the depth of the sheet, but assuming that it is horizontal.

For a deeply buried spherical intrusion of radius  $d$ , the temperature  $T_m$  at the center after a long time  $t$  is approximately

$$T_m = \frac{1}{3}\pi d^3 T_0 (\pi\kappa t)^{-3/2} \quad (34)$$

The results (32) and (34) are simply the

formulas for instantaneous plane and point sources [*Carslaw and Jaeger*, 1959, sections 10.3(4) and 10.2(2)]. More complicated disturbances can be simulated by integrating them in space or time. The effect of the surface can be taken into account by adding 'images.' *Von Herzen and Uyeda* [1963] have used steady sources of various shapes to explain anomalies in heat flow. In this case the solutions are the well-known ones of potential theory. *Rikitake* [1959] has studied the effect of a spherical intrusion on the geothermal gradient.

In a region in which there has been no recent igneous activity, (32) and (33) can be used to estimate whether any effects of earlier activity remain. In active regions, complete solutions such as those referred to above must be used. These refer only to removal of heat by pure conduction, however, and in such cases transport of heat by convective motion of groundwater may be of great importance (see section 9).

### 8. EROSION, SEDIMENTATION, AND UPLIFT

#### 8.1 General Treatment

Erosion and sedimentation may be treated by using the equation of heat conduction in a moving medium. If material is being eroded at speed  $U$ , the effect is equivalent to material below the actual surface moving toward the surface at this speed. Similarly, if material is added by sedimentation, or accreting snow, the material below can be regarded as moving away from the surface.

The equation of heat conduction in one dimension for material moving with velocity  $U$  in the  $z$  direction is

$$\partial T / \partial t + U(\partial T / \partial z) = \kappa \partial^2 T / \partial z^2 \quad (35)$$

and represents a balance between advection and conduction.

If the  $z$  axis is taken vertically downward from the surface  $z = 0$ , positive  $U$  corresponds to accretion or sedimentation, and in these cases the temperature at the surface will probably remain constant. In the case of erosion,  $U$  will be negative, and, since the actual height of the surface above the sea level is changing, the surface temperature can be expected to vary according to (13). If the whole region is being uplifted at a constant rate, its surface tempera-

TABLE 1. Values of  $\Psi(p)$  from Equation 39

$p$	-2	-1	-0.5	0	0.5	1	2
$\Psi(p)$	4.943	1.720	0.701	0	-0.451	-0.720	-0.943

ture will also decrease linearly with time according to (13).

If these processes are supposed to begin at time  $t = 0$  when the initial temperature is  $(T_0 + gz)$ , and if the surface  $z = 0$  is subsequently maintained at temperature  $(T_0 + bt)$ , the temperature at time  $t$  at depth  $z$  is given by

$$T = T_0 + g(z - Ut) + \frac{1}{2}(g + b/U) \left\{ (z + Ut) e^{Uz/\kappa} \operatorname{erfc} \left[ \frac{z + Ut}{2(\kappa t)^{1/2}} \right] + (Ut - z) \operatorname{erfc} \left[ \frac{z - Ut}{2(\kappa t)^{1/2}} \right] \right\} \quad (36)$$

where

$$\operatorname{erfc}(\xi) = 1 - \operatorname{erf}(\xi), \quad \operatorname{erf}(-\xi) = -\operatorname{erf}(\xi) \quad (37)$$

and the error function  $\operatorname{erf}(\xi)$  is defined in (27). The above solution [Carslaw and Jaeger, 1959, section 15.2(7)] covers all the cases referred to above, and it is readily extended to the case of heat production in the medium. Benfield [1949] discusses solution 36 and applies it to Coster's [1947] Persian measurements.

It follows from (36) that the temperature gradient at the surface is

$$[\partial T / \partial z]_{z=0} = g + (g + b/U)\Psi(p) \quad (38)$$

where

$$\Psi(p) = \frac{1}{2}p^2 - (1 + \frac{1}{2}p^2) \operatorname{erf}(\frac{1}{2}p) - (1/\pi^{1/2}) p \exp(-p^2/4) \quad (39)$$

and  $p$  is the dimensionless quantity  $Ut/(\kappa t)^{1/2}$ .  $\Psi(p)$  tends to  $-1$  for  $p$  large and positive and to  $(1 + p^2)$  for  $p$  large and negative. Some values of  $\Psi(p)$  are shown in Table 1.

For sedimentation with constant surface temperature,  $b = 0$ ; for erosion without uplift,  $b = -g'U$  and  $U$  is negative. For example, if 1000 meters is eroded in  $10^6$  years with  $\kappa = 0.01$  cm<sup>2</sup>/sec, then  $p = -0.18$ ,  $\Psi(p) = 0.22$ , and so by (38) such an erosion rate will change the temperature gradient at the surface to  $(1.22g - 0.22g')$  and so will be important.

## 8.2 Birch's Treatment of Topography Combined with Uplift or Erosion

Birch [1950] has extended Jeffreys' [1940] approximate treatment to allow for uplift or erosion. Like Jeffreys, he uses the solution for the semi-infinite solid with prescribed surface temperature as an approximation, but he allows for the effects of uplift or erosion by letting the surface temperature vary linearly with the time.

The fundamental solution then is that for the semi-infinite region  $z > 0$  in which the surface  $z = 0$  is maintained at temperature  $tf(x, y)$  for  $t > 0$ . Under these circumstances [Carslaw and Jaeger, 1959, section 14.9(3)], the temperature at depth  $z$  at time  $t$  is

$$T = \frac{z}{8(\pi\kappa)^{3/2}} \int_0^t \int_{-\infty}^{\infty} \int_{-\infty}^{\infty} \frac{f(x', y')}{(t - t')^{5/2}} \exp\left\{\frac{-R^2}{4\kappa(t - t')}\right\} dt' dx' dy' \quad (40)$$

$$= (zt/2\pi) \int_{-\infty}^{\infty} \int_{-\infty}^{\infty} R^{-3} f(x', y') E(\beta) dx' dy'$$

where

$$R^2 = z^2 + (x - x')^2 + (y - y')^2 \quad (41)$$

$$\beta = R(4\kappa t)^{-1/2} \quad (42)$$

and

$$E(\beta) = (1 - 2\beta^2) \operatorname{erfc}(\beta) + 2\beta\pi^{-1/2} \exp(-\beta^2) \quad (43)$$

For large values of  $t$ ,  $\beta \rightarrow 0$  and  $E(\beta) \rightarrow 1$ , so that the integral in (40) reduces to that in (20). Birch [1950] discusses the estimation of  $f(x', y')$  and the numerical evaluation of (40).

## 9. UNDERGROUND WATER MOVEMENT

The movement of underground water may greatly affect the values of geothermal gradients, particularly those obtained in shallow holes. Large flows of water are frequently found in tunnels, and it is quite common for drill holes to tap water-bearing seams at several levels and for water to flow along them [Jaeger and Sass

1963]. The effects of such flows can usually be recognized easily.

The recognition of the transport of heat by slow movement of water in aquifers is much more difficult. *Bullard and Niblett* [1951] consider the two-dimensional case of a stream of water flowing horizontally at depth  $(D + D_1)$  which suddenly rises to depth  $D$ . If the undisturbed geothermal gradient is  $g$ , the temperature of water at depth  $(D + D_1)$  will be  $g(D + D_1)$ , and this will be its approximate initial temperature as it begins to flow horizontally at depth  $D$ . Suppose that the thickness of the aquifer is  $d$ ,  $c$  is the specific heat of the water, and  $m$  is its rate of flow in  $g/cm^2$  sec. Then if the temperature of water in the aquifer at distance  $x$  from the step is  $T$ , the heat balance, assuming steady conditions, is

$$mcd(dT/dx) = Kg - KT/D \quad (44)$$

where the first term on the right-hand side represents the heat flux from below and the second the steady heat transfer to the surface. For the boundary condition  $T = g(D + D_1)$ , when  $x = 0$ , the solution of (44) is

$$T = g\{D + D_1 \exp(-Kx/mcdD)\} \quad (45)$$

On this simple model the change in the geothermal gradient at  $x = 0$  is from  $g$  to  $g(D + D_1)/D$ , which obviously may be large.

*Kappelmeyer* [1957] discusses the use of surface temperature measurements in studying underground water movement.

Convective motion of fluid in a porous medium is of fundamental importance in geothermal areas. The equations of motion and the mathematics of thermal convection in a porous medium have been discussed by *Lapwood* [1948], *Donaldson* [1962], and *Wooding* [1957, 1963]. Donaldson and Wooding both discuss situations related to the Wairakei geothermal region, New Zealand. A study of conditions in a geothermal area is given in the *Bulletin Waiotapu Geothermal Field* [1963], and a discussion of heat and mass transfer within the Earth is given by Elder in chapter 8 of this volume.

#### 10. THE EFFECT OF LOCAL VARIATIONS IN THERMAL CONDUCTIVITY ON THE GEOTHERMAL GRADIENT

As remarked in section 5, this question must be studied numerically or by analog methods for

specific situations [see *McBirney*, 1963; *Birch*, 1954; *Sbrana and Bossolasco*, 1952]. The fundamental equations for heat flow are identical with those for the flow of electricity. Ohm's law corresponds to the conduction law, potential difference to temperature difference, electrical conductivity to heat conductivity and electrical capacity to heat capacity' [*Ingersoll et al.*, 1954, p. 205]. Hence many known solutions of electrical problems are available, sometimes with great saving of time, for the solution of heat conduction problems. In particular, steady-state flows from sources within long circular cylinders imbedded in a homogeneous region, or the distortion of a uniform flow pattern by spheres, prolate or oblate ellipsoids, cylinders, two-dimensional planar dikes differing in conductivity from their surroundings are available as electrical analogs. In the magnetic method of prospecting, it is assumed that the source field is uniform locally and that the geologic structures differ in magnetic permeability. This method also provides examples of solutions which apply to analogous heat flow problems.

The polarization in uniform fields of ellipsoids of revolution has been tabulated by *Slichter* [1959] in terms of their fineness ratio and the ratio of the external to the internal conductivity. Within a homogeneous ellipsoid, as is well known, the polarization is uniform and parallel to the direction of the external field if the ellipsoid is aligned with an axis parallel to this field.

#### 10.1 An Ellipsoidal Region of Different Conductivity from the Surrounding Medium

The well-known solutions [*Carslaw and Jaeger*, 1959, section 16.4 III] for an ellipsoidal region of conductivity  $K'$  immersed in a medium of conductivity  $K$  in which the undisturbed gradient is  $g$  are occasionally useful as crude approximations. For ellipsoids of revolution the formulas involve only elementary functions.

If a prolate spheroid of axes  $a$  and  $b$  and eccentricity  $e = (a^2 - b^2)^{1/2}/a$  has its long axis parallel to the geothermal gradient  $g$ , the temperature gradient inside it is constant and has the value [*Carslaw and Jaeger*, 1959, section 16.4(16)]

$$g\{1 + (1/Ke^3)(K' - K)(1 - e^2) [\frac{1}{2} \ln [(1 + e)/(1 - e)] - e]\}^{-1} \quad (46)$$

If  $a = b$ ,  $e = 0$ , this reduces to the value for a sphere, namely

$$3Kg/(2K + K') \quad (47)$$

For a very long spheroid of axes  $a$  and  $b$ ,  $a \gg b$ ,  $e$  is approximately  $1 - b^2/2a^2$  and the gradient in the spheroid is approximately

$$g\{1 + (b^2/Ka^2) / (K' - K)[\ln(2a/b) - 1]\}^{-1} \quad (48)$$

Equation 48 has been used to estimate the effect of casing in drill holes.

If an oblate spheroid of eccentricity  $e$  has its short axis parallel to the geothermal gradient  $g$ , the temperature gradient inside it is constant and has the value [Carslaw and Jaeger, 1959, section 16.4(19)]

$$g\{1 + (1/Ke^3)(K' - K) / [e - (1 - e^2)^{1/2} \cot^{-1} \{(1 - e^2)^{1/2}/e\}]\}^{-1} \quad (49)$$

Equations 46 and 49 hold accurately both when the ellipsoids are deeply buried and when their centers are in the surface (but not at depths moderate relative to the dimensions of the ellipsoid). Von Herzen and Uyeda [1963] have used (49) to estimate the effect of a depression in a rock surface filled with sediments of low conductivity.

The formulas for an elliptic cylinder with its axis horizontal are even simpler. If the axes of the ellipse,  $a$  and  $b$ , are vertical and horizontal, respectively, the temperature gradient in the cylinder is vertical and has the value

$$g\{1 - b(K' - K)/(aK + bK')\} \quad (50)$$

If  $a \gg b$ , the gradient is  $g$ . If  $a \ll b$  it has the value  $gK/K'$  associated with a layer of conductivity  $K'$  above material of conductivity  $K$ . For intermediate values, considerable variation is possible, for example, for the case  $b = a$ ,  $K' = 2K$ , the gradient is  $2g/3$ .

Outside the ellipsoid, the formulas for the temperature are more complicated, but they can be used to estimate the way in which the temperature varies as the ellipsoid is approached. Jaeger and Le Marne [1963] discuss the behavior outside an elliptic cylinder.

## 10.2 Refraction at an Interface

Suppose that two uniform mediums of conductivities  $K_1$  and  $K_2$  have a plane surface of

separation and that the values of the heat flux in them are  $f_1$  and  $f_2$ , respectively, in directions inclined at angles  $\alpha_1$  and  $\alpha_2$  to the normal to the plane of separation.

The boundary conditions at the surface are continuity of the normal component of the heat flux and continuity of temperature (and hence of the temperature gradient along the surface). These give

$$f_1 \cos \alpha_1 = f_2 \cos \alpha_2 \quad (51)$$

$$(f_1/K_1) \sin \alpha_1 = (f_2/K_2) \sin \alpha_2 \quad (52)$$

It follows that

$$K_2 \tan \alpha_1 = K_1 \tan \alpha_2 \quad (53)$$

which is the law of refraction at the surface.

Now suppose that a straight drill hole in the plane of  $f_1$  and  $f_2$  makes an angle  $\theta$  with the normal (measured toward  $\alpha_1$ ). If  $f_{1\theta}$  and  $f_{2\theta}$  are the values of the component of heat flux measured along the drill hole in the two mediums,

$$\frac{f_{2\theta}}{f_{1\theta}} = \frac{f_2 \cos(\theta - \alpha_2)}{f_1 \cos(\theta - \alpha_1)} = \frac{\cos \alpha_1 \cos(\theta - \alpha_2)}{\cos \alpha_2 \cos(\theta - \alpha_1)} \quad (54)$$

It follows that the measured flux changes at the interface. If the drill hole is in the direction of  $f_1$ ,  $\theta = \alpha_1$  and (54) becomes

$$f_{2\theta}/f_1 = 1 - [(K_1 - K_2)/K_1] \sin^2 \alpha_1 \quad (55)$$

In the practical case of a dipping contact between two mediums, the isothermals will be curved because of the additional condition that the temperature has to be constant at the Earth's surface. The above relations still hold, but the angle  $\alpha_1$  is only known if the actual shapes of the isothermal surfaces are known. Roy [1963, p. 18] makes the simplifying assumption that the isothermal surfaces are horizontal in the upper medium. In this case  $\alpha_1$  will be the angle of dip of the contact and (55) gives the change in heat flux measured in a vertical drill hole.

## 11. TEMPERATURES AROUND DRILL HOLES

Two fundamental results are often needed. First, if the region  $r > a$  outside a circular hole of radius  $a$  is initially at constant temperature  $T_0$  and the surface of the hole is maintained at  $T_1$  for  $t > 0$ , the heat flux at the surface of the hole is [Carslaw and Jaeger, 1959, section 13.5(8)]

$$[4K(T_1 - T_0)/\pi^2 a] I(\kappa t/a^2) \quad (56)$$

TABLE 2. Values of  $I(\kappa t/a^2)$

$\kappa t/a^2$	0.1	0.3	1	3	10	30	100	300	1000
$I(\kappa t/a^2)$	5.549	3.643	2.427	1.767	1.317	1.052	0.853	0.725	0.620

where  $I(\kappa t/a^2)$  is an integral involving Bessel functions which has been tabulated by *Jaeger and Clarke* [1942]. Some values are given in Table 2. The temperature variation outside the hole has been tabulated by *Jaeger* [1956a]: close to the hole it is given by

$$T - T_1 = 4(T_0 - T_1) \pi^{-2} \ln(r/a) I(\kappa t/a^2) \quad (57)$$

The second useful result is the temperature distribution due to a line source of infinite length which emits  $Q$  units of heat per unit time per unit length for times  $t > 0$  in an infinite medium initially at zero temperature. The temperature at distance  $r$  at time  $t$  is [*Carslaw and Jaeger*, 1959, section 10.4(4)]

$$T = (Q/4\pi K) \int_{r^2/4\kappa t}^{\infty} e^{-u} u^{-1} du \quad (58)$$

$$= - (Q/4\pi K) Ei(-r^2/4\kappa t)$$

where the exponential integral  $Ei(-x)$  is tabulated, and, for large values of  $t$ , (58) is given approximately by

$$T = (Q/4\pi K) Ei(-r^2/4\kappa t) + (r^2/4\kappa t) - (r^4/64\kappa^2 t^2) + \dots \quad (59)$$

### 11.1 Temperature Measurements in Mines and Tunnels

In new tunnels and mine drifts, the usual practice is to drill short holes into the walls and to measure temperatures in these after so short a time that ventilation cooling has not penetrated to the position of the thermometer. If the change in surface temperature due to ventilation is  $T_0$ , the change in temperature at depth  $x$  after time  $t$  will be [*Carslaw and Jaeger*, 1959, section 2.4(10)]

$$T_0 \operatorname{erfc} [x/2(\kappa t)^{1/2}] \quad (60)$$

Taking  $\kappa = 0.01$  cm<sup>2</sup>/sec, this has the value  $T_0/100$  when  $t = 7.6x^2$ , or 84 hours for a depth of 2 meters.

In a working mine, many old exploratory drill holes are found at various levels drilled from drifts which have been cooling according to (57) for some time. After ten years the region

affected by ventilation cooling may extend to 50–80 meters according to the conductivity of the rock. Further, ventilation conditions are frequently not constant. It is desirable to make a series of measurements along each hole and verify that they are consistent with the logarithmic relation 57. The procedure is discussed by *Jaeger and Le Marne* [1963].

### 11.2 The Disturbance of Temperature Caused by Drilling

The process of drilling causes a disturbance of temperature both by the heat generated at the bit and by heat exchange by the drilling fluid.

*Bullard* [1947] estimated the time necessary for this disturbance to die away by representing the operations of drilling by a line source  $Q$  of heat. If drilling has gone on for time  $t_1$ , the temperature  $T_0$  at radius  $a$  will be (according to equation 59) approximately

$$T_0 = (Q/4\pi K) [\ln(4\kappa t_1/a^2) - 0.577] \quad (61)$$

The effect of ceasing to drill at time  $t_1$  can be regarded as that of starting a negative source  $-Q$  at this time, so that the temperature at  $r = a$  at time  $t$  after the cessation of drilling is given by

$$T = (Q/4\pi K) \ln(1 + t_1/t) \quad (62)$$

and the way in which the disturbance dies away is given by

$$T/T_0 = \frac{[\ln(1 + t_1/t)]}{[\ln(4\kappa t_1/a^2) - 0.577]} \quad (63)$$

From this result *Bullard* concluded that, for the hole to return to within 1% of equilibrium,  $t$  must be of the order of  $10t_1$ . *Jaeger* [1956a] obtained a similar result after a more elaborate calculation. *Lachenbruch and Brewer* [1959] and *Cheremenski* [1960] have extended the theory and compared it with observations. *Lachenbruch and Brewer* show that in a practical case temperatures at  $t = 3t_1$  are within 0.05°C of the equilibrium values.

One result of these estimates has been to discourage measurements during drilling or shortly

TABLE 3. Values of  $\kappa t/a^2$  at Which the Temperature Has Fallen to 1/20 Its Initial Value

$\alpha$	0.5	1	1.5	2	4	6	8
$\kappa t/a^2$	22	11	6.5	4.5	1.9	1.1	0.7

after it has ceased, that is, when they are most conveniently made. Some workers [e.g., *Cooper and Jones*, 1959] use bottom-hole temperatures, which may be expected to be least in error. However, a number of observations has suggested that in some cases the disturbance can be quite small. In fact, the situation is quite complicated: drilling fluid is pumped down the drill rods and up the annulus outside, so that the rods act as a counterflow heat exchanger; the fluid in the annulus is also heated by the rock in the lower parts of the hole. *Jaeger* [1961] has attempted to analyze this situation using (56) to describe the heat flow into the rock; he found that the controlling factor is the mass-velocity of drilling fluid. For the relatively small water flows used in small core diamond drilling, the effect on the temperature gradient is negligible except near the top and bottom of the hole, so that measurements can safely be taken about two days after the cessation of drilling. On the other hand, for the large flows used in rotary drilling, mud temperature is the controlling factor (see Chapter 3, section 3.2, in this volume by Beck).

This conclusion is only valid for drilling in a tight formation. If there is water loss in the hole or if groundwater is encountered, conditions may be quite different.

#### 12. THE DISTURBANCE IN TEMPERATURE CAUSED BY THE SUDDEN INTRODUCTION OF A CYLINDRICAL CONDUCTOR AT A DIFFERENT TEMPERATURE

If a cylindrical conductor is lowered rapidly in a bore hole and suddenly brought to rest, the time it takes to come into temperature equilibrium is determined by conduction of heat through the rock into it. For this purpose, a metallic conductor can be regarded as a perfect conductor. A similar effect was discussed by *Bullard* [1954] in connection with the ocean bottom temperature probe in which frictional heating during penetration raises the temperature of the probe instantaneously. The theory [*Carslaw and Jaeger*, 1959, section 13.7I] is

given in detail by *Jaeger* [1956b], who also considers the case of thermal resistance at the contact and gives numerical values.

In the absence of contact resistance, the theory involves two parameters:  $\kappa t/a^2$ , where  $a$  is the radius of the perfect conductor, and  $\kappa$  is the diffusivity of the surrounding medium; and  $\alpha$ , which is defined as twice the ratio of the heat capacity per unit volume of the surrounding medium to that of the perfect conductor. Values of  $\kappa t/a^2$  at which the temperature has fallen to 1/20 of its initial value are shown in Table 3.

In dry holes, the thermal resistance of the air between the probe and the walls of the hole is a dominating factor, and equilibrium is attained much more slowly.

Lovering (personal communication) remarks that in practice it is desirable to keep the initial temperature difference between the probe and rock as small as possible. This can be achieved by holding the probe for a time at a short distance above the point where the temperature is to be measured before lowering it into its final position.

#### 13. TRANSIENT METHODS FOR MEASURING THERMAL CONDUCTIVITY

Many transient solutions of the equation of conduction of heat for bodies of simple shapes can be used as the basis for measurement of one or, in many cases, two of the quantities  $K$ ,  $\kappa$ , and  $K\kappa^{-1/2}$ . One fundamental experimental difficulty lies in ensuring that the boundary conditions postulated (e.g., a sudden change of surface temperature) are adequately satisfied. Another practical difficulty arises in making good thermal contacts between temperature measuring elements and rock samples. Errors from the latter cause become less important as the size of the specimen increases.

The classical methods developed in the last century, and reviewed briefly by *Carslaw and Jaeger* [1959, section 1.11], usually determine  $\kappa$  from the late stages of a temperature-time curve for a body such as a finite cylinder for which the solution takes a simple form.

Since material is so frequently available in the form of core, one-dimensional flow of heat in either short or long pieces of core can easily be used (the curved surface being insulated and loss of heat from it neglected). For a sudden change in temperature at one surface, solutions are given by *Carlsaw and Jaeger* [1959, sections 2.4 and 3.3]. For constant heat supply by a flat heating element switched on at time  $t = 0$ , solutions are given by *Carlsaw and Jaeger* [1959, sections 3.8, 10.4, and 2.9). *Verzhinskaya and Novichenok* [1960] have used the latter method.

If two materials (one with unknown properties  $K, \kappa$  and one with known properties  $K_1, \kappa_1$ ) at different temperatures  $T, T_1$  are brought suddenly into contact over the plane face  $x = 0$ , the temperature in this plane instantaneously assumes the value

$$T + (T_1 - T) \{1 + K\kappa_1^{1/2}/K_1\kappa^{1/2}\}^{-1} \quad (64)$$

provided that there is no thermal resistance at the surface [*Carlsaw and Jaeger*, 1959, section 2.15(5)]. The case of thermal resistance at the surface and the calculation of temperatures away from it are discussed by *Carlsaw and Jaeger* [1959, section 2.15). *Zierfuss* [1963] used this method for the rapid determination of thermal conductivity of material in the form of disks. The thermal comparator [*Powell and Tye*, 1960] is an application of the same principle. In this instrument a metal sphere is brought into contact with the material to be tested, so that the method is nondestructive and elaborate preparation of specimens is avoided.

Many of the methods now in vogue use a line source of heat. Essentially they all depend on a solution of the same type as (59) for the simple line source. It follows from (59) that if  $r^2/4\kappa t$  is small a plot of  $T$  against  $\ln(t)$  is a straight line of slope  $Q/4\pi K$ , and so  $K$  is found immediately. The requirement that  $r^2/4\kappa t$  be small relative to  $\ln(4\kappa t/r^2)$  sets the time scale of the experiment: if  $r = 0.1$  cm, this condition is attained in less than one minute; if  $r = 1$  cm, in an hour or so.

With most transient methods it is easy to obtain a spurious result, either because of inadequacy of the apparatus or theory, or because a linear or logarithmic asymptote is not completely attained. *Jaeger* [1959*b, c*] has advocated methods in which the complete temperature-time curve is used to determine both  $K$  and

$\kappa$ ; if these combine to give a reasonable value of  $\rho c$ , a useful check is obtained. In one such method the ratio  $T(2t)/T(t)$  of measured temperatures at times  $2t$  and  $t$  is compared with the calculated value of this ratio, which for the simple line source (58) has the value

$$T(2t)/T(t) = Ei(-r^2/8\kappa t)/Ei(-r^2/4\kappa t) \quad (65)$$

This gives  $\kappa$ , and comparison of theoretical and experimental curves with this value of  $\kappa$  gives  $K$ .

### 13.1 Probe Methods for In Situ Measurements

In the 'probe' methods a long cylindrical probe of radius  $a$  which contains a heater and a temperature measuring element is used. The idealized model is a perfect thermal conductor of radius  $a$  with heat supply  $Q$  per unit length per unit time immersed in material of conductivity  $K$ , and possibly with thermal resistance at the interface [*Carlsaw and Jaeger*, 1959, section 13.7II]. The theory has been given by *Blackwell* [1954], *Jaeger* [1956*b*], and *De Vries and Peck* [1958]. Solutions are obtained in terms of infinite integrals whose values can be calculated numerically. For large values of time the solutions take a form similar to (59), namely

$$T = (Q/4\pi K) \{ \ln(4\kappa t/a^2) + A + B(a^2/\kappa t) + C(a^4/\kappa^2 t^2) + \dots \} \quad (66)$$

where now  $A, B$ , and  $C$  are constants depending on the thermal mass of the probe, the thermal resistance at its surface, etc.

For soils [*De Vries and Peck*, 1958] and ocean bottom sediments [*Von Herzen and Maxwell*, 1959], 'needle' probes less than 1 mm in diameter are eminently satisfactory; the logarithmic portion of the curve predominates in less than one minute. The technique is described by *Langseth* in chapter 4, section 3.2 of this volume.

For measurements in drilled holes which may be from 3 to 6 cm in diameter, the logarithmic portion of the curve may not be attained for hours: hence either (1) a very long experiment is needed with its attendant possibility of errors by heat loss longitudinally and by convection and possibly vaporization of water; (2) the constants  $A, B$ , and  $C$  in equation 66 must be determined experimentally and theoretically [*Blackwell*, 1954]; or (3) the complete, accurately calculated, temperature-time curve [*Beck et al.*, 1956] can be used. None of these methods is altogether satisfactory. The diffi-

culties are particularly serious with dry holes, because of the high thermal resistance between the probe and the walls of the hole. Further discussion is given by Beck in chapter 3, section 2.3, of this volume.

### 13.2 Laboratory Probe and Line Source Methods

The application of line-source methods to rocks is difficult, since it is hard to drill long holes of small diameter. *Woodside and Messmer* [1961] have used a needle probe with Wood's metal as contact material. *Jaeger* [1959c] and *Jaeger and Sass* [1964] described a number of line source methods suitable for use with cylindrical core in which the heater is either in a slot in the core or between two surfaces. The theory is that of *Carslaw and Jaeger* [1959, section 14.18].

*Shushpanov and Shushpanov* [1960] use the solution for an instantaneous line source of length  $2l$ , obtained as by *Carslaw and Jaeger* [1959, section 10.31]. If the quantity of heat liberated is  $Q$  per unit length per unit time for  $t > 0$ , the temperature at time  $t$  at distance  $r$  from the line in the plane through its midpoint and perpendicular to it is

$$(Q/4\pi Kt) \exp(-r^2/4\kappa t) \operatorname{erf}[l/2(\kappa t)^{1/2}] \quad (67)$$

This has its maximum value when  $t$  is the root of

$$(2/l)(\pi\kappa t)^{1/2}[(r^2/4\kappa t) - 1] \operatorname{erf}[l/2(\kappa t)^{1/2}] = \exp(-l^2/4\kappa t) \quad (68)$$

$\kappa$  can be determined from this time, and  $K$  then follows from the temperature (67).

*Lubimova et al.* [1960] have used the result corresponding to (67) for a cylindrical surface source of radius  $a$  and length  $2l$ , namely [*Carslaw and Jaeger*, 1959, section 10.3(5)],

$$(Q/4\pi Kt) \exp[-(r^2 + a^2)/4\kappa t] I_0(ar/2\kappa t) \operatorname{erf}[l/2(\kappa t)^{1/2}] \quad (69)$$

## 14. ANISOTROPIC THERMAL CONDUCTIVITY

Anisotropic rocks usually have one principal conductivity  $K_3$  perpendicular to the bedding or foliation and  $K_1 = K_2$  parallel to it. The measured conductivity  $K_\theta$  of a section cut in a plane inclined at  $\theta$  to the bedding is [*Carslaw and Jaeger*, 1959, section 1.20 (16)],

$$K_\theta = K_1 + (K_3 - K_1) \cos^2 \theta \quad (70)$$

If a continuous line source runs perpendicular to the bedding, the temperature at distance  $r$  from it at time  $t$  is given by (58) with  $K$  replaced by  $K_1$  so that the conductivity in the direction of the bedding is measured, as might be expected. For all other directions a mean conductivity involving  $K_1$  and  $K_3$  is measured; the theory follows from *Carslaw and Jaeger* [1959, section 10.2(8)]. *Simmons* [1961] had drawn attention to this fundamental difficulty with probe and line source methods in general.

If several holes are available in different directions, all the principal conductivities can be calculated from probe measurements in them. Alternatively the ratio of the principal conductivities can be found by the simple method of *De Senarmont* [1847] [see *Carslaw and Jaeger*, 1959, section 1.19]. I. S. Fatt (personal communication) has shown that this method can be used very simply with thermally sensitive paint on relatively large pieces of material. The transient methods of *Zierfuss* [1963] and *Verzhinskaya and Novichenok* [1960], referred to in section 13, as well as the usual steady-state methods are free from this difficulty if used on core from a vertical drill hole.

If the rock below the Earth's surface  $z = 0$  is anisotropic, the isothermal surfaces will be parallel to the Earth's surface but the direction of the heat flux vector is not perpendicular to them. If  $K_1 = K_2$ , and  $K_3$  is inclined at  $\theta$  to the vertical, the geothermal flux (the component of the heat flux vector normal to the surface) will be [*Carslaw and Jaeger*, 1959, section 1.18(9) and (12)]

$$K_\theta(\partial T/\partial z) \quad (71)$$

where  $K_\theta$  is given by (70). The component of the heat flux parallel to the surface is  $\frac{1}{2}(K_1 - K_3)(\partial T/\partial z) \sin 2\theta$  in the plane containing  $K_3$  and the normal to the surface.

## 15. SUMMARY

The sources of the mathematical theory presently in use for the reduction of geothermal measurements and in the measurement of thermal conductivity have been reviewed in this chapter. Most of the results quoted, or solutions from which they could be written immediately, have been known since the last century. The first (1913) edition of the book by *Ingersoll et al.*

[1954] contains many references to geological problems. Almost the only new mathematics stimulated by geothermal work have been the development of the theory of the conductivity probe and the ocean bottom temperature probe.

One reason for this backwardness has been the fundamental lack of knowledge of the input data, so that there was little point in using any but the simplest mathematical solutions. This applies to the corrections for topography, uplift and erosion, and past climatic changes.

The present state of knowledge of the effects of movement of groundwater and of lateral variations in thermal conductivity is most unsatisfactory. Unlike the topics mentioned above, there are no simple mathematical solutions which allow their effects to be assessed. When anomalous thermal gradients are measured, they are commonly attributed to one or another of these causes, and occasionally attempts are made to calculate orders of magnitude for postulated local conditions. It would be very valuable to have numerical solutions for a variety of simple idealized situations.

Transient methods for the measurement of thermal conductivity have some advantages; for example, they are absolute and also in many cases can be used in situ. A vast amount of theory for various methods is available, but sufficient experimental study of them has not yet been made.

*Acknowledgments.* I am greatly indebted to Dr. T. S. Lovering and Professor L. B. Slichter for their criticism of the manuscript and for many improvements in it.

## REFERENCES

- Andraea, C., La prévision des températures souterraines, *Ann. Ponts et Chaussées*, 128, 37-85, 1958.
- Beck, A. E., J. C. Jaeger, and G. Newstead, The measurement of the thermal conductivities of rocks by observations in boreholes, *Australian J. Phys.*, 9, 286-296, 1956.
- Benfield, A. E., The effect of uplift and denudation on underground temperatures, *J. Appl. Phys.*, 20, 66-70, 1949.
- Berry, F. A., E. Bollay, and N. R. Beers, *Handbook of Meteorology*, McGraw-Hill Book Company, New York, 1945.
- Birch, F., The effects of Pleistocene climatic variations upon geothermal gradients, *Am. J. Sci.*, 246, 729-760, 1948.
- Birch, F., Flow of heat in the Front Range, Colorado, *Bull. Geol. Soc. Am.*, 61, 567-630, 1950.
- Birch, F., The present state of geothermal investigations, *Geophysics*, 19, 645-659, 1954.
- Birch, F., Physics of the crust, *Geol. Soc. Am. Spec. Paper 62*, 101-117, 1955.
- Blackwell, J. H., A transient flow method for determination of thermal constants of insulating materials in bulk, *J. Appl. Phys.*, 25, 137-144, 1954.
- Bullard, E. C., Heat flow in South Africa, *Proc. Roy. Soc. London, A*, 173, 474-502, 1939.
- Bullard, E. C., The disturbance of the temperature gradient in the earth's crust by inequalities of height, *Monthly Notices Roy. Astron. Soc., Geophys. Suppl.*, 4, 360-362, 1940.
- Bullard, E. C., The time necessary for a borehole to attain temperature equilibrium, *Monthly Notices Roy. Astron. Soc., Geophys. Suppl.*, 5, 127-130, 1947.
- Bullard, E. C., The flow of heat through the floor of the Atlantic Ocean, *Proc. Roy. Soc. London, A*, 222, 408-429, 1954.
- Bullard, E. C., and E. R. Niblett, Terrestrial heat flow in England, *Monthly Notices Roy. Astron. Soc., Geophys. Suppl.*, 6, 222-238, 1951.
- Carslaw, H. S., and J. C. Jaeger, *Conduction of Heat in Solids*, second edition, Oxford University Press, London, 1959.
- Chereminski, G. A., Time of re-establishing the thermal conditions disturbed by drilling a borehole, *Izv. Akad. Nauk SSSR, Ser. Geofiz.*, 1960, 1801-1805, 1960.
- Clark, S. P., Jr., and E. A. Ringwood, Density distribution and constitution of the mantle, *Rev. Geophys.*, 2, 35-88, 1964.
- Cooper, L. R., and C. Jones, The determination of virgin strata temperatures from observation in deep survey boreholes, *Geophys. J.*, 2, 116-131, 1959.
- Coster, H. P., Terrestrial heat flow in Persia, *Monthly Notices Roy. Astron. Soc., Geophys. Suppl.*, 5, 131-145, 1947.
- De Senarmont, H., *Compt. Rend.*, 21, 459, 1847.
- De Vries, D. A., and A. J. Peck, On the cylindrical probe method of measuring thermal conductivity with special reference to soils, *Australian J. Phys.*, 11, 255-271, 1958.
- Donaldson, I. G., Temperature gradients in the upper layers of the Earth's crust due to convective water flows, *J. Geophys. Res.*, 67, 3449-3459, 1962.
- Emmons, H. W., *Trans. Am. Soc. Mech. Engrs.*, 65, 607-615, 1943.
- Emmons, H. W., *Quart. Appl. Math.*, 2, 173, 1944.
- Gough, D. I., Heat flow in the Southern Karroo, *Proc. Roy. Soc. London, A*, 272, 207-230, 1963.
- Hotchkiss, W. O., and L. R. Ingersoll, Post glacial time calculations from recent geothermal measurements in the Calumet Copper Mines, *J. Geol.*, 42, 113-122, February and March, 1934.
- Howard, L. E., Heat flow in Australia, thesis, Australian National University, Canberra, 1964.
- Ingersoll, L. R., O. J. Zobel, and A. C. Ingersoll,

- Heat Conduction with Engineering and Geological Applications*, University of Wisconsin Press, 1954.
- Jaeger, J. C., Numerical values for the temperature in radial heat flow, *J. Math. Phys.*, *34*, 316-321, 1956a.
- Jaeger, J. C., Conduction of heat in an infinite region bounded internally by a circular cylinder of a perfect conductor, *Australian J. Phys.*, *9*, 167-179, 1956b.
- Jaeger, J. C., Temperatures outside a cooling intrusive sheet, *Am. J. Sci.*, *257*, 44-54, 1959a.
- Jaeger, J. C., The analysis of aquifer test data or thermal conductivity measurements which use a line source, *J. Geophys. Res.*, *64*, 561-567, 1959b.
- Jaeger, J. C., The use of complete temperature-time curves for determination of thermal conductivity with particular reference to rocks, *Australian J. Phys.*, *12*, 203-217, 1959c.
- Jaeger, J. C., The effect of the drilling fluid on temperatures measured in boreholes, *J. Geophys. Res.*, *66*, 563-569, 1961.
- Jaeger, J. C., Thermal effects of intrusions, *Rev. of Geophys.*, *2*, 443-466, 1964.
- Jaeger, J. C., and M. E. Clarke, A short table of  $I(0, 1; x)$ , *Proc. Roy. Soc. Edinburgh, A*, *61*, 229-230, 1942.
- Jaeger, J. C., and A. Le Marne, The penetration of ventilation cooling around mine openings and extrapolation to virgin rock temperatures, *Australian J. Appl. Sci.*, *14*, 95-108, 1963.
- Jaeger, J. C., and J. H. Sass, Lees' topographic correction in heat flow and the geothermal flux in Tasmania, *Geofis. Pura Appl.*, *54*, 53-63, 1963.
- Jaeger, J. C., and J. H. Sass, A line source method for measuring the thermal conductivity and diffusivity of cylindrical specimens of rock and other poor conductors, *Brit. J. Appl. Phys.*, *15*, 1187-1194, 1964.
- Jeffreys, H., The disturbance of the temperature gradient in the earth's crust by inequalities of height, *Monthly Notices Roy. Astron. Soc., Geophys. Suppl.*, *4*, 309-312, 1940.
- Kappelmeyer, O., The use of near surface temperature measurements for discovering anomalies due to causes at depths, *Geophys. Prospecting*, *5*, 239-258, 1957.
- Kelvin, W. T., The reduction of observations of underground temperature, *Trans. Roy. Soc. Edinburgh*, *22*, 405-427, 1861.
- Lachenbruch, A. H., Thermal effects of the ocean on permafrost, *Bull. Geol. Soc. Am.*, *68*, 1515-1530, 1957.
- Lachenbruch, A. H., and M. C. Brewer, Dissipation of the temperature effect in drilling a well in Arctic Alaska, *U. S. Geol. Surv. Bull.* *1083-C*, 73-109, 1959.
- Lapwood, E. R., Convection of a fluid in a porous medium, *Proc. Camb. Phil. Soc.*, *44*, 508-521, 1948.
- Lees, C. H., On the shapes of the isogeotherms under mountain ranges in radioactive districts, *Proc. Roy. Soc. London, A*, *83*, 339-346, 1910.
- Lovering, T. S., Theory of heat conduction applied to geological problems, *Bull. Geol. Soc. Am.*, *46*, 69-94, 1935.
- Lovering, T. S., Temperatures in and near intrusions, *Econ. Geol.*, *50*, 249-281, 1955.
- Lovering, T. S., *U. S. Geol. Survey Prof. Paper 504*, in press, 1965.
- Lovering, T. S., and H. D. Goode, Measuring geothermal gradients in drill holes less than 60 feet deep, East Tintic District, Utah, *U. S. Geol. Surv. Bull.* *1172*, 1963.
- Lubimova, E. A., L. M. Lusova, F. V. Firsov, G. N. Starikova, and A. P. Shushpanov, Determination of the heat flow at Stary Matsesta, *Izv. Akad. Nauk SSSR, Ser. Geofiz.*, 1960, 1806-1811, 1960.
- McBirney, A. R., Conductivity variations and terrestrial heat flow distribution, *J. Geophys. Res.*, *68*, 6323-6329, 1963.
- Pekeris, C. L., and L. B. Slichter, *J. Appl. Physics*, *10*, 135-137, 1939.
- Powell, R. W., and R. P. Tye, The thermal comparator in non-destructive testing, in *Techniques of Non-Destructive Testing*, pp. 175-189, Butterworth, London, 1960.
- Rikitake, T., Studies of the thermal state of the earth, 2, Heat flow associated with magma intrusion, *Bull. Earthquake Res. Inst. Tokyo Univ.*, *37*, 233-243, 1959.
- Roy, R. F., Heat flow measurements in the United States, Ph.D. thesis, Harvard University, University Microfilm Inc., Ann Arbor, Michigan, 1963.
- Sbrana, F., and M. Bossolasco, Sul Regime termico degli strati superiori della crosta terrestre, *Geofis. Pura Appl.*, *23*, 3-8, 1952.
- Schössler, K., and J. Schwarzlose, Geophysikalische Wärmeflussmessungen, *Freiburger Forschungshefte*, *C75*, *Geophysik*, Springer, Berlin, 1959.
- Shushpanov, A. P., and P. I. Shushpanov, The cylindrical source of heat method of determining thermophysical coefficients, *Inzh. Fiz. Zh.*, *3*, 74-77, 1960.
- Simmons, G., Anisotropic thermal conductivity, *J. Geophys. Res.*, *66*, 2269-2270, 1961.
- Slichter, L. B., Aspects, mainly geophysical, of mineral exploration, *Natural Resources*, 1959, p. 390, 1959.
- Southwell, R. V., *Relaxation Methods in Engineering Science*, Clarendon Press, Oxford, 1940.
- Van Orstrand, C. E., Some possible applications of geothermics to geology, *Bull. Am. Assoc. Petrol. Geologists*, *18*, 13-39, 1934.
- Van Orstrand, C. E., Temperature of the earth in relation to oil location, *Temperature, Its Measurement and Control in Science and Industry*, pp. 1015-1033, American Institute of Physics, Reinhold Publishing Corporation, New York, 1941.
- Verzhinskaya, A. B., and L. N. Novichenok, A new method of determining thermophysical coefficients, *Inzh. Fiz. Zh.*, *9*, 65-68, 1960.
- Von Herzen, R. P., and A. E. Maxwell, The meas-

- urement of thermal conductivity of deep-sea sediments by a needle probe method, *J. Geophys. Res.*, *64*, 1557-1563, 1959.
- Von Herzen, R. P., and S. Uyeda, Heat flow through the Eastern Pacific Ocean floor, *J. Geophys. Res.*, *68*, 4219-4250, 1963.
- Waiotapu Geothermal Field, *New Zealand Dept. Sci. Ind. Res. Bull.* *155*, 1-141, 1963.
- Wooding, R. A., Steady state free thermal convection of liquid in a saturated permeable medium, *J. Fluid Mech.*, *2*, 273-285, 1957.
- Wooding, R. A., Convection in a saturated porous medium at large Rayleigh number or Péclet number, *J. Fluid Mech.*, *15*, 527-544, 1963.
- Woodside, W., and J. H. Messmer, Thermal conductivity of porous media, 2, Consolidated rocks, *J. Appl. Phys.*, *32*, 1699-1706, 1961.
- Zierfuss, H., An apparatus for the rapid determination of the heat conductivity of poor conductors, *J. Sci. Inst.*, *40*, 69-71, 1963.

(Manuscript received June 1, 1964; revised October 12, 1964.)

## Chapter 3. Techniques of Measuring Heat Flow on Land

ALAN E. BECK

*Department of Geophysics, University of Western Ontario, London, Canada*

*Abstract.* Methods used in determining a value for terrestrial heat flow over land are discussed. Some examples of apparatus and techniques for determining the thermal conductivity of rocks and the temperature gradient in the crust are described; the apparatus described can be built up using fairly simple pieces of equipment, and elaborate techniques are not normally required. Problems and possible sources of error associated with the various techniques are also discussed.

### 1. INTRODUCTION

#### 1.1 *Reasons for Measuring Terrestrial Heat Flow*

Since nearly all theories concerned with the origin and development of surface structures rely, either implicitly or explicitly, on forces in which thermal energy plays a dominant role, it is clear that the amount of heat flowing across the surface of the Earth from the interior is a quantity which is of fundamental importance for geophysics. Furthermore, although geothermal methods in exploration geophysics suffered a decline, these methods are now being used more frequently, particularly in areas where geothermal power may be economically developed (see chapter 9 by McNitt, in this volume). It is therefore important that a large number of measurements of terrestrial heat flow be obtained so that eventually it will be possible to contour isoflux lines to obtain a clear over-all picture of the distribution and relationship of the heat flux to surface and subsurface features.

#### 1.2 *Basic Measurements Required and General Problems*

To determine the terrestrial heat flow in any area the temperature gradient ( $\partial T/\partial z$ ) and the thermal conductivity  $K$  of rocks in that area must be measured. Since the measurements are usually made in a small area and over a depth of penetration  $z$  that is small compared with the radius of the Earth, the heat flow  $q$  can be found from the linear steady-state equation

$$q = K(\partial T/\partial z) \quad (1)$$

Since the surface of the Earth departs from a plane of constant temperature, the topography

will cause irregularities in the heat flow. Fortunately, it is only in very mountainous areas that a topographic correction may become serious, but even here the contribution is found to come from an area within a 2 km radius [Bullard, 1938] of the observation position. The topographic correction can be either positive or negative and affects only the temperature gradient. If a number of measurements of temperature gradient are made in a given area, it may not be necessary to put in a topographic correction for each station, since the corrections tend to cancel each other out (for example, compare Beck [1956b], Howard and Sass [1964]). For measurements in tunnels, where the vertical temperature gradient is being determined from a number of measurements along an essentially horizontal plane [Birch, 1950], or in isolated borcholes in mountainous regions, the topographic correction may well be important and have a magnitude that is significantly greater than the other errors encountered in the determination (see chapter 2, section 5, by Jaeger for a detailed analysis of topographic corrections).

Other corrections for the geological history of the area, for example uplift and erosion [Benfield, 1949], can also be made to arrive at what is known as the equilibrium heat flow (see chapter 2 section 6–8 of this volume by Jaeger); this is the flow that would be observed if the Earth and its climate had remained unchanged through the years. Unfortunately, the geological history of many areas is not known with sufficient accuracy for it to be worth while making this difficult and somewhat tedious correction. Nevertheless, it can be seen that if a value for the average equilibrium heat flow of the Earth, or of the various type regions of the Earth, could

be established, then any departure of a measured value from the average value will provide yet another piece of information in tracing the geological development of that area.

Although temperature gradients in the crust of the Earth were measured as long ago as 1744 [Mairan, 1749], with the first measurements of the thermal conductivity of various Earth materials following about 100 years later [Forbes, 1849; Everett, 1861; Thompson, 1861; Herschel and Lebour, 1873], it was not until the 1930's that the importance of using the same borehole for determining the temperature gradient and thermal conductivity of a small area was realized. Benfield [1939] and Bullard [1939] were among the first to make such measurements. However, they were limited in many cases to single holes.

Clearly, in any one area the more measurements of temperature gradients and rock conductivity there are, the more accurate the average value of these quantities will be, and hence the more reliable will be the value of terrestrial heat flow for the area. If possible, a group of surface collared bore holes is used, or else temperature measurements are made in holes drilled from the various levels of a mine. It is usual to make the first measurement at a depth of about 30 meters, since for most places the temperatures at this depth are not affected by the annual variation of temperature at the surface (see chapter 2, section 2, by Jaeger, in this volume). Caution has to be exercised to insure that underground water flows or that longer period surface variations of temperature are not affecting the results. Fortunately these effects, if significant, can usually be very readily seen in the results of the temperature gradient measurements [Misener and Beck, 1960; Diment and Weaver, 1964]. Water flows in mines can sometimes be detected from the tritium dates of water samples collected from various parts of the mine (see section 3.2).

Perhaps the greatest practical problem in the measurement of terrestrial heat flow is the determination of a good mean value of the thermal conductivity of rocks from a particular area. It is usual to select what appears to be a representative number of specimens. But quite often, in an apparently uniform piece of rock core, it

is found that the thermal resistance per centimeter of one disc can be markedly different from that of a contiguous disc. If the boreholes have been cored, the best that can be done is to select representative short sections of the core and prepare samples for laboratory measurements of their thermal conductivity. It is generally of great help to plot the temperature gradient versus depth, since, as with many other geophysical methods, plotting the gradient (or the second derivative) versus depth frequently makes certain changes much more apparent than they are in the original temperature versus depth curve.

If it is assumed that the heat flow is constant along the length of the borehole, then any changes in temperature gradient, even over small sections of the borehole, must be assumed to be due to changes in thermal conductivity. It is frequently found that significant changes of temperature gradient occur which, from a visual inspection of the core, cannot be correlated with changes in the rock type. Conversely, it is often found that significant changes in the lithology are not always accompanied by significant changes in temperature gradient. Thus a plot of temperature gradient versus depth, in addition to the usual temperature versus depth curve, can be of considerable use in deciding how many specimens of rock to select from a given section of the borehole.

Even after the most careful selection of bore core, it is sometimes found that systematic changes in thermal conductivity of the rock from an apparently uniform section may occur. These systematic changes can sometimes be detected from a plot of depth versus the difference between the mean and the measured conductivity at that depth [Beck and Beck, 1958; Diment and Robertson, 1963] and are of great help in interpreting the data.

For uncored holes there are two possibilities: (1) hand specimens of representative rocks from as close to the measuring point as possible are removed, drilled, and prepared for laboratory measurements; and (2) in situ measurements can be made. The relative advantages and disadvantages of laboratory and in situ measurements will be discussed below.

## 2. MEASUREMENT OF THERMAL CONDUCTIVITY

2.1 *Laboratory Methods*

Both transient and steady-state methods have been used in the laboratory for determining the thermal conductivity of rocks. The transient methods are inherently less accurate than the steady-state methods, but in some cases they have the advantage of requiring less experimental time. There are numerous transient methods for determining the conductivity of insulating materials described in the literature, but only two or three appear to have been used specifically for the thermal conductivity of rocks.

In one method [Lubimova *et al.*, 1961], two holes approximately 3 cm apart are drilled in a specimen of rock which is about 5 cm long. Into one hole is placed a heater and in the other a temperature-sensitive element. An essentially impulsive source of heat is applied to the heater, and the thermal conductivity is found from the time required for the temperature maximum to reach the temperature-sensitive element in the second hole. About 10 to 15 minutes are required for the experiment, and the accuracy is approximately  $\pm 5\%$ .

A more recent transient method [Jaeger and Sass, 1964] makes use of a line source on cylindrical specimens. Two longitudinal grooves, at the ends of a diameter, are cut in the specimen, the length being at least five times the diameter. A heater wire is cemented in one groove, and a thermocouple is cemented at the midpoint of the other groove. The temperature rise versus time is recorded, and the heater current is switched off when the logarithmic linear asymptote is attained (see section 2.3). The conductivity and diffusivity are found from a reduction made on the early part of the curve.

Two quasi-steady-state methods may be briefly mentioned: Powell's [1957] is particularly useful for very small samples (about 1 mm cube); Zierfuss' [1963] requires surfaces about 1 cm square. Both methods are based on bringing a hot surface into contact with a smooth surface of the sample, results being obtained in about 30 seconds. In both methods the sample area may be only part of a much larger area. The samples have to be kept for some time in a well insulated box, or constant temperature enclosure, to attain a uniform temperature before an experiment is started. The experimental

time may be too short for coarse grained rocks (see section 2.3).

The needle probe method used on oceanographic sediments is described by Langseth in chapter 4 of this volume.

With further development to improve the accuracy, it seems that transient methods may eventually become more commonly used. However, the method which is by far the most widely used at the present time is that which employs some form of the divided bar apparatus [Lees, 1892]. This apparatus normally consists of two brass rods a few centimeters long and having a cross section to match that of the cores being used; a rock specimen is sandwiched between the two bars. Very small thermocouples, or thermistors, are spaced at regular intervals along each bar. The top end of the one bar is heated while the remote end of the other is cooled. When the system reaches the steady state, the temperatures (accurate to about  $0.01^\circ\text{C}$ ) along the bars are taken and the thermal conductivity of the rock is determined in terms of the conductivity of the brass bars. The conductivity of the brass bars is determined by measurements on materials of well determined thermal conductivities. The thermocouples or thermistors do not have to be very accurately located, since the method is a comparison one, and an error of 10% in the distance between two thermocouples produces an error of less than 1% in the thermal conductivity of the rock.

The effect of the thermal contact resistance between the bars and specimen can be reduced by the application of axial pressure (a few  $\text{kg}/\text{cm}^2$ ) to the ends of the bars, but it is usually eliminated by making observations on three or more discs of different thicknesses. For uniform material and surface finishes of the specimens, a graph of the thermal resistance between the two faces of the brass bars versus the thickness of the specimen should give a straight line. The slope of the line will yield the conductivity of the material, and the intercept at zero thickness will give the thermal contact resistance.

The conductivity of the brass rods is usually found by calibrating them against two sets of discs: one is of crystalline quartz with faces cut parallel to the optic axis, and the other is of fused quartz. The thermal conductivity  $K_c$ , at a temperature  $T^\circ\text{C}$ , of crystalline quartz with heat flowing perpendicular to the optic axis is given

by  $K_o = 10^3/(60.7 + 0.242T)$  mecal/cm sec °C for  $0^\circ\text{C} < T < 100^\circ\text{C}$  [Ratcliffe, 1959]; this gives a conductivity of 14.7 mecal/cm sec °C at  $30^\circ\text{C}$ . The conductivity  $K_f$  of fused quartz at  $T^\circ\text{C}$  is given by  $K_f = (3160 + 4.6T - 0.016T^2) \times 10^{-3}$  mecal/cm sec °C for  $-150^\circ\text{C} < T < 50^\circ\text{C}$ ; this gives a conductivity of 3.28 mecal/cm sec °C at  $30^\circ\text{C}$ . The conductivities of the great majority of rocks lie in this range, so that, if the conductivity of the brass is found to have the same value for both sets of calibrating discs, it can be concluded that the heat losses at the lower end of the range are negligible and that the instrument is therefore reliable for conductivity measurements of rocks.

The equation connecting the conductivity of the specimen  $K$ , the temperature difference  $\Delta T$  between the brass faces in contact with the specimen, and the thickness  $D$  of the disc is

$$R = \Delta T / (dT/dx) = B + (K_1/K)D \quad (2)$$

where  $K_1$  is the conductivity of the brass,  $(dT/dx)$  is the mean steady-state temperature gradient of the two rods,  $B$  is a constant which involves the sum of a contact resistance of the two interface films (which may be air or a water based fluid), and  $R$  is a parameter expressing the total thermal resistance of the disc plus the contact films in terms of the length of brass (or bar material) of the same thermal resistance.

It is fairly simple to control the machining of the surface of the discs so that, whatever medium is used for the contact films, the contact resistance from disc to disc can be assumed to be constant and a plot of total resistance  $R$  against  $D$  for one set of rock discs will give a straight line.

Until recently the hot end of the system was heated electrically, but, because of poor design, the system used to take several hours to reach the steady state. With the introduction of the constant temperature difference type of divided bar apparatus [Beck, 1957], the time to reach equilibrium has been reduced to about 10 minutes, which is close to the theoretical limits.

In this type of apparatus (Figure 1), the ends of the bars remote from the specimen are sprayed by water from thermostatically controlled baths; the hot bath is about  $20^\circ\text{C}$  above the temperature of the cold bath, and both baths are controlled to within  $0.01^\circ\text{C}$ . If the water flows across the ends of the bars are great

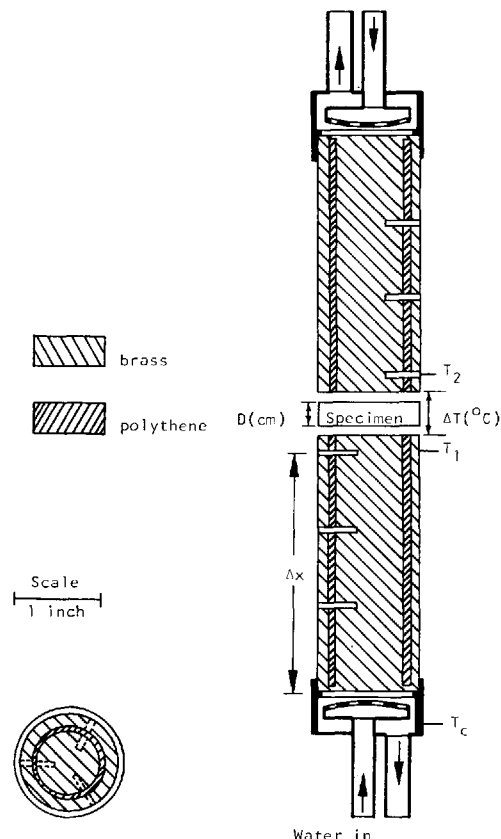


Fig. 1. Constant temperature difference divided bar apparatus with guard ring [Beck, 1957].

enough to keep the input and output temperatures constant to within  $0.01^\circ\text{C}$  (that is, the end of a bar is maintained at the same constant temperature  $T_c$  as that of the respective bath), then only one temperature measurement  $T_1$ , in the bar at a distance  $\Delta x$  from the end of the bar, is required to give the temperature gradient. Equation 2 can then be modified to

$$\Delta T / (T_1 - T_c) = C + (K_1/K)D/\Delta x \quad (3)$$

where  $B = C\Delta x$ .

In the above discussion the contact resistance refers only to the film between the disc and the ends of the brass bars; the temperature gradients in the bars have to be extrapolated to give the temperatures of the surfaces of the bars in contact with the specimens, thus obtaining  $\Delta T$ . This is not really necessary, since if  $\Delta T$  is taken to be the temperature difference  $(T_2 - T_1)$  between the actual thermocouples closest to the

ends of the bars, the slope of the line, and hence the value of  $K$ , given by (2) will remain unchanged; but  $R$ , and therefore  $B$ , now contains the thermal resistance of the brass between the last thermocouple and the face of the bar, as well as the thermal resistance of the contact films. If this procedure is adopted and combined with the method discussed in the preceding paragraph, then (3) can be modified to

$$\frac{(T_2 - T_1)}{(T_1 - T_c)} = C + (K_1/K)D/\Delta x \quad (4)$$

and it is only necessary to measure the ratio of two voltages if differential thermocouples are used to find  $(T_2 - T_1)$  and  $(T_1 - T_c)$ . This ratio can be displayed directly with the aid of an operational amplifier network or with an appropriate ratio meter.

In addition to the short time required to reach equilibrium, this system has the further advantages that a guard ring can be incorporated without additional controls and that the rods, contact films, and specimen are at a given mean temperature, which is usually chosen to be close to the ambient temperature to reduce errors due to possible heat losses from the system. By using a thick guard ring, errors due to small chips in the edges of the specimens and due to small variations in the diameters of the specimens are reduced to negligible proportions [Beck, 1957]. However, for a single disc a correction has to be applied for the finite thickness of insulation between the guard ring and the inner bar. For a typical apparatus, this correction varies from about 2.5% for a disc 0.1 cm thick to about 11% for a disc 1 cm thick. Even this correction can be ignored for a set of discs with thicknesses within the range of thicknesses of the calibrating discs, if the uncorrected slope of the calibration line, and therefore the uncorrected  $K_1$ , is used in (3) with the uncorrected slope of the line obtained for the specimens. Theoretically there should be some curvature of both lines, but in practice the experimental errors hide this effect.

There are many variations of this method which might be applied to a particular series of measurements. The following have all been successfully tried: (1) eliminating one of the bars by placing the specimen directly in contact with a thin copper disc maintained at a constant temperature by a water bath; (2) using crystalline quartz as a bar and measuring the temperature

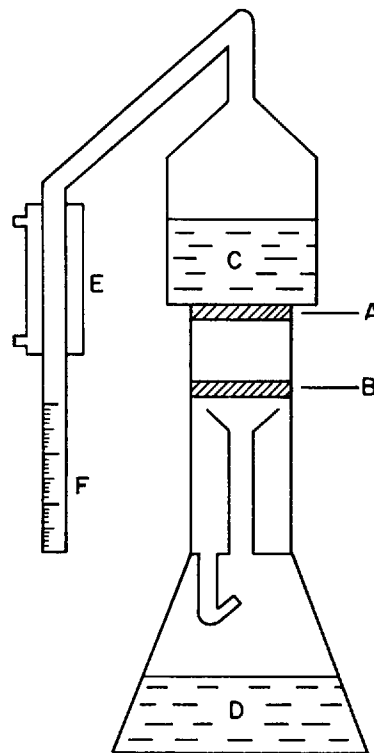


Fig. 2. Constant temperature difference 'latent heat' apparatus [Schröder, 1963].

gradient in it by using a conducting epoxy resin to cement thin discs of brass to each end into which thermocouples are inserted; (3) using solid-state heating and cooling devices at each end of the bars, thus dispensing with the bulky thermostatic baths.

An interesting new approach has recently been described by Schröder [1963]. It has all the difficulties usually associated with a divided bar apparatus, but has the advantage that no temperature measurements are required. It suffers from the great disadvantage that rather complicated glassware is necessary. The principle of the method is illustrated in Figure 2.

A specimen is fitted between two silver plates  $A$  and  $B$ . These plates act as seals to two vessels  $C$  and  $D$  containing pure liquids, with the boiling points chosen so that the liquid in the lower vessel has a boiling point that is about 10 to 20°C higher than the boiling point of the liquid in the upper vessel. A small heating coil is placed around the vessel  $D$ , and current is passed through it in such a way that the liquid in  $D$

just boils. After a steady state is reached, the silver disc *B* is maintained at a constant temperature which is the boiling point of the liquid in *D*, and the heat flowing through the sample causes the liquid in *C* to boil, thus keeping the temperature of the silver plate *A* at the boiling point of the liquid in *C*. There is therefore a constant temperature difference  $\Delta T$  between the two plates. The vapor from the liquid in the upper vessel is condensed in a condenser *E* and the condensate is collected in a graduated container *F*.

After the steady state has been reached, it is only necessary to find how long it takes to distill 1 cc of the liquid in *C* when the thermal conductivity *K* is given by

$$K = (Q_v D) / t A \Delta T \quad (5)$$

where  $Q_v$  is the heat of vaporization for 1 cc of the liquid in *C*, *t* is the time taken for distilling 1 cc,  $\Delta T$  is the temperature difference given by the difference between the boiling points of the two liquids, *D* is the thickness, and *A* is the cross-sectional area of the sample. Thus this is in principle an absolute determination of the thermal conductivity *K*, and its accuracy depends on the accuracy with which  $Q_v$  is known. However, if several samples of known conductivity are available, *K* can be determined from a comparative measurement if the specimens are of the same thickness as the calibrated samples: this procedure has the advantage of eliminating the necessity of knowing the exact values of  $Q_v$  and the boiling points of the two liquids. Alternatively, if specimens of different thicknesses are used, a calibration graph can be drawn. The complicated glassware becomes necessary in arranging for collecting the condensate from the liquids in both *C* and *D* and also in arranging for a guard ring of vapor around the specimen to prevent heat losses or gains.

## 2.2 Problems Associated with the Specimen

The specimens are cut with a diamond saw from cores of a diameter appropriate to the diameter of the apparatus being used. The discs are then ground flat to within 0.002 cm. The important points here are not so much the actual limits of tolerance chosen, but that whatever limits are chosen be consistently adhered to for a given apparatus, and that the final grinding is

always done with the same size grinding powder. Only in this way is it possible to get consistent contact resistances for a given apparatus and tolerances of rock machining.

When enough measurements have been made, it may be possible to find a standard contact resistance for a given apparatus and tolerance of rock machining. Figure 3 is a histogram of contact resistances, using fluid contacts, for 82 sets of discs cut from a wide variety of rocks: there is a mode which corresponds to a contact resistance equivalent to that of 0.5 cm thickness of brass.

To illustrate the effect of this contact resistance, consider a thin disc of rock ( $D = 0.2$  cm) of conductivity 10 kcal/cm sec °C, which is higher than average; the thermal resistance of this disc is roughly equivalent to the thermal resistance of 5 cm of brass. Thus the error in conductivity caused by ignoring the contact resistance would be about 10%. The error would decrease with decreasing conductivity and increasing thickness of the specimens. Furthermore, if the standard contact resistance used for single discs happens to be in error by as much as 20%, subtracting the incorrect value from the observed value of the total thermal resistance *R* will produce an error of only 2% in the thermal conductivity of the rock. Again, this error will decrease with decreasing conductivity and increasing thickness of the specimen.

In view of a number of other difficulties discussed below, it would appear that there is a good case for using single specimens 1 cm thick and either subtracting a nominal contact resistance from *R* to obtain the conductivity of that specimen or ignoring the contact resistance altogether. It should be emphasized that steps must be taken to determine that the contact resistance is in a range that can be ignored with a given size of disc. For instance, if air films are used the contact resistance may be as high as 5 cm brass, and we would need specimens about 10 cm in length, which would lead to other technical difficulties.

It can be seen that the histogram of Figure 3 covers a large range of both negative and positive values of contact resistance. This is a reflection of the scatter of points obtained for a set of discs even for a single rock. For example, Figure 4 shows the results for 48 discs of coarse grained granite used in a detailed study under-

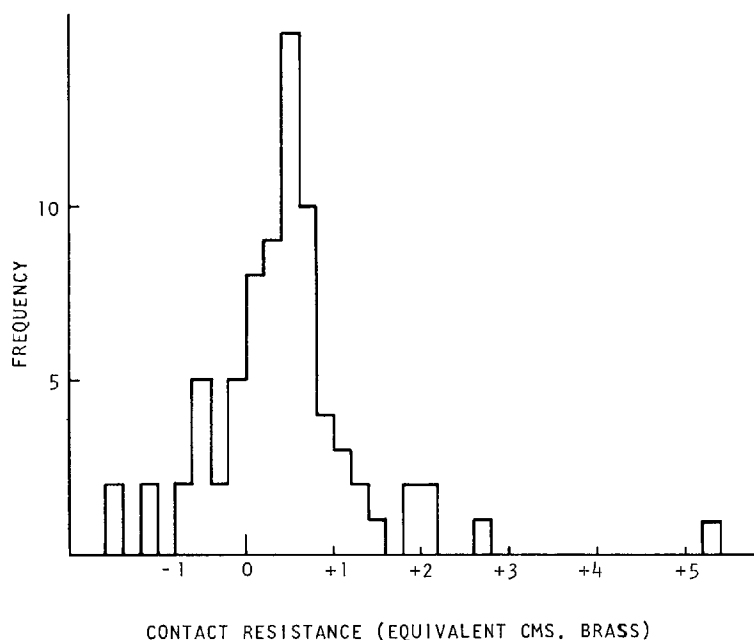


Fig. 3. Histogram of contact resistances for various types of rocks and given apparatus (Figure 1) and tolerances of rock machining.

taken to clarify this behavior. The scatter of points occurs for two reasons: (1) there is a high probability of finding, from disc to disc, a real variation of the proportions of constituent minerals; and (2) as the disc thickness decreases there is an increase in probability of finding a 'parallel' arrangement of highly conducting minerals which will in effect 'short circuit' the heat flow across the disc.

The idea of 'series' and 'parallel' computed conductivities was first introduced by *Birch and Clark* [1940]. It is assumed that the rock is made up of equal-sized cubes of the various minerals. If these cubes are arranged so that homogeneous layers of the minerals are formed lying perpendicular to the direction of heat flow, the rock is said to have a 'series' arrangement of minerals; on the other hand, if the cubes are arranged so that the layers have surfaces lying parallel to the direction of heat flow, then the minerals are said to be arranged in 'parallel.' Clearly, the arrangement of minerals in a rock could be any one of an infinite number of combinations between the extremes of complete parallel arrangement giving maximum conductivity and complete series arrangement giving minimum conductivity.

When sets of three or more discs are used, the parallel arrangement of minerals can cause an apparently negative contact resistance to be observed.

*Bullard* [1939] was the first to comment on the possibility of negative contact resistances, particularly in rocks containing significant quantities of quartz. This can be explained if it is assumed that some of the quartz is in an essentially parallel arrangement, then as the disc thickness decreases the amount of quartz in parallel arrangement increases; because of the high thermal conductivity of quartz, the apparent thermal resistivity of the rock decreases as the disc thickness decreases. Then on the thermal resistance-thickness graph the points obtained for the thinner discs are shifted toward the thickness axis, with the thicker discs having a smaller shift than the thinner discs. When a straight line is drawn through these points, a negative contact resistance can be obtained.

The errors arising from compositional variations and parallel arrangements of minerals are more serious for coarse grained rocks than for fine grained rocks. For instance, the rock used to obtain the results shown in Figure 4 contained

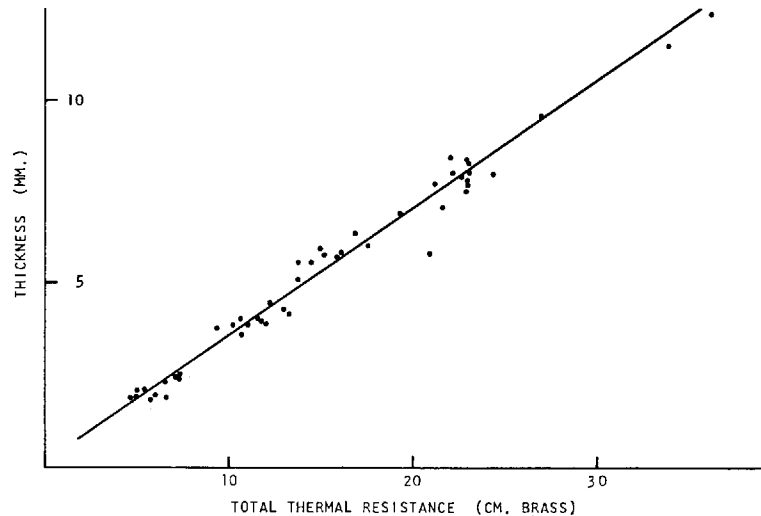


Fig. 4. Thermal resistance versus thickness for 48 discs of a coarse grained granite sampled at intervals over a 400-foot length.

between 20 and 30% quartz and had an average grain size of 0.15 cm, although some grains and clusters of grains were an order of magnitude larger. From this and similar studies [Beck and Beck, 1958, 1965] it appears that a disc with a ratio of thickness  $D$  to average grain size  $G$  greater than about 5, will be free of serious 'parallel' effects. However, because of the possibility of compositional differences between contiguous discs if they are too thin, it was suggested that  $D/G$  should be greater than 15 or 20 to be sure of obtaining a reasonable value for the 'bulk' conductivity; for coarse grained rocks, several discs could be used to achieve this figure.

The term 'bulk conductivity' is often used but has not been specifically defined. A working definition for practical purposes might be postulated as follows: the measured thermal conductivity of a specimen of given thickness is representative of the bulk conductivity of a rock if after the disc thickness is halved there is no significant change in the measured conductivity. This definition assumes that the samples from which the discs are prepared have been chosen from an apparently uniform geological unit.

Although negative contact resistances are normally only observed in rocks containing significant quantities of highly conducting minerals such as quartz or calcite, it must be pointed out that 'short-circuiting' is not the only way in which a negative contact resistance can arise.

For instance, suppose we have a perfectly uniform rock that has a thermal conductivity of 7.0 mcal/cm sec °C and that we have three discs of thicknesses 0.4, 0.8, and 1.2 cm; suppose further that the tolerances on the finishing of the surfaces of these discs and the finish on the ends of the divided bar apparatus in use yield a contact resistance equivalent to the thermal resistance of 0.5 cm of brass. Naturally, with perfect measurement we would expect to get a conductivity of 7.0 from the thermal resistance-thickness graph and a contact resistance equal to 0.5 cm of brass.

Now suppose that because of small experimental errors and slight compositional changes from one disc to another we get conductivities of 7.2 for the thinnest disc, 7.1 for the central disc, and 7.0 for the thickest disc. A least squares straight line through the 3 points would yield a conductivity of 6.9 and give a slightly negative contact resistance. Thus it can be seen that experimental variations of only 2 or 3% can lead to negative contact resistances. The term 'experimental variations' is used to cover composition changes from one disc to another, slight variations in the contact resistance due to slight variations in surface finish for discs, and measurement errors which can normally be kept to less than 2% and, with a little care, to less than 1%.

The sort of error indicated above could also

be caused by an arrangement of minerals such that the disc thicknesses are just becoming small enough to cause a parallel arrangement of minerals. It can readily be seen, however, that there is no way to distinguish the two effects experimentally without further investigations. For those rocks in which the risk of a parallel arrangement of minerals is thought to be significant, further investigation might include the use of four discs, since this would considerably reduce the probability of a consistently decreasing resistivity with decreasing thickness being due only to experimental error.

If a number of sets of discs of the same rock have been used, it can be argued that the contact resistances from the sets of discs should follow a normal distribution curve which has a positive mode, and that the number of negative contact resistances should be roughly balanced by the number of high positive contact resistances.

A measured conductivity can sometimes be checked by a calculation involving the conductivity of the constituent minerals and a modal analysis of the rock. If there are present in a rock  $\alpha\%$  of minerals of conductivity  $K_a$ ,  $\beta\%$  of minerals of conductivity  $K_b$ , and  $\eta\%$  of minerals of conductivity  $K_n$ , then the maximum, or parallel, computed conductivity  $K_p$  is given by

$$100K_p = \alpha K_a + \beta K_b + \dots + \eta K_n \quad (6)$$

and the minimum, or series, computed conductivity  $K_s$  is given by

$$100/K_s = \alpha/K_a + \beta/K_b + \dots + \eta/K_n \quad (7)$$

The approximate mean values of conductivities at 30°C for randomly oriented aggregates of some of the common rock-forming minerals are given in Table 1. With the possible exception of quartz, the values can only be approximate and should be treated with caution, since the determinations on pure minerals are rare and there may be real variations, possibly as much as 30 or 40%, from rock to rock. For instance, recent measurements on a number of feldspars, mainly single crystals, gave conductivities ranging from 3.9 mcal/cm sec °C to 6.9, with a mean of 5.7 [Sass, 1965]; also, *Diment and Werre* [1964] obtained a mean value of 4.5 for micas, compared with the value of 10.0 given by *Birch and Clark* [1940] and 6.0 used by *Beck and Beck* [1958].

TABLE 1. Approximate Conductivities in mcal/cm sec °C of Randomly Oriented Minerals

Minerals	Conductivity
Feldspar, Muscovite, Sericite	5.5
Biotite, Chlorite, Epidote	6.0
Magnetite, Calcite, Topaz	8.5
Hornblende, Pyroxene	10.0
Quartz	17.0

Because these values differ considerably from those generally accepted, a method of testing the various models was devised [Beck and Beck, 1965] which utilized in one equation the measured thermal conductivity and the composition of the specimen but which required a knowledge of only  $(n - 2)$  thermal conductivities in a rock containing  $n$  minerals having  $n$  thermal conductivities. Thus for a three-component system it is necessary to know the thermal conductivity of only one mineral.

For example, assuming the existence of a three-component system, equations 6 and 7 can be arranged to give equations 8 and 9, respectively:

$$(100/\beta)(K_p - K_c) = (\alpha/\beta)(K_a - K_c) + (K_b - K_c) \quad (8)$$

$$\frac{100}{\beta} \left( \frac{1}{K_s} - \frac{1}{K_c} \right) = \frac{\alpha}{\beta} \left( \frac{1}{K_a} - \frac{1}{K_c} \right) + \left( \frac{1}{K_b} - \frac{1}{K_c} \right) \quad (9)$$

It can be seen that if we assume that one of the models is correct, say that given by equation 8, and if  $K_c$  is known, then if  $K_0$  is the measured conductivity a plot of  $(K_0 - K_c)/\beta$  versus  $\alpha/\beta$  should give a straight line with a slope of  $(K_a - K_c)/100$  and an intercept of  $(K_b - K_c)/100$  from which  $K_a$  and  $K_b$  can be determined. Similarly, for equation 9 a plot of  $(1/\beta)(1/K_0 - 1/K_c)$  versus  $\alpha/\beta$  should give a straight line with a slope of  $(1/K_a - 1/K_c)$  and intercept of  $(1/K_b - 1/K_c)$  if the equation represents the model accurately; therefore  $K_a$  and  $K_b$  can again be found.

Effectively, the method consists of assuming a particular model and conductivity of one of the minerals, and then fitting the data to the model in such a way that the values of  $K_a$  and  $K_b$  obtained give the best straight line. In practice, the range of mineral conductivities is such that

the ratio of the maximum to minimum conductivity will rarely exceed 1.5. Thus we might expect both models to be satisfied by a reasonable straight line (but with different values of  $K_a$  and  $K_b$ ). However, it should be possible to tell from the rms deviation of the points which is the better model.

These tests were applied to the 48 discs used in obtaining Figure 4, the composition being found by a modal analysis of both sides of each disc. Assuming the validity of equation 8 and a conductivity value of 17.0 mecal/cm sec °C for quartz, the conductivity of feldspar was found to be 5.7 and of the biotite to be 0.5; assuming the validity of equation 9, the corresponding values were 7.2 and 6.4. Both values for feldspar are significantly higher than that originally assumed. However, neither model appeared to be really satisfactory, since the best value for feldspar in the assumed series model appeared to be too high, and the best value for biotite in the assumed parallel model was certainly too low.

This led to consideration of the Maxwell model; in this model if there are  $n$  minerals then  $(n - 1)$  of them are assumed to be dispersed as small spheres in the  $n$ th medium. This kind of model is certainly more accurate than the other two models and has frequently been used for two-component systems, particularly for investigations into the thermal conductivity of porous mediums and of unconsolidated mediums. The dispersive conductivity  $K_d$  for a three-component system is given by [Brailsford and Major, 1964]

$$K_d = \frac{\alpha + AK_b + BK_c}{(\alpha/K_a) + A + B} \quad (10)$$

where  $A = 3\beta/(2K_a + K_b)$ ,  $B = 3\gamma/(2K_a + K_c)$ ,  $K_a$  is the conductivity of the medium in which the other components of conductivities  $K_b$  and  $K_c$  are dispersed, and  $\alpha$ ,  $\beta$ , and  $\gamma$  have their original meaning. This equation cannot be manipulated into a straight line form for testing in the manner previously described. Fortunately, Woodside and Messmer [1961] found that for a two-component dispersive system the 'geometric' conductivity given by

$$K_g^{100} = K_a^\alpha K_b^\beta \quad (11)$$

is a good approximation to the dispersive conductivity if the mineral conductivities do not differ by an amount approaching an order of magnitude.

If it is assumed that this approximation can be extended to the three-component system, and if logarithms are taken on both sides, the corresponding three-component equation can be manipulated into the straight line form given by equation 12.

$$(100/\beta) \log (K_g/K_c) = (\alpha/\beta) \log (K_a/K_c) + \log (K_b/K_c) \quad (12)$$

It can be seen that if this model is reasonably correct, and if the conductivity  $K_c$  is known, a plot of  $(100/\beta) \log (K_g/K_c)$  versus  $(\alpha/\beta)$  should yield a straight line with a slope of  $\log (K_a/K_c)$  and an intercept of  $\log (K_b/K_c)$  from which  $K_b$  and  $K_c$  can be found. Use of this test with the 48 samples mentioned above, with  $K_c = 17.0$  mecal/cm °C, yielded a feldspar conductivity of 6.7 and a biotite conductivity of 4.8.

Without some additional evidence as to the feldspar or biotite conductivities, little can be said about the accuracy of any of these tests. Fortunately, two of the discs in the group, which had long been a puzzle, contained almost 80% feldspar. Both discs gave a very low value even for the parallel computed conductivity when the earlier conductivity values for biotite and feldspar were used. The new set of values gives a computed conductivity close to the observed value.

All four models represented by equations 8, 9, 10, and 12 were later checked using a computer to obtain the best fit (lowest rms deviation) by (a) assuming the conductivity of quartz to be 17.0 mecal/cm sec °C and varying the feldspar and biotite conductivities and (b) by varying all three conductivities.

It was found that equation 12 was indeed a reasonable approximation of equation 10; for instance, in method (b) the feldspar values were identical, and the quartz and biotite values for equation 12 were found to be 0.3 to 0.5 mecal/cm sec °C higher than those obtained from equation 10. It is therefore reasonable to assume that equation 12 is a fair representation of the dispersive model, and that the equation can be extended to systems having more than three components.

When the discs were arranged in groups in order of thickness, it was found that there was a systematic increase in the rms deviation and in the apparent conductivity of quartz (all 3 conductivities being varied for the best fit) as the

thickness decreased. This is quite consistent with the expected increase in the number of parallel-arranged elements with decrease of thickness.

In the above set of samples the rms deviation for the 16 discs between 7.0 and 12.5 mm thick was surprisingly small (0.23), and the best fitting set of conductivities was feldspar 7.0, quartz 14.0, and biotite 4.9 mcal/cm sec °C.

Until further work is done, not too much significance can be placed on the low quartz value, although it may be genuine. The value of 17.0 usually used is obtained by assuming a random orientation of crystalline quartz with the crystals having perfect thermal contact. It might be expected that thermal contact is not perfect; then the intercrystalline contact resistance would reduce the apparent thermal conductivity of a mass of the randomly oriented quartz. The reported measurements for quartzites cover a wide range of values, some being so high [Bullard, 1939] that they indicate a significant degree of preferred orientation, but the mean values appear to lie in the range 14.0 to 15.5.

To illustrate the type of error that can occur if due care is not exercised, the conductivities, obtained by various methods, from two sets of discs of coarse grained granites are compared in Table 2. In both sets the conductivities are found from the least squares straight line computed for all four discs and also for groups of three discs obtained by omitting each disc in turn. Thus the first column shows which disc has been omitted from the set of four to obtain the value of conductivity shown in column 2 and the standard deviation shown in column 3. For comparison the conductivities of the individual discs obtained by subtracting the standard contact resistance equivalent to 0.5 cm of brass are shown in column 4. Columns 5, 6, 7, and 8 show the computed conductivities, together with their standard deviations, using the dispersive, geometric, series, and parallel models, respectively. The computations are based on conductivities of 14.8 mcal/cm sec °C for quartz, 6.7 for feldspar, and 5.5 for biotite. Columns 9 through 12 give the computed values for all four models using the values originally used by Beck and Beck [1958], namely 17.0 for quartz, 4.5 for feldspar, and 6.0 for biotite.

The least squares straight line results for the second set of discs are particularly noteworthy, since it can be seen that by omitting disc 4 we

TABLE 2. Effect of Treatment of Data on Results of Conductivity

Conductivity from Sets of Discs, mcal/cm sec °C		Conductivity of Individual Discs, mcal/cm sec °C													
		Measured				Computed									
Set Number	Disc Omitted in Least Squares	K from Least Squares Straight Line	Std. Dev., %	8.5	7.9	9.7	9.0	Quartz = 14.8, Feldspar = 6.7, Biotite = 5.5				Quartz = 17.0, Feldspar = 4.5, Biotite = 6.0			
								Mean 8.8 ± 9%	8.6	8.0	8.5	8.8	8.5 ± 4%	8.4 ± 4%	9.1 ± 4%
								Dispersive	Geometric	Parallel	Series	Dispersive	Geometric	Parallel	Series
1	1	13.3	50	8.5	8.6	8.0	8.5	7.3	8.5	9.2	7.9	7.3	7.2	8.8	6.2
	2	9.7	12	7.9	8.0	9.7	7.9	6.6	7.9	8.6	7.5	6.6	6.6	7.9	5.8
	3	9.4	16	9.7	8.5	9.0	8.4	7.4	8.4	9.1	7.8	7.4	7.3	8.8	6.3
	4	10.6	33	9.0	8.8	8.7	8.7	7.5	8.7	9.5	8.1	7.5	9.2	9.2	6.4
	None	10.1	17	Mean 8.8 ± 9%	8.5 ± 4%	8.4 ± 4%	8.4 ± 4%	7.2 ± 6%	9.1 ± 4%	9.1 ± 4%	7.8 ± 3%	7.2 ± 6%	7.2 ± 5%	8.7 ± 6%	6.1 ± 5%
2	1	9.5	68	7.2	7.4	9.2	7.3	6.2	7.3	7.8	7.0	6.2	6.2	7.2	5.6
	2	9.3	35	9.2	8.5	9.4	8.4	7.4	8.4	8.1	7.8	7.4	7.3	8.8	6.3
	3	9.6	7	6.6	7.4	9.0	7.3	5.8	7.3	7.7	7.0	5.8	5.8	6.6	5.3
	4	6.4	31	9.0	8.5	8.4	8.4	7.0	8.4	9.1	7.8	7.0	6.9	8.5	6.0
	None	8.9	26	Mean 8.0 ± 16%	7.9 ± 8%	7.8 ± 8%	7.8 ± 8%	6.6 ± 11%	8.2 ± 8%	8.2 ± 8%	7.4 ± 6%	6.6 ± 11%	6.5 ± 10%	7.8 ± 13%	5.8 ± 8%

obtain a conductivity that is about 25% less than the mean. On the other hand, by omitting disc 3 the discrepancy between the conductivity so obtained and the mean conductivity is not too serious, but a completely erroneous impression of the error is obtained. In addition, comparison of the mean observed conductivities obtained from single discs with the groups of computed conductivities in columns 5 through 8 and 9 through 12 indicate that when computing conductivities from the mineralogical composition it may be more important to know the conductivities of the individual minerals that it is to select the correct model.

To determine the thermal conductivity of a rock by computation involving the analysis of several discs is clearly inefficient compared with the simplicity of measuring thermal conductivity. However, establishing the validity of a reasonable model, such as the dispersive model, is of considerable importance in those holes where only rock chips are available. In such a case, with a reliable model, chips of the rock could be imbedded in a matrix of known conductivity and the conductivity of the discs of composite material determined in the usual way. To obtain a reliable mean value, measurements would have to be made on several discs of this composite material; it may therefore be possible to save time and simultaneously determine the conductivities of two rocks having different conductivities by mixing chips of both of them, in various proportions, into the matrix of known conductivity and using equation 12.

The success of such a method combined with the type of survey of temperatures in oil wells made by *Anglin and Beck* [1965] would open up possibilities of using, for heat flow study, a vast number of hitherto unusable oil wells.

A different approach has recently been made by *Diment and Robertson* [1963], who attempted to relate the thermal conductivity of shales and limestones to the percentage by weight of insoluble residues left after treatment with hydrochloric acid. Although the correlation (Figure 5) is poor, it is good enough to warrant further investigation which, if successful, would also allow the thermal conductivity of calcareous rocks to be estimated from drill cuttings. Attempts have also been made at computing some other thermal properties of rocks [*Somerton*, 1958].

The errors involved in computing the con-

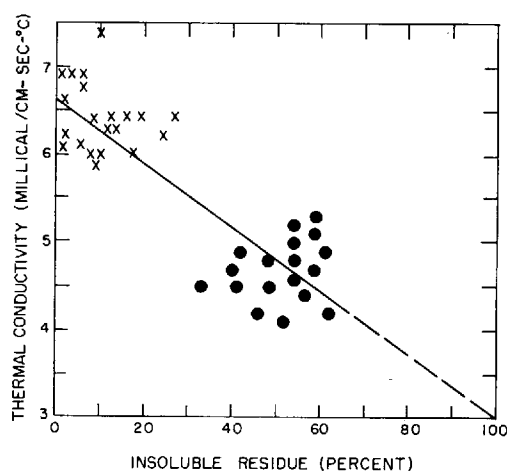


Fig. 5. Relation between thermal conductivity and percentage (by weight) of insoluble residues for limestones (cross) and shales (solid circle) [after *Diment and Robertson*, 1963].

ductivity by any of the above methods may be no worse than the errors that might occasionally occur owing to the inadvertent use of unrepresentative samples in the laboratory determinations of thermal conductivity. It is therefore worth emphasizing that the success of these methods will represent an important step toward the utilization of oil wells for heat flow studies.

The discussion in the preceding sections gives some idea that even though the divided bar apparatus (or, for that matter, any apparatus using somewhat small sizes of specimens) is widely used, its limitations and the practical problems involved must be kept in mind if the results are to be correctly interpreted. Furthermore, there is another set of limitations which apply to all laboratory methods—those imposed by the fact that the observations are not being made under the conditions which prevail at the point in the earth from which the rocks were recovered. Up to the present time this has not presented much of a problem, since it has been shown [*Birch and Clark*, 1940] that for a wide range of igneous rocks the general tendency was for the range of conductivities to decrease from 4–14 mcal/cm sec °C to 4–9 mcal/cm sec °C at 400°C, whereas increasing the pressure tended to increase the conductivity. The effects of rising pressure and temperature therefore tend to cancel each other out.

With the present interest in very deep holes, such as the Mohole, however, the effect of removing the rock from its surroundings may have

more serious consequences. For example, the release of pressure may cause irreversible changes in the structure of the specimen and affect not only its conductivity, but all its physical properties. In addition, laboratory methods are selective in that discs can only be prepared from sound rocks and in that borehole cores cannot be recovered at all from highly altered or sheared zones. For these reasons more attention is now being paid to the development of in situ methods of measuring rock conductivities.

### 2.3 Field Methods

The most easily realized and practical of the in situ methods involves the use of an electrically heated cylindrical probe which, to insure radial heat flow conditions at the central plane normal to its axis, has a length 20 to 30 times the diameter of the hole into which it is inserted [Blackwell, 1956]. Seals at each end of the probe prevent convection losses up and down the hole [Beck et al., 1956], and a temperature-sensitive element is located on the surface of the probe at a point equidistant from the ends of the probe. When the probe is in place and has reached the equilibrium temperature of the borehole at that place, the current is switched on and a record is made of the temperature rise versus time.

The resulting data can be reduced by one of three methods. The first is the method commonly used for all types of probe measurements, whether they are made with needle probes, as in the determination of the thermal conductivity of ocean sediments, or with the large probes used for building materials; it consists of plotting the natural logarithm of the time  $t$  versus the temperature  $T(t)$  and finding the slope of the logarithmic asymptote. If  $Q$  is the heat input per unit length along the section of hole being heated, and  $B$  is a constant, the thermal conductivity  $K$  can be found from the equation

$$T(t) = (Q/4\pi K) \ln(t) + B O(1/t) \quad (13)$$

where the terms  $O(1/t)$  are negligible for long times. The time to reach the asymptotic section of the curve depends on the radius of the borehole involved, the thermal constants of the rocks surrounding the hole, and the thermal contact resistance of the water, or air, layer between the probe and the wall of the borehole. A more detailed discussion of the theoretical aspects is given in chapter 2, section 13, by Jaeger.

The second method [Blackwell, 1954] involves the determination of the thermal contact resistance by the use of an approximate solution to the transient radial heat flow equation for short times; the value obtained is then used in another approximation to the equation for long times. This is equivalent to straightening the curve obtained by the first method somewhat earlier than would otherwise be the case and, theoretically, makes it possible to use shorter experimental times.

The third method [Jaeger, 1956; Beck et al., 1956] uses the exact solution of the transient radial heat flow equation and involves calculating families of theoretical curves using values of the appropriate constants which cover the range of values likely to be found in geophysical work (see appendix to this chapter). The experimental curve of temperature rise versus time is plotted on double logarithmic paper and compared with the families of theoretical curves plotted on the same bases. From the best fit it is theoretically possible to find, from the displacement of the origin, both the thermal conductivity and the diffusivity of rocks. This method requires a shorter experimental time than any other method.

In a series of laboratory experiments designed to compare the various methods of reducing the data [Sass, 1961], it was found that the curve-fitting technique can give very good results. Experiments were carried out in blocks of fine grained concrete of carefully controlled composition, in fine grained granite, and in fine grained limestone; all blocks had a borehole 5 cm in diameter along the long axis. In the concrete, the hole was molded in during casting, and many samples were taken during the casting and from the concrete cylinder (60 cm in diameter, 2 meters high) itself after it had been properly cured. In the two rocks, the holes were drilled with complete core recovery. The object of drilling the holes in the rock and molding the hole in the concrete cylinder was to determine whether there were any serious wall effects due to drilling.

The results of the transient in situ methods were compared with the results from steady-state experiments on the block of concrete, which had thermocouples molded into it at various known radii, and with divided bar measurements

on discs prepared from all the samples noted above.

It was found that under ideal conditions an experimental time of 30 minutes in a water-filled vertical hole was required to determine the conductivity to within  $\pm 5\%$  by the curve-fitting method. When the experiment was run for another hour the same accuracy could be obtained from the slope of the logarithmic asymptote. It was also found that the same experimental time was required if Blackwell's method was to be used to give the same accuracy. In view of the simplicity of using the logarithmic asymptote, the choice of methods of reduction of the data would appear to lie between this and the first method outlined in this section.

For an air-filled borehole, if the annulus between the probe and borehole wall was less than 0.2 cm thick, the time of experiment and the limit of error were doubled. Furthermore, it was found that the usual probe length to diameter ratio could be reduced from 30 to about 15 without introducing serious errors. When similar experiments were carried out under difficult field conditions, the errors were roughly doubled.

In the following discussion it will be seen that there are a number of areas in which compromises have to be made. Any solution will depend not only on the circumstances of experimental environment but also on the amount of money and time available. One cannot therefore be dogmatic about recommending a particular experimental set-up. However, the information in the following paragraphs gives some idea of the practical problems encountered and of the equipment presently being used by the author for holes up to 8 cm in diameter.

In relatively shallow boreholes, say up to about 500 meters deep, the experiments are reasonably easy to carry out, but there are formidable difficulties involved in deep holes. A typical heating requirement, if temperatures are measured to  $0.01^\circ\text{C}$ , is about 0.05 cal/sec/cm length of hole, which will give a temperature rise of about  $3^\circ\text{C}$  for a 3-hour experiment in an 8-cm diameter borehole through a typical rock. If errors or uncertain corrections due to losses in the copper leads are to be avoided, the heating coil should have a high resistance compared with the leads. On the other hand, if the coil resistance is high, the applied potential will also have

to be high to obtain the required power, which leads to insulation difficulties if the equipment is to be kept to easily manageable proportions. For shallow holes a reasonable compromise between the coil resistance and the diameter and weight of the leads can be reached. For deep holes the same compromise would involve a considerable increase in the size of the leads and hence a considerable increase in the weight of cable being used. This in turn would mean heavy and expensive winching equipment. Of course, this difficulty is not insuperable; but the present writer has always been inclined toward the use of apparatus which is light and does not require large quantities of awkward and expensive associated equipment. This preference is based partly on considerations of expense and partly on the fact that the less maneuverable the equipment becomes, the smaller the number of boreholes that can be reached for the experiments.

These considerations lead to one of the primary reasons for seeking methods of treating the data which would require only fairly short experimental times. If the experimental time can be decreased, there is a nonlinear decrease in the power required for logging the borehole, since there is a gain not only on account of the shorter time one has to operate the heater coil, but also because it is possible to reduce the length to diameter ratio and so save power on the length of borehole that has to be heated. On the other hand, if too short an experimental time is used, the depth of penetration of heat into the borehole is small, and, the smaller the experimental time, the less efficient is the method for obtaining an average of the thermal conductivity for a moderately large volume of the rock; this argument also applies to transient methods used in the laboratory. Thus, for fine grained rocks it may be possible to use smaller experimental times, and hence smaller volumes, than would have to be used with coarse grained rocks when the average has to be taken over a reasonably large volume.

To prevent convection losses to other parts of the hole, two types of seal can be used. The first consists of an inflatable seal which can be blown up from the surface. This has the obvious disadvantage that there are complications in the equipment and the support cable if the seals are to be effectively blown up from the surface by,

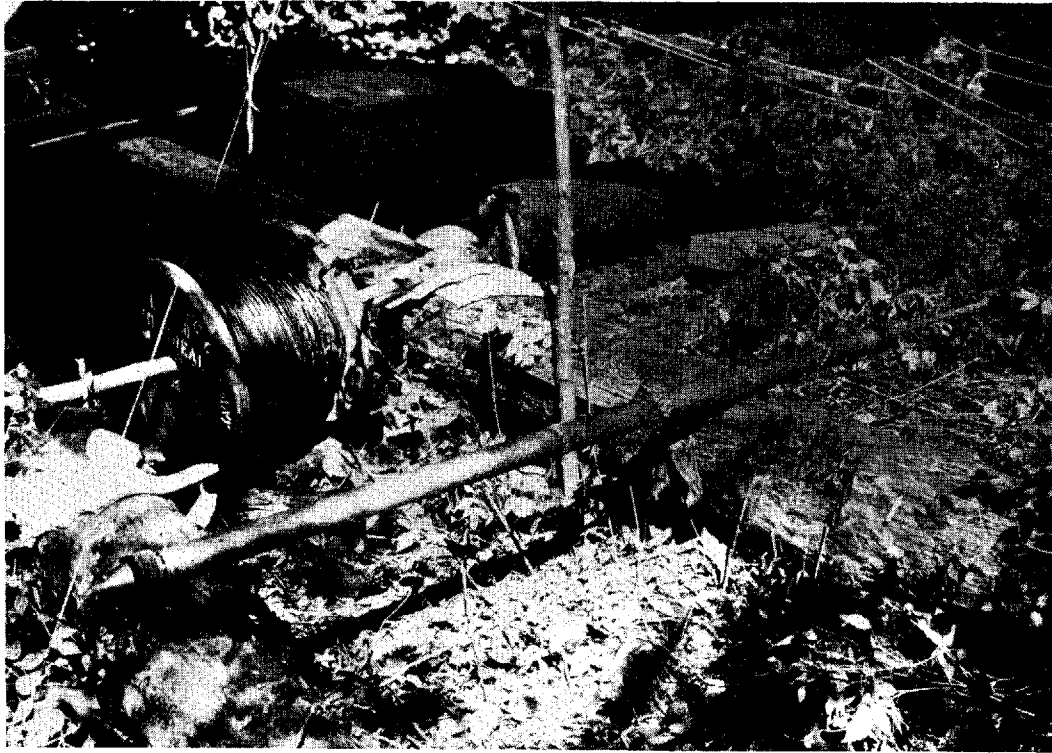


Fig. 6. Photograph of in situ probe for NX hole showing arrangement of external multiple thermocouples and end seals.

for example, a cylinder of gas. There are also limitations on the depth to which this seal can be conveniently used. For this reason the present author prefers the use of the bottle brush type of seal (Figure 6), which consists of a series of rubber washers with nicks in the edge; about ten of these used at each end of the probe, with 0.3-cm thick lucite spacers between them, form an effective seal in boreholes whose diameter is smaller than that of the washers. Under most conditions this type of seal allows the probe to go down the hole fairly easily while keeping it reasonably well centered when the probe is stopped to make an experiment. The rubber washers are at least 0.5 cm greater, and the lucite spacers about 1 cm less, in diameter than the nominal diameter of the borehole; the cuts around the edges of the washers are then taken from the edge of the washer right into the lucite spacer. The main disadvantage of the bottle brush type of seal shows up when a probe happens to be a particularly tight fit in a borehole. In these circumstances a fairly heavy weight is necessary to

pull the probe down the borehole, since there is considerable friction between the walls of the borehole and the rubber washers.

In the only systematic survey in a borehole under difficult field conditions [Beck and Logis, 1964], it was found that an experiment usually required three hours of heating to give the logarithmic asymptote. It was also found that an experimental time of about 2 hours was required to give an unambiguous fit for the curve-fitting method. The conductivity was then obtained from both the logarithmic asymptote and from the curve-fitting method, the correlation between the two giving some idea of the accuracy of the experiment. This check is especially important when very low power inputs are used with a hollow probe, for reasons given below.

The length of a probe is usually between 1.5 and 2 meters, and its diameter is about 1 cm less than the diameter of the borehole (Figure 6). Both hollow and solid probes have been used, with more consistent results from the solid probe, but, when designing equipment for holes

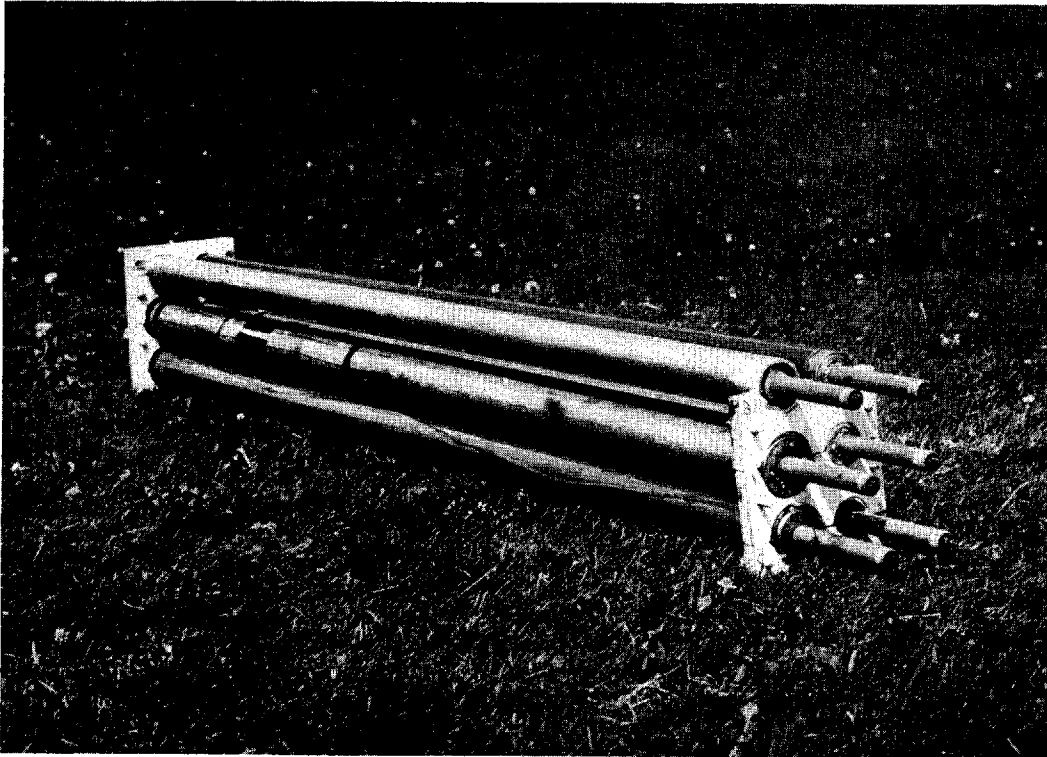


Fig. 7. Group of experimental probes with various geometries. Thermocouples are arranged internally, with some probes having an additional external thermocouple for checking purposes.

8 cm in diameter, a solid probe even of aluminum becomes rather heavy. Figure 7 shows some experimental probes for various sizes of boreholes.

It had been hoped that with a hollow probe fairly efficient convective stirring could be induced with the currents running up the outside of the probe and down the inside, thus making the contact resistance small. This can be done fairly consistently with moderately high heat inputs, but, with the very low power per unit length now normally used, it is difficult to stimulate these currents. It is believed that the inner and outer cells tend to remain independent. The result is that some experiments do not give reliable data. This only happens occasionally, and is easily detected on the logarithmic asymptote, but it is nevertheless a little unnerving to watch the curve when mixing does occur halfway through an experiment.

The heating coil consists of wire, which has a low temperature coefficient of resistance, closely and noninductively wound on to a tube or rod

which is about 0.5 cm less in diameter than the outside diameter of the completely assembled probe. A number of thermocouples connected in series, or a single thermally sensitive element, are then placed around the central plane of the probe. Enough of the thermocouple wire is left so that the cold junctions can be situated between one and two feet below the bottom of the probe. A metal cylinder is then slipped over the whole assembly as a protective cover so that the heating wire and the hot junctions of the thermocouples are all contained within an annulus about 0.1 cm thick. An epoxy resin or a special impregnating wax is then poured into the annulus so that it is completely filled. Since the thermocouples are beneath this filling material and close to the heating wire, the contact resistance presented by the filling material is contained in the contact resistance obtained for the whole experiment. The coil resistance is usually chosen so that the series resistance of the copper wires in a supporting cable does not exceed 10% of the total resistance in the heat-

ing circuit. With the present equipment the lead resistance is 8 ohms and the coil resistance is about 120 ohms. Of course, there are plug and socket arrangements at the top of the probe so that the cable can be easily attached.

Two serious practical difficulties related to the actual diameter of boreholes should be pointed out. The first difficulty came to light during a series of experiments in an NX hole (7.5-cm nominal diameter). The probe had given good results at some shallow depths but at one point it became apparent that serious heat losses were occurring. The probe was lowered about 30 meters and again gave good results; pulling it back 30 meters again resulted in further serious heat losses. It was at first thought that this was a fractured zone, but that idea was not supported by the core. Subsequent experiments showed that the hole at the difficult point was about 9 cm in diameter, and this was between two other regions where the diameter was about 8 cm. The enlarged diameter is probably due to drill rod slap.

The second, and associated, difficulty is illustrated by the fact that it has been found possible to lower a 7 cm diameter rod down a BX hole (6-cm nominal diameter). This enlarged diameter, which is closer to an NX hole than a BX hole, could be due to a number of causes, including a nonstandard drilling bit.

Whatever the causes, it is clear that the term 'nominal diameter' leaves much to be desired, and that wherever possible an attempt should be made to find out if there are any irregularities in the diameter of the borehole before deciding which probe to use.

Some runs with an instrument that continuously records temperature gradient have indicated that after a 1.5-meter section of borehole has been heated for three hours, it takes about two days for this section of the borehole, plus a few meters on either side, to settle back to equilibrium. There does not appear to be any disturbance to parts of the hole above and below the heated sections. It is assumed that the return to equilibrium is due almost entirely to the conduction process and that significant convection currents are not set up after removal of a probe. This, of course, only applies to the setup used in the above experiments, and it is conceivable that with higher heat inputs, and therefore

higher temperature rises, the critical gradient (see section 3.2) could be exceeded in a section of the borehole and important convection currents set up.

### 3. MEASUREMENT OF TEMPERATURE GRADIENT

#### 3.1 *Methods*

For the measurement of temperature gradient, either mercury-in-glass maximum thermometers or thermistors are normally used. Platinum resistance thermometers have been used in the past, but the same problems arise with these as arise with the in situ determinations of conductivities in deep holes. For instance, because of the heavy copper leads required, one set of equipment used in South Africa [Weiss, 1938] weighed more than 2500 kg. All these types of thermometers are usually encased in a pressure-proof, water-tight container to avoid the necessity of applying an uncertain correction for pressure. Both O-ring seals and epoxy resin seals have been successfully used in pressure-proofing containers and sealing the cable into the containers.

The use of thermocouples for absolute determinations to within 0.01° C requires a very stable cold junction and a sensitive galvanometer. On the other hand, thermocouples are useful for direct and continuous recording of temperature gradients. One instrument now in use is essentially a thermopile 1 meter long with an output of approximately 40μv in a temperature gradient of 20° C/km. However, the two most common methods involve the use of a thermistor or maximum thermometers.

In spite of a tendency to drift, thermistors are extremely useful, since they offer two distinct advantages, namely, that they have a temperature coefficient of 4 or 5% (and negative) and they can be obtained with very high resistances. The latter advantage means that it is possible to choose them so that the series resistance of the leads can be neglected. If too high a resistance is chosen, however, then over a long length of cable the insulation resistance of the cable may not be high enough to avoid errors due to its shunting action. In general, for an accuracy of 0.01° C the following inequality should be observed:

$$\frac{\text{insulation shunt resistance}}{\text{element resistance}} > 2000 \quad (14)$$

Consideration must also be given to the self heating effects in a thermistor. This is usually given by the manufacturers in the form of a dissipation constant. The higher the value of this constant, the smaller is the self heating effect for a given thermistor and current. In general, for a given thermistor material and nominal resistance, as the mass of the thermistor increases, the dissipation constant increases; but the time constant also increases, and a suitable compromise may vary from one set of experimental conditions to another.

Referring to (14), if a higher resistance element is chosen to avoid having to take the series lead resistance into account, a fairly heavy cable is required for the insulation resistance to be high enough for the inequality to be true. On the other hand, if a low resistance element is chosen so as to use a cable with lighter insulation, trouble may be experienced with the effect of the series resistance of the leads. Nor is it simply the cable series and shunt resistance at a given temperature that has to be considered; the variation with temperature and pressure must also be known. Corrections can, of course, be applied for all these effects, but they are tedious and not very reliable.

The problem therefore is to find a suitable compromise between the conflicting requirements of (1) having light weight equipment, (2) eliminating the unreliable corrections for series and shunt resistance, (3) eliminating the unreliable corrections for the variation of series and shunt resistance with temperature and pressure, and (4) having the required sensitivity without sacrificing the robustness so necessary for field equipment. Three types of equipment designed to overcome these problems will now be described in order of increasing complexity.

The first equipment [Beck, 1963] meets requirements 2 and 3 by having the four wires in the cable connected in such a way that the series resistance, the shunt resistance, and the variation of these with temperature are automatically compensated. It is thus possible to reduce drastically the size of the wires used, and the cable can be made very light in weight to help achieve requirement 1. In fact, the main criterion for wire size would be the diameter necessary for the strength of the four wires to exceed a given breaking stress selected on the basis of the length of cable required and

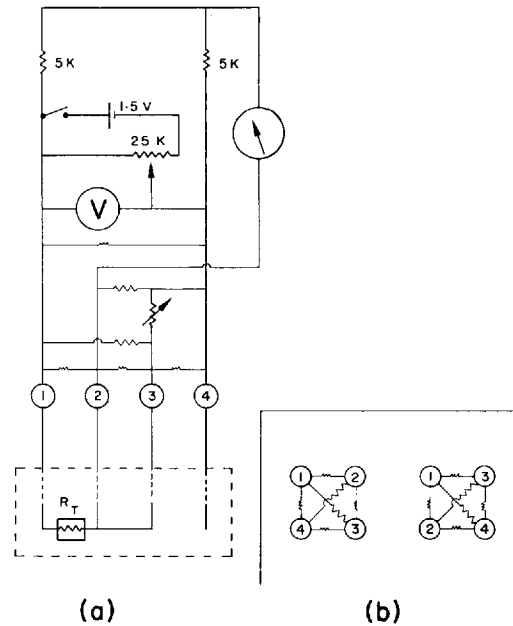


Fig. 8. Circuit diagram of Wheatstone bridge compensated for series and shunt resistance errors; the arrangement of shunt resistances for a four-lead cable are indicated by comparing the circuit diagram resistances of (a) with the coded resistances of (b). Portion in broken line box is in pressure-proof container in borehole [Beck, 1963].

a suitable safety factor. A circuit diagram of the equipment is shown in Figure 8. It can be seen that the circuit is basically a simple Wheatstone bridge with 1 to 1 ratio arms; practically any good Wheatstone bridge with four or five decades can be used.

Compensation for the series lead resistance, and its variation with temperature, is achieved by placing leads 1 and 3 in opposite arms of the bridge. Compensation for the shunt resistances and their variations with temperature is obtained by connecting the surface end of lead 4 to the junction of the variable resistance and the bridge power supply, while leaving the end in the probe electrically unconnected. If cable with good insulation is available, then lead 4 can be dispensed with.

Associated with this equipment is a temperature-compensated direct-coupled transistor amplifier which can be switched in between the bridge and the galvanometer. This amplifier is not necessary for the working of the bridge, since its only function is to increase the sensitivity of

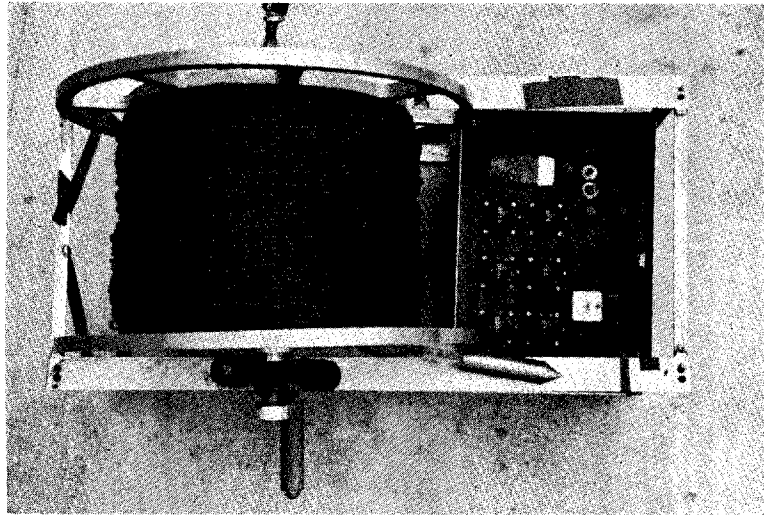


Fig. 9. Photograph of borehole temperature measuring equipment complete with probe and winch. With 1 km of four-lead cable the equipment weighs about 22 kg.

the apparatus. With a 10-k $\Omega$  thermistor and a 1.5-volt battery across the bridge, a sensitivity of 0.1°C can be readily obtained with a quite ordinary meter-type galvanometer. With the amplifier switched in, the sensitivity can be increased to 0.01°C, but the voltage across the bridge may have to be reduced to 0.5 volt to avoid significant self-heating errors at this level of sensitivity. The complete equipment (shown in Figure 9) with 1000 meters of four-lead cable weighs about 22 kg.

In experiments using a 10-k $\Omega$  resistor at the end of a leaky cable (1-M $\Omega$  insulation resistance) 1700 meters long, the accuracy of measurement was better than 0.01°C with the compensation leads connected as shown in Figure 8; without this lead the error was 0.16°C.

The second equipment [Jessop, 1964] requires only three leads, but, by the use of two latching relays in the pressure-proof container which also holds the thermistor, it is possible to provide four separate measuring circuits (Figure 10). Thus with suitable switching arrangements it is possible to measure the insulation resistance, the series resistance, and the resistances of two thermistors. Accurate corrections for the series resistance and the shunt resistance can therefore be applied to the apparent resistance of the thermistor. In this case the bridge is again a simple Wheatstone bridge, but it must be capable of measuring a wide range of resistances; it

should therefore have variable ratio arms. Additional equipment is required for pulsing the relays, which are operated by different currents through their coils.

This method of measuring resistances may be a little tedious, since it requires at least three independent measurements in the field and some computation time in the laboratory. However, it has the distinct advantage that at all times the behavior of the cable is known. With any method which incorporates automatic compensation, such as that previously described, there is always the worry that perhaps the compensation isn't working (it usually is, but it seems difficult to stop worrying).

A sensible modification to that equipment would be to provide a push button to switch the compensating lead in and out to see if it is working properly.

The third apparatus [Doig *et al.*, 1961] is perhaps potentially the most useful. The temperature measuring probe consists of a thermally sensitive oscillator using a thermistor as part of an R-C network. The frequency of the transmitted signal is measured by standard means at the surface and gives the temperature from a previous calibration of frequency versus temperature. The great advantage of this method is that no matter how long the cable or how bad the insulation resistance is, the frequency of the transmitted signal is not changed, so that this

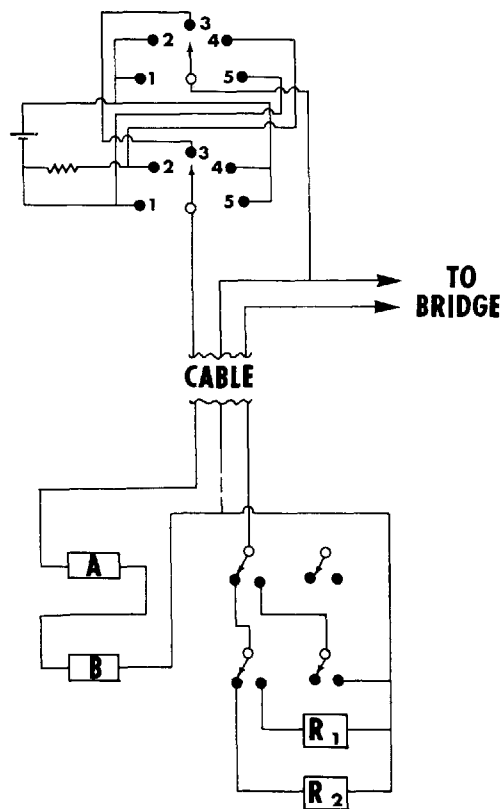


Fig. 10. Circuit diagram showing arrangement of two double pole latching relays for determining series resistance and leakage resistance of cables; portion in broken line box is in pressure-proof container in borehole [Jessop, 1964]. Relay *A* is operated by low voltage; relay *B* is operated by higher voltage. All resistance measurements are made with switch in position 3.

*Operating procedure.* Start in position 3.  $R_2$  connected; measure  $R_2$ . Switch to position 2 and return to 3; operates relay *A*; open circuit; measure shunt resistance. Switch to position 1 and return to 3; operates relay *B*; short circuit; measure series resistance. Switch to position 4 and return to 3; return relay *A* to original position;  $R_1$  connected; measure  $R_1$ . Switch to position 5 and return to 3; return relay *B* to original position;  $R_2$  connected; remeasure  $R_2$ .

equipment is capable of development for use at very great depths. Its disadvantage lies in the fact that it requires fairly complex equipment at the surface as well as in the borehole. At present this equipment is capable of an accuracy of  $0.05^\circ\text{C}$ .

As indicated earlier, one of the drawbacks of thermistors is that an occasional one is found

to be unpredictable. Its 'constants' may start drifting even if it has been observed to be stable for several months. This is why it is so important to check the calibration of thermistors at frequent intervals. Fortunately, it has been found [Beck, 1956a] that for many of the thermistors that drift slowly the drift merely displaces the resistance-temperature curve, and that relative temperatures are still accurate to within  $0.02^\circ\text{C}$  even if the drift is such that the absolute error in temperature is as large as  $1.5^\circ\text{C}$ .

The usual practice is to calibrate thermistors before and after the field trip. If the field area is far away from suitable calibrating facilities, the drift is checked in the field by returning, at suitable intervals, to remeasure the gradient in a conveniently situated borehole. If thermistor drift is suspected or observed, then the absolute temperature in a borehole can be found by comparing the temperature indicated by the thermistor at 30 meters with that observed with a platinum resistance thermometer or with maximum thermometers at the same depth. Having established the temperature and extent of the drift at one point, the rest of the temperatures in the borehole, as indicated by the thermistor, can be adjusted accordingly. Thus, if a careful watch is kept on the thermistor constants, they provide by far the best compromise between accuracy and simplicity of operation and design of associated equipment.

Maximum thermometers have frequently been used, either singly or as groups strung out over a few hundred feet [Mossop, 1950]. In recent years there has been a tendency to regard them as old-fashioned; however, the present author never goes in the field without them. They are not as accurate (approximately  $0.05$  to  $0.1^\circ\text{C}$ ) and do not give results as quickly as the thermistor, but they can be relied on. No matter how careful one is, trouble is likely to arise with electronic gadgetry when it is least expected; batteries go flat, transistors burn out and one has forgotten the spares. In these circumstances the maximum thermometer is a first class standby. Occasionally, it is hotter on the surface than at any point in the hole. In these circumstances a complicated procedure of cooling the thermometer and its container in the borehole has to be followed before a thermometer is lowered to a position where the temperature is higher than the place where the equipment is

cooled. The readings have to be hastily taken when the thermometer is brought to the surface.

### 3.2 Sources of Error in Temperature Gradient Measurements

In boreholes that are cased with metal, the temperature gradient is undisturbed for distances from an end of a casing that are fifty times greater than the diameter [Misener and Beck, 1960]. In general this means that correct results will be obtained 15 meters or more from the collar of the hole.

From a theoretical consideration it is found that once a borehole has been drilled it takes about twenty times the time taken to drill the borehole for thermal equilibrium to be re-established [Bullard, 1947; Jaeger, 1955-1956] (see also chapter 2, section 11, by Jaeger, in this volume). This applies to the whole borehole. For the lower parts of the hole the time is less. It may, therefore, be possible to make measurements in the lower sections of a borehole and get a reasonable temperature gradient only a few weeks after drilling has ceased. Even the upper sections of the borehole may be used before they return to equilibrium if the temperatures, at a number of given depths, are measured at intervals after the drilling has ceased. Then for any given depth  $z$  the equilibrium temperature  $T(\infty)$  can be determined [Lachenbruch and Brewer, 1959] from the equation

$$T(t) - T(\infty) = C \ln(1 + t_1/t_2) \quad (15)$$

where  $T(t)$  is the temperature observed at the time  $t_2$  since the cessation of drilling,  $t_1$  is the interval between the time the drill bit first reached the depth in question and the time the drilling ceased,  $T(\infty)$  is the equilibrium temperature, and  $C$  is a constant which depends on the diameter of the hole, the temperature, the depth, and the temperatures and thermal properties of the fluid and surrounding rock.

Since local and national regulations in a great number of regions require that boreholes be sealed at various levels and capped before they are abandoned, an alternative method of obtaining reasonable values of the undisturbed gradient which is likely to prove useful is to take temperatures at the bottom of the hole at various intervals during the drilling of the hole.

In a recent series of experiments during the

course of diamond drilling an AX hole, 600 meters deep, it was found that virgin rock temperatures at the bottom of the hole could be obtained to better than  $0.05^\circ\text{C}$  after a 12 to 24 hour standing time. Since the water flow through the hole was only about five liters per minute, it should not be expected that similar results could be obtained from rotary-drilled holes of the type normally put down for oil. There are two reasons for this: the first is that the water flows are considerably greater in a rotary-drilled hole, and the second is that there is far more mud to settle out after a rotary-drilled hole has been standing for several hours. It is unlikely that a probe could in fact reach the very bottom of the hole; it is more likely that it will become imbedded in settled mud about five meters from the bottom of the hole. This has been confirmed from the collection of data from several thousand oil wells in western Canada [Anglin and Beck, 1965].

It appears therefore that in diamond-drilled holes, and also in cable-tool-drilled holes, temperatures that are significant to terrestrial heat flow measurements can be obtained by making bottom hole temperature measurements after the hole has been allowed to stand for about a day. Thus, by making such measurements as the hole is drilled, a value of the temperature gradient can be obtained.

Theoretically, boreholes may have uncertain temperature gradients because of convection in the fluid. However, in boreholes deep enough to have one section theoretically stable and another section theoretically unstable, no detectable change in gradient could be found between the two sections [Krige, 1939; Diment and Robertson, 1963]. The criterion of stability [Krige, 1939] is

$$dT/dz < (dT/dz)_c \quad (16)$$

where  $(dT/dz)$  is the actual temperature gradient in the rocks, and  $(dT/dz)_c$  is the critical gradient given by

$$(dT/dz)_c = (gaT/C_p) + (B\nu\kappa/gaa^4) \quad (17)$$

where  $g$  is the acceleration due to gravity,  $a$  is the radius of the borehole,  $T$  is the absolute temperature,  $B$  is a numerical constant equal to 216 for a long tube, and  $\alpha$ ,  $\nu$ ,  $C_p$ , and  $\kappa$  are the coefficient of volume expansion, the kinematic viscosity, the specific heat at constant pressure,

and the diffusivity, respectively, at  $T^\circ\text{K}$ , of the fluid filling the hole.

Underground water flows may also cause large errors. The flows may be local and shallow and are often indicated by water flowing out of a hole. Occasionally water may flow into a hole at one depth and out of a hole at another depth with no observable effect at the surface. In this case, it is often possible to detect the inlet and outlet levels [Misener and Beck, 1960] and sometimes to measure the magnitude of the flow [Newstead and Jaeger, 1956] by thermal means. There also exists the possibility that a large scale but very slow movement of water occurs [Bullard and Niblett, 1951] which is very difficult to detect and evaluate. Care also has to be exercised when measurements are made near oceans or large lakes, since large corrections, which can be broadly classified as topographic corrections, may be required [Birch, 1954; Lachenbruch, 1957]; errors arising in this way can sometimes be combined with errors due to mass flow of water in the region of the shore line [Swartz, 1958].

More recently [Beck, 1962] attempts have been made to determine a pattern of underground water flow in a mine by collecting samples of water from various levels and positions throughout a mine and measuring the tritium content of the samples. Since the half-life of tritium is only about 12 years, the relative tritium content of the water samples would give some indication of the water flow. The results to date do in fact indicate that there is underground flow of water, at least in the upper levels of the mine. But there is now the difficulty of deciding whether the water flow was in progress before the mine started or whether the flows have been induced by the mining activity in the area.<sup>1</sup> The resultant flow may, of course, be a combination of both of these possibilities. From this point of view, it would be desirable to obtain water samples from various depths in a borehole, or, better still, from a grid of boreholes which are unlikely to have disturbed an area as much as a mine. In any event it seems clear that more work along these lines is needed.

<sup>1</sup>Note added in proof. More recent work indicates that the introduction of the mine has a strong influence on the tritium dates [Neophytov, 1965].

#### 4. CALCULATION OF HEAT FLOW

##### 4.1 Combining Gradient and Conductivity

The heat flow is obtained by combining the temperature gradient and the conductivity of the rocks in the area. The simplest method is to divide each hole, or mine, into its respective lithological sections and then to take for each section the product of the arithmetic mean conductivity and the temperature gradient derived from the least squares calculation, thus obtaining a value of heat flux for each section. A mean flux for the area can then be obtained from the values for each lithologic section.

An alternative method [Bullard, 1939] is to combine the observations according to the equation

$$T_z = T_0 + q \sum_i (D_i/K_i) \quad (18)$$

where  $T_z$  is the temperature at depth  $z = \sum_i D_i$ ,  $K_i$  is the thermal conductivity of the  $i$ th homogeneous section of thickness  $D_i$ , and  $T_0$  is a constant. The mean heat flow  $q$  can then be found from the slope of the line resulting from a plot of  $T_z$  versus  $\sum_i (D_i/K_i)$ . Because of the form of (18), the harmonic mean conductivity is sometimes used.

Slight differences in the heat flow value obtained from these methods will usually be observed, but these differences are usually not significant [Diment and Robertson, 1963; Sass and LeMarne, 1963].

This second method gives a value which is an average for all sections down to the maximum depth of penetration, and it makes it a little easier to put error limits on the heat flow value. The first method shows up more clearly any variations of heat flow with depth. If these variations are significant, an explanation must be sought, the two possibilities being an incorrect temperature gradient due to the reasons discussed in section 3.2 (see also chapter 2, sections 5–9, by Jaeger, in this volume), or due to heat production within a particular lithologic section.

The calculation of heat flow is usually made assuming that the flow is normal to the surface of the Earth. If the temperature gradient has been found from measurements in mines, or if a number of boreholes have been used over a reasonably wide area, it is sometimes possible to

detect a horizontal component of heat flow. Except in obviously abnormal geological conditions, the horizontal component rarely exceeds 4% of the vertical component [Mossop and Gafner, 1951; Flugge-de Smidt, 1951].

In some areas, the heat flow lines may be distorted by geological structures such as dikes. For simple cases Roy [1963] assumes a tangential law of refraction from which the following relation is obtained:

$$\sin^2 \alpha = \left(1 - \frac{f_{2v}}{f_1}\right) / \left(1 - \frac{K_2}{K_1}\right) \quad (19)$$

where  $\alpha$  is the dip angle of the dike of conductivity  $K_2$ ,  $K_1$  is the conductivity of the host rock,  $f_{2v}$  is the vertical component of heat flow in the dike, and  $f_1$  is the heat flow in the host rock.

Roy applied this correction to the results from a borehole near Boss, Missouri. This hole passed through a tabular body of andesite ( $K_2 = 5.8$  mcal/cm sec °C) imbedded in a rhyolite mass ( $K_1 = 7.5$ ). The heat flux in the rhyolite was 1.29  $\mu$ cal/cm<sup>2</sup> sec and 1.07 in the andesite. It was found that the difference in heat flows could be accounted for by a value of  $\alpha = 50^\circ$ .

#### 4.2 Sources of Heating

The possible sources of local heat production are oxidation of oil [Van Orstrand, 1934], oxidation of ore bodies [Misener, 1949], and local concentrations of radioactive material [Garland and Lennox, 1962]; none of these appears to be very significant to the levels of accuracy of heat flow measurement at present attainable.

Absorption of neutrinos throughout the Earth has been proposed as a possible source of heat. Estimates range from the effect being negligible to its being able to account for practically all the observed terrestrial heat flow [Saxon, 1949; Cormack, 1954; Isaacs and Bradner, 1964]. The problem here is that neither the neutrino flux nor the mechanisms of the various interactions is very well known.

Sources of excess heat may occur in regions situated over the rising arm of a convection current and in mountainous regions where there is increased radioactivity due to mountain roots. The correlation of geoid highs and heat flow lows (and vice-versa), which can be interpreted [Lee and MacDonald, 1963] as being caused by a fall-

ing arm of convection current, is not very strong and is in any case based on an uneven distribution of data, particularly for the heat flow data. There is some evidence of high (approximately 2.0  $\mu$ cal/cm<sup>2</sup> sec) heat flow values in mountainous regions [Beck, 1956b; Clark and Niblett, 1956; Clark, 1961; Howard and Sass, 1964]. However, there are also values of the same magnitudes in nonmountainous regions. Thus, it is probably fair to say that, although there is evidence that the effects may exist, in neither case is the evidence very strong.

Perhaps the two most significant pieces of information to come from heat flow work are the approximate equivalence of the heat flow values over the ocean basin and over the continents, and the relatively low values for areas lying over a shield compared with the value for areas that lie well away from a shield [Lubimova, 1963; Beck and Logis, 1964; Howard and Sass, 1964; Verma, 1965]. In chapter 6 of this volume Lee and Uyeda present a review of heat-flow observations, and geophysical deductions from observations of heat flow are given in chapter 7 by MacDonald.

## 5. SUMMARY

There are hundreds of methods available for determining temperatures and thermal conductivities. Nearly all these methods are slight variations on a few basic themes, and the variations arise because, for a particular application, one worker's idea of a suitable compromise between mechanical reliability, accuracy, and convenience (which includes cost of equipment and time taken for one measurement) may not coincide with the ideas of another worker with a slightly different application. In a chapter such as this, which is in itself a compromise between a review article for experienced workers and an introductory article for workers planning to enter the field, it is clearly impossible to discuss critically even a small fraction of the methods available without being selective.

The selection of a particular instrument, or method, for discussion has been based on observing the type of instrument most used by workers who have had several years experience in terrestrial heat flow, on the assumption that they continue to use the equipment because it fulfills

their requirements of a good compromise among the three factors mentioned above.

In this respect there seems to be little doubt that the basic instrument used for the determination of the thermal conductivities of rocks is some form of the divided bar apparatus, whether it is in the form of a single disc sandwiched between two relatively long rods or whether it consists of a stack of discs. Since the same basic principle applies to practically any type of divided bar apparatus, only the constant temperature difference type incorporating a thick guard ring has been described in detail. The apparatus is easy to build and use, and measurements on single discs can be completed within ten or fifteen minutes of introducing the disc into the apparatus, the reproducibility being between 1 and 2%. The precision on this, and on many other types of apparatus, can be improved, but improvement is usually considered to be unnecessary. The main reason for describing this particular apparatus in detail is that the use of the guard ring makes it possible to obtain reliable values from discs that are somewhat over or under sized—a very important point if bore cores, which vary in diameter as the drill gets worn, are to be used directly without further drilling in the laboratory.

A new absolute method which avoids the direct measurement of temperature is also described in some detail.

One or two new methods which appear to be promising have been briefly mentioned, but they have not been in use long enough for us to see if they represent a marked improvement over the methods currently in use. This applies particularly to transient methods being developed for measuring the thermal conductivity of rocks in the laboratory.

In striving for a higher precision of measurement in the laboratory, a point that is frequently overlooked is that what is really required is a good average value of the thermal conductivity of a large mass of rock. There is therefore little point in obtaining a highly precise measurement on a single disc if this disc is not truly representative of the rock as a whole. It is better to seek more rapid, rather than more precise, laboratory methods of determining thermal conductivities.

To illustrate the problem of nonrepresentative specimens, the results from a set of discs cut

from a granite core are discussed in some detail. Although the conductivities of the individual discs were probably accurate to within 1 or 2%, other evidence indicated that the mean measured value may be 20 to 40% too high. It is therefore important when dealing with quartz-rich rocks, such as granites, to make a petrological examination and other tests to see whether, in fact, the discs are reasonably representative of the rock as a whole.

An alternative to the approach of making a large number of rapid conductivity measurements on relatively small samples in the laboratory is to make probe measurements in a borehole. In this case, since the probe is a few feet long and the experimental time from several minutes to a few hours long, a large volume of the rock is effectively sampled. Some of the practical difficulties in making these measurements in the field have been discussed; precision of such measurements is not much better than 10%.

For the determination of temperature gradients, temperatures accurate to 0.1°C are generally quite satisfactory, but in some circumstances it may be desirable to measure to 0.01°C. To establish regional trends of underground temperatures and gradients, a large number of readings, with an accuracy of only 0.5 or even 1°C, may be adequate.

Although platinum resistance thermometers, thermocouples, and maximum thermometers have been used, a thermistor is the most common type of thermally sensitive element now in use.

A wide variety of thermistors are available, having different (but all high, approximately 4 or 5%) temperature coefficients of resistance, self heating coefficients, time constants, and geometries. The thermistors should normally be confined in a pressure-tight, water-proof container, but there are some types that do not require pressure-tight containers if measurements are confined to a few hundred meters of water pressure.

Three types of temperature-measuring equipment have been described. The first utilizes any commercially available 2- to 4-lead cable; a third lead is necessary if, as is usually desirable, series resistance compensation is required, and the fourth lead is required if shunt resistance compensation in a leaky cable is desired. The

second instrument is a little more complex and requires three leads and two latching relays. In effect, the relays provide four separate circuits with which the series resistance, shunt resistance, and two thermistor resistances can be measured. Circuit diagrams have been provided for both sets of the equipment. In both cases, practically any commercially available wheatstone bridge and robust galvanometer will allow measurements to an accuracy of 0.1°C. Measurements to 0.01°C require either a large thermistor with negligible self heating effects at high (about 6 volts) bridge voltages or a sensitive laboratory type galvanometer to detect the smaller out of balance voltages obtained at low bridge voltages (about 1/2 volt). The latter may be replaced by one of the many battery operated solid state null detectors, incorporating a simple dc amplifier and robust meter, now commercially available.

The third instrument described is the most complex of them all, but it is potentially the most useful since it makes use of the thermistor in a thermally sensitive oscillator circuit. A frequency-measuring device is required at the surface but, since the temperature is determined from the frequency measurement, only one insulated lead is really required, and the series and shunt resistances can be ignored. To date this instrument has been developed only to an accuracy of 0.05°C, but there are no serious practical difficulties preventing a more accurate version being built.

Possible disturbances, largely geologically controlled, to the equilibrium temperatures have been pointed out.

Various methods of combining conductivities and temperature gradients to obtain the terrestrial heat flow have been discussed; it was found that the slight differences in heat flow values were without real significance in the light of the errors of measurement.

*Acknowledgments.* The author is indebted to the National Research Council of Canada for a continuing grant-in-aid and to the many colleagues, some of them authors of other chapters in this volume, who critically reviewed the manuscript.

This chapter constitutes Canadian contribution 69 to the International Upper Mantle Project.

## REFERENCES

- Anglin, F. M., and A. E. Beck, Regional heat flow pattern in western Canada, *Can. J. Earth Sci.*, **2**, 176-182, 1965.
- Beck, A. E., The stability of thermistors, *J. Sci. Instr.*, **33**, 16-18, 1956a.
- Beck, A. E., The flow of heat through the earth's crust and through rock, Ph.D. thesis, Australian National University, Canberra, 1956b.
- Beck, A. E., A steady state method for the rapid measurement of the thermal conductivity of rocks, *J. Sci. Instr.*, **34**, 186-189, 1957.
- Beck, A. E., Terrestrial flow of heat near Flin Flon, Manitoba, *Nature*, **195**, 368-369, 1962.
- Beck, A. E., Lightweight borehole temperature measuring equipment for resistance thermometers, *J. Sci. Instr.*, **40**, 452-454, 1963.
- Beck, A. E., and J. M. Beck, On the measurement of the thermal conductivities of rocks by observations on a divided bar apparatus, *Trans. Am. Geophys. Union*, **30**, 1111-1123, 1958.
- Beck, A. E., J. C. Jagger, and G. N. Newstead, The measurement of the thermal conductivities of rocks by observations in boreholes, *Australian J. Phys.*, **9**, 286-296, 1956.
- Beck, A. E., and Z. Logis, Terrestrial flow of heat in the Brent Crater, *Nature*, **201**, 383, 1964.
- Beck, J. M., and A. E. Beck, *J. Geophys. Res.*, **70**, in press, 1965.
- Benfield A. E., Terrestrial heat flow in Great Britain, *Proc. Roy. Soc. London*, **A**, **173**, 428-450, 1939.
- Benfield, A. E., The effect of uplift and denudation on underground temperatures, *J. Appl. Phys.*, **20**, 66-70, 1949.
- Birch, F., Flow of heat in the Front Range, Colorado, *Bull. Geol. Soc. Am.*, **61**, 567-630, 1950.
- Birch, F., Thermal conductivity, climatic variation and heat flow near Calumet, Michigan, *Am. J. Sci.*, **252**, 1-25, 1954.
- Birch F., and H. Clark, The thermal conductivity of rocks and its dependence upon temperature and composition, *Am. J. Sci.*, **238**, 529-558 and 613-635, 1940.
- Blackwell, J. H., A transient heat flow method for determination of thermal constants of insulating materials in bulk, *J. Appl. Phys.*, **25**, 137-144, 1954.
- Blackwell, J. H., The axial flow error in the thermal conductivity probe, *Can. J. Phys.*, **34**, 412-417, 1956.
- Brailsford, A. D., and K. G. Major, The thermal conductivity of aggregates of several phases, including porous materials, *Brit. J. Appl. Phys.*, **15**, 313-319, 1964.
- Bullard, E. C., The disturbance of the temperature gradient in the earth's crust by inequalities of height, *Monthly Notices Roy. Astron. Soc., Geophys. Suppl.*, **4**, 360-363, 1938.
- Bullard, E. C., Heat flow in South Africa, *Proc. Roy. Soc. London*, **A**, **173**, 474-502, 1939.
- Bullard, E. C., Time necessary for a borehole to attain temperature equilibrium, *Monthly No-*

- tices Roy. Astron. Soc., Geophys. Suppl.*, 5, 125-130, 1947.
- Bullard, E. C., and E. R. Niblett, Terrestrial heat flow in England, *Monthly Notices Roy. Astron. Soc., Geophys. Suppl.*, 6, 222-238, 1951.
- Clark, S. P., Jr., Heat flow in the Austrian alps, *Geophys. J.*, 6, 54-63, 1961.
- Clark, S. P., and E. R. Niblett, Terrestrial heat flow in the Swiss alps, *Monthly Notices Roy. Astron. Soc., Geophys. Suppl.*, 7, 176-195, 1956.
- Cormack, A. M., Heat generation in the earth by solar neutrinos, *Phys. Rev.*, 95, 580-581, 1954.
- Diment, W. H., and E. C. Robertson, Temperature, thermal conductivity, and heat flow in a drilled hole near Oak Ridge, Tennessee, *J. Geophys. Res.*, 68, 5035-5047, 1963.
- Diment, W. H., and J. D. Weaver, Subsurface temperatures and heat flow in the AMSOC core hole near Mayaguez, Puerto Rico, in *A study of serpentinite*, C. A. Burk, editor, pp. 75-91, *Natl. Acad. Sci.—Natl. Res. Council Publ.* 1188, 1964.
- Diment, W. H., and R. W. Werre, Terrestrial heat flow near Washington, D. C., *J. Geophys. Res.*, 69, 2143-2149, 1964.
- Doig, R., V. A. Saull, and R. A. Butler, A new borehole thermometer, *J. Geophys. Res.*, 66, 4263-4264, 1961.
- Everett, J. D., On a method of reducing observations of underground temperature, with its application to the monthly mean temperatures of underground thermometers, at the Royal Edinburgh Observatory, *Trans. Roy. Soc. Edinburgh*, 22, 429-439, 1859-1861.
- Flugge-de Smidt, R. A. H., Contribution to discussion on Mossop and Gafner's paper, 1951, *J. Chem. Met. Min. Soc. South Africa*, 52, 73-76, 1951.
- Forbes, J. D., Account of some experiments on the temperature of the Earth at different depths, and in different soils, near Edinburgh, *Trans. Roy. Soc. Edinburgh*, 16, 189-236, 1845-1849.
- Garland, G. D., and D. H. Lennox, Heat flow in Western Canada, *Geophys. J.*, 6, 245-262, 1962.
- Herschel, A. S., and G. A. Lebour, Notes on some experiments on the conducting powers for heat of certain rocks, with remarks on the geological aspects of the investigations, *Brit. Assoc. Repts., 43rd Meeting, Trans. of the Sections*, 223-227, 1873.
- Howard, L. E., and J. H. Sass, Terrestrial heat flow in Australia, *J. Geophys. Res.*, 69, 1617-1626, 1964.
- Isaacs, J. D., and H. Bradner, Neutrino and geothermal fluxes, *J. Geophys. Res.*, 69, 3883-3887, 1964.
- Jaeger, J. C., Numerical values for the temperature in radial heat flow, *J. Math. Phys.*, 34, 316-321, 1955-1956.
- Jaeger, J. C., Conduction of heat in an infinite region bounded internally by a circular cylinder of a perfect conductor, *Australian J. Phys.*, 9, 167-179, 1956.
- Jaeger, J. C., and J. H. Sass, A line source method for measuring the thermal conductivity and diffusivity of cylindrical specimens of rock and other poor conductors, *Brit. J. Appl. Phys.*, 15, 1-8, 1964.
- Jessop, A. M., A lead-compensated thermistor probe, *J. Sci. Instr.*, 41, 503-504, 1964.
- Krige, L. J., Borehole temperatures in the Transvaal and Orange Free State, *Proc. Roy. Soc. London, A*, 173, 450-474, 1939.
- Lachenbruch, A. H., Thermal effects of the ocean on permafrost, *Geol. Soc. Am. Bull.* 68, 1515-1529, 1957.
- Lachenbruch, A. H., and M. C. Brewer, Dissipation of the temperature effect of drilling a well in arctic Alaska, *U. S. Geol. Surv. Bull.* 1083-C, 73-109, 1959.
- Lee, W. H. K., and G. J. F. MacDonald, The global variation of terrestrial heat flow, *J. Geophys. Res.*, 68, 6481-6492, 1963.
- Lees, C. H., On the thermal conductivities of crystals and other bad conductors, *Phil. Trans. Roy. Soc. London, A*, 183, 481-509, 1892.
- Lubimova, E. A., Terrestrial heat flow in shields and their recent movements (abstract), Upper Mantle Symposium, *IUGG*, Berkeley, Calif., August 19-31, 1963.
- Lubimova, E. A., L. M. Lusova, F. V. Firsov, G. N. Starikova, and A. P. Shushpanov, Determination of surface heat flow in Mazesta (USSR), *Ann. Geophys.*, 14, 157-167, 1961.
- Mairan, J. J. D., Dissertation sur la glace ou explication physique ou la formation de la glace, et de ses divers phénomènes, Chapter 11, L'Imprimerie Royale, Paris, 1749.
- Misener, A. D., Temperature gradients in the Canadian Shield, *Can. Min. Met. Bull.*, 42, 280-287, 1949; also in *C.I.M. Trans.*, 52, 125-132, 1949.
- Misener, A. D., and A. E. Beck, The measurement of heat flow over land, in *Methods and Techniques in Geophysics*, edited by S. K. Runcorn, pp. 10-61, Interscience Publishers, New York, 1960.
- Mossop, S. C., A multi thermometer method for temperature measurement in boreholes, *J. Chem. Met. Min. Soc. South Africa*, 51, 120-122, 1950.
- Mossop, S. C., and G. Gafner, The thermal constants of some rocks from the Orange Free State, *J. Chem. Met. Min. Soc. South Africa*, 52, 61-73, 1951.
- Ncophytov, J. P., Tritium distribution, dating theory, and hydrological applications, M.Sc. thesis, University of Western Ontario, London, 1965.
- Newstead, G. N., and J. C. Jaeger, The determination of underground water movements from measurements in drill holes, *The Engineer, London*, 202, 76-78, 1956.

- Powell, R. W., Experiments using a simple thermal comparator for measurements of thermal conductivity, surface roughness and thickness of foils or of surface deposits, *J. Sci. Instr.*, *34*, 485-492, 1957.
- Ratcliffe, F. H., Thermal conductivities of fused and crystalline quartz, *Brit. J. Appl. Phys.*, *10*, 22-25, 1959.
- Roy, R. F., Heat flow measurements in the United States, Ph.D. thesis, Harvard University, Cambridge, 1963.
- Sass, J. H., In situ measurement of rock conductivities, M. Sc. thesis, University of Western Ontario, London, 1961.
- Sass, J. H., Geothermal measurements in Australia, Ph.D. thesis, Australian National University, Canberra, 1965.
- Sass, J. H., The thermal conductivity of fifteen feldspar specimens, *J. Geophys. Res.*, *70*, in press, 1965.
- Sass, J. H., and A. E. LeMarne, Heat flow at Broken Hill, New South Wales, *Geophys. J.*, *7*, 477-489, 1963.
- Saxon, D., The neutrinos from the sun and the source of the earth's heat, *Phys. Rev.*, *76*, 986, 1949.
- Schröder, J., Apparatus for determining the thermal conductivity of solids in the temperature range from 20 to 200°C, *Rev. Sci. Instr.*, *34*, 615-621, 1963.
- Somerton, W. H., Some thermal characteristics of porous rocks, *Petroleum Trans.*, *AIME*, *213*, 375-378, 1958.
- Swartz, J. H., Geothermal measurements on Eniwetok and Bikini atolls, *U. S. Geol. Surv. Profess. Paper* 260U, 711-741, 1958.
- Thompson, W., On the reduction of observations of underground temperature, with application to Professor Forbes' Edinburgh observations, and the continued Calton Hill series, *Trans. Roy. Soc. Edinburgh*, *22*, 405-427, 1859-1861.
- Van Orstrand, C. E., Some possible applications of geothermics to geology, *Bull. Am. Assoc. Petrol. Geol.*, *18*, 13-39, 1934.
- Verma, R. K., Terrestrial heat flow in Kolar gold field, India, *J. Geophys. Res.*, *70*, 1353-1356, 1965.
- Weiss, O., Temperature measurements with an electrical resistance thermometer in a deep borehole on the East Rand, *J. Chem. Met. Min. Soc. South Africa*, *39*, 149-166, 1938.
- Woodside, W., and J. H. Messmer, Thermal conductivity of porous media, 1, Unconsolidated sands, 2, Consolidated rocks, *J. Appl. Phys.*, *32*, 1688-1706, 1961.
- Zierfuss, H., An apparatus for the rapid determination of the heat conductivity of poor conductors, *J. Sci. Instr.*, *40*, 69-71, 1963.

(Manuscript received June 1, 1964; revised October 28, 1964.)

## APPENDIX 2

## THEORETICAL TEMPERATURE-TIME CURVES FOR THE CYLINDRICAL THERMAL CONDUCTIVITY PROBE

*Introduction.* The theory of the cylindrical heat source in an infinite medium is used frequently to determine the thermal conductivity of rocks and soils. For large time the temperature ( $V$ ) versus log time ( $\ln t$ ) curve for the cylindrical heater approaches a linear asymptote with slope equal to  $Q/4\pi K$ , where  $Q$  is the heat input and  $K$  is the thermal conductivity of the medium surrounding the heater. This asymptote can be used conveniently with probes of small diameter such as the 'needle probe' [cf. Vos, 1955; Von Herzen and Maxwell, 1959]. With probes of diameter appropriate to diamond-drilled boreholes, the linear asymptote is closely approached only after times of the order of hours (compared with minutes for the needle probe), and a reduction that utilizes the earlier portion of the temperature-time curve is desirable.

A number of these reduction methods have been proposed [cf. Blackwell, 1954; Jaeger, 1956, 1958, 1959]. They all require calculation of theoretical curves for a range of values of the various parameters. Jaeger [1956] has calculated a few theoretical curves. The present work extends the range and interval of Jaeger's curves, resulting in a sufficient number of curves to cover nearly all cases of probes in water-filled holes in rock.

The theory of the probe is that of an infinite region bounded internally by a circular cylinder of a perfect conductor where there is a constant heat flux across the boundary between the probe and the surrounding medium. The temperature rise of the probe [cf. Jaeger, 1956] is given by

$$V = (Q/K) G(h, \alpha, \tau) \quad (1)$$

$$h = K/aH, \quad \alpha = 2\pi a^2 \rho c/S, \quad \tau = \kappa t/a^2 \quad (2)$$

$$G(h, \alpha, \tau) = (2\alpha^2/\pi^3) \int_0^\infty \frac{[1 - \exp(-\tau u^2)]}{u^3 \Delta(u)} du \quad (3)$$

$$\Delta(u) = [uJ_0(u) - (\alpha - hu^2)J_1(u)]^2 + [uY_0(u) - (\alpha - hu^2)Y_1(u)]^2 \quad (4)$$

where  $V$  is the temperature at time  $t$ ;  $K$ ,  $\kappa$ ,  $\rho$ ,

<sup>2</sup> Prepared by J. H. Sass, Geophysics Department, University of Western Ontario, London, Canada.

and  $c$  are the thermal conductivity, thermal diffusivity, density, and specific heat of the rock;  $a$  is the radius of the hole;  $H$ , the coefficient of heat transfer at the interface between probe and rock; and  $S$ , the heat capacity per unit length of the probe;  $J_n(u)$  and  $Y_n(u)$  are the Bessel functions of the first and second kinds and order  $n$ . The function  $G(h, \alpha, \tau)$  has been calculated by numerical integration using an IBM 7040 computer. The integration was carried out using first 120 then 240 values of the integrand. In all cases, convergence to five significant figures between the two determinations was obtained. Tables of  $G(h, \alpha, \tau)$  versus  $\tau$  are given below (pages 52-57) for  $0 \leq h \leq 2.0$ ,  $0.5 \leq \alpha \leq 5.0$ , and  $0.2 \leq \tau \leq 40$ .

This range includes all experimental configurations for which the contact resistance between probe and rock is moderately low. When measurements are made in dry holes, there is an air gap between probe and rock that results in a high value of the parameter ' $h$ .' In these cases the reduction is more difficult and the precision of the measurement not nearly so high as in the cases where ' $h$ ' is small. Fortunately, dry holes can usually be avoided in the field, and, when they cannot, the introduction of a liquid or cement layer between probe and rock is a simple procedure.

The values of  $\tau$  have been chosen so as to fa-

ilitate the calculation of the curves  $G(h, \alpha, 2\tau)/G(h, \alpha, \tau)$  versus  $\tau$  [cf. Jaeger, 1959].

*Acknowledgments.* This work has been supported by a research grant and a post-doctoral fellowship from the National Research Council of Canada. I am indebted to A. F. Beek for advice and criticism and to the University of Western Ontario for providing its computer facilities.

#### REFERENCES

- Blackwell, J. H., A transient-flow method for determination of thermal constants of insulating materials in bulk, *J. Appl. Phys.*, *25*, 137-144, 1954.
- Jaeger, J. C., Conduction of heat in an infinite region bounded internally by a circular cylinder of a perfect conductor, *Australian J. Phys.*, *9*, 167-179, 1956.
- Jaeger, J. C., The measurement of thermal conductivity and diffusivity with cylindrical probes, *Trans. Am. Geophys. Union*, *39*, 708-710, 1958.
- Jaeger, J. C., The use of complete temperature-time curves for determination of thermal conductivity with particular reference to rocks, *Australian J. Phys.*, *12*, 203-217, 1959.
- Von Herzen, R., and A. E. Maxwell, Measurements of thermal conductivity of deep sea sediments by a needle probe method, *J. Geophys. Res.*, *64*, 1557-1563, 1959.
- Vos, B. H., Measurement of thermal conductivity by a non-steady state method, *Appl. Sci. Res.*, *A*, *5*, 425-438, 1955.

(Received May 5, 1965.)

ALPHA = 0.50

TAU	h	0.	0.05	0.10	0.20	0.40	0.60	0.90	1.20	1.50	2.00
0.2	0.01330	0.01364	0.01390	0.01429	0.01475	0.01501	0.01524	0.01538	0.01547	0.01557	
0.3	0.01912	0.01962	0.02004	0.02068	0.02150	0.02199	0.02244	0.02271	0.02290	0.02311	
0.4	0.02459	0.02525	0.02581	0.02671	0.02732	0.02868	0.02939	0.02984	0.03016	0.03050	
0.5	0.02976	0.03057	0.03128	0.03244	0.03406	0.03511	0.03612	0.03678	0.03724	0.03776	
0.6	0.03469	0.03565	0.03649	0.03791	0.03994	0.04130	0.04265	0.04354	0.04417	0.04488	
0.8	0.04389	0.04514	0.04625	0.04817	0.05105	0.05307	0.05514	0.05655	0.05756	0.05873	
1.0	0.05239	0.05389	0.05527	0.05767	0.06139	0.06409	0.06696	0.06894	0.07040	0.07211	
1.2	0.06030	0.06204	0.06365	0.06652	0.07107	0.07447	0.07816	0.08077	0.08271	0.08502	
1.6	0.07465	0.07684	0.07889	0.08261	0.08876	0.09355	0.09895	0.10291	0.10593	0.10960	
2.0	0.08744	0.09001	0.09245	0.09695	0.10459	0.11073	0.11738	0.12326	0.12744	0.13263	
3.0	0.11438	0.11776	0.12101	0.12715	0.13804	0.14730	0.15867	0.16770	0.17499	0.18439	
4.0	0.13624	0.14023	0.14412	0.15155	0.16512	0.17706	0.19228	0.20483	0.21527	0.22915	
5.0	0.15456	0.15904	0.16343	0.17191	0.18767	0.20188	0.22052	0.23634	0.24982	0.26818	
6.0	0.17027	0.17515	0.17994	0.18927	0.20686	0.22300	0.24463	0.26342	0.27974	0.30245	
8.0	0.19610	0.20158	0.20699	0.21761	0.23800	0.25719	0.28370	0.30754	0.32869	0.35962	
10.0	0.21673	0.22263	0.22849	0.24003	0.26244	0.28388	0.31410	0.34195	0.36746	0.40515	
12.0	0.23380	0.24002	0.24620	0.25843	0.28234	0.30546	0.33854	0.36955	0.39845	0.44206	
16.0	0.26085	0.26750	0.27411	0.28727	0.31322	0.33865	0.37568	0.41121	0.44513	0.49787	
20.0	0.28174	0.28865	0.29555	0.30929	0.33653	0.36341	0.40294	0.44141	0.47668	0.53782	
24.0	0.29865	0.30575	0.31284	0.32698	0.35508	0.38293	0.42414	0.46458	0.50413	0.56777	
32.0	0.32498	0.33231	0.33964	0.35427	0.38343	0.41246	0.45568	0.49849	0.54079	0.60996	
40.0	0.34506	0.35253	0.36000	0.37492	0.40470	0.43439	0.47874	0.52284	0.56664	0.63884	

ALPHA = 0.75

TAU	h	0.	0.05	0.10	0.20	0.40	0.60	0.90	1.20	1.50	2.00
0.2	0.01840	0.01904	0.01957	0.02036	0.02133	0.02188	0.02238	0.02268	0.02288	0.02309	
0.3	0.02600	0.02693	0.02773	0.02900	0.03066	0.03169	0.03265	0.03325	0.03366	0.03411	
0.4	0.03297	0.03417	0.03522	0.03695	0.03935	0.04090	0.04241	0.04338	0.04405	0.04480	
0.5	0.03944	0.04088	0.04217	0.04434	0.04748	0.04960	0.05171	0.05310	0.05408	0.05520	
0.6	0.04548	0.04715	0.04866	0.05126	0.05514	0.05784	0.06060	0.06245	0.06378	0.06530	
0.8	0.05654	0.05862	0.06054	0.06393	0.06924	0.07313	0.07726	0.08013	0.08223	0.08471	
1.0	0.06649	0.06893	0.07122	0.07533	0.08199	0.08705	0.09261	0.09659	0.09956	0.10311	
1.2	0.07554	0.07831	0.08092	0.08568	0.09361	0.09982	0.10682	0.11196	0.11585	0.12059	
1.6	0.09155	0.09487	0.09804	0.10394	0.11415	0.12251	0.13236	0.13987	0.14574	0.15307	
2.0	0.10540	0.10917	0.11280	0.11966	0.13184	0.14214	0.15470	0.16458	0.17249	0.18259	
3.0	0.13353	0.13814	0.14264	0.15132	0.16737	0.18169	0.20018	0.21559	0.22851	0.24577	
4.0	0.15549	0.16067	0.16578	0.17574	0.19457	0.21192	0.23516	0.25533	0.27280	0.29699	
5.0	0.17341	0.17903	0.18458	0.19547	0.21637	0.23602	0.26303	0.28716	0.30860	0.33915	
6.0	0.18852	0.19445	0.20034	0.21194	0.23441	0.25584	0.28585	0.31325	0.33809	0.37431	
8.0	0.21293	0.21931	0.22567	0.23826	0.26294	0.28689	0.32125	0.35356	0.38373	0.42928	
10.0	0.23216	0.23885	0.24551	0.25875	0.28488	0.31048	0.34773	0.38342	0.41740	0.47000	
12.0	0.24797	0.25487	0.26175	0.27544	0.30257	0.32930	0.36856	0.40664	0.44336	0.50125	
16.0	0.27295	0.28011	0.28727	0.30154	0.32994	0.35811	0.39987	0.44093	0.48116	0.54605	
20.0	0.29225	0.29958	0.30690	0.32153	0.35069	0.37970	0.42290	0.46567	0.50792	0.57692	
24.0	0.30794	0.31538	0.32282	0.33768	0.36733	0.39688	0.44100	0.48483	0.52832	0.59987	
32.0	0.33251	0.34009	0.34767	0.36281	0.39306	0.42326	0.46845	0.51350	0.55838	0.63272	
40.0	0.35141	0.35907	0.36673	0.38204	0.41264	0.44320	0.48899	0.53469	0.58030	0.65606	

ALPHA = 1.00

TAU	h	0.	0.05	0.10	0.20	0.40	0.60	0.90	1.20	1.50	2.00
0.2	0.02273	0.02372	0.02455	0.02583	0.02745	0.02837	0.02921	0.02973	0.03008	0.03045	
0.3	0.03165	0.03305	0.03426	0.03624	0.03893	0.04063	0.04224	0.04327	0.04397	0.04476	
0.4	0.03966	0.04141	0.04298	0.04561	0.04940	0.05193	0.05443	0.05606	0.05721	0.05851	
0.5	0.04697	0.04904	0.05092	0.05416	0.05902	0.06241	0.06587	0.06818	0.06984	0.07174	
0.6	0.05372	0.05607	0.05823	0.06203	0.06793	0.07218	0.07664	0.07970	0.08191	0.08450	
0.8	0.06584	0.06868	0.07135	0.07616	0.08398	0.08992	0.09644	0.10108	0.10454	0.10866	
1.0	0.07655	0.07980	0.08288	0.08856	0.09812	0.10566	0.11424	0.12055	0.12535	0.13119	
1.2	0.08614	0.08974	0.09319	0.09963	0.11073	0.11978	0.13036	0.13836	0.14456	0.15225	
1.6	0.10280	0.10697	0.11102	0.11870	0.13244	0.14415	0.15849	0.16981	0.17888	0.19046	
2.0	0.11693	0.12156	0.12607	0.13473	0.15061	0.16457	0.18228	0.19673	0.20861	0.22420	
3.0	0.14503	0.15043	0.15576	0.16615	0.18587	0.20407	0.22849	0.24965	0.26795	0.29320	
4.0	0.16652	0.17242	0.17827	0.18978	0.21200	0.23306	0.26227	0.29860	0.31216	0.34595	
5.0	0.18386	0.19011	0.19631	0.20859	0.23255	0.25560	0.28930	0.31854	0.34630	0.38728	
6.0	0.19836	0.20486	0.21133	0.22417	0.24937	0.27388	0.30913	0.34236	0.37342	0.42036	
8.0	0.22168	0.22852	0.23534	0.24892	0.27579	0.30221	0.34088	0.37813	0.41392	0.46972	
10.0	0.24000	0.24706	0.25411	0.26816	0.29506	0.32366	0.36442	0.40425	0.44298	0.50470	
12.0	0.25506	0.26227	0.26947	0.28394	0.31243	0.34082	0.39296	0.42444	0.46514	0.53088	
16.0	0.27888	0.28628	0.29368	0.30845	0.33791	0.36726	0.41104	0.45447	0.49743	0.56802	
20.0	0.29736	0.30488	0.31239	0.32740	0.35738	0.38728	0.43199	0.47649	0.52074	0.59383	
24.0	0.31244	0.32003	0.32762	0.34279	0.37310	0.40336	0.44865	0.49381	0.53881	0.61340	
32.0	0.33615	0.34384	0.35152	0.36689	0.39761	0.42830	0.47428	0.52020	0.56604	0.64225	
40.0	0.35448	0.36222	0.36996	0.38545	0.41640	0.44734	0.49371	0.54005	0.58634	0.66339	

ALPHA = 1.25

TAU	h	0.	0.05	0.10	0.20	0.40	0.60	0.90	1.20	1.50	2.00
0.2	0.02644	0.02780	0.02935	0.03076	0.03309	0.03448	0.03576	0.03654	0.03707	0.03765	
0.3	0.03634	0.03820	0.03994	0.04257	0.04639	0.04887	0.05127	0.05280	0.05387	0.05506	
0.4	0.04509	0.04737	0.04943	0.05298	0.05826	0.06188	0.06553	0.06796	0.06967	0.07164	
0.5	0.05297	0.05560	0.05804	0.06233	0.06898	0.07375	0.07873	0.08213	0.08459	0.08744	
0.6	0.06015	0.06310	0.06586	0.07082	0.07875	0.08465	0.09099	0.09543	0.09869	0.10253	
0.8	0.07290	0.07638	0.07969	0.08579	0.09601	0.10404	0.11310	0.11971	0.12471	0.13076	
1.0	0.08399	0.08790	0.09166	0.09869	0.11089	0.12086	0.13254	0.14135	0.14819	0.15664	
1.2	0.09382	0.09809	0.10222	0.11004	0.12394	0.13564	0.14978	0.16077	0.16947	0.18044	
1.6	0.11069	0.11551	0.12022	0.12929	0.14593	0.16058	0.17911	0.19419	0.20655	0.22268	
2.0	0.12482	0.13006	0.13521	0.14522	0.16396	0.18095	0.20318	0.22192	0.23772	0.25895	
3.0	0.15256	0.15849	0.16436	0.17592	0.19820	0.21925	0.24830	0.27427	0.29733	0.33007	
4.0	0.17353	0.17988	0.18620	0.19970	0.22312	0.24668	0.28015	0.31116	0.33964	0.38169	
5.0	0.19037	0.19700	0.20361	0.21674	0.24257	0.26778	0.30422	0.33876	0.37121	0.42052	
6.0	0.20442	0.21125	0.21807	0.23163	0.25846	0.28482	0.32333	0.36038	0.39575	0.45065	
8.0	0.22696	0.23406	0.24116	0.25530	0.28340	0.31122	0.35235	0.39259	0.43178	0.49431	
10.0	0.24469	0.25195	0.25922	0.27371	0.30259	0.33129	0.37396	0.41606	0.45747	0.52464	
12.0	0.25927	0.26665	0.27403	0.28877	0.31816	0.34744	0.39109	0.43436	0.47717	0.54726	
16.0	0.28239	0.28991	0.29744	0.31248	0.34252	0.37249	0.41731	0.46193	0.50633	0.57969	
20.0	0.30037	0.30798	0.31560	0.33082	0.36124	0.39162	0.43710	0.48246	0.52769	0.60273	
24.0	0.31508	0.32275	0.33043	0.34577	0.37643	0.40707	0.45297	0.49880	0.54454	0.62056	
32.0	0.33829	0.34604	0.35378	0.36927	0.40025	0.43120	0.47761	0.52397	0.57030	0.64740	
40.0	0.35629	0.36407	0.37186	0.38744	0.41859	0.44973	0.49643	0.54310	0.58974	0.66743	

ALPHA = 1.50

TAU	h	0.	0.05	0.10	0.20	0.40	0.60	0.90	1.20	1.50	2.00
0.2		0.02964	0.03136	0.03285	0.03522	0.03834	0.04026	0.04203	0.04312	0.04387	0.04469
0.3		0.04029	0.04258	0.04464	0.04812	0.05314	0.05648	0.05975	0.06187	0.06336	0.06504
0.4		0.04956	0.05232	0.05465	0.05930	0.06609	0.07088	0.07580	0.07911	0.08149	0.08422
0.5		0.05781	0.06096	0.06390	0.06918	0.07759	0.08381	0.09043	0.09504	0.09840	0.10234
0.6		0.06528	0.06876	0.07205	0.07805	0.08794	0.09551	0.10385	0.10973	0.11422	0.11949
0.8		0.07839	0.08241	0.08627	0.09348	0.10591	0.11597	0.12762	0.13630	0.14297	0.15115
1.0		0.08967	0.09412	0.09843	0.10660	0.12113	0.13335	0.14807	0.15946	0.16843	0.17971
1.2		0.09960	0.10438	0.10906	0.11801	0.13428	0.14837	0.16589	0.17985	0.19111	0.20557
1.6		0.11647	0.12178	0.12700	0.13714	0.15611	0.17323	0.19551	0.21413	0.22972	0.25049
2.0		0.13050	0.13619	0.14181	0.15281	0.17375	0.19316	0.21924	0.24182	0.26129	0.28804
3.0		0.15781	0.16410	0.17036	0.18272	0.20682	0.22994	0.26252	0.29278	0.31949	0.35892
4.0		0.17834	0.18499	0.19162	0.20478	0.23068	0.25505	0.29242	0.32691	0.35923	0.40310
5.0		0.19478	0.20167	0.20854	0.22221	0.24927	0.27589	0.31483	0.35235	0.38821	0.44392
6.0		0.20848	0.21553	0.22257	0.23660	0.26446	0.29200	0.33260	0.37216	0.41048	0.47114
8.0		0.23048	0.23774	0.24501	0.25950	0.28837	0.31706	0.35969	0.40174	0.44307	0.51001
10.0		0.24779	0.25518	0.26258	0.27736	0.30684	0.33621	0.38001	0.42345	0.46646	0.53693
12.0		0.26204	0.26953	0.27702	0.29199	0.32188	0.35169	0.39624	0.44055	0.48458	0.55718
16.0		0.28469	0.29230	0.29990	0.31512	0.34551	0.37586	0.42129	0.46661	0.51179	0.58671
20.0		0.30235	0.31002	0.31770	0.33306	0.36375	0.39442	0.44036	0.48623	0.53202	0.60813
24.0		0.31682	0.32454	0.33227	0.34772	0.37861	0.40948	0.45575	0.50197	0.54814	0.62496
32.0		0.33970	0.34748	0.35527	0.37084	0.40197	0.43309	0.47975	0.52639	0.57300	0.65063
40.0		0.35747	0.36529	0.37311	0.38875	0.42003	0.45130	0.49819	0.54507	0.59193	0.66999

ALPHA = 1.75

TAU	h	0.	0.05	0.10	0.20	0.40	0.60	0.90	1.20	1.50	2.00
0.2		0.03243	0.03450	0.03631	0.03926	0.04323	0.04571	0.04803	0.04949	0.05048	0.05158
0.3		0.04364	0.04634	0.04879	0.05302	0.05925	0.06350	0.06773	0.07051	0.07247	0.07469
0.4		0.05329	0.05648	0.05945	0.06474	0.07303	0.07902	0.08520	0.08958	0.09268	0.09628
0.5		0.06180	0.06539	0.06879	0.07497	0.08508	0.09275	0.10109	0.10698	0.11133	0.11648
0.6		0.06944	0.07337	0.07713	0.08407	0.09579	0.10501	0.11538	0.12292	0.12859	0.13543
0.8		0.08275	0.08722	0.09155	0.09972	0.11413	0.12610	0.14029	0.15110	0.15952	0.16998
1.0		0.09412	0.09900	0.10376	0.11288	0.12942	0.14369	0.16130	0.17524	0.18640	0.20064
1.2		0.10406	0.10926	0.11437	0.12423	0.14249	0.15869	0.17931	0.19614	0.20995	0.22799
1.6		0.12086	0.12655	0.13216	0.14313	0.16395	0.18313	0.20867	0.23053	0.24919	0.27453
2.0		0.13476	0.14078	0.14675	0.15850	0.18113	0.20246	0.23173	0.25767	0.28048	0.31247
3.0		0.16167	0.16822	0.17475	0.18769	0.21309	0.23773	0.27300	0.30595	0.33640	0.38165
4.0		0.18183	0.18869	0.19553	0.20915	0.23609	0.26255	0.30117	0.33823	0.37348	0.42785
5.0		0.19796	0.20501	0.21206	0.22612	0.25402	0.28160	0.32225	0.36185	0.40018	0.46073
6.0		0.21140	0.21859	0.22578	0.24013	0.26869	0.29702	0.33902	0.38027	0.42062	0.48541
8.0		0.23298	0.24036	0.24773	0.26247	0.29185	0.32111	0.36472	0.40794	0.45067	0.52052
10.0		0.24998	0.25747	0.26496	0.27993	0.30982	0.33962	0.38416	0.42846	0.47247	0.54502
12.0		0.26401	0.27157	0.27914	0.29426	0.32448	0.35464	0.39977	0.44475	0.48954	0.56369
16.0		0.28632	0.29398	0.30164	0.31697	0.34760	0.37820	0.42404	0.46980	0.51547	0.59135
20.0		0.30375	0.31147	0.31919	0.33463	0.36551	0.39637	0.44262	0.48882	0.53497	0.61175
24.0		0.31805	0.32581	0.33357	0.34909	0.38013	0.41116	0.45768	0.50416	0.55061	0.62794
32.0		0.34070	0.34850	0.35631	0.37194	0.40318	0.43441	0.48125	0.52807	0.57488	0.65284
40.0		0.35832	0.36615	0.37399	0.38968	0.42104	0.45240	0.49942	0.54644	0.59345	0.67177

ALPHA = 2.00

TAU	h	0.	0.05	0.10	0.20	0.40	0.60	0.90	1.20	1.50	2.00
0.2		0.03488	0.03727	0.03940	0.04292	0.04777	0.05086	0.05379	0.05563	0.05690	0.05832
0.3		0.04652	0.04958	0.05241	0.05734	0.06480	0.06999	0.07524	0.07873	0.08121	0.08404
0.4		0.05643	0.06001	0.06338	0.06945	0.07919	0.08640	0.09408	0.09941	0.10329	0.10784
0.5		0.06512	0.06910	0.07290	0.07991	0.09161	0.10070	0.11030	0.11804	0.12345	0.12991
0.6		0.07287	0.07719	0.08135	0.08913	0.10253	0.11333	0.12574	0.13492	0.14191	0.15043
0.8		0.08629	0.09113	0.09595	0.10485	0.12100	0.13473	0.15137	0.16431	0.17452	0.18737
1.0		0.09769	0.10292	0.10805	0.11795	0.13621	0.15231	0.17261	0.18902	0.20237	0.21965
1.2		0.10761	0.11314	0.11859	0.12920	0.14911	0.16712	0.19055	0.21009	0.22639	0.24801
1.6		0.12430	0.13027	0.13619	0.14781	0.17012	0.19099	0.21932	0.24410	0.26561	0.29535
2.0		0.13805	0.14433	0.15057	0.16289	0.18683	0.20968	0.24158	0.27040	0.29619	0.33304
3.0		0.16461	0.17135	0.17808	0.19145	0.21783	0.24360	0.28091	0.31628	0.34946	0.39969
4.0		0.18447	0.19148	0.19848	0.21244	0.24012	0.26745	0.30762	0.34658	0.38408	0.44283
5.0		0.20035	0.20753	0.21471	0.22904	0.25754	0.28580	0.32767	0.36875	0.40886	0.47306
6.0		0.21358	0.22088	0.22818	0.24276	0.27182	0.30071	0.34368	0.38611	0.42798	0.49563
8.0		0.23485	0.24231	0.24977	0.26467	0.29442	0.32408	0.36838	0.41239	0.45606	0.52788
10.0		0.25162	0.25917	0.26673	0.28184	0.31201	0.34212	0.38717	0.43205	0.47674	0.55066
12.0		0.26547	0.27309	0.28071	0.29595	0.32640	0.35681	0.40235	0.44778	0.49308	0.56824
16.0		0.28753	0.29523	0.30294	0.31835	0.34915	0.37993	0.42605	0.47212	0.51813	0.59464
20.0		0.30479	0.31254	0.32029	0.33580	0.36661	0.39781	0.44428	0.49071	0.53711	0.61434
24.0		0.31897	0.32675	0.33454	0.35011	0.38126	0.41240	0.45909	0.50576	0.55241	0.63009
32.0		0.34144	0.34926	0.35709	0.37276	0.40408	0.43540	0.48236	0.52931	0.57625	0.65446
40.0		0.35895	0.36679	0.37465	0.39036	0.42179	0.45321	0.50034	0.54746	0.59457	0.67307

ALPHA = 2.25

TAU	h	0.	0.05	0.10	0.20	0.40	0.60	0.90	1.20	1.50	2.00
0.2		0.03703	0.03974	0.04217	0.04625	0.05200	0.05573	0.05930	0.06157	0.06315	0.06490
0.3		0.04901	0.05241	0.05557	0.06118	0.06984	0.07599	0.08230	0.08656	0.08959	0.09309
0.4		0.05912	0.06303	0.06675	0.07355	0.08467	0.09309	0.10222	0.10863	0.11335	0.11892
0.5		0.06792	0.07224	0.07640	0.08414	0.09733	0.10780	0.11965	0.12829	0.13480	0.14265
0.6		0.07574	0.08039	0.08490	0.09341	0.10835	0.12065	0.13505	0.14589	0.15425	0.16433
0.8		0.08922	0.09437	0.09941	0.10910	0.12679	0.14213	0.16110	0.17611	0.18813	0.20344
1.0		0.10060	0.10612	0.11155	0.12211	0.14184	0.15954	0.18232	0.20109	0.21658	0.23691
1.2		0.11048	0.11628	0.12201	0.13322	0.15451	0.17408	0.20002	0.22207	0.24075	0.26591
1.6		0.12705	0.13325	0.13941	0.15156	0.17505	0.19731	0.22803	0.25538	0.27950	0.31341
2.0		0.14067	0.14715	0.15360	0.16637	0.19134	0.21540	0.24944	0.28072	0.30913	0.35041
3.0		0.16692	0.17381	0.18069	0.19440	0.22150	0.24814	0.28702	0.32429	0.35969	0.41411
4.0		0.18652	0.19365	0.20078	0.21499	0.24324	0.27121	0.31254	0.35292	0.39213	0.45435
5.0		0.20220	0.20948	0.21676	0.23129	0.26024	0.28901	0.33177	0.37393	0.41535	0.48229
6.0		0.21527	0.22265	0.23004	0.24479	0.27422	0.30352	0.34720	0.39043	0.43327	0.50317
8.0		0.23630	0.24381	0.25134	0.26637	0.29640	0.32635	0.37114	0.41572	0.46005	0.53324
10.0		0.25289	0.26049	0.26810	0.28331	0.31369	0.34403	0.38946	0.43476	0.47991	0.55479
12.0		0.26661	0.27426	0.28192	0.29725	0.32787	0.35847	0.40431	0.45006	0.49573	0.57159
16.0		0.28847	0.29620	0.30393	0.31941	0.35034	0.38125	0.42759	0.47388	0.52013	0.59709
20.0		0.30560	0.31337	0.32115	0.33671	0.36782	0.39892	0.44555	0.49215	0.53873	0.61629
24.0		0.31968	0.32747	0.33528	0.35090	0.38213	0.41336	0.46018	0.50699	0.55378	0.63171
32.0		0.34202	0.34985	0.35770	0.37333	0.40477	0.43615	0.48321	0.53026	0.57731	0.65569
40.0		0.35944	0.36729	0.37516	0.39090	0.42237	0.45384	0.50104	0.54824	0.59543	0.67406

MEASURING HEAT FLOW ON LAND

ALPHA = 2.50

TAU	h	0.	0.05	0.10	0.20	0.40	0.60	0.90	1.20	1.50	2.00
0.2		0.03894	0.04194	0.04466	0.04929	0.05594	0.06033	0.06458	0.06732	0.06921	0.07135
0.3		0.05118	0.05488	0.05836	0.06459	0.07442	0.08154	0.08896	0.09401	0.09764	0.10185
0.4		0.06143	0.06565	0.06969	0.07713	0.08957	0.09917	0.10975	0.11729	0.12289	0.12954
0.5		0.07031	0.07493	0.07939	0.08779	0.10235	0.11415	0.12773	0.13778	0.14544	0.15476
0.6		0.07817	0.08310	0.08791	0.09707	0.11339	0.12709	0.14344	0.15594	0.16569	0.17780
0.8		0.09166	0.09707	0.10239	0.11268	0.13171	0.14850	0.16964	0.18668	0.20049	0.21829
1.0		0.10302	0.10877	0.11446	0.12556	0.14654	0.16565	0.19069	0.21167	0.22924	0.25260
1.2		0.11285	0.11886	0.12483	0.13654	0.15897	0.17987	0.20804	0.23240	0.25333	0.28193
1.6		0.12930	0.13569	0.14204	0.15460	0.17907	0.20247	0.23520	0.26482	0.29131	0.32912
2.0		0.14280	0.14943	0.15605	0.16918	0.19497	0.22000	0.25580	0.28915	0.31984	0.36514
3.0		0.16878	0.17578	0.18279	0.19675	0.22443	0.25174	0.29183	0.33061	0.36780	0.42573
4.0		0.18818	0.19539	0.20261	0.21702	0.24571	0.27417	0.31638	0.35784	0.39837	0.46333
5.0		0.20369	0.21104	0.21840	0.23300	0.26239	0.29154	0.33497	0.37794	0.42034	0.48935
6.0		0.21663	0.22407	0.23152	0.24641	0.27612	0.30573	0.34994	0.39385	0.43739	0.50888
8.0		0.23745	0.24501	0.25259	0.26772	0.29796	0.32814	0.37330	0.41830	0.46312	0.53730
10.0		0.25391	0.26154	0.26918	0.28447	0.31502	0.34554	0.39125	0.43686	0.48237	0.55793
12.0		0.26751	0.27519	0.28289	0.29828	0.32904	0.35978	0.40585	0.45185	0.49778	0.57416
16.0		0.28922	0.29697	0.30473	0.32025	0.35128	0.38230	0.42880	0.47526	0.52170	0.59899
20.0		0.30624	0.31402	0.32182	0.33742	0.36861	0.39980	0.44655	0.49329	0.54000	0.61781
24.0		0.32024	0.32805	0.33588	0.35153	0.38282	0.41412	0.46104	0.50796	0.55485	0.63298
32.0		0.34248	0.35032	0.35818	0.37389	0.40533	0.43675	0.48389	0.53102	0.57814	0.65665
40.0		0.35983	0.36769	0.37557	0.39132	0.42283	0.45434	0.50160	0.54886	0.59611	0.67485

ALPHA = 3.00

TAU	h	0.	0.05	0.10	0.20	0.40	0.60	0.90	1.20	1.50	2.00
0.2		0.04217	0.04568	0.04894	0.05461	0.06304	0.06879	0.07449	0.07823	0.08085	0.08381
0.3		0.05476	0.05899	0.06302	0.07039	0.08241	0.09144	0.10113	0.10786	0.11278	0.11954
0.4		0.06519	0.06992	0.07449	0.08309	0.09788	0.10974	0.12322	0.13307	0.14051	0.14948
0.5		0.07416	0.07926	0.08424	0.09375	0.11071	0.12494	0.14187	0.15476	0.16477	0.17716
0.6		0.08205	0.08744	0.09273	0.10295	0.12163	0.13785	0.15794	0.17359	0.18614	0.20203
0.8		0.09552	0.10133	0.10709	0.11834	0.13954	0.15879	0.18384	0.20465	0.22194	0.24473
1.0		0.10679	0.11291	0.11899	0.13095	0.15389	0.17531	0.20420	0.22919	0.25063	0.27987
1.2		0.11652	0.12286	0.12918	0.14166	0.16586	0.18887	0.22070	0.24907	0.27407	0.30914
1.6		0.13276	0.13941	0.14606	0.15926	0.18516	0.21029	0.24617	0.27947	0.30998	0.35474
2.0		0.14605	0.15291	0.15978	0.17344	0.20042	0.22689	0.26532	0.30198	0.33626	0.38835
3.0		0.17159	0.17876	0.18594	0.20029	0.22879	0.25705	0.29887	0.33981	0.37962	0.44292
4.0		0.19066	0.19800	0.20536	0.22007	0.24936	0.27853	0.32195	0.36491	0.40727	0.47613
5.0		0.20592	0.21337	0.22084	0.23577	0.26556	0.29526	0.33961	0.38368	0.42741	0.49925
6.0		0.21866	0.22618	0.23373	0.24882	0.27893	0.30899	0.35394	0.39871	0.44325	0.51685
8.0		0.23918	0.24680	0.25445	0.26974	0.30027	0.33077	0.37645	0.42204	0.46751	0.54300
10.0		0.25542	0.26310	0.27080	0.28621	0.31700	0.34777	0.39387	0.43992	0.48591	0.56238
12.0		0.26886	0.27658	0.28432	0.29982	0.33077	0.36172	0.40811	0.45446	0.50076	0.57783
16.0		0.29034	0.29811	0.30591	0.32151	0.35268	0.38385	0.43058	0.47729	0.52399	0.60175
20.0		0.30720	0.31501	0.32283	0.33850	0.36980	0.40110	0.44804	0.49496	0.54188	0.62003
24.0		0.32109	0.32891	0.33676	0.35247	0.38385	0.41524	0.46232	0.50938	0.55644	0.63485
32.0		0.34317	0.35102	0.35889	0.37466	0.40615	0.43765	0.48489	0.53213	0.57937	0.65808
40.0		0.36041	0.36828	0.37617	0.39196	0.42352	0.45509	0.50243	0.54978	0.59712	0.67601

TAU	h	0.	0.05	0.10	0.20	0.40	0.60	0.90	1.20	1.50	2.00
0.2		0.04695	0.05127	0.05539	0.06282	0.07462	0.08315	0.09198	0.09796	0.10223	0.10715
0.3		0.05989	0.06488	0.06975	0.07891	0.09471	0.10732	0.12154	0.13186	0.13960	0.14887
0.4		0.07046	0.07589	0.08125	0.09153	0.11011	0.12590	0.14484	0.15935	0.17066	0.19468
0.5		0.07945	0.08520	0.09090	0.10198	0.12257	0.14080	0.16370	0.18202	0.19678	0.21564
0.6		0.08731	0.09330	0.09927	0.11093	0.13302	0.15314	0.17931	0.20101	0.21897	0.24256
0.8		0.10064	0.10698	0.11331	0.12580	0.14395	0.17273	0.20381	0.23099	0.25450	0.28679
1.0		0.11174	0.11832	0.12490	0.13794	0.16343	0.18794	0.22238	0.25361	0.28154	0.32133
1.2		0.12129	0.12804	0.13480	0.14823	0.17466	0.20036	0.23717	0.27140	0.30279	0.34882
1.6		0.13719	0.14417	0.15118	0.16513	0.19278	0.22001	0.25979	0.29796	0.33414	0.38949
2.0		0.15018	0.15731	0.16448	0.17878	0.20719	0.23533	0.27686	0.31734	0.35647	0.41803
3.0		0.17513	0.18249	0.18989	0.20467	0.23414	0.26349	0.30723	0.35054	0.39330	0.46291
4.0		0.19377	0.20125	0.20878	0.22382	0.25385	0.28380	0.32858	0.37314	0.41743	0.49044
5.0		0.20871	0.21627	0.22387	0.23907	0.26944	0.29976	0.34515	0.39041	0.43551	0.51023
6.0		0.22119	0.22880	0.23646	0.25177	0.28237	0.31294	0.35873	0.40443	0.45002	0.52575
8.0		0.24134	0.24902	0.25675	0.27220	0.30310	0.33398	0.38026	0.42649	0.47267	0.54950
10.0		0.25730	0.26503	0.27280	0.28835	0.31942	0.35048	0.39706	0.44360	0.49011	0.56755
12.0		0.27054	0.27830	0.28610	0.30170	0.33290	0.36409	0.41086	0.45760	0.50433	0.58216
16.0		0.29174	0.29953	0.30737	0.32305	0.35440	0.38575	0.43276	0.47976	0.52675	0.60504
20.0		0.30841	0.31622	0.32409	0.33981	0.37126	0.40270	0.44985	0.49701	0.54415	0.62270
24.0		0.32215	0.32998	0.33786	0.35362	0.38512	0.41663	0.46389	0.51114	0.55838	0.63711
32.0		0.34403	0.35189	0.35978	0.37558	0.40716	0.43875	0.48613	0.53350	0.58087	0.65982
40.0		0.36115	0.36901	0.37692	0.39274	0.42438	0.45601	0.50346	0.55091	0.59836	0.67743

ALPHA = 5.00

TAU	h	0.	0.05	0.10	0.20	0.40	0.60	0.90	1.20	1.50	2.00
0.2		0.05029	0.05519	0.05996	0.06880	0.08352	0.09472	0.10679	0.11520	0.12134	0.12852
0.3		0.06336	0.06887	0.07431	0.08476	0.10351	0.11921	0.13773	0.15168	0.16240	0.17554
0.4		0.07393	0.07983	0.08570	0.09712	0.11844	0.13733	0.16105	0.17996	0.19514	0.21448
0.5		0.08289	0.08905	0.09521	0.10731	0.13037	0.15153	0.17928	0.20244	0.22168	0.24704
0.6		0.09069	0.09705	0.10343	0.11602	0.14032	0.16314	0.19402	0.22070	0.24353	0.27450
0.8		0.10388	0.11053	0.11721	0.13045	0.15640	0.18141	0.21663	0.24860	0.27719	0.31787
1.0		0.11484	0.12168	0.12856	0.14224	0.16922	0.19558	0.23353	0.26907	0.30185	0.35022
1.2		0.12425	0.13123	0.13825	0.15224	0.17994	0.20719	0.24695	0.28493	0.32074	0.37507
1.6		0.13991	0.14707	0.15428	0.16868	0.19731	0.22569	0.26762	0.30856	0.34819	0.41060
2.0		0.15270	0.15998	0.16732	0.18198	0.21119	0.24023	0.28341	0.32598	0.36775	0.43497
3.0		0.17727	0.18472	0.19224	0.20728	0.23729	0.26723	0.31197	0.35648	0.40069	0.47348
4.0		0.19565	0.20320	0.21082	0.22605	0.25648	0.28687	0.33237	0.37774	0.42297	0.49794
5.0		0.21038	0.21800	0.22568	0.24103	0.27173	0.30239	0.34834	0.39420	0.43999	0.51606
6.0		0.22271	0.23036	0.23809	0.25353	0.28440	0.31525	0.36149	0.40768	0.45381	0.53055
8.0		0.24263	0.25034	0.25812	0.27367	0.30477	0.33586	0.38247	0.42905	0.47560	0.55311
10.0		0.25844	0.26618	0.27399	0.28961	0.32085	0.35208	0.39892	0.44573	0.49253	0.57048
12.0		0.27156	0.27932	0.28716	0.30283	0.33416	0.36549	0.41247	0.45944	0.50639	0.58463
16.0		0.29259	0.30038	0.30824	0.32397	0.35542	0.38687	0.43404	0.48121	0.52836	0.60694
20.0		0.30914	0.31695	0.32483	0.34060	0.37212	0.40365	0.45093	0.49821	0.54548	0.62426
24.0		0.32280	0.33062	0.33852	0.35430	0.38588	0.41745	0.46481	0.51217	0.55952	0.63843
32.0		0.34456	0.35240	0.36031	0.37613	0.40777	0.43941	0.48686	0.53431	0.58177	0.66085
40.0		0.36160	0.36945	0.37737	0.39321	0.42488	0.45656	0.50407	0.55158	0.59909	0.67827

## Chapter 4. Techniques of Measuring Heat Flow through the Ocean Floor <sup>1</sup>

MARCUS G. LANGSETH

*Lamont Geological Observatory  
Columbia University, Palisades, New York*

*Abstract.* Heat flow through the ocean floor is determined by measuring the temperature gradient and thermal conductivity in the ocean sediment. Techniques for these measurements are reviewed here, and some comments are made on procedure. Thermal conditions of the ocean bottom are also briefly examined.

### 1. INTRODUCTION

The measurement of heat flow through the surface of the Earth is fundamental to the study of the thermal state that exists at depth in the crust and the upper mantle. The heat flux at the surface can be determined by measuring the temperature gradient and multiplying by the conductivity of the material between the two points of measurement. The extent to which the heat flux determination reflects the temperature distribution at depth depends on: (1) whether the two temperature measurement points are free of transient thermal disturbances; (2) whether the interval of temperature measurement is free from the flow of mass such as circulating groundwater, which would greatly disturb the conductive heat transfer; and (3) whether the conductivities of the rocks at the site are homogeneous enough to allow meaningful extrapolations of the observed heat flux. For a fuller discussion of these problems, see chapters 2 and 3 by Jaeger and Beck, respectively. Most of the above difficulties can be avoided when heat flow determinations are made on the deep ocean floor. The nearly constant temperature of deep ocean bottom water over a long period of time means that the ocean floor sediment should be in a steady-state thermal condition with the deeper material of the crust.

In 1949, Bullard, Revelle, and Maxwell at the Scripps Institution of Oceanography developed the first successful instrument for measuring temperature gradients in the sediment and hence the heat flux through the ocean bottom. Since then, other institutions have developed heat flow apparatus, notable among them the Lamont

Geological Observatory of Columbia University, Cambridge University, the Earthquake Research Institute of Tokyo University, and the Woods Hole Oceanographic Institution. All the ocean bottom instruments, except for a special probe designed for use with Mohole ocean bottom drilling experiments, can be used from a moderate-sized oceanographic vessel and are designed to measure the vertical temperature gradient in the upper several meters of sediment. A sample of the bottom sediment is collected at or near the site of the measurement to determine thermal conductivity. One of the principal gains of ocean bottom measurements is that closely spaced heat flow measurements can be made over submarine features. This is a great advantage over land heat flow measurements, which are limited to deep excavations such as drill holes, tunnels, and mines. These excavations are seldom located for investigation of a geophysical problem (see chapter 3 by Beck, section 1, in this volume).

### 2. TECHNIQUES OF TEMPERATURE GRADIENT MEASUREMENT IN THE SEDIMENT

Two techniques for measuring the temperature gradient in the sediment in the ocean bottom are now in common use. They both use two or more temperature elements which are spaced vertically some known distance apart in or on a probe which can penetrate the sediment. These elements are driven into the ocean bottom, and the temperature difference between the elements is recorded while the heat of penetration dissipates into the sediment. The basic difference between the two techniques is that one places the thermal elements inside a long, slender, hollow probe 2 to 4 cm in diameter, whereas the other uses very small temperature sensing probes that

<sup>1</sup> Contribution 806 from the Lamont Geological Observatory of Columbia University.

are set out from a penetrating vehicle, usually a coring device. When the first method is used, an auxiliary sediment core must be taken close by for conductivity measurements. A sediment sample is automatically obtained when a corer is used as a penetrating vehicle. Because of a number of advantages, the outriggered instrument is gradually replacing the cylindrical probe. The details of each technique will be described separately.

### 2.1 The Bullard Thermal Gradient Probe

The Bullard instrument consists of a thin, hollow probe containing two thermal elements spaced a known distance apart. In early models of this instrument, probes about 5 meters in length and 2.7 cm in external diameter were used. The thermal elements were spaced 4.5 meters apart, one near the bottom tip and the other near the upper end of the probe. Later model probes are shorter and thinner; for example, a model currently being used by the Scripps Institution of Oceanography (illustrated in Figure 1) is two meters long and 1.9 cm in diameter. The whole probe is made pressure tight at 1 atmosphere; therefore the walls of the probe must be thick enough to withstand expected sea bottom hydrostatic pressures, i.e., up to 1400 atm. These probes are usually made from a malleable alloy of steel, for they almost always bend during recovery from the sediment, and it is necessary that the probe not fracture when straightened.

In operation, the probe is lowered to the bottom on a wire and is allowed to remain for a short time in the nearly isothermal bottom water. It is then driven into the sediment by the momentum of the lowering and the instrument's weight. The temperature difference between the thermal elements inside the probe is recorded as a function of time for a brief period before penetration, while the probe is in the sediment, and after it is withdrawn. After penetration, the lower end of the probe attains a higher temperature than the upper end, owing to the normal thermal gradient in the sediment and frictional heating of the probe tip during penetration. The temperature difference between the extremes of the probe caused by the heat of penetration is of the same order of magnitude as that to be observed for a normal flux measurement (i.e., 0.15 to 0.3°C); therefore, the frictional heat

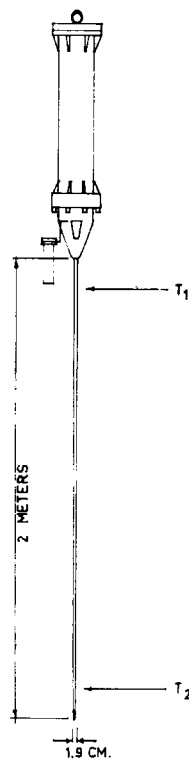


Fig. 1. Cylindrical temperature gradient probe and recorder pressure case. The thermal sensing elements are thermistors fixed at positions  $T_1$  and  $T_2$  [from Von Herzen and Uyeda, 1963, Figure 2].

must be carefully eliminated. The probe is left in the sediment for a period of time ranging from 14 to 40 minutes to allow 80% to 90% of the frictional heat to dissipate into the sediment. (Smaller diameter probes require shorter observation times.) Typical records for high, normal, and low gradients made by this type of probe are shown in Figure 4B. For the normal and low gradients the gradual dissipation of the heat of penetration can be seen.

*Cooling of the probe in the sediment.* Temperature difference between elements in the probe at equilibrium in the sediment is determined on the basis of the cooling of a solid cylinder in a homogeneous infinite medium given by Carslaw and Jaeger [1959] (see chapter 2, section 12, by Jaeger, in this volume). Bullard [1954] has fitted their solution to the initial conditions of a heat pulse applied to a cylinder in a system which is at zero degrees everywhere at times before the pulse is applied. He derives

an expression for the temperature difference  $\Delta T$  at any time in the probe. This expression is written in an abbreviated way as:

$$\Delta T = \Delta T_f + \Delta T_0 F(\alpha, \tau) \quad (1)$$

where  $\Delta T_f$  is the final temperature difference,  $\Delta T_0$  is the initial excess of temperature resulting from the heat of penetration, and  $F(\alpha, \tau)$  is the function which defines the decay of the initial excess of temperature in the probe with time. The analytical form of this expression is:

$$F(\alpha, \tau) = \int_0^\infty e^{-\tau x^2} f(x) dx$$

$$f(x) = 4\alpha/\pi^2 x [\{xY_0(x) - \alpha Y_1(x)\}^2 + \{xJ_0(x) - \alpha J_1(x)\}^2]$$

For times greater than a few minutes, the function  $F(\alpha, \tau)$  closely resembles the two lower curves shown in Figure 4B.  $\tau$  is the characteristic time of the probe,  $\kappa t/a^2$ ; where  $\kappa$  is the diffusivity of the sediment in square centimeters per second,  $t$  is the time in seconds, and  $a$  is the radius of the probe in centimeters.  $\alpha$  is a parameter equal to  $2\pi a^2 \rho c/m$ , where  $\rho$  is the sediment density,  $c$  is the specific heat of the sediment, and  $m$  is the water equivalent mass per unit length of probe (that is, the mass of water that would require the same amount of heat to raise it 1°C as a 1-cm length of probe does).

The shape of the function  $F(\alpha, \tau)$  is not very dependent on  $\alpha$ , so that fitting the observed data to the theoretical expression does not require exact knowledge of the thermal constants of the sediment. For procedures of fitting the observed temperature versus time record of the probe to the function  $F(\alpha, \tau)$ , see Bullard [1954].

The temperature versus time recorder is carried in a pressure vessel at the top of the probe. The weight of the recorder and its case also serves to drive the probe into the sediment. The recording techniques used for all temperature gradient measuring devices are similar, and a detailed description of all the presently used systems will be given in section 2.5.

*Modifications of the Bullard probe.* Several modifications of the Bullard probe have been used. To test whether the heat flow is constant with depth, three temperature measuring elements have been placed inside the probe so that the temperature gradient over two different intervals can be measured. The third element is placed midway down the length of the probe,

so that the temperature difference between the upper and the lower element and the middle and the lower element can be alternately recorded. The two temperature gradients are then compared. Results of tests with this type of instrument are discussed by Bullard and Day [1961].

If the probe does not completely penetrate the sediment, or if it is not vertical, errors in thermal gradient measurements will result. To test full penetration, a small coring tube is attached to the bottom of the recorder pressure vessel near the top of the probe (see Figure 1). This tube will collect a sediment sample if complete penetration is achieved. Two methods have been devised for determining whether the probe is vertical in the sediment. A recording inclinometer has been used, but the most commonly employed method at present is to use a photo flash-bulb coated with wax which is flashed when the probe is in the sediment. The wax melts and drops from the bulb to a plate below. By comparing the position of the drop of wax on the plate with the position of the bulb, the angle of the probe after penetration can be determined to within a few degrees.

Another modification of the Bullard probe has been developed in Japan by Uyeda *et al.* [1961]. A sediment sample is taken simultaneously with the thermal gradient measurement by a coring device which is rigidly attached alongside and parallel to the temperature gradient probe.

## 2.2 The Ewing Technique

In this technique of temperature gradient measurement, the thermal elements are in fine needle probes which are mounted on outriggers on the penetrating vehicle. Piston or gravity coring devices are used to carry the probes into the sediment and thereby obtain a sample of bottom sediment for conductivity measurement. The piston corer can achieve penetrations up to 20 meters, allowing wider separation of the thermal sensing elements, resulting in more accurate gradient measurements and removal of the probes from possible near surface disturbances. Any number of the small probes can be put on the coring tube; three or four are commonly used.

The probes which house the thermal elements are hollow stainless steel tubes about 0.3 cm in outside diameter with a wall thickness great

enough to withstand up to 1000 atm. The probes are mounted in support fins which hold the probe from 7 to 10 cm out from the core pipe wall. The tips of the probes project from 2.5 to 4 cm ahead of the fins. These probes come to thermal equilibrium with the sediment very rapidly: because of their small mass, only about one-half minute is required for the probes to come within a few per cent of their final value. Hence the temperature gradient can be directly measured in two to four minutes, before the thermal disturbances in the sediment caused by coring reach the probes. Because of the short observation time, problems of leaving an instrument in the bottom for a long interval of time are avoided. In some versions of the instrument the temperature at each probe is recorded versus time, whereas in others the temperature difference between thermal elements is recorded. The recorder is carried in a pressure-proof vessel at the top of the corer. The probes are connected to the recorder by wires which lead up the outside of the pipe to the pressure vessel. Electrical connections to the inside of the pressure vessel are made by pressure-proof bulkhead fittings. A typical arrangement of the probes on a coring device is shown in Figure 2.

*Discussion of possible thermal disturbances caused by core penetration.* Observations on core samples taken by the piston corer show that the sediment is usually disturbed up to about 1 cm away from the wall of the core pipe. Therefore, initially the thermal disturbance caused by the penetration should be confined to a zone not more than 1 cm from the core wall. It would require almost an hour for the heat of penetration to be carried out through the sediment to a probe 8 cm away from the wall of the pipe. However, the support fin is also heated on penetration, and the heat which flows from the fin to the probe must be considered. *Lister* [1963] has used the results of *Carshaw and Jaeger* [1959] to study conduction along a slender probe; also, several experiments have been conducted in which a fin is artificially heated and the effect on probe temperature is measured while the whole assembly is submerged in sediment. The principal conclusion is that a probe about 0.3 cm in diameter will feel an insignificant amount of heat if it protrudes 4 cm or more from the fin. Experiments made with 0.3 cm of insula-

tion between the fin and the probe show that it need not protrude more than 2.5 cm.

On occasion, when the fins are excessively heated by penetration into very resistant sediments such as turbidites or compact clays, a measurable amount of heat is conducted out to the probe tip. This is readily detected, since the probe will follow the much slower cooling rate of the fin rather than the normal quick response of the probe.

Because of the fast response of the probes, an almost complete record of thermal events during the penetration and observation period is obtained; even slight movements of the apparatus in the sediment can be observed. In fact, an in situ test of the instrument's ability to measure the sediment gradient can be made by pulling the core device up a short distance, so that the probes are allowed to come to equilibrium at a new position in the sediment. The temperature difference at both positions should be the same, provided that the conductivity does not vary with depth.

### 2.3 *The Technique with Reversing Thermometers*

Russian scientists have briefly reported on a method of measuring the temperature gradient in the bottom sediment with reversing thermometers [*Sisoev*, 1961]. Standard protected reversing thermometers are attached by outriggers to a penetrating probe. The thermometers are held upright by latching arms until they enter the sediment. The latching arms are thrown upward by the penetration so that on recovery of the device the thermometers reverse. The thermometers are said to require five minutes to come to equilibrium with the sediment. However, the thermometers are not well protected from the thermal disturbances of penetration and retrieval of the probe. Judging from experience with other probes, the heat of penetration would not be dissipated in the surrounding sediment in five minutes. The reversing thermometers have also proven to be rather fragile for this type of use.

### 2.4 *Temperature Measuring Elements*

The Bullard and Ewing instruments use similar thermal elements and recording tech-

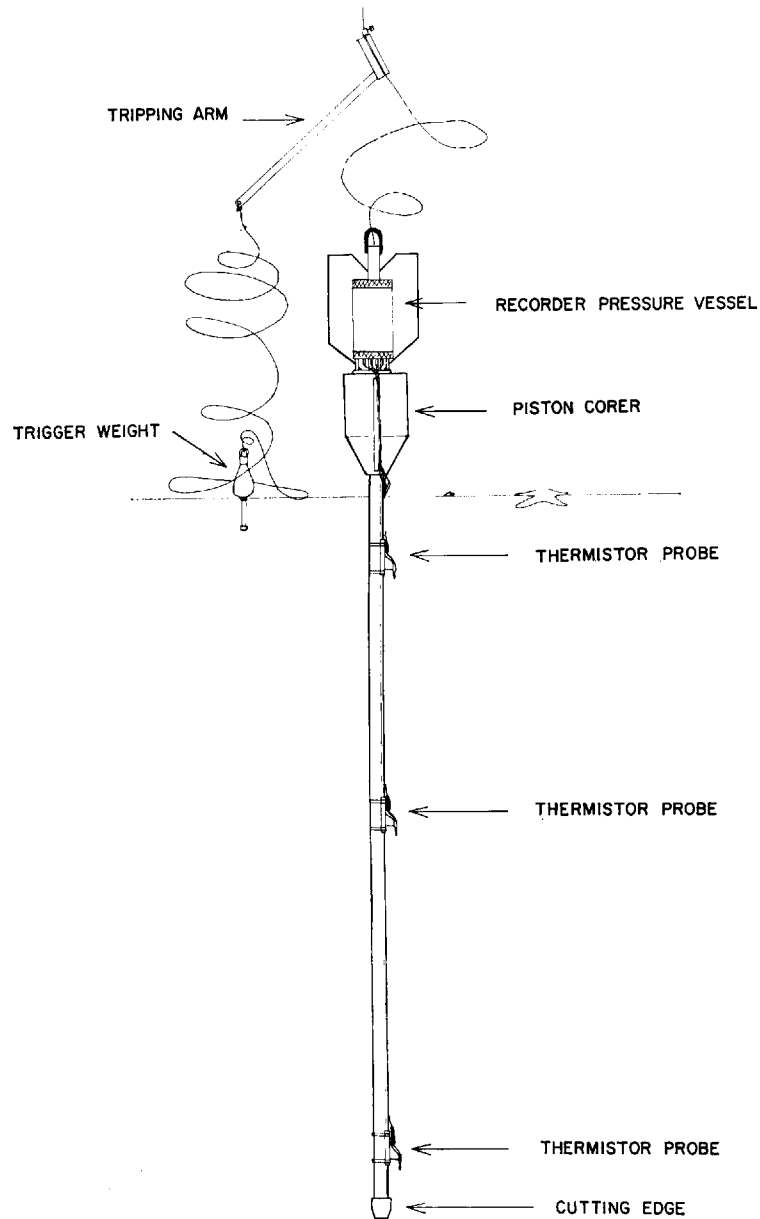


Fig. 2. Outrigged temperature gradient probe attached to a Ewing piston corer.

niques. Therefore, the details of the systems will be described together.

The first thermal gradient probes used thermocouples; however, the most commonly used temperature sensing element at present is the thermistor, a small and rugged resistive element which has a high negative temperature coefficient of resistance  $[(1/R)(\partial R/\partial T) = 4\%]$ . The

resistance of the most commonly used types at  $0^{\circ}\text{C}$  is 2000 to 6000 ohms.

These resistive properties eliminate many of the conductor and connector problems common to thermocouples or less sensitive temperature elements.

The thermistors can be used to measure the temperature of the sediment directly, or a pair

can be used to measure temperature difference. In both cases, the individual thermistors must be calibrated carefully, for the characteristics of each element are different. Thermistors are also known to change characteristics or to 'drift' with time. However, this drift is usually small and is most commonly a displacement of the temperature versus resistance curve rather than a change in slope. Therefore, temperature differences determined from a single thermistor will be little affected by the drift.

Thermistors are heated by the current put through them during the measurement of resistance. This heating will cause the thermistor to have a higher temperature than the medium it is measuring. This effect can be minimized by using very small currents and by initially calibrating the thermistor with the current to be used in the measuring circuit of the instrument. Some resistance detecting circuits that measure temperature difference have been designed to effectively cancel 'self-heating' of the thermistors [for example, see *Von Herzen et al.*, 1962].

The 'sensistor' silicon resistance elements made by Texas Instruments and used by *Lister* [1963] have some desirable features which may make them preferable to thermistors. They have little or no drift, and a small spread of characteristics between elements. However, they have a much smaller and positive temperature coefficient of resistance [ $(1/R)(\partial R/\partial T) = 0.7\%$ ], so that a more sensitive detecting circuit is required than for thermistors.

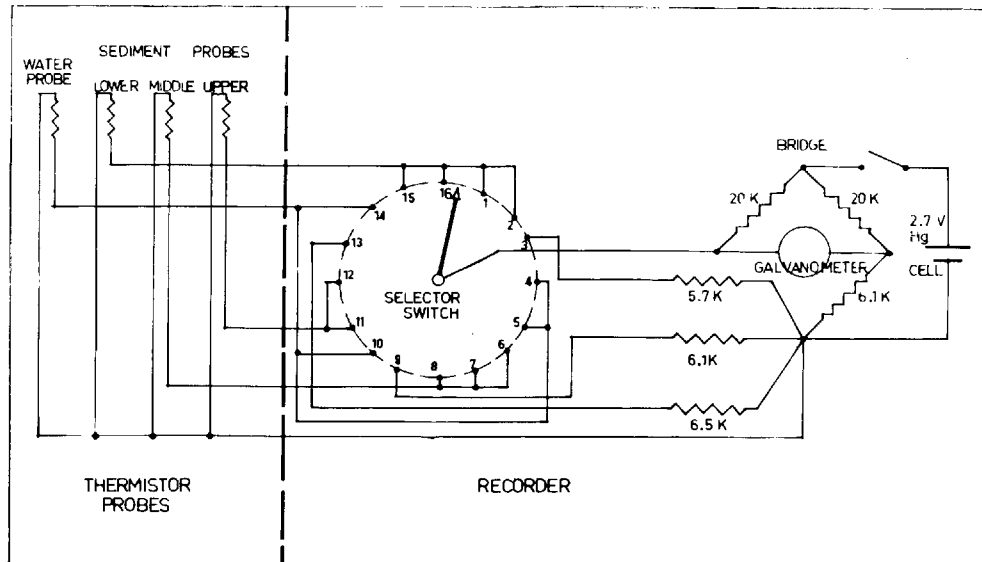
### 2.5 Temperature Detecting and Recording Devices

A wide range of possibilities exists in the design of resistance detecting circuits and recording techniques, and every institution that has constructed a thermogradient probe has felt compelled to devise a new type of recording system. The primary requirements are that they be simple, reliable, compact, and rugged enough to withstand rough handling at sea and the jolts of penetrating the bottom. The recording instruments now in use will be briefly described.

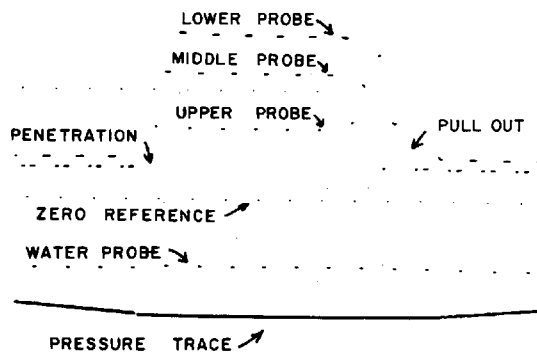
*The Ewing thermograd.* The simplest arrangement is probably that of the Ewing instrument, which is used in conjunction with the outrigger probe technique. A schematic diagram is shown in Figure 3A. The thermistors in the

temperature sensing probes are sequentially placed in one arm of a simple Wheatstone bridge by a 16-position rotating selector switch. The imbalance of the bridge is detected by a sensitive 30-cps galvanometer. Deflections of the galvanometer mirror are recorded photographically on 70-mm film placed about 23 cm from the galvanometer. To repeatedly calibrate the bridge and the galvanometer, three standard resistors which cover the range of expected thermistor resistance near the ocean bottom and in the sediment are placed in the bridge instead of the thermistors on every half-minute cycle of the rotary switch. A typical film record is shown in Figure 3B. The film is driven at a rate of about 0.7 cm/min. The instrument now in use carries enough film to record the temperature of the probes during lowering and hoisting of the instrument. In some instruments, a very small diameter thermistor probe, the 'water probe,' and a pressure gage are used to measure the ocean water temperature and instrument depth. This additional information is very useful in evaluating the stability of the near bottom water.

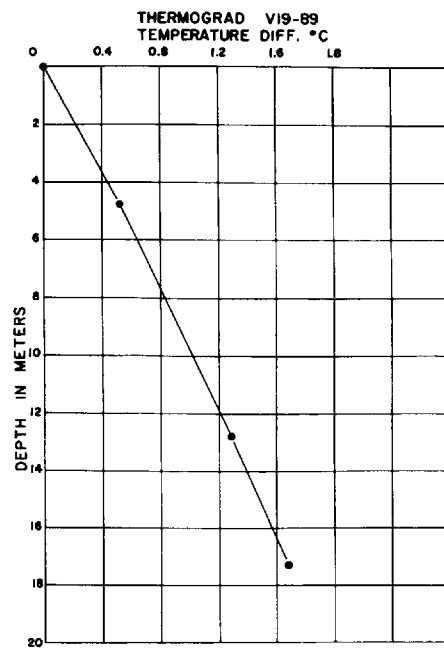
*Scripps Institution of Oceanography recorder.* The details of this recording system for the Bullard probe are more completely given by *Von Herzen et al.* [1962]. The temperature difference between two thermal sensing elements at the extremities of the hollow steel probe is recorded. Each thermal element consists of two thermistors, so that there are four thermistors in the probe which form an all-thermistor bridge. The bridge design is shown in Figure 4A. This arrangement has several advantages for the measurement of temperature difference: (1) the sensitivity of the bridge is doubled by having 2 thermistors in each current path of the bridge; (2) the balanced output of the bridge stays constant for different ambient temperatures; and (3) the output of the bridge is nearly linear for small temperature differences. The bridge output is measured by a self-balancing, null-type potentiometer recorder. In the circuit shown in Figure 4A the output of the bridge is amplified by a solid-state 'chopper' amplifier. The output of the amplifier drives a small servomotor, which rotates a precision potentiometer in series with a mercury reference cell. The potentiometer turns until the voltage on the potentiometer balances out the bridge output. The servomotor also



A



B



C

Fig. 3. (A) Schematic diagram of sensor and detecting circuit of the Ewing thermograd. (B) Typical record of the outriggered probe apparatus. (C) Temperature versus depth in the bottom sediment relative to the bottom water temperature derived from the record shown in B.

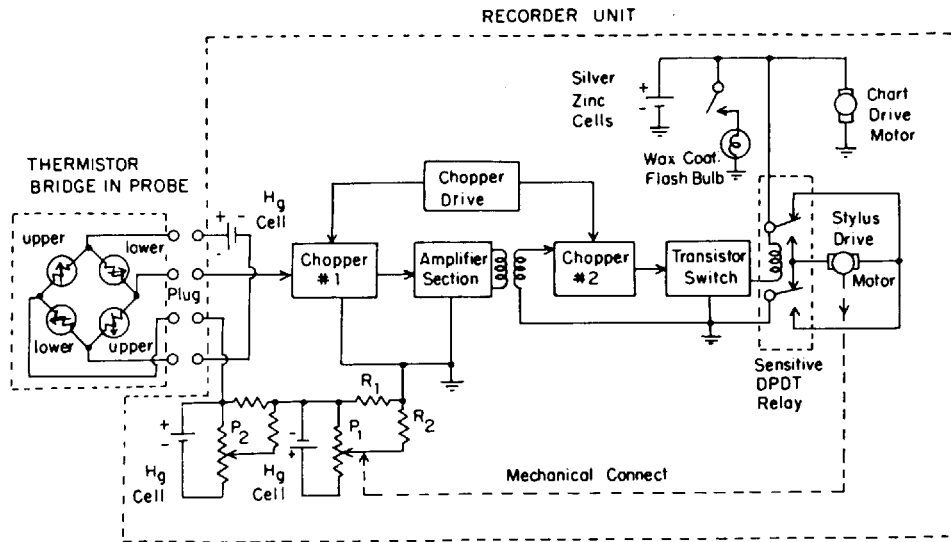


Fig. 4A. Thermistor bridge and recorder circuit for a temperature gradient measurement [Von Herzen et al., 1962].

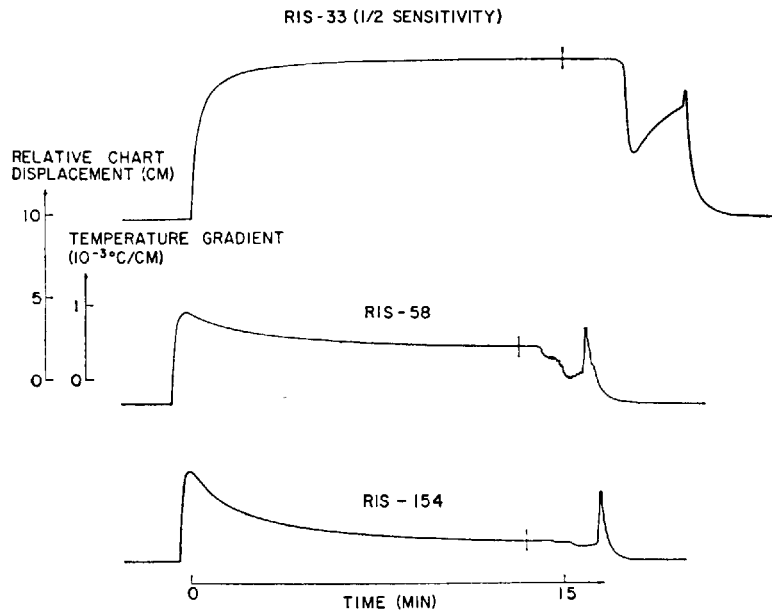


Fig. 4B. Typical recordings for high (RIS 33), normal (RIS 58), and low (RIS 154) heat flow measurements.

drives a recording stylus which makes a record on electro-sensitive paper whose trace displacement is proportional to temperature difference between the elements in the probe. The trace displacement is measured from a zero temperature difference line which is recorded in the nearly isothermal ocean bottom water. With the

use of transistors and solid-state choppers, this unit has been made very compact and rugged.

*The Earthquake Research Institute recorder.* A more complex recording system has been used by Japanese scientists [Uyeda et al., 1961] with the hollow probe technique. A drawing of the mechanical unit and a block and circuit diagram

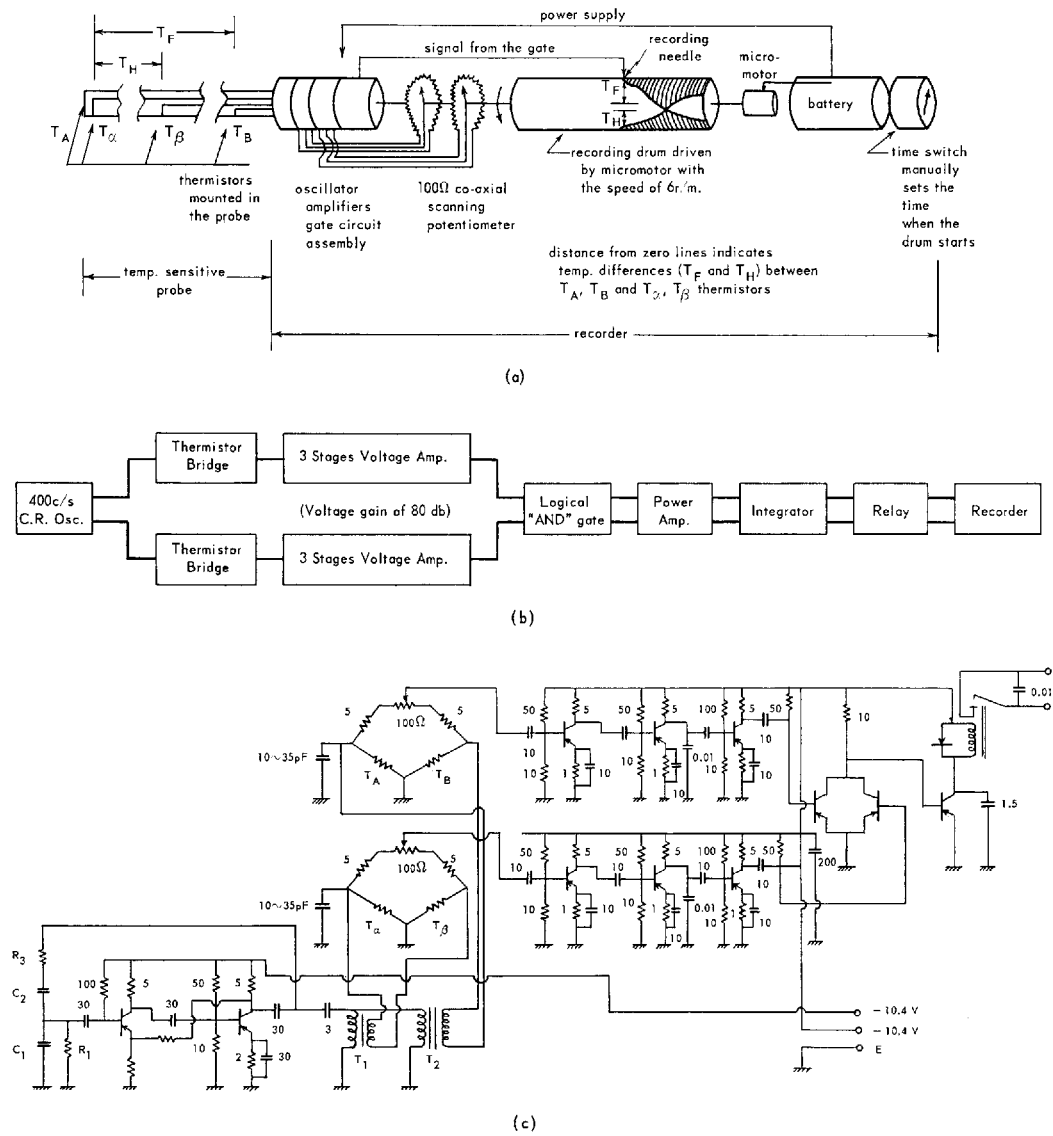


Fig. 5. The Earthquake Research Institute recorder [from Uyeda *et al.*, 1961, Figures 5, 6, and 7]: (a) schematic diagram; (b) simplified block diagram; (c) circuit diagram.

of their instrument are shown in Figure 5. Two pairs of thermistors,  $T_A$ ,  $T_B$ , and  $T_\alpha$ ,  $T_\beta$ , are used to measure the temperature difference between the top and bottom of the probe and between the midpoint and the bottom of the probe, as in the experiments of Bullard and Day [1961]. Each pair of thermistors forms the lower arms of two ac Wheatstone bridges. The two bridges each have a 100-ohm continuously turning potentiometer between the upper reference

arm resistors, so that the 100 ohms first appear in one arm of the bridge and then in the other as the wiper arm of the potentiometer goes from one extreme to the other. In the range of expected temperature differences, each bridge passes through its balance point during a complete turn of the potentiometer. As the bridge passes through the balance point, the ac signal changes phase by  $180^\circ$ . The signals of the two bridges are separately amplified and compared

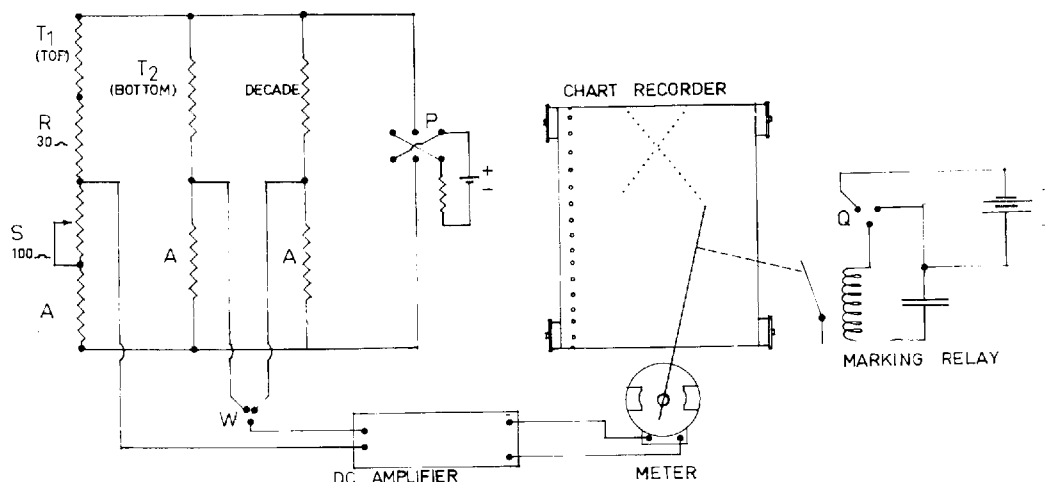


Fig. 6. Simplified circuit diagram of the Woods Hole Oceanographic Institution recorder [after Reitzel, 1961].

by a summing 'gate' circuit. The output of the gate is zero when the phase of the bridge signals is opposite, but is about 10 volts when the phases are the same. The 10-volt output of the gate actuates a relay which produces a record of the 400-cps ac signal on electro-sensitive paper.

The normal operation of the circuit during one revolution of the potentiometers is as follows. Both bridges are unbalanced, and the phases are opposite so that no record is made (the ac signals supplied to the two bridges are out of phase). When one of the bridges passes through the balance point, the phase of the bridge signals immediately becomes the same, and a record is produced. The recording stops when the other bridge passes through the balance point and the phases again become opposite. This recorder is calibrated against resistance change in one arm of both bridges so that the record for each revolution can be converted into temperature difference of the two pairs of thermistors. In practice, the zero temperature difference balance point of each bridge is determined by holding the probe suspended in the deep, nearly isothermal, near bottom water while it records.

The electro-sensitive paper on which the record is made is held on a rotating drum 20 cm long which is directly coupled to the drive of the two 100-ohm potentiometers. Thus one sweep of the paper is made for each complete turn of the potentiometers. One turn takes ten seconds. The recording stylus is slowly

driven along the recording drum by a helical lead screw and traverses the drum in 1.25 or 2.5 hours, depending on the lead screw used. The result is a record of temperature difference versus time for each pair of thermistors.

*The Cambridge University recorder.* In a recording system devised by Lister [1963] for an outriggered probe now used by Cambridge University, the resistance of the thermal elements (sensistors) is balanced against a standard Manganin resistance. The detecting circuit is a Carey-Foster bridge with a Servo-driven precision potentiometer. Cycling cams switch the three elements into the arms of the bridge in sequence. A scratch-sensitive recording paper is used in the Cambridge University instrument which eliminates the high voltage battery needed to mark electro-sensitive paper used in other recorders.

*The Woods Hole Oceanographic Institution recorder.* Another recorder to measure temperature difference has been designed by Reitzel [1963]. The detector is a resistance bridge in which the upper and lower thermistor elements of the probe are the two upper arms of the bridge. In one of the bridge's lower arms is a 100-ohm continuously turning potentiometer ( $S$  in Figure 6) which balances the bridge once every revolution. The configuration is shown in Figure 6. At balance,  $S/A = (T_2 - T_1)/T_2$  plus some small second-order terms. The bridge output is recorded after amplification by an in-

expensive Rustrak recorder. The polarity of the output of the bridge is reversed by switch *P* in Figure 6 thirty-two times during one revolution of the potentiometer *S*. The record marking switch *Q* is mechanically coupled to *S* and *P* and makes thirty-two dots per revolution of *S*. The displacement of the dots is proportional to the bridge output. The resulting record is a series of dots in two straight lines which cross, forming an X. The value of *S* at balance can be determined by finding the number of dots until the two lines cross. This can be estimated roughly to 1/160 of a potentiometer turn, or about 2/3 ohm.

Direct measurements of temperature can be made with this instrument by replacing  $T_1$  by a standard resistor by means of a switch *W* (in Figure 6). In operation, direct temperature measurements are made every few cycles of the potentiometer.

### 2.6 *The Technique Used at the Preliminary Mohole Site*

A 170-meter hole was drilled in the sediment of the ocean bottom near Guadaloupe Island during a preliminary phase of the Mohole project. Temperature measurements to determine the vertical gradient were made in the drill hole by means of a special probe [Von Herzen and Maxwell, 1964]. The probe is 1.5 meters long and 1.27 cm in diameter at the tip and contains a thermistor element in its lower end. The probe is lowered down the drill stem, while the operation is temporarily halted, and is driven into the sediment ahead of the drill bit by hydraulic pressure applied to the top of the probe. The tip of the probe extends far enough below the drill bit so that the temperature measurement can be made before the disturbance of the drilling reaches the thermal element.

The resistance of the thermistor is detected by a resistance-sensitive oscillator in a pressure-proof vessel on top of the probe. The output of the oscillator is sent to the surface by a two-conductor cable, and the frequency of the output is measured aboard the drilling vessel. The probe temperature is calibrated versus oscillator frequency before it is lowered.

Successful measurements of temperature were made at three points below the sediment surface during the drilling of the preliminary Mohole.

Conductivity measurements were made on sediment core samples taken during the drilling. A very important result of these measurements was the direct observation that heat flow was constant, within instrumental error, over the two intervals of gradient measurement [Von Herzen and Maxwell, 1964].

Demonstration of the constancy of heat flow with depth by measuring the temperature gradient over two or more intervals in the sediment is an important test of the validity of the temperature gradient measurements. Many stations have been made with the Ewing instrument where the gradient is measured over two or more intervals. Most of these measurements have shown that the heat flow is constant; however, a very small percentage of values have been measured that appear to be transient heat flow in the sediment shown by gradients which vary greatly with depth.

Another disturbing feature of recent heat flow measurements is that at some stations which are within several miles of each other the observed heat flow differs by an order of magnitude, whereas at other closely spaced stations nearly identical values have been measured. Some cases of large differences in heat flow in relatively short distances are given in Table 1. These results indicate that some regions of the ocean floor probably are subjected to local thermal disturbances, so that the observed gradient does not represent the heat flow through the oceanic crust. Thus an important part of future heat flow measurements should be a careful study of the sediment and hydrographic environment at each station. This topic is discussed briefly in section 5.

### 3. TECHNIQUES OF MEASURING THERMAL CONDUCTIVITY OF THE SEDIMENT

All measurements of thermal conductivity made to date have been made on samples of sediment brought to the surface by coring devices either at or near the site of the temperature gradient measurement. Both steady-state and transient methods of measurement have been used to determine the conductivity of these samples. Conductivity measurements are usually made on board the research vessel or on hermetically sealed samples returned to the laboratory. A good estimate of the conductivity can also

TABLE 1.\* Some Cases of Adjacent Heat Flow Stations That Show Large Variations of Heat Flow over Short Lateral Distances

Case	Station Separation, km	Heat Flow, $\mu\text{cal}/\text{cm}^2 \text{ sec}$		General Area
		Station 1	Station 2	
1	82	2.36	0.19	Continental margin, Baja Calif.
2	151	6.15	0.62	Mouth, Gulf of Calif.
3	18	4.46	1.06	Between Clipperton and Clarion fracture zones, East Pacific
4	35	10	1.15	Tehuantepec Ridge
5	42	7.42	0.67	East Pacific Rise
6	8	5.94	1.98	Southern flank, Carnegie Ridge
7	45	1.13	0.16	Between Tabiti & Tuamotus
8	96	8.14	0.97	Mid-Atlantic Ridge, South Atlantic
9	54	1.30	0.15	Southeastern Atlantic
10	37	7.1	0.5	East Pacific Rise

\* This table is extracted in part from *Langseth et al.* [1965].

be made if the the water content is known. The effective conductivity of the sediment section at a station is determined by making a number of measurements along the length of the core sample and taking the reciprocal of the average thermal resistivities. (Thermal resistivity =  $1/\text{conductivity}$ .) If the core sample is made up of a number of distinct layers of different types of sediment, a weighted average based on the thickness of each layer can be made. The ambient temperature when the measurements are made aboard ship or in the laboratory is usually about  $25^\circ\text{C}$ , so that the values obtained must be adjusted to the ambient temperatures and pressures at the ocean floor (near  $0^\circ\text{C}$  and 700 to 1000 atm). The necessary factor for temperature change can be calculated from the unpublished results of Butler [*Ratcliffe*, 1960], who observed a 6% decrease in sediment conductivity for a temperature change from  $25^\circ\text{C}$  to  $4^\circ\text{C}$ . The effect on the thermal conductivity of pressure change with increasing depth is approximately +1% per 2000 meters. For deep ocean stations, it is common to correct conductivities measured at about  $25^\circ\text{C}$  and 1 atm by  $-4\%$ .

### 3.1 Steady-State Measurements

Steady-state techniques can be used to measure thermal conductivity if the soft sediment is held to a disk shape by a plastic ring of the desired thickness (see chapter 3, section 2.1, by Beck, in this volume). A very suitable arrangement has been used by *Ratcliffe* [1960] (see Figure 7). A metal disc or hot plate containing an

electrical heater is sandwiched between two sediment samples in thin ebonite rings. The other sides of the sediment discs are in contact with a water-cooled disc or cold plate. The apparatus is surrounded by thermal insulation to prevent appreciable side losses of heat. The temperature differences over the sediment samples are measured by thermal elements in fine holes drilled in the hot and cold plates. After the system has come to equilibrium, the heat flow through both samples is easily determined by measuring the power input to the heater. A small correction is

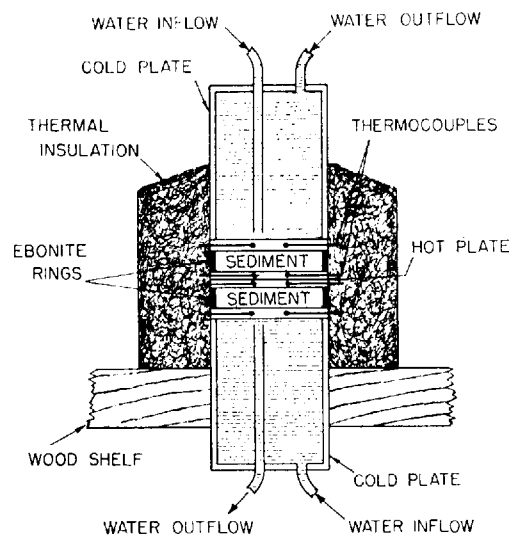


Fig. 7. Disc apparatus (schematic) for measuring the thermal conductivity of ocean sediment [after *Ratcliffe*, 1960].

necessary for the finite area taken by the ebonite rings. This technique measures the average of the conductivity of the two samples.

The steady-state technique is not very suitable for routine measurements on a large number of samples or for shipboard use, because preparation of samples is a tedious job. About half an hour is needed for a sample to reach equilibrium. A more convenient and rapid method is the heated needle probe technique, described below.

### 3.2 Transient Method Using a Fine Needle

In this method [Von Herzen and Maxwell, 1959] a very thin cylinder (or needle) is heated by an internal heater wire at a known and constant rate. The rate of rise of temperature of the needle is measured by a small thermistor which is inside the needle and midway along its length. The needle pictured in Figure 8A is usually 0.5 to 0.9 mm in outside diameter and 6.4 cm long. Such a thin needle can be regarded as a line source of heat in the neighborhood of the thermistor within several seconds after the heater power is turned on. After the heater power has been on for roughly 10 seconds, the temperature  $T$  in degrees Centigrade at the thermistor as a function of time  $t$  in seconds is given by

$$T = (Q/4\pi K) \ln(t) + C \quad (2)$$

where  $Q$  is the heat per unit length per unit time (cal/cm sec),  $K$  is the conductivity (cal/cm sec °C), and  $C$  is a constant. The theory of conductivity measurement by transient techniques is more thoroughly covered by Jaeger in chapter 2, section 13, of this volume.

A record of 4 minutes is made of the temperature rise of the needle. If the temperature is plotted against the logarithm of time (Figure 8B) a straight line results, and the expression  $(Q/4\pi K)$  is the slope of this line. If  $Q$  is measured,  $K$  can be easily calculated.

For a typical probe, the heater is a double length of thin nichrome wire with a nominal value of resistance of 50 ohms. The heater power used is between 0.5 and 1.0 watt supplied by a well regulated power source. The heater raises the probe temperature about 5°C to 7°C during the time interval of between 10 and 400 seconds.

The resistance and hence the temperature of the thermistor can be detected by a Wheatstone bridge and recorded on a strip chart. A con-

ductivity measuring system used by the Scripps Institution of Oceanography is shown in Figure 8A. If the time, temperature, and power input are measured to 1%, the conductivity is determined to approximately 2.5%. Comparison of transient and steady-state measurements on the same sample gives agreement to 3% [Von Herzen and Maxwell, 1959].

### 3.3 The Relation between Sediment Water Content and Conductivity

Most deep sea sediment such as lutites and fine silts can be considered as very fine solid particles in a water medium. The thermal conductivity of the individual solid grains is approximately 4 to 5 times greater than that of sea water. The conductivity of sea water is about 1.4 mcal/cm sec °C at near ocean bottom conditions. The results of Ratcliffe [1960] and Bullard and Day [1961] have shown that there is a linear relation between the thermal resistivity and the water content of ocean bottom sediment in the range of expected values. The relation given by their results after correction to ocean bottom conditions is

$$R \text{ in situ} = (168 \pm 14) + (6.78 \pm 0.31)W$$

where  $R$  is the thermal resistance in cm °C sec/cal, and  $W$  is the water content in per cent water of the wet weight.

A nomogram which relates the conductivity to other parameters of the sediment is given in Figure 9 [from Ratcliffe, 1960].

The original water content of dried sediment samples can also be determined from the percentage of chlorine in the dry sample if it is assumed that all the chlorine in the sediment is due to the evaporation of sea water with a salinity of present-day ocean bottom water.

Published results of conductivity measurements show that the values obtained generally range within  $\pm 25\%$  of 2.00 mcal/cm sec °C. For the uniform deep sea lutites far from the continents, the range of observed values is smaller than that given above, but for turbidites, calcarenites, and volcanic ashes the range can be large. In a single core from abyssal plain type sediment of the Somali Basin in the Indian Ocean, the measured values of conductivity ranged from 1.65 to 2.15 mcal/cm sec °C.

It is possible to make in situ thermal conductivity measurements with the heated needle

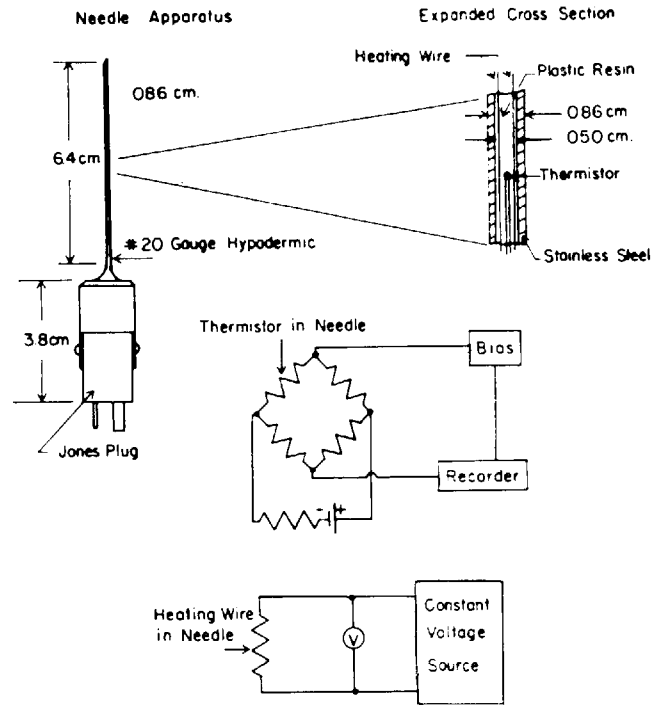


Fig. 8A. Conductivity needle probe and simplified circuit diagram.

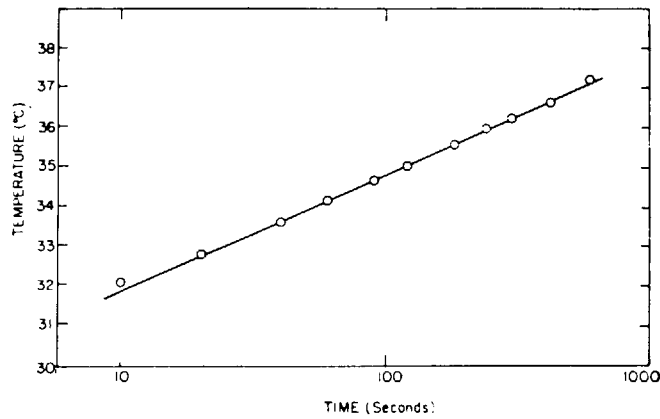


Fig. 8B. Temperature of probe versus logarithm of time for typical measurement [from Von Herzen et al., 1962].

technique. Such instruments have long been discussed but none have been made. It would be very valuable to have one or more in situ checks to compare with the many laboratory and ship-board measurements.

#### 4. SOME NOTES ON PROCEDURE

##### 4.1 Selecting a Site

Early workers in heat flow, particularly if they were the designers and builders of the instru-

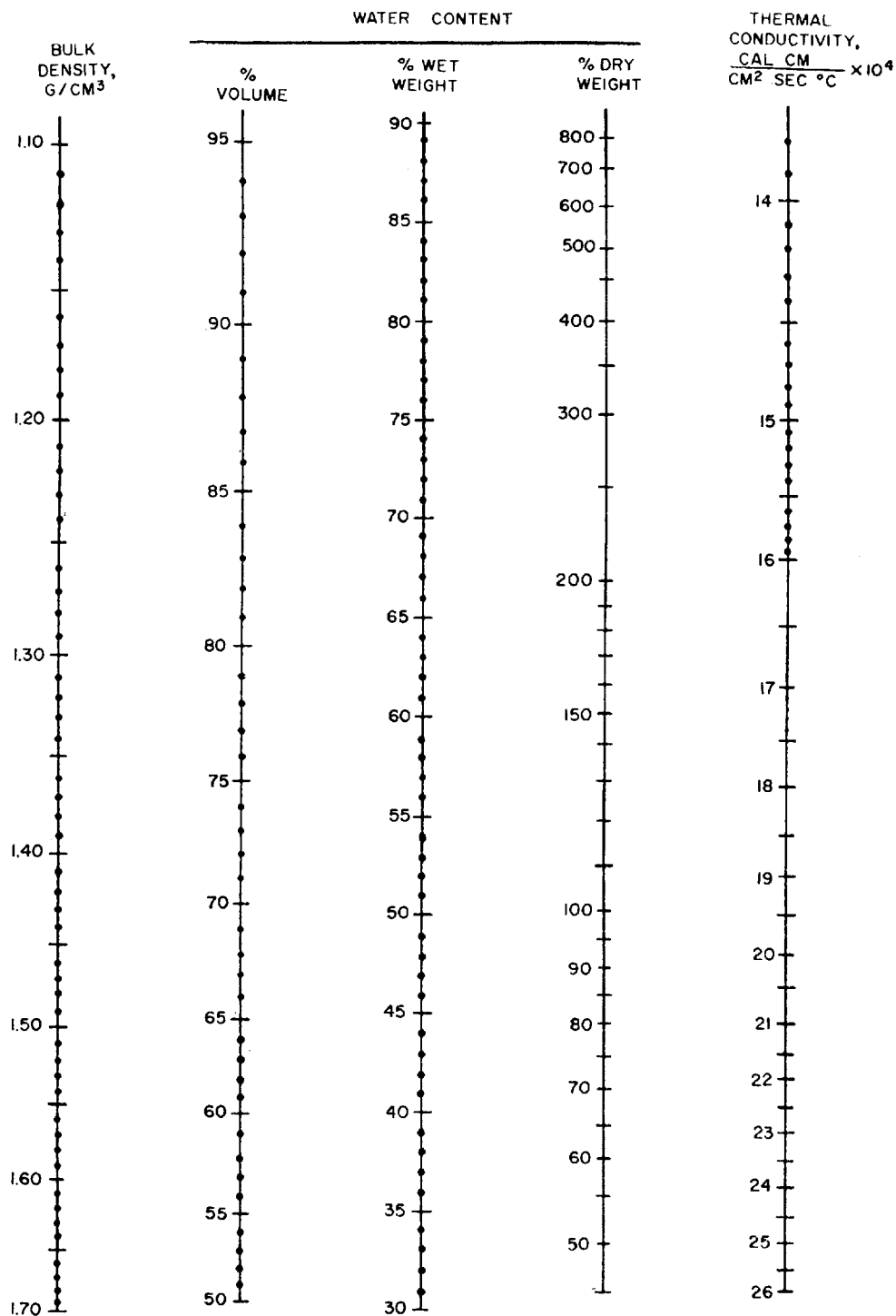


Fig. 9. Nomogram for assessment of thermal conductivity of ocean sediment at 4°C and 1 atm [from *Ratcliffe*, 1960.] The thermal conductivity is given at 4°C and 1 atm. Add 1% per 1000 fathoms and 1% per 4°C temperature increase.

ments, were very careful to select a site which was covered with soft sediments. As a result, the majority of early stations in rough terrain are located in sediment-filled troughs which could bias the results to lower values [Von Herzen and Uyeda, 1963]. Later experience has shown that such care is unwarranted, for the sediment cover on the ocean floor is extensive enough even in the rough topography of the median ridges to allow a high percentage of complete penetrations. Secondly, most instruments are rugged enough to stand up to the few times they are dropped on a hard surface. It is therefore wiser to select stations for their geophysical value rather than the penetrability of the sediment.

The best spacing and distribution for heat flow stations on the ocean floor depend on the problem being studied. Some problems which have been studied might be classified as follows:

(a) The measurement of the average heat flow over a large area to investigate the worldwide variation of heat flux through the surface.

(b) Measurements on prominent geological features such as median ridges, continental margins, etc., to investigate possible variations of heat flow associated with these features.

(c) Closely spaced measurements to investigate single anomalous readings, local topographic and sedimentation effects, or the heat flux over buried structures defined by seismic, gravity, and magnetic surveys.

In the deep ocean basins with nearly uniform sediment thickness, the heat flow has been found to vary little, and the average heat flux can be determined with some confidence by stations spaced a few hundred kilometers apart [Reitzel, 1963].

A greater density of stations is required in an area where the topography is rough and possible local thermal disturbances are suspected. In these areas, a large number of stations will help to negate random errors. The multiprobe instruments have an advantage in these studies, since they can detect recent transient disturbances. Local thermal disturbances are further discussed in section 5.

The investigation of problems of type (c) requires much closer spacing. Measurements that have been published have, by and large, not succeeded in defining small heat flow anomalies of less than 50 km in width completely. The principal difficulty is navigation in an area

several kilometers on a side. Some workers have used anchored buoys for these measurements, and no doubt more will in the future.

Some guide to the proper spacing of stations over buried heat sources is provided by the results of Von Herzen and Uyeda [1963]. They have calculated the heat-flow anomalies over various shaped sources. The vertical dike at high temperature and of infinite extent in the direction of its long axis is of geologic interest. Von Herzen and Uyeda have calculated the half-width of anomalies for various depths and thicknesses. Some of their results are given below. Thickness and depth are lumped as a dimensionless parameter,  $L/2D$ , and half-width is given as  $X/D$ , where  $X$  is the horizontal distance perpendicular to the center line of the dike.

$L/2D$	0	2	4	6	8
Half-width ( $X/D$ )	1.75	3.00	4.90	6.85	8.80

As an example, the anomaly over a dike 5 km below the surface and 1 km thick would have a half-width of about 9 km, so that stations spaced at most 5 km apart are required to define the anomaly.

#### 4.2 Shipboard Operation

The thermal gradient probe, provided that it weighs less than 100 kg in water, is lowered on a hydrographic wire of about 5 mm in diameter. The heavy coring apparatus (600 kg or more) is lowered on heavier steel wire rope 1.27 cm in diameter. For instruments which have water temperature and pressure measuring units, several stops on the way to the bottom should be made to compare the indicated depth on the record with wire out at the stop. If a large angle is being produced by drift during lowering, it can be decreased by maneuvering the ship in the direction of the wire. A straight wire will facilitate leaving the probe in the bottom undisturbed.

'Pingers' which are synchronized with the echo sounder and transponders placed on the wire near the probe are also very useful in determining the instrument's position with relation to the bottom and to the ship. With very short pings the texture of the bottom below the instrument can often be ascertained from the recording of the bottom echo of the transponder pulses.

With the cylindrical probe apparatus, it is now

common to place two Nansen hydrographic bottles a short distance above the probe, spaced about 100 meters apart. The thermometers on the Nansen bottles measure the temperature gradient in the near bottom water, so that the possibility of bottom currents is detected. With outriggered probes, reversing thermometers are sometimes placed on the core head to measure the bottom water temperature. The reversing thermometer measurements are particularly useful as in situ calibration points with the Ewing instrument which measures the probe temperature directly.

The penetration of the probe into the sediment is usually detected aboard the ship by the sudden decrease of tension in the cable. After penetration, the probe must be left undisturbed in the sediment during an observation period of 3 to 40 minutes, depending on the instrument used. This is done by slowly letting out wire as the ship drifts away from the probe.

After the probe is recovered, it is essential to evaluate the results rapidly so that, if an anomalous value is obtained at a station, intermediate stations can be made to better define the heat flow anomaly. The dry paper recorder is advantageous in this regard because, unlike film recorders, it does not require darkroom development before reading. When the pressure case is opened, the recorder, which is cold, acquires a coating of condensation. If this coating is blown off by dry air, little harm is done to the instrument.

If shipboard conductivity measurements are to be made, the sediment core should be taken into an area of constant temperature and allowed to come to room temperature. For cores which are extruded, it is possible to examine the core and decide what type of sampling best gives the over-all conductivity of the sediment.

The time required for a single heat flow observation depends on the technique, the speed of the winch used, and the experience of the operator. For example, the Ewing technique requires about three hours of on-station time for deep water observations.

## 5. CONSTANT THERMAL CONDITIONS OF THE OCEAN BOTTOM

Because the temperature gradient measurements are made in the upper few meters of sedi-

ment, it is necessary that possible disturbing effects which operate on the ocean floor be thoroughly examined. The following possible disturbing factors have been suggested [Bullard *et al.*, 1956; Von Herzen and Uyeda, 1963]: (1) a change of bottom water temperature in recent times; (2) recent rapid deposition or erosion of sediment on the bottom; (3) topographic or sedimentary blanketing effects causing preferential heat flow; (4) mass transfer of heat in the sediment; and (5) heat sources in the sediment.

Most heat flow observations are made in conjunction with other oceanographic and geophysical measurements, so that at each station it is possible to evaluate most of these effects. Unfortunately, full advantage has not been taken of these data in published results to date.

### 5.1 *Recent Changes in the Bottom Water Temperature*

Many heat flow instruments can measure temperature of the near bottom water. Records from these instruments or nearby hydrographic stations can be used to examine the temperature or density structure of the near bottom water. From these data some general inferences about the bottom circulation can be made. For example, if the temperature gradient is nearly adiabatic, shown by a nearly uniform potential temperature with depth in the water, there must be good vertical circulation and very sluggish lateral currents. Adiabatic gradients are common in trenches and small closed basins [Cochrane, 1958]. The bottom water in these basins should have long term temperature stability. Steep temperature gradients to colder water near bottom indicate density stratification and possible currents. In areas near the sources of deep bottom water, for example the Argentine Basin of the western Atlantic and the Agulhas Basin of the Indian Ocean, the near bottom temperature gradients are relatively steep and the velocity of the bottom water appreciable. In these areas variations of the bottom water temperature are possible. It can be stated that generally the deep bottom water (greater than 4000 meters) in the low latitudes is very slow moving and has great temperature stability; however, in polar regions and shallower water, the bottom currents are swifter and more variable. Knowledge of the

hydrography of the bottom water at the measurement site in these regions is essential.

Bottom photography is also a useful tool in detecting the presence of bottom currents. Often scour, ripple marks, or winnowing suggest the velocity and nature of the currents. The effects of changes of surface temperature are discussed by Jaeger in chapter 2 of this volume.

### 5.2 Rapid Deposition or Erosion

Evidence of rapid deposition or erosion can be gained from sedimentary samples taken at the stations and from the topographic settings shown by the depth recorder. Rapid deposition by slumping or turbidity currents is often shown by contorted sediments or graded beds in the sample. A broad knowledge of the sediment sequence of a region is helpful. For example, the deep ocean basin sediments of the western Atlantic are characterized by a few centimeters of soft tan sediment at the surface which is very distinctive and easily recognizable. If this layer is not present, one might suspect recent deposition or erosion. The seismic reflection technique is also very useful in determining the attitude and distribution of the sediment [Ewing and Tirey, 1961].

The effect of continuous and rapid deposition on the temperature gradient can be calculated from results given by Carslaw and Jaeger [1959]. Reitzel [1961] has pointed out that, for a steady sedimentation rate  $U$ , the effect on the surface gradient  $g$  can be expressed as:

$$g = g_0 4i^2 \operatorname{erfc}[Ut/(4\kappa t)^{1/2}]$$

where  $g$  is the present gradient,  $g_0$  the original gradient,  $t$  the time, and  $\kappa$  the diffusivity. At present, it is difficult to obtain exact values for the rates of sedimentation; however, even for rates in deep ocean basins as high as 1 cm/year since glacial times (10,000 years ago), the effect would be very small. Only catastrophic sedimentation such as slumping or turbidity flows would produce a significant disturbance on the regional gradient.

### 5.3 Topographic and Blanketing Effects

The otherwise uniform regional heat flow will be distorted in an area of steep topography. The observed heat flow at the surface in a valley is greater than normal, whereas that on peaks is

below normal, because isotherms in the rock and sediment are distorted to match the nearly isothermal irregular boundary of the ocean floor. Similarly, a variable thickness of low conductivity sediments on a relatively high conductivity rock surface will cause heat to flow preferentially through areas where the sediment is thinner. With continuous precision depth recorders and continuous seismic reflection techniques, the topography and the attitude of the sediment along the track can be determined. Unfortunately, this is usually along only a single line.

If the topography is known, it is possible, by using methods outlined by Carslaw and Jaeger [1959, pp. 424-425] and by Jaeger in chapter 2, section 5, of this volume, or by the use of model topography in electrolytic tanks, to make corrections to the observed heat flow. The effect of some simple models has been calculated.

Von Herzen and Uyeda [1963] give an expression for the effect on the heat flow  $q$  of a semiellipsoidal sediment body with a vertical semi-axis  $l$  and horizontal semiaxes  $m$  and  $n$  in a semi-infinite body of rock. The heat flow is constant over the body and

$$q_s/q = (K_s/K_r)/[1 + (K_s/K_r - 1)F]$$

where

$$F = lmn$$

$$\int_n^\infty \frac{dx}{(x^2 - n^2 - l^2)^{-3/2} (x^2 - n^2 + m^2)^{-1/2}}$$

$q_s$  is the heat flow at the surface of the sediment body, and  $K_s$  and  $K_r$  are the conductivities of the sediment and rock, respectively.

Two special cases are of interest: (1) a trough of semiellipsoidal cross section, i.e.,  $n = \infty$ :

$$F = m/(m + l)$$

and (2) a body which is circular in plan view, i.e.,  $m = n$ :

$$F = m^2(m^2 - l^2)^{-3/2} \{ -\pi/2 + \tan^{-1}[l/(m^2 - l^2)^{1/2}] + (m^2 - l^2)^{1/2}/l \}$$

However, exact calculations at sites of heat flow measurement have not been made owing to the lack of exact information on the topography and the sediment thickness at the specific station. The principal difficulty comes from the loss of precise navigation when the vessel drifts on

station and the lack of a three-dimensional survey.

#### 5.4 Mass Transport of Heat and Heat Production in the Sediment

The upward movement of interstitial water in the sediment could reduce the geothermal gradient by increasing the upward transport of heat. Von Herzen and Uyeda [1963] demonstrate that, if convection exists in the sediment, a vertical velocity of 50 cm/day is required to reduce the regional gradient 10%. For sedimentation rates of 0.1 cm/year or less, the release of interstitial water by steady compaction is insignificant. The only other cause of vertical water movement in the sediment would be juvenile water coming from the rock beneath. To date there is no evidence of such juvenile water.

Heat production by radioactive decay in the upper 50 meters of sediment is many times smaller than the heat flow observed. Heat production or absorption by chemical or bacterial action in the sediments is not known to be great in ocean basin sediments. If unusual heat production is taking place, there should be evidence for it in the core sample taken. Furthermore, chemical or bacterial processes might be expected to be active only in the upper few centimeters of the sediment and would cause temperature gradients which change with depth. Such gradient changes would be detected by multiprobe measurements.

In summary, all the disturbing effects outlined above are believed to be small in the deep ocean basin floor below 4000 meters, which is uniformly covered with sediment. In areas of rough topography or where the environment suggests possible disturbance of the temperature gradient, an evaluation may be possible by means of other oceanographic measurements, although the magnitude of the disturbance can only be estimated. It seems best at present to accept values of heat flow only where auxiliary oceanographic and geophysical measurements show little likelihood of disturbance, and to qualify the results in more questionable areas. Bullard has pointed out, however, that many of these disturbances are random and will not affect the mean of a large number of measurements. In the next chapter Lubimova, Von Herzen, and Udintsev will fur-

ther investigate some problems of heat transfer through the ocean floor.

*Acknowledgments.* I would like to thank Sir Edward Bullard, Richard P. Von Herzen, and W. H. K. Lee for many constructive suggestions that helped in the writing of this article. John Reitzel, John E. Nafe, and J. Lamar Worzel were kind enough to critically read the manuscript. I thank E. H. Ratcliffe, S. Uyeda, and R. P. Von Herzen for allowing some of their illustrations to be reproduced.

#### REFERENCES

- Bullard, E. C., The flow of heat through the floor of the Atlantic Ocean, *Proc. Roy. Soc. London, A*, 222, 408-429, 1954.
- Bullard, E. C., The flow of heat through the floor of the ocean, in *The Sea*, edited by M. N. Hill, vol. 3, pp. 218-232, Interscience Publishers, New York, 1963.
- Bullard, E. C., and A. Day, The flow of heat through the floor of the Atlantic Ocean, *Geophys. J.*, 4, 282-292, 1961.
- Bullard, E. C., A. E. Maxwell, and R. Revelle, Heat flow through the deep sea floor, *Advan. Geophys.*, 3, 153-181, 1956.
- Carslaw, H. S., and J. C. Jaeger, *Conduction of Heat in Solids*, 2nd edition, Oxford University Press, London, 510 pp., 1959.
- Cochrane, J. D., Note on the adiabatic temperature gradient of sea water, in Physical and chemical properties of sea water, *Natl. Acad. Sci. U.S. Publ.* 600, pp. 30-37, 1958.
- Ewing, J. I., and G. B. Tirey, Seismic profiler, *J. Geophys. Res.*, 66, 2917-2927, 1961.
- Gerard, R., M. G. Langseth, Jr., and M. Ewing, Thermal gradient measurements in the water and bottom sediment of the western Atlantic, *J. Geophys. Res.*, 67(2), 785-803, 1962.
- Langseth, M. G., P. J. Grim, and M. Ewing, Heat-flow measurements in the east Pacific Ocean, *J. Geophys. Res.*, 70, 367-380, 1965.
- Lister, C. R. B., Geothermal gradient measurement using a deep sea corer, *Geophys. J.*, 7, 571-583, 1963.
- Ratcliffe, E. H., The thermal conductivities of ocean sediments, *J. Geophys. Res.*, 65, 1535-1541, 1960.
- Reitzel, J., Studies of heat flow at sea, Ph.D. thesis, Harvard University, Cambridge, 66 pp., 1961.
- Reitzel, J., A region of uniform heat flow in the North Atlantic, *J. Geophys. Res.*, 68(18), 5191-5196, 1963.
- Sisoev, N. N., Geothermic measurements in the sediments on the floors of seas and oceans, *Okeanologiya*, 1(5), 886-887, 1961.
- Uyeda, S., Y. Tomoda, K. Horai, H. Kanamori, and H. Futt, Studies of the thermal state of the Earth, 7, A sea bottom thermogradient, *Bull. Earthquake Res. Inst. Tokyo Univ.*, 39, 115-131, 1961.

- Von Herzen, R., and A. E. Maxwell, The measurement of thermal conductivity of deep-sea sediments by a needle-probe method, *J. Geophys. Res.*, 64(10), 1557-1563, 1959.
- Von Herzen, R. P., and A. E. Maxwell, Measurement of heat flow at the preliminary Mohole site off Mexico, *J. Geophys. Res.*, 69(4), 741-748, 1964.
- Von Herzen, R. P., A. E. Maxwell, and J. M. Snodgrass, Measurement of heat flow through the ocean floor, in *Symp. Temperature, 4th*, pp. 769-777, Reinhold Publishing Corporation, New York, 1962.
- Von Herzen, R. P., and S. Uyeda, Heat flow through the eastern Pacific floor, *J. Geophys. Res.*, 68(14), 4219-4250, 1963.

(Manuscript received June 1, 1964; revised December 21, 1964.)

## Chapter 5. On Heat Transfer through the Ocean Floor<sup>1</sup>

ELENA A. LUBIMOVA

*Institute of Physics of the Earth, Academy of Sciences, Moscow, USSR*

RICHARD P. VON HERZEN<sup>2</sup>

*Scripps Institution of Oceanography, La Jolla, California*

GLEB B. UDINTSEV

*Institute of Oceanology, Academy of Sciences, Moscow, USSR*

*Abstract.* Heat flow from the Earth's interior may differ from measured values because of several disturbances in the environment on and near the ocean floor. The effects of water movements in and above the sediments are discussed in the light of recent temperature measurements of near bottom water. Super-adiabatic gradients have been observed near the ocean floor, suggesting convective overturns, although other factors may inhibit these. The velocity of interstitial water required to affect the surface heat flow is found to be several orders of magnitude less than previously suggested values, although still probably much greater than what is likely to occur. To obtain representative heat flow measurements, other controls are desirable to determine the effects of environment. Alternatively, a large number of observations should be made at a locality to reduce the effect of random variables.

### 1. INTRODUCTION

Many heat flow data have been accumulated in recent years, especially from the oceanic areas. These data have been analyzed and interpreted statistically by *Lee* [1963] and *Lee and MacDonald* [1963]. A current review of all available heat flow observations is given by *Lee and Uyeda* in chapter 6 of this volume.

The principal result from heat flow measurements is the approximate equality of the average heat flow on land and that at sea. Also of interest is the discovery of large positive heat flow anomalies on the midoceanic ridges. These two facts have been important in most theories of the thermal state of the Earth. The equality of the average heat flows suggests inhomogeneity of the upper mantle. This implies the existence of horizontal temperature gradients in the earth's interior beneath continents and oceans, which would produce thermoelastic stresses [*Lubimova and Magnitsky*, 1964; *MacDonald*, 1963].

Although the average heat flow for a large area is much the same everywhere, about

1.5  $\mu\text{cal}/\text{cm}^2$  sec, individual values vary greatly, as is indicated by the large standard deviation from the average value, about 1.2  $\mu\text{cal}/\text{cm}^2$  sec (see chapter 6, by *Lee and Uyeda* in this volume). There is an extremely large scattering of oceanic heat flow values, ranging from 0 to 10  $\mu\text{cal}/\text{cm}^2$  sec. In some oceanic areas, especially on and near the ridges, the amplitude of heat flow variation over short distances is large [*Von Herzen and Langseth*, 1965]. For example, *Nason and Lee* [1964] observed heat flow values of 0.3 and 6.5  $\mu\text{cal}/\text{cm}^2$  sec within a distance of 120 km near the crest of the mid-Atlantic ridge. Many other examples demonstrating the irregularity of the geothermal field on a small horizontal scale are given in chapter 6. Such large variations of surface heat flow over short distances suggest disturbances of shallow origin affecting the normal geothermal field. Indeed, many disturbances may affect the heat flow from the Earth's interior at its output from the sediments on the ocean floor. Moreover, the heat exchange between the sediments and the near bottom water may be very different from that on land (for a more detailed discussion of the heat and mass transfer within the Earth, see chapter 9 by *Elder*).

<sup>1</sup> Contribution from the Scripps Institution of Oceanography, University of California, San Diego.

<sup>2</sup> Now at Office of Oceanography, UNESCO, Paris, France.

Many authors have investigated the disturbances affecting the oceanic heat flow. A current review of these investigations is given by *Langseth* in chapter 4 of this volume. We shall examine some of these disturbances and their causes in more detail. There is the possibility that the observed variations of heat flow are due to movement of water in the sediments or in the ocean immediately above the sediments. This problem will be discussed in the light of recent measurements of temperature both in the sediments and in the ocean water above.

The plan of this chapter is as follows:

In section 2, thermal stability of deep ocean water is discussed. Measurements of temperature gradients in near bottom waters which may relate to this stability are described in section 3. Section 4 discusses the heat exchange between the ocean floor and the near bottom, and the influence of heat transfer by migration of interstitial water in sediments is discussed in Section 5.

## 2. THERMAL STABILITY OF DEEP OCEAN WATER

The measurement of oceanic heat flows assumes that thermal equilibrium has been reached on the deep (>2 km) ocean floor. Data on the constancy of temperature and salinity of deep water of the oceans are commonly used to support this assumption. There has been little investigation, however, of the detailed thermal regime of near bottom waters. Significant horizontal differences of temperature and salinity of near bottom waters have been observed [e.g., *Wooster and Volkman*, 1960], but the question of thermal stability of near bottom ocean waters is more closely related to vertical temperature and salinity distributions.

Let us examine the physical process of heat transfer from the ocean floor to the deep water. Close to the bottom there will be a layer of water in which heat transfer is dominated by conduction. We have, by the continuity of heat flow,

$$K_1 (\partial T/\partial z)_1|_{z=0} = K_2 (\partial T/\partial z)_2|_{z=0} \quad (1)$$

where  $K$  is thermal conductivity,  $(\partial T/\partial z)$  is temperature gradient, and  $z = 0$  denotes the water-sediment interface.

Thermal conductivity of oceanic sediments varies only within the narrow limits of about 1.5 to 2.5 mcal/°C cm sec [*Von Herzen and*

*Langseth*, 1965], whereas that of oceanic water in the near bottom layer is approximately 1.3 mcal/°C cm sec [*Sverdrup et al.*, 1942, p. 61]. The latter conductivity is only 30% less than that of the sediments. Hence thermal gradients both within the sediments and in the water must be of the same order of magnitude for heat transfer by conduction. On the average [*Von Herzen and Langseth*, 1965]

$$\begin{aligned} (\partial T/\partial z)_1|_{z=0} &\approx (\partial T/\partial z)_2|_{z=0} \\ &\approx 7 \times 10^{-4} \text{ }^\circ\text{C/cm} \quad (2) \end{aligned}$$

On the other hand, the adiabatic gradient for deep ocean water is [*Sverdrup et al.*, 1942, p. 63]

$$(\partial T/\partial z)_{ad} \approx 1.3 \times 10^{-6} \text{ }^\circ\text{C/cm} \quad (3)$$

The adiabatic gradient is thus far smaller than the average geothermal gradient in the sediments and the possible temperature gradient in the near bottom layer of water as given in (2).

Therefore, the temperature gradient must be super-adiabatic in the near bottom water layer. As deduced in section 4, a normal geothermal gradient in a water layer more than a few centimeters thick implies instability of the fluid—and consequently, the appearance of convection. In the next section we shall present the actual measurements of temperature gradients which confirm the existence of super-adiabatic gradients in the near bottom water layer.

## 3. MEASUREMENTS OF TEMPERATURE GRADIENTS IN NEAR BOTTOM WATERS

Temperature gradients in near bottom water were first measured in the western Pacific by precision thermometers which were attached to a rigid frame placed vertically on the bottom [*Gamutlov et al.*, 1960]. These thermometers were situated 0.5 and 5.5 meters from the sea bottom. Temperature gradients were often observed to exceed the adiabatic and varied from locality to locality. These data appear to indicate the heating of the water from the bottom, that is, by heat flow from the Earth's interior. Such heating apparently affects only a near bottom layer and is not normally detected by the usual hydrographic methods of using thermometers attached to a wire which is suspended from a ship. Positive temperature gradients have also been observed in the deep Atlantic by *Lister* [1963] and in the deep central Pacific

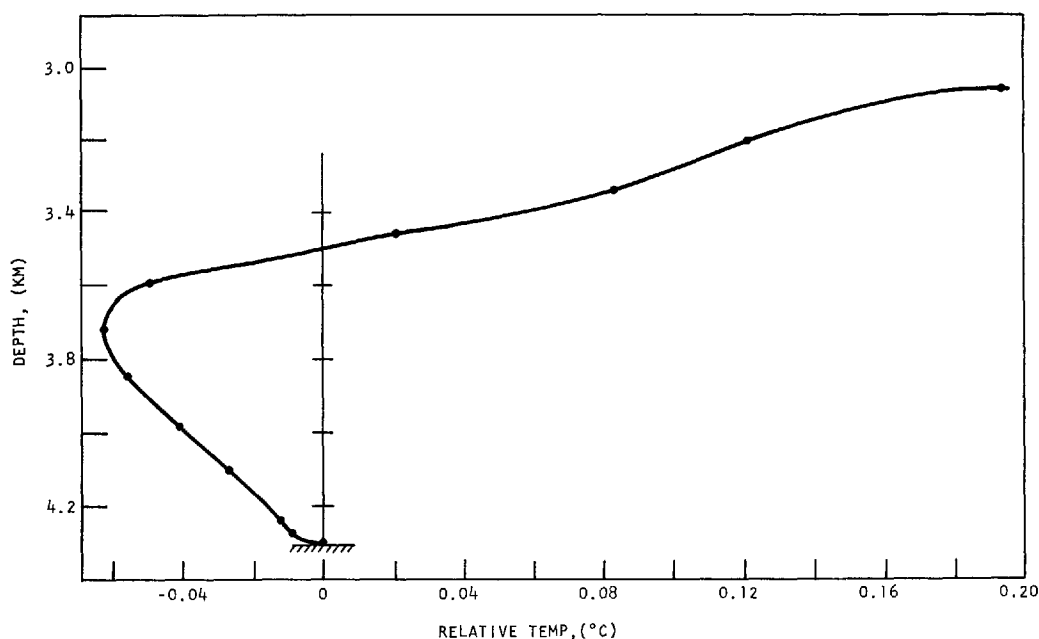


Fig. 1. Typical deep water temperature profile in the east central Pacific Ocean; Station Amph-10, 4°21'S, 125°31'W, 4300 meters deep.

by us. Recently, *Knauss* [1962] has noted the existence of a temperature anomaly of deep waters in the eastern Pacific. He suggests that this anomaly is related to high positive heat flow anomalies on the East Pacific Rise.

On the *Amphitrite* expedition of the Scripps Institution of Oceanography, 1963-1964, we measured temperature gradients in near bottom water of the eastern central Pacific with the same probe used for geothermal measurements in the sediment [see *Von Herzen and Langseth*, 1965]. These measurements were made at distances of 0.5 to 1000 meters from the bottom by a water thermistor which was outside the pressure case of the instrument. It was compared with other thermistors situated along a coring tube, and was also periodically compared with a calibrated resistance. The sensitivity and time constant were sufficient to measure the temperature gradient in the water as the instrument was being retrieved from the bottom.

Figures 1 through 4 show some results of these water temperature measurements in the central Pacific Ocean. Temperatures are plotted relative to those measured by the water thermistor a few centimeters above the bottom when the geothermal gradients in the sediment were being

measured. Water temperatures are estimated to have a general relative accuracy of  $\pm 0.002^\circ\text{C}$ , and the distance above the bottom can usually be measured to an accuracy of about  $\pm 3\%$ .

Figure 1 shows a typical profile in the deep central Pacific. Apart from the layer immediately adjacent to the bottom, the form of the temperature profiles is already well known (see, for example, the temperature data collected by *Fuglister* [1960]). The normal temperature decrease with depth is reversed several hundred meters above the bottom to an approximately adiabatic increase of temperature with depth. Closer to the bottom, usually within only a few meters, a rapid increase of temperature with depth is often observed to exceed the adiabatic rate.

Figures 2 to 4 illustrate some detailed measurements of water temperatures close to the bottom. For these measurements, the probe was lifted at the slowest speed of the winch and stopped for recording at discrete levels. These studies show that the region of super-adiabatic gradient sometimes extended for considerable distances above the sea floor, perhaps as much as 50 meters. Occasionally the temperature gradients appeared to reverse over small vertical

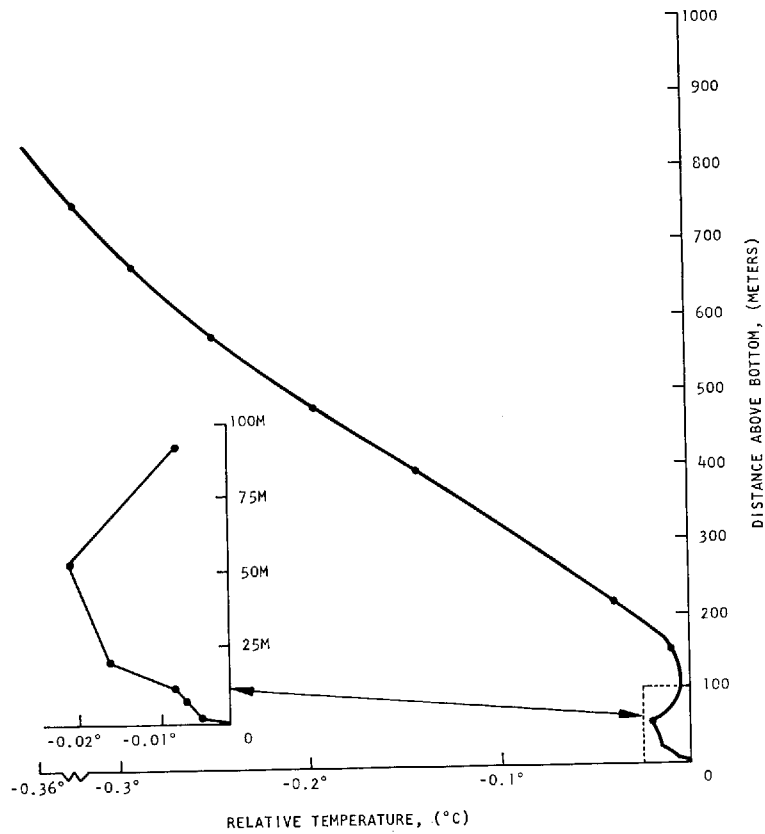


Fig. 2. Detailed profile of deep water temperatures in the east central Pacific Ocean showing complexity near the bottom; Station Amph-62,  $2^{\circ}15'N$ ,  $135^{\circ}08'W$ , 4380 meters deep.<sup>3</sup>

intervals, perhaps because of spurious effects from the instrumentation. However, the reality of a super-adiabatic gradient appeared to be confirmed by measurements at most stations.

#### 4. HEAT EXCHANGE BETWEEN OCEAN FLOOR AND NEAR BOTTOM WATER

The existence of a temperature gradient greater than the adiabatic in the near bottom ocean water suggests a thermodynamic inequilibrium and a possibility of free thermal convection. The solution to the stability problem of fluids is given in terms of the Rayleigh number defined as [Jeffreys, 1962, p. 345]

$$\mathcal{R} = \alpha g (\partial T / \partial z) H^3 / \kappa \nu \quad (4)$$

where  $\alpha$  is the coefficient of thermal expansion,  $g$  is acceleration of gravity,  $H$  is thickness of the

<sup>3</sup> Added in page proof. The authors have ascertained that the data on which this figure is based are not entirely reliable.

layer,  $\kappa$  is thermal diffusivity, and  $\nu$  is kinematic viscosity. These parameters for sea water are  $\alpha g = 10^{-1} \text{ cm/sec}^2 \text{ }^{\circ}\text{C}$ ,  $\kappa \nu = 10^{-3} \times 10^{-2} = 10^{-5} \text{ cm}^4 \text{ sec}^2$ . For the onset of convection in a fluid layer being heated from below,  $\mathcal{R}$  is of the order of  $10^3$ , depending on boundary conditions above and below. Taking  $(\partial T / \partial z) = 7 \times 10^{-4} \text{ }^{\circ}\text{C/cm}$ , the average geothermal gradient (see section 2), we have from (4)

$$H \approx \text{few centimeters}$$

for the values of the parameters given above. This conclusion is not sensibly changed by changing the values of the parameters, since they all enter the equation to the 1/4 power.

The actually observed temperature gradients near the bottom range from about  $10^{-4}$  to  $10^{-6} \text{ }^{\circ}\text{C/cm}$  in excess of adiabatic. In this case, (4) gives

$$\mathcal{R} = H^4 \text{ cm}^{-4} \text{ to } 10^{-2} H^4 \text{ cm}^{-4} \quad (5)$$

Tareev [1960] assumed the upper boundary of

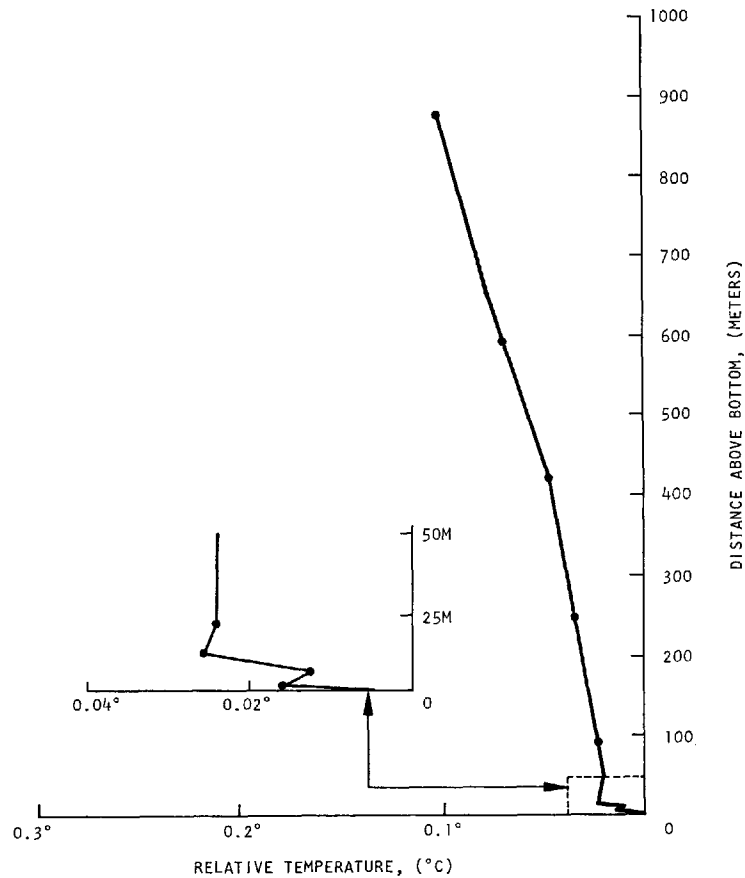


Fig. 3. Detailed profile of deep water temperatures in the east central Pacific Ocean showing complexity near the bottom; Station Amph-63, 3°34'N, 133°11'W, 4300 meters deep.

the layer of instability to occur where there is a zero temperature gradient. It was observed at distances of 10 meters (Figure 3) and 8 meters (Figure 4) above the bottom. The Rayleigh number computed on this basis is of the order of  $10^{10}$  to  $10^{12}$  for  $H = 10$  meters, and  $\mathcal{R} = 10^{14}$  to  $10^{16}$  for  $H = 100$  meters. These Rayleigh numbers are large enough for the flow to be turbulent [Jakob, 1949].

The possibility of turbulent convection in the near bottom water is important for many oceanographic problems, such as oceanic circulation, sedimentation, and the disposal of radioactive wastes in oceans.

Heat transfer in the near bottom water may be influenced, not only by free thermal convection, but also by salinity convection or water movement initiated by other mechanisms. The

salinity convection may result from a decrease of salinity near the bottom, perhaps because of the absorption of dissolved salts in sediments. Salinity gradients have been observed in the near bottom water at many western Pacific localities [Gamutlov *et al.*, 1960].

An estimate of the influence of the flow of the water above the sediments on measured heat flows can be made from the following model. Assume that temperature inhomogeneities are present in the water at a particular locality. Fluctuations of temperature over the bottom can arise either from the convective instability of the bottom water or from horizontal advection of the inhomogeneities past the locality by deep ocean currents. Consider fluctuations of amplitude  $A$  and circular frequency  $\omega$ . We find that the heat flux at the surface has a fluctuating

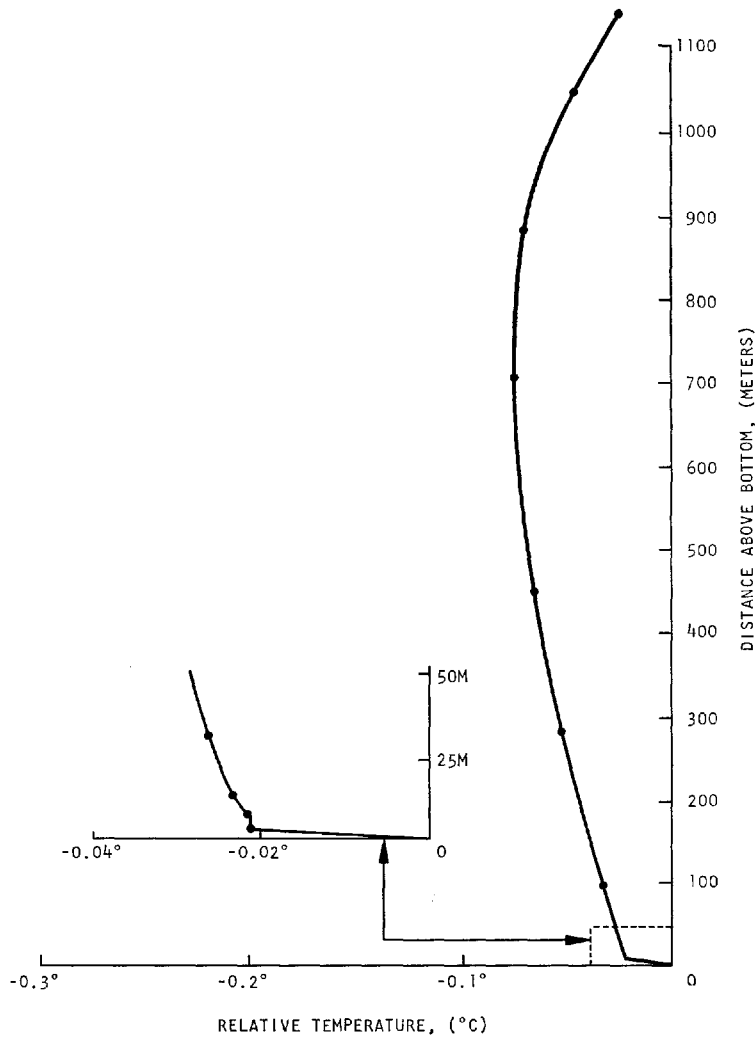


Fig. 4. Detailed profile of deep water temperatures in the east central Pacific Ocean showing complexity near the bottom; Station Amph-64, 8°34'N, 133°39'W, 4975 meters deep.

component of amplitude [*Carlsaw and Jaeger*, 1959, p. 67]

$$q_0 = \sqrt{2} K A (\omega/2\kappa)^{1/2} \quad (6)$$

Let us find  $A$  such that the amplitude  $q_0 = 1$  ucal/cm<sup>2</sup> sec, say, for which the heat flux would vary from 0 to 2 ucal/cm<sup>2</sup> sec. For a period of 1 day, with  $K \approx 1$  mcal/°C cm sec,  $\kappa \approx 10^{-8}$  cm<sup>2</sup>/sec for sea water,  $A \approx 0.01^\circ\text{C}$ . For a period of 100 days,  $A \approx 0.1^\circ\text{C}$ . This would seem to be the range of temperature fluctuations to be expected from consideration of the observations. For periods of 1 day, the temperature fluctuations penetrate only a few tens of centimeters

into the sediment, so that sensors several meters deep in the sediments would not be seriously affected. For periods of 100 days, the temperature fluctuations penetrate deeper into the sediment and may be a source of error for most probes. However, the general constancy of temperature gradient with depth for multiple sensing probes [*Von Herzen and Langseth*, 1965] implies that the effect is not widespread.

The flow velocities involved can be estimated. For convective motion, assume that the bottom layer of thickness of the order of 10 meters is overturned in 100 days. Hence, we require an

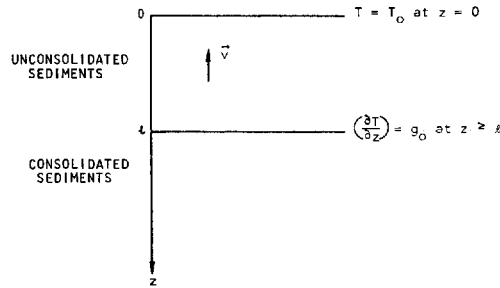


Fig. 5. Schematic diagram illustrating theoretical model of interstitial water movement and boundary conditions of unconsolidated sediments overlying consolidated sediments.

average vertical velocity of the order of  $10^{-4}$  cm/sec. On the other hand, for an advective situation, noting that transverse velocities in a turbulent flow are of the order of 10% of the longitudinal velocities, and considering a current of thickness of the order of 100 meters (see Figure 2), a turnover time of 100 days corresponds to a horizontal velocity of the order of  $10^{-2}$  cm/sec. These values are comparable to those given by *Knauss* [1962] for near bottom currents in the Pacific. He finds velocities of the order of 0.05 to 0.1 cm/sec.

##### 5. THE INFLUENCE OF HEAT TRANSFER BY MIGRATION OF INTERSTITIAL WATER IN SEDIMENTS

*Bullard et al.* [1956] and later *Von Herzen and Uyeda* [1963] examined the heat transfer in sediments by free thermal convection of interstitial water. *Bullard et al.* [1956] also studied the possible effect of the churning activities of burrowing organisms. These studies resulted in very approximate formulas, which implied that velocities of convection of about 50 cm/day were needed to cause any noticeable effect on geothermal gradients. The occurrence of such high velocities in the sediments was considered to be unlikely.

The existence of free thermal convection of such high velocity in the interstitial water also seems unlikely to us, but we shall investigate a similar problem in which much lower velocities seem to be important. This is the uniform expulsion of water from the sediments, resulting in an upward migration of the interstitial water. It could result, for example, from the slow compaction of sediments over geologic time.

We assume that the heat is transported not

only by thermal conduction, where the heat flow is determined by the value  $q = -K(\partial T/\partial z)$ , but also by the mass movement of interstitial water from deeper and thus warmer sedimentary layers. If the velocity of water migration is  $\mathbf{v}$  ( $\mathbf{v}$  is positive for downward movement, Figure 5), then the expression of total heat transfer by conduction and mass movement is

$$q^* = -K(\partial T/\partial z) - v\rho cT \quad (7)$$

where  $c$  = specific heat capacity,  $T$  = temperature of the moving water, and  $\rho$  = water density. In steady state (as a result of the continuous flow of heat and water), we have

$$\nabla \cdot \mathbf{q}^* = 0 \quad (8)$$

With  $v$  and  $K$  being constants, we obtain

$$K(\partial^2 T/\partial z^2) + v\rho c(\partial T/\partial z) = 0 \quad (9)$$

We assume that these processes occur in the layer of soft and unconsolidated sediments with high permeability. We denote the thickness of this layer as  $l$ . We solve (9) under the following boundary conditions (Figure 5):

$$T = T_0 \quad \text{at } z = 0 \quad (10)$$

$$\partial T/\partial z = g_0 \quad \text{at } z \cong l \quad (11)$$

Integrating (9) and applying (11) we obtain the following expression for the gradient in the unconsolidated sediments:

$$\partial T/\partial z = g_0 \exp(pl) \exp(-pz) \quad (12)$$

where

$$p = v\rho c/K \quad (13)$$

A distribution of temperature, in conformity with the gradient caused by interstitial water,

can be obtained by integration of (12) under condition 10:

$$T - T_0 = [g_0 \exp(pl)/p] [1 - \exp(-pz)] \quad (14)$$

From (12) we have the gradient on the boundary between sediments and water ( $z = 0$ ):

$$(\partial T/\partial z)|_{z=0} = g_0 \exp(pl) \quad (15)$$

From (15) we conclude that, as a result of migration of interstitial water, the gradient observed near the surface of the sediments would change by the factor  $\exp(pl)$ . If we assume that the gradient increased by 10 times, i.e.,

$$\exp(pl) = 10 \quad (16)$$

then the value of  $(pl)$  will be, by logarithmic calculation,

$$pl = v\rho cl/K = 2.3 \quad (17)$$

We take the values of the parameters for sea water as:  $\rho = 1 \text{ g/cm}^3$ ,  $c = 1 \text{ cal/}^\circ\text{C g}$ ,  $K = 1.3 \text{ mecal/}^\circ\text{C cm sec}$ , and thus, for a thickness of the sediment layer  $l = 10$  meters, we obtain  $v = 0.5 \times 10^{-5} \text{ cm/sec}$ , or  $0.1 \text{ cm/day}$ . For sediment thickness  $l = 100$  meters, we obtain  $v = 10^{-7} \text{ cm/sec}$ , or about  $0.01 \text{ cm/day}$ . These values are smaller by 100 or even 1000 times than those obtained by Bullard *et al.* [1956] and Von Herzen and Uyeda [1963] on the basis of more approximate estimations. We conclude that very small velocities of migration of interstitial water could make the geothermal gradient near the surface of sediments 10 times greater than the normal, although it would decrease quickly with depth.

For steady-state conditions, it would not be expected that the rate of expulsion of interstitial water would be greater than the rate of sedimentation. Maximum measured rates of sedimentation over most of the deep sea floor range between 1 and 10 cm per 1000 years, which is 3 or 4 orders of magnitude less than the rates used in the above calculations. It seems unlikely that such slow rates could significantly affect the temperature distribution in the unconsolidated sediments.

This conclusion appears to be substantiated by temperature measurements in a hole drilled for the preliminary Mohole project, which penetrated more than 150 meters of unconsolidated sediments [Von Herzen and Maxwell, 1964]. The temperature gradient and heat flow ap-

peared constant over the depth of the hole, and the results agreed well with heat flow measurements in the same vicinity made with a short (2-meter) probe from oceanographic vessels. It will be of interest to look for the effect in deep holes drilled in the ocean floor at other localities.

## 6. SUMMARY

As has previously been deduced by most investigators, the outward flow of heat through the Earth's surface must have its origin in the deep interior. Hence data on the variability of heat flow over the Earth's surface could give information on different parameters affecting its interior, e.g., temperature, heat production, heat transfer, and thermal history. The numerous heat flow measurements on the ocean floor have demonstrated a large variability in values in these regions. However, from repeated and nearby measurements in some areas, some of this variability appears to be of a local origin.

Some of this local variability appears to result from local sources of heat not far beneath the sea floor, such as linear magmatic intrusions or other volcanic events [e.g., Von Herzen and Uyeda, 1963; Von Herzen and Maxwell, 1964]. On the other hand, other sources of local variations may be imposed by the environment near the ocean floor in which heat exchange takes place. Some recent measurements in the water close to the ocean floor in the Pacific indicate vertical temperature gradients considerably in excess of adiabatic, implying possible gravitational instability in near bottom water layers. If these super-adiabatic gradients result from the heat flow itself, quasi-periodic overturns of the unstable near bottom water when a critical point is reached would produce a temperature at the sediment-water interface which is variable in time. This would give a certain 'noise' to the heat flow values, which would be more serious for measurements made with short probe than for those made with a long probe. At present there is no evidence that such overturns take place, other than the frequently large and variable temperature gradients in the water near the bottom. The average heat flow from the interior implies convectional currents in near bottom water of  $10^{-4}$  to  $10^{-2} \text{ cm/sec}$ , which may be important for other oceanographic phenomena.

Variable movements of water near the ocean

floor may also be caused by variable currents which flow over a topographically rough ocean floor. Such currents have been measured to attain horizontal velocities of the order of 10 cm/sec, and vertical velocities of the same order of magnitude are also possible. These variations could produce a variable rate of heat exchange with the ocean floor and, hence, a variable effective temperature at the ocean floor. Also, advected water masses of slightly different temperatures could produce the same effects.

Another possible variable in the oceanic heat flow measurements is the migration of interstitial water in the porous sediments. Very small velocities, of the order of 1 mm/day, are seen to produce significant errors in the measurements. Nevertheless, the presently existing measurements show no evidence of such movement, and the steady-state expulsion of water by the accumulation of sediment on the ocean floor would have much smaller rates.

The variable perhaps most thoroughly investigated by theoretical techniques is the geometric effect of rough topography (see chapter 4, by Langseth, in this volume). Variations of 50% are not uncommon for some typical dimensions and slopes of sea floor features. Verification has been obtained with some models by laboratory experiments, but field measurements correlated with known detailed topography at sea are difficult to achieve. In summary, heat flowing from the deep interior may differ from measured values owing to several disturbances in the environment on and near the ocean floor. To obtain accurate values, individual measurements should have additional control to determine the magnitude of these disturbances, or a sufficient number of measurements should be made at a locality to reduce the effect of random variables.

*Acknowledgments.* We wish to thank the Soviet Geophysical Committee and the Scripps Institution of Oceanography for making this joint work possible on board Scripps' R. V. *Argo*. We are also grateful to C. S. Cox, J. W. Elder, and J. Reitzel for their critical reviews of the manuscript.

This research was supported by the Office of Naval Research under contract Nonr 2216(23) and by the National Science Foundation under grant NSF-G19239.

#### REFERENCES

- Bullard, E. C., A. E. Maxwell, and R. Revelle, Heat flow through the deep sea floor, *Advan. Geophys.*, 3, 153-181, 1956.
- Carslaw, H. S., and J. C. Jaeger, *Conduction of Heat in Solids*, second edition, Oxford University Press, London, 1959.
- Fuglister, F. S., *Atlantic Ocean Atlas*, Woods Hole Oceanographic Institution, Woods Hole, Mass., 1960.
- Gamutilov, A. E., A. D. Dobrovolsky, D. D. Sabinin, and G. B. Udinstev, Opit izuchenia temperaturi i solenosti pridonnoi vodi pri pomezshehi trubki PTR-57, *Tr. Inst. Okeanol. Akad. Nauk SSSR*, 39, 1960.
- Jakob, M., *Heat Transfer*, John Wiley & Sons, New York, 1949.
- Jeffreys, H., *The Earth*, fourth edition, Cambridge University Press, Cambridge, 1962.
- Knauss, J., On some aspects of the deep circulation of the Pacific, *J. Geophys. Res.*, 67, 3943-3954, 1962.
- Lee, W. H. K., Heat flow data analysis, *Rev. Geophys.*, 1, 449-479, 1963.
- Lee, W. H. K., and G. J. F. MacDonald, The global variation of terrestrial heat flow, *J. Geophys. Res.*, 68, 6481-6492, 1963.
- Lister, C. R. B., Geothermal gradient measurement using a deep sea corer, *Geophys. J.*, 7, 571-583, 1963.
- Lubimova, E. A., and V. A. Magnitsky, Thermoelastic stresses and the energy of earthquakes, *J. Geophys. Res.*, 69, 3443-3448, 1964.
- MacDonald, G. J. F., The deep structure of continents, *Rev. Geophys.*, 1, 587-665, 1963.
- Nason, R. D., and W. H. K. Lee, Heat flow measurements in the north Atlantic, Caribbean, and Mediterranean, *J. Geophys. Res.*, 69, 4875-4883, 1964.
- Sverdrup, H. U., M. W. Johnson, and R. H. Fleming, *The Oceans: Their Physics, Chemistry, and General Biology*, Prentice-Hall, Englewood Cliffs, N. J., 1942.
- Tareev, B. A., Contribution to a theory of convective circulation in oceanic deeps, *Bull. Acad. Sci. USSR, Geophys. Ser., English Transl.*, 1960 (7), 683-687, 1960.
- Von Herzen, R. P., and M. G. Langseth, Present status of oceanic heat-flow measurements, *Physics and Chemistry of the Earth*, vol. 6, edited by S. K. Runcorn, Pergamon Press, London, in press, 1965.
- Von Herzen, R. P., and A. E. Maxwell, Measurements of heat flow at the preliminary Mohole site off Mexico, *J. Geophys. Res.*, 69, 741-748, 1964.
- Von Herzen, R., and S. Uycda, Heat flow through the eastern Pacific ocean floor, *J. Geophys. Res.*, 68, 4219-4250, 1963.
- Wooster, W. S., and G. H. Volkmann, Indications of deep Pacific circulation from the distribution of properties at five kilometers, *J. Geophys. Res.*, 65, 1239-1249, 1960.

(Manuscript received August 1, 1964; revised October 15, 1964, and November 2, 1964.)

## Chapter 6. Review of Heat Flow Data <sup>1</sup>

WILLIAM H. K. LEE

*Institute of Geophysics and Planetary Physics  
University of California, Los Angeles*

SEIYA UYEDA <sup>2</sup>

*Department of Geophysics, Stanford University, Stanford, California*

*Abstract.* All available heat flow data (about 2000 observations) are reviewed and analyzed. Statistical methods are used to summarize the data, and numerical techniques are developed to find their essential features. Analysis of nearby and repeated measurements suggests that regional heat flow variations  $>0.2 \mu\text{cal}/\text{cm}^2 \text{ sec}$  are significant. At the 95% confidence level, the world's mean heat flow is  $1.5 \pm 10\% \mu\text{cal}/\text{cm}^2 \text{ sec}$ , and the average over the continents does not differ significantly from that over the oceans. Heat flow results are well correlated with major geological features. On land, the average and standard deviation of heat flow values are  $0.92 \pm 0.17$  from Precambrian shields,  $1.23 \pm 0.4$  from Paleozoic orogenic areas,  $1.54 \pm 0.38$  from post-Precambrian non-orogenic areas, and  $1.92 \pm 0.49$  from Mesozoic-Cenozoic orogenic areas. At sea, they are  $0.99 \pm 0.61$  from trenches,  $1.28 \pm 0.53$  from basins, and  $1.82 \pm 1.56$  from ridges. On a large scale, a negative correlation between heat flow and gravity is found.

### 1. INTRODUCTION

The outflow of heat from the Earth's interior by *conduction* is, energy-wise, the most impressive terrestrial phenomenon. Its present rate of about  $2 \times 10^{20}$  cal/year is orders of magnitude greater than the energy dissipation of earthquakes or heat loss from volcanic eruptions. The study of terrestrial heat flow is fundamental in Earth sciences. It is the most direct observation of the thermal state of the Earth, and geothermal processes play an important role in all theories of the Earth's origin, constitution, and behavior.

*Surface heat flow* from the Earth's interior is the rate of heat transferred across the Earth's surface per unit area per unit time. The unit of heat flow is  $\mu\text{cal}/\text{cm}^2 \text{ sec}$  and will be omitted in this chapter whenever convenient.

All heat flow data reviewed in this chapter are measurements of surface heat flow by *thermal conduction*. The neglect of thermal convection and radiation is justified for most areas of the world, since the upper crust is solid and at a rather low temperature. On land, heat flow observations from geothermal areas are ignored

in the data analysis, because convection and radiation may play an important role (see chapter 8 by Elder, in this volume). At sea, this rejection of data is not possible because the nature of oceanic geothermal areas is poorly known.

Heat flow by conduction,  $\mathbf{q}$ , in a solid is found *experimentally* to be proportional to the temperature gradient  $\nabla T$ :

$$\mathbf{q} = -K \cdot \nabla T \quad (1a)$$

where  $K$  is called the 'thermal conductivity.' In general, the thermal conductivity is a second-rank tensor quantity, but it is a constant for a *homogeneous* and *isotropic* solid. The *surface* heat flow by *conduction*,  $q$ , is therefore the product of thermal conductivity and vertical temperature gradient:

$$q = K(\partial T/\partial z) \quad (1b)$$

where the flow is vertically outward.

To determine surface heat flow by conduction at a location, we measure (1) temperatures through some finite interval of depth and (2) conductivities of the same interval either in situ or in a laboratory on an appropriate number of samples. Techniques for heat flow measurements on land and at sea have been reviewed in chapters 3 and 4 by Beck and Langseth, respectively.

To obtain meaningful values of heat flow from the Earth's interior, measurements of undis-

<sup>1</sup> Publication 409, Institute of Geophysics and Planetary Physics, University of California, Los Angeles.

<sup>2</sup> On leave from Geophysical Institute, University of Tokyo, Tokyo, Japan.

turbed temperatures and representative thermal conductivities are essential. These requirements are difficult to meet in practice, and consequently reliable heat flow values are obtained only through laborious efforts. Modern measurements on land were first made in 1939 by E. C. Bullard and A. E. Benfield, and at sea in 1952 by E. C. Bullard, R. Revelle, and A. E. Maxwell. More than 90% of all existing heat flow measurements were published only after 1960 by R. P. Von Herzen, M. G. Langseth, and many others. Recently Lee [1963] has summarized the data up to early 1963. Statistical analyses of data have also been attempted by Lee [1963] and Lee and MacDonald [1963].

In this chapter we will briefly review and analyze all available heat flow data. Local details are often omitted because abundant literature on heat flow is available (more than 100 papers and theses). Statistical methods are used to summarize the data, and numerical techniques are developed to find their essential features. The chapter closes with a brief summary of the most important results of the investigation. An up-to-date listing of heat flow data with extensive references is given in the appendix. The next chapter, by MacDonald, in this volume, in which geophysical deductions from heat flow observations are presented, is a continuation of the present one.

## 2. HEAT FLOW DATA

As of the end of 1964, about 2000 individual heat flow observations were available (approximately 50% of them published, 30% in press, and 20% unpublished). Excluding unpublished values, preliminary results, very crude estimates, and observations published prior to 1939, over 1300 of the available data have been catalogued by us. Almost all plottings and computations in this chapter have been based entirely on these catalogued data. They are listed as 1162 entries in the Appendix, after values from closely-spaced stations (usually less than 10 km apart) have been averaged.

In the computations, locally anomalous or questionable values have also been discarded, so that only 1043 values were analyzed. In a few cases, some values from the unpublished data were also used, bringing the total number of analyzed data to 1150 values. Criteria for select-

ing data for the analysis will be discussed later at the beginning of sections 3 and 4.

### 2.1 Geographical Distribution of Heat Flow Observations

It is obvious (see Figure 1) that the geographical distribution of heat flow data is very uneven. There are many more oceanic heat flow values than continental ones: 89% versus 11%. Since the oceans occupy some 71% of the Earth's surface, we have about 3 times more data per unit area at sea than on land. Although observations are fairly well distributed over the oceans, measurements tend to be concentrated over anomalous regions, such as the East Pacific Rise. The large gaps are in the massive continental and high latitude regions; there are no measurements in South America, Antarctica, and most of Asia and Africa. The sites of heat flow stations at sea can be randomly chosen along the ship tracks. However, existing measurements have usually been made where the ocean bottom is relatively flat to ensure penetration of the probe. The land stations are mostly in pre-existing oil wells and mines which may not be representative of the continents in general. Locations of heat flow stations are therefore selective, and consequently data analysis is extremely difficult.

### 2.2 Application of Statistics in Summarizing Data

Statistical methods deal with the presentation, analysis, and interpretation of numerical data. A useful statistical manual is *Crow et al.* [1960], which defines the terms we used.

Histogram, modes, mean, and standard deviation are most useful for summarizing a set of numerical data  $\{x_1, x_2, \dots, x_n\}$ . A histogram gives a visual picture of all the data of  $\{x\}$ , and the modes (because there is often more than one peak in the histogram) give the most likely occurring intervals of  $x$ . By using Tchebyshev's inequality [Alexander, 1961, p. 64] with the mean ( $\bar{x}$ ) and standard deviation ( $s$ ), we can easily specify the *center* and *dispersion* of  $\{x\}$ : at least  $(1 - 1/k^2) \times 100\%$  of the data fall within the interval  $(\bar{x} \pm ks)$  for any value of  $k$  and for *any* distribution of  $x$ . In the text, the mean and standard deviation is given in the form

$$\bar{x} \pm s \text{ s.d.} \quad (2a)$$

where s.d. indicates that the value  $s$  preceding it is the standard deviation of  $x_i$ ,  $i = 1, \dots, n$ , from the sample mean  $\bar{x}$ .

In the following sections, a histogram and a few statistics of each set of data will be presented in summarizing numerical values. Although *weighted statistics* can be introduced, every value of  $\{x\}$  is usually considered to be of equal importance, because a weighting factor is hard to assign. Most plottings and all computations are programmed on an IBM 7094 computer in Fortran language.

The set of data  $\{x_1, x_2, \dots, x_n\}$  is usually a *sample* drawn from a *population*  $\{x_1, x_2, \dots, x_m\}$ , where  $m \gg n$ . We are obviously interested in estimating the population characteristics from the sample. If the sample is chosen in such a way that every individual in the population has an equal chance of being chosen, then the sample is called a *random sample* and statistical methods are applicable. In particular, if the population is also *normally distributed*, then at  $100(1 - p)\%$  confidence level, the population mean is

$$\bar{X} = \bar{x} \pm t(p,f)s/\sqrt{n} \quad (2b)$$

where  $t(p,f)$  is the student  $t$  deviate from  $f = n - 1$  degrees of freedom, the probability of exceeding which is  $p$ ; and  $s/\sqrt{n}$  is the standard error.

Suppose we wish to determine the mean heat flow for a region A defined by

$$\bar{q} = \int_A q da / \int_A da \quad (2c)$$

from a sample of heat flow observations  $\{x_1, x_2, \dots, x_n\}$ . If it is a random sample, then we can generally claim that at 95% confidence level

$$\bar{q} = \bar{x} \pm 2s/\sqrt{n} \quad (2d)$$

by using (2b). Normality is, of course, assumed for the population, but it is not critical because deviation from normality will not greatly invalidate (2d);  $n$  is preferably greater than 20, but  $t \approx 2$ , unless  $n$  is less than 5.

Because heat flow stations are selective and heat flow values are not exact (due to measurement errors), there are *additional* error terms in equation 2d. Cochran [1953, pp. 7-10] has considered the effect of a bias in the sampling

procedure. Assuming normality, he found that the effect of bias on the accuracy of an estimate is negligible if the bias ( $B$ ) is less than one-tenth of the standard deviation of the estimate ( $\sigma$ ); and at  $B = \sigma$ , the total probability of error is 0.17, about 3 times the value of 0.05 given in equation 2d. Unfortunately, the amount of bias cannot be properly estimated from the existing heat flow data. A statistically designed heat flow survey over a given region will be useful in estimating the bias and should be made in the future. Furthermore, measurement errors (discussed in the next section) may be even more serious than the sampling bias. For these reasons, we cannot assign confidence limits of heat flow means by equation 2d. Although standard error is usually computed for each set of data and tabulated together with other statistics, one must be cautious in interpreting its significance.

### 2.3 Reliability of Heat Flow Data

In general, *instrumental* errors of heat flow measurements seldom exceed  $\pm 10\%$ . Most observers are careful in testing their equipment, but have little control over effects of the environment. Instruments employed for measurements on land differ widely. Therefore it is difficult to give a comprehensive review of instrumental errors in land observations. Instrumental errors for measurements at sea have been reviewed by *Von Herzen and Langseth* [1965]. They conclude that the error of individual heat flow measurements at sea varies with the geothermal gradient, the sediments covering the bottom, and the techniques used. When the geothermal gradient is average ( $6 \times 10^{-4}$  °C/cm) and the bottom sediment is uniform with depth, the error is no more than 10% for a good station. Otherwise, errors up to 20% are possible.

To ascertain the significance of a heat flow value, measurement errors (due to instrumentation and local effects) must be known. Such errors can be estimated if repeated measurements have been made under the same conditions. Unfortunately repeated observations were very seldom made at the same heat flow station. However, a general estimate of the measurement errors can be obtained by analyzing repeated and closely spaced observations.

Table 1 summarizes the statistics of  $\{x_i - y_i\}$ ,

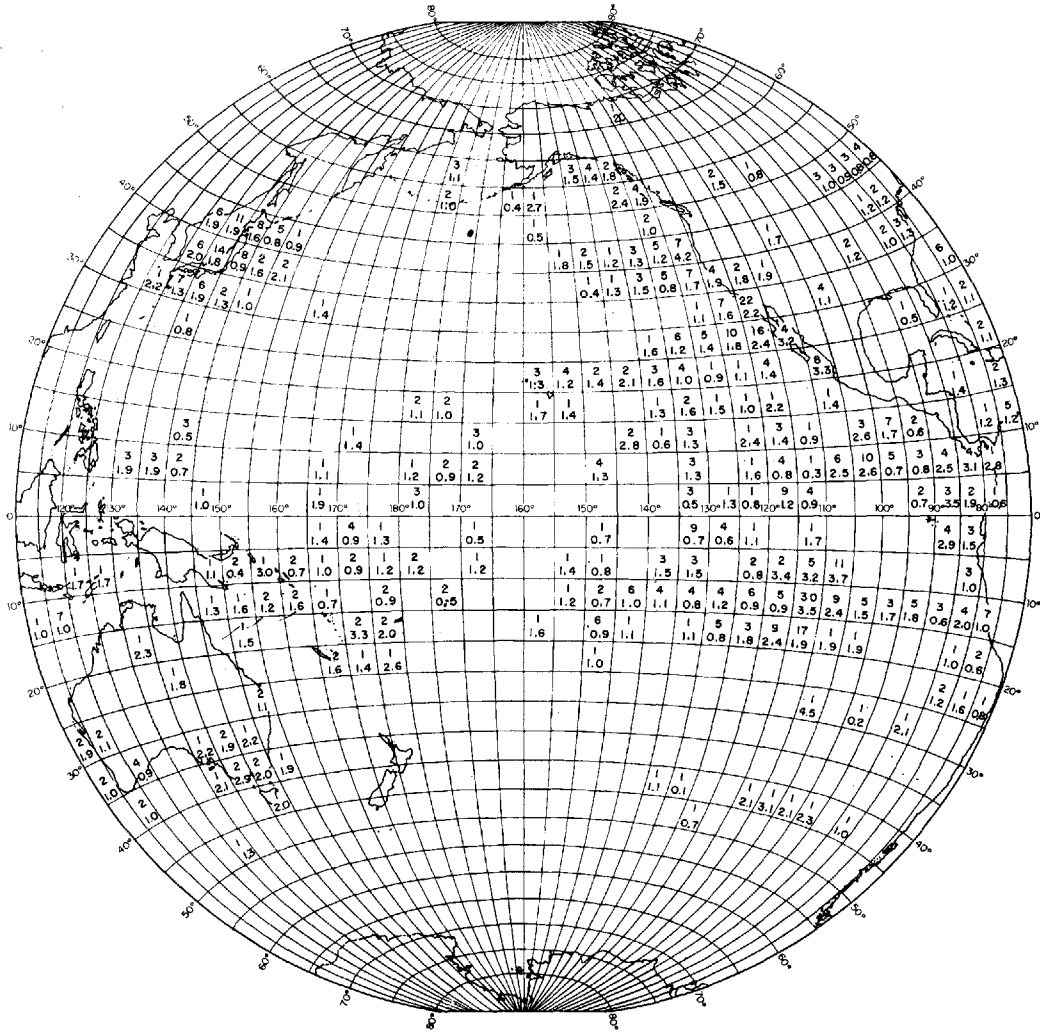


Fig. 1a. Number and arithmetic mean of analyzed heat flow data in  $5^\circ$  by  $5^\circ$  grid.

$i = 1, 2, \dots, n$ , for pairs of heat flow stations that are less than 10 km apart and have heat flow values of  $x_i$  and  $y_i$ . At sea, pairs of such stations are almost indistinguishable in position, and thus they may be considered as pairs of repeated observations. On land, if heat flow variations within 10 km are due to some geological effects (e.g. volcanism), these stations have been excluded from the analysis. It is therefore not surprising that  $\{x - y\}$  is less scattered on land than at sea (see Figure 2). Because land measurements have not usually been repeated by different research groups, some additional systematic errors may be present, and thus  $\{x - y\}$  on land may actually be more

scattered than is shown. For simplicity, we will consider the case at sea as applicable to both land and sea and will estimate the measurement errors as follows.

If  $V_x$  and  $V_y$  are the variances due to measurement errors for  $\{x\}$  and  $\{y\}$  respectively, then the variance of  $\{x - y\}$  is

$$V_{x-y} = V_x + V_y \quad (2e)$$

Let us assume that the measurement errors are essentially the same for  $x$  and  $y$ , so that  $V_x = V_y$ . Then

$$\sigma_x = \pm (1/\sqrt{2}) \sigma_{x-y} \quad (2f)$$

where  $\sigma$ 's denote standard deviations.

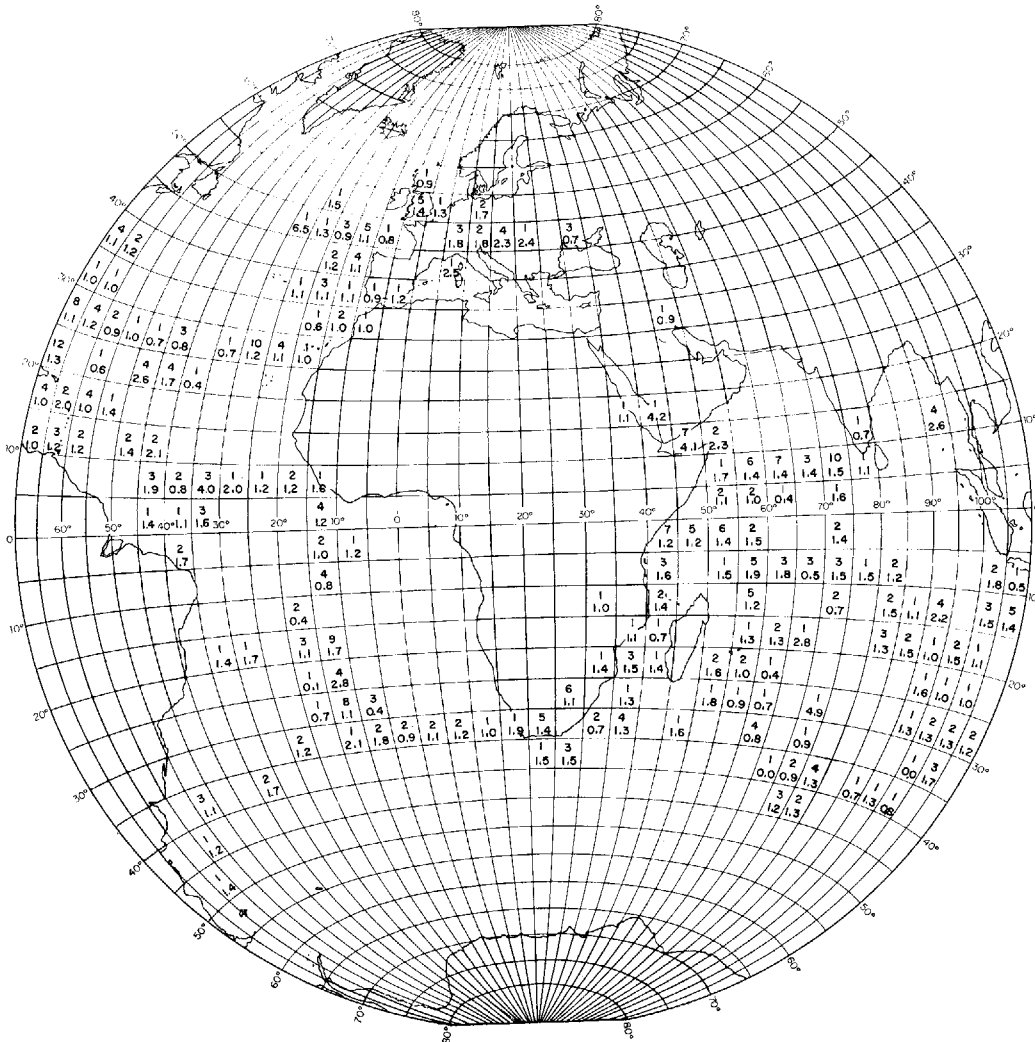


Fig. 1b. Number and arithmetic mean of analyzed heat flow data in 5° by 5° grid.

From Table 2

$$\sigma_x = \pm (1/\sqrt{2}) 0.47 = \pm 0.33 \quad (2g)$$

and hence

$$\sigma_{\bar{x}} = \sigma_x/\sqrt{n} = \pm 0.33/\sqrt{n} \quad (2h)$$

In other words, because of measurement errors the mean heat flow value for a region determined from  $n$  observations can be in error by  $\pm 0.66/\sqrt{n}$  at a 95% confidence level (assuming normality). For  $n = 10$ , this error is about 0.2  $\mu\text{cal}/\text{cm}^2 \text{ sec}$ . Therefore, it is reasonable to assume that regional heat flow variations  $> 0.2 \mu\text{cal}/\text{cm}^2 \text{ sec}$  are significant. Here regional heat flow variations refer to differences in re-

gional mean heat flow values, each of which is determined from a sufficient number ( $> 10$ ) of observations.

As remarked in section 2.2, we cannot simply apply equation 2d because of biased sampling and measurement errors. The standard error calculated from a biased sample of measured values may have already included some of the measurement errors and biased sampling errors. However, we have no sure way of knowing from the existing heat flow data. For this reason, we seldom consider the variations of heat flow means in terms of their computed standard errors.

TABLE 1. Statistics of  $\{x_i - y_i\}$  for Pairs of Heat Flow Stations Less Than 10 km Apart with Heat Flow Values  $x_i$  and  $y_i$  in  $\mu\text{cal}/\text{cm}^2 \text{ sec}$

	Number of Pairs	Arithmetic Mean	Standard Deviation	Standard Error
Land	74	-0.01	0.15	0.02
Ocean	49	0.04	0.47	0.07

### 3. REVIEW OF HEAT FLOW DATA ON LAND

Measuring heat flow on land is rather difficult. Temperature disturbances which affect the heat flow include effects of drilling the hole, variations of surface temperature, past climatic changes, uplift and erosion, topographic and conductivity irregularities, water circulation, and volcanic activity. Knowledge of the local geology is needed to determine some of these disturbances, and, to avoid most of them, it is essential that holes for measurements be deep (>300 meters) and preferably through hard rocks. These disturbances, of which water circulation is the most troublesome, vary from location to location and may require corrections of magnitude comparable to the actual heat flow value. When corrections are large, the data are considered to be unreliable in this chapter. When corrections are small, uncorrected values are adopted, unless the corrected values are favored by the original investigators.

Determining a representative conductivity in the laboratory presents even greater problems because of the difficulty in selecting and preparing adequate samples. Furthermore, conductivity may vary tens of per cent from rock to rock or even from sample to sample of an apparently uniform rock. Techniques of measuring conductivity in situ are in a state of development, and the accuracy of the results obtained from them is still uncertain.

Techniques of heat flow measurement have been reviewed in chapter 3, by Beck, in this volume, and mathematical treatments for various corrections have been given in chapter 2 by Jaeger. The quality of heat flow data on land varies from crude estimates to elaborate determinations. The data have been classified into categories *A*, *B*, and *C*. Category *A* data are derived from 'good' stations, where temperature and conductivity were well measured and disturbances were minor. Category *B* stations are

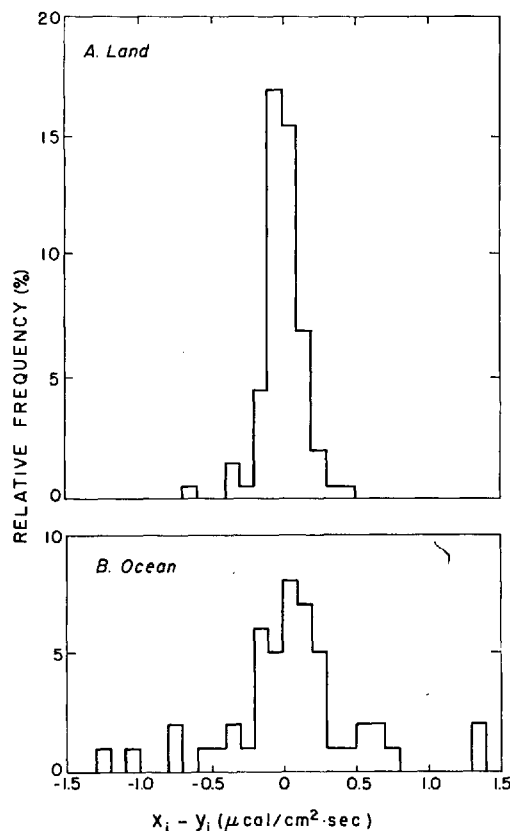


Fig. 2. Histograms of  $\{x_i - y_i\}$  for pairs of heat flow stations less than 10 km apart with heat flow values  $x_i$  and  $y_i$ : (a) for land data and (b) for oceanic data.

'fair' ones because conductivity may have been measured from rock samples nearby, and/or some disturbances may have affected the results. Category *C* data are questionable; they may have been considered to be unreliable by original investigators, may lack conductivity measurements, and/or disturbances may have greatly affected the results. All category *C* data have been rejected from the analysis.

We wish to emphasize, however, that this classification of data is rather subjective, and some data have been classified as lower in quality because of lack of information.

Heat flow data on land are reviewed geographically according to continents. For each region, the literature is briefly reviewed and the data are summarized and discussed with respect to the major features of the continents. Heat flow values are plotted in maps with generalized geology and topography and are alphabetically

TABLE 2. Heat Flow Values in Africa

*MD*, maximum depth in meters; *N*, conductivity samples; *q*, heat flow; *q\**, corrected heat flow; *DC*, data class

Data No.	Station	Type	<i>MD</i>	<i>N</i>	<i>q</i>	<i>q*</i>	<i>DC</i>	Remarks	Reference
Nyasaland									
0018	Lake Nyasa	Lake			~1		<i>B</i>	About 20 measurements using oceanic techniques; disturbances suspected for some measurements	Von Herzen, 1964b
South Africa									
Cape of Good Hope									
0011	Bothadale	Borehole	1457	85	1.28	1.34	<i>A</i>	In southern limit of Karroo system; heat flow increases with depth; climatic correction applied	Gough, 1963
0004	Dubbeldevlei	Borehole	1496	4	1.52		<i>A</i>	From 'old granite' section (lower 670 m) only	Bullard, 1939
0012	Kalkkop	Borehole	300	24	1.21	1.31	<i>A</i>	See Bothadale; hole too shallow to indicate heat flow increase with depth	Gough, 1963
0010	Koegelfontein	Borehole	851	59	1.45	1.57	<i>A</i>	See Bothadale	Gough, 1963
0009	Sambokkraal	Borehole	1760	102	1.39	1.44	<i>A</i>	See Bothadale	Gough, 1963
Orange Free State									
0001	Jacoba-Doornhoutrivier				0.96		<i>A</i>	Average value of 0001A and 0001B; in South African Shield	Bullard, 1939
	A. Jacoba	Borehole	2230	14	0.95		<i>A</i>	Sections were mainly lavas	
	B. Doornhoutrivier	Borehole	1830		0.97		<i>B</i>	Conductivities from Jacoba (5 km away) were used; sections were mainly lavas	
0008	Kestell	Borehole	1402	22	1.29		<i>A</i>	Borehole through bands of sandstone, dolerite, and shale; outside the shield	Carte, 1954
Transvaal									
0002	Gerhardminnebron-Doornkloof				1.24		<i>A</i>	Average value of 0002A and 0002C; in South African Shield	Bullard, 1939
	A. Gerhardminnebron	Borehole	3022	31	1.28		<i>A</i>	Temperature data in dolomite section (upper 1270 m) were discarded because of water circulation; lower sections consisted mainly of quartzite	
	B. Driefontein	Borehole through dolomite	587		0.75		<i>C</i>	Conductivities from Gerhardminnebron were used; heat flow value was discarded by author because of water circulation	
	C. Doornkloof	Borehole	1915		1.20		<i>B</i>	Conductivities from Gerhardminnebron were used; temperature data in dolomite section (upper 1237 m) were discarded because of water circulation	
0005	HB 15	Borehole	1996	32	1.05		<i>A</i>	Temperature data in dolomite section (upper 600 m) were discarded because of water circulation; lower sections were Precambrian lava and quartzite	Carte, 1954
0007	Messina	Borehole	395	13	1.37		<i>A</i>	Borehole in Northern Transvaal through narrow bands of granite, dyke and quartzite; isolated from other heat flow stations; in low-lying area outside the South African plateau	Carte, 1954
0003	Reef-Nigel	Borehole	1430		1.03		<i>B</i>	Conductivities from Jacoba and Gerhardminnebron, about 130 km west, were used; in South African Shield	Bullard, 1939
0006	Roodeport	Borehole	1762	15	0.86		<i>A</i>	Heat flow varied with depth: 0.80 at 400 m, 0.92 at 1380 m	Carte, 1954

tabulated according to geographical location. Numerical data arranged according to the published papers are given in the appendix.

### 3.1 Africa

Reliable heat flow measurements were first made in South Africa and in Great Britain. The classic study by Bullard [1939] in South Africa

has been extended by Carte [1954] and Gough [1963]. Except for attempts to measure heat flow in Lake Nyasa using oceanic techniques (R. P. Von Herzen, private communication), the rest of the African continent remains unexplored. Heat flow values are more numerous in South Africa than in most areas of comparable size; those from South Africa are summarized in Table 2 and in Figure 3.

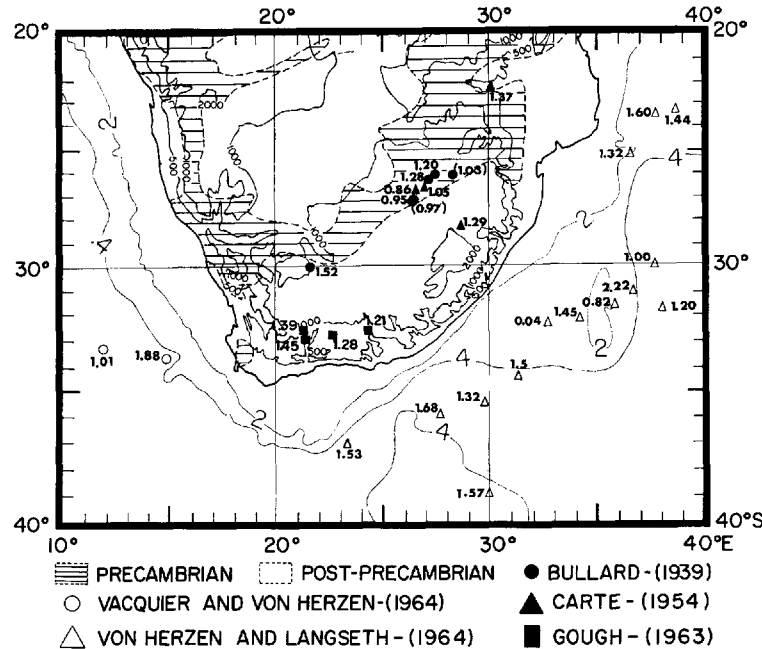


Fig. 3. Heat flow values in South Africa. Topographic contours in meters and bathymetric contours in kilometers. Values in parentheses are fair data (category B).

*General geology.* Geological formations in South Africa extend from Archaozoic to Recent. The oldest rocks include granite, gneiss, and ancient metamorphosed sediments. These are succeeded by the later Precambrian systems (Witwatersrand, Ventersdorp, Transvaal), which have been locally disturbed by Earth movements and by igneous intrusions. Among the systems overlying the Precambrian, the Paleozoic Cape system is strongly folded, forming an orogenic belt in the south. Overlying the Cape system, the Paleozoic-Mesozoic Karroo system consists of about 7500 meters of sediments, mostly sandstones and shales, injected with much dolerite. Except locally, the Karroo beds have not been disturbed by folding and are almost horizontal, forming more than half the surface of South Africa. Post-Karroo formations cover comparatively small coastal areas and synclinal valleys in the Cape folded area.

*South African Shield.* Six of Bullard's [1939] stations were holes drilled relatively close to one another for searching gold-bearing reefs of the Witwatersrand system. They all gave low heat flow values (0.75 to 1.28  $\mu\text{cal}/\text{cm}^2 \text{ sec}$ ), as did two nearby stations of Carte [1954], which have values of 1.05 and 0.86 (see Figure 3).

Both authors discarded results in the dolomite sections because of water circulation in the fissures. The average of the remaining 5 values is  $1.03 \pm 0.13$  s.d. (s.d. is standard deviation from the mean).

*South African non-shield areas.* Bullard [1939] observed a heat flow of 1.52 at Dubbeldevlei bore, which is about 800 km southwest of his shield stations and is drilled through Karroo sandstones and shales and 'old granite.' Outside the shield, Carte [1954] obtained values of 1.37 and 1.29. Gough [1963] measured heat flow from four exploratory boreholes (in search of oil, but no oil was found) in the Southern Karroo system, obtaining values ranging from 1.21 to 1.45 (1.31 to 1.57 when corrected for climatic change). The average of 7 uncorrected heat flow values lying outside the shield is  $1.36 \pm 0.10$  s.d., which is slightly higher (by 0.3  $\mu\text{cal}/\text{cm}^2 \text{ sec}$ ) than the average in the shield.

Carte [1954, p. 671, Table 5] also reported additional heat flow results from other boreholes in Transvaal and Orange Free State. Since the temperature measurements are of low precision, the heat flow values are much less reliable than those reviewed above. Further-

more, the lack of information about these results has prevented us from cataloging them in Table 2 and in the appendix.

*Bullard* [1939] considers that variation of his heat flow values is due both to thermal refraction caused by nonuniform thermal conductivity near the surface and to nonuniform heat generation in the crust. *Carte* [1954] states that both his and Bullard's measurements show little heat flow variation in South Africa. *Gough* [1963] concludes provisionally that the heat flow is appreciably higher in the Southern Karroo than in the shield. Since seismic and gravity studies do not indicate any abnormal crustal thickness in the Southern Karroo region, Gough suggests that attention should be paid to the mantle in seeking an explanation.

R. P. Von Herzen (private communication) measured the heat flow on Lake Nyasa utilizing oceanic techniques. His results show rather large variations in the lake, probably due to rapid local sedimentation or thermal instability of bottom water. Oceanic heat flow values around South Africa [*Vacquier and Von Herzen*, 1964; *Von Herzen and Langseth*, 1965] generally agree with land values in non-shield areas, as shown in Figure 3.

### 3.2 Americas

In North and South America, heat flow measurements have been carried out only in Canada, Puerto Rico, and the United States. Heat flow observations in the United States were initiated by F. Birch in the 1940's, and almost all the measurements were made by Birch and his associates. A. D. Misener and his associates began heat flow measurements in Canada in the early 1950's. At present, extensive programs of measuring heat flow are underway in many areas of the United States and Canada, but most of the results are not yet available.

The results of heat flow observations in North America are summarized in Table 3 and plotted in Figure 4. We shall briefly outline the general geology of North America and then review the heat flow observations in various general geological provinces.

*General geology.* In the north-central part of North America is the *Canadian Shield*, which is made up of ancient Precambrian rocks, mostly granites and gneisses, but including various

kinds of old folded sediments and lavas. This shield has been worn down into a low rolling surface which passes southward and southwestward beneath post-Precambrian sedimentary rocks of the Interior Lowlands. Around the Canadian Shield and Interior Lowlands are various mountain systems which have been formed at different times since the Precambrian. To the southeast is the Paleozoic Appalachian system, extending from Newfoundland to Alabama. To the west is the post-Paleozoic Cordilleran system, extending the entire length of the continent along the Pacific Ocean. Far to the north, there are systems of folded mountains along the oceanward sides of the Arctic Islands and Greenland. Lastly, to the south is the coastal plain of the Gulf of Mexico, where a great thickness of dominantly Tertiary sedimentary rocks marks the edge of the continent.

*The Canadian Shield.* Heat flow measurements have been made in the Canadian Shield by *Misener et al.* [1951] and *Leith* [1952] in the mining regions of Ontario and Quebec; by *Birch* [1954a] in mines and boreholes in Calumet, Michigan; by *Beck* [1962] in a copper mine near Flin Flon, Manitoba; by *Beck and Logis* [1963] in a drill hole at Brent Crater, Ontario; and by *Roy* [1963] in boreholes at Delaware and White Pine, Michigan (see Figure 4). These observations are summarized in Table 3A and in the appendix.

Heat flow values in the Canadian Shield are fairly uniform: 0.69 to 1.07  $\mu\text{cal}/\text{cm}^2 \text{ sec}$ , 50% of the values falling within  $0.9 \pm 0.1$ . The average of 10 values in the shield is  $0.88 \pm 0.13$  s.d., in good agreement with results from shield areas elsewhere.

*The Interior Lowlands.* Heat flow measurements have been made in the Interior Lowlands by *Herrin and Clark* [1956] in oil wells of West Texas and eastern New Mexico; by *Garland and Lennox* [1962] in oil wells at Redwater and Leduc, Alberta; and by *Roy* [1963] in mining exploration holes at Boss and Bourbon, Missouri. Heat flow estimates have also been made by *Birch and Clark* [1945] for an oil well in the West Texas Permian Basin and by *Birch* [1950] in Syracuse, Kansas (see Figure 4). These observations are summarized in Table 3B and in the appendix.

Heat flow values in the Interior Lowlands are slightly higher than those in the Canadian

TABLE 3. Heat Flow Values in North America

*MD*, maximum depth in meters; *N*, conductivity samples; *q*, heat flow; *q\**, corrected heat flow; *DC*, data class

Data No.	Station	Type	<i>MD</i>	<i>N</i>	<i>q</i>	<i>q*</i>	<i>DC</i>	Remarks	Reference
A. THE CANADIAN SHIELD									
Canada									
Manitoba									
0059	Flin Flon	Copper mine	412	?	0.7- 0.9		<i>B</i>	Water flows suspected for lowering observed heat flow in upper section; number of rock samples for conductivity not specified	<i>Beck</i> , 1962
Ontario									
0060	Brent Crater	Borehole	400	8	0.75		<i>A</i>	In a Cambrian crater; temperature measured in three consecutive years; conductivities measured in situ	<i>Beck and Logis</i> , 1963
0048	Kirkland Lake	3 mines	2200	40	1.00		<i>A</i>	Samples mostly syenite porphyry; in Superior Province	<i>Misener et al.</i> , 1951
0050	Larder Lake	Mine	1000	6	0.88		<i>A</i>	Samples mostly carbonate; in Superior Province	<i>Misener et al.</i> , 1951; <i>Leith</i> , 1952
0045	Sudbury	Mine	1500	6	1.01		<i>A</i>	Samples mostly norite; in Superior Province	<i>Misener et al.</i> , 1951
0051	Timmis	2 mines	1500	10	0.73		<i>A</i>	Samples mostly rhyolite; in Superior Province	<i>Misener et al.</i> , 1951
Quebec									
0047	Calumet Island	Mine	400	4	1.32		<i>C</i>	Large probable error was assigned by authors; in Grenville Province	<i>Misener et al.</i> , 1951
0049	Malartic	Gold mine	450	9	0.69		<i>A</i>	Samples mostly diorite and schist; in Superior Province	<i>Misener et al.</i> , 1951
United States									
Michigan									
0028	Calumet	Mine and borehole	2490	90	0.9	0.93	<i>A</i>	In Keweenaw peninsula; topographic correction applied; no definite thermal effect related to past climatic change was found	<i>Birch</i> , 1954a
0036	Delaware	Borehole	270	65	0.85	0.95	<i>A</i>	Near end of Keweenaw peninsula; topographic correction and refraction by heterogeneous conductivity were taken into account; 40 km east of Calumet	<i>Roy</i> , 1963
0037	White Pine	3 nearby boreholes	1000 650 600	156	1.01	1.07	<i>A</i>	Topographic correction applied to temperature gradient; water saturation applied to samples for conductivity measurement; 120 km west of Calumet	<i>Roy</i> , 1963
B. THE INTERIOR LOWLANDS									
Canada									
Alberta									
0056	Leduc	Nonproductive oil well	900		1.6		<i>B</i>	Estimated conductivity from Redwater (80 km SW)	<i>Garland and Lennox</i> , 1962
0057	Redwater	Oil well	900	44	1.46		<i>A</i>	Rock samples (shales and sandstones) for conductivity from nearby wells	<i>Garland and Lennox</i> , 1962
United States									
Kansas									
0024	Syracuse	Oil well			1.4- 1.7		<i>C</i>	Estimated conductivity	<i>Birch</i> , 1950
Missouri									
0034	Boss	Borehole through Cambrian and Precambrian rocks	550	102	1.29		<i>A</i>	Cambrian sections were discarded because of no core and water movement; Precambrian sections consisted of rhyolite (upper half) and andesite (lower half); rhyolite section was taken to be representative of the region because andesite was considered to be a dike	<i>Roy</i> , 1963
0035	Bourbon	Borehole	600	28	1.22		<i>A</i>	160 km north of Boss; geology is similar except the Precambrian is about 250 m deeper	<i>Roy</i> , 1963

TABLE 3. Heat Flow Values in North America (continued)

*MD*, maximum depth in meters; *N*, conductivity samples; *g*, heat flow; *g\**, corrected heat flow; *DC*, data class

Data No.	Station	Type	<i>MD</i>	<i>N</i>	<i>g</i>	<i>g*</i>	<i>DC</i>	Remarks	Reference
<i>B. THE INTERIOR LOWLANDS (continued)</i>									
New Mexico									
0021	Eddy County	5 oil wells			1.1		<i>B</i>	Reliable temperature gradient from 3 of 5 oil wells; only temperature data in salt section were used; conductivity of rock salt was estimated	<i>Herrin and Clark, 1956</i>
0022	Lea County	Oil well			1.2		<i>C</i>	Estimated conductivity of rock salt was used; temperature gradient was considered not reliable by authors	<i>Herrin and Clark, 1956</i>
Texas									
0016	Big Lake No. 1-B	Oil well	2523	4	2.0		<i>C</i>	In West Texas Permian Basin; conductivities were measured on samples from nearby wells; see text	<i>Birch and Clark, 1945</i>
0020	Midland County	Oil well			1.2		<i>C</i>	Estimated conductivity of rock salt was used; temperature gradient was considered not reliable by authors	<i>Herrin and Clark, 1956</i>
0017	Reeves County	Oil well			1.1		<i>B</i>	Estimated conductivity of rock salt was used	<i>Herrin and Clark, 1956</i>
0018	Regan County	12 oil wells			1.1		<i>B</i>	Reliable temperature gradient from 6 of 12 oil wells; estimated conductivity of rock salt was used	<i>Herrin and Clark, 1956</i>
0019	Upton County	Oil well			1.1		<i>B</i>	Estimated conductivity of rock salt was used	<i>Herrin and Clark, 1956</i>
<i>C. THE APPALACHIAN SYSTEM</i>									
Canada									
Ontario									
0044	Toronto	Oil well	300	6	1.03		<i>A</i>	Limestone samples; in foreland of Appalachians	<i>Misener et al., 1951</i>
Quebec									
0055	Loupan-Cartier	2 boreholes through alternating sandstone and shale	250	?	0.82		<i>A</i>	Temperature measured by probe-contained oscillator transmitting temperature-dependent frequency signal; number of samples for conductivity measurement not specified	<i>Saull et al., 1962</i>
0053	Montreal	Borehole	340	?	0.74		<i>A</i>	See Loupan-Cartier; borehole through sandstone, dolomite, and conglomerate	<i>Saull et al., 1962</i>
0054	Ste. Rosalie	Borehole	450	?	0.81		<i>A</i>	See Loupan-Cartier; borehole through beds dipping steeply and having slaty cleavage	<i>Saull et al., 1962</i>
0046	Thetford	Mine	300	8	1.05		<i>A</i>	In metamorphosed zone of Appalachians; samples mostly serpentinized peridotite	<i>Misener et al., 1951</i>
United States									
District of Columbia									
0033	Washington	3 closely spaced boreholes	1058 875 843	35	1.12		<i>A</i>	Borehole through quartz-mica schist in metamorphosed zone of Appalachians	<i>Diment and Werre, 1964</i>
Georgia									
0025	Georgia	2 shallow wells			~1		<i>C</i>	Estimated conductivity; Birch estimated heat flow to be 1.4; later Diment and associates re-estimated heat flow from corrected temperature gradient given by Spicer [1942]	<i>Birch, 1950; Diment and Robertson, 1963; Diment and Werre, 1964</i>
	A. Griffin		213		0.97		<i>C</i>		
	B. LaGrange		188		1.02		<i>C</i>		
Pennsylvania									
0029	Butler County	Oil well in Devonian shales	1500		1.2		<i>B</i>	Conductivity estimated; in Foreland of Appalachians	<i>Joyner, 1960</i>
0030	Potter County	2 oil wells in Devonian shales	1500		1.4		<i>B</i>	Conductivity estimated; in Valley and Range Province of Appalachians	<i>Joyner, 1960</i>
South Carolina									
1134	Aiken	6 boreholes	600		1.0		<i>A</i>	Rock types are schists and gneisses	<i>Diment et al., 1965a</i>

TABLE 3. Heat Flow Values in North America (continued)

*MD*, maximum depth in meters; *N*, conductivity samples; *q*, heat flow; *q\**, corrected heat flow; *DC*, data class

Data No.	Station	Type	<i>MD</i>	<i>N</i>	<i>q</i>	<i>q*</i>	<i>DC</i>	Remarks	Reference
C. THE APPALACHIAN SYSTEM (continued)									
Tennessee									
0032	Oak Ridge	Borehole	880	146	0.73		A	Borehole drilled in Valley and Ridge Province of Appalachians, close to the axis of regional gravity low; samples are mostly limestones and shales	<i>Diment and Robertson, 1963</i>
Virginia									
1133	Alberta	Borehole through granite	312	21	1.1- 1.4		A	In metamorphic zone of Appalachians; rock samples from two large pieces of the core and two samples of gneiss from nearby quarry; difficulty in obtaining representative conductivity value; heat flow value 1.4 is preferred by authors	<i>Diment et al., 1965b</i>
West Virginia									
0031	Doddridge, Marin, and Harrison Counties	3 oil wells	2200		1.2		B	Estimated conductivity from well sample log; in Valley and Range Province of Appalachians	<i>Joyner, 1960</i>
D. THE CORDILLERAN SYSTEM									
Canada									
Northwest Territories									
0058	Norman Wells	Nonproductive oil well	410	17	2.14	2.00	A	In permafrost region; rock samples (shales and limestones) for conductivity from nearby wells; heat flow value corrected for the effect of river nearby	<i>Garland and Lennox, 1962</i>
United States									
Arizona									
0027	Sau Manuel	11 churn drill wells	305	3	~1.2		C	Samples not from the same holes; inflections in temperature-depth relations were interpreted as due to past climatic changes and oxidation of sulfides; heat flow was determined from the least disturbed sections	<i>Lovering, 1948</i>
California									
0015	Bakersfield	Nonproductive oil well	2640	32	1.29		A	About 20 km NE from San Andreas Fault; rocks penetrated were all shale	<i>Benfield, 1947</i>
0042	Barstow	2 boreholes	730 360	250	2.1		A	SW portion of Basin and Range Province; fault zone at about 450 m deep caused small disturbance in gradient	<i>Roy, 1963</i>
0014	Grass Valley	Several mines		29		0.69	B	Temperature measured at 21 levels in several mines and corrected for topographic effect; Spicer estimated the heat flow to be 0.57 to 0.81 using estimated conductivity and uncorrected gradient	<i>Clark, 1957; Spicer, 1941</i>
Colorado									
0023	Colorado Springs (Red Creek)	Borehole	850		1.0- 1.4 1.2- 1.6		C	Estimated conductivity was used; small water flow existed in the well	<i>Birch, 1947a, 1950</i>
0026	Front Range (Adams Tunnel)	Tunnel	1200	123		1.7	A	Tunnel 20 km long under Rocky Mountains at a mean altitude of 2500 m; topographic corrections were applied	<i>Birch, 1947b 1950</i>
Nevada									
0041	Yerington	3 boreholes in and near a magnetite deposit	500 290 280	31	2.36		A	Rock types are mainly metamorphosed limestones, garnetites, and felsites of Triassic age, with later igneous intrusives	<i>Roy, 1963</i>

TABLE 3. Heat Flow Values in North America (continued)

*MD*, maximum depth in meters; *N*, conductivity samples; *q*, heat flow; *q\**, corrected heat flow; *DC*, data class

Data No.	Station	Type	<i>MD</i>	<i>N</i>	<i>q</i>	<i>q*</i>	<i>DC</i>	Remarks	Reference
<i>D. THE CORDILLERAN SYSTEM (continued)</i>									
Utah									
0040	Eureka	Borehole into latite of Middle Eocene age	250	21		3.51	<i>C</i>	Terrain correction was applied; questionable significance because of local heat sources: hot springs activity and possibly oxidizing sulfides	<i>Roy</i> , 1963
0089	Government Canyon	Borehole into latite of Middle Eocene age	330	5		1.9	<i>A</i>	9 km SW of Eureka; Basin and Ridge Province; terrain correction was applied	<i>Roy</i> , 1963
1185	Salt Valley	5 boreholes		167	1.2		<i>B</i>	Average of 5 values; conductivity measured on samples not from the same holes	<i>Spicer</i> , 1964
A.	Reeder		900		1.32		<i>B</i>	In graben area of the Salt Valley anticline	
B.	Crescent		600		1.30		<i>B</i>		
C.	Brendell		450		1.33		<i>B</i>		
D.	Balsley		900		1.10		<i>B</i>	In southern area of Salt Valley anticline	
E.	Hyde		1700		1.01		<i>B</i>	To the east and off the Salt Valley anticline	
Washington									
0038	Metaline	4 boreholes	700 650 360 400	29		2.31	<i>A</i>	In Northern Rocky Mountain Province; topographic corrections applied; complex local geology	<i>Roy</i> , 1963
<i>E. OTHER AREAS</i>									
Canada									
Northwest Territories									
0052	Resolute Bay	Borehole	200	15	2.9	1.25	<i>C</i>	In permafrost region; value corrected by Lachenbruch for the effect of ocean nearby	<i>Misener</i> , 1955, <i>Lachenbruch</i> , 1957
Puerto Rico									
0043	Mayaguez	Borehole	305	18		0.6	<i>A</i>	Drill hole into ultrabasic body (serpentine); local terrain and climatic corrections applied	<i>Diment and Weaver</i> , 1964

Shield. The average of 8 values is  $1.25 \pm 0.18$  s.d. This result is consistent with the fact that there are no significant geological differences between these two regions, except a thin cover of Paleozoic and later sediments in the Interior Lowlands. The study of *Herrin and Clark* [1956] covered a fair size area ( $10^5$  km<sup>2</sup>), and they obtained remarkably uniform heat flow values of  $1.1 \pm 0.1$   $\mu\text{cal}/\text{cm}^2$  sec. They remark that the value (2.0) at Big Lake, Texas, estimated by *Birch and Clark* [1945] is probably too large.

*The Appalachian system.* In the Appalachian area, heat flow has been estimated at Griffin and LaGrange, Georgia, by *Birch* [1947a, 1950], and in Pennsylvania and West Virginia by *Joyner* [1960]; measured in Toronto, Ontario, and Thetford, Quebec, by *Misener et al.* [1951]; in the St. Lawrence lowland by *Saull et al.* [1962]; at Oak Ridge, Tennessee, by *Diment and Robertson* [1963]; near Washington, D.C., by *Diment*

and *Werre* [1964]; near Alberta, Virginia, by *Diment et al.* [1965b]; and near Aiken, South Carolina, by *Diment et al.* [1965a] (see Figure 4). These observations are summarized in Table 3C and in the appendix.

Heat flow values in the Appalachian system show small variations (0.73 to 1.4  $\mu\text{cal}/\text{cm}^2$  sec) despite great diversity in rock type and geological history. The average of 12 values is  $1.04 \pm 0.23$  s.d., which is slightly higher than that of the Canadian Shield, but the difference is not significant. Why the average heat flow value from the Appalachian region is similar to that from the Canadian Shield and the Interior Lowland is not quite apparent, especially when there is a marked difference in geology between these regions.

*The Cordilleran system.* In the Cordilleran system, heat flow measurements have been made by *Spicer* [1941] and *Clark* [1957] at Grass Valley, California; by *Benfield* [1947] near

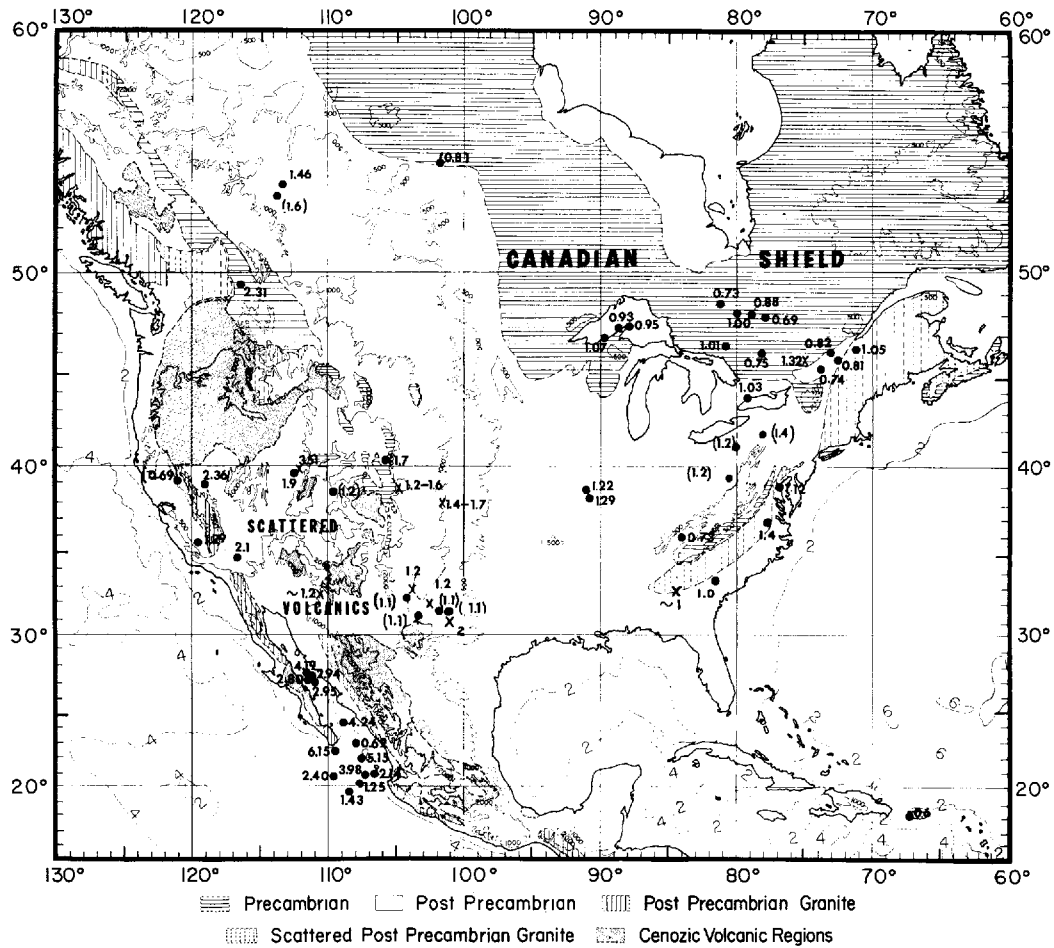


Fig. 4. Heat flow values in North America. Topographic contours in meters and bathymetric contours in kilometers. X is rejected station (category C), and values in parentheses are fair data (category B).

Bakersfield, California; by *Lovering* [1948] in San Manuel, Arizona; by *Birch* [1947a] near Colorado Springs, Colorado; by *Birch* [1947b, 1950] at Front Range, Colorado; by *Garland and Lennox* [1962] at Norman Well, N.W.T.; by *Roy* [1963] at Government Canyon and Eureka, Utah; Yerington, Nevada; Barstow, California; and Metaline, Washington; and finally by *Spicer* [1964] at Salt Valley anticline, Utah (see Figure 4). These observations are summarized in Table 3D and in the appendix. Very recently, T. S. Lovering (private communication) has measured the heat flow in the East Tintic district, Utah. He found an area of about 20 km<sup>2</sup> where the heat flow is anomalous and ranges from 3 to 7  $\mu\text{cal}/\text{cm}^2$  sec; farther

west, however, where the heat flow is normal, it amounts to from 1.7 to 2.2  $\mu\text{cal}/\text{cm}^2$  sec.

Heat flow varies greatly in the Cordillera (0.69 to 2.36  $\mu\text{cal}/\text{cm}^2$  sec, discarding the value 3.51 at Eureka, Utah, as not representative). Values are generally lower in the west and in the east. *Menard* [1960] suggests that the region of high heat flow along the crest of the East Pacific Rise may continue through the Gulf of California into western North America (see Figures 22 and 23). Indeed, heat flow values are high ( $\geq 2$   $\mu\text{cal}/\text{cm}^2$  sec) in the Basin and Range Province. Furthermore, widespread hot spring activities, higher electrical conductivity [*Schmucker*, 1964], and lower seismic velocity in the Basin and Range Province also seem to

favor higher subsurface temperature and consequently higher heat flow. We need more observations, however, to define the extent of the high heat flow region in the Cordillera. The average of 9 values in the Cordillera is  $1.73 \pm 0.53$  s.d., which is considerably greater than averages from other North American areas.

*Other areas.* Misener [1955] reports a heat flow of  $2.9 \mu\text{cal}/\text{cm}^2 \text{ sec}$  at Resolute Bay, Cornwallis Island, Northwest Territories, Canada. However, Lachenbruch [1957] argues that heat flow from such permafrost areas is affected by the unfrozen ocean nearby and suggests a corrected value of 1.25. The value obtained by Diment and Weaver [1964] at Mayaguez, Puerto Rico, will be discussed in section 4.1. These two measurements are summarized in Table 3E and in the appendix.

### 3.3 Asia

Asia occupies 30% of the world's land area, but has only a few heat flow measurements. Extensive heat flow studies have been carried out in Japan, which occupies only 0.9% of Asia's area and geologically is not characteristic of the Asian continent. Elsewhere in Asia, one preliminary determination in India and 18 measurements in Iran have been made. Asian observations are summarized in Table 4 and also in the appendix.

*India.* Verma and Rao [1965] report a preliminary heat flow determination in South India at the Kolar Gold Fields. The heat flow obtained is  $0.66 \mu\text{cal}/\text{cm}^2 \text{ sec}$ , which agrees quite well with values in shield areas elsewhere.

*Iran (Persia).* Coster [1947] determined the heat flow from 18 wells in the Masjid-i-Sulaiman (Masjed Soleyman) oil field in southwest Persia. The study covers a region of about 30 km by 5 km where stratigraphy is complicated and where recent tectonic movements have occurred. Representative sampling of rocks for conductivity was not available, and some temperatures were measured after oil production in some wells. The measured heat flows range from 0.53 to  $1.22 \mu\text{cal}/\text{cm}^2 \text{ sec}$ , with an arithmetic mean of  $0.87 \pm 0.04$  s.e. (s.e. is standard error). A substantial part of the largest regional variation of heat flow may be accounted for by the influence of geological structure. Recent climatic changes may have

decreased the heat flow by about 30% throughout the region. Topographic irregularities, recent tectonic movement, and denudation are found to have insignificant effect on the heat flow. The average of heat flow values corrected for climatic changes is  $1.18 \pm 0.04$  s.e.

*Japan.* In Japan, heat flow work was initiated in 1957 by the Earthquake Research Institute, and to date 39 land observations and 19 measurements in the surrounding seas have been published [Horai, 1959, 1963a, b, c; Uyeda and Horai, 1960, 1963a, b; Uyeda et al., 1958, 1962; Yasui et al., 1963]. Recently, Horai and Uyeda [1963], Uyeda and Horai [1964], and Horai [1964] have presented comprehensive summaries of these results. Of the land stations, 26 are in various metal mines, 4 in coal mines, 2 in oil fields, 3 in natural gas fields, and 4 at other types of sites. Oceanic measurements are conducted under a joint project with the Japan Meteorological Agency and the Hydrographic Department.

All the Japanese results, including 38 new sea measurements [Yasui and Watanabe, 1965], are plotted in Figure 5 (Table 4 contains published land data only, and the appendix contains all data). Because of complex geology, the accuracy at some individual stations may be lower than the average. However, the distribution of heat flow in Figure 5 shows a definite pattern: (I) the basin of the Japan Sea has moderately high heat flow ( $1.84 \pm 0.6$  s.d.); (II) regions of high heat flow ( $2.01 \pm 0.38$  s.d.) also exist in the Japan Sea side of the island arc and branch off toward the Izu-Marianne arc, through the central part of Honshu; (III) most regions of Mesozoic metamorphism have normal heat flow ( $1.58 \pm 0.47$  s.d.); (IV) the Pacific side of northeastern Japan has low heat flow ( $0.70 \pm 0.15$  s.d.); and (V) the Kurile and Japan Trenches also have low heat flow ( $0.99 \pm 0.38$  s.d.). These heat flow zones are labeled in Figure 6 with the relevant geological and topographical features of the Japanese area. The land region of high heat flow coincides precisely with the region of Cenozoic volcanic activity. The zone of low heat flow is just inside the Japan and Kurile Trenches, and in the zones of Mesozoic metamorphism the heat flow is rather normal. Assuming a steady state, Uyeda and Horai [1964] calculate the temperature distribution in the crust under various

TABLE 4. Heat Flow Values in Asia

*MD*, maximum depth in meters; *N*, conductivity samples; *q*, heat flow; *q\**, corrected heat flow; *DC*, data class

Data No.	Station	Type	<i>MD</i>	<i>N</i>	<i>q</i>	<i>q*</i>	<i>DC</i>	Remarks	Reference
India									
0083	Kolar	Mine	2000	10	0.66		A	Temperature measured at 12 levels in gold field in South India; samples are hornblende schists	Verma and Rao, 1965
Iran (Persia)									
0084	Masjid-i-Sulaiman	18 oil wells	1200	35	0.87	1.18	A	Climatic correction applied; other corrections are small; local variations explained by geological structure, using an electrical analog model	Coster, 1947
Japan									
Central Japan									
0101	Ashio	Cu mine	800	2	2.23		B	Temperature measured at 10 levels in mine; geology is a simple rhyolite mass	Uyeda and Horai, 1964;
0103	Chichibu	Fe mine	400	3	1.34		A	2 underground drill holes (120, 180 m deep) in mine; rocks are limestones, little magnetite, and pyrite	Horai, 1964
0096	Hitachi	Cu mine	550	36	0.71		A	Temperature measured at 65 localities (9 levels) in mine; rocks are mainly granites, schists, and pyrite	Uyeda and Horai, 1964
0105	Kamioka	Pb, Zn mine	720	4	1.80		A	2 underground boreholes (400 and 200 m deep) and a level in mine; rocks are mainly gneiss, limestone, and skarn	Uyeda and Horai, 1964;
0098	Kashima	Borehole	900	3	0.76		A	Nonproductive gas well into silt	Horai, 1964
0097	Katsuta	Borehole	900	3	0.91		A	Nonproductive gas well into silt	Uyeda and Horai, 1964;
0107	Kune	Cu mine	560	4	1.60		C	Temperature measured at 13 depths and an underground borehole in mine; rocks are crystalline schists	Horai, 1964
0102	Kusatsu-Shirane	Borehole	250	5	10.8		C	Exploration hole in geothermal area on flank of an active volcano; andesites	Uyeda and Horai, 1964;
0109	Minenosawa	Cu mine	190	4	1.79		B	2 underground drill holes (80, 100 m deep); 80 m deep hole under drilling operation; 5 km south of Nako; crystalline schists	Horai, 1964
0099	Mobara	Borehole	1900	6	0.54		A	5 gas exploration drill holes into sandstone and siltstone (470, 450, 275, 1300, 1900 m deep)	Uyeda and Horai, 1964;
0106	Nakatatsu	Zn, Pb mine	640	4	1.95		A	1 underground drill hole (180 m deep) and 2 levels in mine; rocks are skarn and porphyrite	Horai, 1964
0108	Nako	Cu mine	640	7	1.44		A	Temperature measured at 6 depths in mine; 5 km SE of Kune; rocks are crystalline schists	Uyeda and Horai, 1964;
0104	Sasago	Tunnel	480	2	2.06		B	Tunnel 4647 m long through hornfels and quartz diorite; temperature-depth relation needs correction for topography	Horai, 1964
0100	Tokyo	Borehole	885	3	0.74		A	Research hole at Tokyo Univ., into sand and clay	Uyeda and Horai, 1964;
Hokkaido									
0088	Akabira	Coal mine	700	4	1.07		A	2 drill holes (35, 73 m deep) and 5 points in 2 levels in coal mine; rocks are sandstones and schists	Uyeda and Horai, 1964;
0089	Ashibetsu	Borehole	500	6	1.35		A	Coal-prospecting bore into shale and sandstone	Horai, 1964
0085	Haboro	Borehole	350	5	1.87		B	Coal-prospecting bore; cores for conductivity from a bore 3 km away were used; sandstones and mudstones	Uyeda and Horai, 1964;
0087	Konomai	Au, Ag mine	520	9	2.54		A	17 boreholes (3 nearly vertical, 14 horizontal) in mine; rocks are shales, tuffs, liparites, and propylites	Horai, 1964
0086	Shimokawa	Cu, Fe mine	530	7	1.71		A	Temperature measured at 7 levels in mine; spilitic samples were used for conductivity	Uyeda and Horai, 1964;

TABLE 4. Heat Flow Values in Asia (continued)

*MD*, maximum depth in meters; *N*, conductivity samples; *q*, heat flow; *q\**, corrected heat flow; *DC*, data class

Data No.	Station	Type	<i>MD</i>	<i>N</i>	<i>q</i>	<i>q*</i>	<i>DC</i>	Remarks	Reference
Hokkaido (continued)									
0090	Toyoha	Zn, Pb mine	400		5.		<i>C</i>	Mine in geothermal area; estimated conductivity	<i>Uyeda and Horai, 1964; Horai, 1964</i>
Kyushu									
0120	Izuhara	Borehole, Pb, Zn mine	480	8	2.17		<i>B</i>	3 boreholes (250, 480, 450 m deep) from ground surface and 4 shorter boreholes in mine; in Tsushima Island; rocks are sandstones, shales, and porphyry	<i>Uyeda and Horai, 1964; Horai, 1964</i>
0123	Makimine	Cu, Fe mine	845	6	1.79		<i>A</i>	Temperature measured at 40 localities at 11 depths in mine; rocks are phyllites, sandstones, and greenstones	<i>Uyeda and Horai, 1964; Horai, 1964</i>
0122	Taio	Ag, Au mine	560	11	1.05		<i>B</i>	Temperature measured at 39 localities in mine; temperatures scattered probably because of water movement; rocks are propylites	<i>Uyeda and Horai, 1964; Horai, 1964</i>
0121	Takamatsu	Coal mine	1000	8	1.92		<i>A</i>	Temperature measured at 11 levels in coal mine; rocks are sandstones and shales	<i>Uyeda and Horai, 1964; Horai, 1964</i>
Northeastern Japan									
0092	Innai	Borehole	1050	4	1.49		<i>B</i>	Gradient obtained from bottom temperature of more than 100 oil wells; water saturated silt for conductivity	<i>Uyeda and Horai, 1964; Horai, 1964</i>
0095	Kamaishi	Cu, Fe mine	530	12	0.52		<i>B</i>	Temperature measured at 4 boreholes and 9 depths in mine; temperatures found disturbed probably by water movement; rocks are limestone, skarn, slate, and intrusives	<i>Uyeda and Horai, 1964; Horai, 1964</i>
1136	Matsukawa	Borehole			15		<i>C</i>	Geothermal area	<i>Uyeda and Horai, 1964; Horai, 1964</i>
0094	Nodatamagawa	Mn mine	400	6	1.14		<i>A</i>	Temperature measured at 6 depths in mine; rocks are cherts, sandstones, and shales	<i>Uyeda and Horai, 1964; Horai, 1964</i>
0093	Osarizawa	Au, Ag mine, borehole	300	14	2.24		<i>A</i>	Temperature measured at 1 borehole from surface (300 m deep) and 11 levels in mine; rocks are tuffs, shales, and propylites	<i>Uyeda and Horai, 1964; Horai, 1964</i>
0091	Yabase	Borehole	1700	2	2.01		<i>B</i>	Gradient obtained from bottom temperatures of more than 200 oil wells in shale	<i>Uyeda and Horai, 1964; Horai, 1964</i>
Southwestern Japan									
0119	Besshi	Cu mine	1600	8	1.22		<i>A</i>	3 underground boreholes (150, 530, 705 m deep) in mine; crystalline schists	<i>Uyeda and Horai, 1964; Horai, 1964</i>
0117	Hidaka	Borehole	310	4	2.12		<i>A</i>	Hot-spring exploration borehole into sandstone; nonproductive	<i>Uyeda and Horai, 1964; Horai, 1964</i>
0110	Ikuno	Cu, Zn mine	880	6	1.38		<i>A</i>	Temperature measured at 15 depths in mine; rocks are liparite, tuffs, and andesite	<i>Uyeda and Horai, 1964; Horai, 1964</i>
0113	Isotake	Borehole	170	3	3.49		<i>C</i>	2 boreholes in Pb, Zn mine; temperature disturbed because of shallow depth of bore into gypsum, clay, and phillite	<i>Uyeda and Horai, 1964; Horai, 1964</i>
0115	Kuwayama	Borehole, Cu mine	520	6	1.00		<i>A</i>	2 boreholes (300, 450 m deep) from surface and 1 underground borehole (300 m) in mine; weakly metamorphosed Paleozoic area	<i>Uyeda and Horai, 1964; Horai, 1964</i>
0118	Kiwa	Cu mine	410	6	1.31		<i>B</i>	3 underground boreholes (100, 150, 290 m deep) in sandstones; temperature scattered	<i>Uyeda and Horai, 1964; Horai, 1964</i>
0116	Naka	Cu mine	640	2	1.79		<i>A</i>	Underground borehole 190 m deep in mine; rocks are entirely schist	<i>Uyeda and Horai, 1964; Horai, 1964</i>
0111	Nakaze	Au, Sb mine	365	9	2.21		<i>A</i>	Temperature measured at 5 depths and an underground borehole (100 m deep) in mine; rocks are andesite tuff and schists	<i>Uyeda and Horai, 1964; Horai, 1964</i>
0114	Tsumo	Cu, Zn mine	310	7	1.09		<i>A</i>	2 underground boreholes (200, 140 m deep) in mine; rocks are mainly hornfels	<i>Uyeda and Horai, 1964; Horai, 1964</i>
0112	Yanahara	Borehole	940	6	1.20		<i>A</i>	2 boreholes (200, 940 m) into slate of Fe mine	<i>Uyeda and Horai, 1964; Horai, 1964</i>

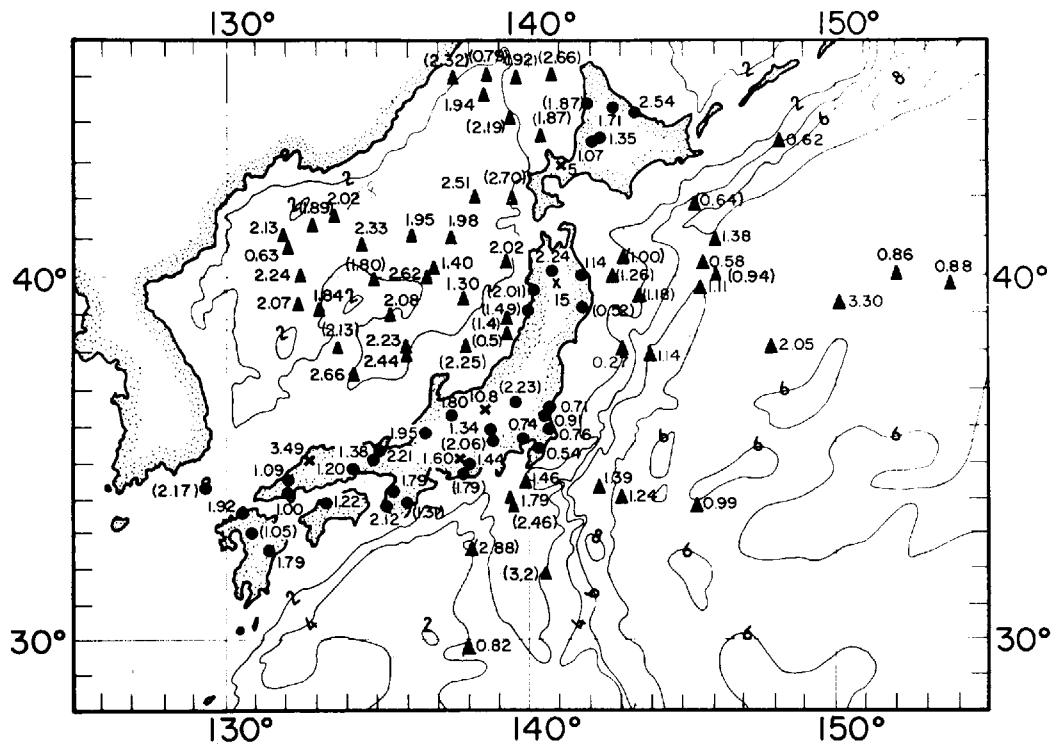


Fig. 5. Heat flow values in and around Japan. Bathymetric contours in kilometers. On land, X is rejected station (category C), and values in parentheses are fair data (category B). At sea, values in parentheses are rejected data.

zones of Japan. Although depending on the assumed radioactivity in the crust, the lateral temperature variation under Japan is shown to be very great: at the Mohorovicic discontinuity, the temperature in the Japan Sea side (high heat flow zone) may be  $800^{\circ}\text{C}$  to  $1200^{\circ}\text{C}$ , whereas it is only about  $200^{\circ}\text{C}$  in the low heat flow zone in the Pacific Ocean side.

Despite pronounced tectonism in island arc areas, the average heat flow in Japan is  $1.53 \pm 0.57$  s.d., which is quite close to the world's average value,  $1.58 \pm 1.14$  s.d. However, the characteristic feature of the heat flow in Japan is the areal distribution of anomalies. *McBirney* [1963] proposes that this distribution is caused by a refraction mechanism due to heterogeneous thermal conductivity. *Uyeda and Horai* [1964] consider, however, that such a pronounced refraction of heat flow is unlikely in Japan.

### 3.4 Australia

Heat flow measurements in Australia were initiated by J. C. Jaeger in the 1950's. Observa-

tions are relatively well distributed. They are plotted in Figure 7 and summarized in Table 5 and in the appendix. Recently, *Howard and Sass* [1964] have presented a comprehensive study of their heat flow measurements and have also summarized all previous works. Since then *Sass* [1964b] has reported additional heat flow observations in eastern Australia. Some oceanic heat flow measurements have been made near Australia by *Von Herzen and Langseth* [1965] and M. G. Langseth (private communication). These oceanic observations are also shown in Figure 7.

*General geology.* Australia is of low elevation, moderate relief, and without young mountains. About two-thirds of it consists of Precambrian rocks. The ancient Australian Shield in the west is usually buried under desert sands. In the east, flanking the narrow coastal plain are a series of deeply eroded ranges and table lands which have been raised in relatively recent geological time. Between the eastern highlands and the western shield is a broad depression. It is

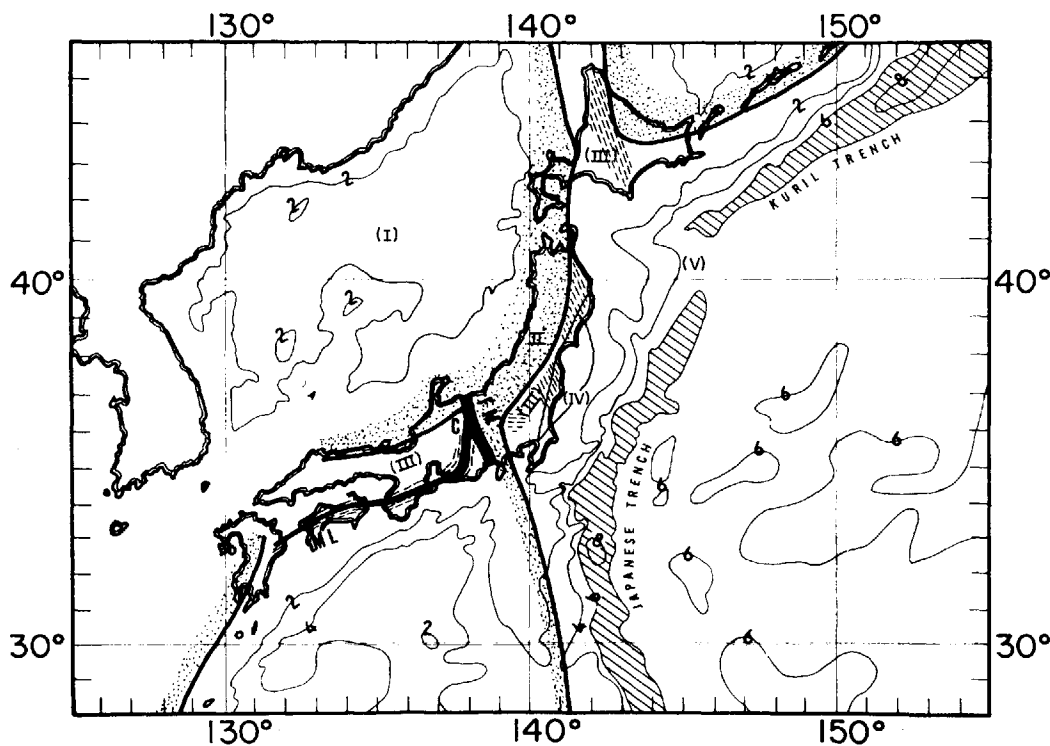


Fig. 6. Map of Japan showing major geological features. Stippled area is late Cenozoic volcanic zone. Dashed area is Mesozoic metamorphic zone. *FM* is Fossa Magna. *ML* is median tectonic line. (I) to (V) correspond to areas described in the text. Bathymetric contours in kilometers.

floored by relatively soft Mesozoic and Cenozoic sedimentary rocks overlying the Paleozoic and Precambrian formations.

Folding had almost ceased in Australia by the end of Paleozoic time, and Australia has remained relatively stable in the last 200 million years. In Miocene time, volcanic activity and lava flows were quite widespread in eastern Australia, and throughout the Cenozoic era Australia was emergent. The generalized geology and the topography of Australia are shown in Figure 7, and radioactive ages from Australian Precambrian rocks and tectonic activities are given in Figure 8.

*The Australian Shield.* Sass [1964a] measured the heat flow at three quite closely spaced stations in the central Archean Gold Fields province of the shield, and obtained values consistently near  $1 \text{ } \mu\text{cal/cm}^2 \text{ sec}$ . Later Howard and Sass [1964] not only confirmed the earlier results, but they have also measured the heat flow at four stations to the west, obtaining

similar values (see Figure 7). These observations are summarized in Table 5A and the appendix. The average of 7 values in the Australian Shield is  $1.02 \pm 0.15 \text{ s.d.}$

*The Australian Interior Lowlands.* LeMarne and Sass [1962], Sass and LeMarne [1963], Howard and Sass [1964], and Sass [1964b] obtained 5 fairly uniform heat flow values of about  $2 \text{ } \mu\text{cal/cm}^2 \text{ sec}$  in the mining areas of New South Wales and South Australia. Howard and Sass [1964] also observed 3 similar values in northern Australia. Values obtained in Rum Jungle are doubtful because of high local radioactivity and disagreement among themselves. In the eastern edge of the Great Artesian Basin that covers a large part of eastern Australia, Sass [1964b] observed two low values of about  $1 \text{ } \mu\text{cal/cm}^2 \text{ sec}$  from oil wells. Whether these low values are representative of the Basin is very uncertain. Observations in the Interior Lowlands (see Figure 7) are summarized in Table 5B and in the appendix. Excluding doubt-

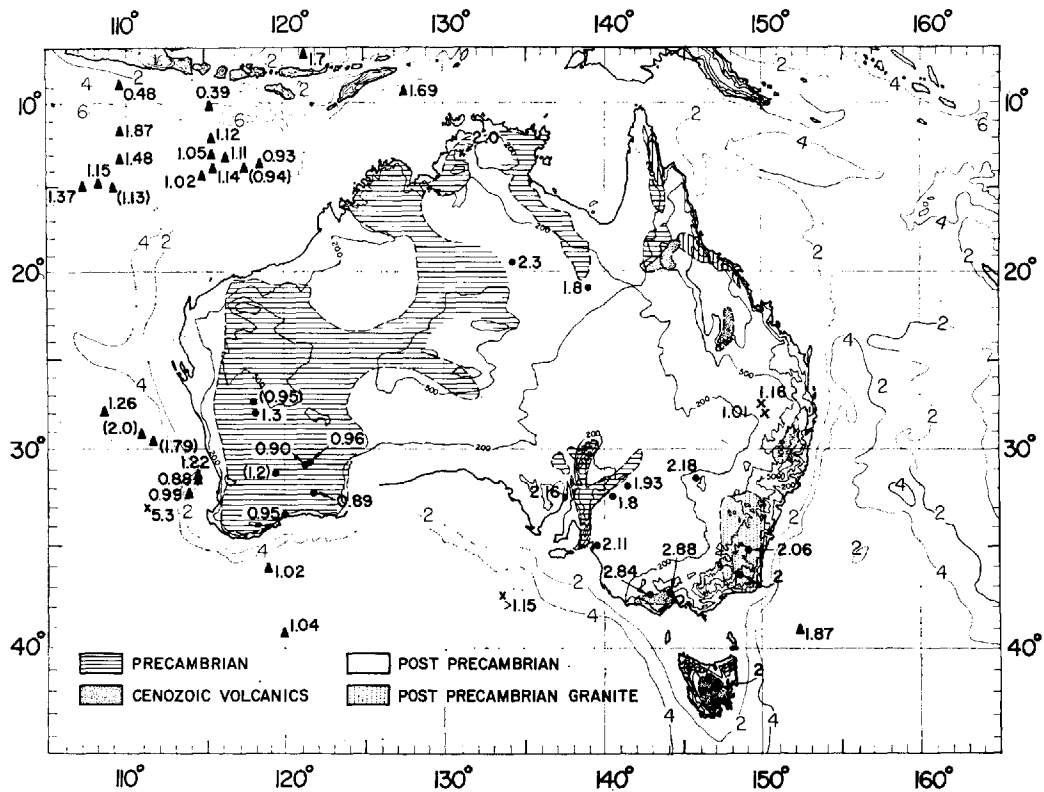


Fig. 7. Heat flow values in and around Australia. Topographic contours in meters. Bathymetric contours in kilometers. X is rejected station (category C), and values in parentheses are fair data (category B).

ful values, the average of 7 values in the Australian Interior Lowlands is  $2.04 \pm 0.18$  s.d., which is much higher than that in the interior lowlands of other continents.

*East Australian Highlands.* *Newstead and Beck* [1953] observed quite high heat flow (2.04 to 2.54  $\mu\text{cal}/\text{cm}^2$  sec) in Tasmania, where the geology is extremely complex. *Jaeger and Sass* [1963] confirmed these results by applying Lees' topographic corrections and also made several new measurements. *Beck* [1956] observed heat flow values of about 2  $\mu\text{cal}/\text{cm}^2$  sec in the Snowy Mountains, which were confirmed later by *Howard and Sass* [1964]. *Sass* [1964b] observed a similar value in a specially drilled hole near Canberra and even higher values of about 3  $\mu\text{cal}/\text{cm}^2$  sec in mines near Stawell and Castlemaine, Victoria, which may be related to Cenozoic volcanism or oxidation of sulfides. All

these observations (see Figure 7) are summarized in Table 5C and in the appendix. The average of 5 values in the East Australian Highlands is  $2.36 \pm 0.38$  s.d.

According to the studies reviewed above, heat flow is low ( $1.02 \pm 0.15$  s.d.) in the Western Australian Shield area and high in eastern Australia ( $2.16 \pm 0.33$  s.d.). This tendency is again confirmed by oceanic heat flow measurements along the south coast of Australia made by Scripps Institution of Oceanography and by Lamont Geological Observatory: four values of about 1.0  $\mu\text{cal}/\text{cm}^2$  sec off the southwest coast and one value of about 1.9 off the southeast coast (see Figure 7).

On the basis of these observations and some plausible assumptions about the radioactive contents and thermal conductivity of the crust, *Howard and Sass* [1964] estimate that the tem-

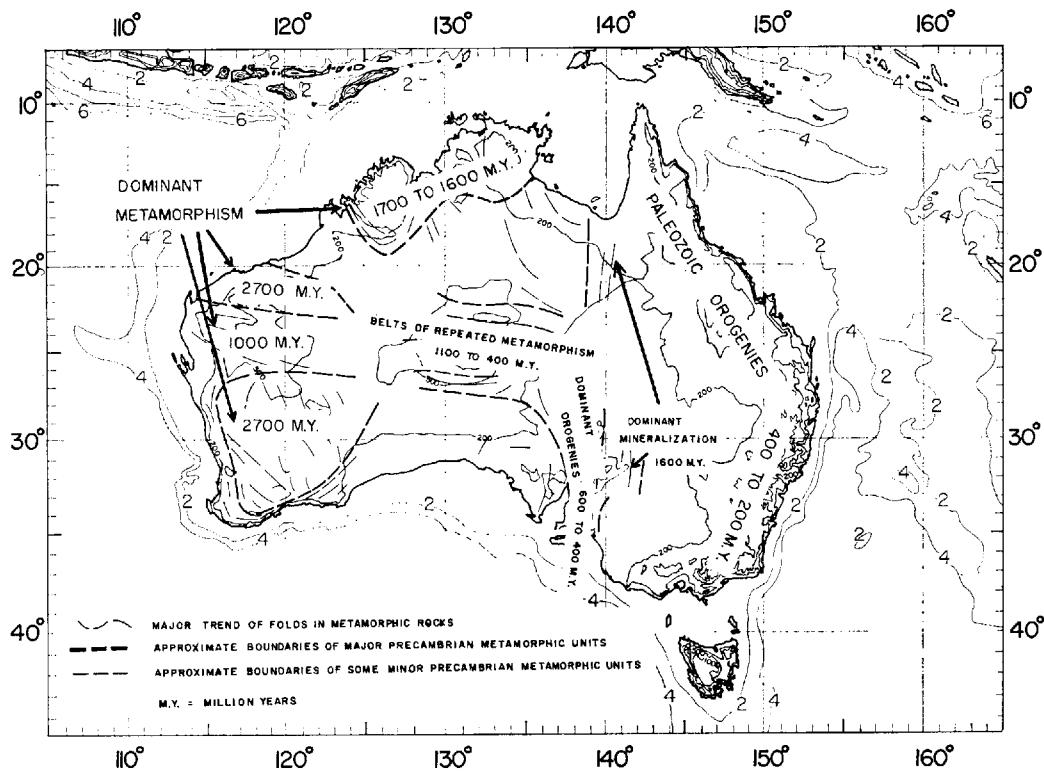


Fig. 8. Radioactive ages from Precambrian rocks and tectonic activities in Australia [after Wilson *et al.*, 1961, Figure 11].

perature difference at the Mohorovicic discontinuity in western and eastern Australia should be at least 200°C.

### 3.5 Europe

Despite the fact that geology and geophysics are well studied in Europe, heat flow measurements are still few in number. The present data are plotted in Figure 9 and are given in Table 6 alphabetically by nations. Numerical data are listed in the appendix. Because of the lack of data, we shall review heat flow observations by countries.

*General geology.* Precambrian sequences are widely distributed only in northern and eastern Europe, with a few scattered ones elsewhere. Apart from older orogenies, the building of the core of the European mainland was completed by the later Precambrian. This core, known as the Baltic-Russian Shield, includes the lowland of Sweden, Finland, Russia, and the Baltic Sea.

During the Paleozoic, the Caledonian, and Variscan orogenic episodes profoundly affected the continent. Alpine diastrophism, beginning in the late Mesozoic and continuing to the present, has culminated in folding and faulting of the Alps and their extensions with widespread volcanism, particularly in southern Europe and Asia Minor. Unlike other large continents, geological provinces in Europe are small in extent.

*Great Britain.* British scientists have pioneered heat flow measurements on land, obtaining some twenty values in Great Britain within an area smaller than 5° by 5°. Benfield [1939] obtained an average heat flow of about 1  $\mu\text{cal}/\text{cm}^2 \text{ sec}$  from five boreholes. Anderson [1940] recalculated some of Benfield's values and also obtained new ones. Plotting these values on a map, Anderson shows that the relatively high heat flows at Glasgow and Durham are in an area coinciding with the southeastern extension of the 'Mull Swarm,' a complex of Tertiary dykes. Since these values are uncertain (see re-

TABLE 5. Heat Flow Values in Australia

*MD*, maximum depth in meters; *N*, conductivity samples; *q*, heat flow; *q\**, corrected heat flow; *DC*, data class

Data No.	Station	Type	<i>MD</i>	<i>N</i>	<i>q</i>	<i>q*</i>	<i>DC</i>	Remarks	Reference
A. THE AUSTRALIAN SHIELD									
Western Australia									
0073	Bullfinch	Mine	370	8	1.2		<i>B</i>	Geology is very complex; mostly dolomitized greenstones; heat flow value 1.2 may be too low because of uncertainty in obtaining a representative conductivity	Howard and Sass, 1964
0066	Coolgardie	2 boreholes 20 km apart	320 300	12	0.90		<i>A</i>	Average of 2 values (1.09 and 0.72); one hole passes through massive granite with about 30 m of greenstone at the top; another penetrates a fine-grained greenstone	Sass, 1964a; Howard and Sass, 1964
0071	Cue	2 boreholes 300 m apart	420 330	19	0.95		<i>B</i>	2 bores gave identical temperature-depth curves; gradient increased with depth; rocks are greenstone	Howard and Sass, 1964
0065	Kalgoorlie	4 boreholes	900 550 300 250	47	0.99	0.96	<i>A</i>	Bores into altered basic and ultrabasic rocks; effect of salt lake is corrected; Howard and Sass from 4 mines to depth of 1100 m and covering 5 km <sup>2</sup> obtained heat flow value of 0.89, using conductivity by Sass	Sass, 1964a; Howard and Sass, 1964
0072	Mount Magnet	Mine	480	10	1.3		<i>A</i>	Gold mine in an area of jaspilite and altered greenstone	Howard and Sass, 1964
0067	Norseman				0.95		<i>A</i>	Average of two values	
	A. Norseman	3 boreholes	390 420 600		1.01		<i>A</i>	Conductivities were measured on samples from the deepest hole	Sass, 1964a
	B. Norseman	3 nearby boreholes	480		0.89		<i>A</i>	Bores pass through altered basic rocks with quartz-porphry dikes	Howard and Sass, 1964
0075	Ravensthorpe	Borehole	330	19	0.95		<i>A</i>	Drill hole into quartz-diorites and basic greenstones	Howard and Sass, 1964
B. THE INTERIOR LOWLANDS									
New South Wales									
0064	Broken Hill	Boreholes, mine	1200	118	1.93		<i>A</i>	18 drill holes covering 500 km <sup>2</sup> and 32 horizontal holes in mine walls; samples are mostly quartzites and gneisses; 4 holes studied by Howard and Sass gave results in good agreement	Sass and LeMarne, 1963; Howard and Sass, 1964
0063	Cobar	2 boreholes 100 m apart	575 340	16	2.18		<i>A</i>	Bores in western edge of Tasman geosyncline through a fairly uniform slate formation with some mineralized zones	LeMarne and Sass, 1962
Northern Territory									
0068	Rum Jungle	3 boreholes	550 300 400	27	2.0 1.9 1.02		<i>C</i>	Low value (1.02) probably not representative because of measurement through narrow and vertical bodies of low conductive amphibolites; the area is known for high radioactivity	Howard and Sass, 1964
0069	Tennant Creek	Borehole, mine	300	16	2.3		<i>A</i>	4 horizontal holes in mine and 1 borehole; in a large area of Precambrian deep marine sediments containing abundant graywackes interbedded with shales, siltstones, conglomerates, and breccias	Howard and Sass, 1964
Queensland									
0076	Cabawin	Oil well	3000	19	1.16		<i>C</i>	In eastern edge of Great Artesian basin; water flow at depth suspected	Sass, 1964b
0077	Moonie	Oil well	1700		1.01		<i>C</i>	See Cabawin; conductivity estimated from Cabawin, 24 km apart	Sass, 1964b
0070	Mount Isa	Borehole	430	12	1.8		<i>A</i>	Drill hole penetrating a uniform shale formation	Howard and Sass, 1964
South Australia									
0080	Kanmantoo	2 boreholes	250 160	16	2.11		<i>A</i>	Both holes pass through andalusite-biotite schists; topographic correction applied for shorter hole; anisotropic conductivity because of schistosity	Sass, 1964b
0074	Radium Hill	7 boreholes	305	30	1.8		<i>A</i>	Holes penetrated into Precambrian paragneisses consisting mainly of micas, quartz, and feldspars	Howard and Sass, 1964
0079	Whyalla	Borehole	185	8	2.16		<i>A</i>	Drill hole into alternating iron ore and amphibolites	Sass, 1964b

TABLE 5. Heat Flow Values in Australia (continued)

*MD*, maximum depth in meters; *N*, conductivity samples; *q*, heat flow; *q\**, corrected heat flow; *DC*, data class

Data No.	Station	Type	<i>MD</i>	<i>N</i>	<i>q</i>	<i>q*</i>	<i>DC</i>	Remarks	Reference
C. THE EAST HIGHLANDS									
A.C.T.									
0078	Canberra	Borehole	225	7	2.06		A	Specially drilled hole penetrating porphyry	<i>Sass</i> , 1964 <i>b</i>
New South Wales									
0062	Snowy Mountains	Tunnel, boreholes	>300	27		2	A	Average of about 10 values from Encumbene-Tumut tunnel area (80 × 15 km); topographic correction applied later by Howard	<i>Beck</i> , 1956, private communication; <i>Howard and Sass</i> , 1964
Tasmania									
0061	Great Lake	Borehole	314	8	2		A	Drill hole into a tholeiite sill; data from 4 other holes were included as corroborative evidence; further studies by Jaeger and Sass confirmed early results	<i>Newstead and Beck</i> , 1953; <i>Jaeger and Sass</i> , 1963
Victoria									
0082	Castlemaine	Borehole	165	5	2.88		A	Drill hole into interbedded slates and sandstones	<i>Sass</i> , 1964 <i>b</i>
0081	Stawell	Borehole	300	7	2.84		A	Drill hole into a fine-grained slate with inclusions of quartz and pyrite	<i>Sass</i> , 1964 <i>b</i>

marks in Table 6), more measurements are needed to clarify this correlation between heat flow and igneous activity.

*Bullard and Niblett* [1951] measured the heat flow in six boreholes in Nottinghamshire and two in north Yorkshire. Four Nottinghamshire bores give high values (~2.5) which were possibly caused by the underground water flow over an anticline. We suggest that the values (~1.6) from the two remaining Nottinghamshire bores are more representative of the regional heat flow, as further supported by two similar values obtained by *Mullins and Hinsley* [1958] in the same area. Four other values obtained by the latter authors at the Nottinghamshire-Yorkshire border are moderately high, which may also be caused by underground water movement.

Heat flow at Cambridge is estimated to be small by *Anderson* [1940]. However, *Chadwick* [1956] determined the heat flow there to be 1.28 from a specially drilled hole.

All British heat flow measurements are summarized in Table 6 and in the appendix under the subheading Great Britain. The average heat flow from 7 reliable values is  $1.31 \pm 0.38$  s.d. It is highly desirable to establish the role of water circulation and to extend measurements in Scotland, Wales, and Ireland.

*Austria and Switzerland.* *Clark and Niblett* [1956] measured the heat flow at three tunnels

in the Swiss Alps: two values (Loetschberg and Simplon) were about  $2 \mu\text{cal}/\text{cm}^2 \text{ sec}$ , and the other (Gotthard) was 1.4. They also estimated the heat flow at tunnels in the eastern Alps (Arlberg and Tauern), but more reliable figures of similar values were obtained later by *Clark* [1961]. In such an area of folded mountains, anisotropy of thermal conductivity due to foliation presents unique problems.

*Hungary, Czechoslovakia, and Italy.* Intensive thermal studies have been conducted in Hungary by *Boldizsar* and associates [*Boldizsar*, 1956*a, b, c*; 1958*a, b*; 1959; 1964*a, b, c*; *Boldizsar and Gozon*, 1963; *Scheffer*, 1963]. Seven determinations, including one in Czechoslovakia, give high values of about  $2.5 \mu\text{cal}/\text{cm}^2 \text{ sec}$ . In addition to these heat flow values, more than 400 underground temperature measurements have been made to show that the Tertiary Hungarian Basin is characterized by high heat flow.

Within the Hungarian Basin, relatively high heat flows occur where the Paleozoic and Mesozoic bottom rocks are elevated, whereas relatively low ones occur where Tertiary sediments are thick owing to the subsidence. There is no indication of present volcanic activity even in the highest heat flow area. *Boldizsar* [1964*a, c*] considers that the Hungarian basin is an isolated geothermal high, surrounded by normal territories.

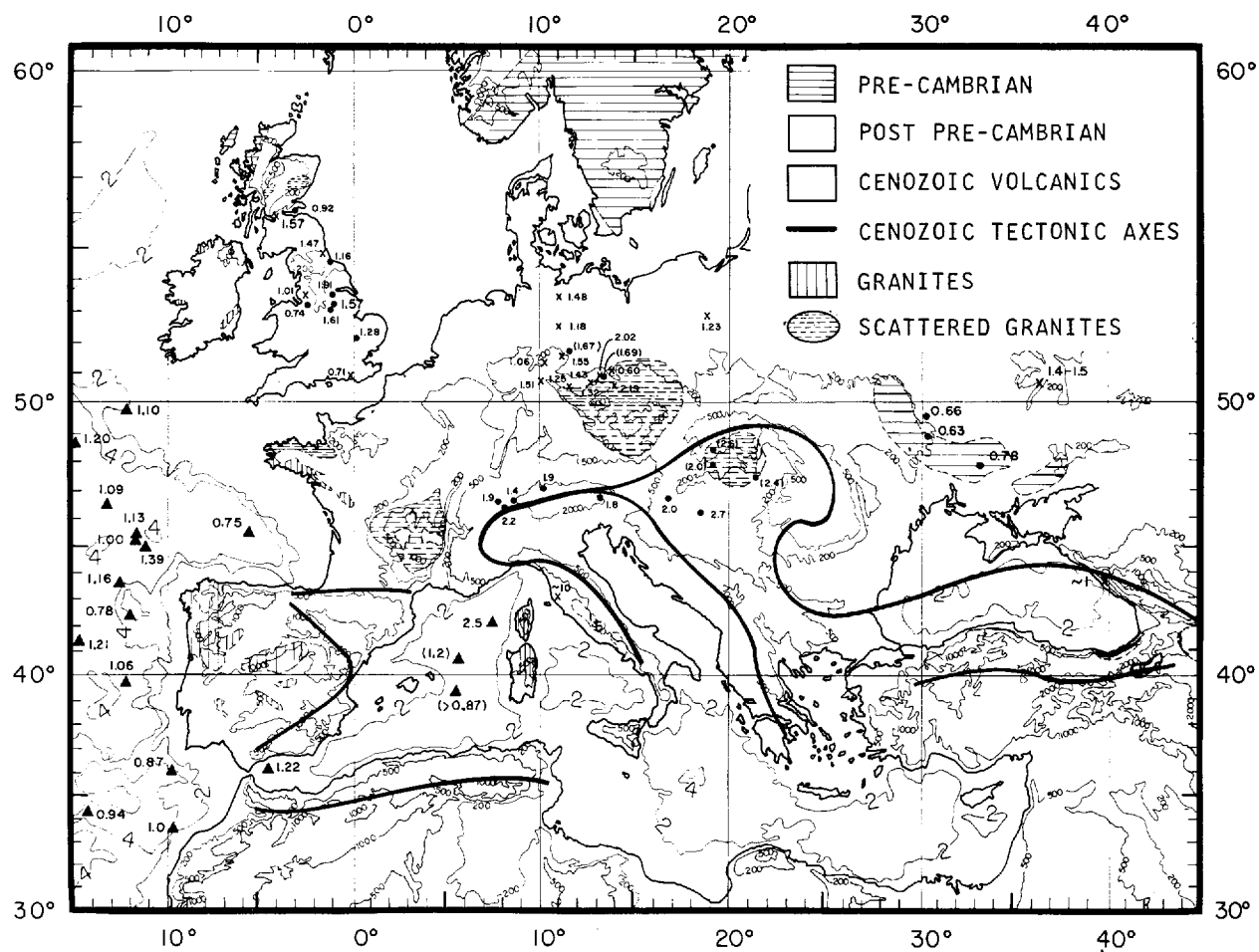


Fig. 9. Heat flow values in Europe. Topographic contours in meters. Bathymetric contours in kilometers. X is rejected station (category C), and values in parentheses are fair data (category B).

TABLE 6. Heat Flow Values in Europe

*MD*, maximum depth in meters; *N*, conductivity samples; *q*, heat flow; *q\**, corrected heat flow; *DC*, data class

Data No.	Station	Type	<i>MD</i>	<i>N</i>	<i>q</i>	<i>q*</i>	<i>DC</i>	Remarks	Reference
Austria									
0188	Arlberg	Tunnel	680	15		1.9	A	Tunnel through gneisses and schists of the pre-Mesozoic basement beneath the Arlberg pass; topographic correction applied; difficulty in sampling for conductivities	Clark, 1961
0139	Tauern	Tunnel	1440	27		1.8	A	Tunnel through granites and granite gneisses; topographic correction applied; 220 km E of Arlberg	Clark, 1961
Great Britain									
0133	Bawtry	4 boreholes	1190 980 970 1140	26	1.91		A	Survey holes in virgin coal areas through sandstone, marls, limestones, and breccia, on Nottinghamshire-Yorkshire border	Mullins and Hinsley, 1958
0130	Cambridge	Borehole	240	>16	1.28	1.48	A	Specially drilled hole; conductivity measured at 16 levels in Paleozoic section (lower half), and external samples were used for Mesozoic section (upper half); climatic correction applied	Chadwick, 1956
0128	Durham	Underground borehole	520		1.47	1.82	C	Estimated conductivity; climatic correction applied	Anderson, 1940
0124	Dysart	2 boreholes			0.92		A	Average value of 0124B and 0124C	Anderson, 1940
	A. Balfore bore		1200		0.68	1.16	B	Conductivities from Boreland bore, 5 km away; climatic correction applied	Benfield, 1939
	B. Balfore bore				0.89	1.20	B	Recalculated value of 0124A; climatic correction applied	Anderson, 1940
	C. Boreland bore		1000	6	0.95	1.28	A	Climatic correction applied	Anderson, 1940
0126	Glasgow	2 boreholes			1.57		C	Average value of 0126C and 0126D	Anderson, 1940
	A. Blythwood bore		100		1.24	1.56	C	Estimated conductivity	Benfield, 1939
	B. South Balfary bore		160		1.53	1.85	C	Estimated conductivity	Benfield, 1939
	C. Blythwood bore				1.41	1.75	C	Recalculated value of 0126A	Anderson, 1940
	D. South Balfary bore				1.73	2.07	C	Recalculated value of 0126B	Anderson, 1940
0127	Hankham	Borehole	235	8	0.71	1.12	C	Uncertainty due to absence of lithological information	Benfield, 1939
0125	Holford	Borehole	295	6	0.74	1.43	A	2 drill holes a few hundred meters apart through marl and rock salt; climatic correction applied	Benfield, 1939
0134	Nottingham	2 boreholes	693 533		1.61		A	Geology similar to Bawtry; same conductivity data as Bawtry	Mullins and Hinsley, 1958
0131	Nottinghamshire		670	60	1.57		A	Average value of 0131E and 0131F; samples mostly sandstones, marls, limestones, and shales	Bullard and Niblett, 1951
	A. Earkring 5		600		2.73		C	} Possibly disturbed by water flow	
	B. Earkring 6		660		2.75		C		
	C. Earkring 64		610		1.97		C		
	D. Earkring 141		605		2.87		C		
	E. Kelham Hill 1		670		1.47		A		
	F. Caunton 11		650		1.67		A		
0132	Yorkshire	2 boreholes	930 900		1.16		A	Some conductivity data from 0131 were also used	Bullard and Niblett, 1951
0129	Wigan	Colliery shaft	730		1.01	1.34	C	Temperature recorded during sinking of shaft in colliery; estimated conductivity; climatic correction applied	Anderson, 1940
Czechoslovakia									
0144	Banska Stiavnica				2.6		B	Tertiary andesite and dacite area; detail to be published	Boldizsar, 1964a, b
East Germany									
0155	Altenberg	Mine	240	?	2.19		C	Reliable temperature only from one level	Schossler and Schwarzlose, 1959
0146	Bleicherode	Mine	470	?	1.06		C	Temperature measured at 2 levels (404, 470 m deep)	Schossler and Schwarzlose, 1959
0153	Brand-Erbisdorf	Mine	?	?	2.02		C	Temperature measured at 2 levels 60 m apart in depth	Schossler and Schwarzlose, 1959

TABLE 6. Heat Flow Values in Europe (continued)

*MD*, maximum depth in meters; *N*, conductivity samples; *q*, heat flow; *q\**, corrected heat flow; *DC*, data class

Data No.	Station	Type	<i>MD</i>	<i>N</i>	<i>q</i>	<i>q*</i>	<i>DC</i>	Remarks	Reference
East Germany (continued)									
0156	Dorndorf	Mine	400	?	1.51		<i>C</i>	Temperature measured at 3 levels (largest vertical distance 55 m)	Schossler and Schwarzlose, 1959
0154	Freiberg	Mine	690	?	1.69		<i>B</i>	Temperature measured at 4 levels (600, 650, 530, 400 m deep)	Schossler and Schwarzlose, 1959
0152	Freitel	Mine		?	0.60		<i>C</i>	Temperature measured at a pair of 2 levels (75, 294 m in vertical distance)	Schossler and Schwarzlose, 1959
0158	Oebisfelde	Borehole	1350		0.91- 1.46		<i>C</i>	Deep hole into porphyry and quartz; estimated conductivity	Schossler and Schwarzlose, 1959
0149	Pechtelsgrün	Quarry	430		1.43		<i>C</i>	Temperature measured at 2 levels (250 m in vertical distance, 350 m in horizontal distance)	Schossler and Schwarzlose, 1959
0157	Rehna I	Borehole	890		1.14- 1.83		<i>C</i>	Limestone section between 700 m and ~890 m was used; estimated conductivity	Schossler and Schwarzlose, 1959
0150	Schmiedfeld	Mine	276	?	1.25		<i>C</i>	2 levels were used for temperature measurement in each of 2 mines 2.5 km apart (131, 176 m deep and 202, 276 m deep)	Schossler and Schwarzlose, 1959
0147	Stassfurt	Mine	614	?	1.67		<i>B</i>	Temperature measured at 4 levels (484, 528, 560, 614 m deep)	Schossler and Schwarzlose, 1959
0148	Strassberg	Quarry	280	?	1.55		<i>C</i>	Temperature measured at 2 levels (190, 280 m deep)	Schossler and Schwarzlose, 1959
0151	Zwickau	Mine	830	?	1.32		<i>C</i>	Temperature measured at 2 levels (730, 830 m deep)	Schossler and Schwarzlose, 1959
Hungary									
0142	Hajduszoboszló				2.2- 2.6		<i>B</i>	In Great Hungarian Plain of Pliocene sediments; details to be published	Boldizsar, 1964a, b
0141	Nagy Lengyel	Oil wells			1.9- 2.0			In Western Hungary	Boldizsar, 1964a, b
0143	Szentendre				2.0		<i>B</i>	Edge of mid-Hungarian Mountains of Oligocene sandstone; details to be published	Boldizsar, 1964a, b
0140	Zobak-Hosszúhetény-Bakonya	Mine	600		2.7		<i>A</i>	Average value of 3 stations in Mecsek Mountains; earlier value at Zobak [Böldizsar, 1956c] of 3.04 was confirmed; for other stations, detail to be published	Boldizsar, 1964a, b
Iceland									
1188	Iceland					4-5	<i>C</i>	Estimated conductivity	Bodvarsson, 1955
Italy									
0145	Larderello	9 boreholes	1400	18	6-14		<i>C</i>	In geothermal area	Boldizsar, 1963
Poland									
0159	Ciechocinek	Deep brine well	1300		1.23		<i>C</i>	Estimated conductivity	Stenz, 1954
Switzerland									
0135	Gotthard	Tunnel	1520	15	1.23	1.4	<i>A</i>	Tunnel through Swiss Alps; topographic correction applied	Clark and Niblett, 1956
0137	Loetschberg	Tunnel	1530	47	1.73	1.9	<i>A</i>	See Gotthard	Clark and Niblett, 1956
0136	Simplon	Tunnel	2050	51	1.98	2.2	<i>A</i>	See Gotthard	Clark and Niblett, 1956
USSR									
0161	Belaya Tserkov	Borehole	120	10	0.63		<i>A</i>	In NW part of Ukrainian Shield; area of present subsidence (< 2 mm/yr)	Lubimova et al., 1964; Lubimova, 1964
0160	Krivoy Rog	3 boreholes	1425 790 360	20	0.78		<i>A</i>	In SE part of Ukrainian Shield; area of present uplift (< 10 mm/yr)	Lubimova et al., 1964; Lubimova, 1964

TABLE 6. Heat Flow Values in Europe (continued)

*MD*, maximum depth in meters; *N*, conductivity samples; *q*, heat flow; *q\**, corrected heat flow; *DC*, data class

Data No.	Station	Type	<i>MD</i>	<i>N</i>	<i>q</i>	<i>q*</i>	<i>DC</i>	Remarks	Reference
USSR (continued)									
0164	Mazesta-Hosta	3 boreholes	2170 1350	15	~1		<i>C</i>	In Black Sea Coast of Caucasus; effect of Black Sea on gradient suspected; rocks obtained from nearby hole for sections above 950 m	<i>Lubimova et al.</i> , 1964; <i>Lubimova</i> , 1964
0162	Uman	Borehole	180	10	0.66		<i>A</i>	In NW part of Ukrainian Shield; 3 other holes (150, 140, 90 m deep) with 8 conductivities gave heat flow values 0.64, 0.63, 0.60 [ <i>Lubimova</i> , 1964]	<i>Lubimova et al.</i> , 1964; <i>Lubimova</i> , 1964
0163	Yakovlevski	2 boreholes	820 380	34	1.4- 1.5		<i>C</i>	Bores into iron ore layer; 100 km south of Kursk; temperature disturbed	<i>Lubimova et al.</i> , 1964

Even more pronounced hyperthermal areas are often found in Italy, where many active volcanoes are known. *Boldizsar* [1963] reports heat flows ranging from 6 to 14  $\mu\text{cal}/\text{cm}^2$  sec in Larderello, Tuscany, where geothermal energy is utilized for large-scale power production (see chapter 9 by McNitt).

*East Germany and Poland.* In the western part of the German Democratic Republic, 13 heat flow determinations in two boreholes and eleven mines have been made [*Schossler and Schwarzlose*, 1959]. Near the Czechoslovakian border, the stations in the Erzgebirge Mountains show high heat flows which have been considered to be related to the relatively strong radioactivity of the granites there.

In Poland, *Stenz* [1954] estimates the heat flow to be 1.23  $\mu\text{cal}/\text{cm}^2$  sec in a deep well at Ciechocinek, which is situated on the border between the old Russian Shield and the folded central Europe.

*West Germany.* *Creutzburg* [1964] has made 10 heat flow measurements in West Germany and has estimated the average heat flow to be 1.6  $\mu\text{cal}/\text{cm}^2$  sec. Very high heat flow values (up to 4.6) were observed in the salt masses in the Lower Saxony area and were not thought to be representative of the regional heat flow. However, these data have not been catalogued because of lack of information concerning their measurements.

*USSR.* The Soviet Union covers an area of about 22 million square kilometers (15% of the world's land area), but so far has only five published heat flow stations. *Lubimova et al.* [1961, 1964] measured the heat flow for three boreholes in the Caucasus near the Black Sea. They point out that the heat flow ( $\sim 1$   $\mu\text{cal}/\text{cm}^2$

sec) may be disturbed by the cooling effect of the neighboring Black Sea and of the Mazesta's springs.

*Lubimova et al.* [1964] also describe in detail the heat flow measurements at four other Soviet locations: Krivoi Rog, Uman, and Belaya Tserkov in the Ukrainian Shield and Yakovlevski Iron Ore Deposit. These observations are summarized in Table 6 under USSR.

*Lubimova* [1964] reviews the above shield measurements and compares them with the data on recent tectonic movements. She postulates that the Krivoi Rog area, which is uplifting, has slightly higher heat flow than the subsiding Kiev area (Uman and Belaya Tserkov). However, *Diment* [1965] suggests that her heat flow values in the Kiev area are about 20% too low and that the heat flow difference between the Kiev and Krivoi Rog areas is not significant.

*Miscellany.* *Kraskovski* [1961], in discussing heat flow in old shields, quotes heat flow estimates of 0.8  $\mu\text{cal}/\text{cm}^2$  sec at Monche-Tundra, 0.8 at Boliden (Sweden), both in the Baltic Shield area, and 0.88 near Krivoi Rog in the Ukrainian Shield. Details, however, are not given.

*Sisoev* [1961] measured the heat flow in the Black Sea with reversing thermometers (see section 2.3, Chapter 4, by Langseth). Since the method is doubtful and the assumed conductivity is too high, the results (data no. 0166 in the appendix) are very uncertain.

*Scheffer* [1964] reviews the European heat flow data and draws a heat flow contour map. As Scheffer notes, Figure 9 seems to suggest that the heat flow is generally high in Central Europe. By comparing this map with the geoid map of Europe [*Heiskanen and Vening-Meinesz*,

1958, p. 286], he maintains that the high heat flow is associated with an elevation of the geoid.

#### 4. REVIEW OF HEAT FLOW DATA AT SEA

In measuring heat flow, we are much more fortunate at sea. The bottom temperature in deep oceans being remarkably constant with space and time, temperature disturbances in the sediment from above are negligible, and the ocean floor sediment is quite easily penetrable by heat flow probes. An important disturbance is the effect of frictional heat generated by the penetration of the probe which has been satisfactorily eliminated by the design of the instrument or by the reduction of the data. The slow sedimentation in deep ocean (normally less than 1 cm per 1000 years) and water circulation in the sediments have negligible effects in disturbing the temperature. Moreover, the conductivity of ocean sediments varies only slightly (see Table 6.5). In early oceanic heat flow measurements, temperature gradients were measured with Bullard-type probes that penetrated a few meters into the sediment, and the conductivities were measured from cores taken at or near the site of temperature measurement. Recently Ewing-type probes have also been introduced. They are less convenient to operate, but they are more reliable because they combine coring (usually piston coring) and temperature gradient measurement into one operation and consequently offer deeper penetration and several temperature-sensing elements. Techniques of measuring heat flow through the ocean floor have been reviewed in chapter 4 by Langseth.

In considering the heat transfer through the ocean bottom, Lubimova et al. in chapter 5 of this volume conclude that to obtain representative heat flow measurements at sea other controls are desirable to determine the effects of environment. Alternatively, large numbers of observations should be made over an area to reduce the effect of random variables. Since measuring heat flow at sea is fast (a few hours per observation) and relatively inexpensive, detailed surveys of heat flow and reduction of data using statistical methods are recommended.

The quality of heat flow data at sea is far more uniform than that on land. We have rejected some oceanic data because of one or more

TABLE 6.5. Statistics of Thermal Conductivity of Oceanic Sediments

Ocean	Number of Values*	Mean	Standard Deviation	Standard Error	Mode
Atlantic	106	2.09	0.19	0.02	2.1
Indian	180	1.98	0.25	0.02	2.1
Pacific	300	1.95	0.20	0.01	2.1
All	586	1.98	0.22	0.01	2.1

\* These values are usually the mean conductivities at different locations, each of which is the average determined from a number of sediment core samples by needle probe or water content methods.

of the following reasons: (1) an upper or a lower or a range of heat flow values is given for a station; (2) conductivity values are adopted from nearby stations and temperature probes have partly penetrated the sediment; and (3) measurements were made over shallow water (e.g.  $\leq 1$  km deep). The oceanic data are reviewed separately for the Atlantic, Indian, Pacific, and Arctic oceans. For each region, the literature is briefly reviewed, and the data are summarized and discussed under major features of the oceans. Heat flow values are plotted on maps and are tabulated in the appendix.

##### 4.1 Atlantic Ocean

The Atlantic is the second largest ocean, covering nearly 20% of the Earth's surface. North of the equator, because of projecting land areas and islands arcs, the Atlantic is characterized by several semi-enclosed seas. Excluding these adjacent seas, the Atlantic Ocean floor can be divided into three major divisions: the continental margins, basins, and the Mid-Atlantic Ridge, each occupying about one-third of the total area. Bathymetric maps for the North and the South Atlantic, with heat flow stations indicated, are given in Figures 10 and 12, respectively.

The pioneering work on heat flow measurements in the Atlantic was carried out by Bullard in 1954. Within a decade, about 250 heat flow values have been obtained (see Figures 11 and 13). The literature includes *Bullard* [1954], *Bullard and Day* [1961], *Reitzel* [1961a, b; 1963], *Gerard et al.* [1962], *Lister* [1962, 1963a, b], *Lister and Reitzel* [1964], *Nason and Lee* [1962, 1964], *Vacquier and Von Herzen* [1964], *Langseth and Grim* [1964], *Birch* [1964], and M. G. Langseth (private communi-

cation). They are summarized in Table 7, and their numerical results are given in the appendix.

*General geology.* The most striking feature of the Atlantic is the continuous, broad, fractured swell known as the Mid-Atlantic Ridge (Figures 10 and 12). It runs along almost the entire length of the ocean and is almost exactly equidistant from Europe and Africa on one side and the Americas on the other. The Ridge rises about two kilometers above the deep basins on either side. It is very mountainous, and some of the highest parts rise above the sea level, forming islands. The crest zone has extremely rugged relief, and *Heezen and Ewing* [1963] maintain that a continuous central rift valley lies along the axis, coinciding with the belt of mid-oceanic earthquake epicenters. In Figures 11 and 13, the crest of the Mid-Atlantic Ridge is indicated by heavy solid lines, and the extent of the ridge is given by dashed lines. Numerous faults, approximately perpendicular to the ridge crest, have displaced much of the Ridge. Recent seismic and gravity studies over the Mid-Atlantic Ridge reveal normal thickness of the crust, lower seismic velocity under the axial zones, and null free air gravity anomaly over the entire ridge [*Le Pichon et al.*, 1965; *Talwani et al.*, 1965].

On either side of the Mid-Atlantic Ridge, many basins are separated by a series of small transverse ridges and rises that extend from the Mid-Atlantic Ridge or out from the continents. Most basins are more than four kilometers deep, and some parts are deeper than six kilometers. In many places, the basin floors are extremely smooth and slope gently toward the deeper parts, constituting the abyssal plains. In other places, the floors are intensely disrupted and have a finely textured relief; these are the abyssal hills. In addition to the abyssal plains and abyssal hills, there are small asymmetric oceanic rises with moderate relief, but they do not occupy much area.

The Atlantic Ocean has only a few small trenches. The Puerto Rico Trench (maximum depth 9200 meters) has a flat floor and can be traced for only about a thousand kilometers, much shorter and shallower than the Pacific trenches.

*Mid-Atlantic Ridge.* *Bullard and Day* [1961] observed a high heat flow of  $6.52 \mu\text{cal}/\text{cm}^2 \text{ sec}$  in the central valley of the Mid-Atlantic Ridge

( $47^\circ\text{N}$ ). The area is very rocky, causing great difficulty in attempts to repeat the measurements. *Reitzel* [1961*a, b*] also obtained a high value of  $>6.2$  in a small valley about 50 km northeast of the Ridge ( $51^\circ\text{N}$ ). The temperature gradient at this station exceeded the range of the instrument, and no core for conductivity measurement was taken. A pipe dredge haul brought up yellow mud with large and abundant shards of fresh volcanic glass. Like the value found by *Bullard and Day*, this high heat flow is attributed to recent volcanism. *Lister and Reitzel* [1964] report a line of six stations along  $29^\circ\text{N}$  across the crest of the Ridge. These successful stations, out of 13 trials, give low values of about  $1 \mu\text{cal}/\text{cm}^2 \text{ sec}$ . Rough rocky bottom caused considerable penetration difficulties, so that these stations may not be representative of the crestal zone. Some 700 km south, *Nason and Lee* [1962, 1964] made a profile of 11 stations across the Ridge. Values as low as  $0.3 \mu\text{cal}/\text{cm}^2 \text{ sec}$  are found on the flanks, and values as high as  $6.5 \mu\text{cal}/\text{cm}^2 \text{ sec}$  at the crest.

*Vacquier and Von Herzen* [1964] made extensive heat flow and magnetic studies of the Mid-Atlantic Ridge. Fourteen crossings ( $30^\circ\text{S}$  to  $6^\circ\text{S}$ ) revealed the presence of a continuous magnetic intensity anomaly characteristic of the crest. Nearly all heat flow values greater than  $2 \mu\text{cal}/\text{cm}^2 \text{ sec}$  lie within 100 km of the apex of the magnetic anomaly. Low heat flow values are observed to be predominant between 300 and 600 km from the crest. Many of these low values do not appear to be associated with unusual local topography and are quite uniformly distributed on the ocean floor.

*Atlantic Basins.* In various Atlantic Basins (including those in the Caribbean Sea), very uniform heat flow values of about  $1.1 \pm 0.2 \text{ s.d.}$  have been observed. *Reitzel* [1963] determined heat flow at sixteen stations regularly spaced over the North American Basin. The results show a remarkable uniformity in heat flow ( $1.14 \pm 0.06 \text{ s.d.}$ ) over  $10^6 \text{ km}^2$  area, which have been further confirmed by later workers. *Lister* [1963*a*] discusses ten measurements forming a close group in the Canary Basin around the Madeira and the Cape Verde abyssal plains. His values range from 1.03 to 1.39, with a standard deviation of 0.11. *Nason and Lee* [1964] also found similar values in the same region.

*Other Atlantic areas.* Heat flow values are

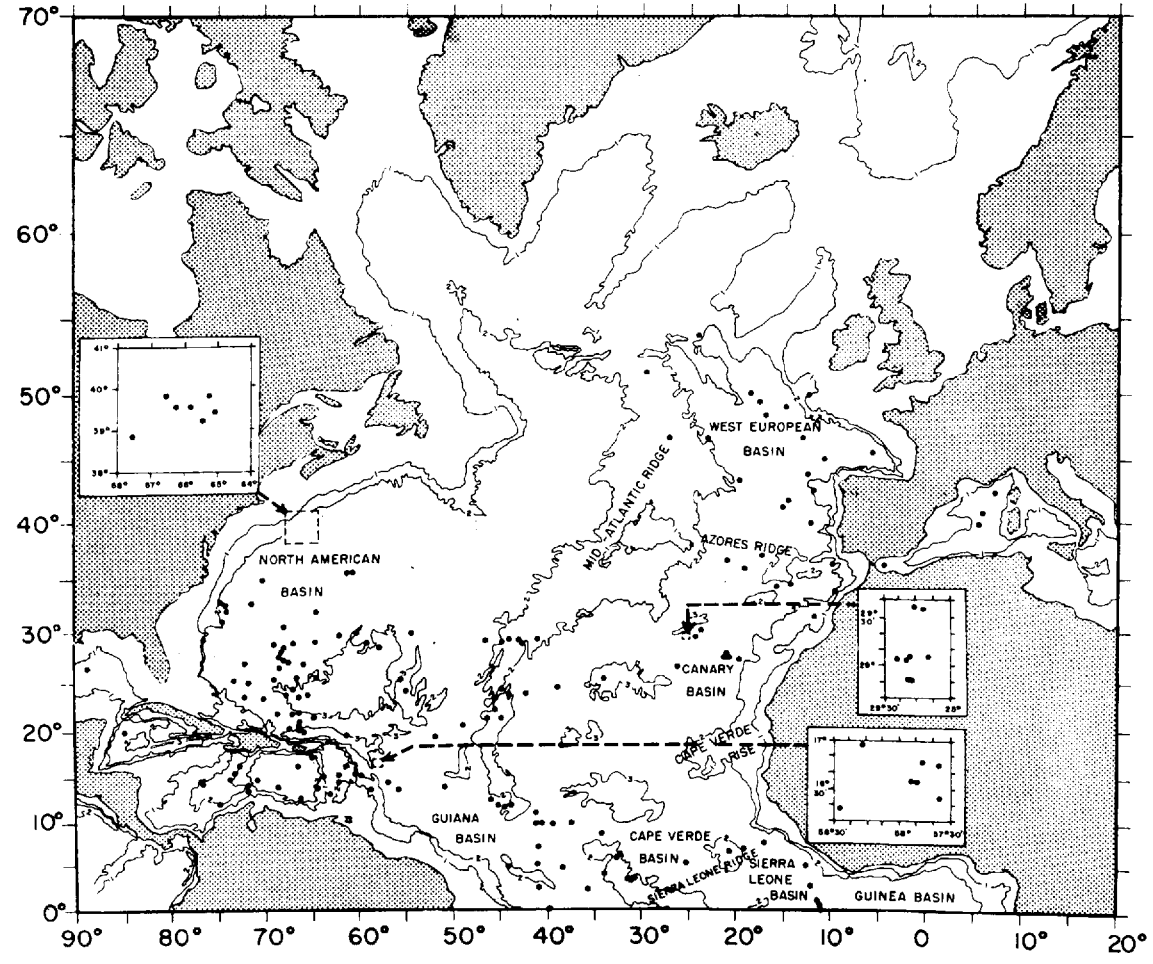


Fig. 10. Bathymetric map of the North Atlantic with locations of heat flow stations. Contours in thousands of fathoms.

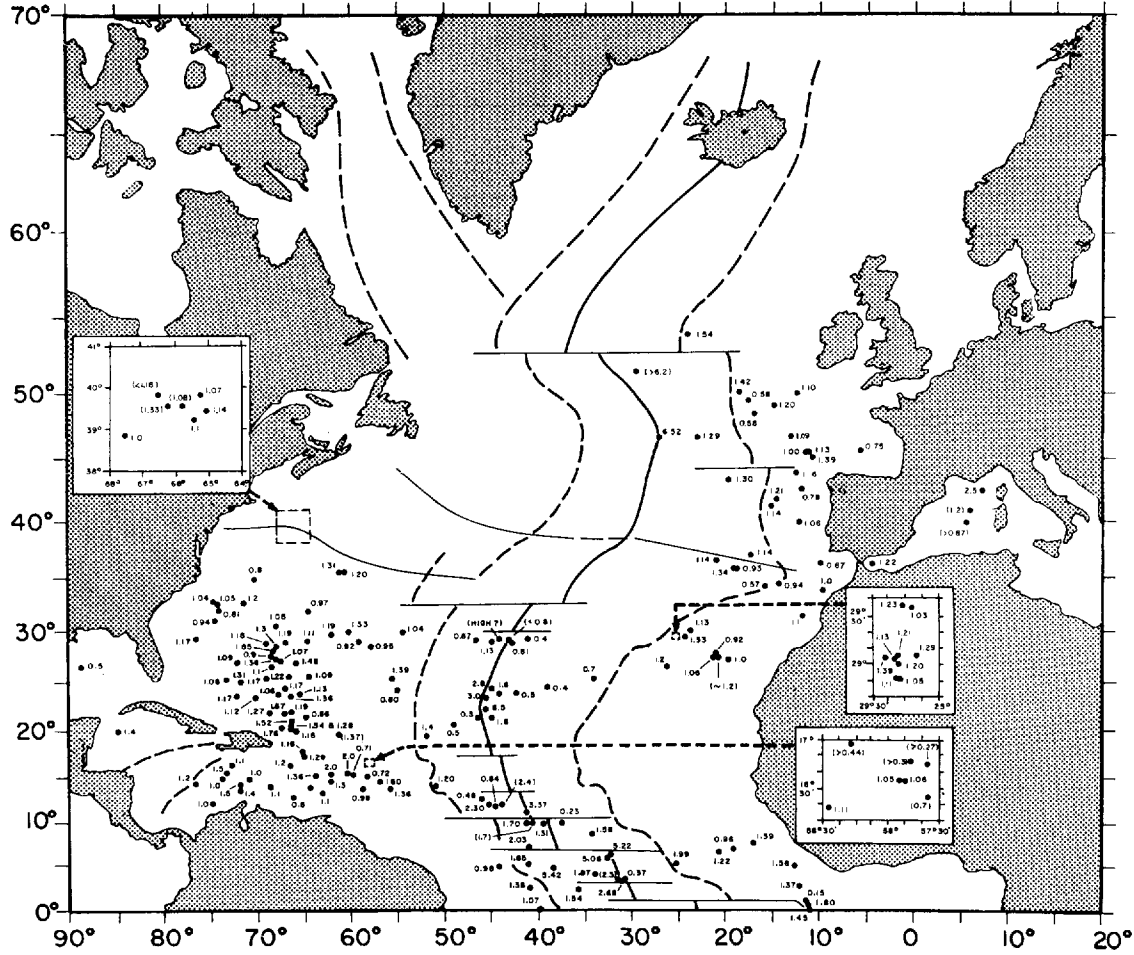


Fig. 11. Heat flow values in the North Atlantic. Values in parentheses are rejected data (category C). Heavy solid lines indicate the crest, and dashed lines the extent of the Mid-Atlantic Ridge (taken from Figure 38).

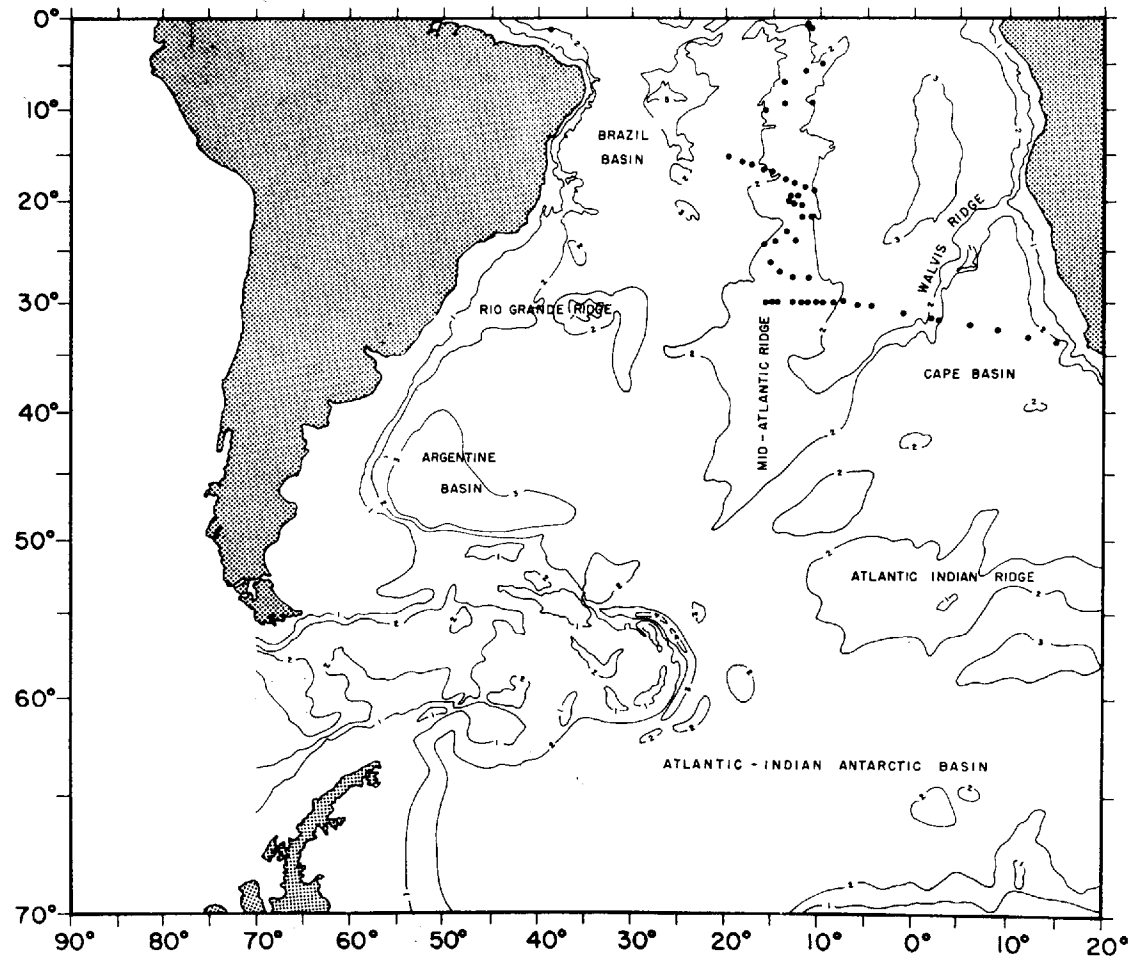


Fig. 12. Bathymetric map of the South Atlantic with locations of heat flow stations. Contours in thousands of fathoms.

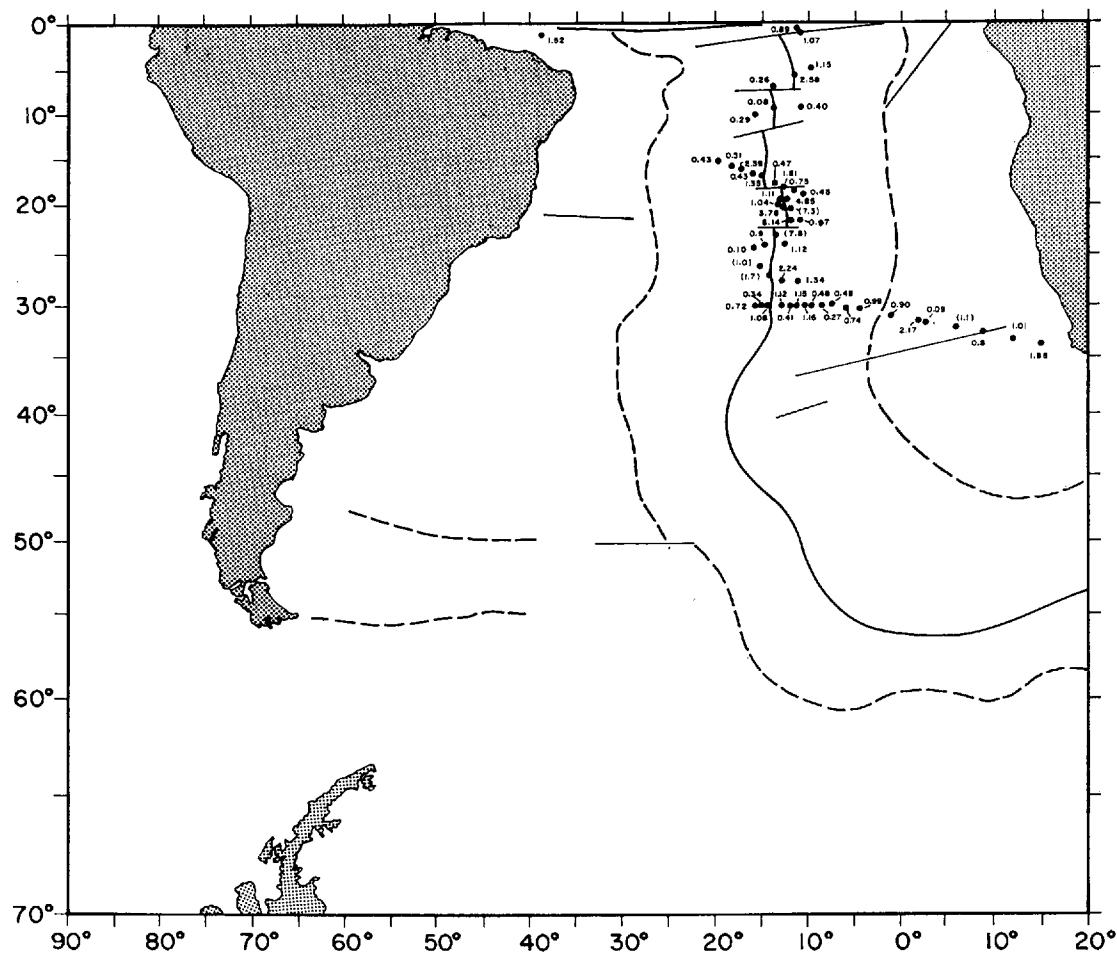


TABLE 7. Summary of Heat Flow Data in the Atlantic Ocean

Reference	Data No.	No. of Stations	Regions	Remarks on Heat Flow Data
<i>Bullard, 1954</i>	0391-0395	5	West European Basin	First measurements in the Atlantic; average value is $0.98 \pm 0.35$ s.d.
<i>Bullard and Day, 1961</i>	0214-0229	16	West European Basin, Mid-Atlantic Ridge, and Mediterranean Sea	Fairly uniform (0.78 to 1.89) values in the Basin and the east flank of the Mid-Atlantic Ridge; high value (6.52) in the central valley of the Ridge; difficult to repeat this measurement because of rocky bottom
<i>Reitzel, 1961a</i>	0230-0233	4	North American Basin and Mid-Atlantic Ridge	Two stations (10 km apart) in the Basin gave similar values (1.20 and 1.31); high value ( $> 6.2$ ) in a small valley about 50 km NE of the crest of the Mid-Atlantic Ridge
<i>Reitzel, 1961b</i> <i>Gerard et al., 1962</i>	0234-0247	14	Various Atlantic Basins, Mid-Atlantic Ridge, and Puerto Rico Trench	Ph.D. thesis; detailed account of <i>Reitzel</i> [1961a] Values are: continental rise off Brazil (1.52 & 1.07), Ceara abyssal plain (1.38), edge of Guiana abyssal plain (1.85), western flank of Mid-Atlantic Ridge (2.08), transverse trough in the Ridge axis (3.37), SE extension of Puerto Rico Trench (1.60), Antilles outer ridge (1.52), Nares abyssal plain (1.36), crest of Antilles outer ridge (1.67), floor of Puerto Rico Trench (1.16), continental rise off U.S. (1.03 & 1.04); conductivity estimated from chlorine content
<i>Lister, 1962</i>				Ph.D. thesis; source material for <i>Lister</i> [1963a, b] and <i>Lister and Reitzel</i> [1964]
<i>Lister, 1963a</i>	0348-0357	10	Around Madeira and Cape Verde abyssal plains (Madcap) in west Canary Basin	Closely spaced ( $\sim 1^\circ \times 1^\circ$ ) stations giving very uniform values: $1.20 \pm 0.11$ s.d.; Madcap caldera causes a reduction in heat flux at its summit as expected from the effect of topographic relief
<i>Lister, 1963b</i>	168, 170, 171, 174, 0348-0370	27	Various Atlantic Basins, Mid-Atlantic Ridge, and Mediterranean Sea	Brief summary of values obtained in <i>Lister</i> [1962]
<i>Lister and Reitzel, 1964</i>	0167-174	8	A profile along $29^\circ\text{N}$ over Mid-Atlantic Ridge; a pair on the outer ridge north of Puerto Rico Trench	6 successful stations out of 13 trials on the ridge have rather low values (0.8-1.1); difficult for the probe to penetrate sediments because of rocky bottom; a pair of stations ( $< 4$ km apart) by two different techniques are 1.28 and 1.54
<i>Nason and Lee, 1962</i>		14	A profile across the Mid-Atlantic Ridge from Martinique to Canary Islands	Preliminary results of some part of <i>Nason and Lee</i> [1964]
<i>Nason and Lee, 1964</i>	0328-0347	20	A profile from Panama to Nice, France, across the Caribbean, various Atlantic Basins, Mid-Atlantic Ridge, and the Mediterranean	Values of $\sim 1.2$ in various basins; low values in the flanks of Mid-Atlantic Ridge and high values in the crest; values obtained in the east of Antilles and the Mediterranean are questionable because of possible thermal disturbances in the sediment
<i>Reitzel, 1963</i>	0175-0194	20	North American Basin; near Puerto Rico Trench; continental slope off U.S.	16 regularly spaced stations over North American Basin between Bermuda and the Bahama Banks show a remarkable uniformity in heat flow ( $1.14 \pm 0.06$ s.d.); value at southern edge of the above area near the Puerto Rico Trench is 1.76; rather low values ( $\sim 1$ ) close to continental slope off U.S.
<i>Vacquier and Von Herzen, 1964</i>	0248-0327	81	14 crossings of the crest of the Mid-Atlantic Ridge between $30^\circ\text{S}$ and $6^\circ\text{S}$ ; a long profile from Freetown, Africa, to the Caribbean	Nearly all heat flow values $> 2$ are within 100 km of the apex of the magnetic anomaly which is characteristic of the crest; between 300 and 600 km from the crest, low values are predominant, and most of them do not seem to be associated with unusual local topography and are systematically distributed on the ocean floor; a somewhat high value (2.7) in the center of Walvis Ridge and low values over its flanks; six values from deep sea to the inside of the Lesser Antilles arc showed higher values near the central part of the island arc
<i>Birch, 1964</i>	0195-0213	19	Barracuda Fault Zone, New England Seamounts, and abyssal hills SE of Bermuda	M.Sc. thesis; details not available to us
<i>Langseth and Grim, 1964</i>	0371-0390	20	Western Atlantic, Caribbean Sea and Gulf of Mexico	Preliminary report; details not available

few over the Puerto Rico Trench and do not indicate any significant feature, except that values on its outer ridge are slightly higher (about 1.5) than the value (1.2) measured on the floor of the trench [*Gerard et al.*, 1962]. *Diment and Weaver* [1964] obtained a low

value of 0.6 from a hole 300 meters deep in a serpentinized ultrabasic body (see Table 3E) near Mayaguez, Puerto Rico.

Around the Antilles island arc, heat flow values are fairly variable (0.3 to 2.0). Because of disturbance observed in the sediment cores,

heat flow values observed over this area are probably not representative of the regional heat flow [Nason and Lee, 1964].

The Mediterranean Sea and the Gulf of Mexico have only a few measurements, and hence no definite conclusions can be drawn.

*Heat flow results.* Histograms of heat flow values from the Atlantic ridges (almost all from the Mid-Atlantic Ridge) and basins are given in Figures 14 and 16. The arithmetic mean for 87 ridge values is  $1.48 \pm 1.48$  s.d., whereas that for 74 basin values is  $1.13 \pm 0.24$  s.d. (see Table 14). Heat flow values in the Mid-Atlantic Ridge are plotted versus distance from the crest in Figure 15. Values exceeding 2.5 are found only within 100 km of the ridge crest. The average of 32 measurements within 100 km of the crestal zone is  $3 \pm 2$  s.d.  $\mu\text{cal}/\text{cm}^2 \text{ sec}$ , which is twice the world average. 75-, 50-, and 25-percentile lines are also given for heat flow values from the Mid-Atlantic Ridge and the Atlantic basins in Figure 15. (For example, the 75-percentile line separates the data into two groups: 75% of the data points are above it, and 25% of the data points below it. In drawing the percentile lines, the horizontal axis is divided into small intervals. Within each interval, a horizontal line separating the number of data points into different percentiles is drawn. Each set of these horizontal lines is then connected smoothly to form the percentile line.) The contrast is obvious: whereas values from the Mid-Atlantic Ridge are widely scattered, those from the Atlantic basins are very uniform. Furthermore, the percentile lines for the values from the Mid-Atlantic Ridge indicate two subgroups: (1) within 100 km of the ridge crest heat flow values are extremely scattered, and (2) beyond 100 km the values become less scattered as the distance from the ridge crest increases.

#### 4.2 Indian Ocean

The Indian Ocean is the second smallest of the four oceans and covers about 15% of the Earth's surface. The major topographic features and locations of heat flow stations are shown in Figure 17. Figure 18 gives the heat flow values and morphologic divisions.

Heat flow measurements were first made in the Indian Ocean by R. P. Von Herzen, and within a few years about 220 heat flow values

have been obtained by four research groups (Cambridge, Lamont, Scripps, and USCGS). (See Figure 18.) The literature includes Von Herzen [1963], Burns [1964], Von Herzen and Langseth [1965], and J. Selater (private communication). They are summarized in Table 8, and their numerical results are given in the appendix. Very recently, V. Vacquier and associates (private communication) have made extensive heat flow measurements in the Indian Ocean. However, the results are too late to be catalogued in this chapter.

*General geology.* The Indian Ocean has a well developed basin and ridge structure [Stocks, 1960]. The Mid-Indian Ocean Ridge system is believed to be part of the seismically active worldwide rift system [Heezen and Ewing, 1963]. It begins in the north as the Carsberg Ridge and extends from the Gulf of Aden southeastward to the equator. It then runs nearly due south, passing to the east of the Seychelles-Mauritius Ridge and branches into two separate ridges at about 25°S. The southwest branch runs around the southern tip of Africa to join the Mid-Atlantic Ridge. The southeast branch runs south of Australia and is continuous with the ridge of the southwestern Pacific Ocean. This ridge system divides the Indian Ocean into three units, western, eastern, and southern. The last unit has hardly been explored.

The three major units of the Indian Ocean are further divided into various basins by minor ridges; e.g., the Laccadive Ridge and Ninety-East Ridge. For the most part these ridges are seismically inactive and extend from the Mid-Indian Ridge system toward the continents, varying in width from 150 to 300 km. Most of the Indian Ocean basins are more than 3.5 km deep, and some parts are deeper than 5 km. The deepest basins and the only trench (Java-Sumatra Trench off the Indonesian arc) occur in the east. In the west the sediments are chiefly globigerina ooze, whereas in the east red clay predominates.

Extensive study of the Indian Ocean is still in progress. The International Indian Ocean Expedition (1960-1965) has yielded much valuable information, but most of it is not yet published.

*Heat flow results.* The most extensive heat flow study of the Indian Ocean is given by Von Herzen and Langseth [1965]. Besides giv-

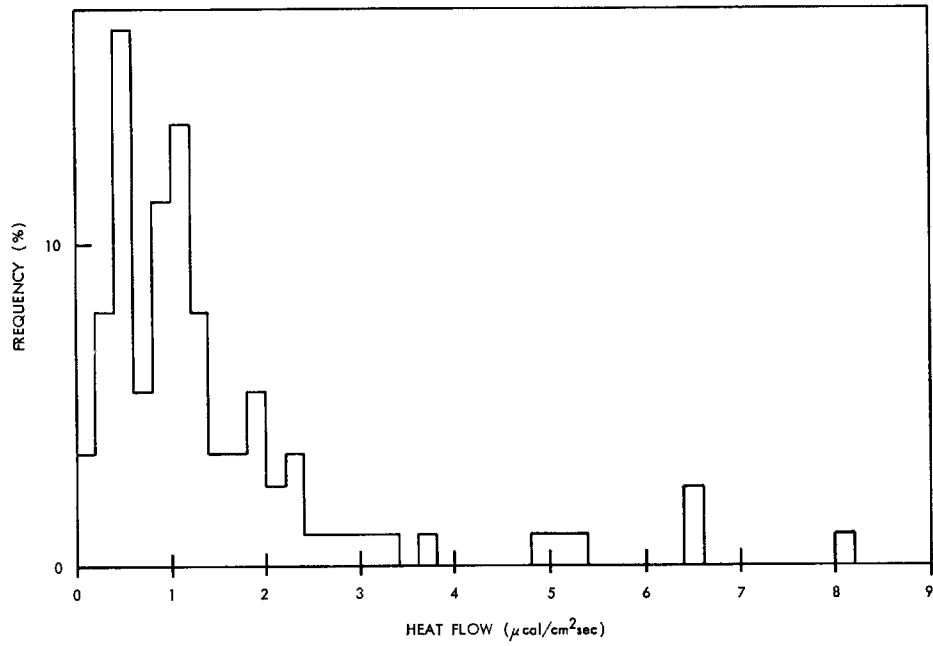


Fig. 14. Histogram of heat flow values from Atlantic ridges.

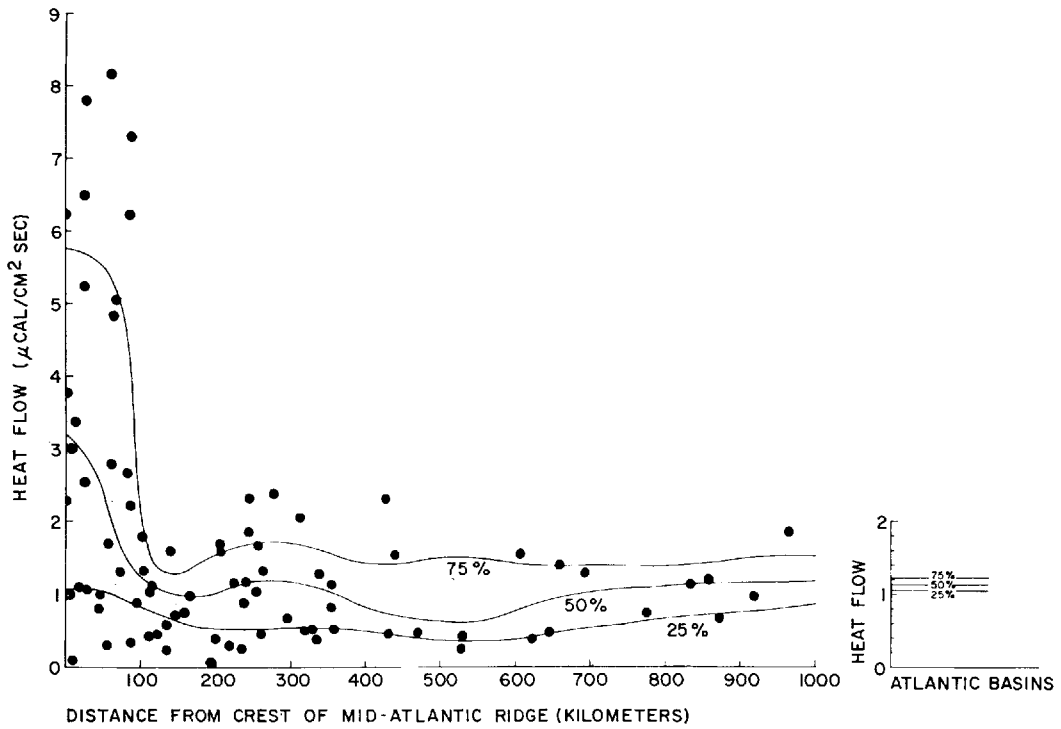


Fig. 15. Heat flow values versus distance from the crest of the Mid-Atlantic Ridge; 75-, 50-, and 25-percentile lines are given for values from the Mid-Atlantic Ridge and the Atlantic basins. For example, the 50-percentile line separates half the data points above and half the data points below it.

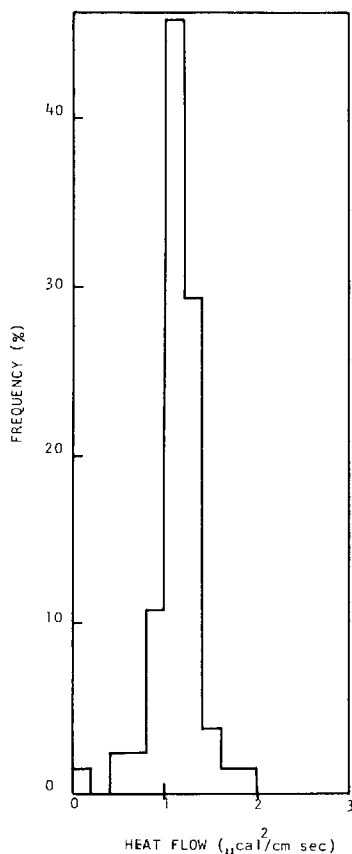


Fig. 16. Histogram of heat flow values from the Atlantic basins.

ing an excellent review of oceanic heat flow measurements in general, they also present a comprehensive account of their heat flow observations in the Indian Ocean. The measurements by Scripps Institution of Oceanography using Bullard-type probes, and those by the Lamont Geological Observatory utilizing the Ewing technique, have been made independently of one another. The authors give a critical

evaluation of measurements by different techniques, and they summarize and discuss their results under major physiographic features.

Histograms of heat flow values from the Indian Ocean ridges and basins are given in Figures 19 and 21. The arithmetic mean of 85 ridge values is  $1.57 \pm 1.17$  s.d., whereas the mean of 90 basin values is  $1.39 \pm 0.42$  s.d. (see Table 14). Heat flow values in the Mid-Indian Ocean Ridge are plotted versus distance from the crest in Figure 20. As for the Mid-Atlantic Ridge (Figure 15), values exceeding 2.5 are found only within about 100 km of the crestal zone. In Figure 20, 75-, 50-, and 25-percentile lines are also given for heat flow values from the Mid-Indian Ocean Ridge and the basins. Although the contrast is not as great as in the Atlantic Ocean, the picture is similar. The percentile lines fall to a minimum at about 300 to 400 km from the crest of the Mid-Indian Ocean Ridge and then increase (Figure 20).

A few measurements from the Java Trench suggest that the inner trench may be a region of low heat flow, whereas the outer trench may have moderately high heat flow. Recently *Vacquier and Taylor* [1965] have made a detailed survey in the trench area off Sumatra. They obtained a mean value of  $1.23 \pm 0.88$  s.d. from 20 measurements in the deep trench and a mean value of  $1.57 \pm 0.84$  s.d. from 37 measurements outside the trench. However, these data were too late to be catalogued.

#### 4.3 Pacific Ocean

The Pacific is the largest ocean and covers about 35% of the Earth's surface. *Menard* [1964] provides an excellent account of the general geology and geophysics of the Pacific. Bathymetric maps for the Pacific and locations

TABLE 8. Summary of Heat Flow Data in the Indian Ocean

Reference	Serial No.	No. of Stations	Regions	Remarks on Heat Flow Data
<i>Von Herzen</i> , 1963	0424-0428	5	Gulf of Aden	High values (2.5 to 6) were obtained; see <i>Von Herzen and Langseth</i> [1964]
<i>Turns</i> , 1964	0587-0590	4	Volcanic trend of the primary arc enclosing the Adaman Sea	Widely different values (0.9 to 5.3) over a nearly straight north-south profile of about 300 km length
<i>Von Herzen and Langseth</i> , 1965	0396-0586	191	Fairly well distributed over the whole Indian Ocean	See text
clater, private communication	0591-0617	27	Red Sea, Gulf of Aden, West Indian Ocean	High values observed in Red Sea and Gulf of Aden; details not available

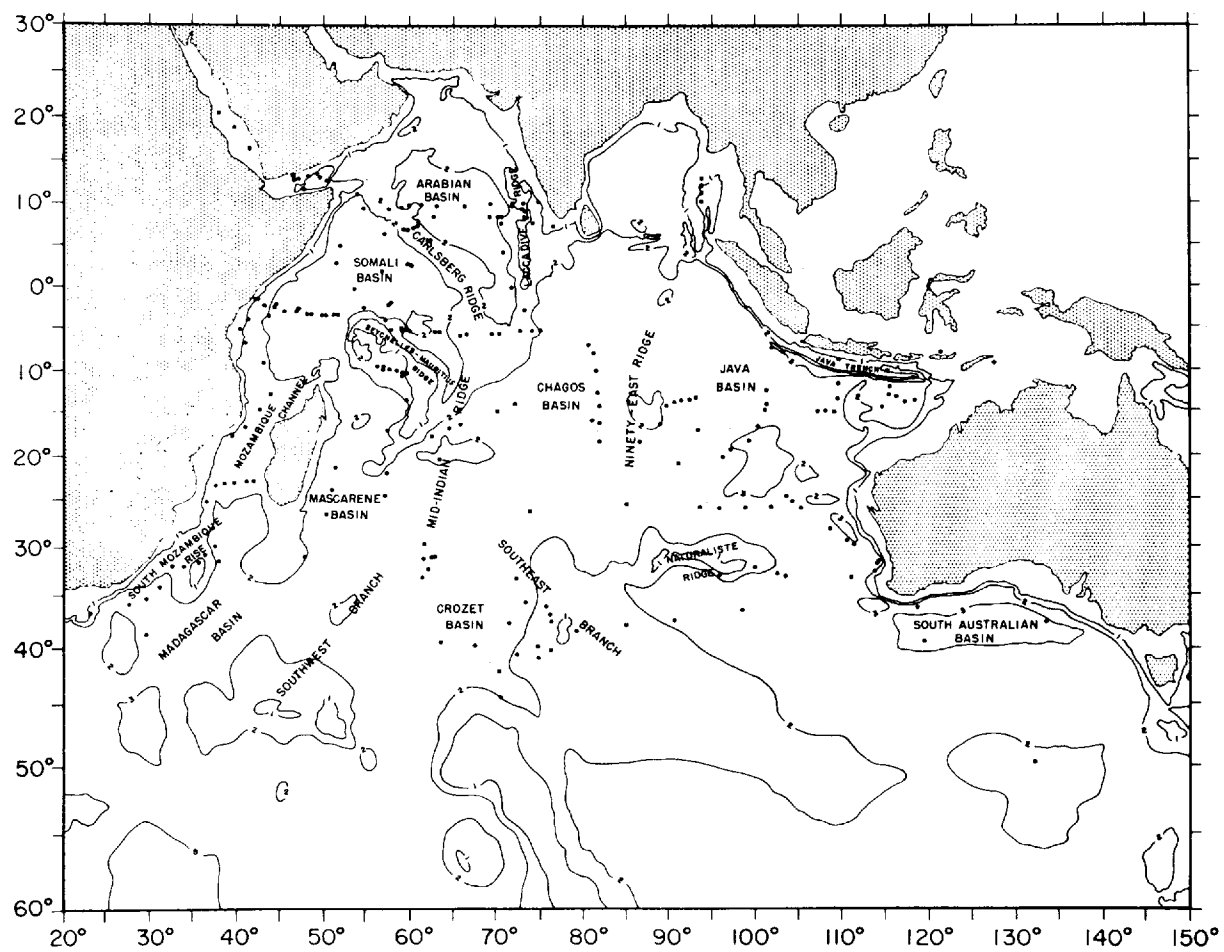


Fig. 17. Bathymetric map of the Indian Ocean with locations of heat flow stations; contours in thousands of fathoms.



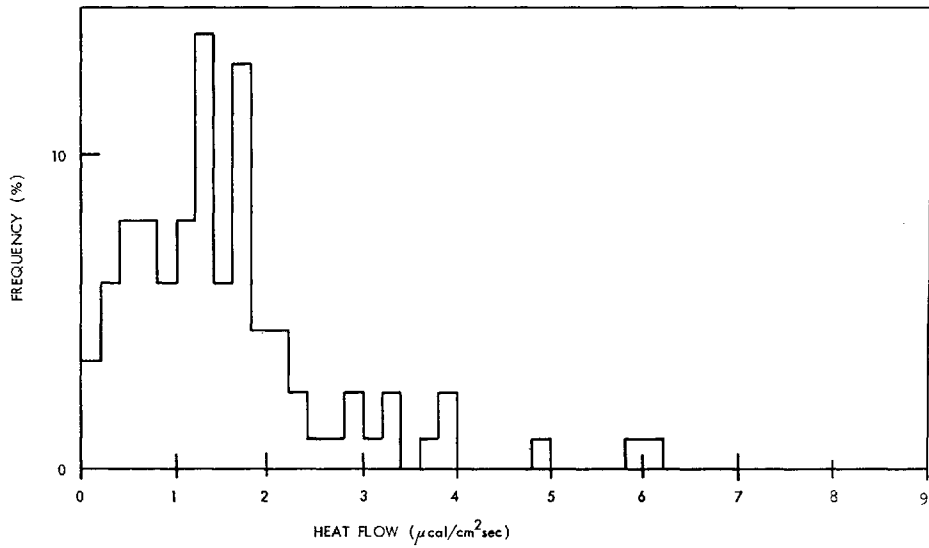


Fig. 19. Histogram of heat flow values from the Indian Ocean ridges.

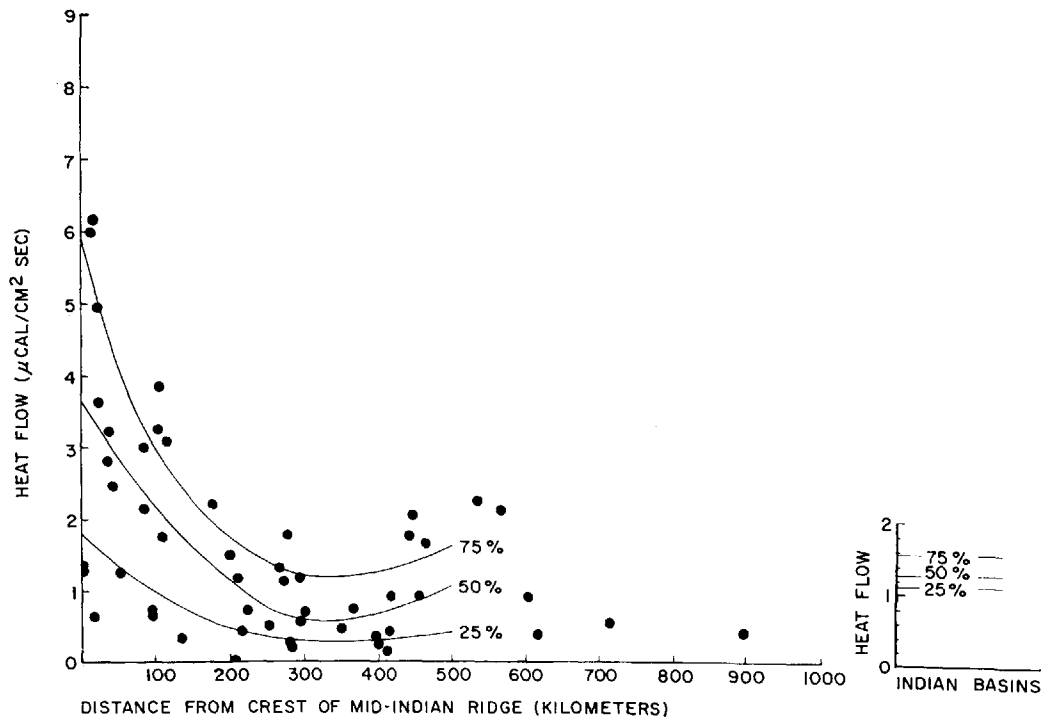


Fig. 20. Heat flow values versus distance from the crest of the Mid-Indian Ocean Ridge; 75-, 50-, and 25-percentile lines are given for values from the Mid-Indian Ocean Ridge and the Indian Ocean basins. For example, the 50-percentile line separates half the data points above and half the data points below it.

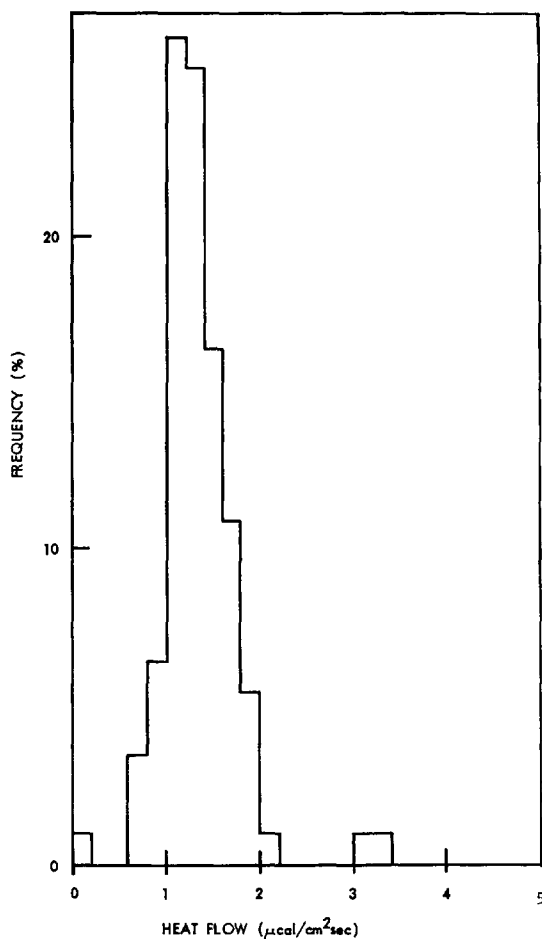


Fig. 21. Histogram of heat flow values from the Indian Ocean basins.

of heat flow stations are given in Figures 22, 24, 26, and 27.

E. C. Bullard, R. Revelle, and A. E. Maxwell pioneered the heat flow measurements in the Pacific in the early 1950's. Since then about 500 heat flow values have been published (see Figures 23, 25, 26, and 27). Unfortunately most data are centered around the central east Pacific. The literature includes *Revelle and Maxwell* [1952], *Bullard et al.* [1956], *Maxwell and Revelle* [1956], *Maxwell* [1958], *Von Herzen* [1959, 1960, 1963, 1964, and private communication], *Uyeda et al.* [1962], *Foster* [1962], *Von Herzen and Uyeda* [1963], *Von Herzen and Maxwell* [1964], *Rhea et al.* [1964], *Uyeda and Horai* [1964], *Langseth et al.* [1965], P. Grim (private communication), and *Yasui and*

*Watanabe* [1965]. They are summarized in Table 9 and their numerical results are given in the appendix.

*General geology.* The northwestern half of the Pacific is relatively deep compared with the southeastern half and is relatively normal: water depth of 5 to 6 km, crustal thickness of about 5 to 6 km, and aseismic. Clusters of volcanoes are common and usually occur along very long faults. The southeastern half is 3 to 5 km deep and has been deformed into a system of elongated, broad rises.

The most prominent of the rises is the East Pacific Rise, a vast, low bulge of the sea floor 2 to 3 km high, 2000 to 4000 km wide, and about 15,000 km long [*Menard*, 1964, p. 118]. Its size is comparable to North and South America, which it roughly parallels and in part overlaps. Both ends are ill-defined, and its boundaries are rather vague (Figures 23 and 25). The southern end may be at about 60°S and 160°W and can be traced as a continuous feature trending northeast, although the crest is offset between 25 and 30°S. The general trend of the rise changes to northwest at the equator, and it is so close to land that the eastern flank begins to be obscured. The crest disappears as an identifiable topographic feature at the southern end of the Gulf of California, and *Menard* suggests that it continues under the Gulf of California and reappears off Oregon. North of the Mendocino fracture zone, the crest of the rise reappears as a belt of ridges and troughs, but again vanishes, because of transverse faulting, at about 50°N. The western flank butts into Alaska, and the crest has not been identified farther north. Seismic refraction studies indicate that the depth to the Mohorovicic discontinuity under the crest of the East Pacific Rise is shallow and upper mantle velocities are low. Shallow earthquakes are also common along the crest.

Most Pacific basins are to the west of the East Pacific Rise. They are usually 5 to 6 km deep and mostly not mountainous. A series of deep ocean trenches almost surrounds the Pacific at the margin. The circum-Pacific margin including these trenches is the most active geological structure on Earth. Special features are the greatest ocean depths, largest gravity anomalies, most extensive volcanism, most intense

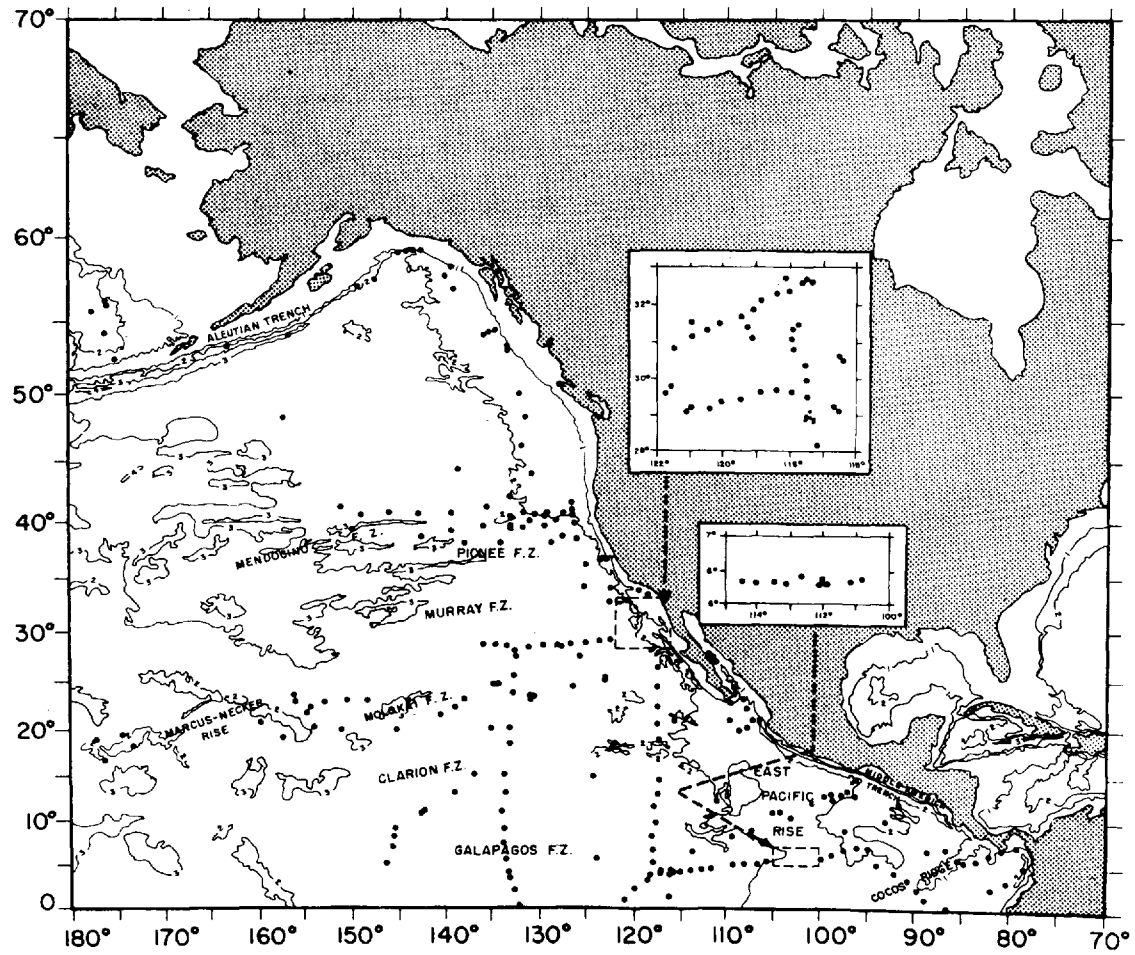


Fig. 22. Bathymetric map of the northeast Pacific with locations of heat flow stations, contours in thousands of fathoms.

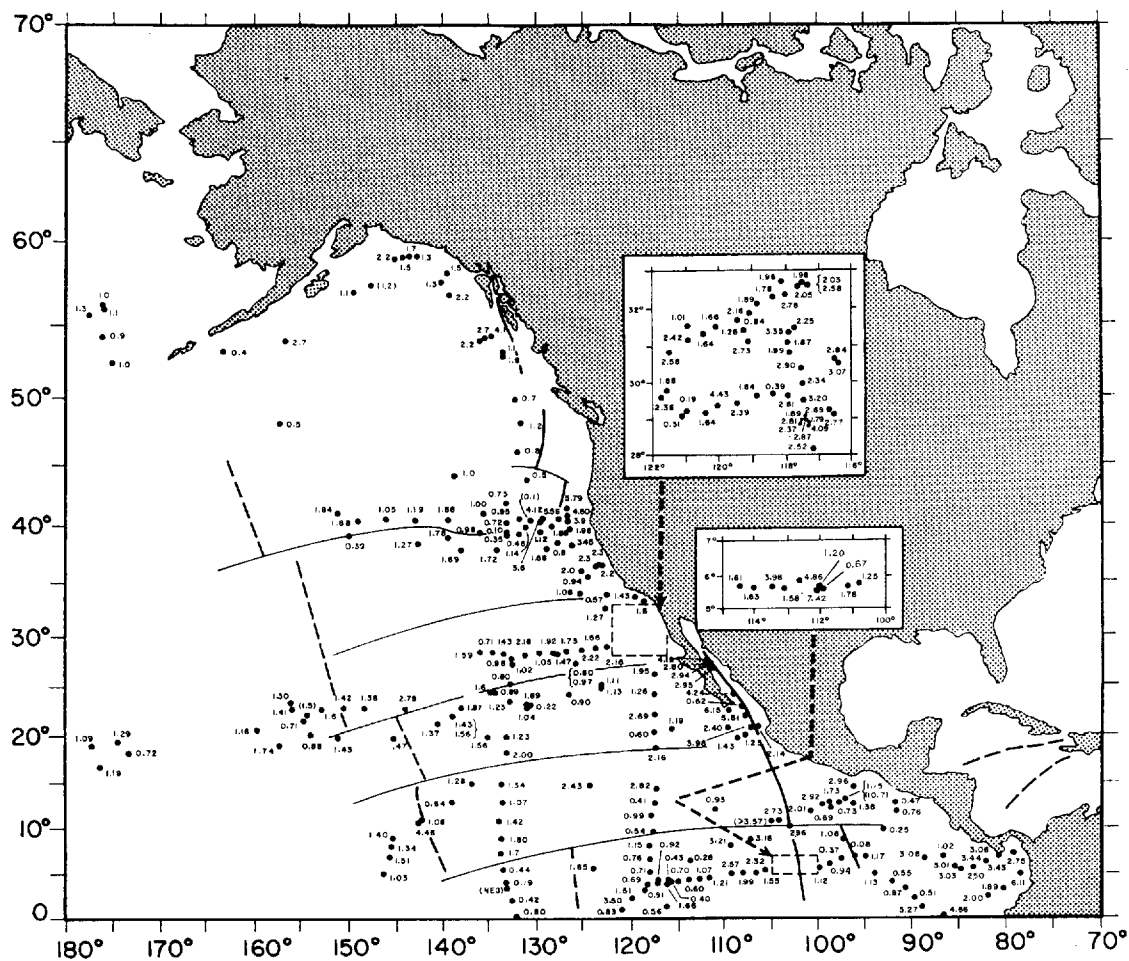


Fig. 23. Heat flow values in the northeast Pacific. Values in parentheses are rejected data (category C). Heavy solid lines indicate the crest and dashed lines the extent of the East Pacific Rise (taken from Figure 38).

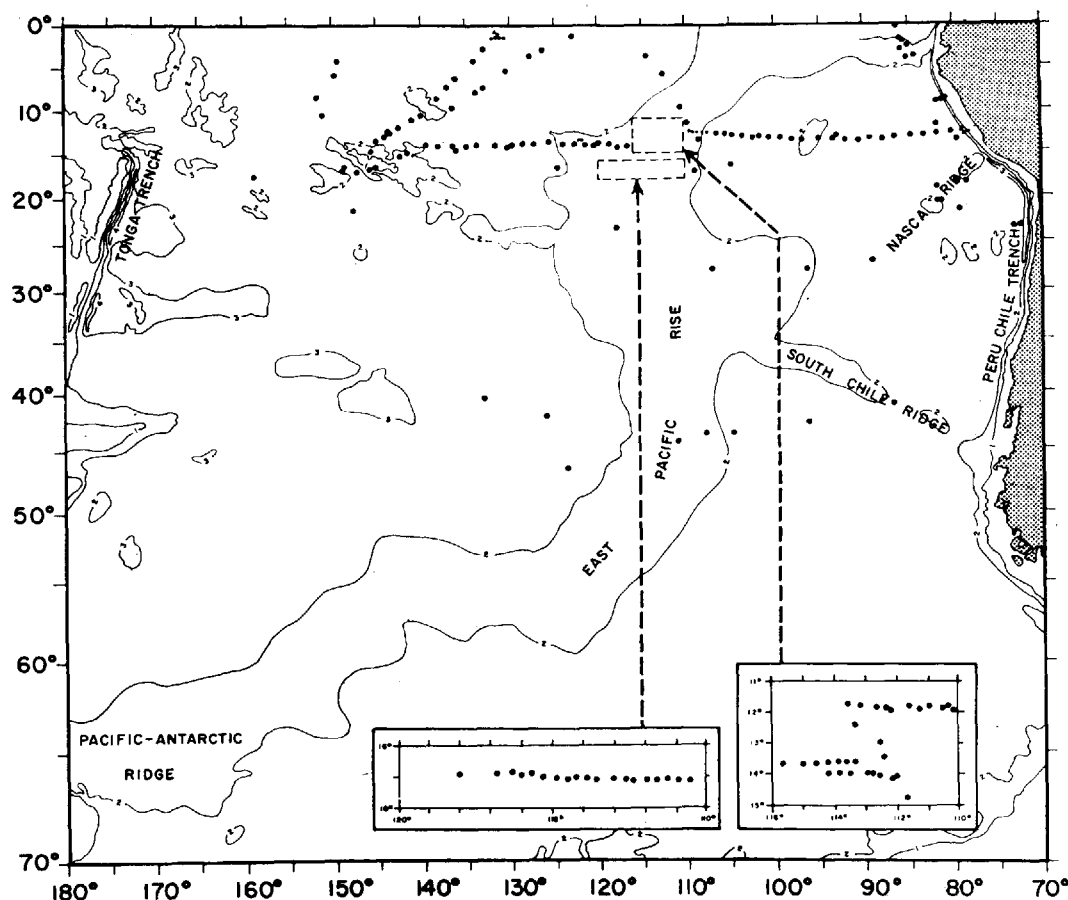


Fig. 24. Bathymetric map of the Southeast Pacific with locations of heat flow stations; contours in thousands of fathoms.

shallow seismicity, and almost all the known deeper earthquakes.

*East Pacific Rise.* Bullard *et al.* [1956] first observed three high heat flow values in the East Pacific Rise. Von Herzen [1959] observed a relatively narrow band of high heat flow in the crest and areas with low heat flow roughly on each side. Von Herzen and Uyeda [1963] made extensive heat flow studies over the Rise and concluded that it is systematically associated with high values, a strip 200 to 300 km wide at the crest having an average heat flow of about  $3 \mu\text{cal}/\text{cm}^2 \text{ sec}$ . Within this strip, the highest values occur in two narrower zones which seem to be parallel and symmetrically oriented to the crest. The source of high heat flow is thought to be a region of unusually high temperature, a few tens of kilometers wide, located about

10 km beneath the ocean. One-fourth of their measurements give low heat flow values ( $\leq 0.8$ ). They find two approximately equidimensional regions near the equator and to each side of the rise showing generally low heat flow. In many areas, isolated low heat flow values are correlated with flat topography, suggesting a local environmental effect. Langseth *et al.* [1965] also found broad variations of heat flow similar to previous findings. A broad heat flow maximum of about  $3 \mu\text{cal}/\text{cm}^2 \text{ sec}$  is found near the East Pacific Rise at  $10^\circ\text{N}$ , while three singular peaks of high heat flow of 3.3, 3.5, and  $7.1 \mu\text{cal}/\text{cm}^2 \text{ sec}$  have been measured over the rise at  $17^\circ\text{S}$ . Another high heat flow area is found to extend from the East Pacific Rise to the Gulf of Panama.

*Other areas.* Extensive heat flow studies have

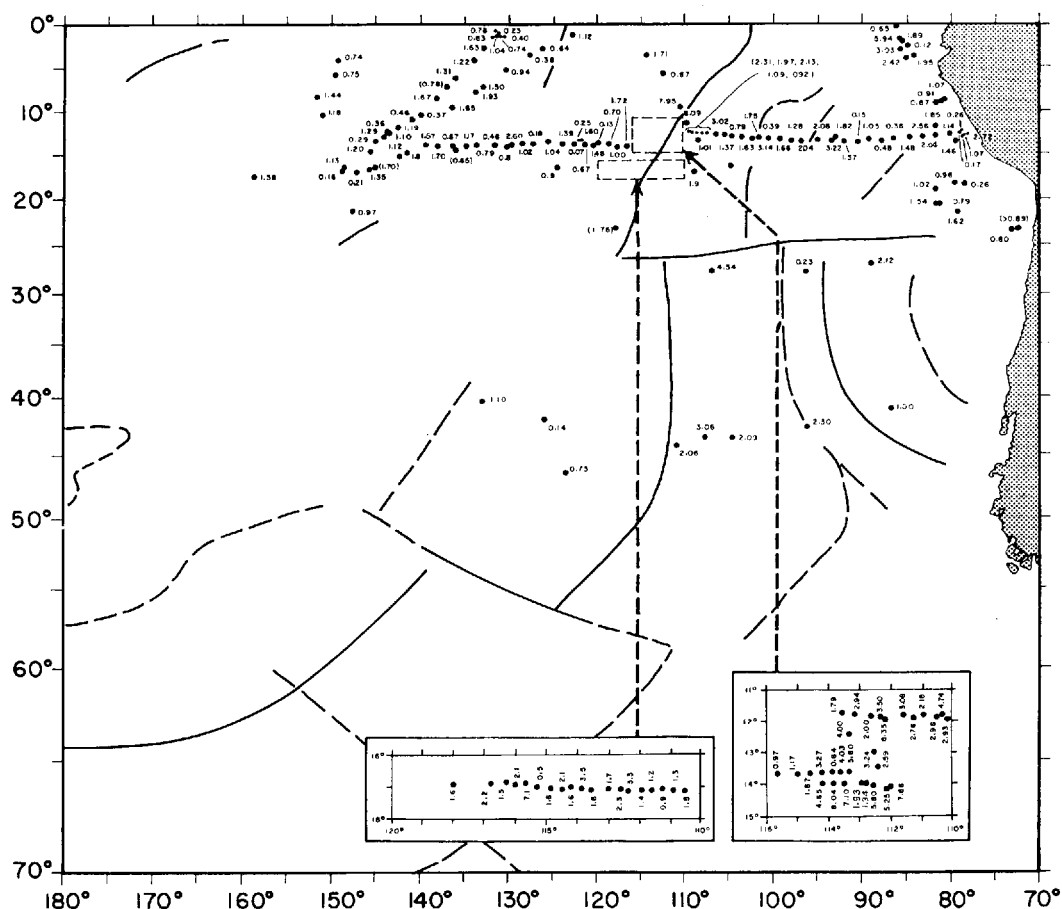


Fig. 25. Heat flow values in the southeast Pacific. Values in parentheses are rejected data (category C). Heavy solid lines indicate the crest and dashed lines the extent of the East Pacific Rise (taken from Figure 38).

been made off the Pacific Coast of the United States and Baja California [Von Herzen, 1964]. Most measurements at the same location have been repeated reasonably well. High heat flow values are observed near the coast, three or four times normal north of the Mendocino fault, and twice normal in the borderland off southern and Baja California. Values observed west of North America range from 0.1 to 6  $\mu\text{cal}/\text{cm}^2$  sec. Some of the large anomalies seem to have wavelengths ranging from about 250 km off Baja to 1000 km off northern California. For the most part the anomalies appear to be uninterrupted across the Mendocino fracture zone.

Between North America and the Hawaiian Islands, Rhea et al. [1964] observed heat flow

values which range from 0.80 to 2.78 and average 1.4  $\mu\text{cal}/\text{cm}^2$  sec. No significant heat flow differences between recognized topographic provinces, including the Hawaiian Ridge and the Molokai fracture zone, are observed.

Foster [1962] observed a low value of 0.4 on the bench just north of the Aleutian Trench off Unimak Pass, whereas a moderately high value of 2.7 was found in the Aleutian Trench proper. Measurements over the Japan and Kurile Trenches and nearby areas have been discussed in section 3.3.

Finally, heat flow has been measured at the preliminary Mohole site, 75 km east of Guadalupe Island [Von Herzen and Maxwell, 1964]. The technique used is different from usual prac-



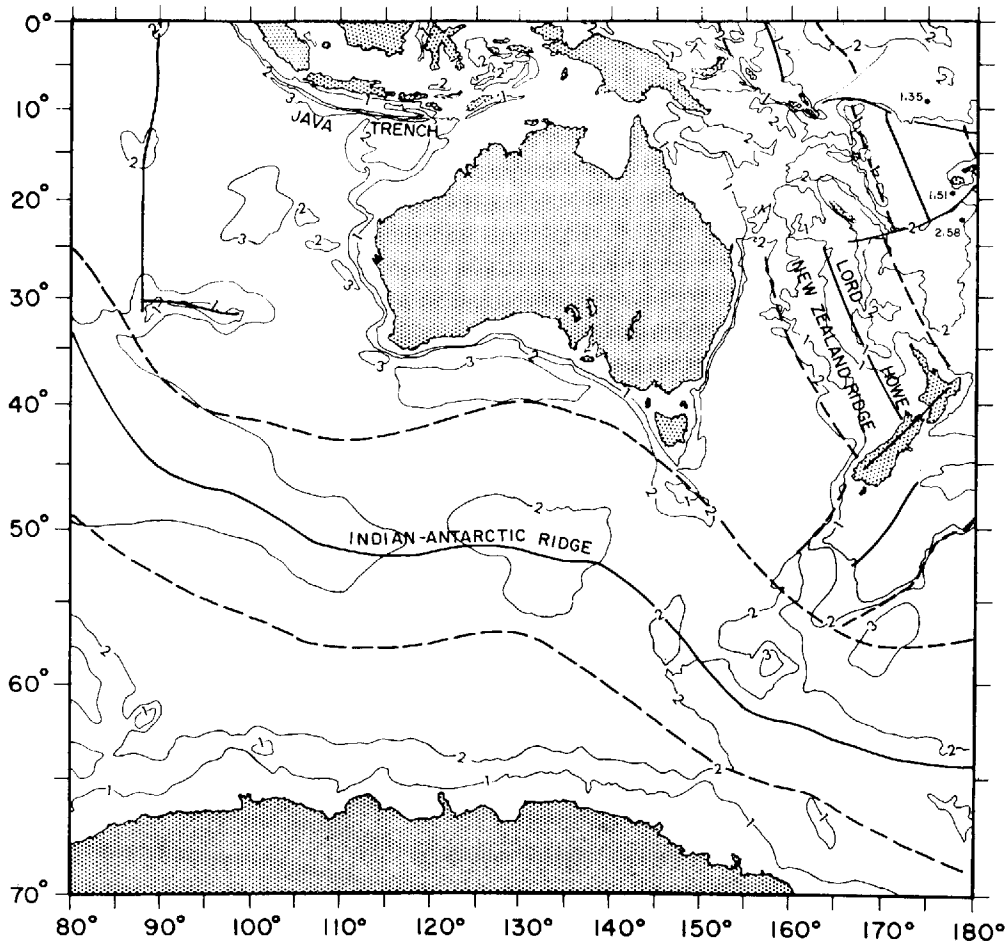


Fig. 27. Bathymetric map of the southwest Pacific with heat flow values. Contours in thousands of fathoms. Geological features are taken from Figure 38. Heat flow values in Indian Ocean are not shown here because they have been plotted in Figure 18.

of the crestal zone. In Figure 29, 75-, 50-, and 25-percentile lines are also given for heat flow values from the East Pacific Rise and the Pacific Ocean basins. The contrast is very obvious, as in the case for the Atlantic and the Indian oceans. The percentile lines drop to a minimum at about 300 km from the crest of the East Pacific Rise (similar to the Mid-Indian Ocean Ridge), increase, and drop again at about 600 to 700 km (Figure 29).

Although heat flow values from Pacific basins are more scattered (Figure 30) than those from the Atlantic and Indian oceans (Figures 16 and 21), their averages (1.18, 1.13, and 1.34  $\mu\text{cal}/\text{cm}^2 \text{ sec}$ ) are similar.

A histogram of heat flow values from the Pacific trenches is shown in Figure 31. The average of 16 trench values is  $0.94 \pm 0.6$  s.d.; modes are 0.9 and 1.1. It appears that the heat flow is low over the trenches, but this conclusion cannot be fully substantiated yet.

#### 4.4 Arctic Ocean

The Arctic Ocean is the smallest ocean, and its features are relatively unknown. Heat flow measurements using a Ewing-type probe have been made by *Lachenbruch and Marshall* [1964] and *Lachenbruch et al.* [1965]. Their measurements are unique in that a drifting ice-island

TABLE 9. Summary of Heat Flow Data in the Pacific Ocean

Reference	Data No.	No. of Stations	Regions	Remarks on Heat Flow Data
<i>Revelle and Maxwell</i> , 1952	1027-1031	6	1 near the base of the main ridge of the Hawaiian Island, 4 in the vicinity of the sunken Mid-Pacific Mountains, and 1 in the deep water off the coast of Southern California	First successful measurements of heat flow through the ocean floor; values (from 0.9 to 1.3) were revised and discussed in detail in <i>Maxwell</i> [1958]. E. C. Bullard has a brief note added after this article
<i>Maxwell and Revelle</i> , 1956 <i>Bullard et al.</i> , 1956				See <i>Bullard et al.</i> [1956]
<i>Maxwell</i> , 1958	1027-1051	25	Values fairly well distributed over the Pacific	Review of all oceanic heat flow values available in 1956; see <i>Maxwell</i> [1958]
<i>Von Herzen</i> , 1959	0759-0794	36	Southeastern Pacific	Ph.D. thesis; detailed account of every station average value is $1.44 \pm 1$ s.d. and the average of 16 values obtained within the deep Pacific Basin is $1.27 \pm 0.4$ s.d.
<i>Von Herzen</i> , 1960				Results (together with Maxwell's) indicated: (1) a narrow band of high heat flow over the crest of the East Pacific Rise and areas of low heat flow on each side, and (2) low values over axes of trenches bordering the eastern Pacific Ocean
<i>Von Herzen</i> , 1963	0746-0758	18	Gulf of California	Ph.D. thesis; detailed account of <i>Von Herzen</i> [1959] and <i>Von Herzen</i> [1963]
<i>Uyeda et al.</i> , 1962	0618-0620	3	Profile along 38°N across the Japan Trench	10 high values (2.4-6.2) and 3 rather low values (0.6-1.4) were observed
<i>Foster</i> , 1962	0795-0830	36	Northeast Pacific, Bering Sea, and Aleutian Trench	Very low value (0.27) on the inner side of the arc, moderately low (1.14) in the trench, and moderately high (2.05) farther to the east
<i>Von Herzen and Uyeda</i> , 1963	0831-1026	196	Eastern Pacific	A low value of 0.4 on the bench just north of the Aleutian Trench off Unimak Pass; a fairly high value of 2.7 in the Aleutian Trench proper; large difference in heat flow (0.1 to 3.6) at station 90 km apart over the extension of the crest of the East Pacific rise off the coast of Oregon
<i>Von Herzen and Maxwell</i> , 1964	0745	1	Preliminary Mohole site, 75 km E of Guadalupe Is.	A strip 200-300 km wide having high heat flow values (~3) at the crest of East Pacific Rise, the highest values being in two narrow zones parallel and symmetrically oriented to the crest; two large areas of low heat flow values near the equator on each side of the Rise; many isolated low values were correlated with topography, suggesting an effect of local environment
<i>Von Herzen</i> , 1964a	0672-0744	78	West of U.S. and Baja California	Heat flow almost constant to a depth of 154 meters; the average value, 2.81, agreed well with other measurements nearby using Bullard-type probes penetrating only a few meters
<i>Rhea et al.</i> , 1964	1114-1132	23	Between North America and the Hawaiian Is.	High heat flow values near the N. American west coast: 3 or 4 times normal north of Mendocino fault and 2 times normal in the borderland of southern and Baja California; heat flow seems to be uninterrupted across the Mendocino fracture zone
<i>Uyeda and Horai</i> , 1964	0621-0636	16	Pacific off Japan	Values ranged from 0.8 to 2.8 and averaged 1.4; no significant differences in heat flow were recognized over various topographic provinces, including the Hawaiian ridge and the Molokai fracture zone
<i>Yasui and Watanabe</i> , 1965	0637-0671 1140-1142	38	Japan Sea	Low heat flow (<1) prevailed in the oceanic area directly east of northeastern Japan
<i>Langseth et al.</i> , 1965	1052-1113	62	East Pacific	Moderately high heat flow (<2) in most parts of Japan Sea Basin
				A broad heat flow maximum (~3) near the East Pacific Rise at 10°N and 3 singular peaks of high heat flow at 17°S; area of high heat flow seems to extend from the East Pacific Rise to the Gulf of Panama

station is used instead of a vessel. Slow drifting of the ice-island permits some twenty closely spaced stations. Remarkably uniform heat flow values ( $1.41 \pm 0.06$  s.d.  $\mu\text{cal}/\text{cm}^2 \text{ sec}$ ) are observed in the abyssal plain of the Canada Basin and lower values ( $1.15 \pm 0.25$  s.d.) over the Alpha Rise. This variation is thought to be caused by nonuniform thermal conductivity.

Heat flow data from the Arctic Ocean have

been catalogued in the Appendix but were received too late to be included in the analysis.

##### 5. GLOBAL REVIEW OF HEAT FLOW DATA

Heat flow data that have been regionally reviewed in the last two sections are now synthesized, with simple generalizations, on a worldwide basis. We shall proceed from large-scale regions to smaller ones.

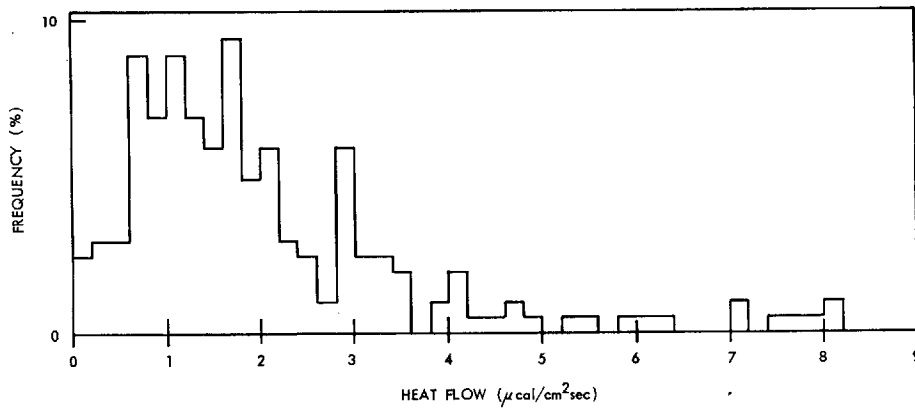


Fig. 28. Histogram of heat flow values from Pacific ridges.

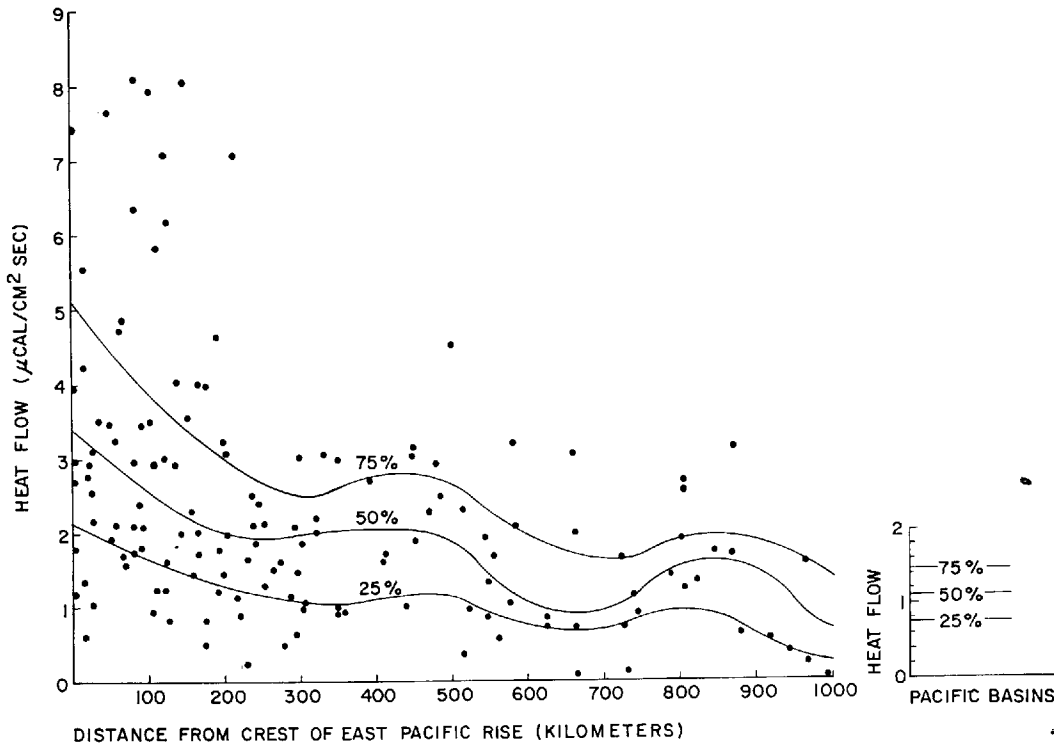


Fig. 29. Heat flow values versus distance from the crest of the East Pacific Rise (50°S to 20°N). 75-, 50-, and 25-percentile lines are given for values from the East Pacific Rise and the Pacific basins. For example, the 50-percentile line separates half the data points above and half the data points below it.

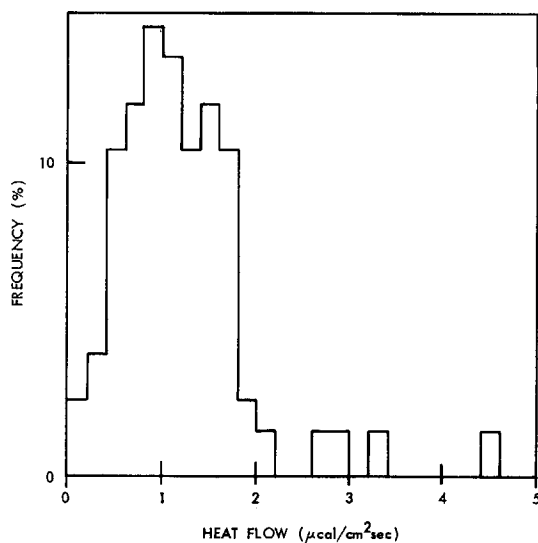


Fig. 30. Histogram of heat flow values from Pacific basins.

### 5.1 World

The global heat flow data have been shown in Figures 1a and 1b, where the number and arithmetic mean of analyzed data in  $5^\circ$  by  $5^\circ$  grid are given.

*Statistics.* A histogram of the world's heat flow values is given in Figure 32a. The mode occurs at  $1.1 \mu\text{cal}/\text{cm}^2 \text{ sec}$ , and the number of data drops off rather rapidly and symmetrically on both sides of this value to 0 and about  $2.5 \mu\text{cal}/\text{cm}^2 \text{ sec}$ , with a long 'tail' toward high values. The slight skewness of the distribution causes the average heat flow to exceed the most frequently observed value. The arithmetic mean of 1043 'published' heat flow values is  $1.58 \pm 1.12 \text{ s.d.}$ ; that for 1150 values including 'unpublished' ones is essentially the same:  $1.58 \pm 1.14 \text{ s.d.}$  For comparison, these results and previous ones are given in Table 10.

Heat flow values greater than  $3 \mu\text{cal}/\text{cm}^2 \text{ sec}$  are uncommon and may not be representative of the conducted heat flow. If these values are excluded, the arithmetic mean of 951 published values (0 to  $3 \mu\text{cal}/\text{cm}^2 \text{ sec}$  only) is  $1.33 \pm 0.63 \text{ s.d.}$  However, we can also argue that a fair amount of low heat flow values (about 120 values are less than  $0.6 \mu\text{cal}/\text{cm}^2 \text{ sec}$ ) are also not representative of the conducted heat flow.

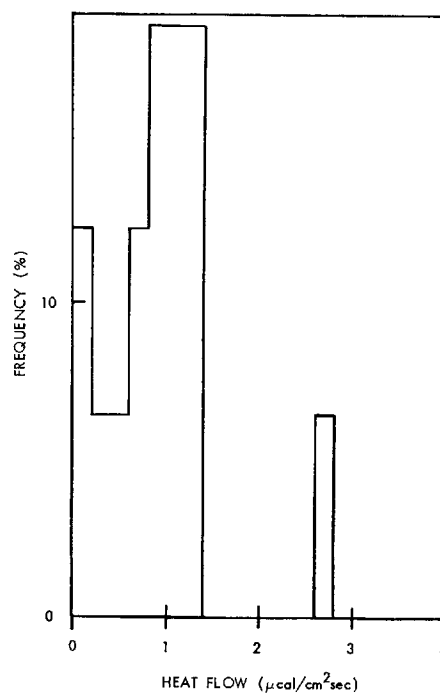


Fig. 31. Histogram of heat flow values from Pacific trenches.

If these low values are excluded, then the arithmetic mean will increase again.

*Weighted statistics.* Because of uneven geographical distribution of observations, Lee [1963] introduced successive averaging weighted according to areas of the grids (bounded by meridians and parallels) chosen. The advantage is in reducing sampling bias, but there is also a danger of over-weighting isolated values. Since grids formed by latitudes and longitudes have unequal area, the averaging process by Lee [1963] does not give an unbiased sample of grid averages. To avoid this difficulty, averages for grids of equal area are computed (for convenience, we take an area of 300 by 300 square nautical miles, i.e.,  $5^\circ$  by  $5^\circ$  at the equator). A histogram of these equal-area averages is given in Figure 32b. The arithmetic mean for 389 such averages is  $1.43 \pm 0.75 \text{ s.d.}$  Smoothing of data is indicated by the decrease of the standard deviation, and sampling bias toward too high a value is reduced by the decrease of the mean.

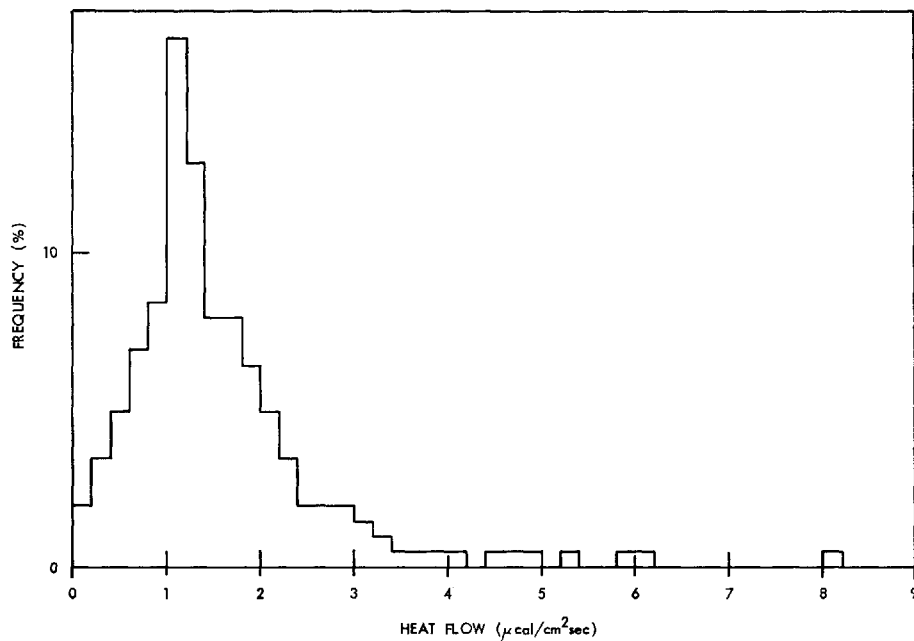


Fig. 32a. Histogram of world's heat flow values.

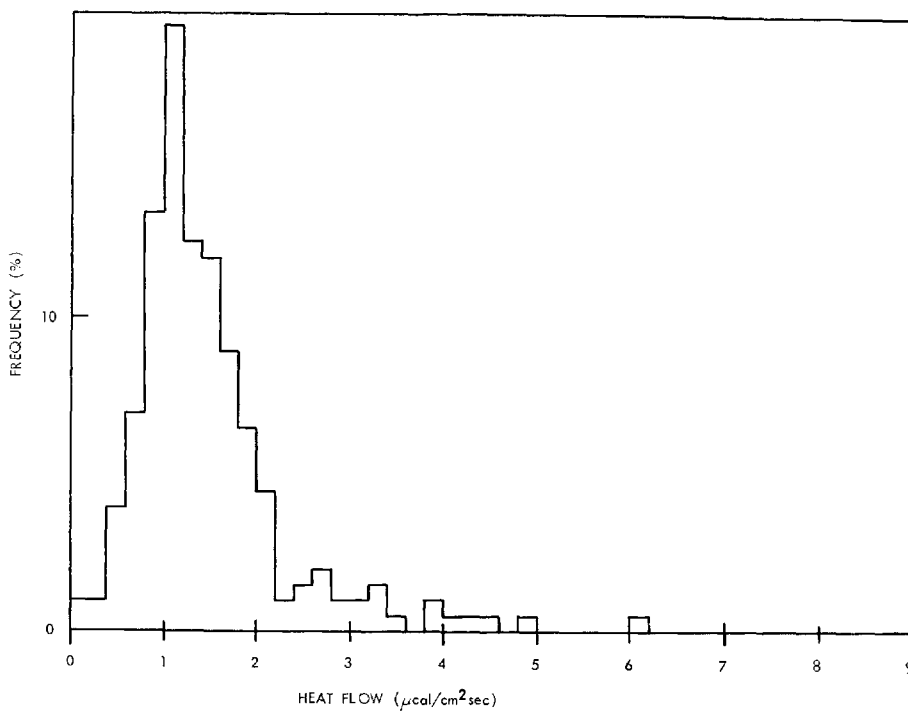


Fig. 32b. Histogram of world's heat flow grid averages ( $9 \times 10^4$  square nautical miles per grid).

TABLE 10. Statistics of World's Heat Flow Values

Date	Number of Values	Mean	Standard Deviation	Standard Error	Mode	Reference
Jan.- 1963	634	1.62	1.21	0.05	1.1	Lee [1963]
June 1963	757	1.61	1.16	0.04	1.1	Lee and MacDonald [1963]
Feb. 1964	987	1.58	1.16	0.04	1.1	Lee [1965]
Dec. 1964	1043 *	1.58	1.12	0.04	1.1	This article
Dec. 1964	1150 †	1.58	1.14	0.03	1.1	This article
Dec. 1964	389 ‡	1.43	0.75	0.04	1.1	This article

\* Published values.

† Published and unpublished values.

‡ Grid (300 by 300 square nautical miles) averages derived from 1150 individual values.

*Mean heat flow.* The world's mean heat flow by conduction is defined as

$$\bar{q} = \int_{\sigma} q d\sigma / \int_{\sigma} d\sigma \quad (3)$$

where the integration is over the entire surface of the Earth. Lee [1963] has estimated  $\bar{q}$  from spherical harmonic analysis and concludes that at the 95% confidence level

$$\bar{q} = 1.5 \pm 10\% \text{ ucal/cm}^2 \text{ sec} \quad (4)$$

Current analysis with twice the amount of data confirms this result.

*Heat loss from the Earth's interior.* The amount of heat losses from the Earth's interior is an important geophysical quantity in considering its origin, constitution, and behavior. The total heat loss by conduction  $Q$  through the Earth's surface can be estimated from the world's mean heat flow and the surface area of the Earth ( $5.1 \times 10^{18} \text{ cm}^2$ ) as

$$Q = 7.7 \times 10^{12} \pm 10\% \text{ cal/sec} \quad (5)$$

To this value of conducted heat, we must add heat loss transported by hot mobile constituents, such as volcanic ash and lavas, steam, and hot water. Lotze [1927] estimates the heat loss from volcanic eruptions to be of the order of  $2 \times 10^{10} \text{ cal/sec}$  for the Earth, and Verhoogen [1946] estimates that the heat escaped during volcanic activity since the Precambrian is of the order of  $3 \times 10^9 \text{ cal/sec}$ . Although these estimates are crude, they are orders of magnitude less than the conducted heat. Hence the amount of heat loss from the Earth's interior is essentially given by the conducted heat:  $7.7 \times 10^{12} \text{ cal/sec}$ .

*Sources of heat.* Radioactivity is probably the main source of heat, and other sources, such as tidal dissipation, initial heat, etc., are believed to be small [Bullard *et al.*, 1956; Gutenberg, 1959]. The observed heat losses from the Earth's interior can be completely accounted for if we assume that the entire Earth has the same potassium, thorium, and uranium content as chondritic meteorites and that the heat arrives at the Earth's surface at the same rate as that at which it is generated. Since the thermal conductivity of solid rock is rather low, it can be shown that the heat generated below a few hundred kilometers has not been conducted to the surface even in billions of years [Slichter, 1941]. To explain the observed heat flow by radioactive decay in a chondritic Earth model, either one or both of the following are required: the radioactive elements are concentrated in the outer few hundred kilometers, or there are other mechanisms to transfer heat more quickly than by the assumed conduction alone. Recently the validity of a chondritic Earth model has been questioned because the K/U ratio for terrestrial rocks is about  $1 \times 10^4$ , whereas that for the meteoritic materials is about  $7 \times 10^4$  [Wasserburg *et al.*, 1964]. The main difficulty is our present ignorance of the radioactivity at depth, and the observed heat flow does not uniquely determine the internal concentration of radioactivity.

## 5.2 Continents and Oceans

The first-order feature of the Earth's surface is its division into continents and oceans by the sea level. Although many shallow water areas

have continental structure, we shall ignore this modification because current oceanic heat flow techniques cannot safely be applied in shallow water.

*Statistics.* Histograms of continental and oceanic heat flow are shown in Figures 33a and 34a, respectively. These two histograms are very different. The continental values do not extend beyond  $3 \mu\text{cal}/\text{cm}^2 \text{ sec}$  because values from geothermal areas on land have been excluded from the analysis. Thus we probably should compare only the part of the histogram from 0 to  $3 \mu\text{cal}/\text{cm}^2 \text{ sec}$ . In this part the land values seem to be divided into two subgroups—around 1 and  $2 \mu\text{cal}/\text{cm}^2 \text{ sec}$ —whereas at sea there is only one group. The modes for both land and sea values are the same: 1.1. The arithmetic mean for 131 continental values is  $q_c = 1.43 \pm 0.56$  s.d., whereas for 793 oceanic values (excluding those  $>3 \mu\text{cal}/\text{cm}^2 \text{ sec}$ ), the mean is  $q_o = 1.31 \pm 0.65$  s.d. (the arithmetic mean for all 913 oceanic values is  $q_o = 1.60 \pm 1.18$  s.d.). Since  $|q_o - q_c| < 0.2 \mu\text{cal}/\text{cm}^2 \text{ sec}$  in both cases, the difference between the heat flow averages on land and at sea is *not* significant (see section 2.3). This conclusion is further supported by considering the weighted statistics.

*Weighted statistics.* As we remarked in section 5.1, averages over grids of equal area tend to reduce sampling bias and hence are more representative values. Histograms for continental and oceanic grid averages ( $9 \times 10^4$  square nautical miles) are given in Figures 33b and 34b, respectively. The arithmetic mean for 51 continental grid averages is  $1.41 \pm 0.52$  s.d., whereas that for 340 oceanic ones is  $1.42 \pm 0.78$  s.d. The difference is clearly insignificant.

*Equality of heat flow.* The equality of heat flow between oceans and continents suggests that radioactivity is roughly the same beneath land and sea. Since the continental and oceanic crusts are very different in thickness and probably in composition, this further suggests that there are differences between the upper mantle under the continents and that under the oceans. Most of the continental heat flow (about 70%) can be easily accounted for by the radioactivity of the continental crust, assuming it has intermediate composition (e.g. granodiorite). Since the continental crust is about 35 km thick, and since some heat must come from below the Mohorovicic discontinuity, the difficulty is not

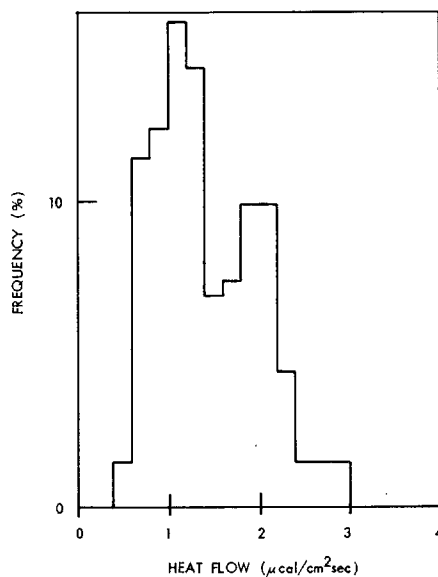


Fig. 33a. Histogram of continental heat flow values.

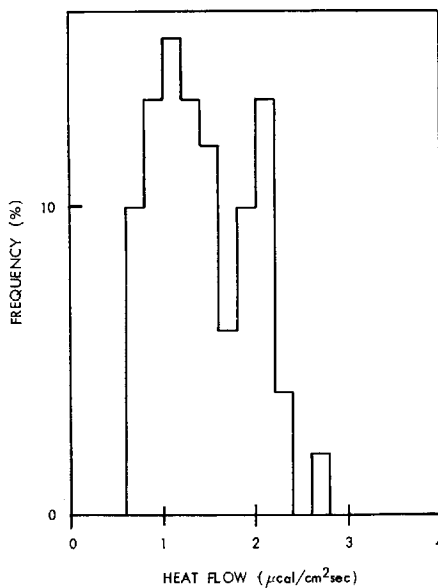


Fig. 33b. Histogram of continental heat flow grid averages ( $9 \times 10^4$  square nautical miles per grid).

the lack of a heat source but to explain why the continental heat flow is not greater than it is. A simple explanation may be that the radioactivity of the continental crust is much less than that of granodiorite. On the other hand,

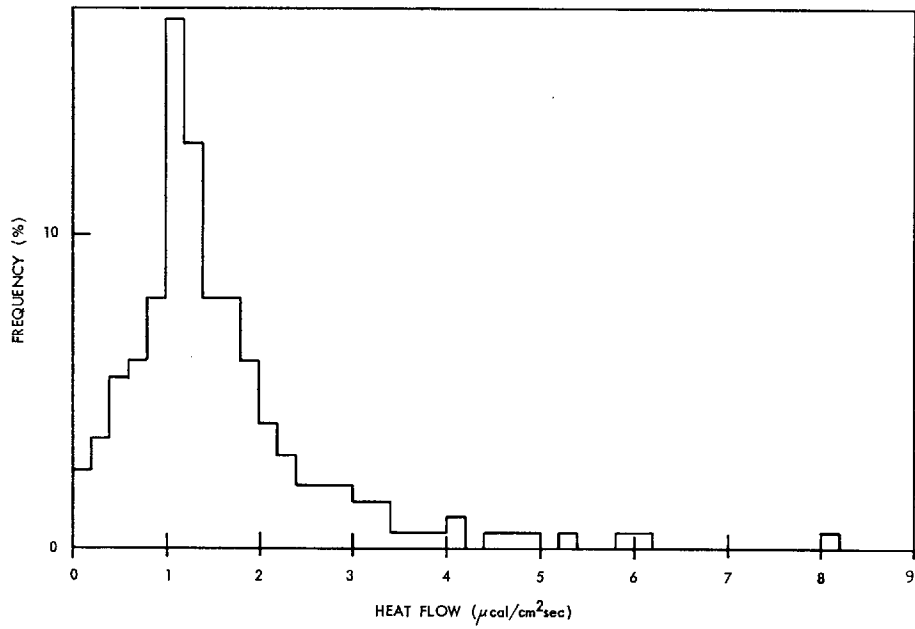


Fig. 34a. Histogram of oceanic heat flow values.

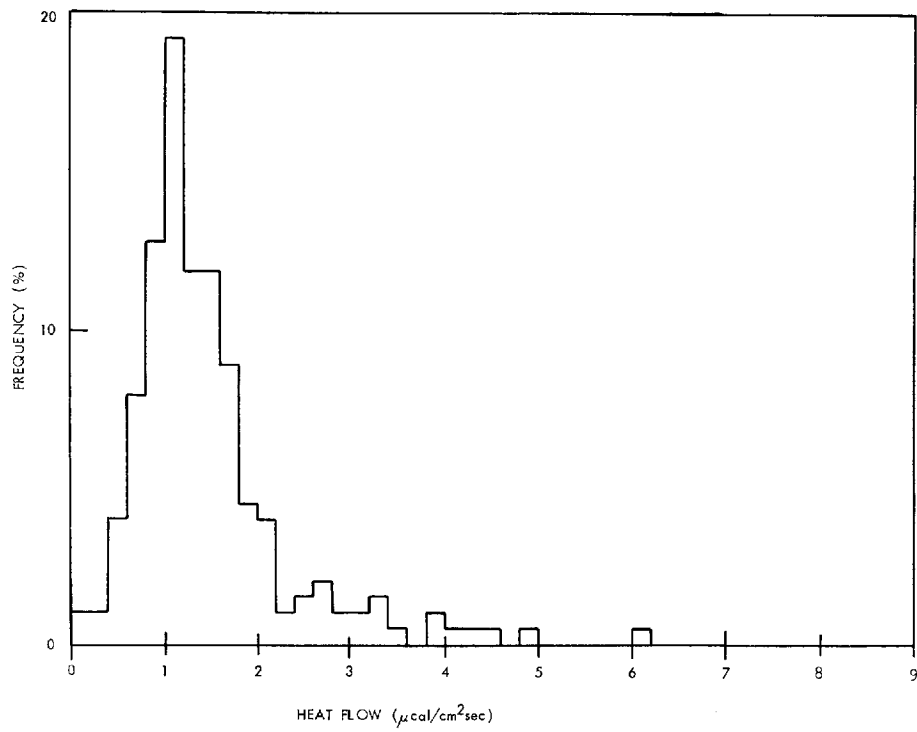


Fig. 34b. Histogram of oceanic heat flow grid averages ( $9 \times 10^4$  square nautical miles per grid).

TABLE 11. Statistics of Heat Flow Values for Various Continents

Continent	Number of Values	Mean	Standard Deviation	Standard Error	Modes	Remark
Africa	13	1.20	0.20	0.06	1.3	Almost all data from South Africa
Asia	37	1.49	0.58	0.10	1.1 and 1.3	Almost all data from Japan
Australia	19	1.75	0.62	0.14	2.1	
Europe	22	1.62	0.60	0.13	0.7 and 1.9	
North America	40	1.19	0.44	0.07	1.1	
All continents	131	1.43	0.56	0.05	1.1	
Grid averages of all continents	51	1.41	0.52	0.07	1.1	$9 \times 10^4$ square nautical miles per grid

the oceanic crust is thin (about 7 km) and may be of basaltic composition, which contains about 30% of the radioactivity of granodiorite. Thus, if the oceanic crust is basaltic, most of the oceanic heat flow (about 90%) must come from below the Mohorovicic discontinuity. The main problem is then to find a source for the heat and a way of getting it to the oceanic surface without invoking a temperature above the melting point at a depth of a few hundred kilometers or contradicting other geophysical evidence. MacDonald in Chapter 7 of this volume shows that a variety of concentrations of radioactive elements within the Earth is consistent with the observed heat flow and with the estimated melting gradient, provided that radiative transfer is effective.

*Various continents.* Statistics of heat flow values for various continents are summarized in Table 11. Since heat flow values are few for individual continents and their distributions are uneven, no definite conclusion can be drawn.

*Various oceans.* Statistics of heat flow values for various oceans are summarized in Table 12 with histograms shown in Figures 35*a* and *b*, 36*a* and *b*, and 37*a* and *b*. Although all oceans have values extending to higher values, the main parts (0 to 3  $\mu\text{cal}/\text{cm}^2 \text{ sec}$ ) of the histograms are quite different. The mean and scattering of values increases from the Atlantic to the Indian Ocean and to the Pacific. These differences may be related to their different structures and histories. However, they may also be caused by nonuniform sampling of measure-

TABLE 12. Statistics of Heat Flow Values for Various Oceans

	Number of Values	Mean	Standard Deviation	Standard Error	Modes
A. Individual values					
Atlantic	206	1.29	1.00	0.07	1.1
Indian	210	1.47	0.89	0.06	1.3
Pacific	497	1.79	1.31	0.06	1.1
All Oceans	913	1.60	1.18	0.04	1.1
B. Grid averages ( $9 \times 10^4$ square nautical miles per grid)					
Atlantic	65	1.21	0.64	0.08	1.1
Indian	94	1.35	0.67	0.07	1.3
Pacific	181	1.53	0.87	0.06	1.1
All Oceans	340	1.42	0.78	0.04	1.1

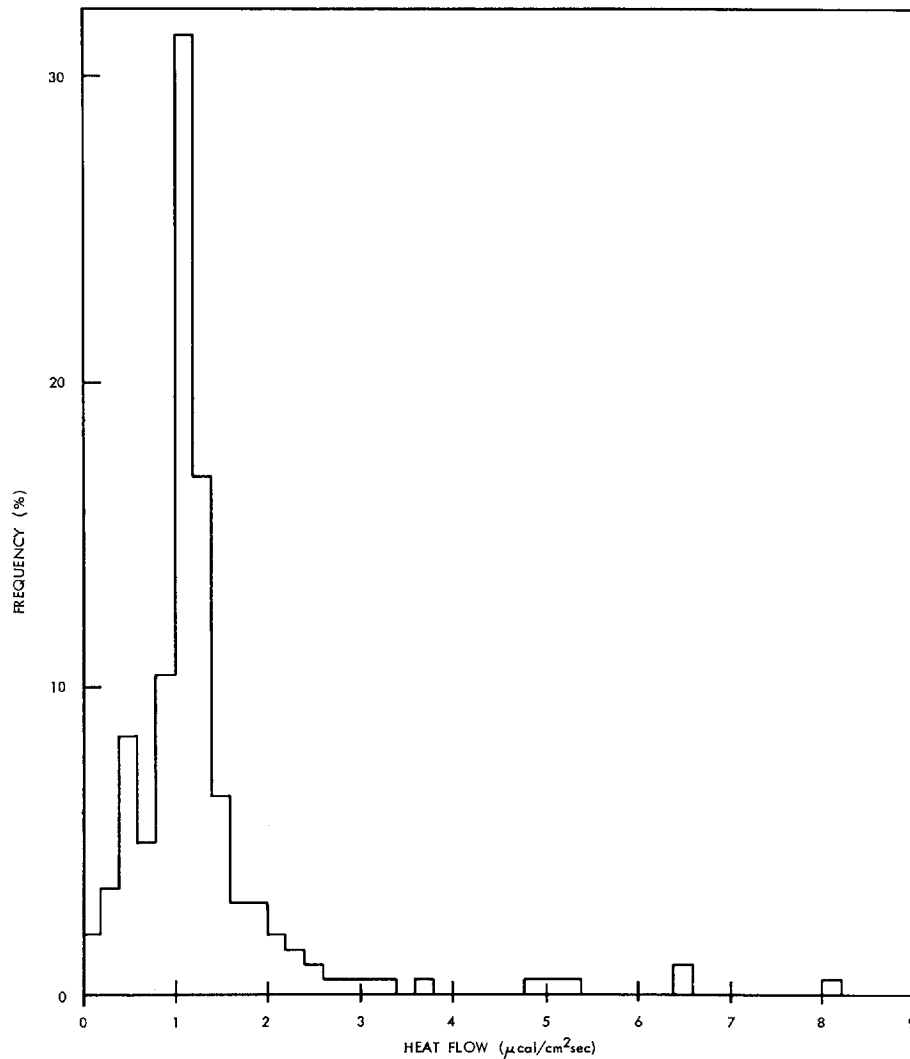


Fig. 35a. Histogram of Atlantic heat flow values.

ments (ratio of number of values from ridges to that from basins varies from about 1:1 in the Atlantic and the Indian oceans to about 2:1 in the Pacific). When grid averages are compared (see Table 12, section *B*), heat flow values are approximately the same for various oceans.

### 5.3 Major Geological Features

Figure 38 shows a *gross* picture of the major geological features of the Earth's surface, and statistics of heat flow values corresponding to these features on land are summarized in Table 13 and those at sea in Table 14.

#### 5.3.1 Land

*Shields and non-shields.* About 80% of the land surface is covered by post-Precambrian rocks. When Precambrian rocks are exposed in large continental areas, they are called *shields*. The shields are generally areas of low relief and have been very stable since the Precambrian. Heat flow results bear witness to their stability. A histogram of shield values is given in Figure 39a, and statistics for them are summarized in section 1 of Table 13. Heat flow values are very uniform in all shield areas, and the average is  $0.92 \pm 0.17$  s.d. On the other hand, heat flow

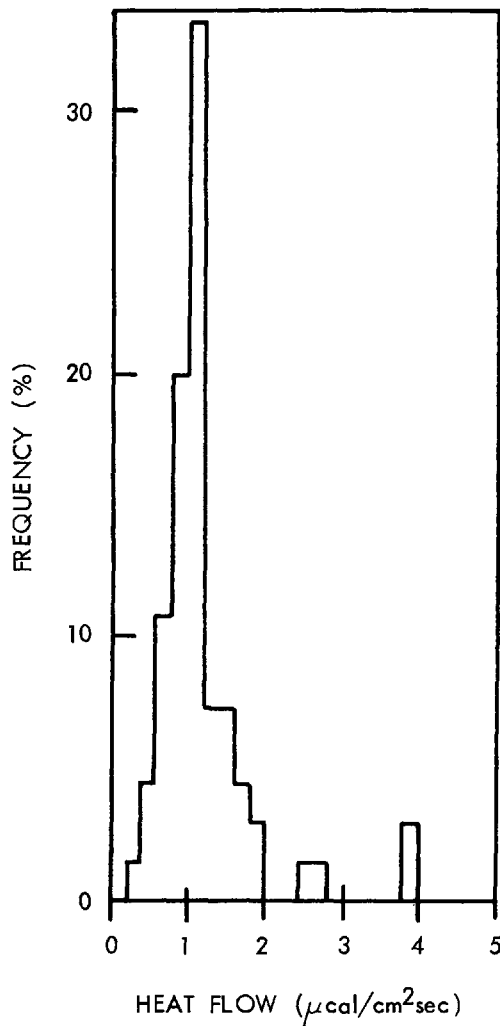


Fig. 35b. Histogram of Atlantic heat flow grid averages ( $9 \times 10^4$  square nautical miles per grid).

values outside the shields are usually higher and have greater variation, as seen in sections 2, 3, and 4 of Table 13.

*Post-Precambrian orogenic and non-orogenic areas.* In areas covered by the post-Precambrian rocks, interior lowlands and mountain belts are generally recognized. The former are little disturbed and underlain by Precambrian formations; the latter have been severely deformed during orogenesis. Sections 2 and 3 in Table 13 and Figures 39b and 39c summarize the results of the heat flow values in these two areas. Their averages are essentially the same, but

heat flow values in the orogenic areas are more scattered. The average heat flow undoubtedly will be higher in the orogenic areas if we include data from Cenozoic volcanic areas.

Heat flow values from the Interior Lowlands of Australia are much higher than those of North America's Interior Lowlands and may be related to Cenozoic volcanism.

With the exception of the East Australian Highlands, the Paleozoic orogenic areas have much smaller heat flow values than later orogenic areas. The Alpine and Cordilleran systems are characterized by relatively high heat flow. Cenozoic volcanic areas are associated with high heat flow, as is expected (see Table 13).

Among island arc areas (Figure 39d), extensive heat flow studies have only been carried out in Japan (see section 3.3).

### 5.3.2 Oceans

The ocean floor consists of three major morphological divisions: (1) continental margin, (2) ocean-basin floor, and (3) mid-oceanic ridge, each occupying about one-third the area [Heezen and Menard, 1963]. For heat flow studies, major features of the oceans are basins, ridges, and trenches (see Figure 38). Basins are characterized by relatively smooth bottom, deep water, normal thickness of oceanic crust, and aseismicity. Trenches are usually associated with island arcs, very deep water, and strong seismicity. Ridges have rugged relief and shallow water, and can be further divided into two groups according to seismicity. The seismic active mid-ocean ridge system is a spectacular feature [Heezen and Ewing, 1963], whereas aseismic ridges are small and occupy little area. Since heat flow data are few over aseismic ridges, we have not made this distinction. For convenience, any stations that do not clearly fall into the three categories of basins, ridges, and trenches are grouped under 'other areas.'

Statistics of heat flow values in basins, ridges, trenches, and other areas are summarized in Table 14, and corresponding histograms are given in Figures 40, 41, 42, and 43. Heat flow values in the ocean basins are fairly uniform and rather low, whereas those in the ridges and 'other areas' are higher and more scattered. The average of the trench values is rather low ( $\sim 1 \mu\text{cal}/\text{cm}^2 \text{ sec}$ ). However, the trench data

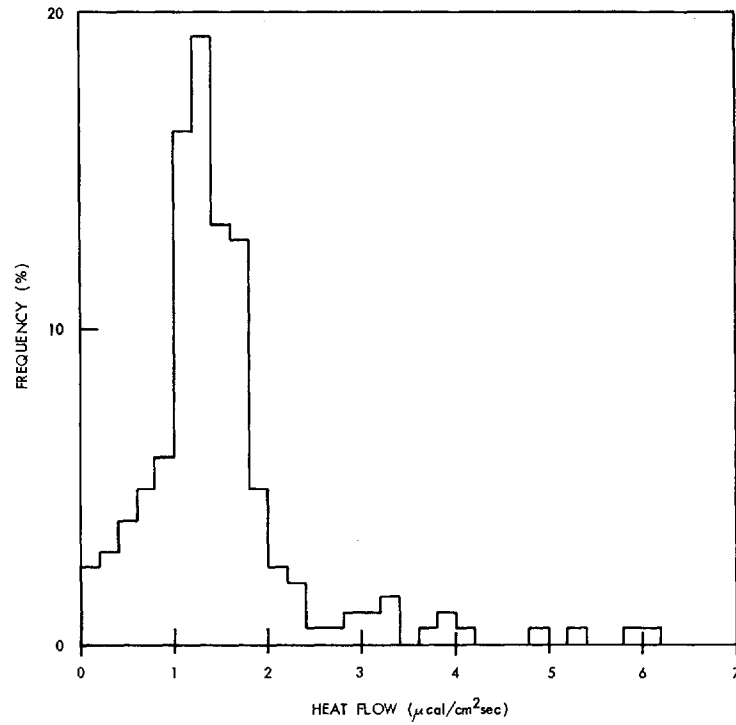


Fig. 36a. Histogram of Indian Ocean heat flow values.

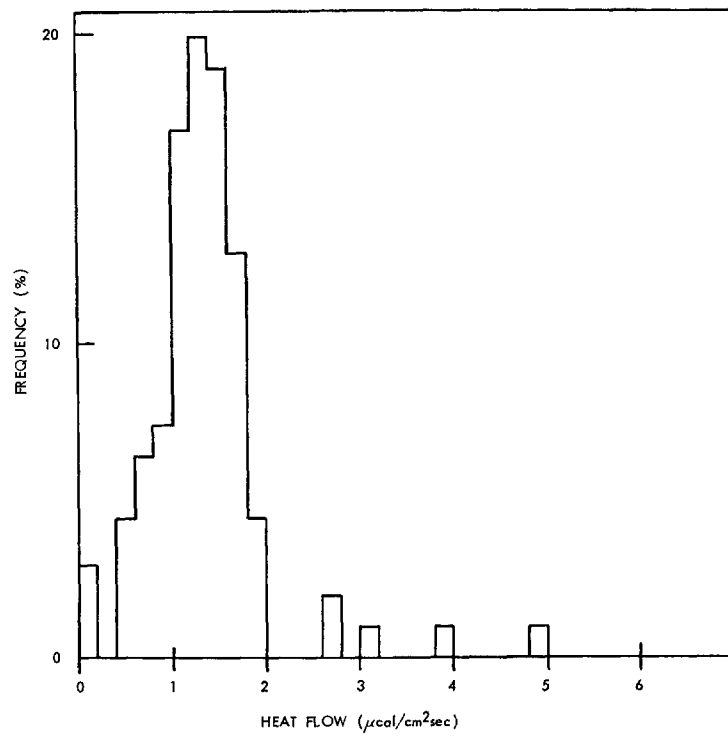


Fig. 36b. Histogram of Indian Ocean heat flow grid averages ( $9 \times 10^4$  square nautical miles per grid).

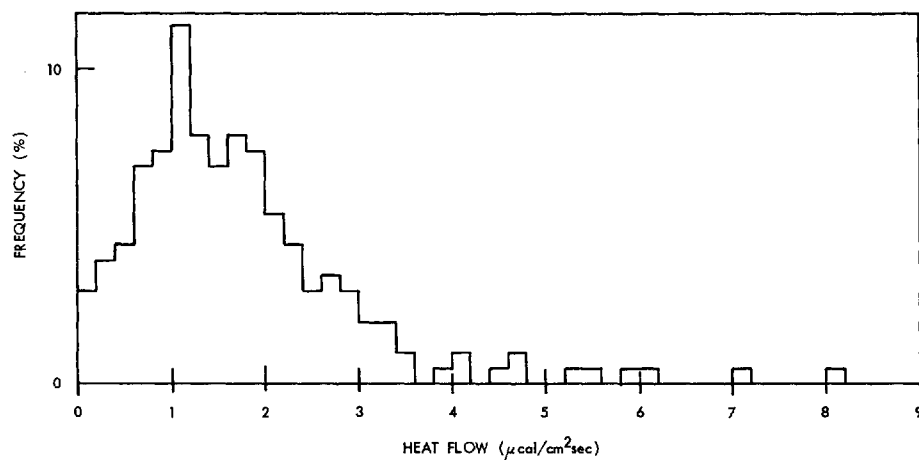


Fig. 37a. Histogram of Pacific heat flow values.

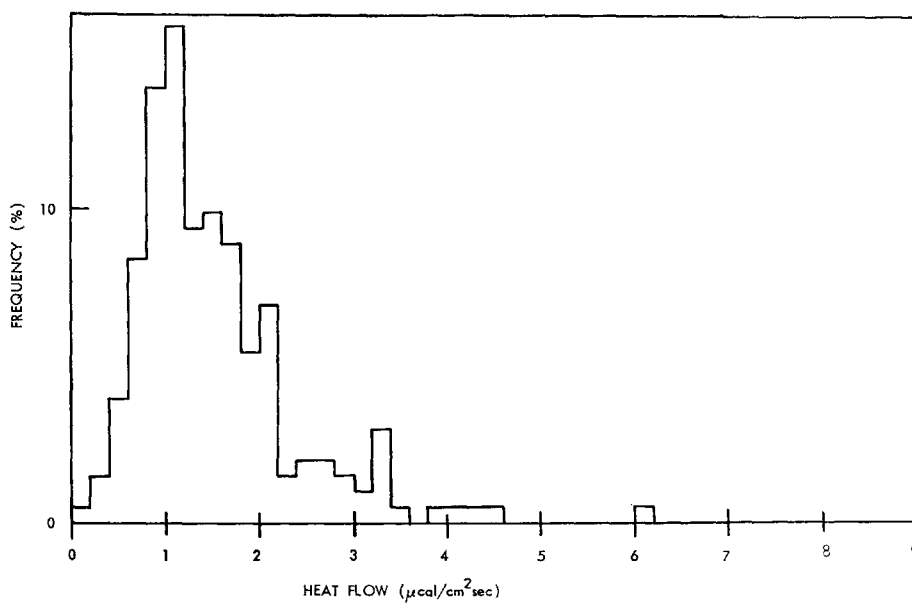


Fig. 37b. Histogram of Pacific heat flow grid averages ( $9 \times 10^4$  square nautical miles per grid).

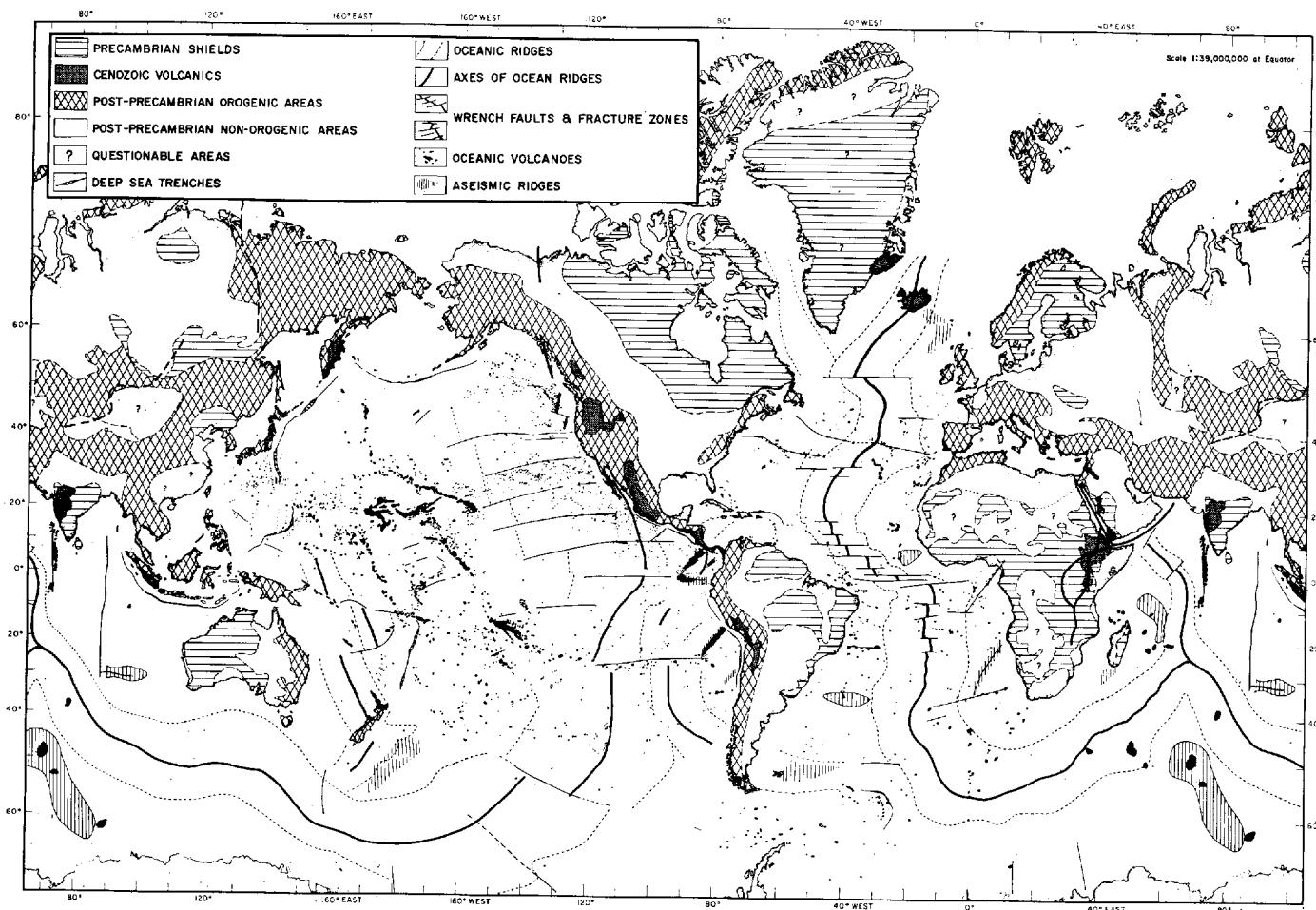


Fig. 38. Major geological features of the Earth. Most oceanic geological features are taken from *Menard* [1965], with a few additional data taken from *Fisher and Hess* [1963], *Heezen* [1962], *Heezen and Ewing* [1963]. Geological features on land are compiled from various geological maps.

TABLE 13. Statistics of Heat Flow Values for Major Geological Features on Land

Geological Feature	Number of Values	Mean	Standard Deviation	Standard Error	Modes
1. Precambrian shields	26	0.92	0.17	0.03	0.9
Australian Shield	7	1.02	0.15	0.06	0.9
Ukrainian Shield	3	0.69	0.07	0.04	0.7
Canadian Shield	10	0.88	0.13	0.04	0.9
Indian Shield	1	0.66			
South African Shield	5	1.03	0.13	0.06	0.9
2. Post-Precambrian non-orogenic areas	23	1.54	0.38	0.08	1.3
Europe	1	1.67			
Interior Lowlands of Australia	7	2.04	0.18	0.07	1.9 and 2.1
Interior Lowlands of N. America	8	1.25	0.18	0.06	1.1
South Africa	7	1.36	0.10	0.04	1.5
3. Post-Precambrian orogenic areas *	68	1.48	0.56	0.07	1.1
Paleozoic orogenic areas	21	1.23	0.40	0.09	1.1
Appalachian system	12	1.04	0.23	0.07	1.1
East Australian Highlands	2	2.03	0.03	0.02	2.0
Great Britain	7	1.31	0.38	0.14	no mode
Mesozoic-Cenozoic orogenic areas	19	1.92	0.49	0.11	1.9 and 2.1
Alpine system	10	2.09	0.38	0.12	1.9 and 2.1
Cordilleran system	9	1.73	0.53	0.18	1.3, 2.1, 2.3
Island Arc areas	28	1.36	0.54	0.10	1.1
4. Cenozoic volcanic areas (excluding geothermal areas)	11	2.16	0.46	0.14	2.1

\* Excluding Cenozoic volcanic areas.

TABLE 14. Statistics of Heat Flow Values for Major Geological Features at Sea

Geological Feature	Number of Values	Mean	Standard Deviation	Standard Error	Modes
1. Ocean basins	273	1.28	0.53	0.03	1.1
Atlantic Ocean	74	1.13	0.24	0.03	1.1
Indian Ocean	90	1.34	0.42	0.04	1.1
Pacific Ocean	75	1.18	0.69	0.08	0.9
Mediterranean seas	8	1.20	0.22	0.08	1.5
Marginal seas	26	1.83	0.60	0.12	1.9
2. Ocean ridges	338	1.82	1.56	0.09	1.1
Atlantic Ocean	87	1.48	1.48	0.16	0.5
Indian Ocean	85	1.57	1.17	0.13	1.3
Pacific Ocean	166	2.13	1.70	0.13	1.7
3. Ocean trenches	21	0.99	0.61	0.13	1.1
4. Other areas	281	1.71	1.05	0.06	1.1
Atlantic Ocean	24	1.16	0.33	0.07	1.1
Indian Ocean	27	1.53	0.85	0.16	1.5
Pacific Ocean	209	1.80	1.13	0.08	1.1
Mediterranean seas	14	1.50	0.87	0.23	1.1
Marginal seas	7	1.71	0.57	0.21	1.7

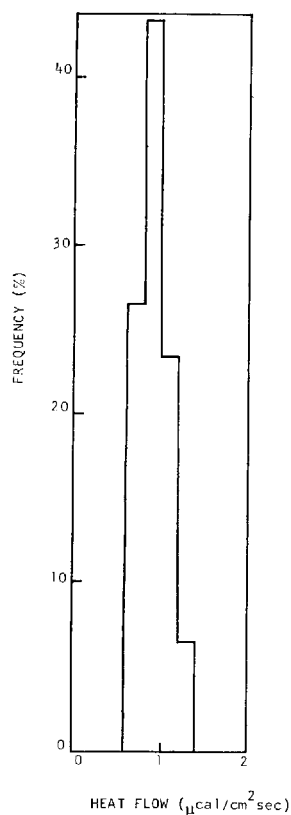


Fig. 39a. Histogram of heat flow values from Precambrian shields.

(21 in number) are still too few to be of great significance.

*Basins.* Heat flow values from basins of various oceans are similar (Figures 16, 21, and 30), although the average is highest for the Indian Ocean and the scattering is greatest for the Pacific (section 1 of Table 14). For basins in adjacent seas, data are still insufficient to draw definite conclusions. The relatively high average for marginal seas is mainly due to moderately high values obtained in the Japan Sea (see section 3.3).

*Ridges.* The crestal zones of ridges are usually characterized by high heat flow and large variations, whereas relatively low values are observed over the flanks. Details for each ocean have been discussed previously. Section 2 in Table 14 summarizes the statistics. High values observed in the crest are undoubtedly related to recent volcanisms, but the low ones are difficult to explain [Von Herzen and Uyeda, 1963].

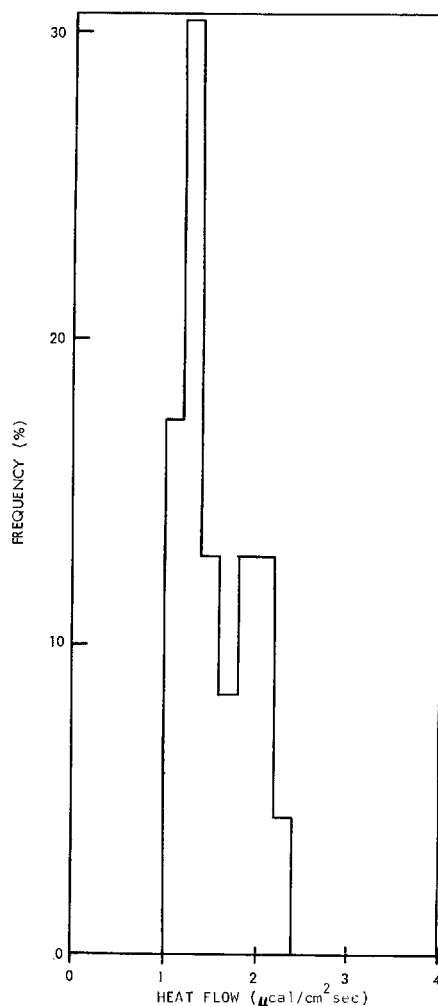


Fig. 39b. Histogram of heat flow values from post-Precambrian non-orogenic areas.

(See section 3.7, chapter 8, by Elder for a suggested explanation.)

## 6. GLOBAL ANALYSIS OF HEAT FLOW OBSERVATIONS

### 6.1 Global Representation

Having a set of heat flow observations, it is desirable to construct a contour map of isoflux that best fits the observations. It is hoped that some general picture of the heat flow pattern will appear in such a contour map, and that explanations for it will be found. Contouring is usually done by 'eye,' but it can be done more

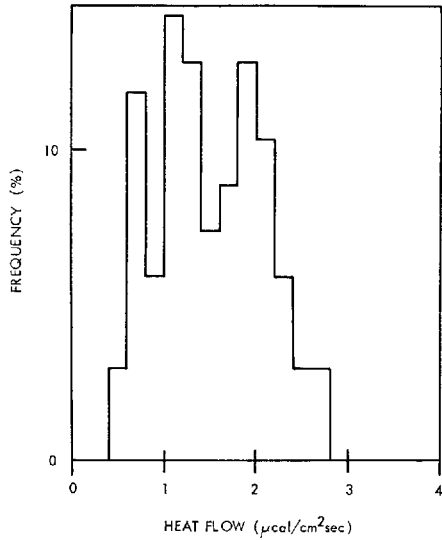


Fig. 39c. Histogram of heat flow values from post-Precambrian orogenic areas.

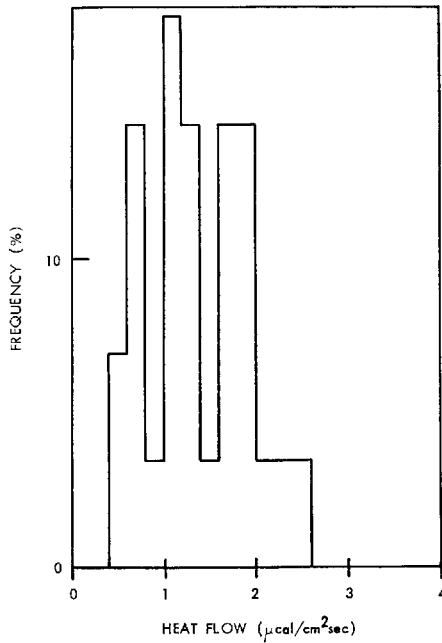


Fig. 39d. Histogram of heat flow values from island arc areas.

objectively by numerical methods using electronic computers. A set of heat flow data  $q(\theta_i, \varphi_i)$ ,  $i = 1, 2, \dots, N$ , where  $\theta_i$  is the colatitude, and  $\varphi_i$  the east longitude of the  $i$ th station, can

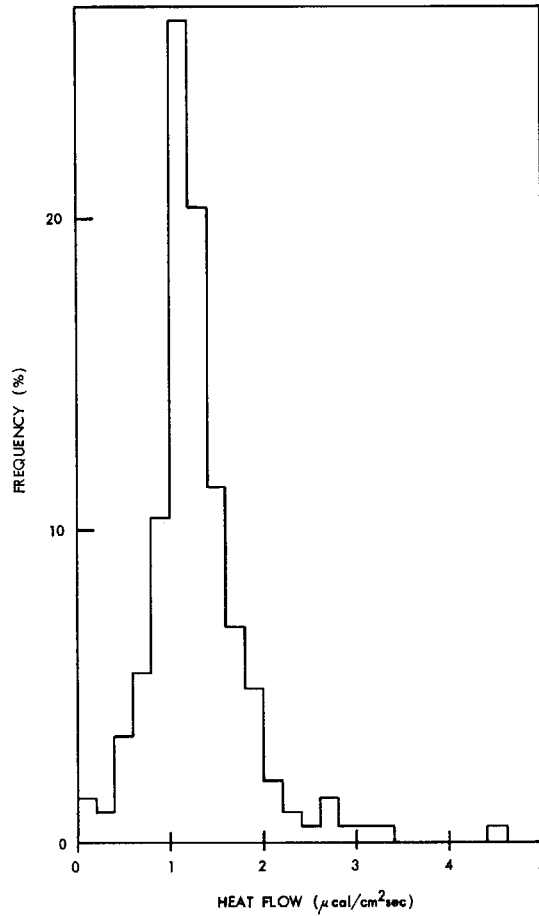


Fig. 40. Histogram of heat flow values from ocean basins.

be fitted by a least squares method to a spherical harmonic expansion of order  $M$ :

$$q(\theta, \varphi) = \sum_{n=0}^M \sum_{m=0}^n [A_n^m P_n^m(\mu) \cos(m\varphi) + B_n^m P_n^m(\mu) \sin(m\varphi)] \quad (6)$$

$$\equiv \sum_{j=1}^k t_j T_j(\theta, \varphi), \quad k \equiv (M+1)^2$$

where  $\mu \equiv \cos(\theta)$ , and the  $P_n^m(\mu)$  are the normalized associated Legendre functions. The coefficients  $t_j$  (and hence  $A_n^m$  and  $B_n^m$ ) are determined from the normal equations:

$$\sum_{j=1}^k t_j \sum_{i=1}^N T_l(\theta_i, \varphi_i) T_j(\theta_i, \varphi_i) = \sum_{i=1}^N q(\theta_i, \varphi_i) T_l(\theta_i, \varphi_i) \quad (7)$$

$l = 1, 2, \dots, k$

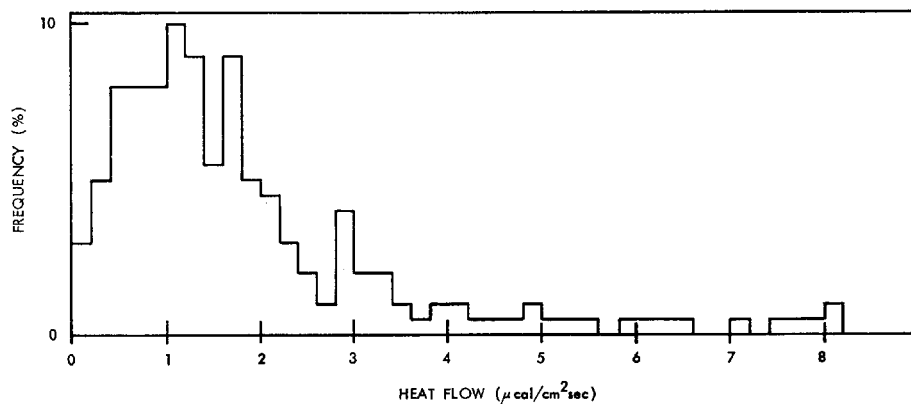


Fig. 41. Histogram of heat flow values from ocean ridges.

For observing stations on a regular grid, (7) is greatly simplified to:

$$t_j = \frac{\sum_{i=1}^N q(\theta_i, \varphi_i) T_j(\theta_i, \varphi_i)}{\sum_{i=1}^N T_j^2(\theta_i, \varphi_i)} \quad (8)$$

$j = 1, 2, \dots, k$

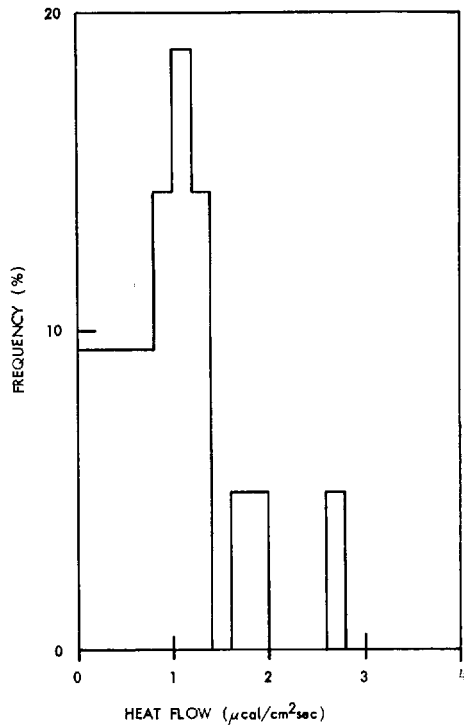


Fig. 42. Histogram of heat flow values from ocean trenches.

Although the geophysical stations are usually irregularly distributed, it is still possible to average over grid squares and use these regularly spaced averages to obtain the spherical harmonic representation. This is essentially the classical method of Gauss. The averaging smooths the values and lowers the 'energy' at wavelengths that are short compared with the intergrid distance. Such a procedure is difficult when the data are limited, for it requires judgment as to the area over which the smoothing should take place. Further, there is the problem of extrapolation into regions where no data exist. However, *Lee* [1963] did not extrapolate in this manner, but solved the set of normal equations 7 directly for  $t_j$  via matrix inversion by Jordan's method. A better computing scheme is to expand the heat flow field in functions orthogonal to the observing stations and to determine the maximum order of spherical harmonic expansion by an objective statistical test of significance [*Lee and MacDonald*, 1963].

A global representation of the heat flow field has been constructed by *Lee and MacDonald* [1963], and a revised one up to third order spherical harmonics is shown in Figure 44. Contour lines over regions where no data exist are dashed. Spherical harmonic coefficients of the heat flow field based on 987 observations are given in Table 15. A recent analysis based on all available observations gives essentially the same picture.

The main features of the heat flow field are highs over the eastern Pacific and east Africa, and lows over the Atlantic and central Pacific. However, it should be emphasized that *the*

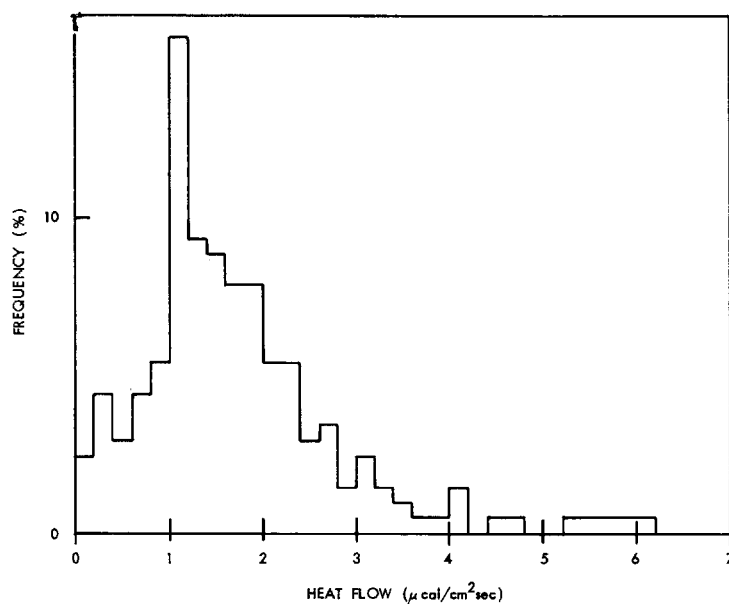


Fig. 43. Histogram of heat flow values from oceanic 'other areas.'

analysis averages out the small-scale variations in the heat flow field, and there is also a possibility that the anomalies in the heat flow field are actually much smaller-scale phenomena than those that can be represented by the low-order harmonics [Lee and MacDonald, 1963]. The resolution of third-order spherical harmonic analysis is about 2000 km; i.e., variations of a scale less than 2000 km will not appear. Nevertheless, on the average and over a large area, the heat flow is high in the eastern Pacific and low in the central Pacific and in the Atlantic. The east African high is uncertain, because there are very few measurements there.

6.2 Comparison with the Gravitational Field

Lee and MacDonald [1963] suggest that the contour representation of the heat flow shows

certain similarities to the geoid (see Figures 44 and 45). The correlation is that where gravity is high the heat flow is low and vice versa. Wang [1963, 1964] reaches similar conclusions independently by using mostly Lee's [1963] data and finds a large negative correlation coefficient of  $-0.82$  between Izsak's [1964] satellite geoid and Lee and MacDonald's [1963] heat flow distribution. Kaula [1965] made a cross-covariance analysis of the gravity and heat flow data, the results of which are shown in Figure 46. The horizontal axis is the angular distance between stations in degrees. The vertical axis is the covariance, i.e. the mean product of heat flow and free-air gravity anomaly pairs adjusted to zero mean product as a function of distance. If heat flow and gravity were not correlated, then the points would all

TABLE 15. Spherical Harmonic Coefficients of the Heat Flow Field

$$\text{The normalization is } \int_0^\pi \int_0^{2\pi} \left[ P_n^m(\mu) \begin{Bmatrix} \cos(m\varphi) \\ \sin(m\varphi) \end{Bmatrix} \right]^2 \sin \theta \, d\theta \, d\varphi = 4\pi$$

$n$	0	1		2		3				
$m$	0	0	1	0	1	2	0	1	2	3
$A_n^m$	1.475	0.118	0.064	-0.107	0.107	-0.044	0.037	-0.162	0.043	0.110
$B_n^m$			-0.018		0.085	0.133		-0.009	0.089	0.219

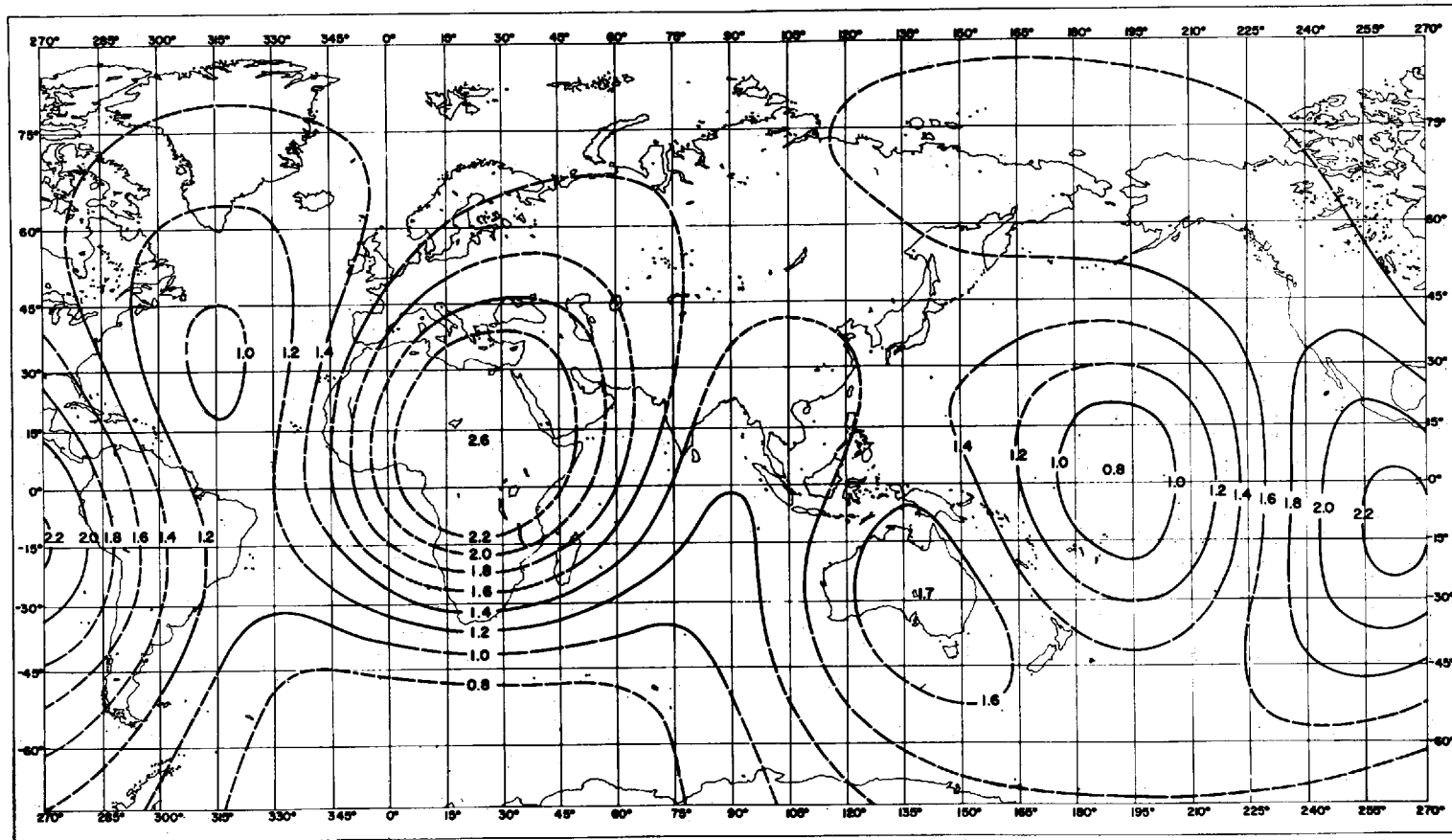


Fig. 44. Orthogonal function representation (to third-order spherical harmonics) of 987 heat flow values. Contour lines are in  $\mu\text{cal}/\text{cm}^2 \text{ sec}$  and are dashed over regions where no data exist.

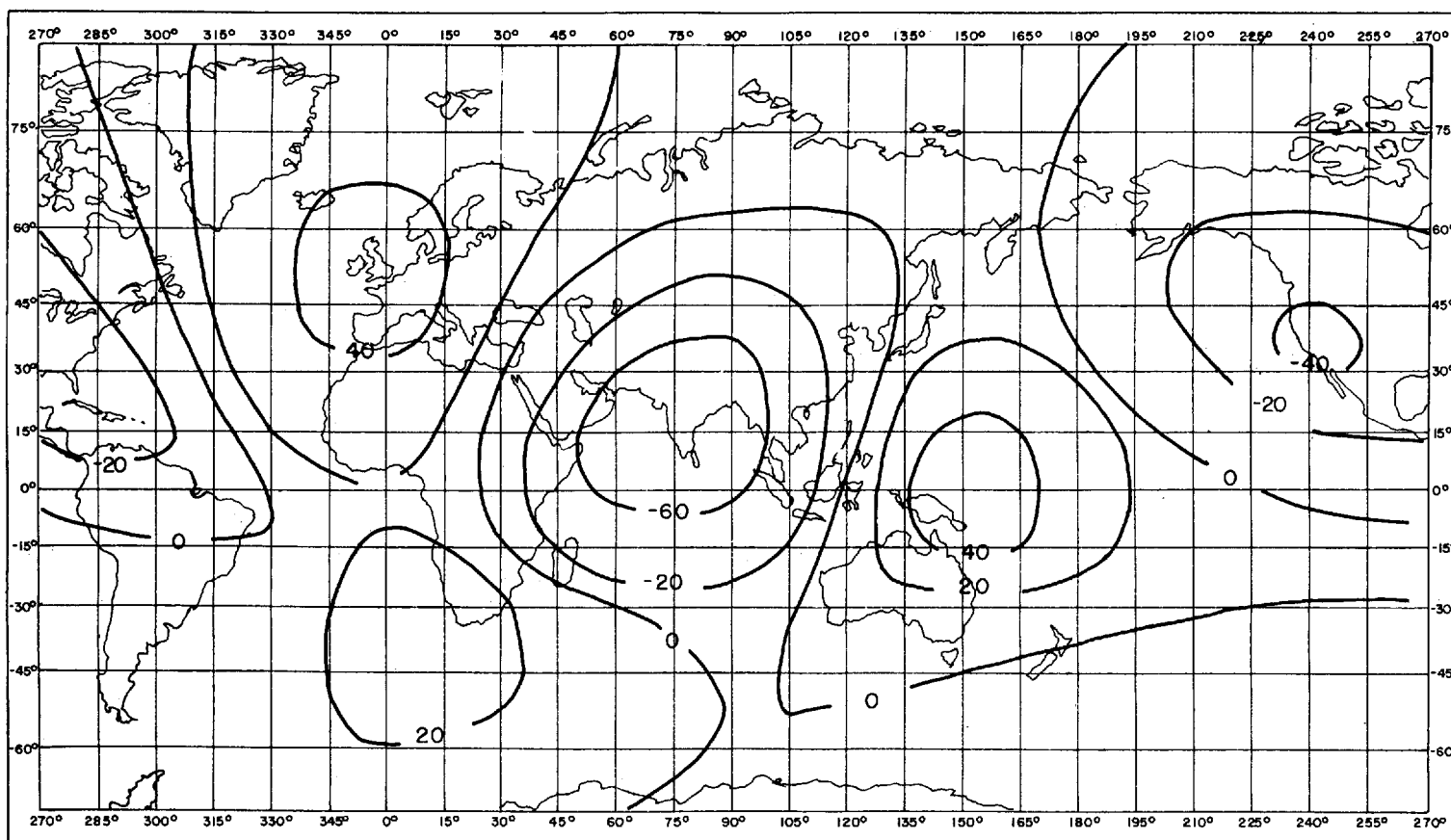


Fig. 45. Geoid heights (in meters, referring to the ellipsoid with a flattening of  $1/298.37$ ) constructed from spherical harmonics up to third order from analysis up to eighth order of the latest artificial satellite data [Guier, 1965].

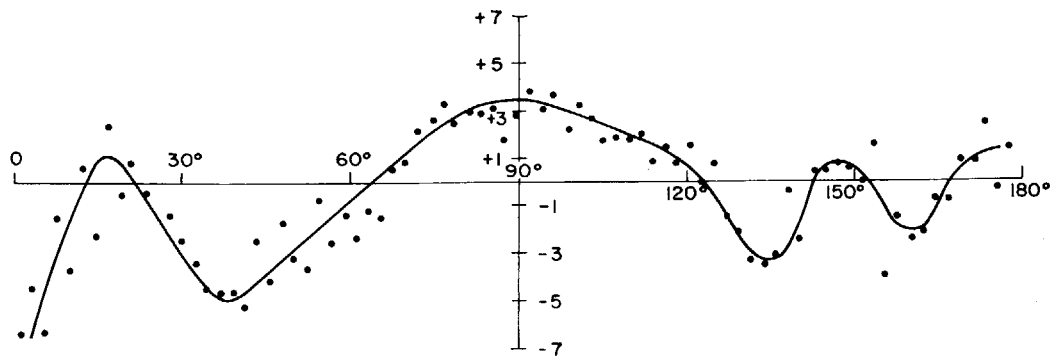


Fig. 46. Cross covariance of heat flow and free-air gravity anomalies (in units of milligal  $\mu\text{cal}/\text{cm}^2 \text{ sec}$ ; taken from *Kaula* [1965, Figure 31]; see text.

fall close to the zero covariance and show no marked pattern. Figure 46 shows negative covariance at  $0^\circ$ —corroborating the negative correlation between heat flow and gravity—but also shows an interesting variation in covariance with extrema at about  $17^\circ$ ,  $38^\circ$ , and  $90^\circ$ . The peak at  $17^\circ$  and the trough at  $38^\circ$  may be produced by convection cells of a wavelength of  $38^\circ$  (i.e., about 4000 km).

The correlation between heat flow and gravity is not yet well established because of the uncertainties of (1) our knowledge of both the heat flow and gravity fields, and (2) their interrelationships. The gravity field reflects the present mass distribution, whereas the surface heat flow field (because of slow thermal conduction) may lag millions of years in indicating the temperature distribution of the corresponding depth in the Earth's interior. A very strong negative correlation between heat flow and gravity would imply that (1) the density irregularities are near the surface and are due to thermal expansion and contraction, rather than chemical variation, and (2) thermal properties are uniform.

Because of the slowness of thermal conduction process, the negative correlation between heat flow and gravity may be more easily explained by convection motions within the mantle. A hot, rising column represents a deficiency in mass and carries an excess of heat, whereas a descending column contains a greater mass and less heat. *Lee and MacDonald* [1963] have demonstrated by an order of magnitude calculation that the anomalies in the gravitational and heat flow fields are consistent with convection currents having velocities of the order of a few centimeters per year. Inhomogeneity in heat sources and in other physical and chemical properties of the Earth's interior may also explain the negative correlation.

genity in heat sources and in other physical and chemical properties of the Earth's interior may also explain the negative correlation.

### 6.3 Heat Flow and Topography

*Lee and MacDonald* [1963] have investigated the distribution of heat flow values with ocean depth. They note that there is some tendency for high values to be associated with a 3000-meter depth (oceanic rises), but on the whole there is a low linear correlation (correlation coefficient =  $-0.33$ ) of the heat flow in oceans with topography.

Figure 47 shows the distribution of heat flow with station elevation or depth. The oceanic part is essentially the same as noted by *Lee and MacDonald*. The land part is too scattered to draw any definite conclusion. On the whole, the linear correlation of heat flow with topography is insignificant (correlation coefficient =  $-0.1$ ).

## 7. SUMMARY

Surface heat flow by conduction is determined as the product of thermal conductivity and vertical temperature gradient. At present, about 2000 observations are available; however, their geographical distribution is extremely uneven, with three times more data per unit area at sea than on land. Analysis of nearby and repeated measurements suggests that in general regional heat flow variations  $>0.2 \mu\text{cal}/\text{cm}^2 \text{ sec}$  are significant.

From spherical harmonic analysis, the global mean heat flow is  $1.5 \pm 10\% \mu\text{cal}/\text{cm}^2 \text{ sec}$  at 95% confidence level. The heat arriving at the Earth's surface is believed to be produced

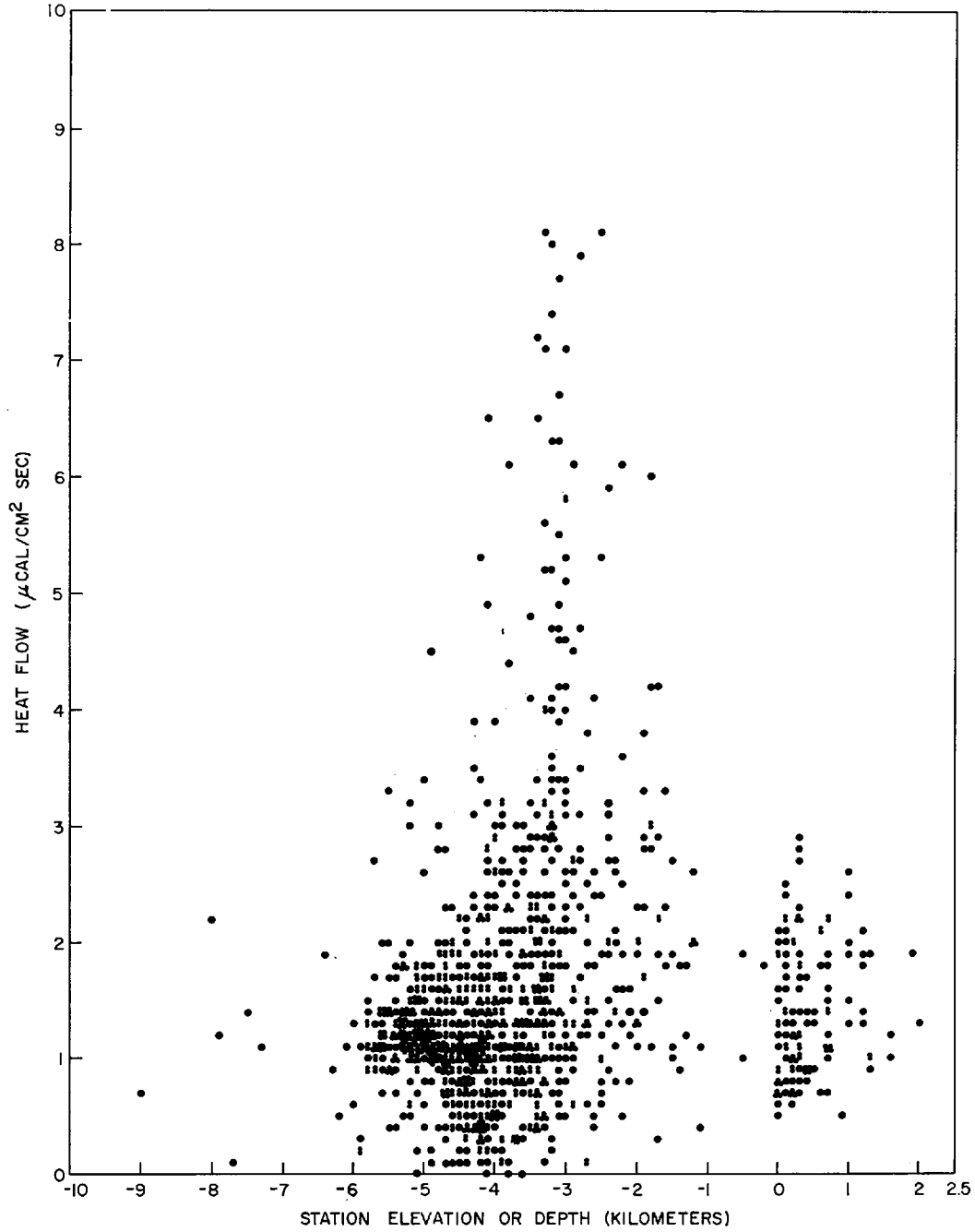


Fig. 47. Distribution of heat flow values with station elevation or depth. Each dot, regardless of its size, represents one data point.

mainly by radioactivity within the Earth [Birch, 1954b]. The average heat flow over the continents does not differ significantly from that over the oceans. This equality of heat flow suggests that radioactivity is approximately the same beneath land and sea, and further implies that there are differences between the upper mantle under the continents and that under the oceans.

Heat flow values are well correlated with major geological features. On land, the average and standard deviations of heat flow values are  $0.92 \pm 0.17$  from Precambrian shields,  $1.23 \pm 0.4$  from Paleozoic orogenic areas,  $1.54 \pm 0.38$  from post-Precambrian non-orogenic areas, and  $1.92 \pm 0.49$  from Mesozoic-Cenozoic orogenic areas. At sea, they are  $0.99 \pm 0.61$  from trenches,  $1.28 \pm 0.53$  from basins, and  $1.82 \pm 1.56$  from ridges.

Global analysis of heat flow data has indicated that the main features of the heat flow field are highs over the eastern Pacific and east Africa and lows over the Atlantic and central Pacific. On a large scale, heat flow seems to be inversely correlated with gravity: where gravity is high, the heat flow is low, and vice versa. The correlation between heat flow and gravity is not yet well established because of uncertainties in the determination of both fields and in their relationships. Moreover, the gravity field reflects the present mass distribution, whereas the surface heat flow field may lag millions of years in indicating the temperature distribution of the corresponding depth in the Earth's interior.

The origin of continents and oceans has long been the object of speculation and debate (see, for example, Hess [1962], Kennedy [1962], and Engel [1963]). A common hypothesis is that the original crust of the Earth is oceanic and that continents are originated and have grown by differentiation of the mantle through geologic time [Menard, 1964, p. 234]. As noted above, heat flow observations are consistent with this theory. It may also be noted that heat flow variations over short distances are most pronounced over active areas (e.g., the crest of the oceanic ridges, and island arc and trench areas). Recently, Ramberg [1964] suggested a model of early-formed global crust of sialic composition. However, postulating an early differentiation over the whole Earth may have difficulty in

explaining the equality of heat flow over land and sea.

In a little more than 25 years, heat flow has become one of the leading topics in geophysical research and has greatly influenced our thought about the Earth's interior. Although progress is accelerating, much remains to be done: development of new experimental techniques, correlation with other geophysical and geological parameters, as well as global and regional surveys. It is extremely important to extend observations to areas where there are no data: most land areas and high-latitude seas. Greater efforts should be made in measuring heat flow around island arc and trench areas, where large heat flow variations occur over short distances. Investigations should also be made to find the reasons for extremely low heat flow values and the role of water circulation from high areas of intake to low areas of discharge.

*Note added in proof.* To keep this review as up-to-date as possible, a brief summary of the heat flow data that came to our knowledge after the completion of the manuscript will be made.

Using the oceanic heat flow technique, Law *et al.* [1965] have made 3 heat flow measurements from sea ice in the northwestern part of the Arctic Archipelago of Canada. They obtained a weighted mean heat flow of  $0.84 \pm 0.09$  s.e.  $\mu\text{cal}/\text{cm}^2 \text{ sec}$ , which has not provided evidence to support the suggestion that the structure responsible for the magnetic variation anomaly at nearby Mould Bay is of thermal origin.

Von Herzen and Vacquier [1965] obtained 60 heat flow values along nine profiles across the Mid-Indian Ocean Ridge. They found results similar to those of the south Mid-Atlantic Ridge reported in Vacquier and Von Herzen [1964].

Several heat flow papers were presented at the 46th Annual Meeting of the American Geophysical Union. The abstracts of these papers were published in the *Transactions, American Geophysical Union*, vol. 46, pp. 174-176, 1965. The following researchers have reported some new data:

Roy and Decker reported 7 preliminary heat flow values (1.2 to 2.2  $\mu\text{cal}/\text{cm}^2 \text{ sec}$ ) in the White Mountains, New England. Three high values ( $>1.9$ ) were interpreted as due to high radioactivity of Conway granite.

Diment, Ortiz, Silva, and Ruiz made the first land measurements in the South American continent in seven boreholes (maximum depth 800 m) at two locations near Vallenar, Chile. Heat flow values are between 0.7 and 1.0  $\mu\text{cal}/\text{cm}^2 \text{ sec}$ . Some uncertainty was associated with the degree of alteration and amount of magnetite in the strata concerned.

Diment, Werre, Baldwin and Saunders made studies on the thermal state in Green Lake, near Fayetteville, N. Y., and found that the computed heat flow is higher than would be expected for the region. Similar attempts in Seneca Lake, N.Y., were reported by Steinhart and Hart. Sub-bottom temperature gradient was measured to a depth of 7 meters, and the heat flow value of 1.7 was obtained.

F. S. Birch (private communication) has revised some of his heat flow values. Data number and revised heat flow values are as follows: 0195, 1.00; 0196, 1.03; 0198, >0.4; 0199, 1.07; 0200, 1.03; 0201, >0.47; 0202, 1.13; 0204, 1.34-1.65; 0205, 1.02; 0206, 1.12; 0207, 1.14; 0209, 1.22-1.56.

#### APPENDIX

##### A LISTING OF HEAT FLOW DATA

The following compilation covers all available heat flow observations up to the end of 1964. It includes many observations in press which have been made available before publication through the kind cooperation of many colleagues. The quality of data ranges from crude estimates to elaborate determinations. When the same data appear in several sources, or when data are modified in later publications, only the latest values are given, and references to the most easily accessible sources (in America) are quoted. Although care has been taken to insure accuracy, errors undoubtedly will occur because of large amounts of data being processed. We will be grateful if readers will inform us about these errors.

The data are arranged in geographical divisions with the following notations:

1. Data number: An arbitrary number is assigned to each heat flow station as it is processed. If several measurements are made or several values are given by different authors, these data are further tabulated under the

given station using letters *A, B, C*, etc., and the average or 'best' value is assigned to the given station.

2. Code: A six digit number is used for classification of each heat flow station.

First digit is geographical code.

- 0 Africa
- 1 Americas
- 2 Australia
- 3 Eurasia
- 4 other lands and Arctic Ocean
- 5 Atlantic Ocean
- 6 Indian Ocean
- 7 Pacific Ocean
- 8 mediterranean seas
- 9 marginal seas

Second digit is geological code.

- 0 post-Precambrian orogenic area
- 1 Precambrian shield
- 2 post-Precambrian non-orogenic area
- 3 Cenozoic volcanic area
- 4 land area where geology is little known
- 5 ocean basin
- 6 oceanic ridge or rise
- 7 ocean trench
- 8 other oceanic area
- 9 complicated area

Third digit indicates type of temperature measurement.

- 0 no measurement
- 1 in borehole
- 2 in mine
- 3 in tunnel
- 4 in other
- 5 using Bullard-type probe
- 6 Bullard-type probe partly penetrating sediments
- 7 using Ewing-type probe
- 8 using other probe
- 9 in boreholes and in mines

Fourth digit indicates type of conductivity measurement.

- 0 no measurement
- 1 using divided bar method
- 2 using transient method
- 3 measured in situ
- 4 using other method
- 5 using needle probe method
- 6 using method of water content

- 7 using method of chlorine content  
 8 using other method  
 9 measurement made on nearby samples
- Fifth digit indicates type of corrections applied.
- 0 no particular correction applied  
 1 water circulation  
 2 climatic changes  
 3 topographic correction  
 4 uplift and erosion  
 5 sedimentation  
 6 effects of nearby lakes, or river, or ocean  
 8 corrections for composite effects
- Sixth digit indicates the quality of data.
- 0 heat flow value not reliable  
 1 lower limit of heat flow value  
 2 upper limit of heat flow value  
 3 average value of a given range of heat flow values  
 4 station located in geothermal area  
 5 no location available  
 6 heat flow disturbed  
 7 'fair' value  
 8 'good' value
3. Station name: first eight characters are used if station name exceeds eight characters.
4. Station latitude in degrees and minutes: S = south, and N = north.
5. Station longitude in degrees and minutes: E = east, and W = west.
6. Station elevation or depth in meters.
7. Temperature gradient ( $\nabla T$ ) in  $10^{-3}$  °C/cm.
8. Thermal conductivity ( $K$ ) in mcal/cm sec °C.
9. Heat flow ( $Q$ ) in  $\mu\text{cal}/\text{cm}^2$  sec.
10. Number of heat flow values available for the station (NO).
11. Reference number (REF); see below.
12. Year of Publication (YR), e.g. 39=1939.
- Reference number (REF) refers to the list below. Complete citations are given in the Reference section of this article.
1. *Von Herzen and Langseth*, 1965
  2. *Burns*, 1964
  3. *Lister and Reitzel*, 1964
  4. *Reitzel*, 1963
  5. *Birch*, 1964
  6. *Bullard and Day*, 1961
  7. *Reitzel*, 1961a
  8. *Gerard et al.*, 1962
  9. *Vacquier and Von Herzen*, 1964
  10. *Nason and Lee*, 1964
  11. *Lister*, 1963a
  12. *Lister*, 1963b
  13. *Langseth and Grim*, 1964
  14. *Nason and Lee*, 1962
  15. *Bullard*, 1954
  16. *Bullard et al.*, 1956
  17. *Reitzel*, 1961b
  18. *Uyeda and Horai*, 1964
  19. *Von Herzen*, 1964a
  20. *Von Herzen and Maxwell*, 1964
  21. *Von Herzen*, 1963
  22. *Von Herzen*, 1959
  23. *Foster*, 1962
  24. *Von Herzen and Uyeda*, 1963
  25. *Maxwell*, 1958
  26. *Revelle and Maxwell*, 1952
  27. *Von Herzen*, 1960
  28. *Langseth et al.*, 1965
  29. *Rhea et al.*, 1964
  30. *Lister*, 1962
  31. *Horai and Uyeda*, 1963
  32. *Maxwell and Revelle*, 1956
  33. *Birch*, 1947b
  34. *Uyeda et al.*, 1962
  35. *Lachenbruch et al.*, 1965
  36. *Yasui et al.*, 1963
  37. *Bullard*, 1939
  38. *Carte*, 1954
  39. *Gough*, 1963
  40. *Von Herzen*, 1964b
  41. *Spicer*, 1941
  42. *Clark*, 1957
  43. *Benfield*, 1947
  44. *Birch and Clark*, 1945
  45. *Herrin and Clark*, 1956
  46. *Birch*, 1947 a, b
  47. *Birch*, 1950
  48. *Lovering*, 1948
  49. *Birch*, 1954a
  50. *Joyner*, 1960
  51. *Diment and Robertson*, 1963
  52. *Diment and Werre*, 1964
  53. *Roy*, 1963
  54. *Diment and Weaver*, 1964
  55. *Lachenbruch and Marshall*, 1964
  56. *Misener et al.*, 1951

57. *Leith*, 1952
58. *Misener*, 1955
59. *Lachenbruch*, 1957
60. *Saull et al.*, 1962
61. *Garland and Lennox*, 1962
62. *Beck*, 1962
63. *Beck and Logis*, 1963
64. *Newstead and Beck*, 1953
65. *Jaeger and Sass*, 1963
66. *Beck*, 1956
67. *Howard and Sass*, 1964
68. *Le Marne and Sass*, 1962
69. *Sass and Le Marne*, 1963
70. *Sass*, 1964a
71. *Sass*, 1964b
72. *Bodvarsson*, 1955
73. *Benfield*, 1939
74. *Anderson*, 1940
75. *Bullard and Niblett*, 1951
76. *Chadwick*, 1956
77. *Mullins and Hinsley*, 1957
78. *Clark and Niblett*, 1956
79. *Clark*, 1961
80. *Boldizar*, 1964a, c
81. *Boldizar*, 1963
82. *Schossler and Schwarzlose*, 1959
83. *Stenz*, 1954
84. *Langseth*, 1964
85. *Grim*, 1964
86. *Yasui and Watanabe*, 1965
87. *Sisoev*, 1961
88. *Sclater*, 1964
89. *Coster*, 1947
90. *Verma and Rao*, 1965
91. *Boldizar*, 1964b
92. *Boldizar and Gozon*, 1963
93. *Boldizar*, 1959
94. *Lubimova et al.*, 1964
95. *Birch*, 1956
96. *Kraskovski*, 1961
97. *Diment et al.*, 1965a
98. *Diment et al.*, 1965b
99. *Spicer*, 1964
100. *Lubimova et al.*, 1961

*Note added in proof.* Note the following changes in heat flow values given on page 166: Data No. 0161 should read 0.63 (instead of 0.66); Data No. 0162 should read 0.66 (instead of 0.63).

DATA NUMBER	STATION CODE	STATION NAME	LATI-TUDE	LONGI-TUDE	ELE./DEPTH	V.T	K	Q	NO	REF	YR	
AFRICA--SOUTH AFRICA												
0001	011108	JACO-DOH	27-18S	26-24E	+1310	.130	7.43	0.96	2	37	39	
	A	011108	JACOBA	27-18S	26-24E	+1310	.128	7.46	0.95	1	37	39
	B	011907	DOORNHOU	27-18S	26-24E	+1300	.131	7.40	0.97	1	37	39
0002	011108	GERH-DOK	26-24S	27-21E	+1590	.092	13.5	1.24	3	37	39	
	A	011108	GERHARDM	26-30S	27-12E	+1520	.095	13.5	1.28	1	37	39
	B	011900	DRIEFONT	25-52S	29-11E	+1000	.070	10.8	0.75	1	37	39
	C	011907	DOORNKLO	26-18S	27-30E	+1660	.089	13.5	1.20	1	37	39
0003	011907	REEF-NIG	26-18S	28-18E	+1565	.103	10.0	1.03	1	37	39	
0004	021108	DUBBELDE	30-30S	21-30E	+ 990	.223	6.80	1.52	1	37	39	
0005	011108	HB15	26-48S	26-54E	+1310	.105	10.0	1.05	1	38	54	
0006	011108	ROODEPOR	26-54S	26-36E	+1300	.119	7.2	0.86	1	38	54	
0007	021108	MESSINA	22-18S	30-06E	+ 518	.269	5.1	1.37	1	38	54	
0008	021108	KESTELL	28-18S	28-42E	+1980	.248	5.2	1.29	1	38	54	
0009	021128	SAMBOKKR	32-42S	21-18E	+ 737	.183	7.6	1.39	1	39	63	
0010	021128	KOEGELFO	33-00S	21-18E	+ 726	.182	7.9	1.45	1	39	63	
0011	021128	BOTHADAL	32-48S	22-36E	+ .952	.178	7.1	1.28	1	39	63	
0012	021128	KALKKOP	32-42S	24-24E	+ .654	.196	6.1	1.21	1	39	63	
AFRICA--LAKE NYASA												
0013	045507	L.NYASA	11-27S	34-29E	- 460	.62	1.6	1.0	20	40	65	
AMERICA--UNITED STATES												
0014	102137	GRASS VA	39-12N	121-03W	+ 667	.095	7.2	0.69	1	42	57	
	A	102137	GRASS VA	39-12N	121-03W	+ 667	.095	7.2	0.69	1	42	57
	B	102000	GRASS VA	39-12N	121-03W	+ 667	.095	7.2	0.69	1	41	41
0015	101108	BAKERSFI	35-28N	119-45W	+ 207	.350	3.7	1.29	1	43	47	
0016	121900	BIG LAKE	31-12N	101-29W	+ 500	.25	8.	2.0	1	44	45	
0017	121907	REEVES C	31-10N	103-14W	+ 700	.083	13.	1.1	1	45	56	
0018	121907	REGAN CO	31-15N	101-28W	+ 700	.083	13.	1.1	12	45	56	
	A	121907	BLU 103	31-15N	101-28W	+ 700	.090	13.	1.2	1	45	56
	B	121900	BLU 106	31-15N	101-28W	+ 700	.088	13.	1.1	1	45	56
	C	121900	BLU 110	31-15N	101-28W	+ 700	.098	13.	1.3	1	45	56
	D	121900	BLU 112	31-15N	101-28W	+ 700	.092	13.	1.2	1	45	56
	E	121907	BLU 115	31-15N	101-28W	+ 700	.076	13.	1.0	1	45	56
	F	121907	BLU 118	31-15N	101-28W	+ 700	.079	13.	1.0	1	45	56
	G	121907	BLU 119	31-15N	101-28W	+ 700	.083	13.	1.1	1	45	56
	H	121900	BLU 124	31-15N	101-28W	+ 700	.085	13.	1.1	1	45	56
	I	121900	BLU 125	31-15N	101-28W	+ 700	.083	13.	1.1	1	45	56
	J	121907	BLU 126	31-15N	101-28W	+ 700	.083	13.	1.1	1	45	56
	K	121907	BLU 127	31-15N	101-28W	+ 700	.086	13.	1.1	1	45	56
	L	121900	UNIV 1	31-15N	101-28W	+ 700	.097	13.	1.3	1	45	56
0019	121907	UPTON CO	31-23N	101-48W	+ 700	.083	13.	1.1	1	45	56	
0020	121900	MIDLAND	31-39N	102-15W	+ 700	.094	13.	1.2	1	45	56	
0021	121907	EDDY COU	32-29N	104-03W	+ 700	.085	12.6	1.1	5	45	56	
	A	121907	SM-1	32-38N	104-14W	+ 700	.103	11.8	1.2	1	45	56
	B	121900	S-1C	32-14N	104-07W	+ 700	.101	11.8	1.2	1	45	56
	C	121900	NMPR 1B	32-24N	104-16W	+ 700	.073	13.	0.9	1	45	56
	D	121907	M-O-1W	32-18N	103-45W	+ 700	.077	13.	1.0	1	45	56
	E	121907	G-7D	32-31N	104-09W	+ 700	.080	13.	1.0	1	45	56
0022	121900	LEA CNTY	32-47N	103-48W	+1000	.092	13.	1.2	1	45	56	
0023	101013	COLORADO	38-49N	104-49W	+1885	.2	7.	1.4	1	47	50	

## REVIEW OF HEAT FLOW DATA

161

DATA NUMBER	STATION CODE	STATION NAME	LATI- TUDE	LONGI- TUDE	ELE./ DEPTH	VT	K	Q	NO	REF	YR	
AMERICA--UNITED STATES (CONTINUED)												
0024	121003	SYRACUSE	37-57N	101-45W	+1051	.28	5.5	1.55	1	47	50	
0025	101000	GEORGIA	33- N	84- W	+ 300	.143	7.	1.0	3	51	63	
	A	101000	GEORGIA	33- N	84- W	+ 300	.2	7.	1.4	1	47	50
	B	101000	GRIFFIN	33- N	84- W	+ 300	.139	7.	0.97	1	51	63
	C	101000	LAGRANGE	33- N	84- W	+ 300	.146	7.	1.02	1	51	63
0026	103138	FRONT RA	40-15N	105-40W	+2500	0.22	7.8	1.7	1	47	50	
0027	101983	SAN MANU	32-37N	110-39W	+ 970	.15	8.	1.2	1	48	48	
0028	119138	CALUMET	47-17N	88-28W	+ 360	.186	5.0	0.93	1	49	54	
0029	101007	1-BUTLER	40-59N	80-08W	+ 200	.29	4.2	1.2	1	50	60	
0030	101007	POTTER	41-54N	77-56W	+ 200	.37	3.8	1.4	2	50	60	
	A	101007	3-POTTER	41-56N	77-51W	+ 500	.39	3.7	1.47	1	50	60
	B	101007	4-POTTER	41-52N	78-00W	+ 500	.35	3.7	1.31	1	50	60
0031	101007	DO-MA-HA	39-20N	80-32W	+ 200	.33	3.6	1.2	3	50	60	
	A	101007	2-DODDRI	39-17N	80-46W	+ 200	.29	4.2	1.22	1	50	60
	B	101007	5-MARIO	39-25N	80-05W	+ 200	.34	3.5	1.20	1	50	60
	C	101007	6-HARRIS	39-18N	80-14W	+ 200	.37	3.4	1.26	1	50	60
0032	101108	OAK RIDG	35-55N	84-19W	+ 240	.12	6.1	0.73	1	51	63	
0033	101108	WASHINGT	39- N	77- W	+ 30	.157	7.13	1.12	1	52	64	
0034	121108	BOSS	37-39N	91-10W	+ 375	.17	7.6	1.29	1	53	63	
0035	121108	BOURBON	38-09N	91-15W	+ 290	.15	8.1	1.22	1	53	63	
0036	111138	DELAWARE	47-24N	88-01W	+ 389	.16	5.3	0.95	1	53	63	
0037	111138	WHITE PI	46-44N	89-34W	+ 281	.16	6.7	1.07	3	53	63	
	A	111138	DDH-N-55	46-45N	89-34W	+ 279	.16	6.7	1.07	1	53	63
	B	111138	DDH-N-65	46-44N	89-34W	+ 305	.16	6.6	1.06	1	53	63
	C	111138	DDH-E-27	46-44N	89-36W	+ 260	.16	6.9	1.10	1	53	63
0038	101138	METALINE	48-54N	117-21W	+ 686	.20	11.6	2.31	4	53	63	
	A	101138	DDH-CS-2	48-55N	117-20W	+ 671	.24	11.	2.67	1	53	63
	B	101138	DDH-CS-9	48-53N	117-21W	+ 734	.21	11.	2.31	1	53	63
	C	101138	DDH-R-1	48-54N	117-21W	+ 664	.20	12.	2.38	1	53	63
	D	101138	DDH-R-4	48-54N	117-20W	+ 675	.19	12.	2.25	1	53	63
0039	101138	GOVERNME	39-52N	112-04W	+1860	.40	4.7	1.9	1	53	63	
0040	131134	EUREKA	39-57N	112-03W	+1702	.80	4.4	3.51	1	53	63	
0041	101138	YERINGTO	38-55N	119-04W	+1034	.27	8.7	2.36	3	53	63	
	A	101138	DDH-L-2	38-55N	119-04W	+1459	.27	8.4	2.26	1	53	63
	B	101138	DDH-L-5	38-56N	119-04W	+1410	.28	8.5	2.39	1	53	63
	C	101137	DDH-L-13	38-56N	119-04W	+1434	.21	9.1	1.9	1	53	63
0042	101138	BARSTOW	34-39N	116-21W	+1245	.24	8.8	2.1	2	53	63	
	A	101106	DDH-M-10	34-39N	116-41W	+1246	.24	6.6	1.59	1	53	63
	B	101138	DDH-M-11	34-39N	116-21W	+1245	.24	8.8	2.10	1	53	63
1133	101108	ALBERTA	36-52N	77-54W	+ 116	.18	7.8	1.4	1	98	65	
1134	101108	AIKEN SC	33-17N	81-40W	+ 100	.15	6.7	1.0	6	97	65	
1135	101907	SALT VLY	38-55N	109-50W	+1500	.385	3.43	1.2	5	99	64	
	A	101907	REEDER 1	38-55N	109-50W	+1500	.374	3.54	1.32	1	99	64
	B	101907	CRESCENT	38-55N	109-50W	+1500	.386	3.38	1.30	1	99	64
	C	101907	BRENDELL	38-55N	109-50W	+1500	.394	3.38	1.33	1	99	64
	D	101907	BALSLEY	38-46N	109-38W	+1500	.314	3.51	1.10	1	99	64
	E	101907	HYDE	38-51N	109-30W	+1500	.194	5.23	1.01	1	99	64

## AMERICA--PUERTO RICO

0043	101188	MAYAGUEZ	18-09N	67-10W	+ 30	.10	6.0	0.6	1	54	64
------	--------	----------	--------	--------	------	-----	-----	-----	---	----	----

DATA NUMBER	STATION CODE	STATION NAME	LATI- TUDE	LONGI- TUDE	ELE./ DEPTH	∇T	K	Q	NO	REF	YR
AMERICA--CANADA											
0044	101108	TORONTO	43-42N	79-25W	+ 100	.160	6.4	1.03	1	56	51
0045	112108	SUDBURY	46-30N	81-01W	+ 200	.158	6.4	1.01	1	56	51
0046	102108	THETFORD	46-06N	71-18W	+ 200	.157	6.7	1.05	1	56	51
0047	112100	CALUMET	45-49N	74-41W	+ 50	.156	8.5	1.32	1	56	51
0048	112108	KIRKLAND	48-10N	80-02W	+ 200	.130	7.7	1.00	3	56	51
A	112108	KL-LS	48-10N	80-02W	+ 200	.130	7.5	0.97	1	56	51
B	112108	KL-TH	48-10N	80-02W	+ 200	.130	7.9	1.03	1	56	51
C	112108	KL-WH	48-10N	80-02W	+ 200	.130	7.7	0.99	1	56	51
0049	112108	MALARTIC	48-09N	78-09W	+ 200	.101	6.8	0.69	1	56	51
0050	112108	LARDER L	48-06N	79-44W	+ 200	.097	9.1	0.88	1	56	51
0051	112108	TIMMINIS	48-30N	81-20W	+ 200	.091	8.0	0.73	2	56	51
A	112108	TIMMIN-D	48-30N	81-20W	+ 200	.092	8.0	0.73	1	56	51
B	112107	TIMMIN-M	48-30N	81-20W	+ 200	.090	8.0	0.73	1	56	51
0052	101180	RESOLUTE	74-41N	94-54W	+ 0	.395	7.3	2.9	1	58	55
0053	101108	MONTREAL	45-15N	073-57W	+ 50	.062	12.0	0.74	1	60	62
0054	101108	STE-ROSA	45-38N	072-40W	+ 49	.159	5.06	0.81	1	60	62
0055	101108	LOUN-CAR	46-05N	073-08W	+ 22	.269	3.03	0.82	1	60	62
0056	121907	LEDUC	53-23N	113-48W	+ 700	.43	3.7	1.6	1	61	62
0057	121908	REDWATER	53-59N	113-07W	+ 700	.30	4.9	1.46	1	61	62
0058	101988	NORMAN W	65-18N	126-51W	+ 100	.65	3.1	2.00	1	61	62
0059	112107	FLIN FLO	54-47N	101-51W	+ 200	.12	6.7	0.8	1	62	62
0060	111308	BRENT CR	46-05N	78-29W	+ 335	.133	5.6	0.75	1	63	63
AUSTRALIA											
0061	231138	GT.LAKE	41-58S	146-11E	+1027	.4	5.	2.	8	65	63
A	231108	NO.1 G.L	41-58S	146-11E	+1027	.43	4.7	2.04	1	64	53
B	231100	NO.2 DTL	41-58S	146-11E	+ 733	.43	4.8	2.06	1	64	53
C	231900	NO.3 DTL	41-58S	146-11E	+ 714	.43	4.8	2.07	1	64	53
D	231100	NO.4 ROS	41-46S	145-34E	+ 198	.30	8.2	2.47	1	64	53
E	231100	NO.5 ROS	41-46S	145-34E	+ 263	.28	9.0	2.54	1	64	53
F	231138	GT.LAKE	41-58S	146-11E	+1000	.338	5.4	1.9	1	65	63
G	231136	STOREY C	42- S	146- E	+ 900	.308	12.2	3.8	1	65	63
H	231186	ROSBERY	41-46S	145-34E	+ 320	.29	8.6	2.5	1	65	63
0062	203108	SNOWY MT	36-30S	148- E	+1000	.226	8.6	2.	2	67	64
A	201108	E-5010	36-30S	148- E	+1000	.213	8.8	1.9	1	66	56
B	203108	EUCUMBEN	36-30S	148- E	+1000	.239	8.4	2.0	1	67	64
0063	221108	COBAR	31-32S	145-50E	+ 300	.205	10.6	2.18	1	68	62
0064	229108	BROKEN H	31-57S	141-28E	+ 300	.199	9.70	1.93	18	69	63
A	221108	BH-1205	31-57S	141-28E	+ 300	.197	9.87	1.94	1	69	63
B	221908	BH-1126	31-57S	141-28E	+ 300	.200	9.53	1.91	1	69	63
C	221108	BH-1093	31-57S	141-28E	+ 300	.196	9.84	1.93	1	69	63
D	221908	BH-1040	31-57S	141-28E	+ 300	.193	10.4	2.01	1	69	63
E	221108	BH-950	31-57S	141-28E	+ 300	.198	10.5	2.07	1	69	63
F	221908	BH-W-1	31-57S	141-28E	+ 300	.187	10.3	1.93	1	69	63
G	221908	BH-305	31-57S	141-28E	+ 300	.199	9.49	1.89	1	69	63
H	221908	BH-678	31-57S	141-28E	+ 300	.198	9.51	1.88	1	69	63
I	221908	G-969	31-57S	141-28E	+ 300	.200	10.1	2.03	1	69	63
J	221908	P-814	31-57S	141-28E	+ 300	.188	9.61	1.81	1	69	63
K	221908	P-820	31-57S	141-28E	+ 300	.193	9.93	1.92	1	69	63
L	221908	P-831	31-57S	141-28E	+ 300	.198	9.58	1.90	1	69	63
M	221908	P-835	31-57S	141-28E	+ 300	.189	9.84	1.86	1	69	63
N	221908	C-834	31-57S	141-28E	+ 300	.202	9.61	1.94	1	69	63

## REVIEW OF HEAT FLOW DATA

163

DATA NUMBER	CODE	STATION NAME	LATI-TUDE	LONGI-TUDE	ELE./DEPTH	∇T	K	Q	NO	REF	YR
AUSTRALIA (CONTINUED)											
O	221908	57-LBH-1	31-57S	141-28E	+ 300	.211	9.47	2.00	1	69	63
P	221908	57-LBH-6	31-57S	141-28E	+ 300	.203	9.61	1.95	1	69	63
Q	221908	59-P-8	31-57S	141-28E	+ 300	.206	9.61	1.98	1	69	63
R	221108	55-C-6	31-57S	141-28E	+ 300	.216	8.40	1.81	1	69	63
0065	211168	KALGOORL	30-45S	121-30E	+ 380	.093	10.1	0.96	2	67	64
A	212108	KALGOORL	30-45S	121-30E	+ 380	.088	10.1	0.89	1	67	64
B	211168	KALGOORL	30-55S	121-33E	+ 380	.098	10.1	0.96	4	70	64
BA	211168	SE-10	30-55S	121-33E	+ 380	.107	9.7	1.04	1	70	64
BB	211168	SE-12	30-55S	121-33E	+ 380	.105	10.4	1.09	1	70	64
BC	211168	SE-6	30-55S	121-33E	+ 380	.084	9.9	0.83	1	70	64
BD	211168	SE-4	30-55S	121-33E	+ 380	.096	9.2	0.83	1	70	64
0066	211108	COOLGARL	30-57S	121-10E	+ 423	.124	7.3	0.90	2	67	64
A	211108	BV-1	30-57S	121-10E	+ 423	.142	7.7	1.09	1	70	64
B	211108	MLS-1	30-57S	121-10E	+ 423	.105	6.9	0.72	1	70	64
0067	211108	NORSEMAN	32-20S	121-37E	+ 305	.131	7.3	0.89	2	67	64
A	211108	NORSEMAN	32-20S	121-37E	+ 305	.119	7.5	0.89	1	67	64
B	210107	NORSEMAN	32-20S	121-37E	+ 305	.143	7.1	1.01	3	70	64
BA	210107	C-79	32-20S	121-37E	+ 305	.151	6.9	1.04	1	70	64
BB	210107	C-80	32-20S	121-37E	+ 305	.154	6.8	1.05	1	70	64
BC	210107	PRS-105	32-20S	121-37E	+ 305	.125	7.5	0.94	1	70	64
0068	241106	RUM JUNG	13- S	131- E	+ 60	.19	10.5	2.0	3	67	64
A	241106	RJ-337	13- S	131- E	+ 60	.148	6.9	1.02	1	67	64
B	241106	RJ-B35	13- S	131- E	+ 60	.174	11.7	2.0	1	67	64
C	241106	RJ-B40	13- S	131- E	+ 60	.201	9.4	1.9	1	67	64
0069	222108	TENNANT	19-34S	134-13E	+ 328	.225	10.2	2.3	1	67	64
0070	221108	MT. ISA	21- S	139- E	+ 300	.189	9.5	1.8	1	67	64
0071	211107	CUE	27-27S	117-52E	+ 454	.108	8.8	0.95	1	67	64
0072	212108	MT. MAGN	28- S	118- E	+ 460	.113	11.4	1.3	1	67	64
0073	212107	BULLFINC	31-14S	119-19E	+ 360	.139	8.8	1.2	1	67	64
0074	221108	RADIUM H	32-30S	140-30E	+ 305	.230	7.8	1.8	1	67	64
0075	211108	RAVENSTH	33-40S	120- E	+ 180	.116	8.2	0.95	1	67	64
0076	221106	CABAWIN	27-30S	150-12E	+ 300	.25	4.6	1.16	1	71	64
0077	221906	MOONIE	27-44S	150-13E	+ 300	.22	4.6	1.01	1	71	64
0078	201108	CANBERRA	35-17S	149-08E	+ 560	.252	8.15	2.06	1	71	64
0079	221108	WHYALLA	33-10S	137-30E	+ 60	.21	10.3	2.16	1	71	64
0080	221108	KANMANTO	35-05S	139-15E	+ 150	.194	10.9	2.11	1	71	64
0081	231108	STAWELL	37-03S	142-47E	+ 300	.271	10.5	2.84	1	71	64
0082	231108	CASTLEMA	37-03S	144-13E	+ 165	.242	11.9	2.88	1	71	64
ASIA--INDIA											
0083	312108	KOLAR	12-55N	78-15E	+ 600	.104	6.28	0.66	1	90	65
ASIA--IRAN											
0084	341128	MASJID-I	31-59N	49-18E	+ 413	.151	5.8	0.87	18	89	47
A	341128	MIS-T171	31-59N	49-18E	+ 580	.164	6.2	1.01	1	89	47
B	341128	MIS-T230	31-59N	49-18E	+ 565	.147	4.4	0.65	1	89	47
C	341128	MIS-K178	31-59N	49-18E	+ 550	.123	6.5	0.80	1	89	47
D	341128	MIS-SH95	31-59N	49-18E	+ 440	.113	4.7	0.53	1	89	47
E	341128	MIS-B162	31-59N	49-18E	+ 350	.133	4.8	0.64	1	89	47
F	341128	MIS-B187	31-59N	49-18E	+ 310	.114	7.3	0.83	1	89	47
G	341128	MIS-B212	31-59N	49-18E	+ 335	.128	7.2	0.93	1	89	47

DATA NUMBER	STATION CODE	STATION NAME	LATI- TUDE	LONGI- TUDE	ELE./ DEPTH	VT	K	Q	NO	REF	YR
ASIA--IRAN (CONTINUED)											
H	341128	MIS-T232	31-59N	49-18E	+ 440	.125	6.4	0.80	1	89	47
I	341128	MIS-CS23	31-59N	49-18E	+ 435	.127	8.9	1.13	1	89	47
J	341128	MIS-B211	31-59N	49-18E	+ 335	.106	6.2	0.66	1	89	47
K	341128	MIS-Q250	31-59N	49-18E	+ 555	.180	5.1	0.92	1	89	47
L	341128	MIS-Q225	31-59N	49-18E	+ 420	.214	5.7	1.22	1	89	47
M	341128	MIS-C209	31-59N	49-18E	+ 335	.181	5.2	0.94	1	89	47
N	341128	MIS-C229	31-59N	49-18E	+ 315	.166	5.4	0.90	1	89	47
O	341128	MIS-C222	31-59N	49-18E	+ 320	.155	6.0	0.92	1	89	47
P	341128	MIS-C240	31-59N	49-18E	+ 335	.150	5.7	0.85	1	89	47
Q	341128	MIS-A244	31-59N	49-18E	+ 305	.186	5.2	0.96	1	89	47
R	341128	MIS-C235	31-59N	49-18E	+ 510	.198	5.3	1.05	1	89	47

## ASIA--JAPAN

0085	301907	HABORO	44-21N	141-52E	+ 100	0.45	4.12	1.87	1	18	64
0086	302108	SHIMOKAW	44-14N	142-41E	+ 350	0.30	5.63	1.71	1	18	64
0087	339108	KONOMAI	44-08N	143-21E	+ 100	0.40	6.41	2.54	1	18	64
0088	302108	AKABIRA	43-32N	142-02E	+ 100	0.25	4.31	1.07	1	18	64
0089	301108	ASHIBETS	43-33N	142-12E	+ 100	0.30	4.38	1.35	1	18	64
0090	332004	TOYOHA	42-54N	141-05E	+ 500	1.13	5.	5.6	1	18	64
0091	331907	YABASE	39-44N	140-06E	+ 10	0.48	4.19	2.01	1	18	64
0092	331907	INNAI	39-16N	139-58E	+ 10	0.48	3.11	1.49	1	18	64
0093	339108	OSARIZAW	40-11N	140-45E	+ 300	0.33	6.70	2.24	1	18	64
0094	302108	NODA-TAM	40-04N	141-50E	+ 0	0.14	8.28	1.14	1	18	64
0095	302107	KAMAISHI	39-16N	141-42E	+ 770	0.09	5.66	0.52	1	18	64
0096	302108	HITACHI	36-38N	140-38E	+ 350	0.11	6.62	0.71	1	18	64
0097	301108	KATSUTA	36-24N	140-30E	+ 0	0.30	3.02	0.91	1	18	64
0098	301108	KASHIMA	35-57N	140-41E	+ 0	0.21	3.57	0.76	1	18	64
0099	301108	MOBARA	35-24N	140-20E	+ 0	0.18	2.94	0.54	1	18	64
0100	301108	TOKYO	35-42N	139-46E	+ 20	0.22	3.36	0.74	1	18	64
0101	332107	ASHIO	36-39N	139-27E	+ 700	0.36	6.25	2.23	1	18	64
0102	331104	KUSATSU-	36-37N	138-34E	+1600	2.47	4.48	10.8	1	18	64
0103	331108	CHICHIBU	36-01N	138-48E	+1020	0.19	7.06	1.34	1	18	64
0104	333907	SASAGO	35-37N	138-48E	+ 650	0.27	7.61	2.06	1	18	64
0105	309108	KAMIOKA	36-21N	137-19E	+ 650	0.28	6.49	1.80	1	18	64
0106	309108	NAKATATS	35-52N	136-35E	+ 600	0.29	6.71	1.95	1	18	64
0107	302100	KUNE	35-05N	137-50E	+ 262	0.20	8.14	1.60	1	18	64
0108	302108	NAKO	35-03N	137-52E	+ 285	0.22	6.65	1.44	1	18	64
0109	301107	MINENOSAX	35-00N	137-51E	+ 300	0.29	6.13	1.79	1	18	64
0110	302108	IKUNO	35-10N	134-50E	+ 370	0.19	7.33	1.38	1	18	64
0111	309108	NAKAZE	35-21N	134-57E	+ 300	0.34	6.51	2.21	1	18	64
0112	301108	YANAHARA	34-57N	134-04E	+ 100	0.20	5.89	1.20	1	18	64
0113	331100	ISOTAKE	35-11N	132-26E	+ 100	0.40	8.65	3.49	1	18	64
0114	301108	TSUMO	34-34N	132-00E	+ 350	0.18	6.08	1.09	1	18	64
0115	301108	KAWAYAMA	34-15N	132-59E	+ 350	0.17	5.85	1.00	1	18	64
0116	301108	NAKA	34-15N	135-25E	- 197	0.30	5.90	1.79	1	18	64
0117	301108	HIDAKA	33-57N	135-05E	+ 0	0.29	7.40	2.12	1	18	64
0118	301107	KIWA	33-50N	135-53E	+ 80	0.18	7.06	1.31	1	18	64
0119	301108	BESSHI	34-01N	133-09E	+ 160	0.25	4.89	1.22	1	18	64
0120	331107	IZUHARA	34-13N	129-14E	+ 150	0.29	7.41	2.17	1	18	64
0121	302108	TAKAMATS	33-52N	130-43E	- 450	0.31	6.27	1.92	1	18	64
0122	302107	TAIO	33-07N	130-52E	+ 600	0.17	6.16	1.05	1	18	64
0123	302108	MAKIMINE	32-38N	131-27E	+ 120	0.26	6.95	1.79	1	18	64
1136	331104	MATSUKAW	40- N	141- E	+ 500			15.	1	18	64

## REVIEW OF HEAT FLOW DATA

165

DATA NUMBER	CODE	STATION NAME	LATI- TUDE	LONGI- TUDE	ELE./ DEPTH	▽T	K	Q	NO	REF	YR
EUROPE--GREAT BRITAIN											
0124	301127	DYSART	56-08N	3-07W	+	0 .22	4.2	0.92	3	74	40
	A 301927	BALFOUR	56-08N	3-07W	+	0 .23	3.0	0.68	1	73	39
	B 301127	BORELAND	56-08N	3-07W	+	0 .20	4.7	0.95	1	74	40
	C 301927	BALFOUR	56-08N	3-07W	+	0 .24	3.7	0.89	1	74	40
0125	301128	HOLFORD	53-20N	2-30W	+	30 .13	5.7	0.74	1	73	39
0126	301020	GLASGOW	55-53N	4-22W	+	20 .41	3.8	1.57	4	74	40
	A 301020	BLYTHSWO	55-53N	4-20W	+	20 .36	3.4	1.24	1	73	39
	B 301020	SOUTH BA	55-53N	4-20W	+	20 .46	3.3	1.53	1	73	39
	C 301020	BLYTHSWO	55-53N	4-24W	+	20 .36	3.9	1.41	1	74	40
	D 301020	SOUTH BA	55-53N	4-24W	+	20 .46	3.8	1.73	1	74	40
0127	301120	HANKHAM	50-55N	0-15W	+	20 .234	3.0	0.71	1	73	39
0128	301020	DURHAM	54-45N	1-38W	+	20 .306	4.8	1.47	1	74	40
0129	304020	WIGAN	53-30N	2-20W	+	20 .327	3.2	1.01	1	74	40
0130	301128	CAMBRIDG	52-12N	0-00E	+	30 .13	9.8	1.28	1	76	56
0131	301108	NOTTINGH	53-08N	0-53W	+	70 .38	4.1	1.57	6	75	51
	A 301106	EAKR-5	53-09N	0-59W	+	83 .743	3.7	2.73	1	75	51
	B 301106	EAKR-6	53-09N	1-00W	+	86 .786	3.5	2.75	1	75	51
	C 301106	EAKR-64	53-08N	0-59W	+	91 .573	3.4	1.97	1	75	51
	D 301106	EAKR-141	53-09N	1-00W	+	79 .718	4.0	2.87	1	75	51
	E 301108	KH-1	53-07N	0-52W	+	52 .364	4.0	1.47	1	75	51
	F 301108	CAUN-11	53-08N	0-54W	+	30 .391	4.2	1.67	1	75	51
0132	301108	YORKSHIR	54-34N	1-03W	+	39 .24	4.9	1.16	2	75	51
	A 301108	KIRK-1	54-35N	1-05W	+	21 .209	5.5	1.15	1	75	51
	B 301108	TOCK-1	54-33N	1-01W	+	57 .277	4.3	1.18	1	75	51
0133	301108	BAWTRY	53-25N	1-00W	+	50 .36	5.3	1.91	4	77	57
	A 301108	MISSON	53-25N	1-00W	+	50 .38	5.3	2.03	1	77	57
	B 301108	RANBY CA	53-25N	1-00W	+	50 .36	5.5	1.98	1	77	57
	C 301108	RANBY HA	53-25N	1-00W	+	50 .34	5.4	1.84	1	77	57
	D 301108	SCAFTWOR	53-25N	1-00W	+	50 .35	5.1	1.79	1	77	57
0134	301108	NOTTINGH	53-00N	1-10W	+	50 .32	5.0	1.61	2	77	57
	A 301108	GOOSE DAG	53-00N	1-10W	+	50 .31	4.9	1.52	1	77	57
	B 301108	PAPPLEWI	53-00N	1-10W	+	50 .34	5.0	1.69	1	77	57
EUROPE--SWITZERLAND											
0135	303988	GOTTHARD	46-25N	8-35E	+1154	.209	6.70	1.4	1	78	56
0136	303988	SIMPLON	46-25N	8-05E	+705	.328	6.70	2.2	1	78	56
0137	303988	LOETSCHB	46-35N	7-45E	+1243	.244	7.77	1.9	1	78	56
EUROPE--AUSTRIA											
0138	303988	ARLBERG	46-55N	10-10E	+1300	.173	11.0	1.9	1	79	61
0139	303988	TAUERN	46-50N	13-05E	+1200	.230	7.83	1.8	1	79	61
EUROPE--HUNGARY											
0140	302108	ZO-HQ-BA	46-10N	18-14E	+300	.43	6.3	2.7	3	80	64
	A 302108	HOSSZUHE	46-10N	18-22E	+270	.41	6.1	2.49	2	80	64
	B 302108	KO-ZORAK	46-12N	18-18E	+300	.45	7.3	3.31	2	80	64
	C 30 7	BAKONYA	46-07N	18-04E	+300			2.4	1	80	64
0141	301108	NAGYLENG	46-46N	16-45E	+200	.46	4.4	1.9	1	80	64
0142	30 7	HAJDUSZO	47-26N	21-23E	+100			2.4	1	80	64
0143	30 7	SZENTEND	47-41N	19-05E	+200			2.0	1	80	64

DATA NUMBER	STATION CODE	STATION NAME	LATI- TUDE	LONGI- TUDE	ELE./ DEPTH	VT	K	Q	NO	REF	YR
EUROPE--CZECHOSLOVIA											
0144	30	7 BANSKA S	48-27N	18-53E	+1000			2.6	1	80	64
EUROPE--ITALY											
0145	331104	LARDEREL	43-12N	10-54E	+ 300	3.4	3.2	10.6	9	81	63
EUROPE--EAST GERMANY											
0146	322400	BLEICHER	51-30N	10-10E	+ 228	0.14	7.60	1.06	1	82	59
0147	322407	STASSFUR	51-40N	11-30E	+ 76	0.22	7.60	1.67	1	82	59
0148	322400	STRASSBE	51-35N	11-00E	+ 340	0.33	4.69	1.55	1	82	59
0149	342400	PECHTELS	50-30N	12-25E	+ 500	0.25	5.70	1.43	1	82	59
0150	342400	SCHMIEDE	50-30N	11-25E	+ 740	0.23	5.56	1.25	1	82	59
0151	342400	ZWICKAU	50-40N	12-35E	+ 328	0.45	2.8	1.32	1	82	59
0152	342400	FREITAL	51-05N	13-40E	+ 250	0.16	3.7	0.60	1	82	59
0153	342400	BRAND ER	51-00N	13-00E	+ 250	0.34	5.95	2.02	1	82	59
0154	342407	FREIBERG	51-00N	13-30E	+ 427	0.31	5.5	1.69	1	82	59
0155	342400	ALTENBER	50-30N	13-50E	+ 790	0.31	7.09	2.19	1	82	59
0156	322400	DORNDORF	50-50N	10-00E	+ 250	0.15	10.3	1.51	1	82	59
0157	321000	REHNA I	53-20N	11-00E	+ 50	0.23	6.5	1.48	1	82	59
0158	321000	OEBISFEL	52-30N	11-00E	+ 50	0.18	6.6	1.18	1	82	59
EUROPE--POLAND											
0159	321000	CIECHOCI	52-53N	18-47E	+ 100	.23	5.3	1.23	1	83	54
EUROPE--U.S.S.R.											
0160	311208	KRIVOI R	48-02N	33-20E	+ 100	.104	7.5	0.78	3	94	64
A	311208	KR-7554	48-02N	33-20E	+ 100	.104	7.13	0.74	1	94	64
B	311000	KR-8123	47-55N	33-20E	+ 100	.091	8.53	0.78	1	94	64
C	311000	KR-8500	47-55N	33-20E	+ 100	.10	7.1	0.71	1	94	64
0161	311208	BELAYA T	49-50N	30-10E	+ 100	.092	7.2	0.66	1	94	64
0162	311208	UMAN	48-45N	30-13E	+ 200	.11	5.8	0.63	1	94	64
0163	321206	YAKOVLEV	50-30N	36-30E	+ 300	.15	9.7	1.45	1	94	64
0164	341906	MAZESTA	43-35N	39-48E	+ 500	.15	6.7	1.	2	94	64
EUROPE--ICELAND											
1138	431000	ICELAND						4.5	1	72	55
EUROPE--BALTIC SHIELD											
1137	319000	BALTIC S				.15	5.	0.8	3	96	61
PACIFIC ISLAND											
0165	741090	ENIWETOK	11-30N	162-15E	+ 0	0.18	5.	0.9	1	95	56

## REVIEW OF HEAT FLOW DATA

167

DATA NUMBER	CODE	STATION NAME	LATI- TUDE	LONGI- TUDE	ELE./ DEPTH	$\nabla T$	K	Q	NO	REF	YR
BLACK SEA											
0166	888000	BLACK S.	-	-	-2269	.48	4.0	1.9	7	87	61
A	888000	4742	-	-	-2179	.30	4.0	1.2	1	87	61
B	888000	4745	-	-	-1714	.45	4.0	1.8	1	87	61
C	888000	4751	-	-	-2216	.55	4.0	2.2	1	87	61
D	888000	4750	-	-	-2170	.65	4.0	2.6	1	87	61
E	888000	4752	-	-	-2197	.45	4.0	1.8	1	87	61
F	888000	4753	-	-	-1840	.50	4.0	2.	1	87	61
G	888000	4754	-	-	-1300	.45	4.0	1.8	1	87	61
ATLANTIC OCEAN											
0167	557608	CH21-1	29-51N	54-36W	-5610	0.50	2.08	1.04	1	3	64
0168	567608	CH21-4	28-56N	46-44W	-4370	0.30	2.24	0.67	1	3	64
0169	567608	CH21-5	28-47N	44-55W	-3940	0.51	2.22	1.13	1	3	64
0170	567602	CH21-10	29-04N	43-12W	-3080	0.4	1.96	0.8	1	3	64
0171	567608	CH21-12	28-51N	42-49W	-3520	0.38	2.11	0.81	1	3	64
0172	567607	CH21-13	29-02N	41-10W	-4060	0.2	1.94	0.4	1	3	64
0173	585508	CH19-C	20-13N	66-35W	-5810	0.56	2.27	1.28	1	3	64
0174	587608	CH19-7-1	20-14N	66-35W	-5770	0.75	2.05	1.54	1	3	64
0175	557608	A-282-3	23-20N	70-02W	-5480	0.54	2.09	1.12	1	4	63
0176	557608	A-282-5	23-28N	72-18W	-5300	0.66	1.77	1.17	1	4	63
0177	557608	A-282-6	25-14N	73-16W	-5310	0.53	2.03	1.08	1	4	63
0178	557608	A-282-7	26-59N	72-13W	-5150	0.58	1.86	1.09	1	4	63
0179	557608	A-282-9	25-18N	69-01W	-5580	0.55	2.11	1.17	1	4	63
0180	557608	A-282-10	23-37N	67-54W	-5650	0.53	2.00	1.06	1	4	63
0181	557608	A-282-11	21-47N	68-51W	-5560	0.61	2.10	1.27	1	4	63
0182	587608	A-282-12	20-22N	67-23W	-5410	0.87	2.01	1.76	1	4	63
0183	557608	A-282-13	21-54N	66-37W	-5640	0.61	1.94	1.19	1	4	63
0184	557608	A-282-14	23-40N	65-37W	-5800	0.59	1.92	1.13	1	4	63
0185	557608	A-282-15	25-29N	64-34W	-5680	0.57	1.92	1.09	1	4	63
0186	557608	A-282-17	25-26N	66-40W	-5580	0.64	1.90	1.22	1	4	63
0187	557608	A-282-18	27-05N	67-56W	-5200	0.57	1.88	1.07	1	4	63
0188	557608	A-282-20	28-44N	69-05W	-5330	0.58	2.06	1.18	1	4	63
0189	557608	A-282-21	28-51N	66-50W	-5240	0.62	1.93	1.19	1	4	63
0190	557608	A-282-22	28-54N	64-39W	-4900	0.61	1.80	1.11	1	4	63
0191	557608	A-282-23	30-27N	67-58W	-5230	0.55	1.91	1.05	1	4	63
0192	587607	AII-1-1	32-02N	74-09W	-4870	0.40	2.05	0.81	1	4	63
0193	587607	AII-1-3	30-56N	74-36W	-3430	0.47	1.99	0.94	1	4	63
0194	587608	AII-1-5	29-10N	76-22W	-4990	0.46	2.51	1.17	1	4	63
0195	557608	C-36-1	21-08N	65-02W	-5696	0.53	1.82	0.96	1	5	64
0196	557603	C-36-3	19-24N	61-30W	-5468	0.73	1.89	1.37	1	5	64
0197	557601	C-36-5	16-45N	57-38W	-5853	0.12	2.28	0.27	1	5	64
0198	557601	C-36-6	16-47N	57-49W	-5853	0.15	2.0	0.3	1	5	64
0199	557608	C-36-7	16-34N	57-52W	-4330	0.54	1.96	1.06	1	5	64
0200	557608	C-36-8	16-35N	57-54W	-4330	0.54	1.93	1.05	1	5	64
0201	557601	C-36-9	16-57N	58-24W	-5890	0.22	2.01	0.44	1	5	64
0202	557608	C-36-10	16-18N	58-37W	-5599	0.60	1.86	1.11	1	5	64
0203	587601	ATS296-4	39-32N	65-50W	-4330	0.47	2.29	1.08	1	5	64
0204	587601	ATS296-6	39-33N	66-17W	-4325	0.56	2.37	1.33	1	5	64
0205	587608	ATS296-7	39-47N	65-16W	-4467	0.48	2.22	1.07	1	5	64
0206	587608	ATS296-8	39-26N	65-09W	-4757	0.54	2.10	1.14	1	5	64
0207	587602	ATS296-9	39-46N	66-28W	-3922	0.56	2.11	1.18	1	5	64
0208	557608	C-39-1	29-00N	59-11W	-5811	0.47	1.96	0.92	1	5	64

DATA NUMBER	CODE	STATION NAME	LATI-TUDE	LONGI-TUDE	ELE./DEPTH	VT	K	Q	NO	REF	YR
ATLANTIC OCEAN (CONTINUED)											
0209	557603	C-39-2	25-18N	55-44W	-5932	0.72	1.93	1.39	1	5	64
0210	557608	C-39-3	24-04N	55-14W	-5984	0.33	1.82	0.60	1	5	64
0211	557608	C-39-5	28-30N	57-59W	-5800	0.48	1.98	0.95	1	5	64
0212	557608	C-39-6	29-56N	60-33W	-5715	0.72	1.84	1.33	1	5	64
0213	557608	C-39-7	29-47N	62-12W	-4865	0.66	1.81	1.19	1	5	64
0214	586607	B-D-6	39-36N	12-13W	-3020	0.46	2.30	1.06	1	6	61
0215	585608	B-D-7	35-59N	9-59W	-4534	0.37	2.31	0.87	1	6	61
0216	885608	B-D-8	35-58N	4-34W	-1251	0.57	2.13	1.22	1	6	61
0217	555608	B-D-9	45-28N	5-47W	-4592	0.33	2.26	0.75	1	6	61
0218	555608	B-D-10	46-32N	13-04W	-4413	0.50	2.17	1.09	1	6	61
0219	565608	B-D-11	46-30N	22-58W	-4084	0.57	2.25	1.29	1	6	61
0220	566607	B-D-12	46-37N	27-18W	-4109	3.15	2.07	6.52	1	6	61
0221	565608	B-D-13	36-20N	21-00W	-4844	0.54	2.12	1.14	1	6	61
0222	566607	B-D-14	35-36N	19-02W	-5375	0.67	2.01	1.34	1	6	61
0223	566607	B-D-15	35-34N	18-56W	-5380	0.46	2.01	0.93	1	6	61
0224	565608	B-D-16	36-39N	17-21W	-5146	0.53	2.13	1.14	1	6	61
0225	555608	B-D-17	44-55N	10-45W	-4844	0.64	2.18	1.39	1	6	61
0226	556607	B-D-18	40-59N	15-09W	-5305	0.49	2.32	1.14	1	6	61
0227	585608	B-D-19	42-18N	11-53W	-3063	0.36	2.18	0.76	1	6	61
0228	556607	B-D-20	41-27N	14-40W	-5260	0.55	2.18	1.21	1	6	61
0229	555608	B-D-21	43-42N	12-39W	-5030	0.51	2.29	1.16	1	6	61
0230	555808	CHAIN-1	35-35N	61-08W	-4590	0.62	1.92	1.20	1	7	61
0231	555808	CHAIN-2	35-35N	61-15W	-4680	0.68	1.92	1.31	1	7	61
0232	565801	CHAIN-3	51-18N	29-35W	-3260	3.7	1.7	6.2	1	7	61
0233	555808	CHAIN-4	53-53N	24-05W	-3350	0.73	2.10	1.54	1	7	61
0234	587708	V-15-3	00-59S	38-10W	-4137	0.66	2.31	1.52	1	8	62
0235	587708	V-15-4	00-12N	39-54W	-4111	0.48	2.23	1.07	1	8	62
0236	557708	V-15-5	02-30N	40-55W	-4285	0.63	2.19	1.38	1	8	62
0237	567708	V-15-6	05-04N	41-01W	-4544	0.83	2.23	1.85	1	8	62
0238	567708	V-15-7	06-59N	41-04W	-4636	0.90	2.25	2.03	1	8	62
0239	567708	V-15-8	10-45N	41-21W	-5002	1.51	2.23	3.37	1	8	62
0240	557707	V-15-10	14-14N	57-06W	-5002	0.73	2.19	1.60	1	8	62
0241	587708	V-15-12	17-21N	65-11W	-4169	0.52	2.23	1.16	1	8	62
0242	587708	V-15-13	20-49N	66-25W	-5227	0.68	2.23	1.52	1	8	62
0243	557708	V-15-14	23-14N	66-36W	-5605	0.61	2.23	1.36	1	8	62
0244	587708	V-15-16	21-34N	67-06W	-5115	0.75	2.23	1.67	1	8	62
0245	577708	V-15-19	19-50N	65-53W	-7934	0.52	2.23	1.16	1	8	62
0246	587708	V-15-23	32-35N	74-24W	-4521	0.46	2.23	1.03	1	8	62
0247	587708	V-15-24	32-47N	74-49W	-4462	0.47	2.22	1.04	1	8	62
0248	555508	LSDA-55	33-45S	15-00E	-4170	0.77	2.45	1.88	1	9	64
0249	555907	LSDA-56	33-15S	11-59E	-4630	0.43	2.37	1.01	1	9	64
0250	556507	LSDA-57	32-30S	09-01E	-5040	0.40	2.01	0.8	1	9	64
0251	556900	LSDA-58B	32-00S	06-06E	-5210	0.55	2.01	1.1	1	9	64
0252	565907	LSDA-59	31-37S	02-47E	-4215	0.04	2.18	0.09	1	9	64
0253	565508	LSDA-60	31-21S	01-58E	-4190	1.00	2.18	2.17	1	9	64
0254	565907	LSDA-61	30-52S	00-56W	-3810	0.41	2.18	0.90	1	9	64
0255	565508	LSDA-63	30-16S	04-21W	-4890	0.46	2.15	0.99	1	9	64
0256	565907	LSDA-64	30-06S	05-45W	-4340	0.34	2.19	0.74	1	9	64
0257	565508	LSDA-65	29-43S	07-16W	-4150	0.22	2.23	0.48	1	9	64
0258	565907	LSDA-66	29-48S	08-24W	-4155	0.12	2.23	0.27	1	9	64
0259	565508	LSDA-67	29-51S	09-25W	-3940	0.21	2.32	0.48	1	9	64
0260	565907	LSDA-68	29-49S	10-18W	-3735	0.51	2.28	1.16	1	9	64
0261	565907	LSDA-69	29-51S	11-07W	-3690	0.50	2.28	1.15	1	9	64

## REVIEW OF HEAT FLOW DATA

169

DATA NUMBER	CODE	STATION NAME	LATI- TUDE	LONGI- TUDE	ELE./ DEPTH	$\nabla T$	K	Q	NO	REF	YR
ATLANTIC OCEAN (CONTINUED)											
0262	565907	LSDA-70	29-55S	11-54W	-3400	0.18	2.28	0.41	1	9	64
0263	565508	LSDA-71	29-51S	12-46W	-3200	0.50	2.24	1.12	1	9	64
0264	565907	LSDA-72	29-45S	14-11W	-3385	0.48	2.24	1.08	1	9	64
0265	565907	LSDA-73	29-50S	14-51W	-3735	0.15	2.24	0.34	1	9	64
0266	565907	LSDA-74	29-50S	15-33W	-3405	0.32	2.24	0.72	1	9	64
0267	565907	LSDA-75	27-22S	12-34W	-3520	0.99	2.27	2.24	1	9	64
0268	565508	LSDA-76	27-27S	10-56W	-3580	0.59	2.27	1.34	1	9	64
0269	566900	LSDA-77	26-47S	13-54W	-2480	0.78	2.27	1.7	1	9	64
0270	566900	LSDA-78	25-58S	14-51W	-3785	0.44	2.27	1.0	1	9	64
0271	565508	LSDA-79	24-03S	15-32W	-4100	0.05	2.18	0.10	1	9	64
0272	565907	LSDA-80	23-47S	14-27W	-4000	0.41	2.18	0.9	1	9	64
0273	565907	LSDA-81	23-42S	12-12W	-3580	0.51	2.18	1.12	1	9	64
0274	566900	LSDA-82	22-43S	13-07W	-3605	3.44	2.27	7.8	1	9	64
0275	565508	LSDA-83	21-21S	11-35W	-2515	3.58	2.27	8.14	1	9	64
0276	565907	LSDA-85	21-15S	10-39W	-3535	0.45	2.18	0.97	1	9	64
0277	566900	LSDA-86	20-10S	11-30W	-2925	3.35	2.18	7.3	1	9	64
0278	565907	LSDA-87	19-53S	12-26W	-2710	1.73	2.18	3.78	1	9	64
0279	565508	LSDA-88	19-44S	12-55W	-3500	0.48	2.18	1.04	1	9	64
0280	565907	LSDA-89	18-58S	12-49W	-3125	0.51	2.18	1.11	1	9	64
0281	565907	LSDA-90	18-58S	12-00W	-2510	2.14	2.27	4.85	1	9	64
0282	565508	LSDA-91	18-32S	10-15W	-3395	0.21	2.15	0.45	1	9	64
0283	565907	LSDA-92	18-08S	11-15W	-3305	0.34	2.18	0.75	1	9	64
0284	565907	LSDA-93	17-39S	12-22W	-3440	0.74	2.18	1.61	1	9	64
0285	565907	LSDA-94	17-15S	13-20W	-3340	0.22	2.18	0.47	1	9	64
0286	565907	LSDA-95	16-46S	14-30W	-3455	0.62	2.18	1.35	1	9	64
0287	565907	LSDA-96	16-15S	15-45W	-3435	0.20	2.18	0.43	1	9	64
0288	565907	LSDA-97	15-48S	16-50W	-3820	1.07	2.18	2.33	1	9	64
0289	565907	LSDA-98	15-23S	17-54W	-4390	0.23	2.18	0.51	1	9	64
0290	565508	LSDA-99	14-55S	19-22W	-4230	0.19	2.24	0.43	1	9	64
0291	565508	LSDA-100	10-00S	15-26W	-3595	0.13	2.23	0.29	1	9	64
0292	565508	LSDA-101	09-11S	13-20W	-2690	0.04	2.16	0.08	1	9	64
0293	565907	LSDA-102	09-03S	10-29W	-3550	0.18	2.23	0.40	1	9	64
0294	565907	LSDA-103	06-43S	13-27W	-3245	0.12	2.18	0.26	1	9	64
0295	565508	LSDA-104	05-41S	11-12W	-2905	1.18	2.18	2.58	1	9	64
0296	565907	LSDA-105	04-57S	09-28W	-3500	0.53	2.18	1.15	1	9	64
0297	565907	LSDA-106	00-56S	10-37W	-4040	0.50	2.12	1.07	1	9	64
0298	565907	LSDA-107	00-28S	10-51W	-4350	0.42	2.12	0.89	1	9	64
0299	565508	LSDA-108	00-03N	11-02W	-4125	0.68	2.12	1.45	1	9	64
0300	565907	LSDA-109	00-26N	11-14W	-4215	0.85	2.12	1.80	1	9	64
0301	555907	LSDA-110	00-52N	11-28W	-4950	0.07	2.12	0.15	1	9	64
0302	555508	LSDA-111	02-38N	12-12W	-4735	0.76	1.81	1.37	1	9	64
0303	555508	LSDA-112	05-01N	12-45W	-4390	0.82	1.91	1.56	1	9	64
0304	555508	LSDA-113	07-24N	17-08W	-4800	0.71	1.95	1.39	1	9	64
0305	565508	LSDA-114	06-47N	19-18W	-4360	0.46	2.09	0.96	1	9	64
0306	565907	LSDA-115	06-21N	20-49W	-3590	0.58	2.12	1.22	1	9	64
0307	565508	LSDA-116	05-07N	25-15W	-4360	0.92	2.16	1.99	1	9	64
0308	565508	LSDA-117	03-21N	30-52W	-2590	0.16	2.34	0.37	1	9	64
0309	565907	LSDA-118	03-18N	31-00W	-2820	1.16	2.31	2.68	1	9	64
0310	566900	LSDA-119	03-15N	31-35W	-2415	1.00	2.31	2.3	1	9	64
0311	565508	LSDA-120	03-57N	34-04W	-3340	0.82	2.28	1.87	1	9	64
0312	565907	LSDA-121	05-42N	32-51W	-2955	2.23	2.28	5.08	1	9	64
0313	565907	LSDA-122	05-59N	32-28W	-3300	2.26	2.31	5.22	1	9	64
0314	565508	LSDA-124	08-26N	34-23W	-4790	0.76	2.04	1.56	1	9	64

DATA NUMBER	CODE	STATION NAME	LATI-TUDE	LONGI-TUDE	ELE./DEPTH	VT	K	Q	NO	REF	YR	
ATLANTIC OCEAN (CONTINUED)												
0315	565907	LSDA-125	09-39N	37-40W	-4045	0.11	2.16	0.23	1	9	64	
0316	565907	LSDA-126	09-34N	39-32W	-3340	0.57	2.28	1.31	1	9	64	
0317	566900	LSDA-127	09-41N	40-49W	-2315	0.74	2.28	1.7	1	9	64	
0318	565907	LSDA-128	09-45N	41-18W	-3295	0.74	2.28	1.70	1	9	64	
0319	566900	LSDA-130	11-35N	44-03W	-2755	1.05	2.28	2.4	1	9	64	
0320	565508	LSDA-131	11-34N	44-48W	-3830	0.40	2.12	0.84	1	9	64	
0321	565907	LSDA-132	11-34N	45-33W	-4105	1.11	2.08	2.30	1	9	64	
0322	565907	LSDA-133	12-17N	46-13W	-4515	0.22	2.08	0.46	1	9	64	
0323	585508	LSDA-134	14-59N	58-19W	-3535	0.32	2.22	0.72	1	9	64	
0324	585508	LSDA-135	15-04N	59-58W	-4480	0.32	2.20	0.71	1	9	64	
0325	586507	LSDA-136	15-04N	60-30W	-2335	0.93	2.15	2.0	1	9	64	
0326	885907	LSDA-137	15-02N	62-15W	-2720	0.93	2.15	2.0	1	9	64	
0327	885508	LSDA-139	15-00N	63-50W	-2082	0.66	2.06	1.36	2	9	64	
	A	885508	LSDA139A	15-00N	63-50W	-2080	0.66	2.06	1.37	1	9	64
	B	885508	LSDA139B	15-00N	63-50W	-2085	0.66	2.06	1.36	1	9	64
0328	855508	ZEP-4	13-36N	71-59W	-4232	0.72	2.0	1.4	1	10	64	
0329	855508	ZEP-5	13-43N	68-38W	-5042	0.53	1.9	1.1	1	10	64	
0330	886507	ZEP-8	14-22N	62-19W	-2877	0.70	1.9	1.3	1	10	64	
0331	555506	ZEP-9	16-24N	57-39W	-4647	0.39	1.8	0.7	1	10	64	
0332	565508	ZEP-11	19-10N	52-03W	-5344	0.81	1.7	1.4	1	10	64	
0333	565508	ZEP-12	20-12N	49-01W	-4632	0.30	1.5	0.5	1	10	64	
0334	865508	ZEP-13	21-06N	46-30W	-3912	0.16	1.9	0.3	1	10	64	
0335	565508	ZEP-14	21-04N	44-57W	-3255	0.84	2.1	1.8	1	10	64	
0336	565508	ZEP-15	21-56N	45-46W	-3372	3.24	2.0	6.5	1	10	64	
0337	565508	ZEP-16	23-06N	45-39W	-3983	1.48	2.0	3.0	1	10	64	
0338	565508	ZEP-17	23-34N	44-14W	-4960	0.81	2.0	1.6	1	10	64	
0339	566507	ZEP-18	23-57N	44-59W	-3493	1.34	2.1	2.8	1	10	64	
0340	566507	ZEP-19	23-36N	42-28W	-4113	0.23	2.1	0.5	1	10	64	
0341	565508	ZEP-20	24-16N	39-06W	-5439	0.19	1.9	0.4	1	10	64	
0342	565508	ZEP-22	25-05N	34-13W	-5602	0.36	1.9	0.7	1	10	64	
0343	555508	ZEP-23	26-14N	26-27W	-5210	0.59	2.0	1.2	1	10	64	
0344	555508	ZEP-25	26-57N	19-58W	-4298	0.46	2.1	1.0	1	10	64	
0345	586507	ZEP-26	31-12N	11-50W	-3210	0.50	2.2	1.1	1	10	64	
0346	585508	ZEP-27	33-35N	9-43W	-4340	0.45	2.2	1.0	1	10	64	
0347	885506	ZEP-32	40-37N	5-50E	-2720	0.56	2.2	1.2	1	10	64	
0348	557608	D 4775	29-02N	25-27W	-5342			1.39	1	11	63	
0349	557608	D 4777	28-60N	25-26W	-5344			1.20	1	11	63	
0350	557608	D 4778	29-03N	25-33W	-5342			1.13	1	11	63	
0351	557608	D 4784	29-04N	25-27W	-5339			1.21	1	11	63	
0352	557608	D 4788	29-05N	25-15W	-5299			1.29	1	11	63	
0353	557608	D 4809	28-51N	25-27W	-4871			1.11	1	11	63	
0354	557608	D 4813	28-50N	25-24W	-4862			1.05	1	11	63	
0355	557608	D 4817	29-34N	25-18W	-5400			1.03	1	11	63	
0356	557608	D 4821	29-35N	25-23W	-5297			1.23	1	11	63	
0357	557608	D 4822	29-08N	24-19W	-5281			1.33	1	11	63	
0358	557607	D 4528	45-19N	11-27W	-4143			1.13	1	12	63	
0359	557608	D 4531	45-19N	11-28W	-4125			1.00	1	12	63	
0360	557608	C19-6-17	31-54N	64-44W	-4262			0.97	1	12	63	
0361	567601	CH21-8	29-04N	44-11W				+	1	12	63	
0362	567608	CH21-14	34-00N	15-51W	-3810			0.57	1	12	63	
0363	567608	CH21-16	34-06N	14-24W	-4315			0.94	1	12	63	
0364	887601	CH21-18	39-31N	05-26E	-2826			0.87	1	12	63	
0365	887607	CH21-19	42-14N	07-09E	-2731			2.5	1	12	63	
0366	557608	D 4790	27-10N	21-06W	-4702			1.06	1	12	63	

## REVIEW OF HEAT FLOW DATA

171

DATA NUMBER	STATION CODE	STATION NAME	LATI-TUDE	LONGI-TUDE	ELE./DEPTH	VT.	K	Q	NO	REF	YR
ATLANTIC OCEAN (CONTINUED)											
0367	557603	D 4794	27-10N	21-00W	-4682			1.2	1	12	63
0368	557608	D 4795	27-13N	21-05W	-4707			0.92	1	12	63
0369	557608	D 4805	29-35N	23-52W	-5240			1.13	1	12	63
0370	567608	D 4824	43-06N	19-50W	-5959			1.30	1	12	63
0371	857007	V18-151	19-51N	84-56W	-4564	0.7	2.0	1.4	1	13	64
0372	887508	V18-153	26-35N	88-49W	-2582	0.22	2.3	0.5	1	13	64
0373	557508	V18-155	26-28N	68-25W	-5284	0.55	2.0	1.1	1	13	64
0374	587508	V18-158	38-45N	67-33W	-4184	0.55	1.8	1.0	1	13	64
0375	587007	V18-159	39-11N	65-26W	-4730	0.55	2.0	1.1	1	13	64
0376	557007	V19-1	34-50N	70-15W	-4716	0.42	1.9	0.8	1	13	64
0377	557007	V19-2	32-36N	71-19W	-5392	0.63	1.9	1.2	1	13	64
0378	557508	V19-3	28-20N	68-06W	-5261	0.68	1.9	1.3	1	13	64
0379	557508	V19-4	27-28N	68-27W	-2858	0.47	1.9	0.9	1	13	64
0380	557007	V19-5	24-16N	67-11W	-5562	0.63	1.9	1.2	1	13	64
0381	857508	V19-6	16-06N	66-29W	-4520	0.6	2.0	1.2	1	13	64
0382	887007	C7-2	13-06N	63-09W	-1060	0.55	2.0	1.1	1	13	64
0383	857007	C7-3	12-34N	66-18W	-4529	0.4	2.0	0.8	1	13	64
0384	857007	C7-4	13-59N	71-43W	-3948	0.75	2.0	1.5	1	13	64
0385	887007	C7-5	12-04N	74-54W	-3611	0.5	2.0	1.0	1	13	64
0386	857007	C7-6	14-11N	76-32W	-4087	0.6	2.0	1.2	1	13	64
0387	887007	C7-9	14-50N	73-50W	-3460	0.5	2.0	1.0	1	13	64
0388	887007	C7-10	15-23N	73-17W	-3324	0.75	2.0	1.5	1	13	64
0389	887007	C7-11	16-08N	72-48W	-2893	0.55	2.0	1.1	1	13	64
0390	857007	C7-12	14-36N	70-57W	-3525	0.5	2.0	1.0	1	13	64
0391	555608	BULLARD1	49-46N	12-30W	-2032	0.426	2.59	1.10	1	15	54
0392	555608	BULLARD2	49-58N	18-33W	-4017	0.548	2.58	1.42	1	15	54
0393	555608	BULLARD3	49-09N	17-38W	-4532	0.237	2.43	0.58	1	15	54
0394	555608	BULLARD4	48-14N	16-58W	-4670	0.254	2.28	0.58	1	15	54
0395	555608	BULLARD5	48-52N	15-00W	-4710	0.455	2.64	1.20	1	15	54

## INDIAN OCEAN

0396	985508	MSN-12	9-14S	127-30E	-3300	0.81	2.09	1.69	1	1	65
0397	985508	MSN-15	7-46S	121-14E	-4840	0.84	2.02	1.7	1	1	65
0398	655508	MSN-16	11-58S	115-26E	-5010	0.63	1.77	1.12	1	1	65
0399	655508	MSN-17	12-48S	115-24E	-5400	0.64	1.65	1.05	1	1	65
0400	675508	MSN-18	10-11S	115-19E	-4330	0.24	1.63	0.39	1	1	65
0401	655508	MSN-20	13-19S	109-34E	-4630	0.80	1.85	1.48	1	1	65
0402	655508	MSN-21	11-39S	109-35E	-4605	1.00	1.87	1.87	1	1	65
0403	675508	MSN-23	8-49S	109-36E	-3300	0.26	1.88	0.48	1	1	65
0404	655508	MSN-24	12-21S	101-25E	-4745	0.78	1.99	1.56	1	1	65
0405	655508	MSN-28	16-59S	93-29E	-5230	0.61	1.63	1.0	1	1	65
0406	665508	MSN-29	18-14S	86-42E	-4455	0.89	1.83	1.63	1	1	65
0407	655508	MSN-30	15-51S	81-10E	-5000	1.01	1.71	1.73	1	1	65
0408	655508	MSN-32	14-05S	72-15E	-5200	0.77	1.55	1.20	1	1	65
0409	665508	MSN-33	14-56S	70-13E	-4460	0.07	2.06	0.14	1	1	65
0410	665508	MSN-34	16-25S	66-01E	-3660	1.40	1.99	2.78	1	1	65
0411	665907	MSN-35	16-58S	64-46E	-4055	1.10	1.99	2.19	1	1	65
0412	665508	MSN-36	17-48S	62-40E	-3740	0.15	2.26	0.34	1	1	65
0413	665508	MSN-38	26-22S	74-08E	-4130	2.48	1.98	4.91	1	1	65
0414	665508	MSN-40	33-20S	72-37E	-4220	0.42	2.19	0.91	1	1	65
0415	665508	MSN-41	37-44S	71-47E	-4260	0.66	2.08	1.38	1	1	65
0416	665508	MSN-42	42-09S	70-37E	-4200	0.80	2.08	1.67	1	1	65

DATA NUMBER	STATION CODE	STATION NAME	LATI- TUDE	LONGI- TUDE	ELE./ DEPTH	VT	K	Q	NO	REF	YR
INDIAN OCEAN (CONTINUED)											
0417	665800	MSN-43	39-50S	75-03E	-3780	-	2.0	-	1	1	65
0418	665907	MSN-44	38-26S	79-34E	-3410	0.25	2.0	0.5	1	1	65
0419	665907	MSN-45	37-50S	85-22E	-3600	0.35	2.0	0.7	1	1	65
0420	655907	MSN-46	37-18S	90-42E	-3855	0.65	2.0	1.3	1	1	65
0421	655508	MSN-47	36-19S	98-41E	-4375	0.39	1.93	0.76	1	1	65
0422	655508	MSN-48	39-18S	119-52E	-4895	0.58	1.78	1.04	1	1	65
0423	665907	MSN-49	49-31S	132-14E	-3500	0.72	1.8	1.3	1	1	65
0424	665508	Z-1	12-27N	47-07E	-1820	2.95	2.03	5.98	1	1	65
0425	665907	Z-2	12-57N	48-16E	-2205	1.68	1.92	3.62	1	1	65
0426	665508	Z-3	13-17N	49-15E	-2425	1.78	1.81	3.22	1	1	65
0427	665907	Z-4	12-54N	49-38E	-2200	1.29	1.92	2.47	1	1	65
0428	665508	Z-5	12-25N	50-33E	-2420	1.53	2.02	3.09	1	1	65
0429	665508	Z-6	9-08N	54-42E	-3705	0.79	2.11	1.66	1	1	65
0430	665907	Z-7	9-09N	57-30E	-3265	0.68	2.01	1.37	1	1	65
0431	665508	Z-8	9-16N	59-00E	-3200	0.91	1.91	1.74	1	1	65
0432	665907	Z-9	9-34N	59-52E	-3895	0.84	2.01	1.68	1	1	65
0433	665508	Z-10	9-32N	61-24E	-4580	0.45	2.10	0.95	1	1	65
0434	656900	Z-11	9-34N	63-06E	-4505	0.10	2.25	0.23	1	1	65
0435	656507	Z-12	9-40N	66-19E	-4450	0.35	2.30	0.8	1	1	65
0436	655508	Z-13	9-48N	69-15E	-4550	0.69	2.17	1.49	1	1	65
0437	665508	Z-14	9-50N	71-50E	-2370	0.58	2.21	1.29	1	1	65
0438	665508	Z-15	9-56N	73-08E	-1925	0.31	2.09	1.70	1	1	65
0439	665508	Z-16	9-59N	74-50E	-2285	0.82	1.92	1.57	1	1	65
0440	655508	LSDA-1	8-13N	70-39E	-4145	0.71	2.03	1.44	1	1	65
0441	656507	LSDA-2	3-57N	70-49E	-4130	0.84	1.91	1.6	1	1	65
0442	666507	LSDA-3	0-05S	71-50E	-4200	0.51	2.15	1.1	1	1	65
0443	666507	LSDA-4	2-40S	73-16E	-2980	0.79	2.28	1.8	1	1	65
0444	655508	LSDA-5	5-21S	75-08E	-5220	0.92	1.64	1.51	1	1	65
0445	665508	LSDA-6	5-23S	72-47E	-2530	0.84	2.28	1.92	1	1	65
0446	665508	LSDA-7	5-40S	70-17E	-3935	0.30	1.88	0.57	1	1	65
0447	665907	LSDA-8	5-52S	66-36E	-4370	0.16	1.90	0.30	1	1	65
0448	665508	LSDA-9	5-34S	63-42E	-4210	0.87	1.91	1.67	1	1	65
0449	666508	LSDA-10	5-26S	59-14E	-3980	1.19	1.97	2.35	2	1	65
A	666507	LSDA-10A	5-26S	59-14E	-3980	1.93	1.97	3.8	1	1	65
B	665508	LSDA-10B	5-25S	59-13E	-3980	0.82	1.97	1.62	1	1	65
0450	665508	LSDA-11	5-30S	57-56E	-2525	0.61	2.02	1.23	1	1	65
0451	665907	LSDA-12	9-56S	57-07E	-4045	0.76	2.03	1.55	2	1	65
A	665907	LSDA-12A	9-57S	57-07E	-4040	0.76	2.03	1.54	1	1	65
B	665907	LSDA-12B	9-56S	57-07E	-4050	0.77	2.03	1.56	1	1	65
0452	665508	LSDA-13	10-21S	58-31E	-3575	0.46	2.02	0.92	1	1	65
0453	665508	LSDA-14	10-34S	59-51E	-2315	0.71	2.04	1.44	1	1	65
0454	665508	LSDA-15	13-42S	59-42E	-3900	0.50	2.00	1.00	1	1	65
0455	665508	LSDA-16	17-20S	57-42E	-4145	0.60	2.21	1.32	1	1	65
0456	655508	LSDA-17	22-01S	57-34E	-4750	0.51	1.77	0.90	1	1	65
0457	655508	LSDA-18	24-34S	57-26E	-5000	0.77	1.57	1.21	1	1	65
0458	665508	LSDA-19	26-53S	58-12E	-5540	0.58	1.58	0.91	1	1	65
0459	665508	LSDA-20	29-53S	61-52E	-4620	0.41	1.70	0.7	1	1	65
0460	665508	LSDA-21B	31-25S	61-56E	-4420	0.24	1.73	0.42	1	1	65
0461	665508	LSDA-22	32-55S	62-25E	-4745	0.43	1.59	0.68	1	1	65
0462	656900	LSDA-23B	39-44S	63-56E	-4810	1.70	2.18	3.7	1	1	65
0463	665508	LSDA-24	44-36S	70-57E	-3580	0.79	1.89	1.49	1	1	65
0464	665508	LSDA-25	35-47S	73-37E	-4380	0.20	1.93	0.38	1	1	65
0465	665508	LSDA-26	36-52S	76-22E	-3925	0.94	2.17	2.03	1	1	65

## REVIEW OF HEAT FLOW DATA

173

DATA NUMBER	CODE	STATION NAME	LATI-TUDE	LONGI-TUDE	ELE./DEPTH	$\nabla T$	K	Q	NO	REF	YR
INDIAN OCEAN (CONTINUED)											
0466	685508	LSDA-30	31-28S	114-24E	-3740	0.52	2.04	1.05	2	1	65
	A	685508	LSDA-30A	31-29S	114-25E	-3730	0.43	2.04	0.88	1	1 65
	B	685508	LSDA-30B	31-27S	114-24E	-3750	0.60	2.04	1.22	1	1 65
0467	655907	LSDA-32	29-42S	111-30E	-5340	0.82	2.18	1.79	1	1	65
0468	655508	LSDA-33	25-03S	104-12E	-5100	0.71	1.63	1.15	1	1	65
0469	665508	LSDA-34	16-25S	89-19E	-5625	0.85	1.64	1.39	1	1	65
0470	655508	LSDA-35	13-48S	90-50E	-5200	0.82	1.59	1.30	1	1	65
0471	656507	LSDA-36	13-09S	93-13E	-5230	1.83	1.64	3.0	1	1	65
0472	655508	LSDA-37	14-56S	108-09E	-5580	0.68	1.70	1.15	1	1	65
0473	655508	LSDA-38	13-46S	115-32E	-5680	0.69	1.65	1.14	1	1	65
0474	655508	LSDA-39	13-31S	118-29E	-5680	0.57	1.64	0.93	1	1	65
0475	655508	LSDA-50	30-08S	37-47E	-4990	0.51	1.97	1.00	1	1	65
0476	685907	LSDA-51	31-04S	36-40E	-4535	0.98	2.26	2.22	1	1	65
0477	685508	LSDA-52	31-39S	35-57E	-2545	0.34	2.40	0.82	1	1	65
0478	685907	LSDA-53	32-14S	34-16E	-2660	0.63	2.30	1.45	1	1	65
0479	685508	LSDA-54	32-22S	32-47E	-3560	0.02	2.12	0.04	1	1	65
0480	665508	LSDH-1	9-07N	72-59E	-2135	0.77	2.08	1.61	1	1	65
0481	665508	LSDH-2	9-03N	73-10E	-2110	0.57	2.08	1.18	1	1	65
0482	656507	LSDH-3	7-24N	70-40E	-4110	0.66	2.19	1.44	1	1	65
0483	665508	LSDH-4	5-22S	74-17E	-4780	1.15	1.64	1.88	1	1	65
0484	665508	LSDH-5	5-40S	69-40E	-3815	0.00	2.00	0.00	1	1	65
0485	665508	LSDH-6	5-53S	65-57E	-4260	0.61	1.90	1.16	1	1	65
0486	665907	LSDH-7	5-31S	63-04E	-4255	1.16	1.94	2.26	1	1	65
0487	655907	LSDH-8	5-28S	60-02E	-4100	0.78	1.97	1.54	1	1	65
0488	666507	LSDH-9	5-26S	59-29E	-3952	1.96	2.02	3.95	2	1	65
	A	666507	LSDH-9A	5-26S	59-29E	-3945	2.28	2.02	4.6	1	1 65
	B	666507	LSDH-9B	5-26S	59-29E	-3960	1.63	2.02	3.3	1	1 65
0489	666507	LSDH-11	4-10S	57-15E	-3765	0.94	2.03	1.9	1	1	65
0490	665508	LSDH-13	9-49S	56-28E	-3885	0.13	2.03	0.27	1	1	65
0491	665907	LSDH-14	10-05S	57-53E	-3935	0.64	2.02	1.29	1	1	65
0492	665508	LSDH-15	10-30S	59-23E	-2858	0.66	1.94	1.28	2	1	65
	A	665508	LSDH-15A	10-30S	59-23E	-2870	0.63	1.94	1.22	1	1 65
	B	665508	LSDH-15B	10-30S	59-23E	-2845	0.69	1.94	1.34	1	1 65
0493	665508	LSDH-18	31-14S	62-58E	-5062	0.14	1.60	0.22	2	1	65
	A	665508	LSDH-18A	31-14S	62-57E	-5065	0.15	1.60	0.24	1	1 65
	B	665508	LSDH-18B	31-14S	62-58E	-5060	0.12	1.60	0.19	1	1 65
0494	665508	LSDH-20	33-16S	61-43E	-4695	1.13	1.56	1.77	1	1	65
0495	655508	LSDH-21	39-54S	67-53E	-4065	0.00	2.18	0.00	1	1	65
0496	665508	LSDH-22	40-47S	72-46E	-4000	0.17	2.30	0.40	1	1	65
0497	665508	LSDH-23	40-58S	75-08E	-4030	0.25	2.16	0.54	1	1	65
0498	665508	LSDH-24	40-19S	76-32E	-3020	0.94	2.25	2.12	1	1	65
0499	665907	LSDH-25	36-05S	75-59E	-3290	0.80	2.17	1.74	1	1	65
0500	665508	LSDH-26	37-21S	76-35E	-3380	0.44	2.10	0.92	1	1	65
0501	665907	LSDH-27	32-58S	96-02E	-4030	0.01	2.1	0.01	1	1	65
0502	666507	LSDH-28	32-06S	100-20E	-2450	1.22	2.37	2.9	1	1	65
0503	655508	LSDH-29	32-45S	102-45E	-4760	0.54	1.71	0.93	1	1	65
0504	655508	LSDH-30	32-59S	103-33E	-5130	0.73	1.70	1.27	1	1	65
0505	656900	LSDH-32	33-01S	111-11E	-4390	2.34	2.26	5.3	1	1	65
0506	655508	LSDH-33	32-17S	113-58E	-4190	0.44	2.26	0.99	1	1	65
0507	656507	LSDH-34	29-16S	110-42E	-5550	0.92	2.18	2.0	1	1	65
0508	655907	LSDH-35	25-40S	105-22E	-4830	0.69	1.63	1.13	1	1	65
0509	655907	LSDH-36	24-33S	103-39E	-5400	0.64	1.63	1.04	1	1	65
0510	655508	LSDH-37	20-11S	96-22E	-4910	0.66	1.59	1.05	1	1	65

DATA NUMBER	STATION CODE	STATION NAME	LATI- TUDE	LONGI- TUDE	ELE./ DEPTH	$\bar{v}$	K	Q	NO	REF
INDIAN OCEAN (CONTINUED)										
0511	655508	LSDH-38	14-12S	89-50E	-5315	0.66	1.63	1.07	1	1 65
0512	655907	LSDH-39	13-39S	91-31E	-5150	0.93	1.59	1.48	1	1 65
0513	655508	LSDH-40	13-23S	92-32E	-5200	1.85	1.73	3.20	1	1 65
0514	655508	LSDH-43	14-06S	101-22E	-5110	1.11	1.63	1.81	1	1 65
0515	655508	LSDH-44	14-56S	107-16E	-5805	0.79	1.74	1.37	1	1 65
0516	655907	LSDH-45	14-58S	109-12E	-5630	0.65	1.74	1.13	1	1 65
0517	655508	LSDH-46	14-13S	114-54E	-5670	0.63	1.62	1.02	1	1 65
0518	655508	LSDH-47	13-09S	116-29E	-5670	0.69	1.60	1.11	1	1 65
0519	655907	LSDH-48	13-41S	117-23E	-5715	0.58	1.62	0.94	1	1 65
0520	657508	V18-54	36-55S	23-24E	-5064	0.63	2.42	1.53	1	1 65
0521	657508	V18-55	38-59S	29-56E	-4202	0.62	2.52	1.57	1	1 65
0522	657508	V18-58	31-12S	48-05E	-4395	0.74	2.23	1.65	1	1 65
0523	657508	V18-59	26-42S	50-28E	-5266	1.08	1.68	1.81	1	1 65
0524	657508	V18-60	23-59S	51-11E	-4928	0.87	1.92	1.67	1	1 65
0525	657508	V18-61	21-26S	51-37E	-4959	0.73	1.99	1.46	1	1 65
0526	667508	V18-63	20-35S	63-32E	-3296	0.16	2.67	0.43	1	1 65
0527	657501	V18-67	25-29S	85-09E	-4559	0.96	2.74	2.64	1	1 65
0528	657508	V18-69	25-47S	93-43E	-4435	0.74	1.75	1.30	1	1 65
0529	657508	V18-70	25-46S	95-58E	-4937	0.75	1.81	1.35	1	1 65
0530	657508	V18-71	25-41S	99-04E	-5365	0.68	1.76	1.20	1	1 65
0531	657507	V18-72	25-41S	101-56E	-4720	0.85	1.82	1.54	1	1 65
0532	657508	V18-73	27-59S	108-40E	-5148	0.63	2.00	1.26	1	1 65
0533	657508	V18-74	36-07S	118-47E	-4590	0.47	2.19	1.02	1	1 65
0534	657501	V18-76	37-27S	133-40E	-5570	0.52	2.22	1.15	1	1 65
0535	677508	V19-54	7-43S	103-15E	-6411	0.96	2.03	1.95	1	1 65
0536	677508	V19-55	7-16S	102-02E	-5663	0.91	1.89	1.72	1	1 65
0537	657508	V19-57	14-31S	101-21E	-5363	0.71	1.69	1.20	1	1 65
0538	657508	V19-58	16-20S	100-33E	-5906	0.60	1.86	1.12	1	1 65
0539	657508	V19-59	18-11S	99-24E	-5754	0.70	1.81	1.26	1	1 65
0540	657508	V19-60	19-02S	97-15E	-5500	0.89	1.91	1.70	1	1 65
0541	657508	V19-61	20-56S	91-12E	-4840	0.83	1.87	1.55	1	1 65
0542	657508	V19-64	18-23S	82-08E	-5224	0.85	1.63	1.38	1	1 65
0543	657508	V19-65	16-11S	82-06E	-5380	0.37	1.77	0.66	1	1 65
0544	657508	V19-66	14-11S	82-08E	-4798	0.74	1.84	1.36	1	1 65
0545	657503	V19-67	12-44S	82-01E	-	1.20	1.68	2.02	1	1 65
0546	657507	V19-68	10-13S	81-37E	-5107	0.97	1.63	1.58	1	1 65
0547	657508	V19-69	7-54S	81-25E	-5229	0.58	1.76	1.02	1	1 65
0548	657507	V19-70	7-04S	80-46E	-5045	0.77	1.79	1.38	1	1 65
0549	687507	V19-72	7-07N	76-33E	-1770	0.49	2.22	1.09	1	1 65
0550	667508	V19-73	7-35N	74-13E	-2769	0.80	2.15	1.72	1	1 65
0551	667507	V19-74	8-07N	73-15E	-2186	0.71	2.32	1.65	1	1 65
0552	657508	V19-75	8-09N	70-38E	-4128	0.76	2.36	1.80	1	1 65
0553	657508	V19-76	8-09N	69-15E	-4650	0.90	2.11	1.90	1	1 65
0554	667508	V19-78	8-07N	62-47E	-4325	0.49	2.32	1.13	1	1 65
0555	667508	V19-79	7-26N	61-04E	-3605	1.19	2.50	2.98	1	1 65
0556	667507	V19-80	6-42N	59-20E	-2857	0.28	2.30	0.64	1	1 65
0557	667508	V19-82	7-04N	60-55E	-2680	0.61	2.02	1.23	1	1 65
0558	667507	V19-83	6-52N	60-42E	-3356	0.25	2.41	0.61	1	1 65
0559	667508	V19-84	6-37N	59-48E	-2923	0.91	2.33	2.12	1	1 65
0560	667507	V19-85	6-10N	57-10E	-4128	0.50	2.31	1.16	1	1 65
0561	657508	V19-87	4-43N	52-05E	-5111	0.54	1.96	1.05	1	1 65
0562	657508	V19-88	2-29N	51-28E	-5095	0.63	1.78	1.12	1	1 65
0563	657508	V19-89	0-29S	53-41E	-4857	0.93	1.92	1.78	1	1 65

## REVIEW OF HEAT FLOW DATA

175

DATA NUMBER	CODE	STATION NAME	LATI- TUDE	LONGI- TUDE	ELE./ DEPTH	VT	K	Q	NO	REF	YR
INDIAN OCEAN (CONTINUED)											
0564	657508	V19-90	2-40S	54-45E	-4186	0.74	2.30	1.71	1	1	65
0565	657908	V19-91	3-34S	51-51E	-5056	0.88	1.89	1.66	1	1	65
0566	657503	V19-92	3-24S	48-46E	-4987	0.58	1.99	1.15	1	1	65
0567	657508	V19-93	3-11S	45-49E	-4607	0.61	1.90	1.15	1	1	65
0568	657508	V19-94	3-43S	43-52E	-4089	0.56	2.32	1.30	1	1	65
0569	687508	V19-95	4-13S	41-33E	-2722	0.52	2.44	1.27	1	1	65
0570	687508	V19-96	5-20S	40-26E	-1863	0.74	2.34	1.72	1	1	65
0571	687508	V19-97	6-59S	41-11E	-3369	0.62	2.39	1.48	1	1	65
0572	687508	V19-98	9-28S	43-19E	-3643	0.69	2.18	1.50	1	1	65
0573	687508	V19-100	13-08S	44-09E	-3548	0.65	2.10	1.37	1	1	65
0574	657508	V19-101	14-53S	42-51E	-3250	0.58	2.30	1.33	1	1	65
0575	667507	V19-102	16-56S	41-06E	-2548	0.29	2.51	0.72	1	1	65
0576	687507	V19-103	17-54S	39-30E	-2314	0.50	2.23	1.12	1	1	65
0577	687507	V19-106	22-57S	42-10E	-3175	0.64	2.18	1.40	1	1	65
0578	687500	V19-107	22-58S	41-22E	-3885	-	-	-	1	1	65
0579	687508	V19-108	23-11S	39-58E	-3345	0.70	2.19	1.54	1	1	65
0580	687508	V19-109	23-22S	38-51E	-3087	0.61	2.36	1.44	1	1	65
0581	687508	V19-110	23-31S	37-51E	-2903	0.80	1.99	1.60	1	1	65
0582	687508	V19-111	25-20S	36-47E	-2203	0.56	2.34	1.32	1	1	65
0583	657508	V19-112	31-42S	38-10E	-5018	0.59	2.03	1.20	1	1	65
0584	687503	V19-114	34-24S	31-25E	-4124	0.67	2.23	1.50	1	1	65
0585	687508	V19-115	35-30S	29-57E	-4565	0.53	2.49	1.32	1	1	65
0586	687507	V19-116	35-55S	27-45E	-4656	0.63	2.67	1.68	1	1	65
0587	687608	AND-1	10-01N	93-45E	-4206	3.1	1.70	5.27	1	2	64
0588	687608	AND-2	11-01N	93-42E	-2562	1.3	1.83	2.38	1	2	64
0589	687608	AND-3	11-56N	93-22E	-1390	0.5	1.79	0.90	1	2	64
0590	687608	AND-4	12-44N	93-58E	-2151	1.1	1.76	1.94	1	2	64
0591	667607	DIS 5116	5-35N	61-57E	-3560	.663	2.02	1.34	1	88	65
0592	667608	DIS 5122	5-35N	61-56E	-3560	.642	2.01	1.29	1	88	65
0593	667608	DIS 5125	2-45N	60-15E	-4806	.265	1.70	0.45	1	88	65
0594	667608	DIS 5135	2-55N	59-53E	-4697	.412	1.77	0.73	1	88	65
0595	657608	DIS 5139	1-54N	56-10E	-4812	.728	1.73	1.26	1	88	65
0596	687607	DIS 5144	1-41S	42-13E	-2255	.700	2.00	1.40	1	88	65
0597	687608	DIS 5149	2-24S	43-24E	-3552	.643	1.96	1.26	1	88	65
0598	657608	DIS 5152	2-32S	44-56E	-4160	.618	1.86	1.15	1	88	65
0599	657608	DIS 5155	2-48S	47-03E	-4812	.610	1.77	1.08	1	88	65
0600	657608	DIS 5160	3-30S	49-40E	-5042	.723	1.77	1.28	1	88	65
0601	657608	DIS 5165	3-33S	51-29E	-5100	.418	1.70	0.71	1	88	65
0602	667600	DIS 5171	2-10S	57-25E	-4402	.221	2.26	0.50	1	88	65
0603	667608	DIS 5177	2-12S	57-20E	-4402	.519	2.12	1.10	1	88	65
0604	657608	DIS 5180	6-39S	54-16E	-3824	.748	2.06	1.54	1	88	65
0605	657608	DIS 5190	2-51S	47-00E	-4800	.659	1.82	1.20	1	88	65
0606	657608	DIS 5194	2-34S	44-53E	-4180	.597	1.91	1.14	1	88	65
0607	687607	DIS 5201	1-42S	42-15E	-2046	.613	2.04	1.25	1	88	65
0608	657607	DIS 5204	3-31S	48-23E	-4940	.761	1.80	1.37	1	88	65
0609	657608	DIS 5207	3-34S	50-29E	-5082	.710	1.83	1.30	1	88	65
0610	657907	DIS 5215	2-25S	54-45E	-4360	.750	2.00	1.50	1	88	65
0611	667608	DIS 5226	11-07N	54-03E	-4028	.745	2.09	1.55	1	88	65
0612	667608	DIS 5227	11-39N	47-50E	-1900	1.80	2.14	3.85	1	88	65
0613	667608	DIS 5229	12-29N	47-02E	-2197	2.69	2.29	6.15	1	88	65
0614	667608	DIS 5230	12-56N	46-36E	-1600	1.50	2.16	3.25	1	88	65
0615	887608	DIS 5231	15-58N	41-31E	-1735	1.81	2.31	4.18	1	88	65
0616	887608	DIS 5232	18-24N	39-47E	-1480	.404	2.62	1.06	1	88	65
0617	887600	DIS 5234	20-27N	37-55E	-0870		2.75	+	1	88	65

DATA NUMBER	CODE	STATION NAME	LATI-TUDE	LONGI-TUDE	ELE./DEPTH	VT	K	Q	NO	REF	YR
PACIFIC OCEAN											
0618	785108	E1	38-09N	142-58E	-1710	.130	2.10	0.27	1	34	62
0619	775108	E2	37-59N	143-58E	-7345	.542	2.11	1.14	1	34	62
0620	755108	E6	38-12N	147-55E	-5631	1.05	1.95	2.05	1	34	62
0621	755007	F20	33-39N	161-39E	-5605	.681	2.00	1.36	1	18	64
0622	775108	F23	34-23N	142-15E	-7490	.630	2.21	1.39	1	18	64
0623	776107	F24	34-04N	142-56E	-5110	.598	2.07	1.24	1	18	64
0624	756107	F25	33-53N	145-26E	-5770	.549	1.81	0.99	1	18	64
0625	756107	AKK0 7	39-22N	150-03E	-5480	1.74	1.90	3.30	1	18	64
0626	785503	AKK0 8	39-30N	143-28E	-2800	.546	2.16	1.18	1	18	64
0627	786507	MYJ 1	34-32N	139-46E	-1710	.574	2.54	1.46	1	18	64
0628	755508	AKK0 11	29-53N	137-56E	-3960	.397	2.06	0.82	1	18	64
0629	756507	AKK0 12	32-35N	138-06E	-3970	1.20	2.42	2.88	1	18	64
0630	786507	G1	40-02N	142-31E	-810	.702	1.75	1.26	1	18	64
0631	775808	G12	43-26N	148-15E	-5175	.407	1.53	0.62	1	18	64
0632	786500	G202	40-28N	142-59E	-1550	.464	2.16	1.00	1	18	64
0633	775508	G*2	39-42N	145-25E	-5315	.610	1.82	1.11	1	18	64
0634	755508	G*5	40-24N	145-40E	-5215	.344	1.67	0.58	1	18	64
0635	776507	G*10	41-52N	145-09E	-4435	.356	1.80	0.64	1	18	64
0636	775508	G*11	41-02N	146-00E	-5495	.568	2.44	1.38	1	18	64
0637	755500	AKK0 M1	38-11N	133-45E	-0970	1.08	1.98	2.13	1	86	65
0638	955508	AKK0 M2	40-47N	132-04E	-3080	0.35	1.78	0.63	1	86	65
0639	955508	AKK0 M3	40-48N	134-24E	-3400	1.30	1.79	2.33	1	86	65
0640	955508	AKK0 M4	38-01N	135-57E	-2550	1.39	1.75	2.44	1	86	65
0641	955508	AKK0 M5	40-13N	136-52E	-2525	0.80	1.70	1.40	1	86	65
0642	955508	AKK0 M6	40-59N	137-24E	-3422	0.96	2.08	1.98	1	86	65
0643	955508	AKK0 M7	40-23N	139-11E	-2670	1.18	1.95	2.02	1	86	65
0644	955508	AKK0 M8	39-29N	137-59E	-2508	0.72	1.81	1.30	1	86	65
0645	985500	EN 1	39-00N	139-10E	-0720	0.83	1.67	1.4	1	86	65
0646	985500	EN 2	38-32N	139-10E	-0320	0.26	1.82	0.5	1	86	65
0647	755508	H 11	39-50N	153-52E	-5560	0.50	1.74	0.88	1	86	65
0648	755508	H 12	40-05N	152-01E	-5475	0.51	1.68	0.86	1	86	65
0649	776507	H 14A	40-02N	146-02E	-5150	0.59	1.59	0.94	1	86	65
0650	955507	MAKKO 1	37-21N	134-07E	-2440	1.45	1.83	2.66	1	86	65
0651	955507	MAKKO 2	39-10N	133-02E	-2720	1.18	1.57	1.84	1	86	65
0652	955507	SAIKO 3	40-01N	132-29E	-3330	1.36	1.65	2.24	1	86	65
0653	955507	SAIKO 4	41-01N	131-54E	-3470	1.34	1.59	2.13	1	86	65
0654	956507	SAIKO 5	41-20N	132-48E	-3600	1.21	1.56	1.89	1	86	65
0655	955507	MAKKO 3	41-34N	133-35E	-3650	1.29	1.56	2.08	1	86	65
0656	955500	MAKKO 4	39-55N	134-50E	-1450	1.09	1.65	1.80	1	86	65
0657	955507	MAKKO 5	38-58N	135-25E	-3180	1.23	1.69	2.08	1	86	65
0658	955507	MAKKO 6	38-02N	135-57E	-2740	1.35	1.65	2.23	1	86	65
0659	985500	MAKKO 7	38-13N	137-52E	-1970	1.25	1.80	2.25	1	86	65
0660	955507	MAKKO 8	39-13N	132-25E	-2340	1.06	1.96	2.07	1	86	65
0661	955507	MAKKO 9	40-08N	136-44E	-2650	1.47	1.78	2.62	1	86	65
0662	955507	MAKKO 10	41-03N	136-06E	-3450	1.25	1.55	1.95	1	86	65
0663	955507	MAKKO 11	42-00N	138-10E	-3670	1.33	1.88	2.51	1	86	65
0664	955500	MAKKO 12	41-59N	139-23E	-1480	1.41	1.92	2.70	1	86	65
0665	985500	MAKKO 13	43-32N	140-20E	-0700	1.15	1.62	1.87	1	86	65
0666	985500	MAKKO 14	43-59N	139-20E	-1710	1.22	1.80	2.19	1	86	65
0667	955507	MAKKO 15	44-31N	138-26E	-2430	1.13	1.72	1.94	1	86	65
0668	985500	MAKKO 16	44-59N	137-29E	-1630	1.34	1.73	2.32	1	86	65
0669	986507	MAKKO 17	45-00N	138-36E	-2150	0.45	1.80	0.79	1	86	65
0670	985500	MAKKO 18	45-02N	139-37E	-0885	1.00	1.92	1.92	1	86	65

## REVIEW OF HEAT FLOW DATA

177

DATA NUMBER	CODE	STATION NAME	LATI- TUDE	LONGI- TUDE	ELE./ DEPTH	VT	K	Q	NO	REF	YR
PACIFIC OCEAN (CONTINUED)											
0671	986500	MAKKO 19	45-05N	140-44E	-0330	1.31	2.04	2.66	1	86	65
1140	766502	TOKKO-1	31-58N	140-29E	-	1.58	2.10	3.2	1	86	65
1141	766507	TOKKO-3	33-44N	139-34E	-	1.54	1.60	2.46	1	86	65
1142	765507	TOKKO-4	33-55N	139-14E	-	1.12	1.60	1.79	1	86	65
0672	785508	MEN-2A	33-45N	119-31W	-1900	0.72	2.00	1.43	1	19	64
0673	785508	MEN-3	33-58N	122-34W	-4200	0.30	1.89	0.57	1	19	64
0674	785508	MEN-4	34-02N	125-15W	-4640	0.60	1.81	1.08	1	19	64
0675	785508	MEN-5	36-04N	125-04W	-4450	0.50	1.87	0.94	1	19	64
0676	785508	MEN-6	38-25N	126-09W	-4230	1.70	2.03	3.45	1	19	64
0677	785508	MEN-7	39-47N	126-21W	-4140	0.96	2.04	1.96	1	19	64
0678	786507	MEN-8	40-33N	126-31W	-3150	1.89	2.06	3.9	1	19	64
0679	785508	MEN-9	40-56N	126-31W	-3120	2.35	1.96	4.60	1	19	64
0680	785508	MEN-10	41-30N	126-32W	-2960	3.06	1.89	5.79	1	19	64
0681	785508	MEN-11	40-36N	127-25W	-3280	2.84	1.96	5.56	1	19	64
0682	785508	MEN-12	40-07N	128-10W	-4510	0.98	1.92	1.88	1	19	64
0683	785508	MEN-13	40-40N	129-13W	-3220	2.01	2.05	4.12	1	19	64
0684	785508	MEN-14	40-00N	131-00W	-4520	0.60	1.90	1.14	1	19	64
0685	785508	MEN-15	42-02N	133-07W	-3870	0.40	1.87	0.75	1	19	64
0686	785508	MEN-16	40-25N	133-06W	-4070	0.36	2.00	0.72	1	19	64
0687	785508	MEN-17	39-30N	133-05W	-4750	0.17	2.07	0.35	1	19	64
0688	785508	MEN-18	41-06N	135-32W	-4060	0.48	2.08	1.00	1	19	64
0689	785508	MEN-19	41-07N	151-22W	-5100	0.91	2.03	1.84	1	19	64
0690	785508	MEN-20	39-21N	149-56W	-5500	0.19	2.04	0.39	1	19	64
0691	785508	MEN-21	40-38N	149-01W	-4840	0.91	2.07	1.88	1	19	64
0692	785508	MEN-22	40-47N	146-00W	-4720	0.50	2.11	1.05	1	19	64
0693	785508	MEN-23	40-41N	142-52W	-4730	0.61	1.96	1.19	1	19	64
0694	785508	MEN-24	40-44N	139-22W	-4520	0.91	2.06	1.88	1	19	64
0695	785508	MEN-26	38-40N	142-36W	-5290	0.63	2.02	1.27	1	19	64
0696	785508	MEN-27	39-05N	139-26W	-5290	0.87	2.05	1.78	1	19	64
0697	785508	MEN-28	38-02N	137-58W	-5380	0.86	1.97	1.69	1	19	64
0698	785907	MEN-29	39-33N	135-59W	-5140	0.49	2.00	0.98	1	19	64
0699	785508	MEN-30	38-00N	134-00W	-4810	0.85	2.02	1.72	1	19	64
0700	785508	MEN-31	39-32N	133-05W	-4740	0.05	2.07	0.10	1	19	64
0701	785508	MEN-33	39-30N	131-47W	-4510	0.23	2.02	0.46	1	19	64
0702	785508	MEN-34	40-44N	131-45W	-3640	0.49	1.95	0.95	1	19	64
0703	785907	MEN-36	39-36N	129-31W	-4540	0.59	1.90	1.12	1	19	64
0704	785907	MEN-37	38-01N	128-46W	-4750	0.83	2.03	1.68	1	19	64
0705	785508	MEN-38	32-36N	118-06W	-2010	0.99	1.97	1.96	1	19	64
0706	785508	MEN-39	32-32N	117-31W	-1240	1.1	1.83	2.03	1	19	64
0707	785907	GU-1	32-32N	117-31W	-1230	1.41	1.83	2.58	1	19	64
0708	785508	GU-2	32-29N	118-03W	-1890	1.47	1.89	2.78	1	19	64
0709	785508	GU-3	32-14N	118-27W	-1630	0.95	1.88	1.78	1	19	64
0710	785508	GU-4	32-03N	118-50W	-1480	0.95	1.99	1.89	1	19	64
0711	785508	GU-5	31-50N	119-06W	-1690	1.15	1.88	2.16	1	19	64
0712	785508	GU-6	31-37N	119-35W	-3720	0.44	1.93	0.84	1	19	64
0713	785508	GU-7	31-26N	120-04W	-3970	0.89	1.87	1.66	1	19	64
0714	785508	GU-8	31-14N	120-32W	-3840	0.87	1.88	1.64	1	19	64
0715	785508	GU-9B	31-01N	120-55W	-3970	1.30	1.98	2.58	1	19	64
0716	785508	GU-10	30-48N	121-31W	-4100	1.20	2.02	2.42	1	19	64
0717	785508	GU-11	29-03N	121-04W	-4160	0.15	2.10	0.31	1	19	64
0718	785508	GU-12	29-09N	120-35W	-3910	0.83	1.97	1.64	1	19	64
0719	785508	GU-13	29-16N	120-04W	-3830	2.30	1.93	4.43	1	19	64
0720	785508	GU-14	29-22N	119-35W	-3710	1.20	1.99	2.39	1	19	64

DATA NUMBER	STATION CODE	STATION NAME	LATI- TUDE	LONGI- TUDE	ELE./ DEPTH	VT	K	Q	NO	REF	YR	
PACIFIC OCEAN (CONTINUED)												
0721	785508	GU-15B	29-35N	118-56W	-3800	0.81	2.02	1.64	1	19	64	
0722	785508	GU-16	29-37N	118-27W	-3570	0.19	2.06	0.39	1	19	64	
0723	785508	GU-17	29-33N	117-59W	-3580	1.29	2.02	2.61	1	19	64	
0724	785508	GU-18	28-59N	117-28W	-3542	1.48	1.94	2.87	6	19	64	
	A	785508	GU-18A	28-59N	117-28W	-3570	1.37	1.94	2.66	1	19	64
	B	785508	GU-18B	28-59N	117-28W	-3570	1.31	1.94	2.55	1	19	64
	C	785508	GU-18C	28-59N	117-28W	-3570	1.43	1.94	2.77	1	19	64
	D	785508	GU-18D	28-59N	117-28W	-3570	1.35	1.94	2.62	1	19	64
	E	785508	GU-18E	28-59N	117-28W	-3530	1.27	1.94	2.46	1	19	64
	F	785508	GU-18F	28-59N	117-28W	-3440	2.14	1.94	4.15	1	19	64
0725	785907	GU-19	28-52N	117-26W	-3550	2.11	1.94	4.09	1	19	64	
0726	785907	GU-20	28-58N	117-21W	-3550	0.92	1.94	1.79	1	19	64	
0727	785907	GU-21	29-06N	117-28W	-3620	0.97	1.94	1.89	1	19	64	
0728	785508	GU-22	29-54N	117-36W	-2840	1.12	2.03	2.34	1	19	64	
0729	785508	SB-1	31-16N	117-45W	-1930	1.06	2.12	2.25	1	19	64	
0730	785508	SB-2	31-15N	117-46W	-1950	1.58	2.12	3.35	1	19	64	
0731	785508	SB-3	30-54N	117-53W	-2050	0.92	2.03	1.87	1	19	64	
0732	785508	SB-4	30-53N	117-53W	-2040	0.98	2.03	1.99	1	19	64	
0733	785508	SB-5	30-18N	117-31W	-3250	1.42	2.04	2.90	1	19	64	
0734	785508	SB-6A	29-18N	117-29W	-3950	1.58	2.03	3.20	1	19	64	
0735	785508	SB-8	28-57N	117-31W	-3480	1.14	2.07	2.37	1	19	64	
0736	785508	SB-9	29-09N	116-43W	-4060	1.29	2.08	2.69	1	19	64	
0737	785508	SB-10	29-08N	116-42W	-4070	1.33	2.08	2.77	1	19	64	
0738	785508	SB-11	30-30N	116-30W	-2840	1.50	2.04	3.07	1	19	64	
0739	785508	SB-12	30-31N	116-33W	-2840	1.39	2.04	2.84	1	19	64	
0740	785508	H-1	31-27N	120-59W	-3835	0.53	1.89	1.01	1	19	64	
0741	785907	H-2	29-41N	121-36W	-4000	0.96	1.95	1.88	1	19	64	
0742	785907	T-1	32-35N	117-31W	-1225	1.12	1.83	2.05	1	19	64	
0743	785907	T-2	32-33N	117-31W	-1220	1.08	1.83	1.98	1	19	64	
0744	785508	EHF-1	31-11N	119-16W	-3690	0.63	2.04	1.28	1	19	64	
0745	788508	MOHOLE	28-59N	117-30W	-3570	1.38	2.04	2.81	1	20	64	
0746	765508	V-1	27-08N	111-38W	-1840	1.58	1.77	2.80	1	21	63	
0747	765508	V-2	27-17N	111-22W	-1870	1.78	1.65	2.94	1	21	63	
0748	765508	V-3	27-38N	111-44W	-1775	2.55	1.64	4.19	1	21	63	
0749	765508	V-4	26-46N	111-04W	-1750	1.68	1.75	2.95	1	21	63	
0750	765508	V-5	24-09N	108-55W	-3020	2.13	1.99	4.24	1	21	63	
0751	765508	V-6	22-58N	108-04W	-2900	0.34	1.81	0.62	1	21	63	
0752	765508	V-7	21-59N	107-41W	-3055	2.96	1.86	5.51	1	21	63	
0753	765508	V-8	21-00N	107-04W	-3300	2.11	1.89	3.98	1	21	63	
0754	765508	V-9	20-55N	106-25W	-4450	1.07	2.00	2.14	1	21	63	
0755	765508	V-10	20-10N	107-43W	-3290	0.71	1.76	1.25	1	21	63	
0756	765508	V-11	19-45N	108-28W	-2600	.79	1.82	1.43	1	21	63	
0757	765508	V-12	20-48N	109-34W	-2910	1.33	1.81	2.40	1	21	63	
0758	765508	V-13	22-33N	109-29W	-2860	2.96	2.08	6.15	1	21	63	
0759	755508	D-1	1-23S	131-31W	-4450	0.06	2.29	0.14	1	22	59	
0760	755508	D-2	14-59S	136-01W	-4510	0.35	1.86	0.65	1	22	59	
0761	755508	D-3	21-40S	147-41W	-4760	0.56	1.74	0.97	1	22	59	
0762	765508	D-4	40-37S	132-52W	-5120	0.61	1.80	1.1	1	22	59	
0763	765508	D-5	42-16S	125-50W	-4620	0.08	1.71	0.14	1	22	59	
0764	765508	D-6	46-44S	123-18W	-4140	0.35	2.09	0.73	1	22	59	
0765	765508	D-7	44-27S	110-44W	-3180	0.92	2.24	2.06	1	22	59	
0766	765508	D-8	43-43S	107-33W	-3180	1.34	2.28	3.06	1	22	59	
0767	765508	D-9	43-44S	104-25W	-3850	1.03	2.03	2.09	1	22	59	

REVIEW OF HEAT FLOW DATA

179

DATA NUMBER	CODE	STATION NAME	LATI-TUDE	LONGI-TUDE	ELE./DEPTH	∇T	K	Q	NO	REF	YR
PACIFIC OCEAN (CONTINUED)											
0768	765508	D-10	42-44S	96-03W	-4580	1.48	1.55	2.30	1	22	59
0769	765508	D-11	41-06S	86-38W	-3310	0.51	2.0	1.0	1	22	59
0770	755501	D-12	23-23S	72-10W	-4110	0.49	1.82	0.89	1	22	59
0771	755508	D-13	23-28S	72-58W	-3750	0.41	1.96	0.80	1	22	59
0772	755508	D-14	21-33S	79-09W	-4550	0.89	1.82	1.62	1	22	59
0773	765508	D-15	20-49S	81-08W	-2340	0.35	2.26	0.79	1	22	59
0774	765508	D-16	20-48S	81-09W	-2400	0.68	2.26	1.54	1	22	59
0775	755508	D-17	13-35S	79-09W	-4440	0.79	1.84	1.46	1	22	59
0776	785508	D-18	12-49S	77-53W	-2260	1.35	2.02	2.72	1	22	59
0777	785508	D-19	12-54S	78-06W	-3700	0.56	1.91	1.07	1	22	59
0778	775508	D-20	12-38S	78-38W	-5950	0.08	2.09	0.17	1	22	59
0779	775508	D-21	12-59S	78-21W	-5900	0.08	1.94	0.17	1	22	59
0780	765508	D-22	18-26S	78-16W	-4220	0.14	1.86	0.26	1	22	59
0781	765508	D-23	18-20S	79-21W	-3090	0.46	2.14	0.98	1	22	59
0782	755508	D-24	19-01S	81-29W	-4230	0.55	1.86	1.02	1	22	59
0783	765508	D-25	27-04S	88-53W	-3880	1.04	2.04	2.12	1	22	59
0784	765508	D-26	28-00S	96-20W	-3200	0.10	2.25	0.23	1	22	59
0785	765508	D-27	27-55S	106-57W	-2910	2.10	2.16	4.54	1	22	59
0786	765503	D-28	23-15S	117-48W	-3500	0.92	1.90	1.76	1	22	59
0787	765508	D-29	14-44S	112-06W	-3060	3.45	2.22	7.66	1	22	59
0788	765508	D-30	13-30S	108-31W	-3580	0.43	2.34	1.01	1	22	59
0789	765508	D-31	11-39S	109-48W	-3280	3.61	2.24	8.09	1	22	59
0790	765508	D-32	9-55S	110-39W	-2840	3.90	2.04	7.95	1	22	59
0791	755508	D-33	5-56S	112-29W	-4040	0.44	2.00	0.87	1	22	59
0792	755508	D-34	3-40S	114-13W	-4330	0.94	1.82	1.71	1	22	59
0793	755508	D-35	1-28N	116-04W	-3810	0.28	1.97	0.56	1	22	59
0794	765508	D-36	4-06N	115-41W	-4200	0.20	2.13	0.43	1	22	59
0795	785508	LFG-1	33-13N	118-36W	-1300	1.00	1.8	1.8	1	23	62
0796	785508	LFG-2	36-40N	123-03W	-3320	1.1	2.0	2.2	1	23	62
0797	785508	LFG-3	36-39N	123-16W	-3470	1.10	2.1	2.3	1	23	62
0798	785907	LFG-5	36-34N	123-41W	-3770	1.10	2.1	2.3	1	23	62
0799	785508	LFG-7	44-17N	138-36W	-4220	0.45	2.2	1.0	1	23	62
0800	785507	LFG-8	48-20N	157-22W	-5220	0.25	2.0	0.5	1	23	62
0801	985508	LFG-11	52-33N	175-09W	-3240	0.59	1.7	1.0	1	23	62
0802	955508	LFG-12	54-17N	176-15W	-3740	0.60	1.5	0.9	1	23	62
0803	955508	LFG-13	55-41N	177-40W	-4160	0.81	1.6	1.3	1	23	62
0804	955508	LFG-14A	56-05N	176-10W	-3690	0.69	1.6	1.1	1	23	62
0805	955508	LFG-14B	56-13N	176-18W	-3670	0.62	1.6	1.0	1	23	62
0806	785508	LFG-16	53-23N	163-20W	-4230	0.21	1.9	0.4	1	23	62
0807	775907	LFG-17	54-08N	156-52W	-5680	1.42	1.9	2.7	1	23	62
0808	785508	LFG-19	57-11N	149-38W	-2950	0.55	2.0	1.1	1	23	62
0809	785907	LFG-20	57-34N	147-37W	-4880	0.50	2.4	1.2	1	23	62
0810	785508	LFG-22	59-05N	145-05W	-4220	0.92	2.4	2.2	1	23	62
0811	785508	LFG-24	59-07N	144-20W	-4000	0.56	2.7	1.5	1	23	62
0812	785508	LFG-25	59-09N	143-39W	-3920	0.74	2.3	1.7	1	23	62
0813	785508	LFG-27	59-14N	142-50W	-2670	0.62	2.1	1.3	1	23	62
0814	785508	LFG-28	58-11N	139-31W	-2910	0.68	2.2	1.5	1	23	62
0815	785508	LFG-29	57-42N	140-08W	-3310	0.72	1.8	1.3	1	23	62
0816	785508	LFG-30	56-58N	139-32W	-3340	0.92	2.4	2.2	1	23	62
0817	785907	LFG-35	54-27N	134-41W	-2560	1.86	2.2	4.1	1	23	62
0818	785508	LFG-37	54-13N	135-27W	-2900	1.35	2.0	2.7	1	23	62
0819	785508	LFG-38	54-07N	135-51W	-2740	1.22	1.8	2.2	1	23	62
0820	785508	LFG-39	53-07N	133-27W	-2900	0.94	1.7	1.6	1	23	62

DATA NUMBER	STATION CODE	STATION NAME	LATI- TUDE	LONGI- TUDE	ELE./ DEPTH	$\nabla T$	K	Q	NO	REF	YR
PACIFIC OCEAN (CONTINUED)											
0821	785508	LFG-40	53-15N	133-30W	-2910	0.61	1.8	1.1	1	23	62
0822	785508	LFG-41	50-04N	132-25W	-3100	0.30	2.3	0.7	1	23	62
0823	785508	LFG-42	48-19N	131-38W	-3050	0.52	2.3	1.2	1	23	62
0824	785508	LFG-43	46-15N	131-59W	-3290	0.36	2.2	0.8	1	23	62
0825	785508	LFG-44	43-51N	130-55W	-3320	1.45	2.2	3.2	1	23	62
0826	785508	LFG-45	42-19N	130-39W	-3430	0.24	2.1	0.5	1	23	62
0827	785500	LFG-46	40-36N	130-26W	-3760	0.05	2.0	0.1	1	23	62
0828	785507	LFG-47	40-35N	129-22W	-3240	1.71	2.1	3.6	1	23	62
0829	785507	LFG-48	38-35N	127-45W	-4630	.30	2.0	0.6	1	23	62
0830	785508	LFG-50	36-19N	125-56W	-4620	1.11	1.8	2.0	1	23	62
0831	785508	MSN-2	23-15N	130-46W	-4930	0.11	2.04	0.22	1	24	63
0832	785508	MSN-3	20-02N	135-11W	-5180	0.75	2.08	1.56	1	24	63
0833	755508	MSN-64	10-34S	151-05W	-5070	0.73	1.62	1.18	1	24	63
0834	755508	MSN-65	8-17S	151-36W	-5190	0.87	1.65	1.44	1	24	63
0835	755508	MSN-66	5-55S	149-39W	-5160	0.47	1.59	0.75	1	24	63
0836	755508	MSN-67	4-22S	149-29W	-4600	0.44	1.69	0.74	1	24	63
0837	755508	MSN-68	5-20N	146-13W	-5090	0.64	1.62	1.03	1	24	63
0838	755508	MSN-69	7-02N	145-38W	-5100	0.91	1.66	1.51	1	24	63
0839	755508	MSN-70	8-07N	145-24W	-5000	0.80	1.67	1.34	1	24	63
0840	755508	MSN-71	9-06N	145-18W	-5300	0.79	1.77	1.40	1	24	63
0841	755907	MSN-72	10-59N	142-37W	-4890	2.77	1.61	4.46	1	24	63
0842	755508	MSN-73	11-03N	142-28W	-5000	0.66	1.61	1.06	1	24	63
0843	765508	MSN-74	13-04N	138-59W	-5000	0.41	1.58	0.64	1	24	63
0844	765508	MSN-75	15-11N	136-52W	-4990	0.70	1.83	1.28	1	24	63
0845	785508	MSN-76	24-18N	126-30W	-4750	0.43	2.10	0.90	1	24	63
0846	785508	MSN-77	29-07N	121-03W	-4080	0.10	2.00	0.19	1	24	63
0847	785508	MSN-78	31-01N	119-04W	-3620	1.43	1.91	2.73	1	24	63
0848	785508	RIS-1	28-02N	117-12W	-3900	1.22	2.07	2.52	1	24	63
0849	785508	RIS-2	26-11N	117-18W	-4000	0.91	2.14	1.95	1	24	63
0850	785508	RIS-3	24-12N	117-23W	-3935	0.62	2.02	1.26	1	24	63
0851	785508	RIS-4	22-13N	117-21W	-3890	1.29	2.08	2.69	1	24	63
0852	785508	RIS-5	20-18N	117-27W	-4010	0.33	1.83	0.60	1	24	63
0853	785508	RIS-6	18-46N	117-14W	-4090	1.20	1.80	2.16	1	24	63
0854	765508	RIS-8	14-26N	117-12W	-4110	1.60	1.76	2.82	1	24	63
0855	765508	RIS-9	12-54N	117-24W	-4230	0.24	1.69	0.41	1	24	63
0856	765508	RIS-10	11-28N	117-38W	-4310	0.52	1.90	0.99	1	24	63
0857	765508	RIS-11	9-43N	117-32W	-4230	0.33	1.63	0.54	1	24	63
0858	765508	RIS-12	8-06N	117-51W	-3880	0.59	1.95	1.15	1	24	63
0859	765508	RIS-13	6-45N	117-51W	-4000	0.41	1.87	0.76	1	24	63
0860	765508	RIS-14	5-20N	117-52W	-4355	0.38	1.88	0.71	1	24	63
0861	765508	RIS-15	3-54N	118-08W	-4110	0.35	1.99	0.69	1	24	63
0862	765907	RIS-16	4-03N	117-01W	-4160	0.46	1.99	0.91	1	24	63
0863	765907	RIS-17	4-03N	115-53W	-4120	0.78	2.13	1.66	1	24	63
0864	765907	RIS-18	4-03N	115-36W	-4170	0.19	2.13	0.40	1	24	63
0865	765907	RIS-19	4-13N	114-58W	-4210	0.34	2.06	0.70	1	24	63
0866	765508	RIS-20	4-25N	113-41W	-3980	0.30	1.98	0.60	1	24	63
0867	765907	RIS-21	4-34N	112-31W	-3950	0.54	1.98	1.07	1	24	63
0868	765508	RIS-22	4-44N	111-33W	-4060	0.65	1.87	1.21	1	24	63
0869	765508	RIS-24B	5-04N	109-11W	-3980	1.25	2.06	2.57	1	24	63
0870	765907	RIS-25	5-13N	107-59W	-3760	0.98	2.04	1.99	1	24	63
0871	765508	RIS-26	5-14N	106-33W	-3820	1.15	2.02	2.32	1	24	63
0872	765907	RIS-27	5-24N	105-41W	-3645	0.79	1.95	1.55	1	24	63
0873	765508	RIS-28	5-37N	104-27W	-3570	0.86	1.87	1.61	1	24	63

## REVIEW OF HEAT FLOW DATA

181

DATA NUMBER	CODE	STATION NAME	LATI- TUDE	LONGI- TUDE	ELE./ DEPTH	VT	K	Q	NO	REF	YR
PACIFIC OCEAN (CONTINUED)											
0874	765907	RIS-29	5-43N	103-29W	-3305	2.26	1.76	3.98	1	24	63
0875	765907	RIS-30	5-37N	104-03W	-3400	0.87	1.87	1.63	1	24	63
0876	765508	RIS-31	5-34N	103-08W	-3300	0.90	1.76	1.58	1	24	63
0877	765907	RIS-32B	5-41N	102-36W	-3130	2.76	1.76	4.86	1	24	63
0878	765508	RIS-33	5-39N	102-06W	-3175	4.24	1.75	7.42	1	24	63
0879	765907	RIS-34B	5-42N	101-43W	-3440	0.36	1.84	0.67	1	24	63
0880	765508	RIS-35	5-36N	101-09W	-3250	0.92	1.93	1.78	1	24	63
0881	765907	RIS-36	5-41N	100-50W	-3405	0.64	1.94	1.25	1	24	63
0882	765907	RIS-37	5-44N	101-56W	-3285	0.69	1.75	1.20	1	24	63
0883	765508	RIS-38	5-43N	99-55W	-3420	0.58	1.94	1.12	1	24	63
0884	765907	RIS-39	6-05N	98-47W	-3470	0.54	1.74	0.94	1	24	63
0885	765508	RIS-40	6-41N	97-25W	-3520	0.21	1.74	0.37	1	24	63
0886	785907	RIS-41	6-58N	96-06W	-3785	0.05	1.67	0.08	1	24	63
0887	785508	RIS-42	6-57N	94-58W	-3740	0.73	1.60	1.17	1	24	63
0888	785907	RIS-43	5-05N	93-56W	-3540	0.66	1.72	1.13	1	24	63
0889	785508	RIS-44	4-07N	92-09W	-3150	0.28	1.95	0.55	1	24	63
0890	785907	RIS-45	3-16N	90-42W	-2360	0.44	2.00	0.87	1	24	63
0891	785508	RIS-46	2-17N	89-28W	-2160	0.24	2.09	0.51	1	24	63
0892	785508	RIS-47B	1-13N	88-32W	-2480	2.79	1.89	5.27	1	24	63
0893	785907	RIS-48B	0-15N	86-23W	-2760	2.52	1.85	4.66	1	24	63
0894	785508	RIS-49	0-09S	85-58W	-2750	0.36	1.81	0.65	1	24	63
0895	785907	RIS-50	1-41S	85-33W	-2440	3.11	1.91	5.94	1	24	63
0896	785907	RIS-51	1-45S	85-31W	-2385	1.00	1.98	1.98	1	24	63
0897	785508	RIS-52	2-44S	85-29W	-3220	1.53	1.98	3.03	1	24	63
0898	785907	RIS-53	3-52S	84-50W	-3395	1.22	1.98	2.42	1	24	63
0899	775508	RIS-54	9-07S	81-33W	-4700	0.50	1.75	0.87	1	24	63
0900	775907	RIS-55	8-51S	80-53W	-6280	0.46	2.00	0.91	1	24	63
0901	775907	RIS-56	8-47S	80-35W	-2975	0.54	2.00	1.07	1	24	63
0902	775907	RIS-57	12-34S	78-35W	-5940	0.12	2.09	0.26	1	24	63
0903	785907	RIS-58	12-46S	80-00W	-4630	0.64	1.79	1.14	1	24	63
0904	785508	RIS-59	12-59S	81-32W	-4800	1.21	1.68	2.04	1	24	63
0905	785907	RIS-60	13-04S	82-58W	-4990	1.51	1.70	2.56	1	24	63
0906	785508	RIS-61	13-11S	84-25W	-4740	0.86	1.72	1.48	1	24	63
0907	785907	RIS-62B	13-24S	86-15W	-4500	0.21	1.69	0.36	1	24	63
0908	785508	RIS-63	13-32S	87-26W	-4240	0.29	1.66	0.48	1	24	63
0909	785907	RIS-64	13-33S	89-05W	-4080	0.58	1.80	1.05	1	24	63
0910	785508	RIS-65	13-43S	90-30W	-3900	0.08	1.93	0.15	1	24	63
0911	785907	RIS-66	13-40S	92-00W	-3830	0.78	2.01	1.57	1	24	63
0912	785508	RIS-67	13-35S	93-28W	-3880	1.55	2.08	3.22	1	24	63
0913	785907	RIS-68	13-37S	94-58W	-3720	1.00	2.08	2.08	1	24	63
0914	785508	RIS-69	13-37S	96-44W	-4150	1.10	1.86	2.04	1	24	63
0915	785508	RIS-70	13-32S	97-48W	-3740	0.62	2.05	1.28	1	24	63
0916	785907	RIS-71	13-26S	99-11W	-3950	0.87	1.91	1.66	1	24	63
0917	785508	RIS-72	13-23S	100-30W	-4210	0.22	1.77	0.39	1	24	63
0918	785907	RIS-73	13-16S	101-24W	-4300	1.74	1.80	3.14	1	24	63
0919	765508	RIS-74B	13-18S	102-18W	-4430	0.79	2.22	1.75	1	24	63
0920	765907	RIS-75	13-11S	103-30W	-4170	0.78	2.10	1.63	1	24	63
0921	765508	RIS-76	13-03S	104-41W	-3720	0.40	1.98	0.79	1	24	63
0922	765907	RIS-77	12-59S	105-31W	-3910	0.64	2.13	1.37	1	24	63
0923	765508	RIS-78	12-54S	106-29W	-3720	1.33	2.27	3.02	1	24	63
0924	765907	RIS-79	12-50S	107-31W	-3710	0.41	2.22	0.92	1	24	63
0925	765508	RIS-80	12-48S	107-59W	-3550	0.50	2.16	1.09	1	24	63
0926	765907	RIS-81	12-43S	108-32W	-3550	0.98	2.17	2.13	1	24	63

DATA NUMBER	CODE	STATION NAME	LATI- TUDE	LONGI- TUDE	ELE./ DEPTH	$\nabla T$	K	Q	NO	REF	YR
PACIFIC OCEAN (CONTINUED)											
0927	765907	RIS-82	12-44S	109-02W	-3415	0.91	2.17	1.97	1	24	63
0928	765907	RIS-83	12-40S	109-30W	-3405	1.06	2.17	2.31	1	24	63
0929	765508	RIS-84	12-39S	110-01W	-3255	1.34	2.18	2.93	1	24	63
0930	765907	RIS-85	12-35S	110-29W	-3180	2.17	2.18	4.74	1	24	63
0931	765907	RIS-86	12-35S	110-15W	-3165	1.36	2.18	2.96	1	24	63
0932	765907	RIS-87	12-33S	110-47W	-3010	1.20	1.82	2.18	1	24	63
0933	765508	RIS-88B	12-33S	111-13W	-3105	1.52	1.82	2.76	1	24	63
0934	765907	RIS-89	12-32S	111-29W	-3030	1.64	1.88	3.08	1	24	63
0935	765907	RIS-90	12-33S	112-01W	-3075	3.27	1.94	6.35	1	24	63
0936	765907	RIS-91	12-32S	112-16W	-3175	1.75	2.00	3.50	1	24	63
0937	765508	RIS-92	12-30S	112-37W	-3170	0.98	2.05	2.00	1	24	63
0938	765907	RIS-93	12-26S	113-05W	-3230	1.43	2.05	2.94	1	24	63
0939	765907	RIS-94	12-25S	113-31W	-3325	0.87	2.05	1.79	1	24	63
0940	765907	RIS-95	13-02S	113-17W	-3240	2.10	1.90	4.00	1	24	63
0941	765508	RIS-96	13-36S	112-42W	-3025	1.85	1.75	3.24	1	24	63
0942	765907	RIS-97	14-02S	112-20W	-2960	1.48	1.75	2.59	1	24	63
0943	765907	RIS-98	14-47S	112-32W	-3020	0.69	2.22	1.34	1	24	63
0944	765907	RIS-99	14-47S	112-54W	-3065	0.92	2.09	1.93	1	24	63
0945	765508	RIS-100	14-41S	113-30W	-3010	3.62	1.96	7.10	1	24	63
0946	765907	RIS-101	14-40S	113-45W	-3170	4.10	1.96	8.04	1	24	63
0947	765907	RIS-102	14-38S	114-02W	-2975	2.38	1.95	4.65	1	24	63
0948	765907	RIS-103	14-15S	113-11W	-3045	3.14	1.85	5.80	1	24	63
0949	765907	RIS-104	14-15S	113-33W	-3020	2.07	1.95	4.03	1	24	63
0950	765508	RIS-105	14-15S	113-50W	-3045	0.43	1.94	0.84	1	24	63
0951	765907	RIS-106	14-15S	114-09W	-3015	1.69	1.94	3.27	1	24	63
0952	765907	RIS-107	14-17S	114-32W	-3120	0.96	1.94	1.87	1	24	63
0953	765907	RIS-108	14-17S	114-59W	-3210	0.57	2.04	1.17	1	24	63
0954	765508	RIS-109	14-18S	115-37W	-3440	0.45	2.14	0.97	1	24	63
0955	765907	RIS-110	14-15S	116-23W	-3280	0.79	2.17	1.72	1	24	63
0956	765508	RIS-111	14-14S	117-35W	-3440	0.45	2.20	1.00	1	24	63
0957	765907	RIS-112	13-59S	118-33W	-3380	0.32	2.19	0.70	1	24	63
0958	765508	RIS-113	14-00S	119-39W	-3270	0.06	2.19	0.13	1	24	63
0959	765907	RIS-114B	14-04S	120-16W	-3600	0.69	2.13	1.48	1	24	63
0960	765907	RIS-115	14-03S	121-17W	-3680	0.31	2.13	0.67	1	24	63
0961	765508	RIS-116	14-01S	122-28W	-3935	0.03	2.07	0.07	1	24	63
0962	765907	RIS-117	14-07S	123-47W	-3860	0.67	2.07	1.39	1	24	63
0963	765907	RIS-118	13-33S	121-48W	-3640	0.75	2.13	1.60	1	24	63
0964	765907	RIS-119	13-33S	121-50W	-3665	0.12	2.13	0.25	1	24	63
0965	765508	RIS-120	13-52S	125-20W	-3680	0.47	2.20	1.04	1	24	63
0966	765907	RIS-121	14-02S	127-07W	-3930	0.09	2.05	0.18	1	24	63
0967	765508	RIS-122	14-02S	128-25W	-3995	0.54	1.90	1.02	1	24	63
0968	755907	RIS-123	14-02S	129-48W	-4120	1.49	1.74	2.60	1	24	63
0969	755907	RIS-124	14-03S	130-18W	-4090	0.47	1.74	0.82	1	24	63
0970	755508	RIS-125	14-03S	131-44W	-4010	0.30	1.58	0.48	1	24	63
0971	755907	RIS-127	14-02S	133-45W	-4290	0.50	1.57	0.79	1	24	63
0972	755508	RIS-128	14-02S	134-55W	-4220	0.75	1.56	1.17	1	24	63
0973	755907	RIS-129	14-03S	136-34W	-4290	0.36	1.56	0.57	1	24	63
0974	755508	RIS-130	14-09S	138-06W	-4040	1.10	1.55	1.70	1	24	63
0975	755508	RIS-131	14-03S	139-35W	-3925	0.86	1.94	1.67	1	24	63
0976	785907	RIS-132	14-55S	141-34W	-2610	0.84	2.15	1.8	1	24	63
0977	785508	RIS-133	15-15S	142-26W	-3725	0.52	2.15	1.12	1	24	63
0978	785503	RIS-134	16-30S	145-07W	-1440	0.79	2.14	1.70	1	24	63
0979	785508	RIS-135	16-52S	145-49W	-2750	0.66	2.05	1.35	1	24	63

## REVIEW OF HEAT FLOW DATA

183

DATA NUMBER	CODE	STATION NAME	LATI- TUDE	LONGI- TUDE	ELE./ DEPTH	T	K	Q	NO	REF	YR.
PACIFIC OCEAN (CONTINUED)											
0980	785508	RIS-136	17-05S	147-13W	-4190	0.12	1.72	0.21	1	24	63
0981	785907	RIS-137	16-46S	148-52W	-4200	0.09	1.75	0.16	1	24	63
0982	785508	RIS-138	16-34S	148-30W	-4250	0.65	1.75	1.13	1	24	63
0983	785508	RIS-140	14-43S	145-40W	-2770	0.54	2.20	1.20	1	24	63
0984	785508	RIS-141	13-37S	145-03W	-4390	0.17	1.72	0.29	1	24	63
0985	755508	RIS-142	13-03S	144-03W	-4960	0.58	2.24	1.29	1	24	63
0986	755907	RIS-143	12-46S	143-34W	-4480	0.64	1.71	1.10	1	24	63
0987	755508	RIS-144	11-58S	142-27W	-4520	0.73	1.62	1.19	1	24	63
0988	755907	RIS-145	11-05S	140-57W	-4270	0.22	2.11	0.46	1	24	63
0989	785508	RIS-146	10-30S	139-59W	-4140	0.18	2.11	0.37	1	24	63
0990	785508	RIS-147	8-38S	138-18W	-4030	0.83	2.01	1.67	1	24	63
0991	755903	RIS-148	7-27S	137-11W	-4400	0.43	1.82	0.78	1	24	63
0992	755508	RIS-149	6-23S	136-11W	-4350	0.80	1.64	1.31	1	24	63
0993	755508	RIS-151	4-06S	133-59W	-4445	0.63	1.95	1.22	1	24	63
0994	755907	RIS-152	2-46S	132-58W	-4350	0.82	1.98	1.63	1	24	63
0995	755508	RIS-153	1-40S	131-52W	-4345	0.31	2.01	0.63	1	24	63
0996	755907	RIS-154	1-21S	131-31W	-4510	0.11	2.01	0.23	1	24	63
0997	755907	RIS-155	1-25S	131-04W	-4480	0.37	2.01	0.74	1	24	63
0998	755907	RIS-156	1-27S	130-34W	-4580	0.20	2.01	0.40	1	24	63
0999	755907	RIS-157	0-47S	131-42W	-4425	0.39	2.01	0.78	1	24	63
1000	755907	RIS-158	0-18N	132-00W	-4410	0.41	1.96	0.80	1	24	63
1001	755508	RIS-159	2-04N	132-32W	-4305	0.22	1.91	0.42	1	24	63
1002	755900	RIS-160	3-36N	133-00W	-4375	0.00	2.00	-0.01	1	24	63
1003	755907	RIS-161	3-58N	133-09W	-4375	0.10	2.00	0.19	1	24	63
1004	755508	RIS-162	5-38N	133-26W	-4390	0.21	2.08	0.44	1	24	63
1005	765907	RIS-163	7-14N	133-47W	-4410	0.82	2.08	1.7	1	24	63
1006	765508	RIS-164	9-03N	133-40W	-4980	1.08	1.67	1.80	1	24	63
1007	765907	RIS-165	10-57N	133-56W	-4910	0.85	1.67	1.42	1	24	63
1008	765907	RIS-166	12-56N	133-36W	-4810	0.64	1.67	1.07	1	24	63
1009	765508	RIS-167	14-58N	133-42W	-4775	0.74	1.82	1.34	1	24	63
1010	785508	RIS-169	18-15N	133-06W	-5190	1.05	1.91	2.00	1	24	63
1011	785907	RIS-170	19-59N	133-03W	-5060	0.64	1.91	1.23	1	24	63
1012	785907	RIS-172	23-30N	132-43W	-4880	0.61	2.02	1.23	1	24	63
1013	785508	RIS-173	25-19N	132-37W	-4530	0.38	2.13	0.80	1	24	63
1014	785907	RIS-174	27-15N	132-28W	-4815	0.49	2.10	1.02	1	24	63
1015	785508	RIS-175	28-26N	135-54W	-4740	0.77	2.07	1.59	1	24	63
1016	785907	RIS-176	28-29N	134-35W	-4660	0.36	2.00	0.71	1	24	63
1017	785508	RIS-177	28-18N	133-21W	-4385	0.74	1.92	1.43	1	24	63
1018	785907	RIS-178	27-54N	132-37W	-3700	0.51	1.92	0.98	1	24	63
1019	785907	RIS-180	28-10N	131-04W	-4550	1.10	1.96	2.16	1	24	63
1020	785508	RIS-181	28-17N	129-36W	-4740	0.52	2.00	1.05	1	24	63
1021	785907	RIS-182	28-21N	127-59W	-4660	0.97	1.98	1.92	1	24	63
1022	785508	RIS-183	28-27N	126-37W	-4500	0.88	1.96	1.73	1	24	63
1023	785907	RIS-184	28-35N	125-00W	-4445	1.13	1.96	2.22	1	24	63
1024	785508	RIS-185	28-47N	123-37W	-4370	0.94	1.77	1.66	1	24	63
1025	785907	RIS-186	28-56N	122-27W	-4220	1.10	1.96	2.16	1	24	63
1026	785907	RIS-187	29-33N	121-44W	-4005	1.15	2.05	2.36	1	24	63
1027	755108	MP-21	20-48N	159-42W	-4500	0.65	1.79	1.16	1	25	58
1028	755108	MP-32	18-18N	173-23W	-3900	0.35	2.05	0.72	1	25	58
1029	755108	MP-35-2	19-28N	174-35W	-4900	0.62	2.07	1.29	1	25	58
1030	755108	MP-36	16-45N	176-24W	-5040	0.66	1.80	1.19	1	25	58
1031	755108	MP-38	19-02N	177-19W	-4750	0.69	1.57	1.09	1	25	58
1032	785007	STN-1	32-35N	122-30W	-4000	0.67	1.90	1.27	1	25	58
1033	755108	CAP-2B	0-40N	169-17E	-4310	0.76	2.48	1.88	1	25	58

DATA NUMBER	CODE	STATION NAME	LATI-TUDE	LONGI-TUDE	ELE./DEPTH	$\nabla T$	K	Q	NO	REF	YR
PACIFIC OCEAN (CONTINUED)											
1034	785108	CAP-58	9-04S	174-51E	-5000	0.72	1.87	1.35	1	25	58
1035	785108	CAP-9B	18-59S	177-36E	-2700	0.63	2.40	1.51	1	25	58
1036	785108	CAP-10B	21-56S	178-33E	-3900	1.25	2.07	2.58	1	25	58
1037	755108	CAP-31B	17-28S	158-40W	-4880	0.86	1.83	1.58	1	25	58
1038	755108	CAP-33B	12-48S	143-33W	-4300	0.21	1.71	0.36	1	25	58
1039	765108	CAP-40B	14-45S	112-11W	-3020	2.15	2.44	5.25	1	25	58
1040	765108	CAP48B	5-52N	123-55W	-4100	0.73	2.26	1.65	1	25	58
1041	765108	CAP-50B	14-59N	124-12W	-4350	1.24	1.96	2.43	1	25	58
1042	775108	ACA-B5-1	13-08N	91-57W	-6170	0.24	1.92	0.47	1	25	58
1043	785108	ACA-B6	11-55N	91-37W	-3600	0.46	1.67	0.76	1	25	58
1044	785108	ACA-B8	9-49N	93-02W	-3730	0.14	1.76	0.25	1	25	58
1045	765108	ACA-B9	12-14N	98-44W	-3500	0.40	1.72	0.69	1	25	58
1046	765101	ACA-B11	10-52N	105-04W	-3300	1.83	1.95	3.57	1	25	58
1047	765907	ACA-B11B	10-54N	104-25W	-2950	1.40	1.95	2.73	1	25	58
1048	765007	ACA-B13	12-12N	111-04W	-3600	0.48	1.95	0.93	1	25	58
1049	785108	ACA-B13A	20-44N	115-42W	-3910	0.59	2.02	1.19	1	25	58
1050	785108	GUA-P6	25-01N	123-04W	-4300	0.48	2.30	1.11	1	25	58
1051	785108	GUA-P7	24-54N	123-05W	-4200	0.49	2.30	1.13	1	25	58
1052	757508	V18-100	09-42S	136-28W	-4329	0.96	1.72	1.65	1	28	65
1053	757508	V18-101	08-00S	133-30W	-4696	1.24	1.56	1.93	1	28	65
1054	757508	V18-102	07-20S	133-03W	-4477	0.99	1.52	1.50	1	28	65
1055	757508	V18-105	05-19S	130-22W	-4661	0.57	1.65	0.94	1	28	65
1056	757508	V18-107	03-37S	127-41W	-4564	0.23	1.66	0.38	1	28	65
1057	757507	V18-108	02-51S	126-12W	-4612	0.36	1.78	0.59	1	28	65
1139	757507	V18-109	01-06S	124-37W	-4550	0.28	2.16	0.60	1	28	65
1058	767508	V18-110	01-14S	122-55W	-4389	0.48	2.33	1.12	1	28	65
1059	767508	V18-111	01-03N	120-46W	-4371	0.36	2.31	0.83	1	28	65
1060	767907	V18-112	02-12N	119-40W	-4332	1.52	2.30	3.50	1	28	65
1061	767508	V18-113	03-10N	118-28W	-4217	0.71	2.13	1.51	1	28	65
1062	765508	V18-114	04-14N	117-00W	-4161	0.42	2.19	0.82	1	28	65
1063	765508	V18-116	06-23N	113-32W	-4104	0.15	1.85	0.28	1	28	65
1064	765508	V18-118	08-01N	109-18W	-4065	1.92	1.67	3.21	1	28	65
1065	765508	V18-119	08-46N	107-09W	-3488	1.74	1.83	3.18	1	28	65
1066	765508	V18-122	10-16N	103-05W	-3190	1.91	1.55	2.96	1	28	65
1067	765507	V18-125	11-54N	100-44W	-3360	1.22	1.65	2.01	1	28	65
1068	765508	V18-126	12-38N	99-27W	-3426	1.78	1.64	2.62	1	28	65
1069	765907	V18-127	12-54N	98-52W	-3342	0.96	1.80	1.73	1	28	65
1070	765507	V18-128	12-49N	97-47W	-3720	0.42	1.72	0.46	1	28	65
1071	765907	V18-129	13-09N	97-07W	-3590	0.64	1.80	1.15	1	28	65
1072	765500	V18-130	13-19N	96-51W	-2757	5.78	1.85	10.	1	28	65
1073	765508	V18-131	14-31N	96-18W	-3890	1.55	1.91	2.96	1	28	65
1074	765508	V18-134	12-47N	96-17W	-3987	0.76	1.82	1.38	1	28	65
1075	765508	V18-135	08-49N	97-16W	-3793	0.66	1.61	1.06	1	28	65
1076	785508	V18-140	06-37N	88-24W	-3247	1.91	1.60	3.06	1	28	65
1077	785508	V18-141	06-44N	86-30W	-2892	0.56	1.82	1.02	1	28	65
1078	785508	V18-142	06-04N	85-43W	-1819	1.53	1.97	3.01	1	28	65
1079	785507	V18-143	05-42N	85-16W	-1840	1.41	2.15	3.03	1	28	65
1080	785508	V18-144	05-18N	84-45W	-3005	1.40	1.78	2.50	1	28	65
1081	785508	V18-145	05-34N	83-24W	-3064	1.95	1.76	3.43	1	28	65
1082	785907	V18-146	06-06N	82-05W	-3031	1.91	1.80	3.44	1	28	65
1083	785907	V18-148	06-42N	80-42W	-3424	1.70	1.80	3.06	1	28	65
1084	785508	V19-8	07-04N	78-59W	-3345	1.63	1.69	2.75	1	28	65
1085	785508	V19-9	04-56N	78-16W	-3819	2.83	2.16	6.11	1	28	65
1086	785508	V19-10	03-12N	80-08W	-1711	0.91	2.08	1.89	1	28	65

## REVIEW OF HEAT FLOW DATA

185

DATA NUMBER	CODE	STATION NAME	LATI-TUDE	LONGI-TUDE	ELE./DEPTH	VT	K	Q	NO	REF	YR
PACIFIC OCEAN (CONTINUED)											
1087	785508	V19-11	02-28N	81-42W	-2398	1.12	1.79	2.00	1	28	65
1088	785508	V19-14	02-22S	84-39W	-2724	0.07	1.78	0.12	1	28	65
1089	785508	V19-15	03-35S	83-56W	-3153	1.17	1.67	1.95	1	28	65
1090	785508	V19-19	11-59S	81-31W	-4749	1.21	1.53	1.85	1	28	65
1091	785508	V19-23	13-13S	92-53W	-3647	0.83	2.19	1.82	1	28	65
1092	765507	V19-26	16-21S	104-48W	-4199	0.78	2.42	1.8	1	28	65
1093	765507	V19-27	17-01S	108-52W	-3624	0.76	2.49	1.9	1	28	65
1094	765907	V19-28	17-01S	110-23W	-3449	0.71	2.1	1.5	1	28	65
1095	765507	V19-29	17-00S	110-51W	-3438	0.58	2.23	1.3	1	28	65
1096	765507	V19-30	17-00S	111-12W	-3537	0.44	2.06	0.9	1	28	65
1097	765907	V19-31	17-01S	111-33W	-3320	0.57	2.1	1.2	1	28	65
1098	765907	V19-32	17-02S	111-53W	-3256	0.67	2.1	1.4	1	28	65
1099	765907	V19-33	17-02S	112-12W	-3184	1.57	2.1	3.3	1	28	65
1100	765907	V19-34	17-01S	112-34W	-2981	1.10	2.1	2.3	1	28	65
1101	765907	V19-35	17-01S	112-55W	-3175	0.81	2.1	1.7	1	28	65
1102	765907	V19-36	17-01S	113-31W	-3056	0.86	2.1	1.8	1	28	65
1103	765907	V19-37	17-02S	113-54W	-2830	1.67	2.1	3.5	1	28	65
1104	765907	V19-38	17-00S	114-11W	-3177	0.76	2.1	1.6	1	28	65
1105	765907	V19-39	17-00S	114-32W	-3139	1.00	2.1	2.1	1	28	65
1106	765907	V19-40	17-00S	114-53W	-3157	0.76	2.1	1.6	1	28	65
1107	765907	V19-41	16-58S	115-12W	-3270	0.24	2.1	0.5	1	28	65
1108	765907	V19-42	16-58S	115-33W	-3300	3.38	2.1	7.1	1	28	65
1109	765907	V19-43	16-58S	115-56W	-3336	1.00	2.1	2.1	1	28	65
1110	765907	V19-44	16-57S	116-18W	-3407	0.71	2.1	1.4	1	28	65
1111	765907	V19-45	16-58S	116-48W	-3374	1.05	2.1	2.2	1	28	65
1112	765907	V19-46	16-59S	117-53W	-3422	0.76	2.1	1.6	1	28	65
1113	765907	V19-48	16-39S	124-23W	-3760	0.43	2.1	0.9	1	28	65
1114	785508	H-4	28-14N	127-38W	-4580	.710	2.07	1.47	1	29	64
1115	785508	H-5	24-46N	134-30W	-4530	.632	1.97	1.25	2	29	64
A	785508	H-5A	24-46N	134-28W	-4530	.452	1.97	0.89	1	29	64
B	786507	H-5B	24-46N	134-31W	-4530	.812	1.97	1.6	1	29	64
1116	785907	H-7	23-03N	137-55W	-5295	.935	2.00	1.87	1	29	64
1117	785508	H-8	23-00N	143-58W	-4850	1.32	2.10	2.78	1	29	64
1118	785907	H-9	22-58N	148-24W	-5470	.726	1.90	1.38	1	29	64
1119	785508	H-10	23-00N	150-38W	-5580	.763	1.86	1.42	1	29	64
1120	756507	H-11	22-59N	152-59W	-5060	.860	1.86	1.6	1	29	64
1121	756900	H-12	22-29N	154-26W	-4390	.758	1.98	1.5	1	29	64
1122	756507	H-15	19-08N	157-20W	-4610	1.04	1.68	1.74	1	29	64
1123	755508	H-17	23-36N	156-07W	-4260	.695	1.87	1.30	1	29	64
1124	755508	H-18	21-56N	154-48W	-4660	.353	2.01	0.71	1	29	64
1125	755508	H-19	23-07N	156-07W	-4260	.742	1.90	1.41	1	29	64
1126	756507	LSDH-68	20-15N	154-13W	-5480	.527	1.67	0.88	1	29	64
1127	755508	LSDH-69	19-59N	151-09W	-5305	.773	1.85	1.43	1	29	64
1128	755508	LSDH-70	20-06N	145-16W	-5410	.774	1.90	1.47	1	29	64
1129	785508	LSDH-71	21-26N	140-23W	-5200	.672	2.04	1.37	1	29	64
1130	785508	LSDH-72	22-12N	138-57W	-5100	.721	2.08	1.50	2	29	64
A	755508	LSDH-72A	22-12N	138-57W	-5100	.688	2.08	1.43	1	29	64
B	755508	LSDH-72B	22-12N	138-57W	-5100	.750	2.08	1.56	1	29	64
1131	755508	LSDH-73	23-10N	130-58W	-4870	.659	2.07	1.36	2	29	64
A	755508	LSDH-73A	23-11N	130-58W	-4860	.816	2.07	1.69	1	29	64
B	755508	LSDH-73B	23-11N	130-58W	-4860	.816	2.07	1.69	1	29	64
1132	755508	LSDH-73C	23-10N	130-57W	-4880	.502	2.07	1.04	1	29	64
1133	785508	LSDH-74	27-30N	125-47W	-4483	.441	2.02	0.89	2	29	64
A	755508	LSDH-74A	27-30N	125-47W	-4450	.396	2.02	0.80	1	29	64
B	755508	LSDH-74B	27-30N	125-47W	-4515	.480	2.02	0.97	1	29	64

DATA NUMBER	CODE	STATION NAME	LATI-TUDE	LONGI-TUDE	ELE./DEPTH	∇T	K	Q	NO	REF	YR
ARCTIC OCEAN											
1143	457508	FL-1	82-30N	156-26W	-3747	.683	2.13	1.45	1	35	65
1144	457508	FL-2	82-12N	156-24W	-3742	.674	2.07	1.40	1	35	65
1145	457508	FL-3	82-31N	156-54W	-3741	.672	2.20	1.48	1	35	65
1146	457508	FL-6	82-42N	158-04W	-3740	.625	2.11	1.32	1	35	65
1147	457508	FL-8	82-39N	157-28W	-3742	.665	2.19	1.46	1	35	65
1148	457508	FL-9	82-46N	156-51W	-3743	.634	2.16	1.37	1	35	65
1149	467508	FL-10	82-57N	155-54W	-3507	.496	2.72	1.35	1	35	65
1150	467508	FL-11	83-00N	156-07W	-3520	.547	2.60	1.42	1	35	65
1151	467508	FL-12	83-06N	156-01W	-3473	.552	2.67	1.47	1	35	65
1152	467508	FL-13	83-08N	156-47W	-3577	.540	2.60	1.40	1	35	65
1153	467508	FL-14	83-08N	157-18W	-3216	.394	2.76	1.09	1	35	65
1154	467508	FL-15	82-60N	158-16W	-3137	.295	2.63	0.78	1	35	65
1155	467508	FL-16	83-01N	159-03W	-2247	.338	2.68	0.91	1	35	65
1156	467508	FL-17	82-60N	159-02W	-2215	.296	2.61	0.77	1	35	65
1157	467508	FL-19	83-03N	162-52W	-3417	.440	2.43	1.07	1	35	65
1158	467508	FL-21	83-01N	163-37W	-3494	.478	2.66	1.27	1	35	65
1159	457508	FL-22	82-53N	163-17W	-3750	.666	2.14	1.43	1	35	65
1160	457508	FL-23	82-39N	162-49W	-3748	.676	2.18	1.47	1	35	65
1161	457508	FL-24	82-22N	162-07W	-3743	.570	2.52	1.44	1	35	65
1162	457508	FL-25	82-26N	160-40W	-3760	.631	2.10	1.32	1	35	65

*Acknowledgments.* We thank H. W. Menard for supplying his oceanic geological data before publication and F. S. Birch, W. H. Diment, P. Grim, A. H. Lachenbruch, M. G. Langseth, T. S. Lovering, B. V. Marshall, J. Selater, V. Vacquier, R. K. Verma, R. P. Von Herzen, T. Watanabe, and M. Yasui for making their heat flow data available to us in advance of publication. We are indebted to W. Hamilton, W. M. Kaula, G. Oertel, J. Verhoogen, and R. P. Von Herzen for their critical comments and to S. C. Calvert, A. Cox, C. S. Cox, J. W. Elder, D. I. Gough, A. H. Lachenbruch, T. S. Lovering, C. A. Nelson, P. Taylor, and G. A. Thompson for their valuable suggestions. We also thank C. E. Corbato and M. C. Gilbert for advice on geologic maps and S. Mak for processing the data.

This work was supported by grants from the National Aeronautics and Space Administration (NsG 216-62) and by the Computing Facility, University of California, Los Angeles. It was carried out while one of us (Uyeda) held a visiting professorship at the Department of Geophysics, Stanford University, on a National Science Foundation Senior Foreign Scientist Fellowship.

#### REFERENCES

- Alexander, H. W., *Elements of Mathematical Statistics*, John Wiley & Sons, New York, 1961.
- Anderson, E. M., The loss of heat by conduction from the Earth's crust in Britain, *Proc. Roy. Soc. Edinburgh*, 60, 192-209, 1940.
- Beck, A. E., The measurement of the flow of heat through the crust of the Earth, Ph.D. Thesis, Australian National University, 1956.
- Beck, A. E., Terrestrial flow of heat near Flin Flon, Manitoba, *Nature*, 195, 368-369, 1962.
- Beck, A. E., and Z. Logis, Terrestrial flow of heat in the Brent Crater, *Nature*, 201, 383, 1963.
- Benfield, A. E., Terrestrial heat flow in Great Britain, *Proc. Roy. Soc. London, A*, 173, 428-450, 1939.
- Benfield, A. E., A heat flow value for a well in California, *Am. J. Sci.*, 245, 1-18, 1947.
- Birch, F., Temperature and heat flow in a well near Colorado Springs, *Am. J. Sci.*, 245, 733-753, 1947a.
- Birch, F., Crustal structure and surface heat flow near the Colorado Front Range, *Trans. Am. Geophys. Union*, 28, 792-797, 1947b.
- Birch, F., Flow of heat in the Front Range, Colorado, *Bull. Geol. Soc. Am.*, 61, 567-630, 1950.
- Birch, F., Thermal conductivity, climatic variation, and heat flow near Calumet, Michigan, *Am. J. Sci.*, 252, 1-25, 1954a.
- Birch, F., Heat from radioactivity, in *Nuclear Geology*, edited by H. Faul, pp. 148-174, John Wiley & Sons, New York, 1954b.
- Birch, F., The present state of geothermal investigation, *Geophysics*, 19, 645-659, 1954c.
- Birch, F., Heat flow at Eniwetok Atoll, *Bull. Geol. Soc. Am.*, 67, 941-942, 1956.
- Birch, F., and H. Clark, An estimate of the surface flow of heat in the West Texas Permian Basin, *Am. J. Sci.*, 243A, 69-74, 1945.
- Birch, F. S., Some heat flow measurements in the Atlantic Ocean, M.S. thesis, University of Wisconsin, 1964.
- Bodvarsson, G., Terrestrial heat balance in Iceland, *Timarit Verkfræðingafélags Islands*, 39, 1-8, 1955.

- Bodvarsson, G., and G. P. L. Walker, Crustal drift in Iceland, *Geophys. J.*, *8*, 285-300, 1964.
- Boldizsar, T., Terrestrial heat-flow in Hungary, *Nature*, *178*, 35, 1956a.
- Boldizsar, T., Terrestrial heat flow in Hungary, *Geofis. Pura Appl.*, *34*, 66-70, 1956b.
- Boldizsar, T., Measurement of terrestrial heat flow in the coal mining district of Komlo, *Acta Tech. Acad. Sci. Hung.*, *15*, 219-227, 1956c.
- Boldizsar, T., New terrestrial heat flow values from Hungary, *Geofis. Pura Appl.*, *39*, 120-125, 1958a.
- Boldizsar, T., Geothermic investigations in the Hungarian plain, *Acta Geol.*, *5*, 245-254, 1958b.
- Boldizsar, T., Terrestrial heat flow in the Nagylengyel oilfield, *Publ. Fac. Mining Sopron*, *20*, 27-34, 1959.
- Boldizsar, T., Terrestrial heat flow in the natural steam field at Larderello, *Geofis. Pura Appl.*, *56*, 115-122, 1963.
- Boldizsar, T., Heat flow in the Hungarian basin, *Nature*, *202*, 1278-1280, 1964a.
- Boldizsar, T., Geothermal measurements in the twin shafts of Hosszuheteny, *Acta Tech. Acad. Sci. Hung.*, *47*, 293-308, 1964b.
- Boldizsar, T., Terrestrial heat flow in the Carpathians, *J. Geophys. Res.*, *69*, 5269-5276, 1964c.
- Boldizsar, T., and J. Gozon, The geothermic flow at Komlo-Zobak (in Russian), *Acta Tech. Acad. Sci. Hung.*, *43*, 467-476, 1963.
- Bullard, E. C., Heat flow in South Africa, *Proc. Roy. Soc. London, A*, *173*, 474-502, 1939.
- Bullard, E. C., Warmefluss aus der Erdkruste, *Landolt-Bornstein*, *3*, 385-386, 1952.
- Bullard, E., The flow of heat through the floor of the Atlantic Ocean, *Proc. Roy. Soc. London, A*, *222*, 408-429, 1954.
- Bullard, E. C., The flow of heat through the floor of the ocean, in *The Sea*, edited by M. N. Hill, vol. 3, pp. 218-232, Interscience Publishers, New York, 1963.
- Bullard, E. C., The flow of heat through the Earth, *ICSU Rev. World Sci.*, *6*, 78-83, 1964.
- Bullard, E. C., and A. Day, The flow of heat through the floor of the Atlantic Ocean, *Geophys. J.*, *4*, 282-292, 1961.
- Bullard, E. C., A. E. Maxwell, and R. Revelle, Heat flow through the deep sea floor, *Advan. Geophys.*, *3*, 153-181, 1956.
- Bullard, E. C., and E. R. Niblett, Terrestrial heat flow in England, *Monthly Notices Roy. Astron. Soc., Geophys. Suppl.*, *6*, 222-238, 1951.
- Burns, R. E., Sea bottom heat-flow measurements in the Andaman Sea, *J. Geophys. Res.*, *69*, 4918-4919, 1964.
- Carte, A. E., Heat flow in the Transvaal and Orange Free State, *Proc. Phys. Soc. B*, *67*, 664-672, 1954.
- Chadwick, P., Heat-flow from the Earth at Cambridge, *Nature*, *178*, 105-106, 1956.
- Clark, S. P., Jr., Heat flow at Grass Valley, California, *Trans. Am. Geophys. Union*, *38*, 239-244, 1957.
- Clark, S. P., Jr., Heat flow in the Austrian Alps, *Geophys. J.*, *6*, 45-63, 1961.
- Clark, S. P., Jr., and E. R. Niblett, Terrestrial heat flow in the Swiss Alps, *Monthly Notices Roy. Astron. Soc., Geophys. Suppl.*, *7*, 176-195, 1956.
- Clark, S. P., Jr., and A. E. Ringwood, Density distribution and constitution of the mantle, *Rev. Geophys.*, *2*, 35-88, 1964.
- Cochran, W. G., *Sampling Techniques*, John Wiley & Sons, New York, 1953.
- Coster, H. P., Terrestrial heat flow in Persia, *Monthly Notices Roy. Astron. Soc., Geophys. Suppl.*, *5*, 131-145, 1947.
- Creutzburg, H., *Investigation of the Heat Flow of the Earth in West Germany* (in German), vol. 4, part 3, pp. 73-108, Kali und Steinsalz, Hanover, 1964.
- Crow, E. L., F. A. Davis, and M. W. Maxfield, *Statistical Manual*, Dover Publications, New York, 1960.
- Diment, W. H., Comments on paper by E. A. Lubimova, 'Heat flow in the Ukrainian Shield in relation to recent tectonic movements,' *J. Geophys. Res.*, *70*, 2466-2467, 1965.
- Diment, W. H., I. W. Marine, J. Neiheisel, and G. E. Siple, Subsurface temperatures, thermal conductivity, and heat flow near Aiken, South Carolina, *J. Geophys. Res.*, *70*, in press, 1965a.
- Diment, W. H., R. Raspet, M. A. Mayhew, and R. W. Werre, Terrestrial heat flow near Alberta, Virginia, *J. Geophys. Res.*, *70*, 923-930, 1965b.
- Diment, W. H., and E. C. Robertson, Temperature, thermal conductivity, and heat flow in a drilled hole near Oak Ridge, Tennessee, *J. Geophys. Res.*, *68*, 5035-5047, 1963.
- Diment, W. H., and J. D. Weaver, Preliminary analysis of subsurface temperatures and heat flow in a hole near Mayaguez, Puerto Rico, in A study of serpentinite: The AMSOC core hole near Mayaguez, Puerto Rico, *NAS-NRC Pub. 1188*, 75-91, 1964.
- Diment, W. H., and R. W. Werre, Terrestrial heat flow near Washington, D. C., *J. Geophys. Res.*, *69*, 2143-2149, 1964.
- Engel, A. E. J., Geologic evolution of North America, *Science*, *140*, 143-152, 1963.
- Fisher, R. L., and H. H. Hess, Trenches, in *The Sea*, edited by M. N. Hill, vol. 3, pp. 411-436, Interscience Publishers, New York, 1963.
- Foster, T. D., Heat-flow measurements in the northeast Pacific and in the Bering Sea, *J. Geophys. Res.*, *67*, 2991-2993, 1962.
- Garland, G. D., and D. H. Lennox, Heat flow in western Canada, *Geophys. J.*, *6*, 245-262, 1962.
- Gerard, R., M. G. Langseth, Jr., and M. Ewing, Thermal gradient measurements in the water and bottom sediment of the western Atlantic, *J. Geophys. Res.*, *67*, 785-803, 1962.
- Gough, D. I., Heat flow in the southern Karroo, *Proc. Roy. Soc. London, A*, *272*, 207-230, 1963.
- Grim, P., private communication, 1964.
- Guier, W. H., Recent progress in satellite geodesy,

- Johns Hopkins Univ., Appl. Phys. Lab., preprint, 24 pp., 1965.
- Gutenberg, B., *Physics of the Earth's Interior*, pp. 121-148, Academic Press, New York, 1959.
- Heezen, B. C., The deep-sea floor, in *Continental Drift*, edited by S. K. Runcorn, pp. 235-288, Academic Press, New York, 1962.
- Heezen, B. C., and M. Ewing, The mid-oceanic ridge, in *The Sea*, edited by M. N. Hill, vol. 3, pp. 388-410, Interscience Publishers, New York, 1963.
- Heezen, B. C., and H. W. Menard, Topography of the deep-sea floor, in *The Sea*, edited by M. N. Hill, vol. 3, pp. 233-280, Interscience Publishers, New York, 1963.
- Heiskanen, W. A., and F. A. Vening-Meinesz, *The Earth and Its Gravity Field*, McGraw-Hill Book Company, New York, 1958.
- Herrin, E., and S. P. Clark, Jr., Heat flow in West Texas and eastern New Mexico, *Geophysics*, 21, 1087-1099, 1956.
- Hess, H. H., History of ocean basins, in *Petrologic Studies: A Volume to Honor A. F. Buddington*, edited by A. Engel, H. James, and B. Leonard, pp. 599-620, Geological Society of America, New York, 1962.
- Horai, K., Studies of the thermal state of the Earth, 3, Terrestrial heat flow at Hitachi, Ibaraki Prefecture, Japan, *Bull. Earthquake Res. Inst. Tokyo Univ.*, 37, 571-592, 1959.
- Horai, K., Studies of the thermal state of the Earth, 10, Terrestrial heat flow measurements in Tohoku District, Japan, *Bull. Earthquake Res. Inst. Tokyo Univ.*, 41, 137-147, 1963a.
- Horai, K., Studies of the thermal state of the Earth, 11, Terrestrial heat flow measurements in Kyushu District, Japan, *Bull. Earthquake Res. Inst. Tokyo Univ.*, 41, 149-165, 1963b.
- Horai, K., Studies of the thermal state of the Earth, 12, Terrestrial heat flow measurements in Hokkaido District, Japan, *Bull. Earthquake Res. Inst. Tokyo Univ.*, 41, 167-184, 1963c.
- Horai, K., Studies of the thermal state of the Earth, 13, Terrestrial heat flow in Japan (a summary of terrestrial heat flow measurements in Japan up to December, 1962), *Bull. Earthquake Res. Inst.*, 42, 94-132, 1964.
- Horai, K., and S. Uyeda, Terrestrial heat flow in Japan, *Nature*, 199, 364-365, 1963.
- Howard, L. E., and J. H. Sass, Terrestrial heat flow in Australia, *J. Geophys. Res.*, 69, 1617-1625, 1964.
- Izsak, I. G., Tesseral harmonics in the geopotential and corrections to station coordinates, *J. Geophys. Res.*, 69, 2621-2630, 1964.
- Jaeger, J. C., and J. H. Sass, Lees' topographic correction in heat flow and the geothermal flux in Tasmania, *Geofis. Pura Appl.*, 54, 53-63, 1963.
- Joyner, W. B., Heat flow in Pennsylvania and West Virginia, *Geophysics*, 25, 1229-1241, 1960.
- Kaula, W. M., Global harmonic and statistical analysis of gravimetry, *Proc. IAG Symp. on Extrapolation of Gravity Anomalies to Unsurveyed Areas, Columbus, Ohio*, Nov. 16-18, 1964, Publ. Inst. Geod. Photogr. and Cart., in press, 1965.
- Kennedy, G. C., The origin of continents, mountain ranges, and ocean basins, in *Study of the Earth*, edited by J. F. White, pp. 349-362, Prentice-Hall, Englewood Cliffs, 1962.
- Kraskovski, S. A., On the thermal field in Old Shields (English translation), *Izv. Akad. Nauk SSSR, Ser. Geofiz.*, 1961, 247-250, 1961.
- Lachenbruch, A. H., Thermal effects of the ocean on permafrost, *Bull. Geol. Soc. Am.*, 68, 1515-1530, 1957.
- Lachenbruch, A. H., G. W. Greene, and B. V. Marshall, Permafrost and the geothermal regime, in *Bioenvironmental Features of the Ogotoruk Creek Area, Cape Thompson, Alaska*, in press, 1965.
- Lachenbruch, A. H., and B. V. Marshall, Heat flux from the Arctic Ocean Basin, preliminary results (abstract), *Trans. Am. Geophys. Union*, 45, 123, 1964.
- Langseth, M. G., private communication, 1964.
- Langseth, M. G., and P. J. Grim, New heat-flow measurements in the Caribbean and Western Atlantic, *J. Geophys. Res.*, 69, 4916-4917, 1964.
- Langseth, M. G., P. J. Grim, and M. Ewing, Heat flow measurements in the east Pacific Ocean, *J. Geophys. Res.*, 70, 367-380, 1965.
- Law, L. K., W. S. B. Patterson, and K. Whitham, Heat flow determination in the Canadian Arctic Archipelago, *Can. J. Earth Sci.*, 2, 59-71, 1965.
- Lee, W. H. K., Heat flow data analysis, *Rev. Geophys.*, 1, 449-479, 1963.
- Lee, W. H. K., Results of heat flow measurements, in *International Dictionary of Geophysics*, edited by S. K. Runcorn, Pergamon Press, New York, in press, 1965.
- Lee, W. H. K., and G. J. F. MacDonald, The global variation of terrestrial heat flow, *J. Geophys. Res.*, 68, 6481-6492, 1963.
- Leith, T. H., Heat flow at Kirkland Lake, *Trans. Am. Geophys. Union*, 33, 435-443, 1952.
- Le Marné, A. E., and J. H. Sass, Heat flow at Cobar, New South Wales, *J. Geophys. Res.*, 67, 3981-3983, 1962.
- Le Pichon, X., R. E. Houtz, C. L. Drake, and J. E. Nafe, Crustal structure of mid-ocean ridges, 1, Seismic refraction measurements, *J. Geophys. Res.*, 70, 319-339, 1965.
- Lister, C. R. B., Heat flow through the ocean floor, Ph.D. Thesis, Cambridge University, 1962.
- Lister, C. R. B., A close group of heat-flow stations, *J. Geophys. Res.*, 68, 5569-5573, 1963a.
- Lister, C. R. B., Geothermal gradient measurement using a deep sea corer, *Geophys. J.*, 7, 571-583, 1963b.
- Lister, C. R. B., and J. S. Reitzel, Some measurements of heat flow through the floor of the north Atlantic, *J. Geophys. Res.*, 69, 2151-2154, 1964.
- Lotze, F., Die Joly'sche Radioaktivitäts-hypothese zur Erklärung der Gebirgsbildungen, *Nachr. Ges. Wiss. Göttingen Math. Physik Kl.*, 1927, 75-114, 1927.

- Lovering, T. S., Geothermal gradients, recent climatic changes, and rate of sulfide oxidation in the San Manuel District, Arizona, *Econ. Geol.*, **43**, 1-20, 1948.
- Lubimova, E. A., Heat flow in the Ukrainian Shield in relation to recent tectonic movements, *J. Geophys. Res.*, **69**, 5277-5284, 1964.
- Lubimova, E. A., L. M. Lusova, F. V. Firsov, G. N. Starikova, and A. P. Shushpanov, Determination of surface heat flow in Mazesta (USSR), *Ann. Geofis.*, **14**, 157-167, 1961.
- Lubimova, E. A., L. M. Lusova, and F. V. Firsov, Determination of heat flow from the Earth's interior and some results of the measurements, in *Geothermal Research*, edited by E. A. Lubimova (Russian edition), pp. 5-104, USSR Academy of Sciences, Moscow, 1964.
- MacDonald G. J. F., The deep structure of continents, *Science*, **143**, 921-929, 1964.
- Maxwell, A. E., The outflow of heat under the Pacific Ocean, Ph.D. thesis, University of California, 1958.
- Maxwell, A. E., and R. Revelle, Heat flow through the Pacific Ocean Basin, *Publ. Bur. Cent. Seism. Intern. Trav. Sci.*, **19**, 395-405, 1956.
- McBirney, A. R., Conductivity variations and terrestrial heat flow distribution, *J. Geophys. Res.*, **68**, 6323-6329, 1963.
- Menard, H. W., The East Pacific Rise, *Science*, **132**, 1737-1746, 1960.
- Menard, H. W., *Marine Geology of the Pacific*, McGraw-Hill Book Company, New York, 1964.
- Menard, H. W., Sea floor relief and mantle convection, in *Physics and Chemistry of the Earth*, edited by L. H. Ahrens et al., vol. 6, Pergamon Press, London, in press, 1965.
- Misener, A. D., Heat flow and depth of permafrost at Resolute Bay, Cornwallis Island, N.W.T., Canada, *Trans. Am. Geophys. Union*, **36**, 1055-1060, 1955.
- Misener, A. D., L. G. D. Thompson, and R. J. Uffen, Terrestrial heat flow in Ontario and Quebec, *Trans. Am. Geophys. Union*, **32**, 729-738, 1951.
- Mullins, R., and F. B. Hinsley, Measurement of geothermic gradients in boreholes, *Trans. Inst. Mining Engr.*, **117**, 379-393, 1957-1958.
- Nason, R. D., and W. H. K. Lee, Preliminary heat-flow profile across the Atlantic, *Nature*, **196**, 975, 1962.
- Nason, R. D., and W. H. K. Lee, Heat flow measurements in the north Atlantic, Caribbean, and Mediterranean, *J. Geophys. Res.*, **69**, 4875-4883, 1964.
- Newstead, G., and A. Beck, Borehole temperature measuring equipment and the geothermal flux in Tasmania, *Australian J. Phys.*, **6**, 480-489, 1953.
- Ramberg, H., A model for the evolution of continents, oceans and orogens, *Tectonophysics*, **1**, 159-174, 1964.
- Reitzel, J., Some heat-flow measurements in the north Atlantic, *J. Geophys. Res.*, **66**, 2267-2268, 1961a.
- Reitzel, J., Studies of heat flow at sea, Ph.D. thesis, Harvard University, 1961b.
- Reitzel, J., A region of uniform heat flow in the north Atlantic, *J. Geophys. Res.*, **68**, 5191-5196, 1963.
- Revelle, R., and A. E. Maxwell, Heat flow through the floor of the Eastern North Pacific Ocean, *Nature*, **170**, 199-200, 1952.
- Rhea, K., J. Northrop, and R. P. Von Herzen, Heat-flow measurements between North America and the Hawaiian Islands, *Marine Geol.*, **1**, 220-224, 1964.
- Roy, R. F., Heat flow measurements in the United States, Ph.D. thesis, Harvard University, 1963.
- Runcorn, S. K., editor, *Continental Drift*, Academic Press, New York, 1962.
- Sass, J. H., Heat-flow values from the Precambrian shield of Western Australia, *J. Geophys. Res.*, **69**, 299-308, 1964a.
- Sass, J. H., Heat-flow values from eastern Australia, *J. Geophys. Res.*, **69**, 3889-3894, 1964b.
- Sass, J. H., and A. E. LeMarne, Heat flow at Broken Hill, New South Wales, *Geophys. J.*, **7**, 477-489, 1963.
- Saull, V. A., T. H. Clark, R. P. Doig, and R. B. Butler, Terrestrial heat flow in the St. Lawrence lowland of Quebec, *Can. Mining Met. Bull.*, **65**, 63-66, 1962.
- Scheffer, V., The regional values of the geothermic gradient in the area of the Carpathian Basins, *Acta Tech. Acad. Sci. Hung.*, **43**, 429-436, 1963.
- Scheffer, V., The European values of terrestrial heat flow, *Geofis. Meteorol.*, **13**, 99-103, 1964.
- Schmucker, U., Anomalies of geomagnetic variations in the southwestern United States, *J. Geomag. Geoelec.*, **15**, 193-221, 1964.
- Schossler, K., and J. Schwarzlose, Geophysical heat flow measurements (principles and results) (in German), *Freiberger Forschungsh.*, **C**, **75**, *Geophysik*, 120 pp., 1959.
- Sclater, J., private communication, 1964.
- Sisoev, N. N., Geothermal measurement in sediments of the bottom of oceans and seas (in Russian), *Okeanologiya*, **1**, 886-887, 1961.
- Slichter, L. B., Cooling of the Earth, *Bull. Geol. Soc. Am.*, **52**, 561-600, 1941.
- Spicer, H. C., Geothermal gradient at Grass Valley, Calif.: A revision with a note on the flow of heat, *J. Wash. Acad. Sci.*, **31**, 495-501, 1941.
- Spicer, H. C., Observed temperatures in the Earth's crust, *Geol. Soc. Am. Spec. Papers*, **36**, 281-292, 1942.
- Spicer, H. C., Geothermal gradients and heat flow in the Salt Valley anticline, Utah, *Boll. Geofis. Teorica Appl.*, **6**, 263-282, 1964.
- Stenz, E., Deep-well temperatures and geothermal gradient at Ciechocinek, *Geophys. Polon.*, **2**, 159-168, 1954.
- Stocks, T., Für Bodengestalt des Indischen Ozeans, *Erdkunde*, **14**, 161-170, 1960.
- Swartz, J. H., Geothermal measurement on Eni-

- wetok and Bikini Atolls, *Geol. Surv. Prof. Paper 260-U*, 1958.
- Talwani, M., X. Le Pichon, and M. Ewing, Crustal structure of mid-ocean ridges, 2, Computed model from gravity and seismic refraction data, *J. Geophys. Res.*, **70**, 341-352, 1965.
- Uyeda, S., and K. Horai, Studies of the thermal state of the Earth, 6, Terrestrial heat flow at Innai Oil field, Akita Prefecture and at three localities in Kanto-District, Japan, *Bull. Earthquake Res. Inst. Tokyo Univ.*, **38**, 421-436, 1960.
- Uyeda, S., and K. Horai, Studies of the thermal state of the Earth, 7, Terrestrial heat flow measurements in Kanto and Chubu Districts, Japan, *Bull. Earthquake Res. Inst. Tokyo Univ.*, **41**, 83-107, 1963a.
- Uyeda, S., and K. Horai, Studies of the thermal state of the Earth, 8, Terrestrial heat flow measurements in Kinki, Chugoku, and Shikoku Districts, Japan, *Bull. Earthquake Res. Inst. Tokyo Univ.*, **41**, 109-135, 1963b.
- Uyeda, S., and K. Horai, Terrestrial heat flow in Japan, *J. Geophys. Res.*, **69**, 2121-2141, 1964.
- Uyeda, S., K. Horai, M. Yasui, and H. Akamatsu, Heat-flow measurements over the Japan trench, *J. Geophys. Res.*, **67**, 1186-1188, 1962.
- Uyeda, S., T. Yukutake, and I. Tanaoka, Studies of the thermal state of the Earth, 1, Preliminary report of terrestrial heat flow in Japan, *Bull. Earthquake Res. Inst. Tokyo Univ.*, **36**, 251-273, 1958.
- Vacquier, V., and P. T. Taylor, Heat flow and magnetic measurements off Sumatra, in press, 1965.
- Vacquier, V., and R. P. Von Herzen, Evidence for connection between heat flow and the mid-Atlantic ridge magnetic anomaly, *J. Geophys. Res.*, **69**, 1093-1101, 1964.
- Verhoogen, J., Volcanic heat, *Am. J. Sci.*, **244**, 745-771, 1946.
- Verma, R. K., and R. U. M. Rao, Terrestrial heat flow in Kolar gold field, India, *J. Geophys. Res.*, **70**, 1353-1356, 1965.
- Von Herzen, R., Heat-flow values from the south-eastern Pacific, *Nature*, **183**, 882-883, 1959.
- Von Herzen, R. P., Pacific Ocean floor heat flow measurements, their interpretation and geophysical implications, Ph.D. thesis, University of California, 1960.
- Von Herzen, R. P., Geothermal heat flow in the Gulfs of California and Aden, *Science*, **140**, 1207-1208, 1963.
- Von Herzen, R. P., Ocean-floor heat-flow measurements west of the United States and Baja California, *Marine Geol.*, **1**, 225-239, 1964a.
- Von Herzen, R. P., private communication, 1964b.
- Von Herzen, R. P., and M. G. Langseth, Present status of oceanic heat-flow measurements, in *Physics and Chemistry of the Earth*, edited by L. H. Ahrens et al., vol. 6, Pergamon Press, London, in press, 1965.
- Von Herzen, R. P., and A. E. Maxwell, Measurements of heat flow at the preliminary Mohole site off Mexico, *J. Geophys. Res.*, **69**, 741-748, 1964.
- Von Herzen, R. P., and S. Uyeda, Heat flow through the eastern Pacific Ocean floor, *J. Geophys. Res.*, **68**, 4219-4250, 1963.
- Von Herzen, R. P., and V. Vacquier, Heat flow on the Mid-Indian Ocean, *Proc. Roy. Soc. London*, in press, 1965.
- Wang, C., On the distribution of surface heat flows and the second order variations in the external gravitational field, *Res. Space Sci., Spec. Rept.*, **134**, 1-13, Smithsonian Institute Astrophysical Observatory, 1963.
- Wang, C., Figure of the Earth as obtained from satellite data and its geophysical implications, Ph.D. thesis, Harvard University, 1964.
- Wasserburg, G. J., G. J. F. MacDonald, F. Hoyle, and W. A. Fowler, Relative contributions of uranium, thorium, and potassium to heat production in the Earth, *Science*, **143**, 465-467, 1964.
- Wilson, A. F., W. Compston, P. M. Jeffery, and G. H. Riley, Radioactive ages from the Precambrian rocks in Australia, *J. Geol. Soc. Australia*, **6**, 179-195, 1960-1961.
- Yasui, M., K. Horai, S. Uyeda, and H. Akamatsu, Heat flow measurement in the western Pacific during the JEDS-5 and other cruises in 1962 aboard M/S *Ryofu Maru*, *Oceanog. Mag.*, **14**, 147-156, 1963.
- Yasui, M., and T. Watanabe, Studies of the thermal state of the Earth, 16, Terrestrial heat flow in the Japan Sea (I), *Bull. Earthquake Res. Inst. Tokyo Univ.*, **43**, in press, 1965.

(Manuscript received January 25, 1965; revised March 5, 1965.)

## Chapter 7. Geophysical Deductions from Observations of Heat Flow <sup>1</sup>

GORDON J. F. MACDONALD

*Institute of Geophysics and Planetary Physics  
University of California, Los Angeles*

*Abstract.* It is well known that the Earth's surface heat flow is in approximate balance with the heat production in an Earth of chondritic composition. The ratio of  $K/U$  in crustal rocks, peridotite, dunite, and eclogite is about  $1 \times 10^4$ , in contrast to the ratio in chondrites of about  $7.5 \times 10^4$ . Numerical calculations demonstrate that Earth models which have uranium concentration 3 to 4 times that observed in meteorites and with  $K/U = 10^4$  yield the observed heat flow. The computations clearly show that the present heat flow implies melting at depth unless either the thermal conductivity increases substantially with depth or radioactivity is concentrated at depths less than 300 to 400 km.

The general features of temperature-depth curves are similar for many models in which the energy is transmitted by radiation as well as by ordinary lattice conduction. The gradient of temperature is high near the surface but decreases within the Earth as the effective conductivity increases with increasing temperature. The temperature distribution depends sensitively on the parameters chosen. The computations do not attempt to account for the initial temperature gradient, nor are nonradioactive heat sources included.

### 1. INTRODUCTION

Despite advances on many fronts, the distribution of temperature within the Earth remains uncertain, as does the principal mechanism by which heat is transported. At low temperatures, a solid transports heat by ordinary thermal conduction; at higher temperatures, large amounts of heat may be transported by radiation through the optically transparent silicates. However, the combined effects of ordinary conduction plus radiation may be swamped by convection, provided that the material making up the mantle can undergo organized mass motion.

Any theory of the origin of the principal features of the Earth must, in the end, include assumptions or deductions for its thermal history. Since Kelvin's classic investigation, several important studies in which ordinary thermal conduction was assumed to be a principal mechanism for heat transport have been devoted to the determination of the Earth's thermal history. *Holmes* [1915, 1916] first calculated the internal temperature distribution using the measured values of heat generation by radioactivity. He determined that about three-fourths of the heat escaping at the surface is radiogenic and one-

fourth is contributed by the original heat content, supposing that the Earth were originally molten. *Adams* [1924] reexamined *Holmes*' solution and determined temperature distribution for an Earth cooling from a fluid. *Slichter* [1941] studied the steady-state temperature distributions for a number of Earth models. In this work, *Slichter* clearly emphasized the long time scale associated with the diffusion of heat in the Earth and the large thermal inertia of the Earth. *Jacobs and Allan* [1954] carried out detailed numerical calculations taking into account the previously neglected time dependence of radioactive heat production. All these early studies demonstrate that the temperature distribution that will emerge from calculations will depend on the choice of parameters. Our knowledge of certain of these parameters, radioactive content of rocks, and surface heat flow has improved greatly in the last decade, but the difficulties of estimating temperatures within the Earth remain.

In the present chapter, we will consider the major factors which influence the internal distribution of temperature. It is useful to discuss the problem in terms of the development of the temperature distribution from a set of initial conditions. In addition to the initial conditions, we require the distribution of heat sources within the Earth, and the radial variation of such

<sup>1</sup> Publication 396 of the Institute of Geophysics and Planetary Physics, University of California, Los Angeles.

parameters as thermal conductivity, heat capacity, and density.

The framing of the discussion about the initial value problem for the development of the internal temperature is a convenient way of illustrating the interplay between certain of the variables that enter into the determination of the internal temperature. Proceeding in this fashion, however, does not imply that conduction and radiation are the sole mechanisms for heat transport.

Calculations provide estimates of the present-day distribution of temperature and surface heat flux if, indeed, conduction plus radiative transfer is the principal mechanism for the transport of heat. Predictions can then be compared with observations. In addition to the requirement of the observed heat flow, there is also the fact that the outer mantle of the Earth is solid. The present distribution of temperature must, therefore, lie below the melting point of matter making up the mantle. The melting points of multi-component silicate systems at high temperatures and pressures are still unknown, but preliminary data for simple systems allow a crude assessment.

In the next section, evidence on the radioactivity of the Earth is reviewed. The review includes a discussion of the observed ratios of radioactive isotopes in terrestrial materials. Rather broad limits to the concentration of  $K^{40}$  within the Earth are set by the abundance of argon in the atmosphere, and the relevant data regarding the argon and helium within the Earth are examined. The limit to the internal temperature is placed by the melting point gradient within the Earth. Active studies of the variation of melting temperatures with pressure in multi-component silicate systems are underway in a number of laboratories, and preliminary results suggest a lower melting temperature than was previously accepted.

In section 3 the mechanism of heat transport within silicates is discussed, and some general statements are made about the possibility of large-scale, mantle-wide convection. The section ends with the consideration of detailed calculations of surface heat flow and internal temperature distribution based on arbitrary, but perhaps reasonable, models of the internal distribution of radioactivity.

## 2. OBSERVATIONAL EVIDENCE ON RADIOACTIVITY

### 2.1 *Radioactivity of the Earth*

The radioactivity of the Earth manifests itself in the outward flow of heat at the Earth's surface. Initial heat, present since the formation of the Earth, may also contribute to the heat flow, and the heat flow may lag behind heat production; thus, the observed heat flow does not uniquely determine either the current production of heat or the internal concentration of radioactivity.

Radioactive isotopes that have produced significant amounts of heat over geologic time are distinguished by two characteristics: the product of the isotopic abundance and the rate of heat production is relatively large, and the half-life of the isotope is of the same order as the age of the Earth. The known isotopes that meet the two requirements are  $U^{238}$ ,  $U^{235}$ ,  $Th^{232}$ , and  $K^{40}$ . A number of workers [MacDonald, 1959, 1961, 1963; Clark, 1961] have based calculations of the thermal history on the assumption that the abundance of radioactive isotopes within the Earth equals that of chondritic meteorites. The concentrations used by MacDonald are  $U = 1.1 \times 10^{-8}$  g/g,  $Th = 4 \times 10^{-8}$  g/g,  $K = 8 \times 10^{-4}$  g/g.

A number of arguments have been proposed in support of the assumption that the Earth has a chondritic composition. These arguments include the rough agreement of chondritic abundances with solar abundances, the consistency of the meteoritic model of the Earth's interior with seismic evidence, the rough uniformity of chemical composition of many chondrites (although the carbonaceous chondrites show a wide range of composition), and the approximate equality of surface heat flow and the present rate of heat generation in a chondritic Earth. This last argument is usually given most weight. If the entire Earth is made up of chondrites, and if the heat currently produced is reaching the surface, the heat flow would average  $1.42 \mu\text{cal}/\text{cm}^2 \text{ sec}$ . If only the mantle were of chondritic composition, the heat flow would be  $0.96 \mu\text{cal}/\text{cm}^2 \text{ sec}$ . A recent analysis of terrestrial heat flow gives an average heat flow of about  $1.53 \mu\text{cal}/\text{cm}^2 \text{ sec}$  [Lee and MacDonald, 1963]; a current review of heat flow observations is given in chapter 6, by Lee and Uyeda, in this volume. Initial heat and the higher rate of heat production in the

past both tended to raise the heat flow above the current rate of heat production, whereas a deep burial of heat sources tends to lower surface heat flow below the current heat production. Despite the considerable uncertainties, there is a striking coincidence between the heat flow and the heat production in a chondritic Earth.

*Gast* [1960] and, more recently, *Tilton and Reed* [1963], *Wasserburg et al.* [1964], and *Urey* [1964] question the validity of the chondritic Earth model. *Gast* noted that the concentrations of potassium (also rubidium and cesium) in the Earth's crust were anomalous when compared with uranium (also barium and strontium) for a chondritic Earth model. *Gast* suggests that either the bulk radioactivity of the Earth differs from that of chondrites, or there is an extensive differentiation in which uranium (also strontium and barium) is concentrated in the crust relative to potassium (also rubidium and cesium). Such a differentiation of uranium from potassium is difficult to interpret in terms of current understanding of silicate chemistry, though there may be undiscovered effects of extreme pressures on differentiation. The observations of *Gast* require a higher K/U ratio in the mantle material than in crustal rocks.

*Hoyle and Fowler* [1964] propose that the uranium content of the solar system and, in particular, of the Earth, differs from that of chondrites. Arguing from a nuclear theory of the origin of elements, *Hoyle and Fowler* require a uranium (and thorium) concentration some three or four times greater than that found in chondrites. Their estimate depends on the manner in which the abundance of the elements synthesized by the  $r$  process are normalized relative to the standard element, silicon. Their normalization is based on a comparison of the calculated abundances with those observed in meteorites for elements between Te and Yb.

*Hoyle and Fowler* thus presume that the meteoritic abundances of elements between Te and Yb (also Os, Ir, and Pt) are representative of solar system material, while the uranium and thorium contents of meteorites are not. A further uncertainty in the *Hoyle and Fowler* argument is the time of galactic nucleosynthesis, which they set at  $7.7 \times 10^9$  years. The present Th abundance (Th mean-life =  $20.1 \times 10^9$  years) does not depend sensitively on the choice of the time scale, but the abundances of  $U^{238}$

and  $U^{235}$  do. *Hoyle and Fowler* leave open the question of the abundance of  $K^{40}$ , since they argue that this isotope was produced at the time of the origin of the solar system, rather than in the galactic nucleosynthesis, and therefore may well have had a different fractionation history than did  $K^{39}$  and  $K^{41}$ .

The observed concentrations of uranium, thorium, and potassium in terrestrial materials range widely; however, the ratios of potassium to uranium and of thorium to uranium in a great variety of rocks exhibit rather constant values (see Table 1). Data on the radioactivities of rocks have been summarized by *Wasserburg et al.* [1964]. Within a magmatic differentiation series, in which the bulk composition changes, the ratio of potassium to uranium remains relatively constant. Studies by *Adams* [1954] on a series of volcanic rocks from the Lassen volcanic area show a remarkable constancy in the K/U ratio. The differentiates of the Duluth lopolith have been studied by *Heier and Rogers* [1963], who show that the total range of the K/U ratio is  $0.5 \times 10^4$  to  $4 \times 10^4$ , with only 2 samples in 22 having a ratio greater than  $2 \times 10^4$ . The rocks in the lopolith range from anorthosites and gabbros to granophyres. The rocks of the southern California batholith also show a constancy in the K/U ratio [*Heier and Rogers*, 1963; *Rogers and Ragland*, 1961; *Whitfield et al.*, 1959].

In addition to these studies of differentiation series, there are numerous analyses of various rock types. *Nockolds* [1954], *Senftle and Keevil* [1947], and *Evans and Goodman* [1941] report a large number of results. In a summary of 755 granites, *Heier and Rogers* [1963] report a mean K/U ratio of  $0.8 \times 10^4$ . They also find a ratio of  $1.4 \times 10^4$  for basalts. *Tilton and Reed* [1963] and *Heier* [1963] have analyzed eclogites from igneous and metamorphic environments. They did not find any samples with a K/U ratio greater than  $2.5 \times 10^4$ , and the average ratio calculated from their results is  $1.2 \times 10^4$ . The only reliable measurements of uranium in ultramafic rock are those reported by *Tilton and Reed*. However, the uranium was undetectable on one sample for which potassium was measured.

Values of the average potassium, uranium, and thorium content of chondrites, achondrites, and terrestrial rocks are shown in Table 1. The

TABLE 1. Heat Production in Rocks

Rock	Average Concentration, parts per million			K/U	Average Total Heat Production, $\times 10^{-8}$ cal/g yr
	Uranium	Potassium	Thorium		
Granite <sup>a</sup>	4.75	37,900	18.5	$8.0 \times 10^3$	810
Intermediate <sup>b</sup>	2.0	18,000		$9.0 \times 10^3$	340
Basalt <sup>a</sup>	0.6	8,400	2.7	$1.4 \times 10^4$	119
Eclogite <sup>c, d, e</sup>					
Low uranium	0.048	360	0.18	$7.4 \times 10^3$	8.1
High uranium	0.25	2,600	0.45	$1.0 \times 10^4$	34.0
Peridotite <sup>c</sup>	0.016	12		$7.5 \times 10^3$	0.91
Dunite <sup>c</sup>	0.001	10		$1.0 \times 10^4$	0.19
Chondrites <sup>f</sup>	0.012	845	0.0398	$2.0 \times 10^4$	3.94

<sup>a</sup> Heier and Rogers [1963].

<sup>b</sup> Evans and Goodman [1941], Senftle and Keevil [1947].

<sup>c</sup> Tilton and Reed [1963].

<sup>d</sup> Heier [1963].

<sup>e</sup> Lovering and Morgan [1963].

<sup>f</sup> Wasserburg et al. [1964].

K/U ratio for terrestrial rocks is relatively constant for samples ranging in uranium concentration from  $4.8 \times 10^{-8}$  g/g to  $4.75 \times 10^{-6}$  g/g. For chondrites, the average value of  $1.1 \times 10^{-8}$  g/g, obtained by Hamaguchi et al. [1957], is probably to be preferred.

The relative constancy of the K/U ratio obtained in the wide variety of chemically distinct igneous rock in magmatic differentiation series provides a good estimate of the K/U ratio for the Earth, and indicates that this value may be distinctly lower than that of chondrites. Alternatively, it may be supposed that the Earth is indeed of chondritic composition, but that the crust and upper mantle have undergone marked differentiation. However, this hypothesis supposes an unknown mechanism for the differentiation.

## 2.2 Argon in the Atmosphere

The high ratios of  $\text{Ar}^{40}/\text{Ar}^{36}$  and  $\text{Ar}^{40}/\text{Ar}^{38}$  in the Earth's atmosphere imply that the majority of the argon came from the decay of  $\text{K}^{40}$ . The total abundance of argon in the atmosphere,  $1.93 \times 10^{23}$  atoms/cm<sup>2</sup>, can be used to provide a rough estimate of the potassium content of the Earth. If all the gas produced by the decay of  $\text{K}^{40}$  were, at present, reaching the surface, then

the present flux of argon should be  $2.7 \times 10^5$  atoms/cm<sup>2</sup> sec, if the average K content of the mantle and crust were  $10^{-4}$  g/g. The relatively short half-life of  $\text{K}^{40}$  means that 4.5 aeons ago (1 aeon =  $10^9$  years) argon was produced at about 11 times the present rate, so that the average flux of argon over geologic time would be  $1.1 \times 10^6$  atoms/cm<sup>2</sup> sec. If all the argon produced reached the surface, the present argon content of the atmosphere would be  $1.5 \times 10^{23}$  atoms, or about 20% less than the observed abundance. If the average K content were  $3 \times 10^{-4}$  g/g, then, on the average, 1 out of 2.3 argon atoms has reached the surface. On a chondritic mantle hypothesis, only 1 out of 7 argon atoms has escaped from the mantle.

The average rate of escape of argon from the crust-mantle can be used to estimate the present  $\text{He}^4$  flux into the atmosphere. An average mantle concentration of U of  $3 \times 10^{-8}$  g/g ( $\text{Th}/\text{U} = 3.7$ ) produces helium at the rate of  $4.8 \times 10^6$   $\text{He}^4$  atoms/cm<sup>2</sup> sec. If the release of helium by the crust and mantle equals that of argon, then  $2 \times 10^6$   $\text{He}^4$  atoms/cm<sup>2</sup> sec are entering the atmosphere. The ratio of  $\text{He}^4$  to argon entering the atmosphere in this model of radioactivity is 5.7, and this ratio is independent of the uranium concentration for a fixed K/U ratio.

Measurements of natural gases [Zartman *et al.*, 1961] showed that the He/Ar ratio varies from 2 to 200, a value of about 10 being the most frequent. Wasserburg *et al.* [1963] conclude that the ratio of the present flux of helium to argon lies between 2 and 20, so that a model mantle with an average U content greater than about  $1.2 \times 10^{-8}$  g/g and with  $K/U = 10^4$  is consistent with the observed ratio of  $He^4/Ar$  in natural gases and with the total Ar abundance of the atmosphere.

### 2.3 Melting Relations at High Pressures

Seismic evidence of the solid nature of the mantle provides an important restriction on the possible thermal conditions at depth. In earlier considerations of temperatures at depth, MacDonald [1959] assumed that the melting curve of diopside indicated the highest temperature that could be reached within the upper mantle. The material in the upper mantle is undoubtedly chemically more complex than diopside and, in a multi-component silicate system, melting will take place at temperatures lower than those of simpler systems. Melting relations for such possible constituents as peridotite and dunite have not been investigated at high pressures, but Yoder and Tilley [1962] reported an important investigation on the melting of basalt and eclogite at pressures up to 30,000 bars. They found that in the pressure range 1–14 kb eclogite is transformed into basalt or gabbro before melting begins, and eclogite so transformed would, of course, melt in the same fashion as basalt or gabbro. Above 19 kb the two major minerals of eclogite, garnet and clinopyroxene, begin melting together and coexist with the liquid over most of the narrow melting range of about 85°C. The liquidus temperature rises at a rate of about 11°C/kb. The tentative melting curve obtained by Yoder and Tilley [1962] is shown in Figure 1, where their results are linearly extrapolated from 30 to 70 kb. There are no experimental data in the pressure range 14–19 kb.

Boyd and England [1963] have determined the melting point of diopside at pressures up to 50 kb. The melting curve they obtained is extrapolated by use of the Simon equations to 70 kb in Figure 1.

The melting relations shown in Figure 1 illustrate the range of possibilities in the upper

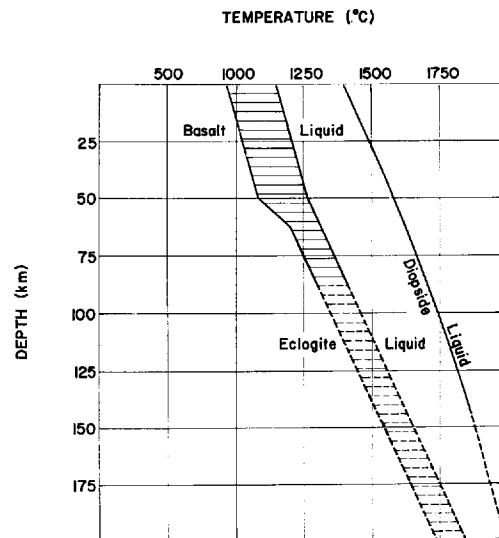


Fig. 1. Approximate melting relations for basalt-eclogite and diopside within the upper mantle. The basalt-eclogite melting relations are taken from Yoder and Tilley [1962]. Their experimental results extend to 30 kb and have been linearly extrapolated. The diopside melting curve is after Boyd and England [1963]. Experimental data yield values to 50 kb, and the extrapolation has been on the basis of the Simon equation.

mantle. If the mantle is predominantly olivine-pyroxene, rather than garnet-pyroxene, then the melting curve will lie at temperatures above the eclogite melting curve but probably below the diopside fusion curve.

### 2.4 Surface Heat Flows

Lee and MacDonald [1963] analyzed more than 900 measurements of surface heat flow. An orthogonal function representation of 757 values yields a global mean of  $1.53 \pm 0.08$   $\mu\text{cal}/\text{cm}^2 \text{ sec}$ . The average over continents is 1.65  $\mu\text{cal}/\text{cm}^2 \text{ sec}$ , while the oceanic average is 1.48  $\mu\text{cal}/\text{cm}^2 \text{ sec}$ . These averages are about 25% greater than those Birch derived [1954] using 65 determinations.

On an equilibrium basis, the mean value of surface heat flow can be accounted for by an average heat production through the crust or mantle of  $1.93 \times 10^{-15}$  cal/g sec. For the terrestrial ratios,  $K/U = 1 \times 10^4$  and  $Th/U = 3.7$ , the combined rate of heat production due to these three elements is  $5.47 \times 10^{-8}$  cal/sec per gram of uranium. Hence, the mean uranium

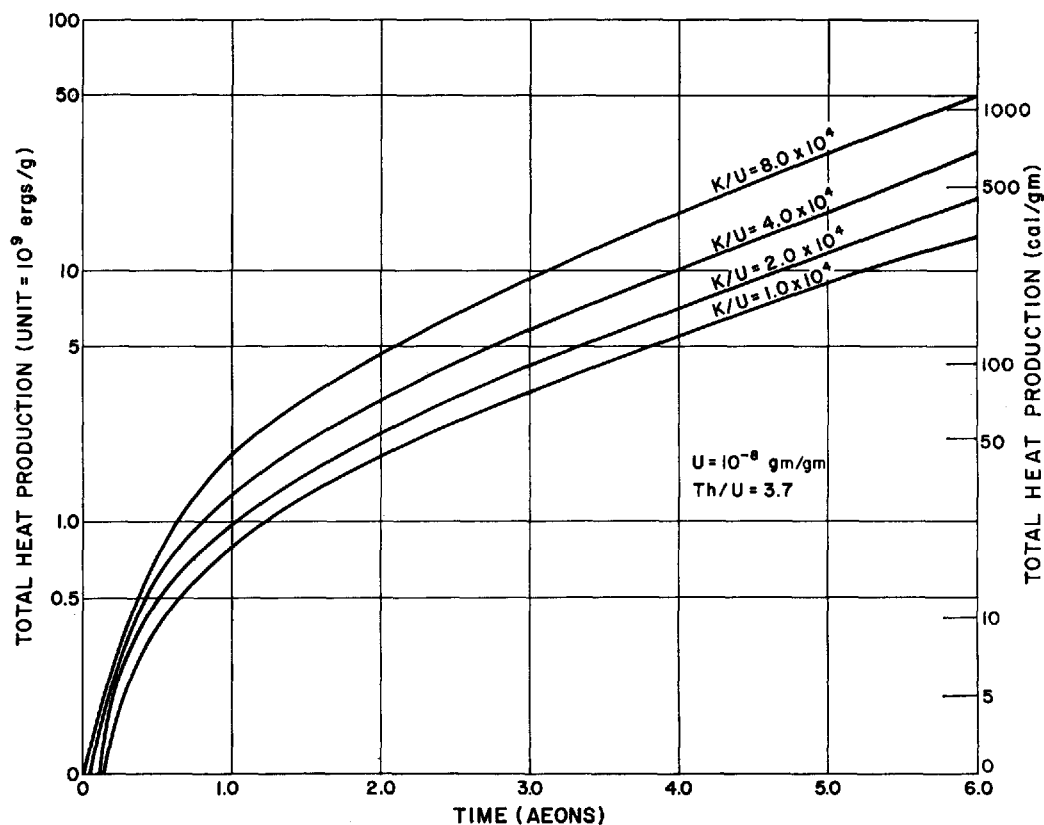


Fig. 2. The integrated heat production for various ratios of potassium to uranium. The uranium concentration is taken to be  $1.0 \times 10^{-8}$  g/g, Th/U = 3.7.

content of the crust and mantle required to produce an equilibrium heat flow equal to the observed value is  $3.52 \times 10^{-8}$  g/g. If the heat flow lags behind the heat production, the heat production in the past might be a more appropriate value to compare with the present heat flow. With the terrestrial ratios of K/U and Th/U, the K production per gram of uranium, 1 and 2 aeons ago, is  $6.06 \times 10^{-8}$  cal/sec and  $6.86 \times 10^{-8}$  cal/sec, respectively. If the average lag in heat flow is 1 aeon, the average crust and mantle concentration of U required for the present heat flow is  $3.18 \times 10^{-8}$  g/g; for a time lag of 2 aeons, the required concentration is  $2.81 \times 10^{-8}$  g/g.

If the contribution of initial heat to the surface heat flow is small, the current heat flow is consistent with an average concentration of uranium of 2.5 to  $3.5 \times 10^{-8}$  g/g. Still higher average concentrations of uranium are per-

mitted, provided that the radioactivity is buried sufficiently deep for the rate of heat loss to be low. Figure 2 illustrates the total heat production in 1 gram of material having a present concentration of U of  $1.0 \times 10^{-8}$  g/g, a Th/U ratio of 3.7, and various ratios of K/U. The total heat production more than 4.5 aeons for a material in which  $U = 1.0 \times 10^{-8}$  g/g,  $K/U = 10^4$  is 17.2 cal/sec. Assuming a heat capacity of 0.31 cal/g °C, the above concentration of radioactivity will raise the temperature of the material 553°C over 4.5 aeons. A concentration of U of  $3 \times 10^{-8}$  g/g would then produce an increase of temperature of 1565°C over 4.5 aeons, if there were no heat losses. This can be compared with a temperature increase of 1900°C produced by a chondritic concentration of radioactivity.

The above considerations imply that a substantial amount of radioactivity can be buried at

depth without producing melting, provided that the initial temperature of aggregation is sufficiently low. The melting temperature of silicates in the deep mantle may be of the order of 2500°C (see Figure 1). If the initial temperature were 1000°C, then the heat produced by a concentration of U of  $3 \times 10^{-8}$  g/g would be sufficient, over 4.5 aeons, to raise the solid material just to the melting point.

### 2.5 Interpretation of Continent-Ocean Heat Flow

Radioactive heat production of rocks exposed at or near the surface in continents and ocean basins differs greatly. If heat flows through the continental surface and ocean bottoms are approximately equal, the consequent differences in vertical distribution of radioactive materials requires quantitative assessment [Bullard, 1954]. Let us suppose that the values for intermediate rock listed in Table 1 represent the heat production in the continental crust. The heat production within the crust is then about 1.1  $\mu\text{cal}/\text{cm}^2$  sec. If the range of values included in the intermediate rock category is examined, then the heat production might lie between 0.72 and 1.43  $\mu\text{cal}/\text{cm}^2$  sec. Since the continental heat flow is about 1.6  $\mu\text{cal}/\text{cm}^2$  sec, the heat flowing from below a depth of 30–40 km is between 0.2 and 0.9  $\mu\text{cal}/\text{cm}^2$  sec. In the ocean, the material above 35 km produces heat at a rate of about 0.07–0.12  $\mu\text{cal}/\text{cm}^2$  sec, provided that the volcanic material in the ocean basins is basalt, the sediments have a radioactivity of intermediate rock, and subcrustal material is eclogite or peridotite. A flux in oceanic regions of 1.5  $\mu\text{cal}/\text{cm}^2$  sec implies that between 1.3 and 1.4  $\mu\text{cal}/\text{cm}^2$  sec must be flowing from the interior into the region above 35 km. The difference in flux between continents and oceans at a depth of 35 km is then between 0.41 and 1.2  $\mu\text{cal}/\text{cm}^2$  sec. Even when we take the extreme limits of error in the values of heat production and heat flow as a basis of calculation, we find a considerable difference in the amount of heat flowing into the crust beneath land and sea. The difference in outward heat flow at a depth of 35 km implies deep-seated differences in temperatures under continents and oceans [MacDonald, 1963, 1964].

## 3. THERMAL CONDITIONS OF THE EARTH'S INTERIOR

### 3.1 Calculation of Internal Thermal Conditions

The internal thermal state of the Earth can be investigated by assuming an initial temperature distribution, a distribution of heat sources, and a distribution with depth of such parameters as density, heat capacity, thermal conductivity, and opacity. The temperature at the outer surface is assumed to be constant with time. The rate of heat flow from the interior is about 20,000 times less than that arriving from the sun when it is overhead. The temperature of the surface is, therefore, controlled by the sun and not by the heat-producing radioactive elements. Given the initial temperature distribution, the problem is then to determine the temperature distribution at later times. The equation governing the development of the temperature field is

$$\frac{\partial T}{\partial t} = -\frac{1}{\rho c_p} [\nabla \cdot (K \nabla T) + A] - \mathbf{v} \cdot \nabla T \quad (1)$$

where

$\rho$  is specific density,  $\text{g}/\text{cm}^3$ .

$c_p$  is heat capacity at constant pressure,  $\text{cal}/\text{g}^\circ\text{C}$ .

$K$  is thermal conductivity,  $\text{cal}/\text{cm} \text{ sec } ^\circ\text{C}$ .

$A$  is rate of heat production,  $\text{cal}/\text{cm}^3 \text{ sec}$ .

$\mathbf{v}$  is velocity,  $\text{cm}/\text{sec}$ .

The term containing thermal conductivity is a measure of the heat flux in and out of a unit volume.  $A$  is the rate at which heat is produced within the unit volume by radioactivity and is a function both of the position coordinate and of time, because of the slow decay of the radioactive elements. If a radioactive element is producing heat at a rate  $dQ/dt$  today, it produced heat at a rate  $e^{\lambda t} x dQ/dt$  at a time  $T$  years ago, where  $\lambda$  is the disintegration constant of the radioactive element.

The term involving the velocity on the right-hand side of (1) is the time rate of change of temperature resulting from the advection of heat into the unit volume. It is this last term which couples the thermal equation to the equations of motion. The problem is much simplified if this term can be neglected. If large-scale horizontal convection takes place in the mantle, this term dominates the thermal transport. We consider the possibility of large-scale horizontal con-

vection in the next section. The mantle may behave more or less elastically, with magma transporting heat vertically. At present, it is seen that the transport of heat by penetrative convection of magma is relatively small compared with the outward heat flow due to finite conductivity. Estimates of the rate at which lava is presently deposited on the surface vary considerably. *Kuenen* [1950] suggests a value of about 1 km<sup>3</sup> per year. The total heat loss by 1 gram of lava crystallizing and cooling from 1000° to 0°C is about 400 cal/g. Of this, 100 cal/g comes from the latent heat and 300 cal/g comes from the specific heat. The average contribution of a cubic kilometer of lava to the surface heat flow is only 0.007 μcal/cm<sup>2</sup> sec. The contribution of lava poured on the surface to the total heat flow is thus completely negligible if the estimate of a cubic kilometer per year is relevant. An alternative estimate follows from assuming that the total mass of the crust has, at one time or another, arrived at the surface as fresh lava. For a crustal mass of  $2.45 \times 10^{25}$  grams, produced in a time of 4.5 aeons, the average rate of addition is  $5.4 \times 10^{15}$  g/year compared with the estimate of  $3 \times 10^{15}$  g/year discussed by *Kuenen*. Though the global contribution of volcanic activity is negligible, local volcanic activity can dominate and lead to an abnormally high heat flow in the vicinity. In heat flow studies, volcanic regions are avoided in continental areas, but the sampling of the ocean floor is more nearly random.

For an elastic mantle, the advective term is small, since ordinary thermal expansion leads to small velocity, and  $\mathbf{v} \cdot \nabla T$  is small compared with  $A/\rho c_p$  [*MacDonald*, 1963].

### 3.2 Thermal Conductivity of Silicates

*Birch and Clark* [1940] showed that the thermal conductivity of a wide variety of rocks showed surprisingly small variation with composition. Recent measurements at room temperature further establish the narrow variation of conductivity with composition [*Clark and Niblett*, 1956; *Birch*, 1950]. The temperature dependence of conductivity has not been thoroughly explored experimentally. *Birch and Clark* measured conductivities up to 600°C and found that conductivities of poor conductors, such as feldspar and quartz, increase with tem-

perature, whereas the conductivities of most materials decrease slightly as the temperature increases. No experimental studies have been carried out on the variation of conductivity with pressure. To a good approximation, the mean thermal conductivity of rocks is 6 mecal/cm sec °C.

At high temperatures, energy may be transferred within the solid by radiation rather than by lattice vibrations. *Clark* [1957] shows that the contribution of radiation to thermal conductivity is approximated by

$$K_R = 16n^2sT^3/3\epsilon \quad (2)$$

In this expression,  $n$  is the effective index of refraction of the material,  $s$  is the Stefan-Boltzman constant,  $\epsilon$  is the sum of the absorption and scattering coefficients averaged over all wavelengths, and  $T$  is the temperature in degrees Kelvin. The striking feature of the contribution of radiation to conductivity is the strong temperature dependence. The higher the temperature, the greater will be the energy transfer by radiation, provided that the variation of index of refraction and opacity do not overwhelm the  $T^3$  dependence.

The opacity  $\epsilon$  and the index of refraction are determined by the properties of the material, and, in general, will be functions of temperature and pressure. The variation of index of refraction of a given material with pressure has not been investigated experimentally. An estimate can be made by noting that, for materials of different composition, the index varies linearly with density. If a law of corresponding states holds, then the index should vary linearly with pressure. Within the mantle, density varies from about 3.3 to 5.7 g/cm<sup>3</sup>, so that over the mantle of the Earth a variation by a factor of 2 would be expected, the material at depth having a higher index of refraction than at the Earth's surface.

The rate at which radiation is transferred through a solid depends on the frequency of the radiation. Various mechanisms are known by which solids can absorb radiation, and these become important at different frequencies. Absorption due to excitation of lattice vibrations by the radiation is strong in the infrared. This lattice absorption is relatively unimportant, since at high temperatures the energy density is low at these long wavelengths. Intrinsic absorp-

tion is due to the excitation of valence electrons to the conduction band across the fundamental energy gap. Intrinsic absorption is important in the ultraviolet for wavelengths less than about 0.4 micron. The transparency of silicates to radiation is thus limited at long wavelengths by the infrared absorption due to lattice vibrations, and at short wavelengths by the absorption in the ultraviolet due to the excitation of electrons to the conduction band.

The region of high transparency in silicates lies in the visible to near infrared. This is not true for a semiconductor, such as silicon or germanium, which is opaque in the visible. Because of the lower energy gap, the absorption edge in these materials lies at much longer wavelengths than in silicates. Within the visible and near infrared regions of transparency, two processes can lead to absorption. Characteristic absorption peaks are associated with the presence of transition elements. The energy levels of the unfilled electron shells are split by the crystalline field, and certain transitions between these split levels are allowed. These transitions lead to characteristic absorption bands of the transition elements. In silicates, the most important transition element is iron, which has a strong absorption peak at about one micron. Titanium, manganese, and other elements will give rise to absorption bands.

Absorption between the peaks determines the contribution of the radiation to thermal conductivity. If there is one perfectly transparent region, then the material has an infinite thermal conductivity. The general level of absorption between absorption bands limits the energy transported by radiation. This general absorption is primarily due to free electrons. In the classical theory, free electrons will absorb at all wavelengths. The dependence of the opacity  $\epsilon$  on the electrical conductivity is given by  $60 \pi \sigma / n$ , where both the electrical conductivity  $\sigma$  and the index of refraction  $n$  vary with frequency. If we assume that the dc electrical conductivity is a sufficiently good approximation, the variation of opacity with temperature can be written as

$$\epsilon = \epsilon_0 + (60 \pi \sigma_0 / n) \exp(-E/kT) \quad (3)$$

where  $\epsilon_0$  is the opacity at low temperatures, and where the second term on the right-hand side takes into account the temperature dependence

of the conductivity, and  $E$  is the characteristic excitation energy.

Most estimates of the contribution of radiation to thermal conductivity are based on the determination of the absorption spectrum, rather than on actual measurements. In a few cases, the measurement of the spectrum can be made as a function of temperature. These indicate the closing off at high temperatures of the region of transparency for materials containing transition elements. The opacities found by Clark for different materials varied considerably among silicate minerals, but olivine and pyroxene showed opacities of less than  $10 \text{ cm}^{-1}$ .

### 3.3 Convection

The principal uncertainty, in addition to that connected with the radioactivity of the Earth, is the problem of whether or not large-scale mantle convection transports appreciable amounts of heat. Recently, *Knopoff* [1964] suggested that mantle-wide convection is unlikely because the inhomogeneity in Bullen's region *C* is large enough to prevent the convection; this conclusion holds, whether or not the inhomogeneity is due to a phase transition or to chemical inhomogeneity. However, convection still may be important in the upper mantle.

*MacDonald* [1963] has argued against large-scale horizontal convection in the upper mantle, on the basis of both continental structure and the mechanical properties of the mantle. Gravity observations, coupled with observations of heat flow, clearly indicate that differences between continents and oceans extend to depths on the order of hundreds of kilometers. This conclusion is substantiated by studies of surface wave dispersion, which show that there are differences between surface waves that travel predominantly oceanic paths and those that travel predominantly continental paths. If, indeed, continental structure extends to depths of the order of hundreds of kilometers, it is difficult to imagine large-scale horizontal motion. Horizontal convection extending to near the surface would tend to homogenize the upper mantle and destroy differences between continent and ocean structure. This objection to upper mantle convection is emphasized by considerations of the thermal time scale; the thermal time scale for a layer 500 km thick is of the order of  $10^9$  years

or longer, depending on the efficiency of radiative transfer [MacDonald, 1959]. The long time scale implies that the presently observed differences between continents and oceans have persisted for times on the order of  $10^9$  years.

A further obstacle to mantle-wide convection is posed by observations of the mechanical properties of the mantle. As Runcorn [1962] has properly emphasized, the anelasticity observed at high frequencies and small amplitudes has little application to problems connected with mantle convection. Gravity observations provide data on the mechanical response of the mantle to deformations with a time scale of  $10^7$  years and with large amplitudes. The result is that, if one wishes to assume an elastoviscous material, the mantle must have a viscosity on the order of  $10^{26}$  egs [MacDonald, 1963]. This viscosity is so high that, in order to drive the convection currents, a heat flow an order of magnitude larger than that observed would be required. Alternatively, the inequality in figure, as determined from satellite observations, may represent the disequilibrium response of material with a creep strength of 100 to 200 bars. The mechanics of convection in such a material, which departs so widely from Newtonian viscosity, remain very uncertain.

#### 3.4 Calculation of Heat Flow as a Function of Radioactivity

Lubimova [1958], MacDonald [1959, 1961], and Clark [1961] have made detailed calculations on the development of temperature within a spherically symmetrical Earth. MacDonald [1963] has extended these calculations, taking into account the differing distributions of heat sources under continents and oceans. Before considering two-dimensional calculations, several general features of the spherically symmetrical calculations should be noted. The principal effect of the radiative transfer of energy on the distribution of temperature is the flattening of the temperature gradient with depth. Because of the contribution from radiation, the temperature required to remove heat from the deep interior decreases as the conductivity increases with temperature. Near the surface, the temperature gradient is dependent only on the lattice conductivity of the solid and the near-surface distribution of heat sources. For a wide variety of

models of the Earth, a near-surface gradient of 10–20°C/km results. Since the temperature gradients are greatest near the surface, the melting temperatures are most closely approached in the outer few hundred kilometers of the Earth.

The effects of the variation of the total radioactivity on the Earth's internal field have been investigated in a number of numerical models. The numerical techniques are those employed by MacDonald [1963] in the study of the effects of a nonsymmetrical heat source distribution on the temperature within the Earth. The equation governing the transfer of heat is

$$b(r) \frac{\partial T(r, \theta, t)}{\partial t} = \frac{1}{r^2} \frac{\partial}{\partial r} \left[ r^2 K(r, \theta) \frac{\partial T(r, \theta, t)}{\partial r} \right] + \frac{1}{r^2 \sin \theta} \frac{\partial}{\partial \theta} \left[ \sin \theta K(r, \theta) \frac{\partial T(r, \theta, t)}{\partial \theta} \right] + A(r, \theta, t) \quad (4)$$

where  $b = \rho c_p$ . The density  $\rho$  is assumed to depend only on the radial coordinates, and, in the numerical calculations discussed below, the density variation is taken to be that given in Bullen's Model A [Bullen, 1953]. The conductivity  $K$  contains both a term due to radiation and a term due to lattice conduction.

Of the quantities appearing in (4), the most uncertain is the production term  $A$ ; it is the term which, in the long run, determines the distribution of temperature and the surface heat flow. In the following, three vertical distributions of heat sources will be investigated. In one set, the radioactivity is uniformly distributed throughout the mantle with no upward differentiation; this is the uniform model. A second, intermediate distribution assumes a concentration of radioactivity in the upper 1500 km of the Earth, with a greater concentration above 465 km. In this oceanic structure, the uranium content of the upper 465 km is 18 times as great as that of the lower region. The third vertical distribution of radioactivity investigated models a continental structure. In this structure, all the radioactivity is concentrated in the upper 1500 km, with a concentration below 465 km equal to that of the oceanic structure. A second region extends from 465 to 45 km, and the concentration in this region equals 3.29 times the concentration of uranium in the region 465–1500 km. In all models,  $K/U = 1.0 \times 10^4$  and  $Th/U = 3.7$ , and there is no vertical differentia-

TABLE 2. Description of Vertical Distribution of Heat Sources Employed in Model Calculations  
 $K/U = 1 \times 10^4$ ,  $Th/U = 3.7$

Model	Distribution of Heat Sources
Uniform	Uniform concentration by weight of U
Oceanic	All radioactivity above 1500 km $\frac{U(1500 - 465 \text{ km})}{U(465 - 0 \text{ km})} = 18.2$
Continental	All radioactivity above 1500 km $U(1500 - 465 \text{ km}) : U(465 - 45 \text{ km}) : U(45 - 0 \text{ km}) = 1 : 3.29 : 40.0$

tion of potassium with respect to uranium. The vertical distribution of heat sources is summarized in Table 2.

### 3.5 Initial Temperature Distribution

We assume that the initial temperature distribution can influence, in a substantial way, the present heat flow and internal temperature distribution. As an example, we consider a chondritic mantle radioactivity concentrated in the outer 1500 km. The mass in the outer 1500 km is  $2.3 \times 10^{27}$  grams, so that, on the average, the heat produced per gram for the radioactivity concentrated in this region is  $9.4 \times 10^2$  cal/g, with a heat capacity of 0.31 cal/g °C. An increase in the average temperature of 1000° requires 310 cal/g. The initial heat resulting from an average temperature of 100°C is then one-third of the heat produced by the chondritic radioactivity. If the heat flow were influenced by the heat sources distributed to the depth of 1500 km, then heat flow might vary as much as 30% if the average initial temperature is changed by 1000°C. Detailed calculations carried out by *MacDonald* [1959, 1961] show that the initial temperature, if averaged about 1500°C, contributes about 15-20% of the present heat flow. The initial temperature thus plays an important, but not dominating, role in determining the subsequent evolution of the temperature field of surface heat flow.

In all the calculations discussed below, the initial temperature is assumed to increase linearly from 0°C at the surface to 1000°C at a depth of 600 km, and to remain at 1000° to the center of the Earth.

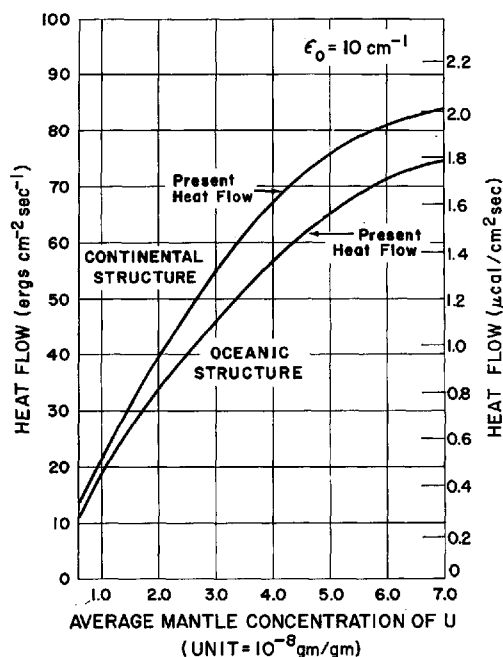


Fig. 3. The variation of heat flow with average mantle concentration of uranium. The opacity is  $10 \text{ cm}^{-1}$ ,  $K/U = 1.0 \times 10^4$ ,  $Th/U = 3.7$ .

### 3.6 Dependence of Heat Flow on Radioactivity

The dependence of the present surface heat flow on the average mantle concentration of uranium is shown in Figures 3-5 for varying vertical distributions of heat sources and different opacities. Figure 3 illustrates the variation of heat flow with uranium concentration for an oceanic and a continental structure having an opacity of  $10 \text{ cm}^{-1}$ . The present oceanic heat flow is about  $1.48 \text{ } \mu\text{cal/cm}^2 \text{ sec}$ , so that, on the basis of the model, a uranium concentration of

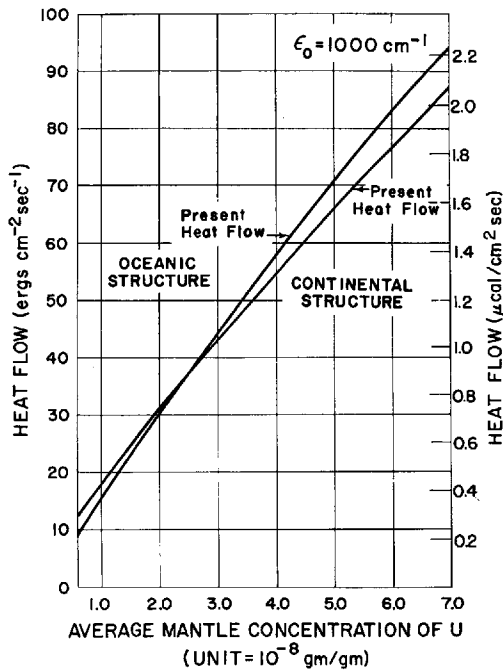


Fig. 4. The variation of heat flow with the average mantle concentration of uranium. The opacity is uniform and equal to  $1000 \text{ cm}^{-1}$ ,  $K/U = 1.0 \times 10^4$ ,  $\text{Th}/U = 3.7$ .

$4.6 \times 10^{-8} \text{ g/g}$  yields the observed heat flow. The present continental heat flow of about  $1.65 \text{ } \mu\text{cal}/\text{cm}^2 \text{ sec}$  can be explained on the basis of this model, provided that the uranium concentration is  $4.2 \times 10^{-8} \text{ g/g}$ . It should be noted that in these models there is a difference of about  $0.24 \text{ } \mu\text{cal}/\text{cm}^2 \text{ sec}$  between the continental and oceanic heat flow, the continental heat flow being larger for concentrations of uranium greater than  $4 \times 10^{-8} \text{ g/g}$ . This result differs from that obtained by MacDonald [1963]. In MacDonald's models, a chondritic radioactivity is assumed, and there is a differentiation of potassium relative to uranium, with the potassium concentrated toward the outer layers, rather than the uniform ratio of the two elements assumed in the present models. In addition, MacDonald used an initial temperature averaging about  $500^\circ$  greater than the initial temperature used in the present calculations.

A comparison of Figure 4 with Figure 3 illustrates the effect of radiative transfer on the present heat flow. In the models represented in Figure 4, the opacity is  $1000 \text{ cm}^{-1}$ , so that the

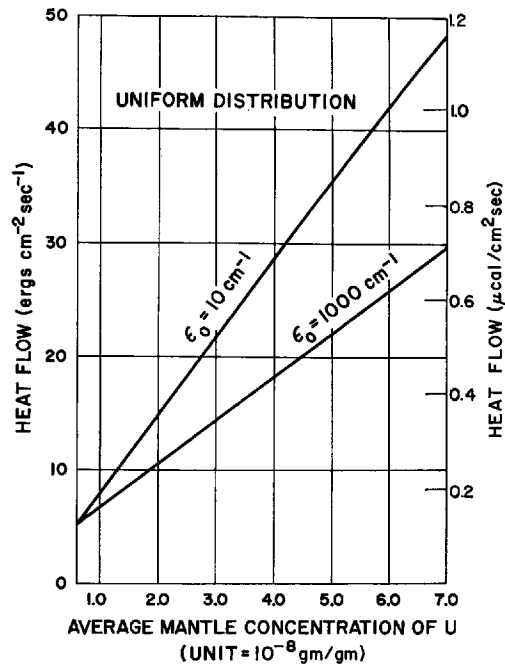


Fig. 5. The variation of heat flow with average mantle concentration of uranium. The heat sources are uniformly distributed throughout the mantle.  $K/U = 1.0 \times 10^4$ ,  $\text{Th}/U = 3.7$ .

contribution of radiative transfer to the conductivity is negligible. In this case, the heat flow in the oceanic areas exceeds that of a continental structure. In the continental structure, the near-surface concentration of the heat sources permits the near-surface heat to escape readily, and there is little contribution from the deeply buried radioactivity because of the low conductivity. For  $\epsilon_0 = 1000 \text{ cm}^{-1}$ , a concentration of uranium of  $4.3 \times 10^{-8} \text{ g/g}$  is required to explain the oceanic heat flow, while the continental heat flow requires a concentration of uranium of  $5.3 \times 10^{-8} \text{ g/g}$ .

Figure 5 shows the variation of heat flow for a uniform distribution of heat sources throughout the mantle and for two values of the opacity. At an average concentration of uranium of  $5.0 \times 10^{-8} \text{ g/g}$ , the heat flow, if radiation makes no contribution to the conductivity, is  $0.57 \text{ } \mu\text{cal}/\text{cm}^2 \text{ sec}$ , while an opacity of  $10 \text{ cm}^{-1}$  increases the heat flow to  $0.85 \text{ } \mu\text{cal}/\text{cm}^2 \text{ sec}$ .

The variation of heat flow with time for an oceanic structure with an opacity equal to  $10 \text{ cm}^{-1}$  is shown in Figure 6. The variation with

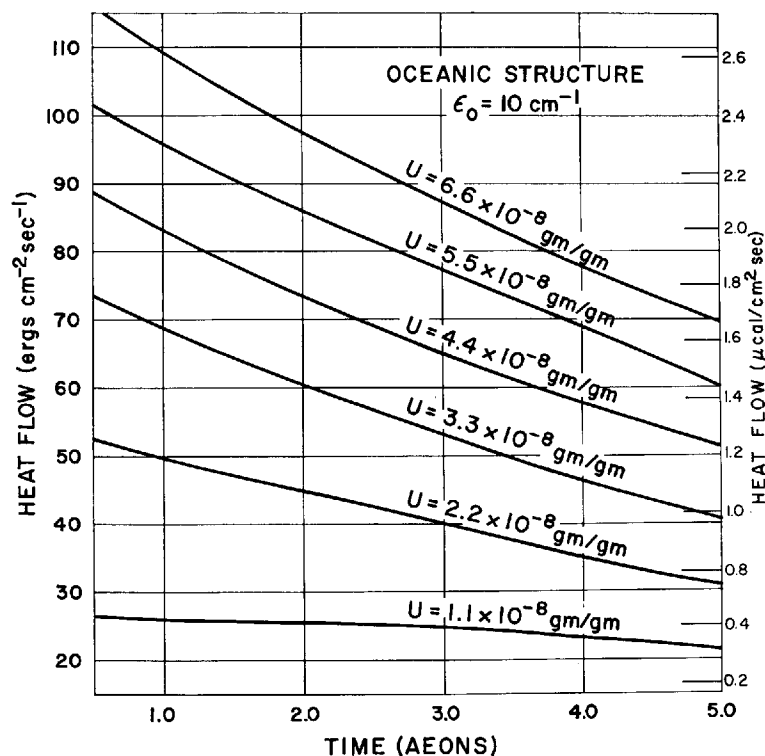


Fig. 6. The variation with time of the surface heat flow for various concentrations of uranium. The structure is oceanic, and the opacity is  $10 \text{ cm}^{-1}$ .  $K/U = 1.0 \times 10^4$ ,  $\text{Th}/U = 3.7$ .

time of the heat flow for a continental structure is shown in Figure 7. A comparison of Figures 6 and 7 demonstrates that continents lose heat at a much greater rate than do oceanic regions, particularly during the early stages. The rate of heat production per unit area is the same under continental and oceanic structure. As a result of the greater heat loss of the continental structure, the temperature at depths under the continental structure will be lower than temperatures under oceanic crust.

Figures 8 and 9 show the development of the heat flow with time for oceanic and continental structures, provided that radiation makes no contributions to the conductivity. In the early stages, the heat flow increases with time, and the amount of heat loss over time in these models is less than in the case where the radiative conductivity makes an important contribution. As a result, the internal temperature for these models will be considerably higher than when radiation permits heat to escape. The variation of heat flow with time for a uniform mantle con-

centration of radioactivity is shown in Figures 10 and 11. The heat flow is much less than in the case where radioactivity is concentrated near the surface. As a result, the final internal temperatures are much higher.

### 3.7 Internal Temperature Distribution

The variation of temperature with depth under continental and oceanic structure is shown in Figure 12 for a uranium abundance of  $3.3 \times 10^{-8} \text{ g/g}$ . The maximum temperatures reached are in the oceanic structure, where they are of the order of  $1800^\circ\text{C}$ . The temperatures under the continental structure are lower, with a maximum of about  $1500^\circ\text{C}$ . In the calculation, a zero flux boundary condition is used over the surface of the sphere at a depth of 1500 km. This implies that additional radioactivity can be buried at depth without perturbing the surface conditions. If the initial temperature were  $1000^\circ\text{C}$  at depth, then the radioactivity needed to raise the temperature at depth to  $1800^\circ\text{C}$  under oceans or  $1500^\circ\text{C}$  under continents would

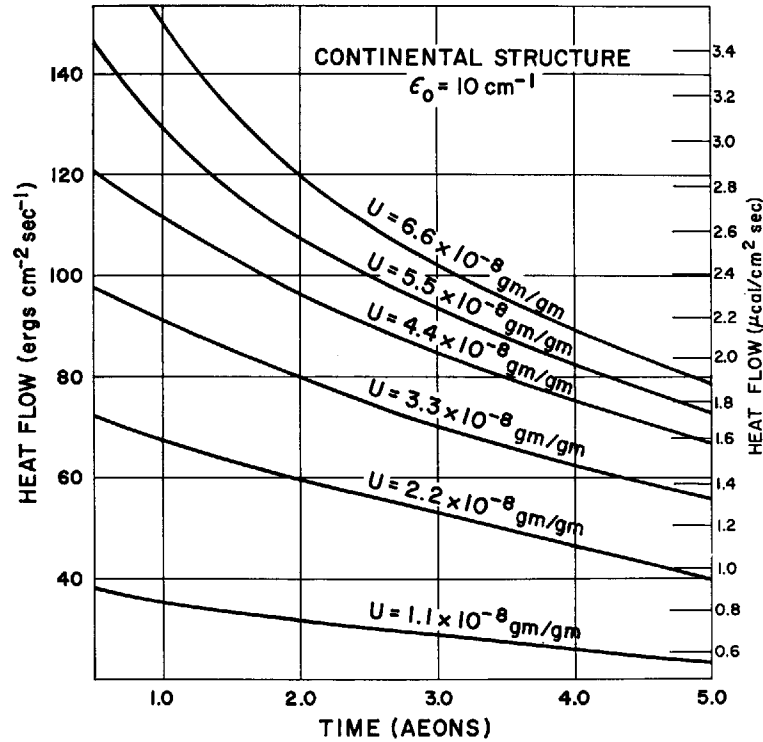


Fig. 7. The variation with time of the surface heat flow for a continental structure. The opacity is  $10 \text{ cm}^{-1}$ ,  $K/U = 1.0 \times 10^4$ ,  $\text{Th}/U = 3.7$ .

be  $1.4 \times 10^{-8} \text{ g/g}$  and  $0.87 \times 10^{-8} \text{ g/g}$  of U, respectively. These concentrations, equal to 24 and 15% of the corresponding concentrations above the 1500-km level, could exist at depths greater than 1500 km without disturbing the temperature distribution in the upper few hundred kilometers.

The drastic effects of radiation on the temperature distribution are illustrated by comparing Figures 13 and 12. In Figure 13, the average uranium concentration is taken to be  $3.3 \times 10^{-8} \text{ g/g}$ , with an opacity of  $1000 \text{ cm}^{-1}$ . The maximum temperature reached under the oceanic structures is of the order of  $3000^\circ\text{C}$ , while temperatures reach only  $2000^\circ\text{C}$  under the continental areas. This large difference between temperatures under continents and oceans and the high average temperature reflect the lower rate of outward heat flow in the oceanic regions over geologic time. Temperatures reached under the oceanic regions far exceed the melting temperature of materials, as illustrated in Figure 1.

The effect of raising the average content of

radioactivity on the internal temperature distribution is illustrated by comparing Figure 14 and Figure 12. In Figure 14, the temperature is shown as a function of depth for a model in which the opacity is  $10 \text{ cm}^{-1}$ . Maximum temperatures reached under the oceans are about  $1000^\circ\text{C}$ , while the maximum temperature under continental areas is  $250^\circ\text{C}$  less. Under oceans, a temperature of  $1000^\circ\text{C}$  is reached at a depth of 88 km if the uranium content is  $3.3 \times 10^{-8} \text{ g/g}$ . If the uranium concentration is raised to  $5.5 \times 10^{-8} \text{ g/g}$ , then a  $1000^\circ\text{C}$  isotherm under oceans is reached at a depth of 58 km. The radial distributions of temperature under oceanic areas are compared with the melting temperature in Figure 15. For a uranium content of  $3.3 \times 10^{-8} \text{ g/g}$ , the temperature lies well below the melting temperature. At a concentration  $5.5 \times 10^{-8} \text{ g/g}$ , the melting region is intersected at a depth of 110 km. It should be noted (see Figure 3) that the concentration of uranium required to equal the heat flow in oceanic areas is  $4.6 \times 10^{-8} \text{ g/g}$ . At this concentration, the melt-

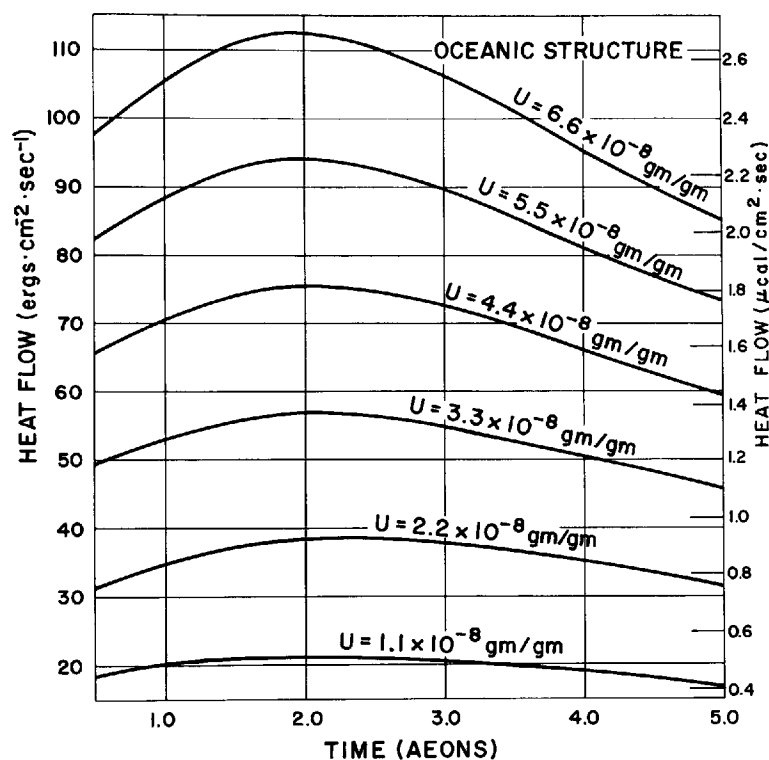


Fig. 8. The variation with time of the surface heat flow for an oceanic structure. The opacity is  $1000 \text{ cm}^{-1}$ ,  $K/U = 1.0 \times 10^4$ ,  $\text{Th}/U = 3.7$ .

ing region shown in Figure 15 would be approached but not exceeded.

#### 4. SUMMARY

The near coincidence of the rate of heat production of a chondritic Earth and the present-day heat flow cannot be used as a unique argument in favor of a chondritic model for the Earth [Wasserburg *et al.*, 1964]. The calculations described above clearly show that radioactive compositions other than that of chondritic meteorites yield surface heat flows and internal temperature distributions compatible with observations. Using terrestrial ratios for the radioactive isotopes, models in which radioactivity is concentrated in the upper 1500 km give the observed heat flow, provided that the average uranium content of the mantle is between  $4$  and  $5 \times 10^{-8} \text{ g/g}$ . An average mantle concentration in excess of  $5.5 \times 10^{-8} \text{ g/g}$  will yield internal temperature distributions in which the melting temperature is exceeded, provided that the

radioactivity has the radial distribution given by the oceanic model. There is a dependence of these results on the assumed initial temperature distribution, which in the models was taken to be  $1000^\circ\text{C}$  at 600 km. A higher initial temperature would require lower radioactive abundances, so that the present temperature would not exceed the melting temperature.

The calculations also illustrate the importance of radiation in transferring heat. If radiative transfer is not effective, then the temperatures required to produce the present surface heat flows are far in excess of the melting temperatures. The marked near-surface concentration of radioactivity (continental model) is sufficient to lower the internal temperatures below the melting point. The fact that the radioactivity must be buried at depth under oceanic areas, and yet the melting temperature is not exceeded, argues strongly for the importance of radiation as a mechanism by which heat is transported. However, a concentration of radioactivity under oceans intermediate to the continent and ocean

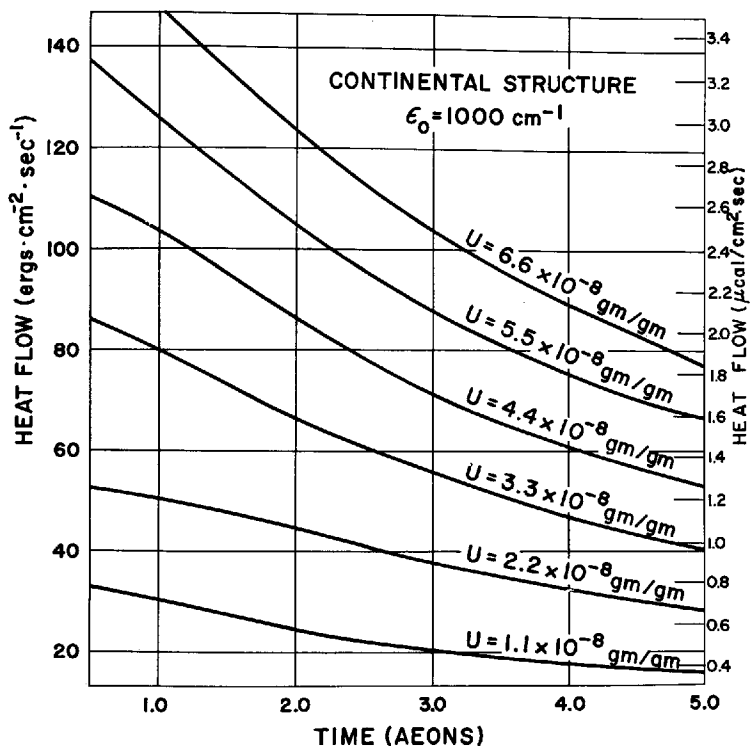


Fig. 9. The variation of heat flow with time for a continental structure. The opacity is  $1000 \text{ cm}^{-1}$ ,  $K/U = 1.0 \times 10^4$ ,  $\text{Th}/U = 3.7$ .

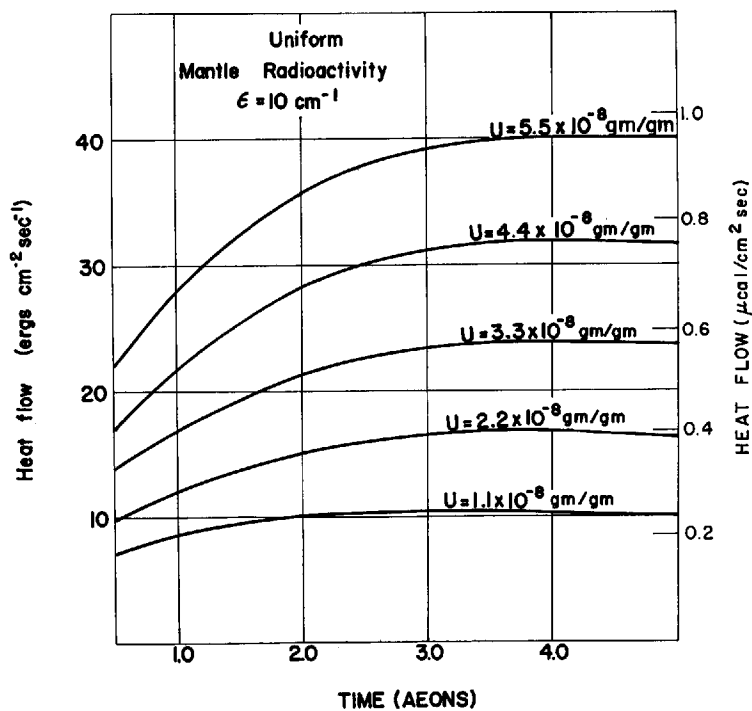


Fig. 10. The variation with time of heat flow for a mantle with a uniform concentration of radioactivity. The opacity is  $10 \text{ cm}^{-1}$ ,  $K/U = 1.0 \times 10^4$ ,  $\text{Th}/U = 3.7$ .

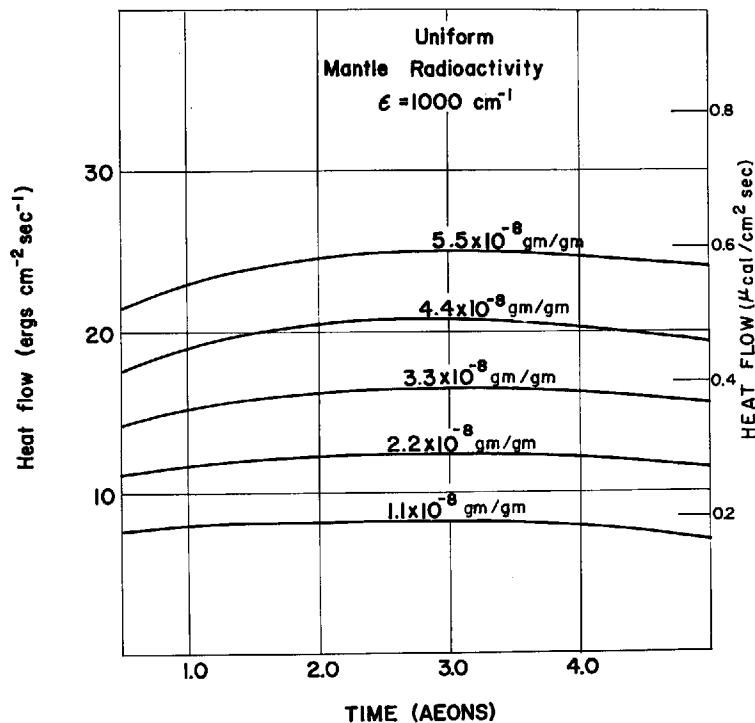


Fig. 11. The variation of heat flow with time for a mantle having a uniform concentration of radioactivity. The opacity is  $1000 \text{ cm}^{-1}$ ,  $K/U = 1.0 \times 10^4$ ,  $\text{Th}/U = 3.7$ .

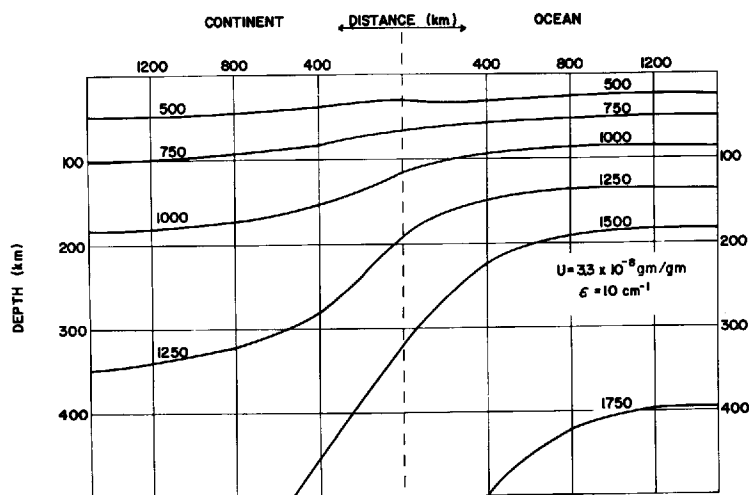


Fig. 12. Internal distribution of temperatures under oceans and continents for a mantle having an average concentration of uranium of  $3.3 \times 10^{-8} \text{ g/g}$ . The opacity is  $10 \text{ cm}^{-1}$ .

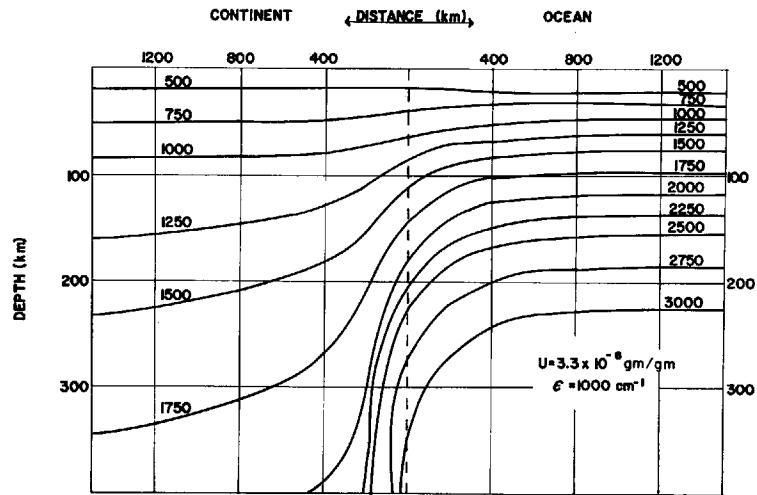


Fig. 13. The radial distribution of temperature under continental and oceanic structure. The uranium concentration is  $3.3 \times 10^{-8} \text{ g/g}$ . The opacity is  $1000 \text{ cm}^{-1}$ .

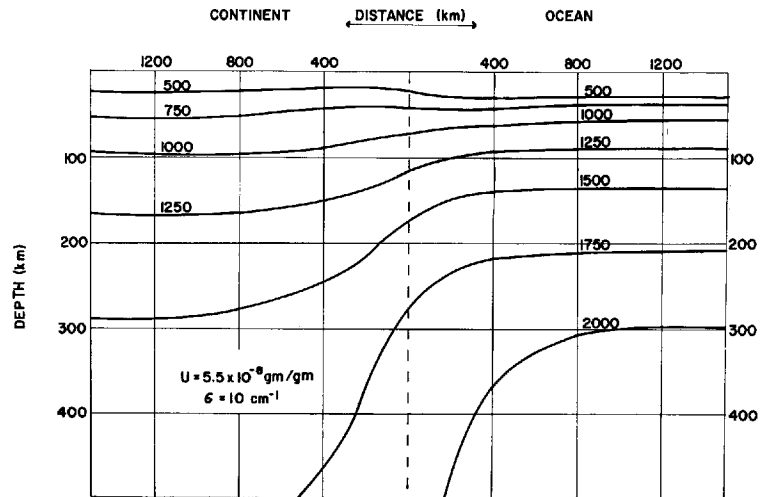


Fig. 14. The radial distribution of temperature under continents and oceans. The uranium concentration is  $5.5 \times 10^{-8} \text{ g/g}$ . The opacity is  $10 \text{ cm}^{-1}$ .

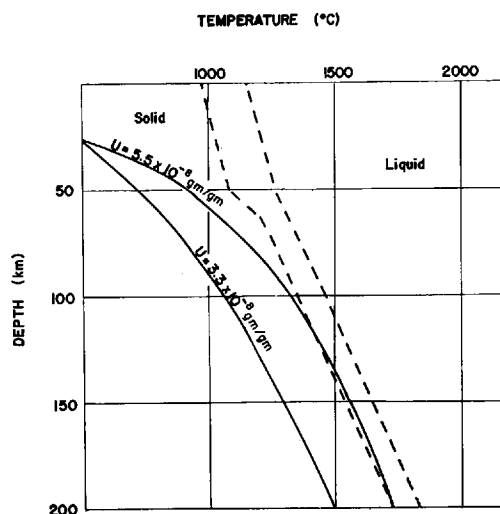


Fig. 15. The vertical temperature distribution for an oceanic structure at uranium concentrations of  $3.3 \times 10^{-8}$  g/g and  $5.5 \times 10^{-8}$  g/g. The dashed lines correspond to the melting relations for basalt and eclogite [Yoder and Tilley, 1962].

model would lead to temperatures lower than the melting temperature.

Hoyle and Fowler [1964] suggest a value of the uranium concentration in the mantle of  $5.6 \times 10^{-8}$  g/g, corresponding to about  $3.6 \times 10^{-8}$  g/g for the whole Earth. In Figures 14 and 15, we note that such a concentration in an oceanic structure will not give rise to severe difficulties with the melting curve. The heat flow resulting from such a concentration is  $1.62 \mu\text{cal}/\text{cm}^2 \text{ sec}$  for an oceanic structure, and  $1.86 \mu\text{cal}/\text{cm}^2 \text{ sec}$  for a continental structure. Both these values are somewhat in excess of those observed. However, as has been noted, it would be possible to construct a model in which sufficient radioactivity is concentrated in the upper 1500 km to provide the observed heat flow, and in which additional radioactivity is buried at greater depths. For example, let the uranium concentration in the upper 1500 km equal  $7.9 \times 10^{-8}$  g/g, which is equivalent to  $4.5 \times 10^{-8}$  g/g for the mantle as a whole. The concentration in the lower mantle would then have to be  $2.7 \times 10^{-8}$  g/g for the total mantle to have an average concentration of uranium of  $5.6 \times 10^{-8}$  g/g. A concentration of  $2.6 \times 10^{-8}$  g/g in the lower mantle would produce  $2.6 \times 1.7 \times 10^2 \text{ cal/g}$ , which, with a heat capacity of  $0.31 \text{ cal/g } ^\circ\text{C}$ , will in-

crease the temperature by  $1440^\circ\text{C}$  over 4.5 aeons. If the initial temperature were as low as  $1000^\circ\text{C}$ , then the temperature at depth in the Hoyle-Fowler model would be  $2440^\circ\text{C}$ . From the presently available experimental melting relations, it is uncertain whether the deep burial of radioactivity would produce melting. It is thus seen that it may be possible to accommodate the Hoyle-Fowler radioactivity within the Earth, provided that the initial temperature of aggregation is low and that radiation makes an important contribution to thermal conductivity. This last condition is not necessary. A distribution in which the concentration of radioactivity toward the surface is intermediate between that of the continental and oceanic structures would be compatible with the postulated melting curves.

*Acknowledgments.* I wish to thank Dr. L. H. Adams and Dr. L. B. Slichter for their kind criticisms of the manuscript.

#### REFERENCES

- Adams, J. A. S., Uranium and thorium content of volcanic rocks, in *Nuclear Geology*, edited by H. Fall, pp. 89-98, John Wiley & Sons, New York, 1954.
- Adams, L. H., Temperatures at moderate depths within the Earth, *J. Wash. Acad. Sci.*, **14**, 459-472, 1924.
- Birch, F., The flow of heat in the Front range, Colorado, *Geol. Soc. Am. Bull.*, **61**, 567-630, 1950.
- Birch, F., The present state of geothermal investigations, *Geophysics*, **19**, 645-659, 1954.
- Birch, F., and H. Clark, The thermal conductivity of rocks and its dependence upon temperature and composition, *Am. J. Sci.*, **238**, 529-558 and 613-635, 1940.
- Boyd, F. R., and J. L. England, Effects of pressure on the melting of diopside,  $\text{CaMgSi}_2\text{O}_6$ , and albite,  $\text{NaAlSi}_3\text{O}_8$ , in the range up to 50 kilobars, *J. Geophys. Res.*, **68**, 311-324, 1963.
- Bullard, E. C., The flow of heat through the floor of the Atlantic Ocean, *Proc. Roy. Soc. London*, **A**, **222**, 408-429, 1954.
- Bullen, K. E., *An Introduction to the Theory of Seismology*, Cambridge University Press, London, 1953.
- Clark, S. P., Absorption spectra of some silicates in the visible and near infrared, *Am. Mineral.*, **42**, 732-742, 1957.
- Clark, S. P., Heat flow from a differentiated Earth, *J. Geophys. Res.*, **66**, 1231-1234, 1961.
- Clark, S. P., and E. R. Niblett, Terrestrial heat flow in the Swiss Alps, *Monthly Notices Roy. Astron. Soc., Geophys. Suppl.*, **7**, 176-195, 1956.

- Evans, R. D., and C. Goodman, Radioactivity of rocks, *Geol. Soc. Am. Bull.*, *52*, 459-490, 1941.
- Gast, P. W., Limitations on the composition of the upper mantle, *J. Geophys. Res.*, *65*, 1287-1297, 1960.
- Hamaguchi, H., G. W. Reed, and A. Turkevich, Uranium and barium in stoney meteorites, *Geochim. Cosmochim. Acta*, *12*, 337-347, 1957.
- Heier, K. S., Uranium, thorium, and potassium in eclogitic rocks, *Geochim. Cosmochim. Acta*, *27*, 849-860, 1963.
- Heier, K. S., and J. J. Rogers, Radiometric determination of thorium, uranium, and potassium in basalts and in two magmatic differentiation series, *Geochim. Cosmochim. Acta*, *27*, 137-154, 1963.
- Holmes, A., Radioactivity in the Earth and the Earth's thermal history, *Geol. Mag.*, *2*, 60-71 and 102-112, 1915.
- Holmes, A., Radioactivity in the Earth's thermal history, *Geol. Mag.*, *3*, 265-274, 1916.
- Hoyle, F., and W. A. Fowler, On the abundance of uranium and thorium in solar system material, in *Isotopic and Cosmic Chemistry*, North-Holland Publishing Company, Amsterdam, 1964.
- Jacobs, J. A., and D. W. Allan, Temperatures and heat flow within the Earth, *Trans. Roy. Soc. Can.*, *48*, 33-39, 1954.
- Knopoff, L., The convection current hypothesis, *Rev. Geophys.*, *2*, 89-122, 1964.
- Kuenen, P. H., *Marine Geology*, John Wiley & Sons, New York, 1950.
- Lee, W. H. K., and G. J. F. MacDonald, The global variation of terrestrial heat flow, *J. Geophys. Res.*, *68*, 6481-6492, 1963.
- Lovering, J. F., and J. W. Morgan, Uranium and thorium abundance in possible upper mantle materials, *Nature*, *197*, 138-140, 1963.
- Lubimova, E. A., Thermal history of the Earth with consideration of the variable thermal conductivity in the mantle, *Geophys. J.*, *1*, 115-134, 1958.
- MacDonald, G. J. F., Calculations on the thermal history of the Earth, *J. Geophys. Res.*, *64*, 1967-2000, 1959.
- MacDonald, G. J. F., Surface heat flow from a differentiated Earth, *J. Geophys. Res.*, *66*, 2489-2493, 1961.
- MacDonald, G. J. F., The deep structure of continents, *Rev. Geophys.*, *1*, 587-665, 1963.
- MacDonald, G. J. F., The deep structure of continents, *Science*, *143*, 921-929, 1964.
- Nockolds, S. R., Average chemical compositions of some igneous rocks, *Bull. Geol. Soc. Am.*, *65*, 1007-1032, 1954.
- Rogers, J. J., and P. C. Ragland, Variation of thorium and uranium in selected granitic rocks, *Geochim. Cosmochim. Acta*, *25*, 99-109, 1961.
- Runcorn, S. K., Towards a theory of continental drift, *Nature*, *193*, 311-314, 1962.
- Senftle, F. E., and N. B. Keevil, Thorium-uranium ratios in the theory of genesis of lead ores, *Trans. Am. Geophys. Union*, *28*, 732-738, 1947.
- Slichter, L. B., Cooling of the Earth, *Bull. Geol. Soc. Am.*, *52*, 561-600, 1941.
- Tilton, G. R., and G. W. Reed, Radioactive heat production in eclogite and some ultramafic rocks, in *Earth Science and Meteoritics*, pp. 31-44, North-Holland Publishing Company, Amsterdam, 1963.
- Urey, H. C., A review of atomic abundances in chondrites and the origin of meteorites, *Rev. Geophys.*, *2*, 1-34, 1964.
- Wasserburg, G. J., E. Mazor, and R. E. Zartman, Isotopic and chemical composition of some terrestrial natural gases, in *Earth Science and Meteoritics*, pp. 219-240, North-Holland Publishing Company, Amsterdam, 1963.
- Wasserburg, G. J., G. J. F. MacDonald, F. Hoyle, and W. A. Fowler, The relative contributions of uranium, thorium and potassium to heat production in the earth, *Science*, *143*, 465-467, 1964.
- Whitfield, J. M., J. J. Rogers, and J. A. S. Adams, The relationship between the petrology and the thorium and uranium contents of some granitic rocks, *Geochim. Cosmochim. Acta*, *17*, 248-271, 1959.
- Yoder, H. S., and C. Tilley, Origin of basalt magmas, an experimental study of natural and synthetic rock systems, *J. Petrol.* *3*, 342-532, 1962.
- Zartman, R. E., G. J. Wasserburg, and J. H. Reynolds, Helium, argon, and carbon in some natural gases, *J. Geophys. Res.*, *66*, 277-306, 1961.

(Manuscript received June 1, 1964; revised September 8, 1964.)

## Chapter 8. Physical Processes in Geothermal Areas

JOHN W. ELDER

*Institute of Geophysics and Planetary Physics  
University of California, San Diego*

*Abstract.* The role of the movement of water and, to a lesser extent, magma in the flow of heat within the Earth, primarily in or just below the crust, is considered. The surface distribution of heat flow shows two major regions: normal areas, covering more than 99% of the surface, with heat flux of  $1.5 \mu\text{cal}/\text{cm}^2 \text{ sec}$ ; and thermal areas, in which the heat flux is an order of magnitude or more greater. Models based on radioactive heat transferred by thermal conduction and radiation give an adequate description of normal areas. In thermal areas, it is necessary to invoke mass transfer. At the surface, the heat flow is discharged as radiation, by warming the ambient air or water, or as water vapor produced by flashing or by evaporation at the water table. The water-vapor mechanism predominates in land thermal areas. Specific reference is made to the Tuscan steam zone of Italy. Beneath land thermal areas, a body of freely circulating hot water is identified and discussed in terms of convection in a porous medium. Such a hydrothermal system can transfer heat several orders of magnitude faster than thermal conduction. Model experiments are compared with the Taupo hydrothermal systems of New Zealand. Thermal areas derive their energy from sources at depth. It is suggested that these sources arise from the upper mantle by penetrative convection. Within the lower mantle a highly disordered free convective motion is envisaged. The great unknown is the rheological nature of the mantle.

### 1. INTRODUCTION

The purpose of this chapter is to consider possible convective mechanisms within the Earth, especially those responsible for thermal areas, and to discuss in the light of available observations those mechanisms that are probable.

Our direct knowledge of heat flow within the Earth is limited to the surface distribution of heat flux, the form of which is summarized schematically in Figure 1. More detailed information is given by Lee and Uyeda in chapter 6 of this volume. The ocean ridge schematic follows the measurements in the eastern Pacific given by Bullard [1963] and Von Herzen and Uyeda [1963]. The land thermal area schematic follows measurements made in New Zealand by Thompson [1960].

Two distinct regions can be recognized:

1. Normal areas, covering more than 99% of the Earth's surface, are those in which the heat flux lies in the range 0 to  $3 \mu\text{cal}/\text{cm}^2 \text{ sec}$ , with an average of about  $1.5 \mu\text{cal}/\text{cm}^2 \text{ sec}$  [Lee, 1963]. The vertical temperature gradient is nearly constant to depths exceeding 1 km, and the surface heat flux variations are gradual, usu-

ally being negligible over distances of the order of 1 km.

2. Thermal areas are those in which the heat flux can reach  $10^5 \mu\text{cal}/\text{cm}^2 \text{ sec}$ , though it is generally much smaller, with possible average values of the order of  $10^2 \mu\text{cal}/\text{cm}^2 \text{ sec}$  over areas of the order of  $10^3 \text{ km}^2$ . Large horizontal variations of heat flux and vertical variations of vertical temperature gradient are possible over distances of 1 meter.

A schema—not to be taken too literally—of the various convective systems to be considered is shown in Figure 2. The diagrams cover a range of length scales from 0.1 to  $10^3 \text{ km}$ : (a) mantle convection, (b, c) penetrative convection in the upper mantle and crust, (d) surface volcanism, especially in relation to convection of water, and (e) surface discharge in thermal areas by flow of water and steam.

In section 2 we investigate the mechanisms by which heat is lost from the Earth. Only the upper  $10^2$  meters or so need be considered, it being assumed at this stage that the matter and energy are supplied from a limitless reservoir at depth (see Figure 2e). On land the bulk of the energy from normal areas is lost as radiation or by slight warming of the air, but in thermal areas the bulk of the energy is transported as

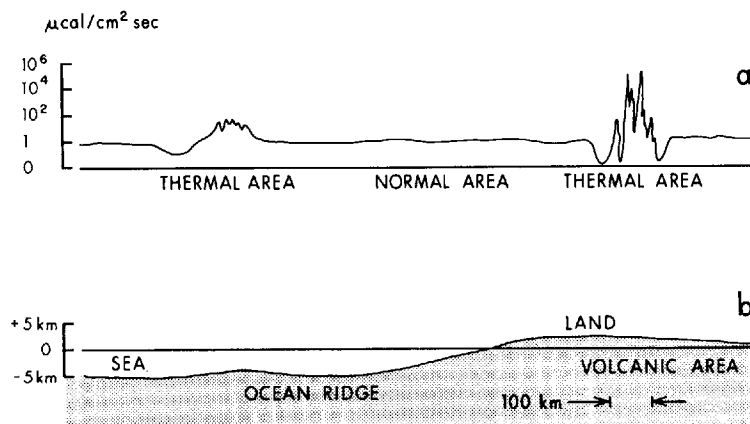


Fig. 1. Schematic profiles: (a) net heat flux at the Earth's surface and (b) corresponding topography.

water vapor. Indeed, water vapor transport plays a role, but a minor one, in normal areas. In the ocean both normal and thermal areas lose their energy by slightly warming the sea water (see chapter 5 by Lubimova et al. in this volume).

In section 3 it is suggested that land thermal areas are driven by circulation of water down to depths of the order of 10 km. This is the central topic of the chapter. There is at the moment little evidence to decide whether or not oceanic thermal areas are similar to those on land. Nevertheless, both types of thermal area must derive their energy ultimately from the mantle.

If for no other reason than that the ultimate origin of the energy released in thermal and volcanic areas must be sought, it is necessary to make conjectures about convection in the mantle. This is the task of sections 4 and 5. Though the laboratory experiments are fairly clear, their comparison with possible flows in the mantle is little more than speculation.

Thus the argument considers first the phenomena with the smallest length scales and proceeds to phenomena of progressively larger scale. On the largest scale it would be necessary to formulate entire thermal histories of the Earth, but this is not our task.

## 2. SURFACE MECHANISMS

The purpose of this section is to identify the surface heat flow mechanisms, especially those

found in land thermal areas. Section 2.1 presents a classification of discharges in land thermal areas. These are then discussed in turn. Our objective is to show that they all arise in the upper 10–100 meters of the crust from a body of hot water at depth, by evaporation or flashing of steam. This section is therefore a necessary preliminary to the discussion in section 3 of the body of hot water itself.

There is an important distinction between the surface discharge mechanisms of land and ocean thermal areas. On land, evaporation can occur at the air-water interface at the water table; this possibility does not exist in the ocean areas. Further, the sediment on the ocean bottom is much more homogeneous than the rock near the land surface. It is therefore to be expected that on land the surface heat flux in thermal areas will be extremely patchy, but in the ocean the heat flux will be more uniform, with much smaller local maximum values. This is the situation indicated in Figure 1.

### 2.1 Classification of Surface Discharges in Land Thermal Areas

The behavior of the fluid discharged at the surface in a thermal area is influenced by two factors:

(a) The discharge may proceed by direct flow of the fluid of the discharge system to the surface without change of phase. These wet and dry passive *spring-type* discharges are dominated by the flow rather than by the pres-

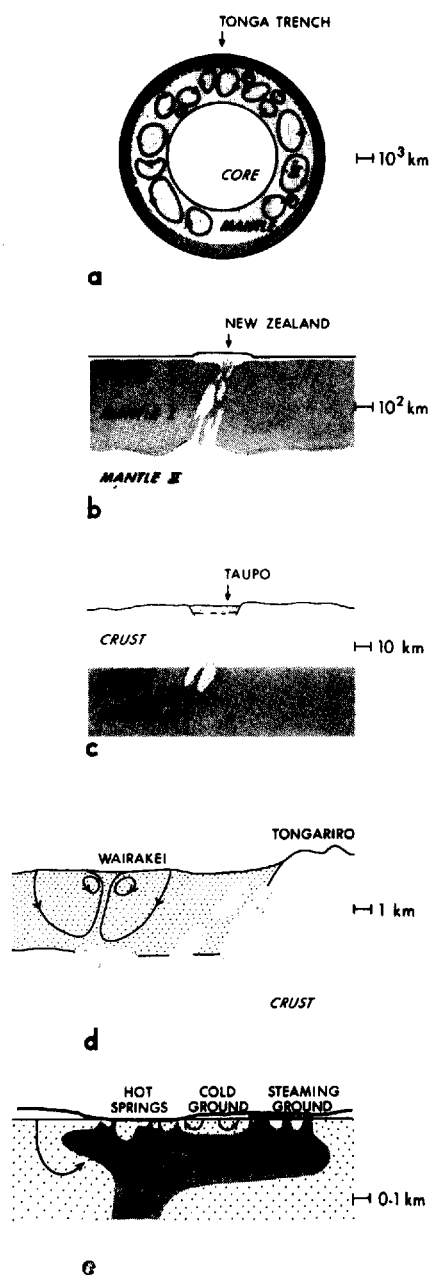


Fig. 2. Diagrams of the model systems considered. Schematic section of (a) the Earth as a whole, (b) the upper mantle near New Zealand, (c) the crust of the Taupo area, (d) the Taupo depression, and (e) the Wairakei hydrothermal system. The length scales of successive diagrams are in the ratio 10:1.

ence of the surface, which is merely the level at which the discharge occurs, and their features are those of the discharge system at depth (section 3). Similarly, surface volcanism will be regarded simply as a magma spring whose properties are essentially those of the system at depth (Section 4).

(b) If the fluid in the surface zone is water, the discharge may be dominated by the phase change of water to vapor or steam. This may occur by *flashing* of water to steam within the *body* of a volume of water hotter than the surface boiling point or by the *evaporation* of vapor at a water-air surface either at the ground surface or at depth, and not necessarily at the boiling point. Both of these processes occur independently of the level of the water table, whereas for a spring the water table must be at the surface. Evaporation will always occur; discharges in which flashing is dominant are called 'flashing-type,' where it is negligible 'pool-type.'

The interaction of flow and phase change leads to a sequence of increasingly intense discharges:

1. Warm ground: weak steaming ground marginal to the intense areas and running out to cold ground of zero gradient and more distant normal ground.
2. Steaming ground.
3. Dry fumaroles.
4. Surface pools without overflow.
5. Springs: wet or dry (slightly superheated fumaroles) with continuous discharge.
6. Geysers: intermittent wet fumaroles and mud volcanoes.
7. Wet fumaroles: bores and mud pools with continuous discharge of wet steam.
8. Phreatic explosions and hydrothermal eruptions.

Numbers 1-4 are pool-type, numbers 6-8 are flashing-type discharges; but springs, though dominated by the flow, can be strongly affected by both evaporation and flashing, so that they are a combination of pool-type and flashing-type discharges.

The bulk of the energy lost from a thermal area comes from pool-type discharges. These are considered first. Flashing discharges are then described. The section concludes with a discussion of the remarkable thermal area near

Larderello, Italy, which can be interpreted as a pool-type discharge area.

## 2.2 Rate of Discharge from Pools

Pool-type discharges are maintained by evaporation at a water-air boundary at the surface of a pool, in a void at depth, or in the pores and joints of the rock. It is assumed that the rate of evaporation  $m$  per unit area of interface is determined by the temperature of the water and the conditions in the air in the immediate vicinity of the interface. *Banwell* [1957] has obtained experimental data for  $m$  for open surfaces up to 20 meters<sup>2</sup>. For still air,

$$m = \sigma(P_s - P_2) \quad (1)$$

where  $\sigma = \text{constant} = 6.55 \times 10^{-4}$  g/cm<sup>2</sup> sec atm,  $P_s$  is the saturated vapor pressure at the interface temperature  $T_2$ , and  $P_2$  is the partial pressure of water vapor in the adjacent atmosphere just above the interface. Above the boiling point bubbles of steam will arise in the body of water, producing a great increase in the mass flux.

Let us see how this simple idea can be applied to the well-known New Zealand fumarole Karapiti. Karapiti discharges 4.5 kg/sec of slightly superheated steam of temperature 114°C. On the assumption that (a) the water-air interface is also at 114°C, the saturated vapor pressure  $P_s = 1.63$  atm [*Faxen*, 1953], and (b)  $P_2 = 0$ ,  $m = 1.07 \times 10^{-3}$  g/cm<sup>2</sup> sec by (1). The water area required to evaporate 4.5 kg/sec at this rate is 420 meters<sup>2</sup>. If the steam arises within the porous rock, of porosity about 0.3, the gross area required is about 1400 meters<sup>2</sup>.

If Karapiti were supplied with the 250°C water of the deep part of the Wairakei discharge system and this water were not cooled or diluted by surrounding groundwater, then each gram of water at 250°C would have enough energy to evaporate 0.25 gram of steam and leave 0.75 gram of water at 114°C to leak away into the surrounding country (incoming 120°C water would require a 0.99-gram leak). This leak is just part of the local convective system required to maintain the fumarole.

## 2.3 Steaming Ground

Steaming ground can be considered to be the result of filling in a surface pool with Earth and

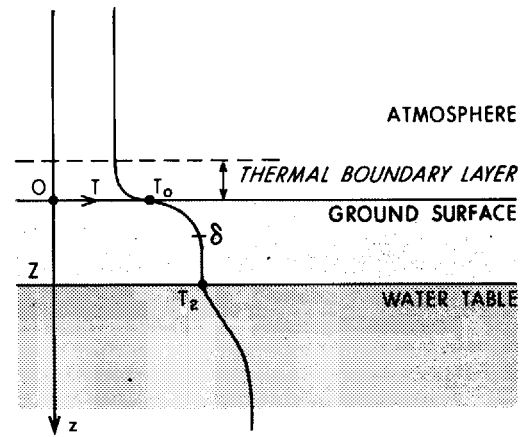


Fig. 3. Schema for steaming ground.

lowering the water table. The deeper the water table, the less intense the area becomes, until the upward flow of the evaporated vapor is completely impeded and the heat flow becomes conductive. Figure 3 shows a schema for steaming ground. Heat reaches the water table by transfer from the hot water at depth; the evaporated vapor rises through the permeable overburden and enters the atmosphere. When the vapor flow is sufficiently strong over a large area, a microclimatic effect is produced [*Robertson and Dawson*, 1964].

It will be assumed that the vertical mass flux is  $em$ , where  $e$  is the effective porosity at the interface of the rock permeable to the vapor, and  $m$  is given by (1) in which  $P_2$ , the vapor pressure near the interface, is considered to be the external ambient vapor pressure  $P_0$  plus the vapor pressure required to drive the vapor through the overburden above the interface. The role of the ambient air is completely ignored, so that this model is a poor approximation when  $P_s \ll 1$  atm. For a shallow overburden of thickness less than about 10 cm, the heat flux is given directly by  $em$  with  $P_2 = 0$ ; otherwise it is necessary to consider the details of the flow of the vapor through the overburden by means of the equations of continuity, flow, and energy [*Elder*, 1965].

Let  $\rho u$  be the mass flux of fluid of viscosity  $\mu \equiv \rho\nu$ , density  $\rho$ , and kinematic viscosity  $\nu$ , through a porous medium of permeability  $k$ . (The dimensions of permeability are square centimeters. A common unit of permeability is the darcy: 1 darcy =  $0.987 \times 10^{-8}$  cm<sup>2</sup>.) In

steady flow, with a pressure gradient  $\nabla P$ , Darcy [1856] found [cf. Wooding, 1957]

$$\rho \mathbf{u} = -(k/v)(\nabla P + \rho g \mathbf{k}) \quad (2)$$

where  $\mathbf{k}$  is a unit vector pointing upward. Here the flow ( $\rho \mathbf{u} = em\mathbf{k}$ ) is assumed to be entirely vertical and dominated by the gradient of the vapor pressure. Hence,

$$dP/dz = em\mu/\rho k \quad (3)$$

The vapor is compressible, and its density near saturation is given by Faxen [1953] as

$$\rho = \zeta P/T \quad T \text{ in deg K} \quad (4)$$

where  $\zeta = 0.22, 0.24,$  and  $0.31 \text{ g deg cm}^{-3} \text{ atm}^{-1}$  at 100, 200, and 300°C. Therefore (3) can be written

$$d(P^2)/dz = 2\mu emT/\zeta k \quad (5)$$

The energy equation is

$$\rho cv T + K_m dT/dz = \text{constant} \quad (6)$$

$K_m$  is the thermal conductivity of the medium, and  $v$  is the vertical velocity of the vapor of specific heat  $c$ . Hence, requiring  $T = T_0$  on  $z = 0$ ,  $T = T_2$  on  $z = Z$ , the depth to the water table, from (6),

$$\begin{aligned} (T - T_0)/(T_2 - T_0) \\ = (1 - e^{-z/\delta})/(1 - e^{-Z/\delta}) \end{aligned} \quad (7)$$

where

$$\delta = K_m/\rho cv$$

In intense steaming ground areas  $\delta \ll Z$ , so that  $T \approx T_2$  except for a narrow region of extent  $\delta$  near the ground surface. Hence for the purpose of integrating (5) it is a good first approximation to take  $T = T_2$  throughout the steam zone. Therefore

$$P_2^2 - P_0^2 = 2\mu em T_2 Z/\zeta k \quad (8)$$

Substituting for  $m$  from (1), this is a quadratic equation for  $\mathbf{p}_2$ . Writing

$$\mathcal{P} = P_0/P_s \quad \mathcal{E} = \sigma \mu e T_2 Z/\zeta k \mathbf{p}_s \quad (9)$$

we have

$$1 - P_2/P_s = (1 + \mathcal{E}) - [(1 + \mathcal{E})^2 - (1 - \mathcal{P}^2)]^{1/2} \quad (10)$$

The mass flux can now be calculated from (1) and (10).

Figure 4 shows the heat flux as a function of  $T_2$  and  $Z$  for a typical case in which  $e = 0.1$ ,  $k = 0.1$  darcy,  $P_0 = 0$ . With this combination

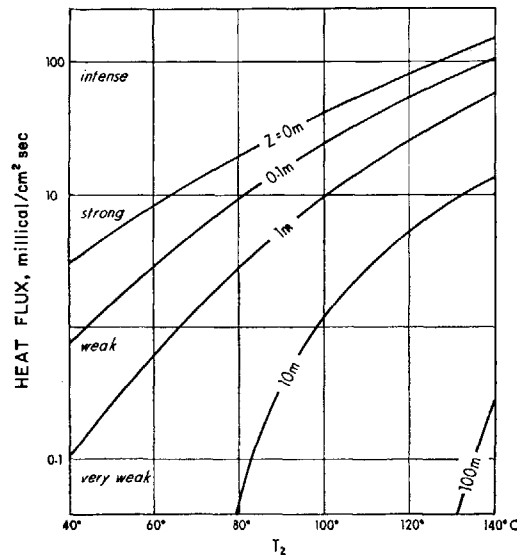


Fig. 4. Heat flux in steaming ground as a function of water table temperature  $T_2$ ; depth to water table  $Z = 0, 0.1, 1, 10,$  and  $100$  meters. Computed from equations 1 and 10 with  $e = 0.1$ ,  $k = 0.1$  darcy.

of values, the calculations fit the Wairakei field data given by Thompson *et al.* [1961] sufficiently well. It is seen that large values of  $\mathcal{E}$  substantially reduce the heat flux, and that for  $Z > 100$  meters even with high  $T_2$  the output is small. Inspection of the maps of shallow temperature surveys, such as that given by Thompson [1960] for Wairakei (see Figure 12), shows that the steaming areas are confined to patches within the  $0.1 \text{ mecal/cm}^2 \text{ sec}$  contour; outside this contour the ground temperature will be established by heat conduction or by downward-moving cold groundwater. The labels in Figure 4 (intense, strong, weak, very weak) correspond to those of field measurement [Banwell, 1957; Benseman, 1959; Dawson, 1964].

#### 2.4 Flashing Discharges

Flashing discharges are maintained by the partial boiling of water at temperatures greater than the surface boiling point; the extra volume of fluid produced can be evaluated from the steam tables if the temperature and pressure are known. It is assumed that the enthalpy of the fluid mixture is conserved. The consequent discharge is limited by the linear resistance of the ground to fluid entering the vent, together with

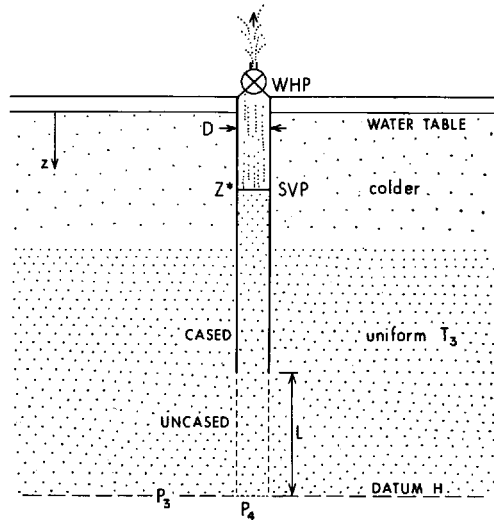


Fig. 5. Diagram of a borehole. SVP is saturated vapor pressure, WHP is well head pressure.

the nonlinear hydrodynamic resistance of the high Reynolds' number flow of the compressible fluid in the vent. An explicit mathematical solution is not possible at the present time, but an adequate semi-empirical treatment is possible [Elder, 1965] for the simplest example, a steadily discharging wet fumarole—a bore discharging vertically through a well head valve into the atmosphere.

Consider a bore of diameter  $D$  (cross-sectional area  $A = \pi D^2/4$ ), cased length  $(H - L)$ , and uncased length  $L$  imbedded in homogeneous ground of permeability  $k$ , as shown in Figure 5. Let the uncased part be in a region at uniform temperature  $T_3 > 100^\circ\text{C}$ , as in common, and let the water pressure at depth  $H$  (datum) be  $P_3$  and within the bore  $P_4$ . Initially, for a non-discharging bore  $P_3 = P_4$ , since the temperature of the bore water will be the same as that of the adjacent groundwater. However, suppose the volume of water in the bore is disturbed and  $P_4$  is reduced (say by injecting compressed air into the water of the bore). If  $P_4$  is reduced enough, local boiling will commence at some level in the bore, and  $P_4$  will continue to fall. Also the pressure difference  $(P_3 - P_4)$  will drive water from the country into the bore, so that water at temperature  $T_3$  is forced higher up the bore, and this will further accelerate boiling. Flashing will spread and  $P_4$  will fall until a balance is established between the amount of

water entering from the ground and that discharged by the bore. If the ground permeability is too small, a continuous discharge is not possible [Elder, 1965]. Because the water is at a nearly uniform temperature below a certain depth (400 meters at Wairakei), the pressure difference driving fluid into the bore is uniform over the uncased portion. Assuming that Darcy's law is valid, the volume of fluid entering the bore per second,  $U$ , is such that,

$$U \approx 2\pi Lk(P_3 - P_4)/\mu \ln(2L/D) \quad (11)$$

The flow velocity in the ground at radius  $r$  is  $U/2\pi Lr$ . Except near the largest bores, this is small enough for Darcy's law to be valid. It is therefore not always necessary to invoke Reynolds' number effects in the porous medium.

Within the bore, as the fluid rises, at some level  $z = z^*$  it reaches the saturated vapor pressure SVP, corresponding to temperature  $T_3$ , and boiling commences. The pressure  $P_4$ , neglecting the small hydrodynamic loss below  $z^*$ , is

$$P_4 = \text{SVP} + \rho_3 g(H - z^*) \quad (12)$$

As the fluid rises above  $z^*$ , the pressure will continue to fall and the proportion by weight of steam  $\eta$  will rise from  $\eta = 0$  at  $z = z^*$  to  $\eta = \eta_0$  at the well head. Assume that at each level the fluid is in thermodynamic equilibrium and that the enthalpy  $E$  remains constant at a value corresponding to  $T_3$ . Values of  $\eta$  at the corresponding pressure and temperature can then be calculated from the steam tables [Faxen, 1953].

As the compressible fluid flashes and expands in moving from  $z = z^*$  to  $z = 0$ , it must not only overcome the hydrostatic head of the overlying fluid together with the pressure at the well head (WHP), but also the hydrodynamic resistance. High Mach numbers will often be found near the well head, but the net effect is barely appreciable for even the largest bores; the resistance is largely hydrodynamic. Two-phase flow has recently been reviewed by Tek [1961], but the numerical procedures required are unnecessarily elaborate for the present problem. Here we simply assume that the behavior is similar to that of a single phase flow [cf. Allen, 1951]. Hence the pressure gradient in the bore can be written

$$dP/dz = \rho g + \lambda \rho W^2/2D \quad (13)$$

a sum of hydrostatic and hydrodynamic terms.  $W$  is the mean velocity of the fluid of density  $\rho$

across the cross section of the bore, and  $\lambda$  is a dimensionless function of the Reynolds' number  $\mathcal{R} = WD/\nu$  and the wall roughness  $\varepsilon/D$  [Schlichting, 1960].

Wairakei bores operate near  $\mathcal{R} = 10^7$ , and in this region  $\lambda$  is determined by  $\varepsilon/D$ ; that is, the pipe is *hydrodynamically rough*, and  $\lambda$  is *almost independent* of  $R$ . For the 8-inch Wairakei bores  $\lambda = 0.015$ , corresponding to  $\varepsilon/D = 0.0003$ , that is,  $\varepsilon = 0.0024$  inch.

Natural wet fumaroles will also be hydrodynamically rough. For example, a 1-liter/sec discharge through a 10-cm diameter vent has  $\mathcal{R}$  of the order of  $10^5$ , so that for  $\varepsilon/D \geq 0.01$ ,  $\lambda$  is independent of  $\mathcal{R}$ . Natural roughness will usually exceed 0.01.

Noting that the mass flow  $M \equiv \rho U = \rho AW$ , (13) can be integrated numerically to give  $M(\eta_0, z^*)$ . Combining this with (11) and (12), the output  $M$  is obtained as a function of well head pressure. Figure 6 shows a number of such output characteristics with parameters chosen for the Wairakei thermal area. Curves *a* and *b* correspond to the typical range of Wairakei bores. Curve *c* corresponds to that of a fumarole. Calculated curves fit field data [Studdt, 1957; Banwell, 1957; Smith, 1958] quite well.

### 2.5 Eruptive Discharges

The intermittent wet fumarole known as a geyser can be regarded simply as a wet fumarole which is intermittent because of the relatively small ground permeability and whose behavior is modified by the existence of reservoirs and ground leakage [Benseman, 1965].

In mud pools, mud volcanoes, and hydrothermal eruptions, the rock takes an active part in the system.

Mud is the viscous water-saturated, decomposed rock. In mud pools the steam rises slowly as bubbles rather than by the uniform permeation of ordinary steaming ground; the mud itself is almost impermeable. The flow about the bubbles will be Stokesian, and the mud transported by this flow will tend to circulate in the pool; as hot water and mud come from depth, quiet flashing produces the steam which accumulates in bubbles. Mud volcanoes are merely geysers with a superimposed mud pool; mud is thereby ejected with the flashing discharge.

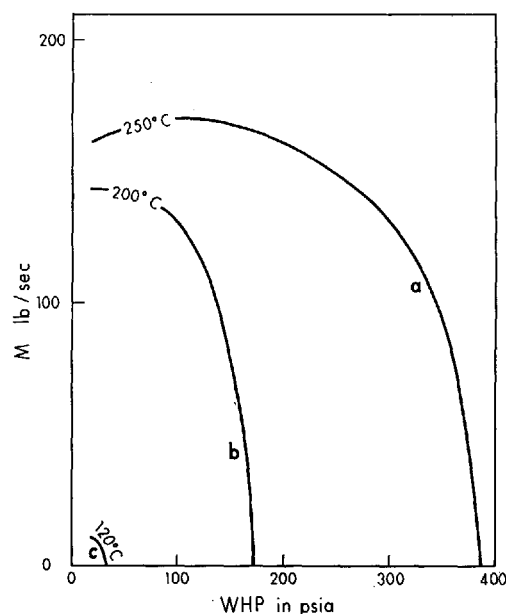


Fig. 6. Bore output characteristics; mass output  $M$  in lb/sec for an 8-inch bore, against well head pressure  $WHP$  in psia: (a)  $k = 0.1$  darcy,  $H = 1400$  feet,  $L = 800$  feet,  $T_s = 250^\circ\text{C}$ , similar to Wairakei bore 20; (b) as for (a) with  $T_s = 200^\circ\text{C}$ ; (c) as for (a) with  $k = 0.4$  darcy,  $T_s = 120^\circ\text{C}$ .

Hydrothermal eruptions are possible when water at depth approaches the boiling point. It is possible for the saturated vapor pressure to exceed the lithostatic load (i.e., pressure due to the weight of the rock above), there being enough thermal energy that after an adiabatic expansion to atmospheric pressure there is a large excess of kinetic energy [Goguel, 1953]. For example,  $250^\circ\text{C}$  water has a saturated vapor pressure of 40 atm, so that an overburden of density  $2 \text{ g/cm}^3$  is in balance at 200 meters depth with available energy of 50 joule/cm<sup>3</sup>. If this region is extensive, an explosion is possible, ranging from pits of diameter 10 meters to craters. In spite of the enormous instantaneous power developed in these explosions, the total energy released is not large compared to that of a thermal area such as Wairakei. Wairakei discharges  $10^8$  Mwatt; Usu-san [Minakami *et al.*, 1951] developed of the order of  $10^6$  Mwatt and transported a total of 0.5 Mwatt-year. These eruptions are possible in a thermal area, and it is not necessary to invoke exclusively a

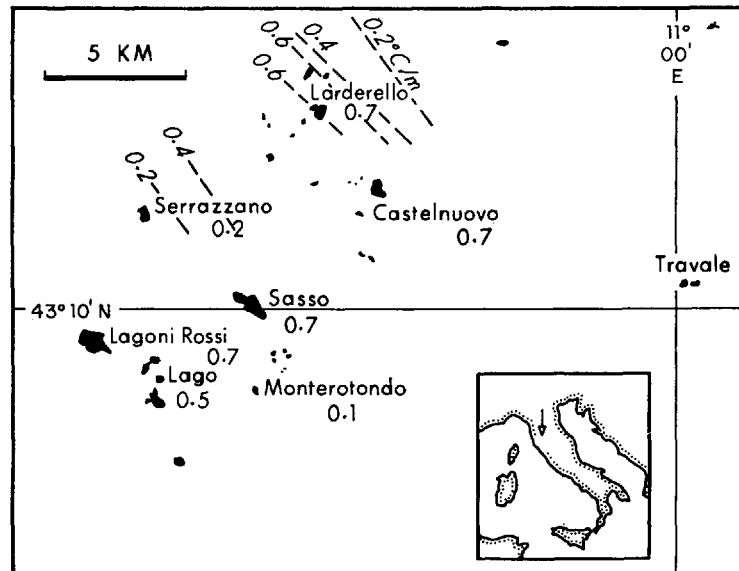


Fig. 7. Location of the thermal areas of the Tuscan thermal district; area indicated in square kilometers (estimated heat flow  $10^8$  cal/km<sup>2</sup> sec), surface temperature gradient in °C/meter; after *Burgassi* [1961].

magmatic injection as the energy source. In a thermal area the explosions will be shallow, however, since below 500 meters the temperature no longer increases rapidly with depth.

### 2.6 A Model of the Tuscan Steam Zone

The earliest large-scale investigation and exploitation of geothermal energy was in the Tuscan thermal area near Larderello shown in Figure 7 [Penta, 1954; Burgassi, 1961; Burgassi *et al.*, 1961]. More details are given by McNitt in chapter 9.

The model presented here (see Figure 9) considers the Tuscan hydrothermal systems as not fundamentally different from those in New Zealand, but in this model the water table is at great depth (2 km) and the discharge mechanism is similar to that of steaming ground. This deduction relies principally on two sets of observations: the pressure transients, and the slight but increasing superheat during the observation period.

One of the outstanding characteristics of the Larderello project is the absence of a steady state during the last 50 years of intensive exploitation.

1. A change in the setting of the well head valve of a bore results in a slow change (10–

100 hours) to a new steady state. For example, Figure 8 shows the growth of the shut-in pressure after closing the well head valve on two Larderello bores [Nencetti, 1961].

2. Whereas the output of a single bore in an unexploited area remains constant over a period of 10 years, in an exploited area not only does the output of individual bores continuously decrease, but so does the total output; to maintain production at Larderello, a continuous drilling program is necessary. A rather crude average for individual outputs  $M$  is,

$$M = M_i \exp(-0.14t \text{ year}) \quad (14)$$

corresponding to a fall to  $0.5 M_i$  in 5 years [Penta, 1954].

Assuming the existence of a steam reservoir, an immediate explanation of these transients is possible. The mass of a compressible fluid contained in a reservoir is a function of the pressure distribution; any change in the pressure distribution will require a mass transport to adjust the mass to its new value. A transient response will occur during the time of this flow.

For example, in one-dimensional flow of a compressible fluid in a porous medium, conservation of mass requires

$$e \frac{\partial \rho}{\partial t} + \frac{\partial}{\partial z} (\rho v) = 0 \quad (15)$$

where  $e$  is the total porosity, not just that of the joints and fractures. Hence using (2) and (4), and neglecting buoyancy effects,

$$\frac{\partial P}{\partial t} = \frac{k}{e\mu} \frac{\partial}{\partial z} \left( P \frac{\partial P}{\partial z} \right) \quad (16)$$

This is a diffusion equation in which for small changes in  $P$  we have a diffusion coefficient  $k\bar{P}/e\mu$ , where  $\bar{P}$  is a mean pressure. Hence if fluid is removed or added to a volume of length scale  $Z$  the pressure will change with a time scale  $\tau$  of the order of

$$\tau = e\mu Z^2 / 2k\bar{P} \quad (17)$$

The volume affected by the manipulations of the well head valve of a single well is a roughly spherical volume with  $Z$  of the order of  $L$ , the length of the well production zone. Take  $\tau$  as the time required to effect 90% of the total pressure change in Figure 8; bore  $B$  gives  $\tau = 12$  hours, which with  $e = 0.1$ ,  $P = 15$  atm,  $\mu = 0.02$  centipoise,  $Z = 100$  m, gives  $k = 0.2$  darcy, in agreement with the output characteristics of the strongest bores. Bore  $C$  gives  $\tau = 600$  hours corresponding to  $k = 0.003$  darcy, a very small value, similar to that of homogeneous rock.

A single bore affects only its immediate vicinity to a distance  $L$ , but with an extensive area of closely spaced bores (Larderello spacing is 400–500 meters) it is possible to affect the distribution of pressure throughout the steam reservoir itself. Here we notice that while pressure adjustments can be made rapidly in the more permeable zones (see equation 17) the ultimate response will be dominated by the movement into and out of the rock pores, for which the permeability is very small; laboratory measurements give a few millidarcy. Hence, choosing the above figure of 0.003 darcy and noting from (14) that  $\tau = 16$  years, with  $e = 0.1$  we require  $Z \approx 2$  km. This figure is of course exceedingly crude. Nevertheless it does support the view that beneath Larderello there is a deep steam zone.

There is another remarkable observation. Whereas the early wells at Larderello (and not just those penetrating only into the superficial near surface groundwater zone) gave steam that was either saturated or very nearly saturated, in the last 50 years of intensive exploitation the degree of superheat has steadily risen: a well head temperature increase of as much as 40°C

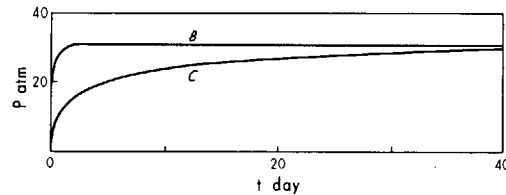


Fig. 8. Growth of shut-in pressure  $P$  in atmospheres in two Larderello steam bores, referred to here as  $B$  and  $C$ , after the sudden closing of the well head valve of wells previously discharging steadily to atmosphere; after *Nencetti* [1961].

has been reported. The maximum steam enthalpy at Larderello is at present about 685 cal/g, though the maximum possible enthalpy of saturated steam is 670 cal/g!

At this point we must modify the view of a static steam reservoir and consider the origin of the steam. Here it is suggested that the system is a 'wet convector' but *with evaporation occurring at the water surface* as in steaming ground, a schema similar to that of steaming ground but with the water table at a great depth, of the order of 2 km (Figure 9). It is therefore possible to consider much higher water surface temperatures than for normal steaming ground.

We will now apply the theory of steaming ground developed in section 2.3 to the Tuscan steam zone. In the original state there are good indications that the steam zone was confined by a perched water layer. In this case,  $P_0 \approx P_s$ , the gas enthalpy is nearly equal to the saturation value at  $T_2$ , for example, a maximum of 670 cal/g at 235°C.

During exploitation it has been engineering practice at Larderello to set the bore *WHP* at 5 atm, and, as can be shown, loss of pressure as the fluid ascends a bore is negligible, so that ground pressure  $P_0$  has been reduced from values at least as large as 30 atm to 5 atm. Hence  $\mathcal{P}$  changes from near 1 to 0.1–0.2. Hence an order of magnitude increase in heat flow is easily possible. This implies a fall in  $P_2/P_s$ . Inspection of the steam tables shows (Figure 10) in the region of interest, at the same temperature, an increase in vapor enthalpy with reduction in pressure. For example, the observed increase to 685 cal/g for  $T_2 = 235^\circ\text{C}$  is given by a change in  $P_2$  from 30 to 20 atm.

It is important to emphasize that the main

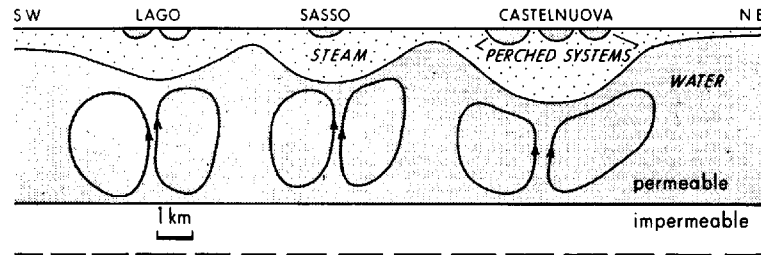


Fig. 9. Possible distribution of water and vapor in the Tuscan hydrothermal systems. Section through Castelnuova and Lago (see Figure 7). Recharge not shown.

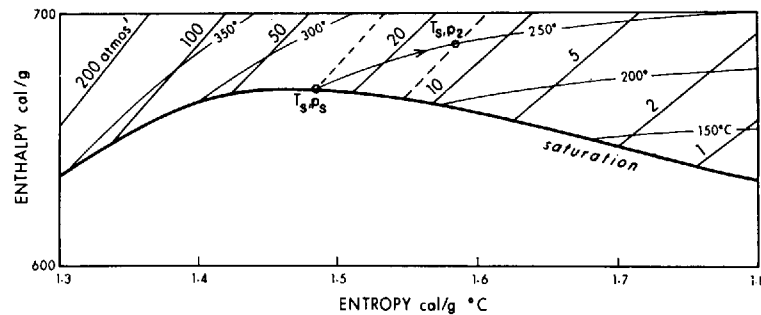


Fig. 10. Portion of the enthalpy-entropy diagram for water [after Faxen, 1953]. The saturation line corresponds to steam and water in thermodynamic equilibrium. Pressure in atmospheres, temperature in degrees centigrade.

assumption is that the evaporated vapor in the immediate vicinity of the evaporative surface is at pressure  $P_2 < P_s$  but at the same temperature as the water surface  $T_2$ .

### 3. CONVECTION OF WATER IN THE CRUST

Of the numerous speculations [reviewed by Banwell, 1957, 1963] about the nature of thermal areas, the work of Einarsson [1942] on the weak hot springs of west Iceland is the first quantitative and comprehensive exposition. He contends that these springs are not physically different from ordinary cold springs except that, because of the greater depth of penetration of the water, it has become heated, and that this heat does not necessarily come directly from volcanism but comes simply from the normal heat flux through the ground.

Bodvarsson [1948, 1949, 1950, 1954, 1961] has elaborated Einarsson's work and attempted to apply it to the intense areas of central Iceland. The 1961 paper is an excellent summary. He notices in these areas the high thermal gradient near the surface and shows how this could

arise from a slowly moving vertical current of hot water which is cooled near the surface by conduction of heat to the surface. At this point the broad features of a *spring-type* or single-pass hydrothermal system are established. He draws attention to the limiting case of a column of water everywhere at its boiling point—the so-called boiling point with depth relation exploited by Banwell [1957].

Lapwood [1948] appears to have been the first to point out and consider quantitatively the possibility of free convection of water in the water-saturated 'porous' rock. He showed that convection in a horizontal layer uniformly heated from below could not occur unless the temperature difference across the layer were sufficiently high. Wooding [1957, 1958, 1959, 1960a, b, 1962, 1963] has made a series of elaborate studies of convection in a porous medium. Elder [1958] constructed laboratory scale models of the Taupo systems and demonstrated that an intense free convective system could transport sufficient heat. Donaldson [1962] has considered weak free convection in a horizontal permeable layer below which is an

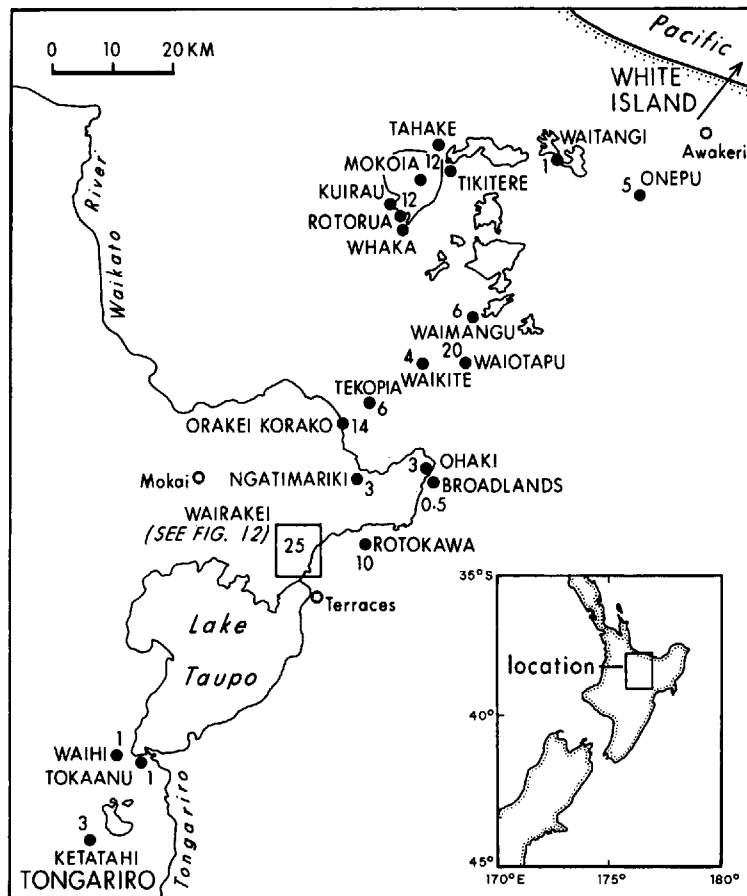


Fig. 11. Location and heat flows of the thermal areas of the Taupo district, New Zealand (after Healy, see text). Units  $10^7$  cal/sec.

impermeable region with specified temperature at a given depth. The view of these workers is of a hydrothermal system based on the continuous circulation of water.

### 3.1 The Taupo Hydrothermal Systems

Beneath the surface zone of a thermal area, in which the details of the surface discharge mechanisms are established, there exists a body of hot water. It is the purpose of this section to discuss the conditions in this body. In order to be specific, I will concentrate attention on the Wairakei hydrothermal system, which is in the Taupo district of New Zealand, simply because it has been extensively explored and it is the area with which I am most familiar. Details of this and other thermal areas are given in chapter 9 by McNitt.

The Taupo thermal areas of New Zealand occur in a zone running NNE between the Tongariro and White Island volcanoes as shown in Figure 11 [Grindley, 1961; Healy, 1962, 1964]. Within this zone geological, gravity, magnetic, and seismic studies reveal a depression of depth 5 km filled with broken block structures, penetrated by rhyolitic volcanic complexes and volcanic debris [Modrniak and Studt, 1959]. The surface heat flow for each of the thermal areas shown in Figure 11 has been determined by Healy [Grange, 1955]. More recent work indicates the need to multiply his values by about 2. This is a matter of present discussion, but I have done this here. The revised values are shown alongside each area in Figure 11; a total of  $Q_0 = 1.3 \times 10^9$  cal/sec. Included in the area of 2500 km<sup>2</sup> are: 2 intense

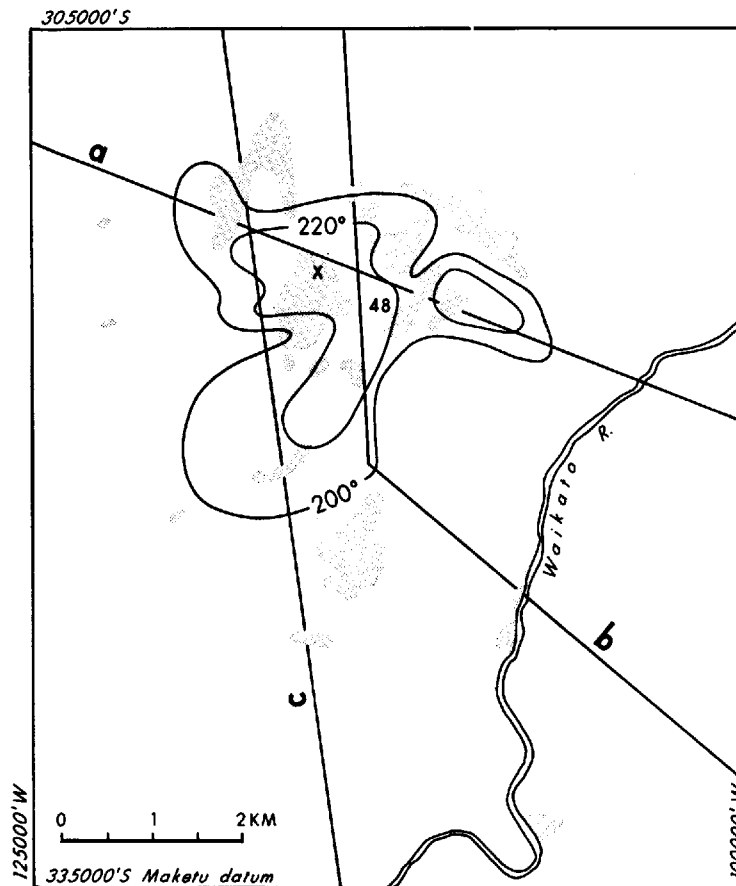


Fig. 12. Distribution of hot areas at Wairakei with heat flux greater than 10 mcal/cm<sup>2</sup> sec; after *Thompson et al.* [1961] and *Thompson* [1960]. The total heat flow from the area shown is  $2.5 \times 10^8$  cal/sec. Superimposed are the 200 and 220°C isotherms at 350 meters below datum; after *Banwell* [1961].

groups, Waiotapu and Wairakei, with flows of the order of  $3 \times 10^8$  cal/sec; 4 moderate groups, Rotorua, Tikitere, Rotokawa, and Orakei Korako, with flows of the order of  $1 \times 10^8$  cal/sec; 7 small groups with flows of the order of  $0.3 \times 10^8$  cal/sec, and 4 very small groups with flows of the order  $0.1 \times 10^8$  cal/sec. The regional average heat flux is 50  $\mu$ cal/cm<sup>2</sup> sec, with values averaged over the more intense parts of each area of the order of 10 mcal/cm<sup>2</sup> sec.

Detailed surface surveys have been made of some of these areas. Figure 12 shows the main features of the Wairakei area obtained by *Thompson* [1960] and *Thompson et al.* [1961]. Patches of steaming ground of area of the order of 1 km<sup>2</sup> are scattered over the area.

The temperature distribution with depth at Wairakei, obtained from several hundred bore holes, is well known to a depth of 500 meters, poorly known from 500–1500 meters, and unknown below 1500 meters. The data presented here are based on the compilations of *Banwell* [1957, 1961].

Superimposed on Figure 12 are the 200°C and 220°C isotherms at 350 meters below datum (500 meters above sea level, near ground level).

Further details are revealed in Figure 13, which shows the temperature distribution in the vertical sections *a*, *b*, *c* of Figure 12. These reveal a body of water-saturated rock at 200°C or more, 4 km wide and 1.4 km deep.

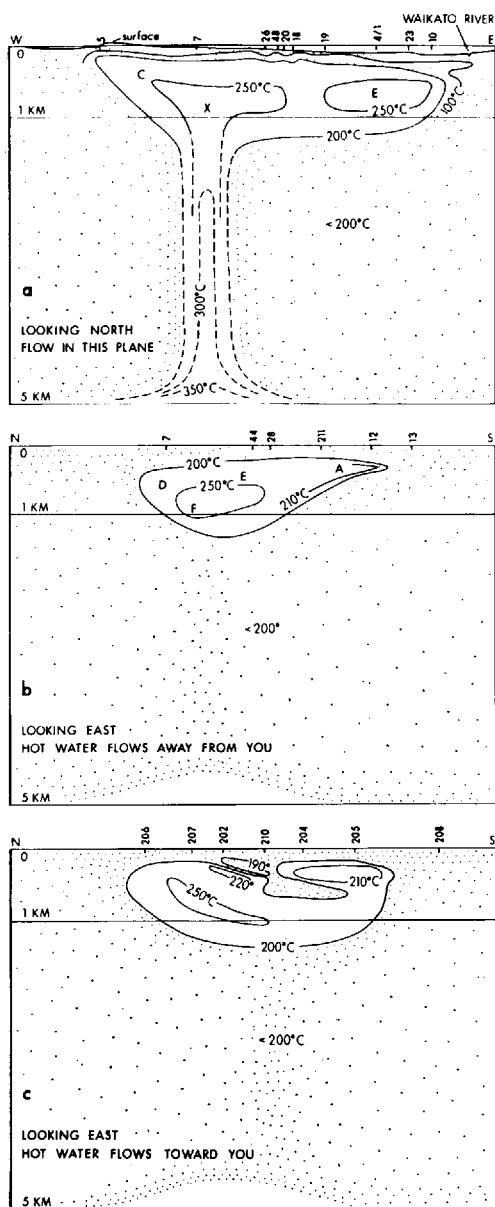


Fig. 13. Isotherms for sections *a*, *b*, *c*, of Figure 12. The location of numbered Wairakei bores is indicated on the datum of 500 meters above mean sea level; after *Banwell* [1961].

### 3.2 Identification of the Elements of a Hydrothermal System

A hydrothermal system is a heat transfer mechanism in the Earth's crust relying for its operation on the transport of water, but not

necessarily the discharge of water at the Earth's surface, and producing at the surface a so-called thermal area in which the heat flow is *different* from normal.

The bulk of the phenomena exhibited by a hydrothermal system can be described merely in terms of a *hot water and rock* reservoir deposited at depth at some previous time. The total heat flow would be considered to arise solely from the energy stored in the reservoir.

In the natural state the water level is generally found to be stationary, and yet fluid is continually discharged from the reservoir. A water recharge system must then exist. The recharge water may be meteoric, originate at depth, or be a mixture of both. There is strong evidence on chemical grounds that the water is meteoric [*White*, 1957]. Certainly rainfall is more than sufficient. For example, only 5% of the rainfall on the Taupo catchment area of  $4 \times 10^3 \text{ km}^2$  of  $1.6 \times 10^5$  liter/sec is needed to supply the natural discharge of  $5 \times 10^3$  liter/sec.

From the known temperatures, the total energy stored in the Wairakei system at the moment can be estimated to be about  $2 \times 10^{18}$  cal, equivalent to  $20 \text{ km}^3$  of rock of specific heat  $0.5 \text{ cal/cm}^3 \text{ }^\circ\text{C}$  at  $200^\circ\text{C}$ . This would be exhausted at the present discharge rate of  $2.5 \times 10^8$  cal-sec in 250 years. There is, however, little doubt that no gross changes in temperature have occurred at Wairakei in  $10^3$  years, since Maori legend goes back to circa 1200 A.D. and there is geological evidence of volcanic and hydrothermal activity for  $10^6$  years [*Healy*, 1962]. Thus the reservoir must be continuously supplied with energy from depth, although the rate of supply need not be constant.

A further possible feature of a hydrothermal system not revealed by a consideration solely of the total mass and energy balance of the system is the recirculation of some of the hot water. This feature will appear when the details of the flow within the system are discussed below.

Thus the elements of a hydrothermal system are: a heat source, a recharge system, a recirculation system, and a surface discharge system.

Given these elements alone, it is of interest to construct a pipe model of a thermal area. Such a model for Wairakei is shown in Figure 14. It is based on the data of *Thompson et al.* [1961],

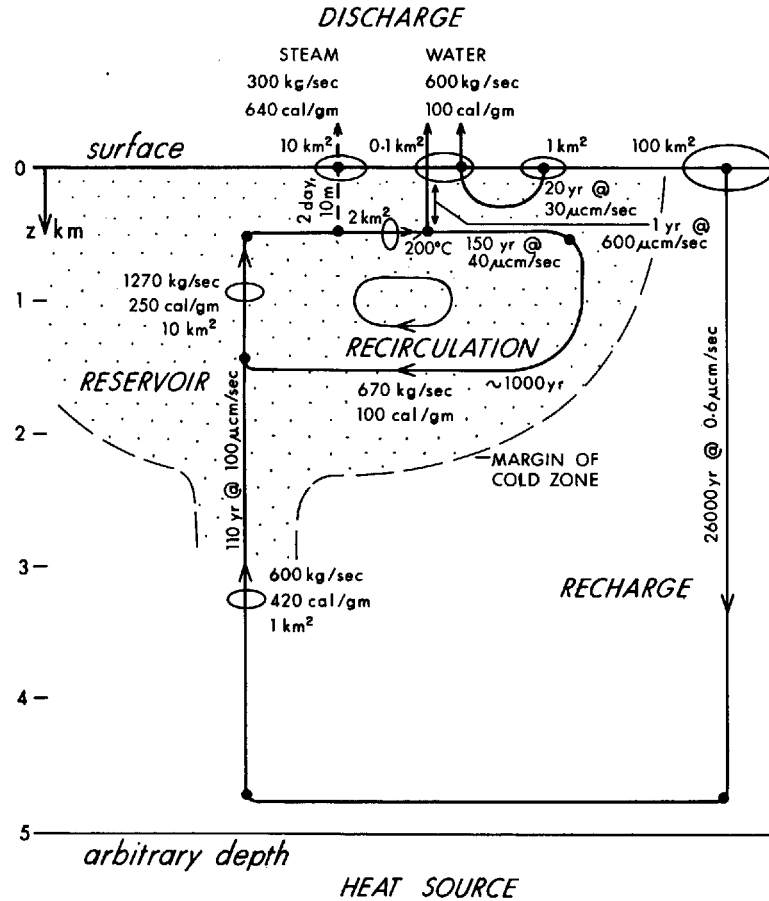


Fig. 14. Schema of a *pipe* model of Wairakei: flow in kilograms per second, enthalpy in calories per gram, cross-sectional areas in square kilometers, velocities in microcentimeters per second, time in years.

who find a steam discharge of 300 kg/sec and a water discharge equivalent to 300 kg/sec of deep water and 300 kg/sec of locally heated groundwater. Included in Figure 14 are estimated areas of the 'pipe' cross sections and the corresponding percolation velocities. Such a model is clearly extremely crude, but it is valuable for calculating orders of magnitude and should be an initial step in exploring a new area. The times revealed are surprising, both for their magnitude and the large range of scales: of the order of  $10^5$  years for the deep recharge,  $10^3$  years for the recirculation, and 10 years for the surface water discharge.

To proceed further it is necessary to consider in some detail the motion of the fluid within the hydrothermal system.

### 3.3 Formulation of the Free Convection Problem in a Porous Medium

Consider a horizontal slab of homogeneous saturated porous material of thickness  $H$ , permeability  $k$ , and thermal conductivity  $K_m$  saturated with a fluid of density  $\rho$ , specific heat  $c$ , and kinematic viscosity  $\nu$ . A Cartesian coordinate system  $OXYZ$  has its origin in the lower surface;  $z$  is measured downward. The upper surface is maintained at temperature  $T_0$ ; a part of the lower surface, the 'heat source,'  $|x| \leq L/2$ , is at temperature  $T_0 + \Delta T$ .

The motions to be considered arise from the buoyancy forces produced by imbalanced density variations in a field of nonuniform temperature. Thus if the fluid density  $\rho =$

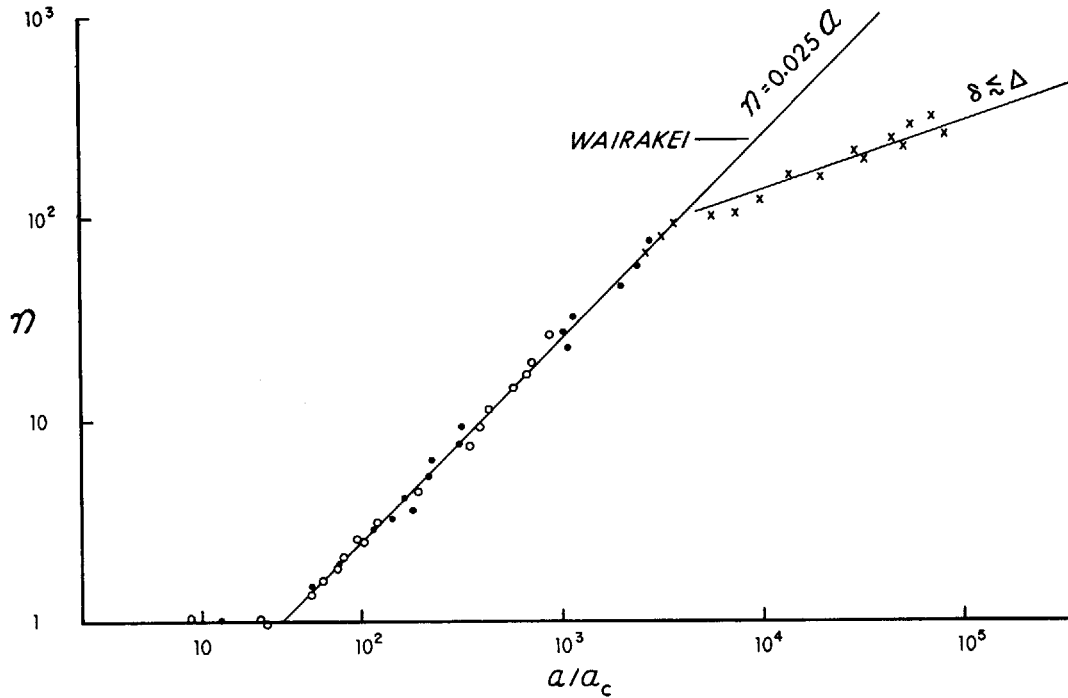


Fig. 15. Heat transfer characteristic for free convection in a porous medium; Nusselt number  $\mathcal{N}$  as a function of Rayleigh number  $\mathcal{R}$ .

Open circle, Hele-Shaw cell,  $a = 0.475$  cm,  $L = 8$  cm, Ondina oil.  
 Solid circle, circular pot of 3, 5, 8 mm glass spheres,  $L = 8$  cm, water.  
 Crosses, circular pot of 6 mm expanded plastic balls,  $L = 35.5$  cm, water.

$\rho_0(1 - \alpha(T - T_0))$ , where  $\alpha$  is the coefficient of cubical expansion, the equation of motion given by Darcy's law (2) can be written, making the Boussinesq [1903] approximation that density variations are important only insofar as they generate buoyancy forces,

$$\rho_0 \mathbf{u} = -\frac{k}{\nu} (\nabla P - \alpha g \rho_0 [T - T_0] \mathbf{k}) \quad (18)$$

Here  $P$  is the departure of the pressure from its value when  $T = T_0$  everywhere.

In nonisothermal flow, heat will be transported at a rate of  $\rho c u \cdot \nabla T$ , where  $\rho c$  is the thermal capacity of the fluid, but will be conducted at a rate  $K_m \nabla^2 T$ , where  $K_m$  is the thermal conductivity of the fluid saturated medium. A crude estimate of  $K_m$  is given by

$$K_m \approx (1 - e) K_s + e K_f \quad (19)$$

where  $e$  is the porosity, the void volume per unit volume of medium, and  $K_s, K_f$  are the conductivities of the solid and the fluid. Thus the effective thermal diffusivity is  $\kappa_m \equiv K_m / \rho c$ .

The problem is now specified by  $k/\nu, \kappa_m, H, L, \alpha g \Delta T$ . These five numbers involve only the dimension of length and time. Three dimensionless parameters are therefore necessary to define the system; a convenient choice is:

$$\begin{aligned} \mathcal{P} &= \nu / \kappa_m && \text{Prandtl number for the medium} \\ \mathcal{R} &= k \alpha g \Delta T H / \kappa_m \nu && \text{Rayleigh number} \\ \mathcal{L} &= L / H && \text{aspect ratio} \end{aligned} \quad (20)$$

A quantity of prime interest will be the power  $Q$  transmitted through the slab, for which we define a Nusselt number  $\mathcal{N}$ , a dimensionless conductivity, such that

$$Q = \mathcal{N} K_m (\text{heated area}) \Delta T / H \quad (21)$$

When the heat transported by convection is negligible, write  $\mathcal{N} = \mathcal{N}_0$ . For  $\mathcal{L} \gg 1, \mathcal{N}_0 = 1$ .

### 3.4 Heat Transfer Measurements

Some heat transfer measurements obtained with laboratory models filled with glass spheres are shown in Figure 15 [Elder; 1958, 1965].

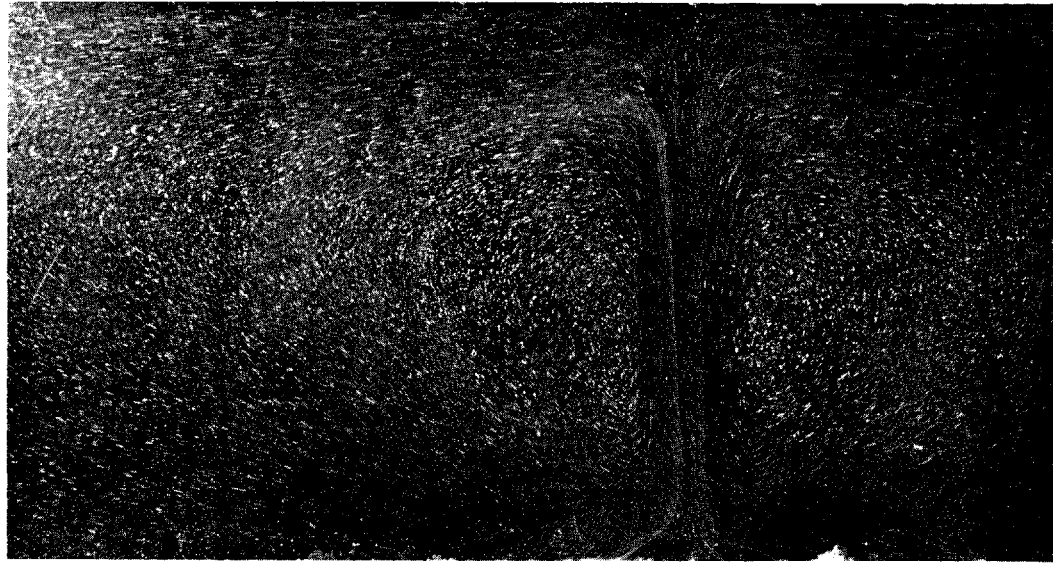
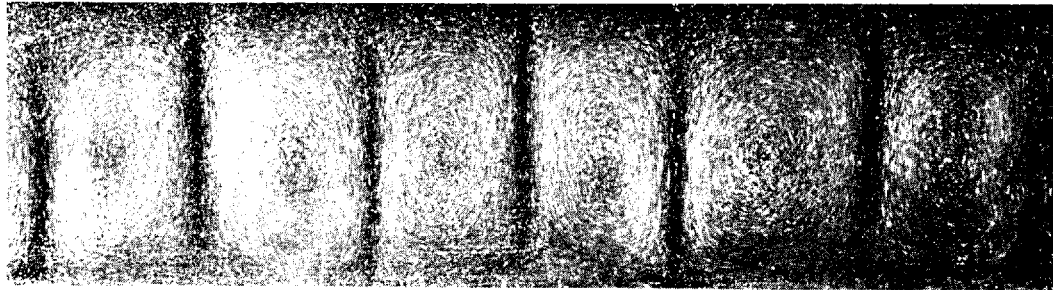
(b)  $\mathcal{L} = 1$ ,  $\mathcal{A} = 10^3$ (a)  $\mathcal{L} \gg 1$ ,  $\mathcal{A} = 2\mathcal{A}_c$ 

Fig. 16. Photographs of free convection in a Hele-Shaw cell.

Note here  $\mathcal{L} \gg 1$ . Below  $\mathcal{A} = 40$ ,  $\mathcal{N} = \mathcal{N}_0$ , so that the heat transfer is entirely by conduction. At  $\mathcal{A} = 40$  there is an abrupt change in  $\mathcal{N}(\mathcal{A})$ . These experiments give this critical value as

$$\mathcal{A}_c = 40 \pm 10\% \quad (22)$$

consistent with the prediction,  $4\pi^2$ , of *Lapwood* [1948]. Above  $\mathcal{A}_c$  the points lie reasonably close to

$$\mathcal{N} = \mathcal{A}/40 \pm 10\% \quad (23)$$

In dimensional form this becomes

$$Q/(\text{heated area}) = k\rho c a g(\Delta T)^2/40\nu \quad (24)$$

a quadratic relation between  $Q$  and  $\Delta T$ . We note that the right-hand side is independent of  $L$ ,  $H$ , and  $K_m$ . The relation 23 can still be valid for  $\mathcal{A}$  at least as large as  $100\mathcal{A}_c$ , the greatest range available in the experiments. At suffi-

ciently large  $\mathcal{A}$ , departures from (23) do occur. These changes occur when the boundary layer thickness  $\delta \equiv H/2\mathcal{N}$  becomes comparable to the scale of the porous medium; for these values of  $\mathcal{A}$  the flow is essentially the same as in a viscous fluid. *Schneider* [1963] has also obtained an extensive series of measurements of  $\mathcal{N}(\mathcal{A})$ .

### 3.5 Measurements in a Hele-Shaw Cell

*Hele-Shaw* [1898] showed that in a cavity of width  $a \ll H, L$  the motion is similar to that in a porous medium of permeability  $k = a^2/12$ . The theory can be found in *Lamb* [1932, section 330]. Although the motion in a Hele-Shaw cell is only two-dimensional, there is the great advantage that the flow can be visualized, e.g., by means of suspended aluminum particles. Figure 16 shows two photographs obtained by this

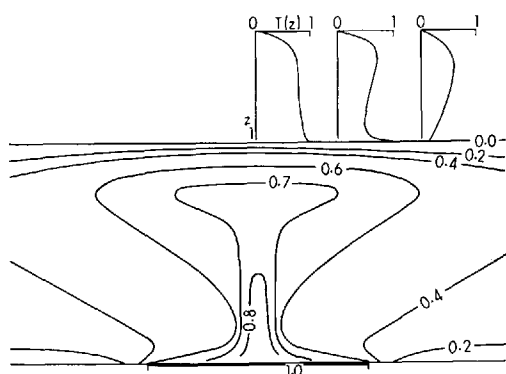


Fig. 17. Temperature distribution corresponding to Figure 16b.

method. Figure 16a shows the flow at  $\mathcal{A} = 2\mathcal{A}_c$  and  $\mathcal{L} = 10$ . A pattern of nearly square cells can be seen. This situation corresponds to the theory of *Lapwood* [1948] and *Donaldson* [1962]. Figure 16b at  $\mathcal{A} = 10^3$ ,  $\mathcal{L} = 1$  shows a single cell. This is the situation of geophysical interest.

The temperature distribution can be measured with a small thermocouple probe. The results for the above cell are shown in Figure 17. The temperature distribution reveals strong vertical thermal gradients near the heater and the upper surface. Above the heater is a mushroom-shaped distribution. Shown also are three typical temperature profiles  $T(z)$  at  $x = 0, 0.75, 1.50$ . Note that on  $x = 0$  the profile is monotonic, with strong gradients near  $z = 0, 1$  but more nearly constant elsewhere. The other profiles show a maximum with depth where the point penetrates the head of the mushroom.

The velocity distribution reveals a plume rising above the heater. Clearly the bulk of the heat is carried in this plume.

Because of its relevance to the geothermal problem, some experiments were performed in which fluid was continuously withdrawn from the cell by a syphon from a small hole in the wall at  $x = 0, z = 0.2$ . At the same time cold fluid was replaced at an equal rate by means of a constant head apparatus at the ends of the apparatus. The effect on the temperature distribution is shown schematically in Figure 18 for various values of  $Q'/Q$ , where  $Q'$  is the power withdrawn by the syphon. Figure 19 is a photograph of one of these flows. The most striking observation, however, is the sharp

boundary between the cold recharge water and the recirculating hot water. At small discharge rates there is little change in the temperature distribution, but as the rate is increased the mushroom distribution collapses to a mere column of heated fluid. The situation is now largely one of forced convection, but we notice that the temperature distribution near the heat source is hardly altered. Indeed, throughout the experiment  $\eta$  remained constant at the value given by (24). This demonstration shows strikingly that the heat transfer for  $\mathcal{A} \gg \mathcal{A}_c$  is determined by conditions near the heat source.

### 3.6 Application to the Taupo Area

Evidence for the existence of convection relies largely on two groups of data, temperatures measured in shut-in boreholes and estimates of the total heat flow.

In Figure 12 *Banwell's* [1961] data for the 200°C and 220°C isotherms at 350 meters below datum (500 meters above mean sea level) have been superimposed on the surface heat flow distribution. The isotherms are centered below the surface thermal areas and are considerably simpler in form than the surface distribution. This pattern is just what would be expected from a section across the upper part of a 'mushroom' which is distorted by outward flowing lobes of hot water. The vertical sections shown in Figure 13 emphasize this observation. Provided that the system is in a steady state, only a system dominated by the flow of water could produce such distributions; water rises vertically from depth below point X of Figure 13 until in the upper 1 km it runs away horizontally.

The most striking evidence for convection is the pronounced occurrence of cold water to depth of the order of 1 km around the immediate margin of the 'mushroom.' It was especially clearly demonstrated in the model experiments that when fluid is continuously discharged the region in which recirculation of hot fluid occurs is surrounded by cold meteoric water (Figures 18 and 19). These observations, together with the estimate obtained by *Thompson et al.* [1961] that  $Q'/Q = 0.96$  (i.e. 96% of the heat is lost by mass flow), demonstrate that Wairakei is close to being a single pass system. This was already evident in the pipe model

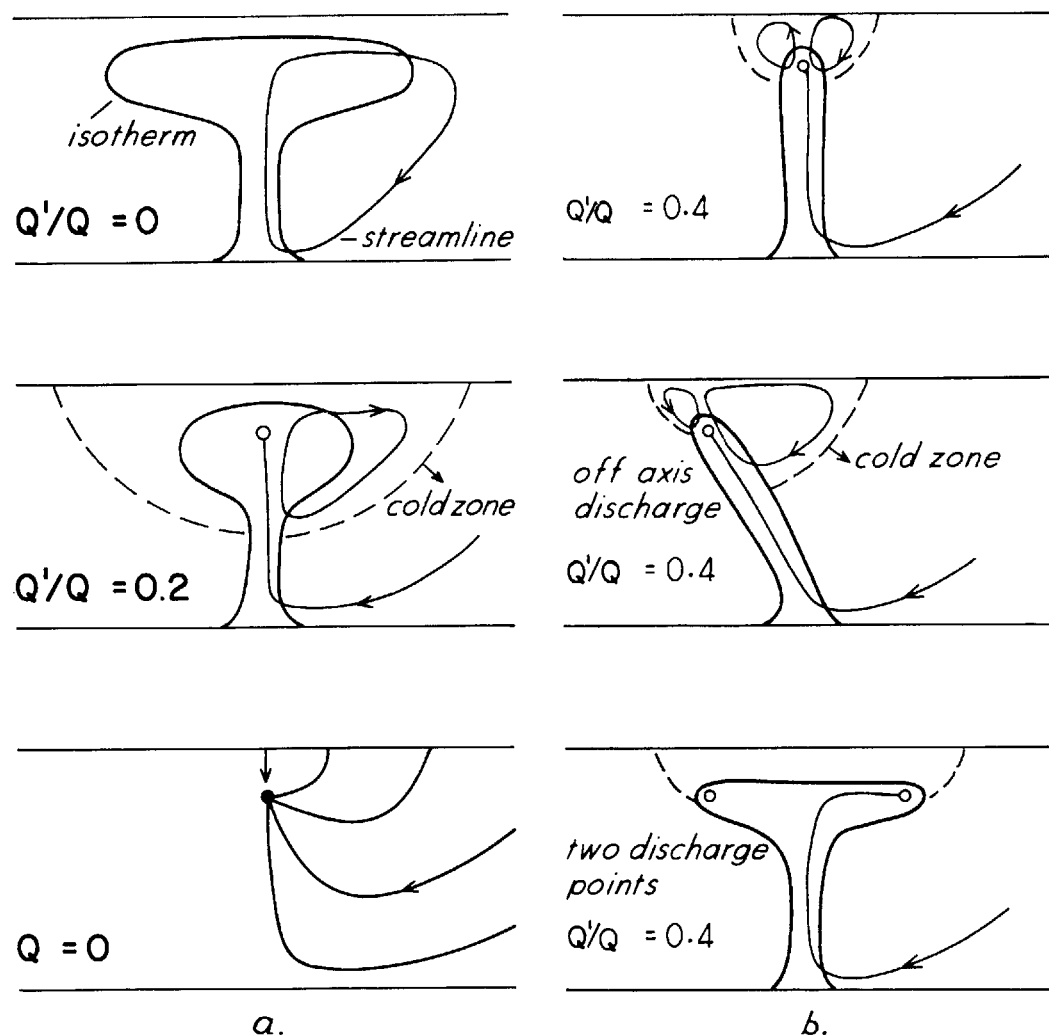


Fig. 18. Influence of discharge on the temperature velocity distribution: (a)  $Q'/Q = 0$ ,  $0.2$ ;  $Q = 0$ ; (b)  $Q'/Q = 0.4$  with the discharge point displaced and with two discharge points.  $Q$  is the power input,  $Q'$  is the power output of the water discharge.

shown in Figure 14, where the heat flow in the recirculation system is only 21% of that in the surface system.

Wairakei lies within the Taupo depression which is known from geological, seismic, magnetic, and gravity surveys to be filled with water-saturated volcanic debris to a depth of the order of 5 km. Extrapolated borehole temperatures suggest a temperature of the order of  $400^{\circ}\text{C}$  at the base of the depression. The heat flow by conduction alone with a temperature gradient of  $400^{\circ}\text{C}/5\text{ km}$  is about  $2 \times 10^{-6}\text{ cal/cm}^2\text{ sec}$ , very much smaller than the average value  $50\text{ }\mu\text{cal/}$

$\text{cm}^2\text{ sec}$ . Clearly, convection is the dominant mode of heat transfer.

There is a difficulty in applying (24). In the laboratory with  $\Delta T$  small,  $\alpha/\nu$  is reasonably constant, but in thermal areas this is no longer the case. We find, rather crudely, with  $T$  in degrees centigrade [c.f. Wooding, 1957]

$$\alpha = 4.2 \times 10^{-6}T \text{ (deg}^{-1}\text{)} \quad 100^{\circ}\text{C} < T < 300^{\circ}\text{C} \quad (25)$$

$$\nu = 0.33(13 + T) \sim 0.33/T \text{ (cm}^2\text{/sec)} \quad T < 200^{\circ}\text{C} \quad (26)$$

Noting that the heat transfer is dominated by

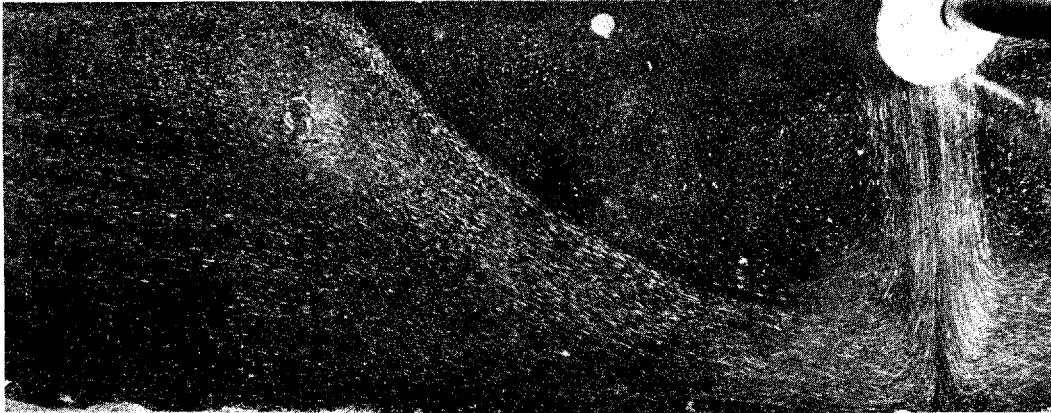


Fig. 19. Photograph of free convection in a Hele-Shaw cell with water discharge.

conditions near the heat source, and that nearly cold water is incident on the heater, the best that can be done is to evaluate  $\alpha$ ,  $\nu$  at  $(T_0 + \frac{1}{2}\Delta T)$ . Then (24) becomes

$$Q = 2.6 \times 10^{-8} k g \rho_0 c (\Delta T)^4 (\frac{1}{4} \pi L^2)^\circ C^{-4} \quad (27)$$

In situ values of  $k$  for the upper 1 km of the system have been found from borehole tests to be in the range  $1-5 \times 10^{-9}$  cm<sup>2</sup>, so that a possible value at depth is of the order of  $10^{-9}$  cm<sup>2</sup>. Hence with  $T = 350^\circ\text{C}$ —a best estimate—we have  $L = 7.5$  km,  $\mathcal{A} = 1.0 \times 10^4$ , and  $Q_l = 250$ . These are reasonable values. In particular, it has been shown that free convection in a porous medium can transport the large heat flows found in thermal areas. Incidentally, values of  $Q_l$  could well be of the order of  $10^3$  in some cases, so that, e.g., bodies of kilometer scale which would cool in  $10^4$  years by conduction can cool in of the order of 10 years by convection. There is a possibility that this is the explanation of the rapid cooling of the volcano on Oshima Island, Japan, following an eruption [Rikitake and Yokoyama, 1955].

Recently Wooding [1963] has given an elaborate analysis of the rising column of hot fluid by showing that when the Peclet number is sufficiently large (viz.,  $WA^{1/2}/\kappa_m > O(10)$ ) the hot column behaves like a jet. He has given a detailed analysis of the validity of the approximation, presented supporting experimental evidence, and applied the ideas to Wairakei. Lateral diffusion on the margin of the jet is found to follow a similarity relation; the horizontal scale of the jet margin is  $X = (4\kappa_m z/W)^{1/2}$  so that, for example, with  $z = 5$  km,  $\kappa_m = 3 \times 10^{-3}$

cm<sup>2</sup>/sec,  $W = 10^4$  cm/sec, we have  $X = 80$  meters. This value is fairly close to that proposed by Wooding in his model *i*.

### 3.7 Ocean Thermal Areas

It is worth while to consider the possibility of hydrothermal systems existing in oceanic thermal areas. For a hydrothermal system to be possible, a source of heat and water is required, together with a layer of sufficiently high permeability. The high heat flows on ocean ridges certainly indicate a source of heat. Sea water, rather than meteoric water, is available. Here there is the possibility of progressive closing of permeable paths by deposition of salt, but this is only likely where vaporization of water occurs. The major problem is the question of the permeability. Permeability will be a rapidly decreasing function of pressure, owing to the compaction of the voids in the rock. Nevertheless, in a region disturbed by surface volcanism it can be anticipated that permeabilities in the upper few kilometers of the ocean crust could be of the order of 0.01 darcy. This would be sufficient to allow regional heat flows of the order of  $10 \mu\text{cal}/\text{cm}^2 \text{ sec}$ . There is already sufficient indication from the observations of lower maximum values of heat flow in oceanic thermal areas compared with land thermal areas that the permeability is somewhat lower in oceanic areas.

The boundary conditions at the surface of an oceanic hydrothermal system differ from those on land: there is no air-water interface, and the sea water exists both above and below

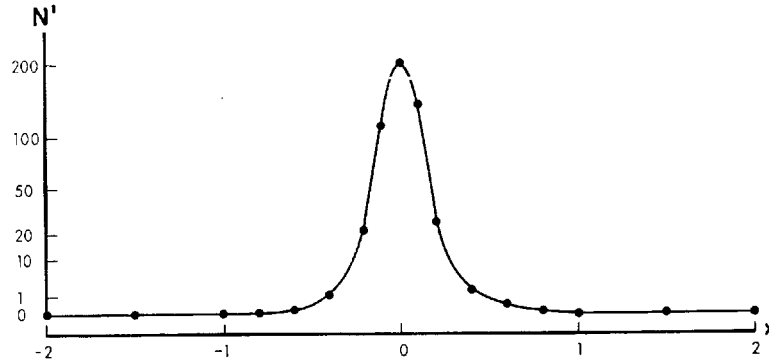


Fig. 20. Local surface heat flux  $q = Q_l K_m (\Delta T / H)$  in model of oceanic thermal area. Hele-Shaw cell with  $Q_l = 50$ ,  $\mathcal{A} = 2 \times 10^3$ . Values are for  $Q_l$ .

the surface. This can be simulated in a laboratory model by joining the upper surface of a Hele-Shaw cell into a wide cavity representing the ocean. The distribution of surface heat flux obtained in such an experiment is shown in Figure 20. It is seen that on the margins of the area the heat flux is zero, corresponding to the region of recharge of cold sea water. In the middle of the area is a region of intense heat flow that is somewhat narrower than the heat source.

Such considerations are merely suggestive. It is not proposed that all the heat discharged in the oceanic thermal areas is transferred in hydrothermal systems. But it should not be overlooked that some of the features of oceanic thermal areas may be explicable in terms of hydrothermal systems.

#### 4. INFERENCES ABOUT CONVECTION IN THE MANTLE

At the outset it should be noted that as far as the normal heat flow areas are concerned convection in the mantle is an unnecessary hypothesis. The heat flow could arise solely from radioactive decay as discussed by MacDonald in chapter 7 of this volume. The great uncertainties in the radioactive hypothesis are the total rate of heat production and its distribution with depth. At the moment it would be simplest to assume that all the normal heat flow arose from radioactive decay, the radioactive material being distributed over sufficient depth that the heat flux through oceans and continents was the same within the limits of observation.

Possible global variations of heat flow proposed by *Lee and MacDonald* [1963] could arise from global variations in the concentration of radioactive material.

As has been pointed out in section 3, however, the Taupo thermal area needs, for a lifetime of  $10^6$  years, a supply of energy equivalent to that in a column of rock of depth  $10^2$  km and temperature excess  $5 \times 10^2$  °C, together with a transport mechanism to transfer the energy from the rock at depth to the base of the Taupo hydrothermal systems. Thermal conduction is inadequate. Some dynamic mass transfer process must be present. Certainly, immediately below the Taupo area, at least to depths of the order of  $10^2$  km, mass transfer occurs. There remains, however, the question of how this large body of rock acquired its energy. It is difficult to escape the conclusion that local energy sources are inadequate: radioactive sources would need to be of the order of  $10^2$  stronger than in the rocks of normal areas, and surely in such a closely explored area some evidence of this would have been reported; chemical energy could perhaps release of the order of  $10^2$  cal/g, but this would be exhausted in  $10^6$  years. There remains the possibility that the energy required for volcanism is not produced locally but is transported to the volcanic zone by large-scale convection in the mantle. Certainly, only the Taupo area has been investigated thoroughly enough to draw this conclusion. For the moment it must remain as a hypothesis that all thermal areas derive their energy from mantle convection.

At the moment there are numerous specula-

tions about mantle convection [e.g. *Vening Meinesz*, 1958; *Runcorn*, 1962]. The present task, however, is restricted to a consideration of the possible contribution of convection to heat flow within the mantle, particularly insofar as such convection could provide an energy source for volcanism. Our point of view will be that developed in a recent review by *Knopoff* [1964], who discusses the possibility of convection in a viscoelastic mantle in terms of the *Rayleigh* [1916] convection problem and a theory of thermal turbulence due to *Malkus* [1954]. The problem in this section is not to question how convection could commence, but rather to find sufficient conditions under which convection would persist and to ask if the convection can transport enough energy.

The crucial assumption is that the mantle is viscoelastic. If this is accepted, there can be little doubt that the mantle is convective.

The basis of the convection hypothesis is that motion is generated by buoyancy forces. Buoyancy forces are those produced in a gravitational field by *imbalanced* density variations. Here it is assumed that the imbalanced density variations arise from variations in temperature. As *Jeffreys* [1930] pointed out, in a compressible fluid the density variations must be measured relative to a reference state of equilibrium. This reference state corresponds to a state of no motion and entropy independent of position, so that

$$T = T_0 \exp(\alpha g z / c_p) \quad (28)$$

where  $T_0$  is the temperature on  $z = 0$ . With  $\alpha = 10^{-5} \text{ deg}^{-1}$ ,  $c_p = 1 \text{ joule/g } ^\circ\text{C}$ , so that  $\alpha g / c_p = 10^{-9} \text{ cm}^{-1}$ , the temperature at the bottom of the mantle in the reference state, for  $T_0 = 300^\circ\text{K}$ , is  $400^\circ\text{K}$ . In the present state of the mantle, however, temperatures are at least of the order of  $10^3 \text{ }^\circ\text{K}$ , so that a strongly superadiabatic situation exists.

The heat transfer process can be evaluated in two stages by considering, first, penetrative convection in the upper mantle and, second, large-scale convection in the lower mantle. Numerous possibilities can be found in the literature; here only certain gross features of a simple convective model which appears to be relevant to the Taupo volcanic area are evaluated. No attempt is made to discuss the many

other geological and geophysical aspects of the problem.

#### 4.1 *Observational Evidence for Penetrative Convection in the Upper Mantle*

Recently *Healy* [1964] has discussed the structures within the Taupo depression in terms of 'ring complexes and associated cauldron subsidences.' These structures are remarkably similar to those associated with salt domes [*Dobrin*, 1941]. We note that the essential mechanical features of the rise of a buoyant element through the more viscous crust are its lower density and viscosity compared with the surrounding rock, together with extensive fracturing of the upper crust as the element approaches the surface. Healy's observations provide strong evidence of penetrative convection.

A study of the spatial distribution of earthquake foci by *Eiby* [1964] indicates the immediate energy source of the buoyant elements. *Eiby* notes that, while earthquakes at depths less than 40 km are widely scattered in New Zealand, deeper earthquakes lie in a zone of width about 100 km and depth 300–400 km. He has called this the New Zealand subcrustal rift. By consideration of the gravity anomalies, he infers that within the rift densities are about  $0.03 \text{ g/cm}^3$  less than the surrounding rocks. Hence, with  $\alpha = 2 \times 10^{-5}/^\circ\text{C}$  and  $\rho = 3 \text{ g/cm}^3$ , this could arise from a mean temperature excess of  $500^\circ\text{C}$ .

The direct observational evidence for penetrative convection in the upper mantle is most convincing. Much of this is discussed in an interesting review of physical volcanology by *Sakuma and Nagata* [1957]. At the time of a volcanic eruption and for a period of years before an eruption, earthquake foci are found near and below the volcano. Before the eruption the earthquake foci are at considerable depth, often of the order of 50 km, but they gradually migrate vertically [*Sakuma and Nagata*, 1957, section 9; *Eaton*, 1962]. During this period the ground surface wells up at rates of the order of 10 cm/day [*Sakuma and Nagata*, 1957, Figure 10, p. 990].

A possible explanation of these phenomena is that a hot body of less viscous material is penetrating the surrounding cooler, more viscous rock. Unfortunately, the rheological na-

ture of the mantle is almost unknown. *Gutenberg* [1958] has discussed a number of possibilities. Of these, a model of current interest is that of a viscoelastic material of Maxwell type. For such a material and motions of sufficient duration, the flow can be described in terms of viscosity. More recently, a concept of the mantle has been proposed by F. C. Frank (personal communication). The mantle is considered to consist of grains of solid between which there is a small fraction of melt, the mantle behaving rather like a porous medium. An immediate attraction of Frank's model is that motion corresponding to that in a material of viscoelastic viscosity of the order of  $10^{20}$  poise is readily contemplated. With Frank's model the matrix itself need not move. In this case it would be possible to have convective heat transfer in the mantle without implying 'continental drift.'

The penetration of a less dense, less viscous bubble through a denser, more viscous material has been studied in the laboratory in connection with the rise of salt domes [*Dobrin*, 1941; see also *Fultz*, 1961, section 4.2]. For the case in which the viscosity in the bubble (or dome) is very much less than the viscosity  $\mu_0$  of its surroundings, *Dobrin* found

$$g\Delta\rho a^2/W\mu_0 \approx 40 \quad (29)$$

where  $W$  is the steady velocity of rise of the bubble of radius  $a$ , and  $\Delta\rho$  is the density difference between the surroundings and the bubble. This expression indicates a balance between viscous forces and buoyancy forces. Inserting the typical values  $\alpha = 2 \times 10^{-5}/\text{deg}$ ,  $\Delta T = 50^\circ\text{C}$ ,  $W = 10^{-4}$  cm/sec [*Sakuma and Nagata*, 1957, Figure 10], and  $r = 1$  km requires  $\mu_0 = 2.5 \times 10^{12}$  poise. This is the order of magnitude to be expected, since seismic waves would be heavily damped for  $\mu_0 < 10^8$  poise, and in non-volcanic areas the upper mantle has a viscosity of the order of  $10^{20}$  poise. The corresponding Reynold's number is of the order of  $10^{-11}$ , so that the motion is indeed resisted solely by viscous forces.

The corresponding heat flux  $\rho c W \Delta T \sim 10^{-2}$  cal/cm<sup>2</sup> sec. This is quite adequate. Such a heat flux over 0.01% of the Earth's surface would produce a total heat flow equal to that from normal areas.

Rather than consider the rising body as a homogeneous bubble, it is possible to consider

that the rising material is a fraction of the rock above its melting point (as in Frank's model). This molten fraction will be less dense than the solid rock and will percolate upward as if it were in a porous medium. The bubble will rise as if it were in a viscous fluid of viscosity  $\mu_m a^2/k$ , where  $\mu_m$  is the viscosity of the melt and  $k$  is the permeability of the solid matrix.

#### 4.2 Origin of the Instability of the Upper Mantle

In their simplest form, studies of penetrative convection consider the instability and subsequent motion of two superimposed layers of fluid of different densities and viscosities. This is the so-called Rayleigh-Taylor instability, after the fundamental work of *Rayleigh* [1900] and *Taylor* [1950]. A full discussion is given by *Chandrasekhar* [1961, chapter 10]. To apply such ideas to the mantle, however, requires a much more elaborate model. Only some reasonable possibilities are suggested here.

Consider the following model. A layer of viscous fluid has a distribution of heat sources falling exponentially from the surface. Let the temperature on  $z = 0$  be zero and at depth be  $2 \times 10^3$  °C, a possible value for the deep mantle. In the steady state, with no motion,

$$T = 2 \times 10^3 (1 - e^{-z/\zeta}) \quad \zeta = \text{constant} \quad (30)$$

This corresponds to a distribution of heat sources  $10^{-13} \exp(-z/\zeta)$  cal/cm<sup>3</sup> sec. With  $\zeta = 100$  km, (30) is in moderate agreement with the petrological models of *Clark and Ringwood* [1964]. Also taking the thermal conductivity  $10^{-2}$  cal/cm deg sec, the surface heat flux is  $1 \mu\text{cal/cm}^2$  sec.

Further, assuming that the viscosity of the fluid behaves as  $\exp(\text{constant}/T^\circ\text{K})$ , the data reported by *Sakuma and Nagata* [1957] give roughly

$$\nu = 10^8 \exp(3 \times 10^4/T^\circ\text{K}) \text{ cm}^2/\text{sec} \quad (31)$$

for acid rocks, an order of magnitude less for basic rocks. I have assumed that the ratio of viscosity below and above the melting point is  $10^6$ .

The stability of the layer will vary with level in the manner suggested by *Rayleigh* [1916]. Figure 21 shows values of  $\mathcal{R} = agT_\alpha a^4/\kappa\nu$  for  $\alpha = 10^{-5}/\text{deg}$ ,  $\kappa = 10^{-2}$  cm<sup>2</sup>/sec,  $a = 30$  km, and the above forms of  $T$ ,  $\nu$ . It is immediately ap-

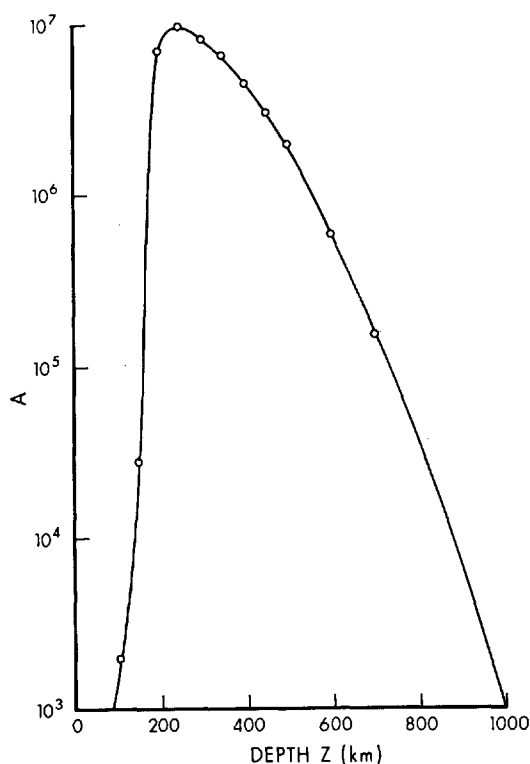


Fig. 21. Instability of the upper mantle as a function of depth for a blob of radius 30 km. Values are for  $\bar{A}$ .

parent that there is a sharp maximum at depth 250 km with a very rapid decrease in instability as the surface is approached. Rayleigh's result implies that any given disturbance to an element will be damped only if  $\bar{A}(a) \lesssim 10^3$ . Thus, in this example, elements of diameter 60 km or larger are unstable for all depths 100–1000 km, but the region of the most vigorous production of buoyant elements will be from depths 200 to 300 km.

Unfortunately, adequate laboratory and theoretical studies of penetrative convection do not exist. If, however, a region of fully developed penetrative convection is at all similar to the thermal sublayer in a layer of fluid heated from below [Townsend, 1959], we can anticipate that blobs of fluids will arise from the source region more or less at random. The blobs will rise easily to about 100 km. Above this level, however, the viscosity rapidly increases. For example, in this model, arising from 250 km, the blob kinematic viscosity is  $1.4 \times 10^{14}$  cm<sup>2</sup>/sec, but

the fluid at 50 km has kinematic viscosity of  $1.7 \times 10^{20}$  cm<sup>2</sup>/sec. At this level a blob is similar to a rising salt dome. Only if its initial buoyancy is high enough will it penetrate the ground surface. Only a small proportion of these blobs will penetrate to the level of the hydrothermal systems, thereby providing a heat source which will fluctuate with time.

#### 4.3 Formulation of the Problem of Mantle Convection

The subsequent discussion is based on investigations of the model convective system first studied by Benard [1901] and Rayleigh [1916]. Consider a layer of thickness  $H$  and horizontal extent  $L$  of fluid of density  $\rho$ , kinematic viscosity  $\nu$ , thermal diffusivity  $\kappa$ . The lower surface  $z = 0$  is maintained at temperature  $\Delta T$  above the temperature in the reference state; the upper surface  $z = H$  is maintained at zero temperature above that in the reference state. Making the Boussinesq [1903] approximation that density variations are significant only in their generation of buoyancy forces, and that other fluid parameters are constant, the problem is defined by:  $\nu, \kappa, \alpha g \Delta T, H, L$ . Since these involve only the dimensions of length and time, three dimensionless parameters are needed to specify the problem; a convenient set is:

$$\begin{aligned} \mathcal{P} &= \nu/\kappa && \text{Prandtl number} \\ \bar{\mathcal{A}} &= \alpha g \Delta T H^3 / \kappa \nu && \text{Rayleigh number} \\ \mathcal{L} &= L/H && \text{aspect ratio} \end{aligned} \quad (32)$$

Since  $\alpha \Delta T \sim 10^{-2}$ , the Boussinesq approximation will be a good one: indeed, even in studies of penetrative convection, where the entire density range 3–6 g/cm<sup>3</sup> may need to be considered, errors on this account would be no more than a factor of 2. However, these uncertainties are dwarfed by ignorance of  $\kappa$  and  $\nu$ . The diffusivity  $\kappa$  is probably of the order of  $10^{-2}$  cm<sup>2</sup>/sec, but in the deep mantle where photons, excitons, and holes may be in abundance, it could be of the order of 1 cm<sup>2</sup>/sec or higher. This is serious enough, but estimates of  $\nu$ , possibly of the order of  $10^{20}$  cm<sup>2</sup>/sec, are given by various authors in the range  $10^{20 \pm 10}$  cm<sup>2</sup>/sec.

Laboratory experiments indicate that the Rayleigh number is the dominant parameter. The aspect ratio plays a role only in laminar convection. Unfortunately no laboratory experi-

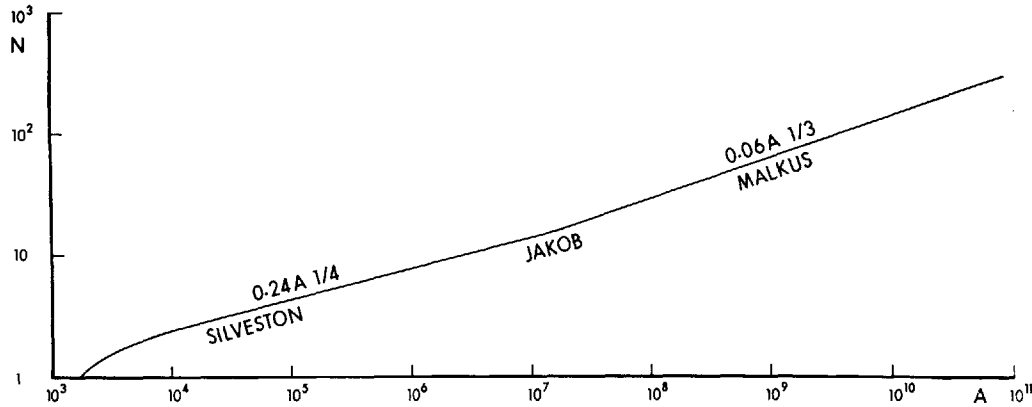


Fig. 22. Heat transfer characteristic for free convection in a viscous fluid. Nusselt number against Rayleigh number. After *Silveston* [1958], *Jakob* [1949], and *Malkus* [1954]. Values are for  $\mathcal{N}$  and  $\mathcal{A}$ .

ments even approach the very large Prandtl number  $10^{22}$  of the mantle, so that on this count alone the comparison of laboratory experiments with the mantle should be viewed with suspicion. *Knopoff* [1964] has discussed also the effects of the sphericity of the Earth and its rotation, together with second-order compressibility effects on the results of this model. These effects are minor.

The quantity of major interest will be the power  $Q$  transmitted through the convecting layer, for which we define the Nusselt number  $\mathcal{N}$ , a dimensionless conductivity such that

$$Q = \mathcal{N}K (\text{heated area}) \Delta T/H \quad (33)$$

where  $K$  is the thermal conductivity of the convecting material. A summary of measurements of  $\mathcal{N}(\mathcal{A})$  is shown in Figure 22. For  $\mathcal{A} \leq \mathcal{A}_c = 1700$ ,  $\mathcal{N} = 1$ , there is no motion in the fluid and the heat is transferred solely by conduction [*Chandrasekhar*, 1961, chapter 1]. The motion is laminar or quasi-laminar for  $\mathcal{A}_c < \mathcal{A} < 10^7$ ; at higher Rayleigh numbers the motion is turbulent and

$$\mathcal{N} = 0.06\mathcal{A}^{1/3} \quad (34)$$

This relation is accurate enough for our present purpose, provided that  $\mathcal{A} > 10^4$ .

The relation 34 implies that the heat transferred through the convecting layer is independent of  $H$ . It is therefore appropriate to define a thermal boundary layer thickness  $\delta$  such that  $\mathcal{N} = H/2\delta$ . Then

$$\delta = 6.6(\kappa\nu/αg\theta)^{1/3} \quad (35)$$

where  $\theta = \frac{1}{2}\Delta T$  is the temperature drop across the thermal boundary layer on one wall.

#### 4.4 Application to the Mantle

At the outset we note that a super-adiabatic temperature difference of  $1^\circ\text{C}$  across a layer of thickness  $10^3$  km gives a Rayleigh number, using the values above, of  $10^4$ . Since much greater temperature differences can be expected in the mantle, the possibility of convection is assured. Indeed, as *Knopoff* [1964] has pointed out, the mantle may be turbulent.

It is believed that the viscosity decreases rapidly with depth in the mantle [*Gutenberg*, 1958]. As a first approximation, therefore, consider an upper layer of thickness  $h$  of material of sufficient rigidity that it takes no direct part in the convection below. It can still be considered plastic, but the time scale of any motions produced in it, either internally or by the stresses at its lower boundary, arising from the convection at depth, are assumed to be much greater than the time scale of the convective motion. *Knopoff* [1964] has made an equivalent suggestion based on the estimated density distribution in the mantle by noting that the rapid density increase from 400- to 1000-km depth presents a barrier to convection.

If the only source of energy is the thermal energy of the Earth, an upper bound for  $h$  is set by the observed heat flux  $1.5 \mu\text{cal}/\text{cm}^2 \text{ sec}$  and the limit of infinite Rayleigh number of the convecting part of the mantle. With  $K =$

$10^{-2}$  cal/cm deg sec, and the temperature of the convecting mantle  $1500^{\circ}\text{C}$ , say, we require  $h \leq 150$  km. Actually, this value would be quite acceptable. It is about the level of isostatic equilibrium and the beginning of the pronounced changes from the upper to the lower mantle.

It should be noted that there is ample thermal energy. For example, a loss of 100 cal/gm (equivalent to about  $500^{\circ}\text{C}$ , or about the value of the latent heat of rock) throughout the mantle of mean density about  $4.5$  g/cm $^3$ , at the present rate of loss of  $1.5$   $\mu\text{cal}/\text{cm}^2$  sec, would be sufficient for  $3 \times 10^9$  year—quite an acceptable value.

There is certainly some radioactive heat generated in *crustal* rocks, however. From petrological models *MacDonald* [1959] estimates of the order of  $0.5$   $\mu\text{cal}/\text{cm}^2$  sec from the crust; *Clark and Ringwood* [1964] estimate  $0.7$   $\mu\text{cal}/\text{cm}^2$  sec from the upper 400 km of the Earth. In view of *Lee's* [1963] analysis, which gives an expected value for a single measurement of  $1.6 \pm 1.2$  s.d.  $\mu\text{cal}/\text{cm}^2$  sec, it is not possible to make discriminatory arguments based on fluxes of the order of  $0.5$   $\mu\text{cal}/\text{cm}^2$  sec which are much less than the standard deviation. Clearly local deposits of radioactive material exist, and their great variability could be a principal contributor to the variability of the heat flux. Nevertheless, if the Rayleigh number is sufficiently high, radioactive heating may be a minor present-day source of the Earth's heat flux.

Consider now a model in which the Rayleigh number is finite and there are radioactive heat sources present in the upper mantle, as sketched in Figure 23. Let the temperatures be  $T_1$ ,  $T_2$  and the heat fluxes  $q_1$ ,  $q_2$  at the top and bottom of the lower mantle. In both cases the mantle temperature outside the thermal boundary layers will be close to adiabatic, so that, writing  $T_1'$ ,  $T_2'$  for the temperatures just outside the thermal boundary layers,

$$T_2' = T_1' \exp \alpha g (H - h) / c_p \quad (36)$$

Hence, assuming  $T_2' = 2000^{\circ}\text{C}$ , say, with  $(H - h) = 3 \times 10^8$  km and  $\alpha g / c_p = 10^{-9}$  cm $^{-1}$ ,  $T_1' = 1470^{\circ}\text{C}$ .

Let the upper mantle have a uniform distribution of heat sources of strength  $A$  cal/cm $^3$  sec. The energy equation for the upper mantle in the steady state is

$$KT_{zz} = -A \quad (37)$$

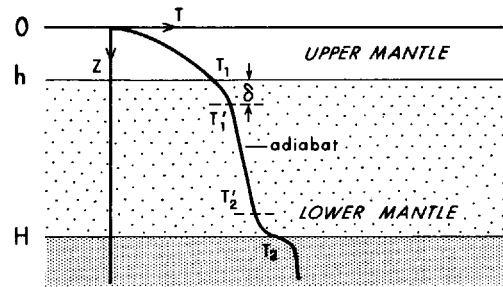


Fig. 23. Schema of the mantle.

so that

$$KT = q_0 z - \frac{1}{2} A z^2 \quad (38)$$

If the temperature and heat flux at  $z = h$ , the base of the upper mantle, are  $T_1$ ,  $q_1$ , we need

$$h = 2KT_1 / (q_0 + q_1) \quad (39)$$

$$A = (q_0 - q_1) / h \quad (40)$$

Hence by (35) with  $\theta = (T_1' - T_1)$

$$q_1 = K\theta / \delta \quad (41)$$

Table 1 shows some values of  $h$  for typical values of the parameters. The values found for  $A$  are similar to those suggested by *Clark and Ringwood* [1964, Table 4]. Note the relatively sharp cutoff at  $\theta = 420^{\circ}\text{C}$ . Even if *Clark and Ringwood's* estimates of  $A$  are only order of magnitude, there is a strong suggestion here that the upper mantle must be at least 100 km thick. If it is 300 km or more thick, there is negligible heat flux from the lower mantle. Accepting, for example, *Clark and Ringwood's* estimate of about  $0.3$   $\mu\text{cal}/\text{cm}^2$  sec from the lower mantle, Table 1 suggests that the upper mantle has a depth of the order of 200 km, and that at this depth the temperature is about  $1300^{\circ}\text{C}$ . Clearly the values used here are somewhat arbitrary, but such simple models place strong constraints on the combination of parameters chosen on other grounds.

If similar calculations are made for  $q_2 \neq 0$ , it is necessary to consider the energy balance of the whole Earth to obtain a closed system of equations. This involves a study of the thermal history of the Earth, but it is not our present purpose.

#### 4.5 Energy Supply for Volcanism

The total rate of loss of heat from thermal areas (including surface volcanism) is probably

TABLE 1. Depth of Upper Mantle  $h$ , Source Strength  $A$ , Obtained from equations (39)–(41)

$T_3 = 2 \times 10^3$  °C,  $q_0 = 1$   $\mu\text{cal/cm}^2$  sec,  $K = 10^{-2}$  cal/cm deg sec,  $\kappa = 10^{-2}$   $\text{cm}^2/\text{sec}$ ,  $\nu = 10^{20}$   $\text{cm}^2/\text{sec}$ ,  $\alpha = 10^{-5}/\text{deg}$ .

$\theta$ , deg C	$T_1$ , deg C	$h$ , km	$A$ , $10^{-14}$ cal/cm <sup>3</sup> sec	$q_1$ , $\mu\text{cal/cm}^2$ sec
20	1450	285	3.45	0.02
50	1420	268	3.52	0.06
100	1370	238	3.59	0.15
200	1270	185	3.38	0.38
300	1170	143	2.52	0.64
400	1070	110	0.48	0.95
420	1050	105	0.00	1.00

of the order of  $5 \times 10^{10}$  cal/sec, i.e. 1% of the total rate of loss in normal areas. This value is equivalent to 40 Taupo areas of output  $1.3 \times 10^9$  cal/sec. Since the bulk of the thermal areas are unmeasured, the value is little more than a guess. A value of 0.1% would clearly be too small, while even an optimistic estimate of total measured output is less than 10%.

There is no difficulty in accounting for  $5 \times 10^{10}$  cal/sec by means of convection from the mantle. Indeed, as has been shown in section 4.3, nearly all the Earth's heat loss could be accounted for by invoking convection in the mantle.

##### 5. A SPECULATION ON THE DEVELOPMENT OF THE EARTH

The above point of view can be conveniently summarized by means of a model thermal history of the Earth. The model merely provides a frame of reference. It is, however, one of the models currently under discussion. It arises from a suggestion by *Urey* [1952] on the growth of the Earth's core. *Runcorn* [1962] and others have paid some attention to it.

Consider an initially cold Earth. Radioactive heat sources will begin to warm the interior. Except near the surface, heat transfer by thermal conduction will be negligible. If the strength of the radioactive heat sources is great enough, the temperature will ultimately approach the melting point. A small fraction of melt will then be produced. The buoyancy of this melt fraction will cause it to percolate between the remaining rock grains and lumps after the manner of Darcy's law. Rising and falling bodies will begin to move through the Earth material in the manner of the salt domes dis-

cussed in section 4. A very rapid segregation of the heavy and light materials will ensue. This process could be largely complete in  $10^6$  years. At the end of this time the temperature at depth would be nearly everywhere close to the melting point.

Subsequently, as the intense penetrative convection dies away, the less vigorous free convection of the viscous rock becomes more important. The essential features of the present Earth are established. Penetrative convection persists, but only weakly and in a sporadic form in the upper mantle to produce the volcanic zones. The contribution of convection in the mantle and core at this time contributes little to the Earth's heat flux, which largely arises from the near surface radioactive layer. Ultimately, of course, since the radioactive sources diminish exponentially with time, convective heat transfer will predominate, but it too will diminish as the Earth cools further. Finally, only thermal conduction will be important.

As the buoyant bubbles in a zone of penetrative convection rise toward the surface, they are slowed by the higher viscosity of the surrounding rocks. Nevertheless, the surrounding rocks will be partially warmed. Near the surface some melting will occur, either of the rising mantle material itself, or of the surrounding rocks. Some of this melt will penetrate the surface and produce surface volcanism. Even if the hot rising elements do not reach the surface, at shallow depths they may warm groundwater and produce hydrothermal systems.

The energy from depth is ultimately lost to the atmosphere and ocean by warming the ambient environment or by discharge of hot water and steam.

Our view has been of a cascade of energy from large-scale motions of the scale of  $10^3$  km through a succession of motions of progressively smaller scale to the ultimate dissipation of the energy in a surface layer of the scale of 1 meter. The interactions between the various scales of motion have been more sharply drawn than they would be in nature.

## 6. SUMMARY

Our knowledge of the surface distribution of heat flow and the distribution of temperature with depth in normal areas of the Earth can be described solely in terms of stored thermal energy, together with energy released by radioactive decay, transferred by thermal conduction and radiation. In thermal areas it is necessary to consider heat transferred by the movement of water and magma.

A discussion of the surface discharge mechanisms in land thermal areas is possible largely in terms of the evaporation and flashing of water into steam, provided that there exists a body of hot water and rock below the surface. Energy is transferred in this body by the convection of water. However, the energy in this body would be rapidly exhausted if it were not supplied with energy from depth. The amount of energy required is large enough that there is little alternative to assuming that it is derived ultimately by transfer of matter from the mantle.

A possible mechanism of volcanism is based on the hypothesis that the mantle is viscoelastic and that the viscosity decreases rapidly with depth. Thence nearly everywhere the upper part of the mantle is stable while the lower part is convecting. Occasionally, however, parts of the upper mantle can become unstable, owing to the presence of a large positive temperature fluctuation in the lower mantle. Penetrative convection can then occur in the upper mantle.

*Acknowledgments.* Much of the work reported here was performed during 1958–1961 at Geophysics Division, Department of Scientific and Industrial Research, Wellington, New Zealand. I wish especially to thank Dr. E. I. Robertson, F. E. Studt, and C. J. Banwell. I am extremely grateful for the assistance of Mr. W. J. P. MacDonald. Professor D. Walker, Victoria University of Wellington, kindly arranged laboratory facilities. It is a pleas-

ure to acknowledge my debt to Dr. Masami Haya-kawa, Geological Survey of Japan, and Dr. D. Lenzi of the Societa Larderello.

I wish to thank Professor F. C. Frank for a very searching reading of the draft of this chapter, and Dr. R. A. Wooding and Dr. Walter M. Elsasser for many valuable comments.

The manuscript was written while I was supported from National Science Foundation grant GP-2414 and Office of Naval Research contract Nonr-2216.

## REFERENCES

- Allen, W. F., Flow of a flashing mixture of water and steam through pipes and valves, *Am. Soc. Mech. Engr. Trans.*, *73*, 257–265, 1951.
- Banwell, C. J., in Physics of the New Zealand thermal area, *New Zealand Dept. Sci. Ind. Res. Bull.* *123*, 1957.
- Banwell, C. J., Geothermal drillholes—physical investigations, U. N. Conf. on New Sources of Energy, Rome, paper G53, 1961.
- Banwell, C. J., Thermal energy from the Earth's crust: Introduction and Part 1, Natural hydrothermal systems, *New Zealand J. Geol. Geophys.*, *6*, 52–69, 1963.
- Benard, M., Les tourbillons cellulaires dans une nappe liquide transportant de la chaleur par convection en régime permanent, *Ann. Chim. Phys.*, *23*, 62–144, 1901.
- Benfield, A. E., Terrestrial heat flow in Great Britain, *Proc. Roy. Soc. London, A*, *173*, 428–450, 1939.
- Benioff, H., Internal constitution of the Earth, edited by B. Gutenberg, p. 391 ff., Dover Publications, New York, 1951.
- Benseman, R. F., The calorimetry of steaming ground in thermal areas, *J. Geophys. Res.*, *64*, 123–126 and 1057–1062, 1959.
- Benseman, R. F., The components of a geyser, *New Zealand J. Sci.*, *7*, 1, 1965.
- Birch, F., Elasticity and constitution of the Earth's interior, *J. Geophys. Res.*, *57*, 231, 1952.
- Bodvarsson, G., On thermal activity in Iceland, Geothermal Dept., State Electricity Authority, Reykjavik, Iceland, 1948.
- Bodvarsson, G., Drilling for heat in Iceland, *Oil and Gas J.*, *47*, 191–199, 1949.
- Bodvarsson, G., Geophysical methods in prospecting for hot water in Iceland (in Danish), *Timarit Verkfraed. Islands*, *35*, 49–59, 1950.
- Bodvarsson, G., Terrestrial heat balance in Iceland, *Timarit Verkfraed. Islands*, *39*, 69–76, 1954.
- Bodvarsson, G., Physical characteristics of natural heat resources in Iceland, U. N. Conf. on New Sources of Energy, Rome, paper G6, 1961.
- Boussinesq, J., *Théorie Analytique de la Chaleur*, *2*, p. 172, Gauthier-Villars, Paris, 1903.
- Bullard, E. C., The flow of heat through the floor of the ocean, in *The Sea*, edited by M. N. Hill, Vol. 3, pp. 218–232, Interscience, John Wiley & Sons, New York, 1963.

- Bullard, E. C., A. E. Maxwell, and R. Revelle, Heat flow through the deep sea floor, *Advan. Geophys.*, 3, 153-181, 1956.
- Bullen, K. E., *An Introduction to the Theory of Seismology*, Cambridge Univ. Press, London, 1953.
- Burgassi, R., Prospecting of geothermal fields, U. N. Conf. on New Sources of Energy, Rome, paper G65, 1961.
- Burgassi, R., F. Battini, and J. Mouton, Geothermal prospecting for endogenous energy, U. N. Conf. on New Sources of Energy, Rome, paper G61, 1961.
- Chandrasekhar, S., *Hydrodynamic and Hydromagnetic Stability*, Clarendon Press, Oxford, 1961.
- Chierici, A., Planning of a geothermal power plant, U. N. Conf. on New Sources of Energy, Rome, paper G62, 1961.
- Clark, S. P., and A. E. Ringwood, Density distribution and constitution of the mantle, *Revs. Geophys.*, 2, 35-88, 1964.
- Darcy, H. P. G., *Les fontaines publiques de la ville de Dijon*, Victor Dalmont, Paris, 1856.
- Dawson, G. B., The nature and assessment of heat flow from hydrothermal areas, *New Zealand J. Geol. Geophys.*, 7, 155-171 (see also pp. 134-143 and 144-154), 1964.
- Dobrin, M. B., Some quantitative experiments on a fluid salt-dome model and their geological significance, *Trans. Am. Geophys. Union*, 22, 528-542, 1941.
- Donaldson, I. G., Temperature gradients in the upper layers of the earth's crust due to convective water flows, *J. Geophys. Res.*, 67, 3449-3460, 1962.
- Eaton, J. P., Crustal structure and volcanism in Hawaii, in *Am. Geophys. Union Monograph 6*, edited by G. A. Macdonald and H. Kuno, pp. 13-29, 1962.
- Eiby, G. A., The New Zealand sub-crustal rift, *New Zealand J. Geol. Geophys.*, 7, 109-133, 1964.
- Einarsson, T., The nature of the hot springs of Iceland (in German), *Rit. Visind. Isl.*, 26, 1-89, 1942.
- Elder, J. W., Ph.D. thesis, Cambridge, England, 1958.
- Elder, J. W., Hydrothermal systems, *New Zealand D.S.I.R. Bull.*, in preparation, 1965.
- Ewing, M., J. Brune, and J. Kuo, Surface wave studies of the Pacific Crust and Mantle, *Am. Geophys. Union Monograph 6*, edited by G. A. Macdonald and H. Kuno, pp. 30-40, 1962.
- Faxen, O. H., *Thermodynamic Tables in the Metric System for Water and Steam*, Nordisk Roto-gravvyr, Stockholm, 1953.
- Fultz, D., Developments in controlled experiments on larger scale geophysical problems, *Advan. Geophys.*, 7, 1-103, Academic Press, New York, 1961.
- Goguel, J., The thermal regime of subterranean water (in French), *Ann. Mines, Paris*, 10, 3-32, 1953.
- Grange, L. I., editor, Geothermal steam for power in New Zealand, *New Zealand Dept. Sci. Ind. Res. Bull. 117*, 1955.
- Griggs, D., A theory of mountain building, *Am. J. Sci.*, 237, 611-650, 1939.
- Grindley, G. W., Geology of New Zealand geothermal steam fields, U. N. Conf. on New Sources of Energy, Rome, 1961.
- Gutenberg, B., in *Rheology, Theory and Applications*, edited by F. R. Eirich, vol. 2, 401-431, Academic Press, New York, 1958.
- Healy, J., Structure and volcanism in the Taupo volcanic zone, New Zealand, in *Am. Geophys. Union Monograph 6*, edited by G. A. Macdonald and H. Kuno, pp. 151-157, 1962.
- Healy, J., Volcanic mechanisms in the Taupo volcanic zone, New Zealand, *New Zealand J. Geol. Geophys.*, 7, 6-23, 1964.
- Heiskanen, W. A., and F. A. Vening Meinesz, *The Earth and Its Gravity Field*, McGraw-Hill Book Company, New York, 1958.
- Hele-Shaw, H. S. J., *Trans. Inst. Naval Architects*, 40, 21, 1898.
- Horton, C. W., and F. T. Rogers, Convection currents in a porous medium, *J. Appl. Phys.*, 16, 367-370 (see also 22, 1476), 1945.
- Jakob, M., *Heat Transfer*, John Wiley & Sons, New York, 1949.
- Jeffreys, H., The instability of a compressible fluid heated from below, *Proc. Cambridge Phil. Soc.*, 26, 170-172, 1930.
- Knopoff, L., The convection current hypothesis, *Revs. Geophys.*, 2, 89-122, 1964.
- Lamb, H., *Hydrodynamics*, Cambridge University Press, London, 1932.
- Lapwood, E. R., Convection of a fluid in a porous medium, *Proc. Cambridge Phil. Soc.*, 44, 508-521, 1948.
- Lee, W. H. K., Heat flow data analysis, *Revs. Geophys.*, 1, 449-479, 1963.
- Lee, W. H. K., and G. J. F. MacDonald, The global variation of terrestrial heat flow, *J. Geophys. Res.*, 68, 6481-6492, 1963.
- Lloyd, E. F., The hot springs and hydrothermal eruptions of Waiootapu, *New Zealand J. Geol. Geophys.*, 2, 141-176, 1959.
- MacDonald, G. J. F., Calculations on the thermal history of the Earth, *J. Geophys. Res.*, 64, 1967-2000, 1959.
- Macelwane, J. B., in *Internal Constitution of the Earth*, edited by B. Gutenberg, Dover Publications, New York, 1951.
- Malkus, W. V. R., Discrete transitions in turbulent convection, *Proc. Roy. Soc. London, A*, 225, 185-195, 1954.
- Mario, P. di, The operation of the geothermal power stations at Larderello, U. N. Conf. on New Sources of Energy, Rome, paper G68, 1961.
- Minakami, T., T. Ishikawa, and K. Yagi, The 1944 eruption of volcano Usu in Hokkaido, Japan, *Bull. Volcan. Naples*, [2]11, 45-157, 1951.
- McNitt, J. R., Geology of the geysers thermal area, California, U. N. Conf. on New Sources of Energy, Rome, paper G3, 1961.
- Modriniak, N., and F. E. Studt, Geological structure and volcanism of the Taupo-Tarawera District, *New Zealand J. Geol. Geophys.*, 2, 654-684, 1959.

- Nencetti, R., Methods and apparatus used for well mouth measurements, U. N. Conf. on New Sources of Energy, Rome, paper G75, 1961.
- Parker, T. J., and A. N. McDowell, Model studies of salt dome tectonics, *Bull. Am. Assoc. Petrol. Geol.*, 39, 2384-2470, 1955.
- Pekeris, C. L., Thermal convection in the interior of the earth, *Monthly Notices Roy. Astron. Soc., Geophys. Suppl.*, 3, 343-367, 1953.
- Penta, F., Studies of exhalative hydrothermal phenomena (in Italian), *Ann. Geofis.*, 7, 317-408, 1954.
- Priestley, C. H. B., *Turbulent Transfer in the Lower Atmosphere*, University of Chicago Press, Chicago, 1959.
- Ramadas, L. A., and S. L. Malurkar, *Ind. J. Phys.*, 7, 1, 1932.
- Rayleigh, Lord, Investigation of the character of the equilibrium of an incompressible heavy fluid of variable density, *Scientific Papers*, vol. 2, pp. 200-207, Cambridge, England, 1900.
- Rayleigh, Lord, On convective currents in a horizontal layer of fluid when the higher temperature is on the under side, *Phil. Mag.*, 32, 529, 1916.
- Reid, W. H., and D. L. Harris, Some further results on the Benard problem, *Phys. Fluids*, 1, 102-110, 1958.
- Richardson, J. G., Flow through porous media, in *Handbook of Fluid Dynamics*, edited by V. L. Streeter, McGraw-Hill Book Company, New York, 1961.
- Rikitake, T., and I. Yokoyama, Volcanic activity and changes in geomagnetism, *J. Geophys. Res.*, 60, 165-172, 1955.
- Robertson, E. I., and G. B. Dawson, Geothermal heat flow through the soil at Wairakei, *New Zealand J. Geol. Geophys.*, 7, 134-143, 1964.
- Runcorn, S. K., editor, *Continental Drift*, Academic Press, New York, 1962.
- Sakuma, S., and T. Nagata, Physical Volcanology, in *Handbuch der Physik*, 48, edited by J. Bartels, Springer-Verlag, Berlin, 1957.
- Schlichting, H., *Boundary Layer Theory*, Pergamon Press, London, 1960.
- Schneider, K. J., 11th Intern. Congress of Refrigeration, paper 11-4, Munich 1963.
- Silveston, P. L., Warmedurchgang in waagerechten Flüssigkeitsschichten, *Forsch. Ing.*, 24, 29-32 and 52-69, 1958.
- Smith, J. H., Production and utilization of geothermal steam, *New Zealand Eng.*, 13, 354-375, 1958.
- Sparrow, E. M., R. J. Goldstein, and V. K. Jonsson, Thermal instability in a horizontal fluid layer: Effect of boundary conditions and non-linear temperature profile, *J. Fluid Mech.*, 18, 513-528, 1964.
- Studt, F. E., Wairakei hydrothermal system and the influence of ground water, *New Zealand J. Sci. Tech.*, B, 38, 596-622, 1957.
- Studt, F. E., Geophysical reconnaissance at Kawerau, New Zealand, *New Zealand J. Geol. Geophys.*, 1, 219-246, 1958a.
- Studt, F. E., The Wairakei hydrothermal field under exploitation, *New Zealand J. Geol. Geophys.*, 1, 703-723, 1958b.
- Studt, F. E., Magnetic survey of the Wairakei hydrothermal field, *New Zealand J. Geol. Geophys.*, 2, 746-754, 1959.
- Taylor, G. I., The instability of liquid surfaces when accelerated in a direction perpendicular to their planes, 1, *Proc. Roy. Soc. London, A*, 201, 192-196, 1950.
- Tek, M. R., Two-phase flow, in *Handbook of Fluid Dynamics*, edited by V. L. Streeter, McGraw-Hill Book Company, New York, 1961.
- Thompson, G. E. K., Shallow temperature surveying in the Wairakei-Taupo area, *New Zealand J. Geol. Geophys.*, 3, 553-562, 1960.
- Thompson, T. E. K., C. J. Banwell, G. B. Dawson, and D. J. Dickinson, Prospecting of hydrothermal areas by surface thermal surveys, U. N. Conf. on New Sources of Energy, Rome, paper G54, 1961.
- Townsend, A. A., Temperature fluctuations over a heated horizontal surface, *J. Fluid Mech.*, 5, 209, 1959.
- Urey, H. C., *The Planets*, Oxford University Press, London, 1952.
- Vening Meinesz, F. A., Major tectonic phenomena and the hypothesis of convection currents in the earth, *Quart. J. Geol. Soc. London*, 103, 191-206, 1958.
- Verhoogen, J., Heat balance of the Earth's core, in *The Earth Today*, edited by A. H. Cook and T. S. Gaskell, pp. 276-281, The Royal Astronomical Society, London, 1960.
- Von Herzen, R. P., and S. Uyeda, Heat flow through the eastern Pacific floor, *J. Geophys. Res.*, 68, 4219-4250, 1963.
- White, D. E., Thermal waters of volcanic origin, *Bull. Geol. Soc. Am.*, 68, 1637-1657 and 1659-1682, 1957.
- Wooding, R. A., Steady state free thermal convection of liquid in a saturated permeable medium, *J. Fluid Mech.*, 2, 273-285, 1957.
- Wooding, R. A., An experiment on free thermal convection of water in saturated permeable material, *J. Fluid Mech.*, 3, 582-600, 1958.
- Wooding, R. A., The stability of a viscous liquid in a vertical tube containing porous material, *Proc. Roy. Soc. London, A*, 252, 120-134, 1959.
- Wooding, R. A., Instability of a viscous liquid of variable density in a vertical Hele-Shaw cell, *J. Fluid Mech.*, 7, 501-515, 1960a.
- Wooding, R. A., Rayleigh instability of a thermal boundary layer in flow through a porous medium, *J. Fluid Mech.*, 9, 183-192, 1960b.
- Wooding, R. A., Free convection of fluid in a vertical tube filled with porous material, *J. Fluid Mech.*, 13, 129-144, 1962.
- Wooding, R. A., Convection in a saturated porous medium at large Rayleigh number or Peclet number, *J. Fluid Mech.*, 15, 527-544, 1963.
- Zierep, J., Cellular convection with non-uniform heating from below (in German), *ZAMM*, 41, 114-125, 1961.

(Manuscript received October 1, 1964; revised November 10, 1964, and December 20, 1964.)

## Chapter 9. Review of Geothermal Resources

JAMES R. McNITT

*California Division of Mines and Geology, San Francisco*

*Abstract.* The geothermal power plants operating in Italy, New Zealand, and the United States have proved the practical value of using natural steam and hot water as a source of energy within the economic framework of these countries. The success of these projects has stimulated additional exploration within the three countries, and has initiated or intensified other investigations, principally in Iceland, Japan, Russia, and Mexico.

All the thermal areas under development occur in regions of late Cenozoic volcanic activity, and their heat is probably derived from shallow intrusive bodies. These intrusives are found in two contrasting tectonic environments: (1) regions of Quaternary uplift of several hundreds of meters and (2) regions of late Tertiary and Quaternary subsidence of several thousands of meters. These tectonic environments determine the local structural and stratigraphic characteristics of the thermal fluid reservoirs. Structure and permeability of the reservoir greatly influence the thermal gradients measured in an area and the heat content of the thermal fluid. In permeable reservoirs, thermal gradients approximate the boiling point curve of water. Gradients as high as 800°C/km have been measured at depths of 30 meters in impermeable rock above the reservoir, but deeper drilling has shown that such high gradients do not persist. A gradient of 180°C/km, however, has been measured to a depth of 1000 meters. Thermal fluid enthalpies as high as 690 kcal/kg have been reported.

Chemical investigations have determined some of the complex reactions that occur between the thermal fluid, which is predominantly of the sodium chloride type, and its enclosing reservoir rock. These data aid in determining the paths of migration of the thermal fluid through the reservoir. In addition, isotopic studies indicate that probably 95% of the thermal fluid discharged from a given area is meteoric in origin. The exploration of thermal areas has been supplemented by numerous geophysical techniques including gravity, magnetic, and heat flow surveys. These investigations, although providing specific geologic information on hydrothermal systems, still leave unanswered fundamental questions about heat transfer within the crust.

### I. INTRODUCTION

In a general sense, 'geothermal energy' simply refers to the natural heat of the Earth. However, this term is now applied specifically to the useful energy extracted from naturally occurring steam and hot water, which are referred to collectively in this paper as 'thermal fluid.' These fluids constitute the main geothermal resources and are found in the Earth's volcanic and young orogenic zones, where their surface manifestations include hot springs, fumaroles, and geysers.

The principal use of natural thermal fluid is for the generation of electric power. The power is harnessed by releasing the thermal fluid through drill holes and conducting it through a system of pipe lines to a turbine-generator unit. Thermal fluid is also used, although to a lesser extent, for space heating, industrial processing, and for the chemical by-products which it may contain.

The economics of geothermal power have been discussed recently by several authors. *Facca and Ten Dam* [1963] have calculated the cost of generating electricity by means of geothermal energy in Italy, New Zealand, and the United States, and have compared these cost figures with that of conventional thermal, nuclear, and hydroelectric plants. The following table summarizes their conclusion that geothermal power is the cheapest source of energy now available:

Energy Source	mills/kwh
Geothermal	2-3
Conventional thermoelectric	5.47-7.75
Nuclear	5.42-11.56
Hydroelectric	5-11.36

Using a 51% plant factor, instead of the 92% factor used by *Facca and Ten Dam* [1963], and applying the present tax structure of the United States, *Kaufman* [1964a, b] concluded that geothermal power is, indeed, competitive

with the more conventional means of generating electricity. The following table summarizes the results of Kaufman's calculations:

Energy Source	mills/kwh
Geothermal plant, producing own steam	6.70
Geothermal plant, purchasing steam	7.43
Coal-fired plant	6.96
Oil-fired plant	6.74
Gas-fired plant	7.04

A factor not yet evaluated in published economic studies, but which may greatly affect the economics of at least one prospective thermal area, is the content of recoverable chemicals in the thermal fluid. Exploratory wells drilled in the Niland thermal area of southern California discharge a thermal fluid that not only has a heat content favorable for power generation but may also contain commercial quantities of potash.

The *United Nations* [1962] has published a report summarizing the favorable economic position of geothermal power; more specific information about the economics of New Zealand's geothermal power installation are given by *Armstead* [1961].

Although the geothermal energy investigations are basically commercial endeavors, they are also of considerable scientific interest. In general, these investigations are concerned with the manner of generation and transport of abnormally large quantities of heat within certain restricted regions of the upper crust and the accumulation of this heat at easily exploitable depths. Ultimately, the goal of these investigations is the assignment of quantitative values to the following parameters:

The size, geometry, depth, and heat content of the heat source.

The rate and mechanism of heat transfer from the source to a thermal fluid.

The size, geometry, and storage capacity of the structures through which the thermal fluid is transferred to the Earth's surface.

The variation of temperature, pressure, and enthalpy of the fluid within the circulating system.

The steady-state rate of mass and heat flow, both under the conditions of natural flow from a thermal area and under conditions of artificial discharge from wells.

Even in the most intensely investigated ther-

mal areas, only a few of the above values are known, and most of these only within an order of magnitude.

The purpose of this chapter is to introduce the nonspecialist to the rapidly growing field of geothermal energy research by (1) briefly outlining the type and status of geothermal investigations now in progress, (2) summarizing some of the data obtained, and (3) discussing some of the more difficult problems encountered thus far. Section 2 describes the history and status of projects in various countries. The geologic environment of developing thermal areas is discussed in section 3. Thermal fluid reservoirs and physical characteristics of thermal systems are given in sections 4 and 5. Section 6 reports chemical investigations, and section 7 discusses problems of exploration, development, and management of geothermal resources. The chapter ends with section 8, summary and conclusions. Throughout this chapter, the discussion is oriented toward the geological point of view. A physical discussion of mass and heat transfer within the Earth with particular reference to geothermal areas has been given by Elder in chapter 8 of this volume.

More than one-fourth of the papers referred to in this review were presented at the 1961 United Nations Conference on New Sources of Energy held in Rome. Thirty-nine papers on the geologic investigation of thermal areas and twenty-eight papers on the harnessing of geothermal energy were presented, thereby constituting the largest published collection of technical data in this field. Those United Nations papers concerned with geologic and geophysical investigations are summarized by *Elizondo* [1961].

Extensive bibliographies to the literature of geothermal energy, exclusive of the United Nations papers, have been published in three papers [*Penta*, 1959, 1960; *Penta and Bartolucci*, 1962]. These papers contain tabulated data, including depth and number of wells drilled and temperature and pressure encountered, from thermal areas being developed throughout the world.

## 2. HISTORY AND STATUS OF PROJECTS

Although for centuries Iceland has utilized natural hot water for heating, and Italy has been

generating electricity from natural steam for more than fifty years, it has only been since about 1950 that attempts have been made to develop geothermal energy on comparable scales elsewhere in the world. These recent attempts have advanced most rapidly in New Zealand and the western United States, where geothermal power stations are now in operation. However, investigations in other countries, notably Japan and Russia, have met with encouraging preliminary results.

### 2.1 Italy

The utilization of natural steam began in Italy during the latter half of the eighteenth century, when it was discovered that boric acid, valuable as a soldering flux, could be extracted from hot spring vapors. The area of hot springs, called the Boraciferous Region, is midway between Siena and the Tyrrhenian coast at what is now called Larderello. By constant improvement of concentrating techniques, the most important of which was the drilling of wells to collect the steam, the thermal region of Tuscany became one of the principal world producers of borax during the last century, in spite of increasing competition from the newly discovered borax deposits of California. In 1904, after a dispute with the local electric company, the natural steam was used for the first time to generate electric power. The geothermal power plant, a turbogenerator unit utilizing a heat exchanger to extract energy from the steam, lighted four lamps. The present capacity of the Larderello plants is more than 370,000 kw.

Exploration for thermal fluid capable of producing electric power in Italy has not been limited to Larderello. Several thermal areas in Tuscany and Latium, as well as the Phlegrean fields and the Island of Ischia, both in the Naples region, have been investigated by either geophysical surveys or exploratory drilling or both. The thermal areas under investigation in Latium and Tuscany (Figure 1) extend to the northwest from Tolfa [Marchesini, 1961], located 50 km north of Rome, through Viterbo [Penta, 1954; Cassinis, 1960], Mt. Amiata [Burgassi, 1961], Roccastrada [Battini and Menut, 1961], and Larderello [Burgassi, 1961] to Montecatini, located 200 km northwest of Rome. So far, exploration has been successful

at two thermal areas outside the main Larderello fields. These areas, which as yet produce only limited amounts of electric power, are near the volcanic center of Mt. Amiata: Bagnore on the southwest side of the mountain, and Piancastagnaio on the southeast side. The 1964 production capacity at Bagnore was 9500 kw, and Piancastagnaio, which was only in the early development stage in 1963, had a production capacity of 3500 kw in 1964.

Although many exploratory wells have been drilled on the Island of Ischia and in the Phlegrean fields, no commercial production of thermal fluid has been obtained, in spite of the fact that historic volcanic eruptions, as well as many hot springs and fumaroles, indicate high heat flow in the area. The geology of this volcanic district and the results of the exploratory drilling are discussed by Penta [1949, 1954, 1955, 1963] and Minucci [1961].

### 2.2 New Zealand

The second country to develop geothermal power on a large scale was New Zealand. The necessity for rapid development of power during the post-war period prompted the New Zealand government to initiate a geothermal power project at Wairakei, North Island, in 1950. In contrast to the South Island, the North Island has limited hydroelectric power potential, but contains many of the world's most extensive hot spring areas. The Wairakei project has already resulted in the drilling of 91 wells, ranging from 160 to 1300 meters in depth, and the construction of a 145,000-kw power station. The goal of the Wairakei project is to reach a capacity of approximately 250,000 kw.

Wairakei, 10 km north of Lake Taupo, is only one of the numerous thermal areas extending in a northeast belt across the center of North Island (Figure 2). Two other areas within this belt have been explored for natural steam: Waiotapu, 40 km northeast of Wairakei, and Kawerau, about 100 km northeast of Wairakei and only 20 km from the Bay of Plenty. The Waiotapu investigation, which has not proceeded beyond the initial stages, is for the purpose of developing steam for electric power generation, while the Kawerau project was successful in developing natural steam to be utilized in wood pulp processing. Some recent papers summariz-

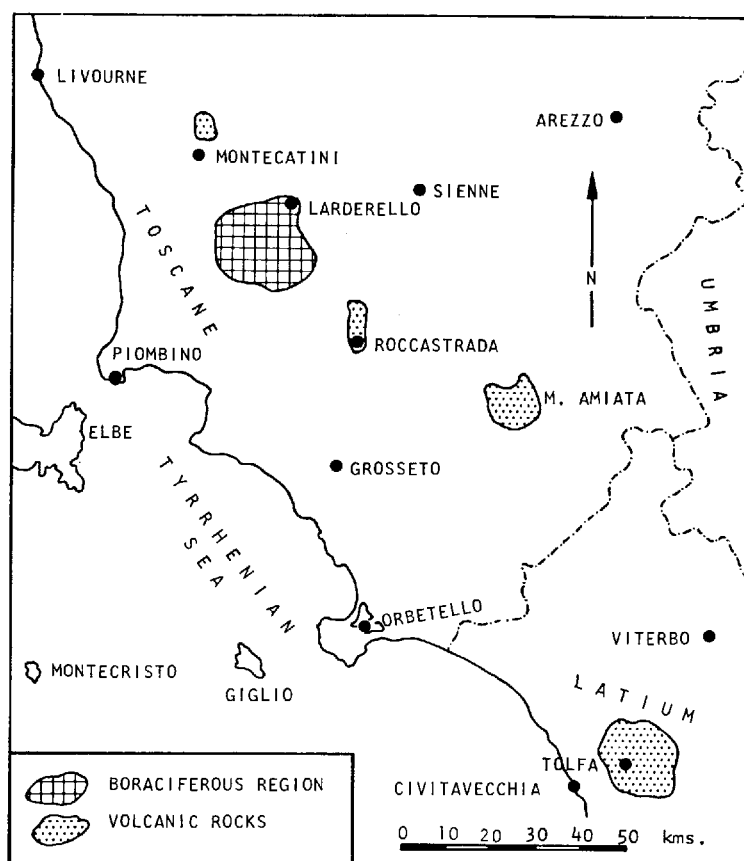


Fig. 1. Map of Latium and Tuscany showing Boraciferous region and distribution of volcanic rocks; after R. Burgassi.

ing the development of geothermal power in New Zealand include those by *Studd and Doyle* [1960], *Banwell* [1961], *Grindley* [1961, 1963], and *Healy* [1961, 1964a, b].

Investigations were underway in 1964 to extend the producing area of Wairakei further to the east and west and to explore the Ngawha thermal area, located in the hitherto untested volcanic region north of Auckland.

### 2.3 United States

As of 1964, more than 20 thermal areas have been drilled in the western United States in search of commercial quantities of natural steam (Figure 3). This drilling activity has taken place within the last decade except for two unsuccessful attempts at commercial development in California during the 1920's [*Laizure*, 1926; *Rook and Williams*, 1942], the scientific

investigations at Yellowstone in the 1930's [*Fenner*, 1936], and minor, sporadic activity elsewhere. Sixteen of the recently drilled areas are in California; the rest are in Nevada, Oregon, New Mexico, and Hawaii. It is interesting to contrast this limited number of explored areas with the fact that approximately 1000 hot springs are known in the western United States, mainly concentrated in Idaho, California, Nevada, and Oregon [*Stearns et al.*, 1935].

Of the twenty or more drilled areas, only The Geysers, in the north Coast Ranges of California, has been developed to the extent of actually producing electric power. Exploration drilling at Niland, Casa Diablo, Brady's Hot Springs, and Beowawe has been successful, and it is probable that commercial quantities of steam can be developed in these areas. Although hot water or steam has been encountered in most of the wells

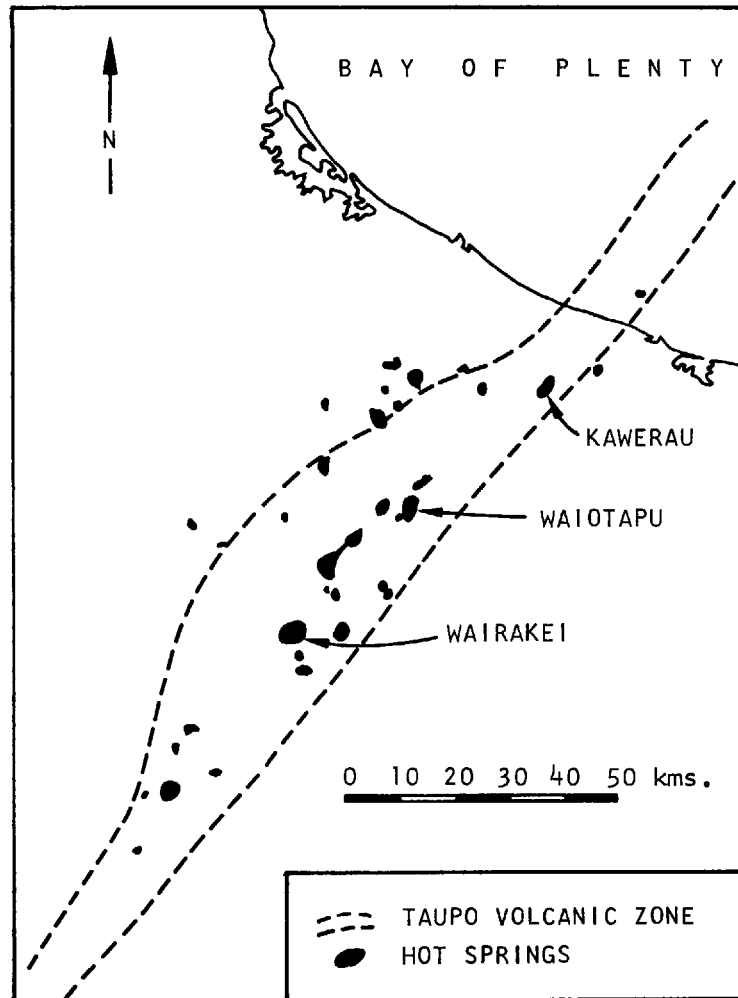


Fig. 2. Distribution of hot springs in the Taupo Volcanic Zone; after J. Healy.

drilled in the other areas shown on Figure 3, data from most of these areas are as yet insufficient for determining whether an adequate supply of steam will be available for power production.

The results of much of this recent exploration activity in California, Nevada, and Oregon are summarized by *Decius* [1961], and the developments at The Geysers, Casa Diablo, and Niland are discussed by *McNitt* [1963].

Wells were first drilled at The Geysers for the purpose of exploring for natural steam in 1921, and by 1925 eight wells were completed. *Allen and Day* [1927] give a detailed account of this early development, including data on the physi-

cal and chemical characteristics of the natural hot spring water and the steam produced from the drill holes. Although these wells were successful, the project was abandoned because there was no market for the energy. A second development project was initiated in 1955, which by 1963 resulted in approximately 15 more wells ranging from 120 to 600 meters in depth and a power plant operating at a capacity of 27,000 kw.

During the winter of 1963-1964, exploration drilling was continued  $1\frac{1}{2}$  km to the west of The Geysers, on what is probably the same steam-bearing fault zone that feeds The Geysers thermal area. Although this new exploration

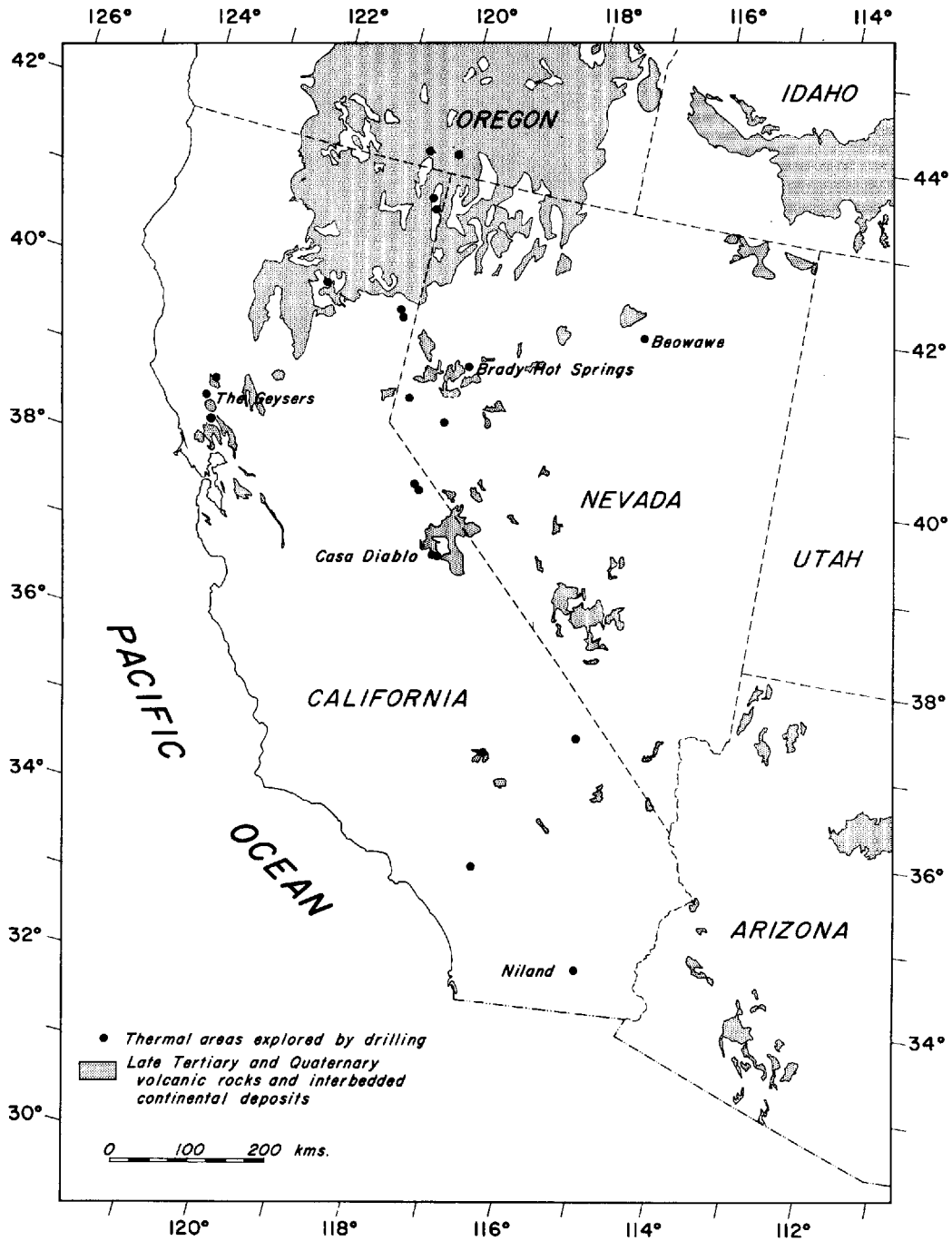


Fig. 3. Location of areas explored for geothermal power in western United States (exclusive of New Mexico), including distribution of late Tertiary and Quaternary volcanic rocks and interbedded continental deposits; base and volcanic rock distribution after U.S. Geological Survey.

project was not completed by June 1964, the cumulative production from nine wells, ranging in depth from 250 to 920 meters, was approximately equal to The Geysers production. A 27,500-kw generating unit has been authorized for this new area.

Early attempts to develop natural steam in the Niland area of southern California are described by *Rook and Williams* [1942]. Although unsuccessful in developing sufficient quantities of steam, this venture resulted in the discovery of a carbon dioxide field which was developed continuously from 1932 to 1954. The gas was obtained from wells 60 to 210 meters deep, which were drilled over an area of about 15 km<sup>2</sup>. The field produced more than 70 million cubic meters of carbon dioxide gas.

In 1957, a well was drilled to a depth of 1400 meters, 10 km south-southwest of the carbon dioxide field in search of oil. Instead, a large flow of steam and concentrated brine was encountered. By the first half of 1964, eight more wells, ranging in depth from 1400 to more than 2400 meters had been drilled on a northeast trend, 9 km long, between this discovery well and the old carbon dioxide field. Although production data on only two of these wells have been reported [*McNitt*, 1963], it is probable that individual generating capacities are in the range of 3000 to 10,000 kw, or slightly higher if low pressure generating equipment is used.

By 1964, only eight wells had been drilled at Casa Diablo, approximately five wells at Beowawe, and five at Brady's Hot Springs. The potential power capacity has been estimated at 40,000 kw for Beowawe and 15,000 kw at Casa Diablo.

#### 2.4 Iceland

The modern exploitation of natural heat in Iceland began in 1925, and by 1962 about 50,000 people in the Reykjavik area were living in houses heated by natural hot water. Expansion of this program is continuing, and, in addition, the Icelandic government is considering the installation of a 15,000-kw geothermal power station in the Hengill area.

#### 2.5 Japan

Since 1947, approximately twenty-two thermal areas in Japan have been prospected for

natural steam by private electric and drilling companies, as well as various research organizations including the Geological Survey of Japan. As of 1961, however, no commercial quantities of steam had been found. The primary reason geothermal power development has not proceeded more rapidly in Japan is that most of the thermal areas having significant surface expression are already being used as hot spring resorts. Because drilling might change the surface characteristics of the thermal system, exploration is avoided in the vicinity of these resorts and must be carried out in less promising areas.

*Saito* [1961] tabulates data obtained from the 20 prospected areas. These tables include number and depth of wells; down-hole temperature; and temperature, pressure, and mass flow of the effluent. Included in *Saito's* paper are detailed descriptions of the exploration projects centered at Onikobe and Matsukawa in northern Honshu and at Showashinzan on Hokkaido.

*Harada and Mori* [1961] also summarize the results obtained from exploration drilling in Japan. Most of the wells ranged in depth from 100 to 400 meters, except for several which reached a maximum depth of 900 meters. The drilling was performed in the vicinity of fumaroles and hot springs near Pliocene and Quaternary volcanoes.

In 1964 personal correspondence with J. Healy of the New Zealand Department of Scientific and Industrial Research, M. Hayakawa of the Geological Survey of Japan reported a successful new exploratory well at Matsukawa. This 950-meter-deep well apparently produced 70 tons of steam per hour without water, and another exploratory well is being drilled. The test wells drilled at Matsukawa, as indicated by *Saito* [1961], are on the southern margin of a caldera collapse structure. A dissected, andesitic Quaternary volcano occupies the center of the caldera. The seismic prospecting of this area has been described by *Hayakawa and Mori* [1962].

#### 2.6 USSR

Since 1958, the USSR Academy of Sciences and the Ministry of Geology and Subsurface Resources have been exploring for natural steam

in the region of the Pauzhetsk river in southern Kamchatka. This project, and the results obtained to 1961, are described by *Piip et al.* [1961]. By 1964, twenty-one exploration wells had been drilled, of which eighteen were productive. These wells range from 200 to 800 meters in depth. Also, by 1964, construction had begun on a 5000-kw generating station to utilize the Pauzhetsk thermal fluid.

A 12,000-kw capacity station to utilize the hot waters at Daghestan in the north Caucasus is in the planning stage.

### 2.7 Mexico

Three thermal areas are in various stages of investigation in Mexico. Two, the Pathé and Ixtlán areas, are in the east-west volcanic belt which crosses the country in the latitude of Mexico City. The third, the Mexicali area, is in northern Mexico 30 km southeast of Mexicali, in the same structural depression as the Niland area which is being developed in the United States. These three exploration projects are described by *de Anda* [1957] and *de Anda et al.* [1961].

As of 1963, fourteen wells had been drilled at Pathé, and electric power is generated by a small 3500-kw plant connected to one of the wells. Three exploration wells were drilled at the Mexicali area during 1960, which ranged from 400 to 700 meters in depth, and two more exploration wells were drilled in 1964.

### 2.8 Other Areas

The following are short papers which either discuss the possibilities of geothermal power development or give the results of preliminary exploration projects in those areas where comparatively little work has been done to develop natural steam: El Salvador [*Durr*, 1961], Kenya [*McCall*, 1957], New Britain [*Fooks*, 1961; *Studt*, 1961], Java [*van Padang*, 1960], and Fiji Islands [*Monro*, 1964].

## 3. GEOLOGIC ENVIRONMENT

All the thermal areas being developed throughout the world are located in regions of Cenozoic volcanism. It appears, therefore, that the source of heat for these areas is related in some manner to the processes of volcanism and magmatic

intrusion. If this is true, then it is reasonable to assume that thermal areas derive their heat either from buried flows of volcanic rock or from still cooling intrusive bodies which may be wholly or partially crystallized. Although it is difficult to evaluate the relative importance of extrusive rock as compared to intrusive bodies as heat sources, the intrusive bodies would seem to be the more significant. Certainly at Larderello and The Geysers, where late Cenozoic volcanic flows do not underlie the steam fields, heat must be derived from an intrusive source. Cenozoic lava flows found in the region of these steam fields testify to youthful volcanic activity and, therefore, to the probable presence of magmatic activity at depth.

If shallow magma bodies are the source of heat for the thermal systems now being exploited, then it is important for the purpose of future exploration and development to be able to recognize the geologic environments in which shallow magma bodies are formed and also to understand the processes responsible for these environments. Moreover, because geologic structure plays such an important part in defining the geometry of the thermal fluid reservoir, the relationship of the magma body to its tectonic environment is of particular importance. As yet, however, only a few generalizations can be made about the geologic and tectonic environments of thermal systems.

For the purpose of this discussion, it is useful to distinguish two structural environments which seem to characterize most of the regions now being explored for geothermal power. One environment, characteristic of the regions surrounding the Larderello, Mt. Amiata, and The Geysers steam fields, is an orogenic belt which has undergone late Pliocene and Quaternary uplift. The other environment, typified by the Wairakei steam field and the Niland and Casa Diablo thermal areas, is characterized by deep structural depressions which involve late Tertiary and Quaternary displacements of 3000 to 6000 meters. Whether there is an important genetic difference in the thermal systems related to these two structural environments remains to be learned.

### 3.1 Regions of Uplift

The complex geology of the Larderello region has been summarized recently by *Cataldi et al.*

[1963], and the regional geology of the northern Apennines is described by *Migliorini* [1948] and *Merla* [1951]. Although the steam fields of the Larderello area are associated with local structural highs within a larger basin, which attains depths of 1500 meters, *Marchesini et al.* [1962] point out that both the Larderello and Mt. Amiata regions have undergone differential post-Pliocene uplift. These uplifts are of 700 and 1000 meters, respectively, as compared to the 300 to 500 meters of post-Pliocene uplift of the surrounding region. At Mt. Amiata, the post-Pliocene uplift is culminated by the Quaternary volcano of the same name; at Larderello, however, there is no such obvious association of the uplift with magmatic activity. The local structural highs within the Larderello basin are either basement horst blocks formed in early or middle Miocene or superficial diapiric structures, no younger than late Pliocene. There is evidence, however, that a structural high approximately 10 km southwest of the Larderello basin is spatially related to the rise of a magmatic intrusion [*Cataldi et al.*, 1963]. This uplift is included within the differential post-Pliocene uplift associated with the Larderello area.

The Geysers is one of several hot spring and fumarole areas which occur along a 10-km length of a long northwest-trending fault zone in the Mayacmas Mountains of northern California. The Mayacmas Mountains, which also trend northwest, are a post-Pliocene uplift, and in the vicinity of The Geysers are approximately 17 km wide.

As yet there is no synthesis of California's north Coast Range geology, but geologic maps of the region surrounding The Geysers have recently been compiled on the scale of 1/250,000 by *Koenig* [1963] and *Jennings and Strand* [1960].

The internal structure of the Mayacmas Mountains is that of differentially uplifted fault blocks, which are tilted 30° to 40° to the northeast. The majority of faults dip steeply to the southwest, and vertical movement on individual faults ranges from 1.5–3 km. A schematic geologic cross section of the uplift, drawn northeast, perpendicular to its major structural trend, is shown in Figure 4. The major fault zones near the center of the Mayacmas uplift, including the present steam-bearing fault zone, have been min-

eralized in numerous localities by mercury-bearing solutions. Indeed, mercury has been reported as one of the minor constituents of The Geysers steam [*White*, 1957]. These deposits and the geology of the Mayacmas mercury district are described by *Bailey* [1946] and *Yates and Hilpert* [1946].

The thermal areas near Mt. Amiata are similar to The Geysers area in that they are also spatially associated with a mercury mining district. In addition, *Tonani* (personal communication) has spectographically detected several parts per million of mercury in incrustations formed on the inside of Larderello steam wells.

The existence of anomalously high heat flow in the Larderello and The Geysers areas is, undoubtedly, the strongest evidence suggesting that magma bodies exist at a shallow depth below these areas. A more permissive line of reasoning, but one that may be helpful in future prospecting for geothermal energy, also suggests that the Larderello and The Geysers areas are underlain by magma bodies. This evidence is found in the late Tertiary geologic history of the respective regions. It can be demonstrated that in the north Coast Ranges of California volcanism and associated tectonic processes have migrated northward from the vicinity of San Francisco Bay to the region just north of The Geysers area, a distance of more than 160 km, through the time interval from lower Pliocene to late Pleistocene. In other words, present magma generation would be expected at the north end of this volcanic trend.

*Marinelli* [1961, 1963] has outlined a similar trend of magmatic processes, including intrusion, mineralization, and structural movements in the northern Apennines. Tracing these processes through space and time, *Marinelli* [1961, 1963] concludes that they should be most active at the present time in the Larderello region. It should be emphasized, however, that neither the Larderello nor The Geysers area is underlain by Cenozoic volcanic rock (Figures 1 and 3).

### 3.2 Regions of Subsidence

The Wairakei area of New Zealand, and the Niland and Casa Diablo areas of California, are examples of thermal systems located in regions of late Cenozoic subsidence.

Although hot springs are scattered widely

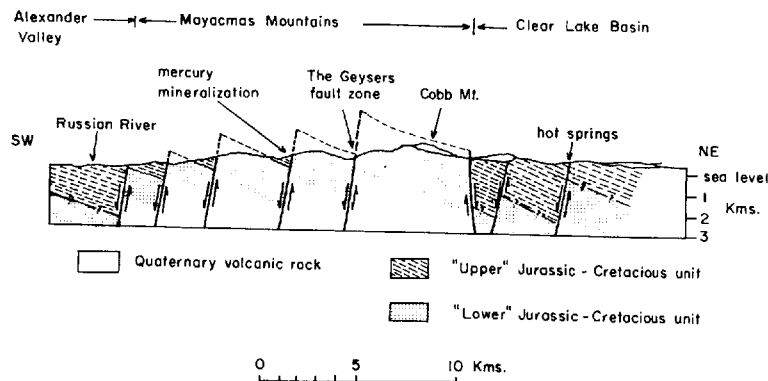


Fig. 4. Schematic geologic cross section through The Geysers.

throughout New Zealand, the hottest and most extensive, including Wairakei, are confined to the Taupo volcanic zone, which extends north-eastward for 300 km across the middle of the North Island (Figure 2). The zone is approximately 40 km wide near its midpoint in the vicinity of Wairakei and narrows to 16 km at both ends. The two ends are marked by large active andesitic volcanoes, and the wider central part is dominated by acid igneous activity, including rhyolite domes, pyroclastic pumice deposits, and ignimbrites. These volcanic rocks, which are described in detail by *Thompson* [1964], occupy a zone of subsidence which is flanked in the central part by plateaus of flat-lying ignimbrite sheets. The regional geology of the zone is discussed by *Grange* [1937] and *Grindley* [1960], and regional seismicity and gravity and their relation to the crustal setting are described by *Eiby* [1964].

Nearly 4000 cubic miles of lava and pyroclastic rocks were erupted from the Taupo volcanic zone during late Pliocene and Quaternary time. *Healy* [1962, 1964a] believes that this large volume of acid volcanic rock is the result of shallow melting of a thin granitic layer rather than differentiation of basic rocks in the mantle. The shallow melting was followed by eruption of large masses of molten material and the formation of grabens and calderas, which constitute the zone of subsidence. Detailed gravity surveys of the central part of the structural depression indicate that basement rocks (Mesozoic and Paleozoic graywacke) have been down-faulted to depths of at least 3700 meters [*Modriniak and Studdt*, 1959].

The Wairakei steam field is on a horst block within the area of general subsidence (Figure 5). This horst has been elevated approximately 1200 meters relative to the surrounding rocks. The steeply dipping faults flanking the horst block feed hot water through an ignimbrite sheet and into an overlying aquifer where it spreads laterally beneath an impermeable mudstone.

The Niland and Casa Diablo areas have not been drilled to the extent of the Wairakei field, and therefore most of the information available for these areas is based on geophysical data.

The Niland thermal area is at the south end of the Salton Sea in the vicinity of five small rhyolite domes which protrude through the sediments of Imperial Valley. The geology of Imperial Valley, which is part of a structural depression extending northwest from the Gulf of California, is described by *Dibblee* [1954]. The late Tertiary sediments filling the depression reach depths of more than 6000 meters. A gravity survey [*Kovach et al.*, 1962] shows the volcanic domes are located on a positive gravity anomaly which is about 16 km in diameter. This gravity anomaly also corresponds to a positive magnetic anomaly of approximately the same areal extent [*Kelley and Soske*, 1936].

The Casa Diablo thermal area is one of several hot springs in the Long Valley structural depression. This depression, adjacent to the steep east front of the Sierra Nevada range, is elliptical in plan, about 40 km long by 20 km wide, and has its long axis oriented east-west. The geology of the area is described by *Rinehart and Ross* [1964].

Gravity studies [*Pakiser*, 1961, 1964] indi-

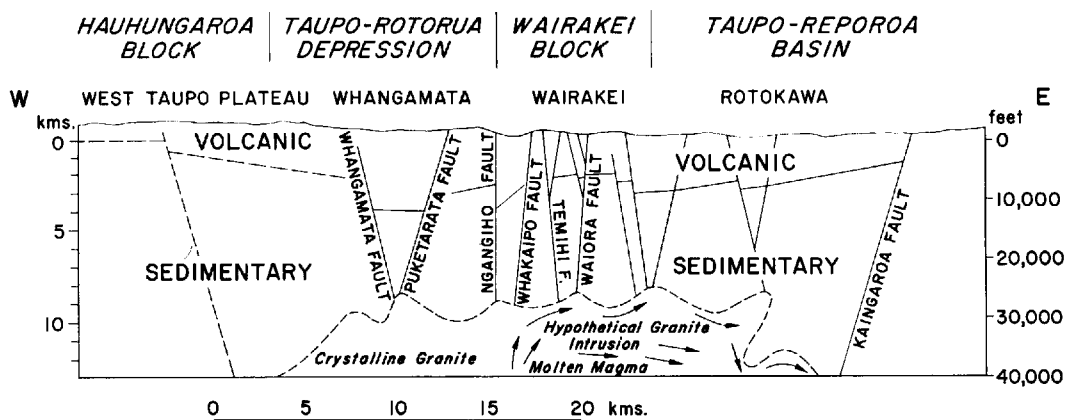


Fig. 5. Geologic cross section through Wairakei; after G. W. Grindley.

cate that the floor of the Long Valley depression is an eastward-tilted fault block, approximately 1500 meters below the surface on the west and 3600 meters below the surface on the east. Late Cenozoic volcanic rocks, as well as alluvial, lacustrine, and glacial deposits, fill the Long Valley basin. An aeromagnetic survey of the region [Henderson *et al.*, 1963] disclosed a sharp magnetic high, having a relief of from 2500 to 5000  $\gamma$ , near the center of the depression.

Because neither the Niland nor Casa Diablo area has been extensively drilled, the significance of the local gravity and magnetic anomalies spatially associated with the steam fields is not known. Three preliminary hypotheses, however, can be advanced: (1) the anomalies may represent local structural highs within the depression, similar to the horst block associated with the Wairakei field; (2) the anomalies may be caused by magma bodies, or (3) they may be due to the metamorphic effect of such magma bodies on the surrounding country rock.

Sviatlovsky [1960] attempts to demonstrate a process of structural inversion by which large depressions evolve into volcano-tectonic 'upheavals.' The particular stage which this process has reached, according to Sviatlovsky, determines the nature of the thermal fluid reservoir found in the region.

#### 4. THERMAL FLUID RESERVOIR

The geometry of the thermal fluid reservoir, its permeability, and the permeability of the

rocks surrounding it, are key factors determining both the heat content of the thermal fluid and temperature distribution within the reservoir.

If the fissures conducting thermal fluid into the reservoir are beneath a structural depression filled with porous sediments and volcanic debris, the ascending thermal fluid will mix with the cold groundwater that saturates the porous rock. These conditions generally pertain to those thermal systems occurring in regions of subsidence and are exemplified by the Wairakei reservoir.

In 1961 the area over which production wells were drilled at Wairakei was approximately 2.5 km long by 0.8 km wide. The quality of the thermal fluid produced from the wells is not uniform across the field, but varies with local variations of temperature and porosity within the reservoir.

The Wairakei reservoir [Grindley, 1961; Healy, 1961] consists of a pumice breccia aquifer, ranging from 450 to more than 900 meters in thickness, in which hot water has accumulated to form a large heat reservoir. The aquifer is capped by a sequence of relatively impermeable mudstones, ranging between 60 and 150 meters thick. The base of this sequence is between 180 and 300 meters below the surface. This capping formation is overlain by a younger sheet of pumice breccia or lapilli tuff, which is exposed at the ground surface. The aquifer is underlain by a thick, dense ignimbrite, which has been penetrated by the drill at one point and found to be underlain by pumice breccia (Healy, personal communication). Ther-

mal fluid enters the reservoir from faults in the underlying ignimbrite and flows upward and laterally into the porous aquifer.

The Waiotapu and Kawerau fields are similar in many respects to the Wairakei field; their geologic features are described by *Grindley* [1961, 1963]. Geophysical investigations at the Kawerau field are described by *Studd* [1958a].

Because of the lateral porosity of the pumice breccia aquifer, the aerial extent of the Wairakei field, as known in 1961, was approximately 2 km<sup>2</sup>. Because of this same porosity, however, cold groundwater is able to mix with the thermal fluid and lower its heat content. Thermal systems occurring in this type of environment have been found to produce only saturated steam mixed with hot water.

If, in contrast to the above case, the fissures conducting thermal fluid to the surface intersect only impermeable rocks, as may be the case in areas of recent uplift, the thermal fluid will be only slightly diluted by local surface water. Such a thermal system may yield dry or even superheated steam, depending on its initial enthalpy. Although the enthalpy of the fluid found in this type of reservoir may be more than 600 kcal/kg, the aerial extent of the reservoir is small in comparison to reservoirs having greater lateral porosity. At The Geysers, which characterizes this type of system, slightly superheated steam is produced from a steeply dipping fault zone in dense, impermeable graywacke. So far, steam production in The Geysers area has been obtained from two 500-meter lengths of the fault zone. The width of these production areas is of the order of 100 meters, giving a cumulative production area of approximately 0.1 km<sup>2</sup>.

The reservoir at Larderello fits neither of the extreme cases exemplified by Wairakei and The Geysers, but combines the favorable aspects of each. Although Larderello is in an upland area, rather than in an alluvial-filled basin, the fissures carrying the thermal fluid intersect a Triassic sequence of highly porous dolomite, limestone, and anhydrite. These rocks, which are capped by impermeable shale, form a reservoir which not only has a considerable lateral extent, similar to the Wairakei field, but also produces a superheated thermal fluid similar to that produced at The Geysers. The geology of the

Larderello field and its relationship to the regional geology of the Appennines are outlined by *Burgassi* [1961], *Marchesini et al.* [1962], and *Cataldi et al.* [1963].

The Larderello steam field consists of eight separate production centers whose cumulative area is approximately 40 km<sup>2</sup>. These eight centers are distributed over a roughly rectangular area 15 km long by 10 km wide. Approximately 175 wells, out of approximately 240 wells drilled, produce thermal fluid from depths between 220 meters and 1000 meters. This drilling, as well as resistivity [*Mazzoni and Breusse*, 1954] and gravity [*Vecchia*, 1960] surveys, has disclosed dominant northwest-trending faults and subordinate northeast-trending faults in the reservoir rock. Although the major faults do not extend through the overlying cover, these two trends can be recognized in a surface fracture pattern [*Marchesini et al.*, 1962]. Vertical movements of up to 800 meters have occurred on these steeply dipping faults, and the reservoir rock is most productive where it has been faulted into a structurally high position. Although it is generally agreed that the relatively impermeable shale acts as a cap rock, confining the thermal fluid within the underlying pervious reservoir, there is some disagreement about the role played by the faults. Some geologists believe the faults merely act to increase the reservoir permeability, thereby promoting vertical convective circulation; others believe that the major faults also act as conduits which bring the thermal fluid into the reservoir from greater depth.

The geology of the Mt. Amiata area, which is 70 km southeast of Larderello and 50 km from the Tyrrhenian coast, is similar in many respects to the geology of Larderello. Thermal fluid is produced from the same reservoir rocks, which are structurally elevated by faulting and covered by an impervious shale. Local structural sections drawn from resistivity surveys are presented by *Alfano* [1960].

The Mt. Amiata area differs from Larderello in two respects: (1) the surface manifestations of high heat flow are limited to minor warm springs (temperatures between 20°C and 50°C), and (2) it is near Quaternary volcanic rocks, that is, the extinct volcano covered with ignimbrite that constitutes Mt. Amiata.

TABLE 1. Physical Characteristics of Selected Thermal Systems Reported as of 1961

Field	Maximum Reservoir Temperature, deg C	Maximum Well Head Pressure, kg/cm <sup>2</sup>	Enthalpy, kcal/kg	Mass Discharge, kg/sec	Heat Discharge, kcal/sec	References
Italy Larderello	245	33	680-690	790	542,000	<i>Burgassi, 1961; Chierici, 1961</i>
United States The Geysers	208	10	667	100	67,000	<i>McNitt, 1961, 1963</i>
Casa Diablo	180	3.5	150-280	332	70,000	
Niland	300+	—	310-320	—	—	
New Zealand Wairakei	266	27	250 (mean)	960	240,000	<i>Banwell et al., 1957; Banwell, 1961; Dench, 1961; Grange, 1955; Healy, 1961; Studt and Doyle, 1960</i>
Waiotapu	295	22	332-600	133	30,700	
Iceland Hveragerdi	233	13.5	230-280	460	122,700	<i>Bodvarsson and Palmason, 1961; Einarsson, 1961</i>
USSR Pauzhetsk	195	6.9	160-188	150	26,100	<i>Päp et al., 1961</i>
Japan Otake	185	6.5	350-480	3.2	1,443	<i>Harada and Mori, 1961; Saito, 1961</i>
Matsukawa	189	5.1	550	.36	200	

##### 5. PHYSICAL CHARACTERISTICS OF THERMAL SYSTEMS

The hydrodynamic treatment given the physical properties of hot, subterranean fluids by *Goguel* [1953] affords an excellent background for reviewing the data summarized in this section.

Table 1 summarizes some physical characteristics of selected thermal systems now being investigated. This list is by no means complete, but represents the best published information available in 1961. Development work has continued since that time, so that mass and heat discharges have been considerably increased in several of the fields.

###### 5.1 Temperature

Because of the extreme conditions of temperature and pressure, and owing to the presence of corrosive fluids, accurate temperature gradients are difficult to measure in high temperature thermal systems. Although maximum recording thermometers have been used, their ability to record negative gradients, which are not uncommon, is questionable. Before about 1962, the

most reliable device used for temperature measurement under these difficult conditions was the 'geothermograph' developed for measuring downhole temperatures in the Wairakei field [*Banwell, 1955*]. In principle, the device consists of a differential-expansion temperature element which drives a writing stylus across a smoked-glass plate. The plate is advanced by jerking the instrument's supporting cable. It was necessary to use this mechanical device, which does not give a continuous temperature record, because the insulation on cables relaying information from electric instruments was insufficient to withstand the extreme conditions in the field. Recently, however, a continuously recording, electrical temperature measuring device has been developed by a private company in California. This instrument is reported to be capable of measuring temperatures in thermal fields as high as 380°C.

The form of the temperature gradient measured in a thermal field is dependent on many different factors, some of which vary, not only from field to field, but from one well to another in the same field. The most important of these factors are: (1) conductive heat flow in the

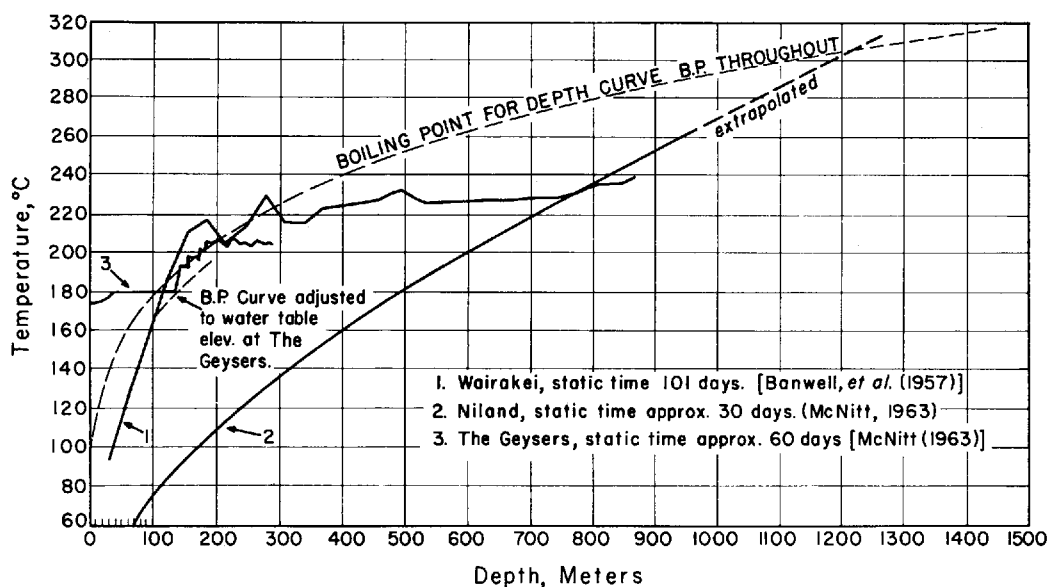


Fig. 6. Representative thermal gradients from Wairakei, Niland, and The Geysers.

reservoir rock; (2) thermal characteristics of the reservoir rock; (3) geometry and porosity of the reservoir; (4) heat content and physical state of the thermal fluid; (5) convection in the thermal fluid; and (6) length of time fluids have remained static in the well used to measure the gradient. The variability of these factors often makes the interpretation of specific gradients very difficult. In general, however, a gradient measured in an open, porous reservoir, having few structural complications, tends to approximate the boiling point–depth curve of water, while a gradient measured in a less porous reservoir is less affected by the thermal fluid but reflects the thermal characteristics of the reservoir rock and the heat being conducted through it. Three thermal gradients, representative of the thermal fields in which they were measured, are shown in Figure 6.

Curve 1 of Figure 6 was measured in hole 18 of the Wairakei field [Banwell *et al.*, 1957] and reflects the general characteristics of gradients measured in the more permeable areas of that reservoir. There is a rapid increase in temperature with depth down to the base of the confining mudstone. At this point, temperatures are commonly close to, or above, the boiling point corresponding to the theoretical hydrostatic pressure for this depth below the water

table (about 200°C). Although the measured temperatures in the upper parts of hole 18 lie above the boiling-point curve for some distance, the well head pressure of 4.43 kg/cm<sup>2</sup> at the time of measurement was sufficient to keep the water below boiling point over most of this region. The temperature gradient through the aquifer is much reduced, reaching 230°C at about 450 meters depth in hole 18. The hottest parts of the Wairakei reservoir (those areas closest to the feeding fissures) reach 250°C at 450 meters depth. Below about 600 meters, the gradient is either very small or negative.

In contrast to this gradient, which is considerably influenced by permeability variations in the reservoir and the thermodynamic characteristics of the thermal fluid, the gradient observed in the Niland area (curve 2, Figure 6) is much more linear, reflecting a closer relation to conductive heat flow. All production from the Niland field is from below 1200 meters, which is the approximate point of intersection of the thermal gradient with the boiling-point curve of water. Although temperatures of more than 400°C have been reported at a depth of 2400 meters in the Niland field, this value may be only an extrapolation of the approximately 180°C/km gradient measured in the upper 900 meters of sediments.

The thermal gradient measured at The Geysers well T7 (curve 3, Figure 6) does not resemble either of the gradients described above. From 40 to 130 meters, the temperature is constant. This indicates that a vapor phase existed in the well, even though the well had been static for two months. A well head pressure of 10.1 kg/cm<sup>2</sup> was registered while the temperature log was being taken, indicating that the vapor at 180°C was saturated. Seven other wells, which had been static for time intervals shorter than the two months, contained a superheated gas phase in the constant temperature interval [McNitt, 1961, 1963]. The degree of superheat ranged from 8°C to 19°C. The rising temperature interval below the constant temperature zone (from 130 to 230 meters in well T7) lies above the boiling-point depth curve calculated for 7 of the 8 wells tested. These data, plus the fact that only superheated steam is produced from The Geysers field, lead the author to conclude that superheated steam exists in the narrow, steeply dipping fault zone that constitutes The Geysers reservoir. Further data and a more detailed discussion of the hydrology and thermodynamics of The Geysers reservoir are given by McNitt [1961, 1963].

Thermal gradients in the Larderello reservoir, which also produces superheated steam, have not been published. *Facca and Tonani* [1961, 1962a, 1963], however, discuss the hydrology and thermodynamics of a hypothetical reservoir model whose geologic characteristics are based on the Larderello field. These authors consider the effects of reservoir structure and permeability on the variation with depth of the quality and quantity of thermal fluid. One of their conclusions is that superheated steam does not exist in the Larderello reservoir, but is produced under flowing conditions by the addition of heat, through loss of kinetic energy, to vapor which has separated from a fluid phase. Some superheat, they believe, is already added to the separated steam by isenthalpic flow at 670 kcal/kg.

*Facca and Tonani* [1962b] also offer an interpretation of the temperature gradients measured under static conditions at The Geysers. They conclude that the superheated condition found in the wells does not necessarily reflect the same condition in The Geysers reservoir, which, they believe, contains water rather than

superheated steam. This conclusion, in part, is based on assumptions (1) about the time necessary for the static wells to reach temperature equilibrium with the surrounding wall rock and thermal fluid, (2) about the value of downhole pressures, and (3) that some of the reported gradients are erroneous. To resolve this interesting problem of whether or not a superheated gas phase can exist, as such, in a reservoir, it will be necessary to obtain more satisfactory temperature and pressure measurements in those fields producing superheated steam.

## 5.2 Pressure

Very few downhole pressure readings have been reported from thermal fields. More commonly, either the static well head pressure or the variation of well head pressure with mass discharge is given. In reservoirs containing only a liquid phase, static well head pressures are generally consistent with pressures at the bottom of the water-filled well which are close to hydrostatic. Well head pressures measured under flowing conditions from a hot water reservoir are directly related to the amount of ebullition and consequent 'gas lift' in the well. This ebullition, in turn, is a function of the pressure differential between the reservoir and the well head, in addition to the temperature and heat content of the thermal fluid.

In New Zealand, where temperature data have indicated the general absence of a vapor phase, reservoir pressures are calculated by utilizing water level measurements, static well head pressure, and water densities corrected for temperature. With this method, *Studt* [1958b] was able to construct piezometric surfaces for the Wairakei field. These surfaces define the direction of flow within the thermal fluid reservoir and are useful for planning efficient exploitation of the field.

Calculation of reservoir pressures from well head measurements is much more uncertain for reservoirs containing a vapor phase or mixed liquid-vapor phases than for a reservoir containing only a liquid phase of known density. McNitt [1961, 1963] concludes that static well head pressures measured at The Geysers are related to the hydrostatic pressure of groundwater which overlies a superheated steam phase. The steam is confined laterally within the porous

fault zone, which forms the reservoir, and is prevented from escaping vertically to the surface, except for minor fumaroles, by the groundwater which fills the upper, near-surface part of the fault zone. The balance of heat flow into and out of the groundwater body is assumed to be responsible for maintaining the density inversion of the two phases in the open and flowing system.

*Nekhoroshev* [1960] presents a theoretical discussion on the relation of flow velocity to temperature, pressure, and heat content of a thermal fluid.

### 5.3 Heat Flow

Three types of heat flow data have been reported from thermal areas: (1) natural conductive heat flow; (2) natural convective heat flow; and (3) the heat contained in effluent discharged from wells. This third type is referred to here as heat discharge rather than heat flow.

Heat discharge is merely the product of the mass flow from the wells multiplied by the enthalpy of the thermal fluid produced from the field. These data are vital for the design of power generating equipment and, therefore, have been measured for most thermal fields under active development. In Table 1, note the high enthalpy of the effluent from the Larderello and The Geysers fields, which produce a superheated steam phase, in contrast to the lower enthalpy of effluent from the other fields, which produce a two-phase mixture of saturated steam and water. The techniques used to measure mass flow and enthalpy are described for the Wairakei field by *Hunt* [1961] and *James* [1961], for the Larderello field by *Nencetti* [1961*b*], and for the Pauzhetsk field by *Averiev* [1961].

Natural heat flow measurements are of less immediate value than well discharge measurements, and, consequently, natural heat flow information, with the exception of that for the Wairakei and Larderello fields, is not as generally available.

The techniques of measuring natural heat flow from thermal areas in New Zealand have been described by *Benseman* [1959*a, b*], *Thompson et al.* [1961], and *Dawson* [1964]. The methods used to measure heat flow through soil, as well as heat flow from boiling water surfaces,

fumaroles, overflow from geysers and springs, and seepage to nearby lakes and rivers, are discussed in these papers.

By study of the variation of temperature with depth at Wairakei, *Robertson and Dawson* [1964] showed that conduction is the dominant mechanism of heat transfer through near-surface soil until the difference between the temperature at the surface and at a depth of 1 meter reaches about 25°C. For higher ground temperatures, heat transport by convection of a mixture of air and water vapor becomes progressively more important, and the conductive effect becomes insignificant. *Dawson and Fisher* [1964] measured the thermal diffusivity and conductivity of the Wairakei pumice soil and the variation of these parameters with moisture content of the soil. They concluded that the heat flow at the surface is 40  $\mu\text{cal}/\text{cm}^2 \text{ sec}$ , which is about 30 times greater than the world average.

The above heat flow value does not include convective heat flow from steam vents, evaporation and radiation from water surfaces, overflow from geysers and springs, and underground seepage to streams. *Fisher* [1964] reports on the variation with time of total natural heat flow at Wairakei, including flow from these various paths of heat escape. He concludes that the natural geothermal heat flow during 1958 was approximately the same as during 1951–1952, namely 100,000 kcal/sec relative to 12°C, in spite of the fact that heat draw-off through wells increased from 10,000 kcal/sec in 1951 to 160,000 kcal/sec in 1958 [*Hunt*, 1961]. During this same period, there was a steady decline in the mass discharge of the natural thermal springs from 440 to 345 kg/sec, but an increase in enthalpy from 245 to 305 kcal/kg. *Banwell et al.* [1957] attribute these relative changes of mass flow and enthalpy to increased local draw-off, which produces an upward displacement of the isotherms, thereby increasing the enthalpy. At the same time, the limited permeability of the reservoir leads to some limitation in total mass flow.

By 1964, the wells at Wairakei discharged nearly six times the original natural heat flow of 100,000 kcal/sec, and at Kawerau the well discharges were nearly twice the natural heat flow [*Healy*, 1964*a*].

In comparison with the natural heat flow at

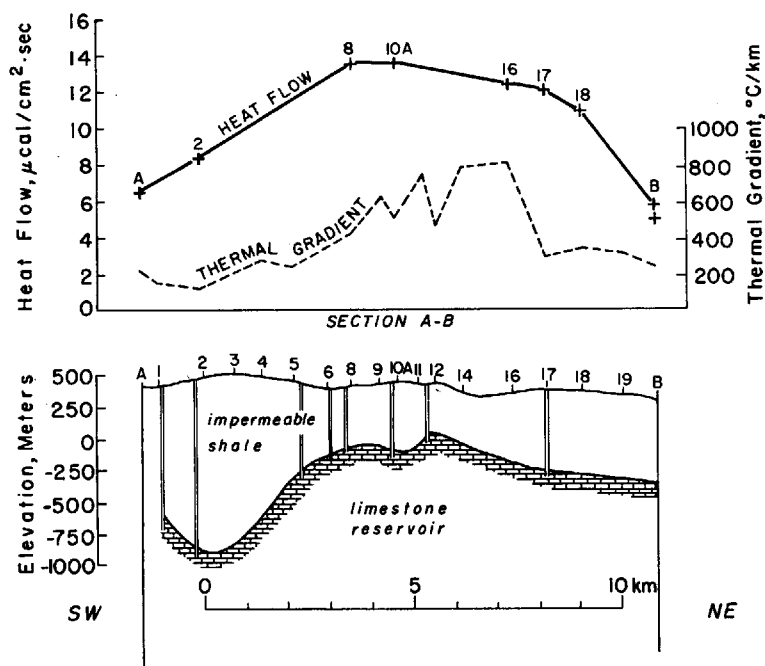


Fig. 7. Geologic cross section, with thermal gradient and heat flow profiles, through Larderello; after T. Boldizzar.

Wairakei, the two nearby thermal areas of Rotorua and Taupo have respective heat flows of 90,000 and 50,000 kcal/sec [Banwell, 1963]. The total natural heat flow within a circle having a 7.5-km radius, therefore, is about 240,000 kcal/sec.

Thermal gradients in the impermeable shale cover that overlies the Larderello reservoir have been reported by Burgassi *et al.* [1961]. Using these gradients, plus conductivity data for the shale, Boldizzar [1963] has calculated conductive heat flow from the Larderello region. Figure 7 shows the relation of the structural high at Larderello to a high heat flow anomaly. Gradients as high as 800°C/km are found over the productive, structurally high part of the Larderello field. This high gradient, however, does not persist through the reservoir. Even in the nonproductive zones at the ends of the section, the gradients average about 150°C/km, considerably higher than the world average of 30–40°C/km.

Although measurements of conductive heat flow have not been reported from Iceland, Bodvarsson [1949, 1960, 1961] has estimated the amount of heat flowing from Iceland's hot

springs. In making this estimate, two types of thermal areas have been distinguished: (1) low temperature areas, mainly located in Tertiary volcanic regions and characterized by hot springs and subsurface temperatures below 150°C, and (2) high temperature areas (Figure 8), located in Quaternary volcanic districts and characterized by steam vents, large areas of hot ground, and by temperatures above 200°C at shallow depth. The total heat output of the low temperature areas is estimated at 100,000 kcal/sec, whereas the high temperature areas appear to have an output of the order of 1,000,000 kcal/sec.

In the high temperature areas, such as at Hveragerdi, where the installation of a 15,000-kw generating station has been proposed, temperatures of 230°C have been measured at a depth of 600 meters. The upper part of the gradient at Hveragerdi, that is, above 400 meters [Bodvarsson and Palmason, 1961], parallels the boiling point–depth curve of water, and the high temperatures found in this system are clearly related to convective flow of heat in the thermal fluid. In nonthermal areas, the observed temperature gradients, which are fairly linear, range

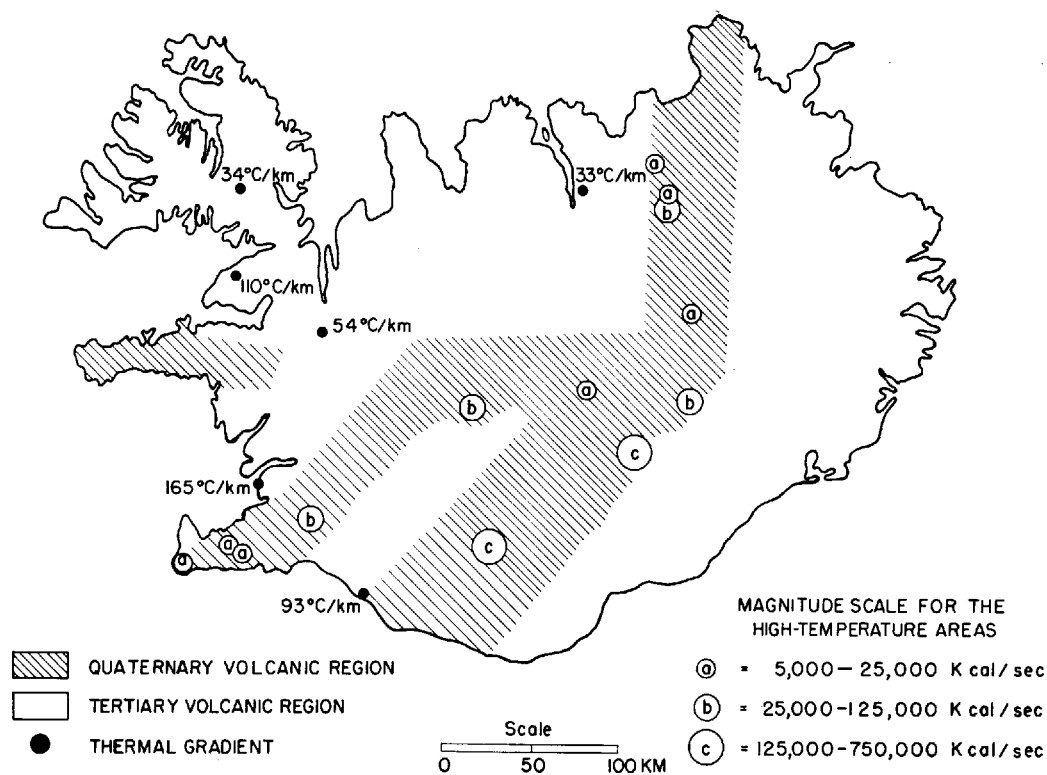


Fig. 8. Post-glacial volcanism, high temperature areas, and thermal gradients in Iceland; after G. Bodvarsson.

from 33°C/km to as high as 165°C/km [Bodvarsson and Palmason, 1961]. As is shown in Figure 8, the lower values of these gradients are found in the Tertiary volcanic districts.

Additional papers about the abnormal heat flow in Iceland include a summary of the geology and volcanic history of the island by Askelsson *et al.* [1960], detailed descriptions of some of the more important hot springs by Barth [1950], and flow data from eight steam wells drilled at Hveragerdi reported by Einarsson [1961].

#### 6. CHEMICAL INVESTIGATIONS

Geochemical investigations have been emphasized at Wairakei since development first began in 1950. This work consists of detailed sampling and chemical analysis of natural hot spring and well discharges at regular time intervals. Wilson [1961] gives a general discussion of the chemistry of the surface thermal water, and Ellis [1961] presents a similar report on

the water discharged from the steam wells. The steam well discharge contains, in general, almost 0.3% sodium chloride in solution and is close to saturation with silica and calcium carbonate.

Methods used in sampling the wells are given by Mahon [1961], and general analytical procedures are described by Ritchie [1961a]. The analysis of specific chemical constituents and their geochemistry are discussed in the following papers: alkali ions [Golding and Speer, 1961; Ellis and Wilson, 1960], bromine and iodine [Ellis and Anderson, 1961], arsenic and antimony [Ritchie, 1961b], boron [Ellis and Sewell, 1963], and noncondensable gases [Ellis, 1962; Mahon, 1962a].

The geochemistry of the Kawerau hot springs and steam well effluent is discussed by Mahon [1962b], and Lloyd [1959] presents geochemical data from the hot springs of Waiotapu.

Interpretation of geochemical data at Wairakei has been extremely difficult because of the complex chemical reactions occurring between the

thermal fluid and the country rock and the varying amounts of mixing and dilution of the thermal fluid with surface water. *Steiner* [1953, 1955] has shown that the rising thermal water at Wairakei interacts with the country rock to form several characteristic zones of alteration at specific intervals of depth. Hydrothermal alteration in the Waiotapu field has also been described by *Steiner* [1963]. The essential changes in the chemistry of the water, resulting from its interaction with the reservoir rock, include loss of some potassium and rubidium; slight loss of lithium, caesium, and magnesium; and gain of calcium. As a result of these reactions, low Na/K and Na/Rb ratios, or high Na/Ca and Li/Ca ratios, indicate the least contact with the reservoir rocks. Consequently, the drillholes which discharge water reflecting the above ratios are assumed to be located closest to the region where the thermal fluid enters the reservoir from greater depths [*Ellis and Wilson*, 1960; *Ellis*, 1961].

From the chemical point of view, undoubtedly the Niland thermal fluid is the most extraordinary found so far. A representative analysis of the effluent produced from the Niland wells indicated the following major constituents: 3.4% by weight of calcium, 7% sodium, 2.4% potassium, 20% chlorine, and 0.4% iron. The interesting geochemistry of this brine, including an abnormally high content of copper and silver, is discussed by *White* [1963]. The developers of the Niland area hope that, in addition to obtaining geothermal power, it will be economically possible to recover potash and perhaps other chemicals from the thermal fluid.

Data about the noncondensable gas content of thermal fluids, and the variation of this content with time, are of vital importance for the proper design of power-generating equipment. In 1958, the superheated steam from The Geysers contained from 0.68 to 0.83% by weight of noncondensable gases, of which 89% was carbon dioxide, 5% was methane, and the remaining 6% was made up of hydrogen sulfide, ammonia, hydrogen, nitrogen, and argon [*McNitt*, 1963]. By 1964, the noncondensable gas content decreased by approximately half.

*Nencetti* [1961b] reports on the methods used to collect and analyze superheated steam from the Larderello wells. This steam [*Nencetti*, 1961c] contains 4.5% by weight of noncon-

densable gas, of which 96% is carbon dioxide, 1.8% is hydrogen sulfide, and the remaining 2.2% is composed of boric acid, ammonia, methane, hydrogen, nitrogen, and argon. Additional information about the chemistry and physics of the Larderello thermal fluid is given by *Nasini* [1930], *Mazzoni* [1948], and *Penta* [1954].

Characteristics of the thermal fluid produced from the Bagnore field near Mt. Amiata are given by *Gennai* [1960] and *Burgassi* [1961]. This fluid, which is also slightly superheated, has a very high noncondensable gas content. When the field was opened in April 1959, the gas content, principally carbon dioxide, was 81.0% by weight. By March 1961, the gas content had dropped to 23.2%, and by 1964 it was reported to be 15%.

*White* [1957], in his classification of thermal waters, notes that natural spring systems associated with dry or superheated steam fields are characterized by acid-sulfate springs with insignificant chloride content, as opposed to the high chloride content of thermal spring waters associated with fields producing hot water and saturated steam. *White* [1957, 1961] concludes that chloride is transported from the heat source in an alkali chloride solution. If a steam phase forms in the thermal system, chloride is left behind in the liquid phase rather than being transported through to the surface with the steam. This mechanism may provide a convenient method for predicting whether a thermal area will produce dry steam or saturated steam and water.

*White's* theory also offers an explanation for the decrease of noncondensable gas content with time as observed in the steam produced at The Geysers and, more notably, at Bagnore. It is probable that the steam is produced from a reservoir which contains a vapor phase overlying liquid water deep within the system. Under conditions of natural equilibrium, the vapor becomes enriched in CO<sub>2</sub> and other gases. Under conditions of sustained production, however, the steam depleted from the upper part of the reservoir is replenished by steam boiling off the liquid water deeper in the system. This causes a continuous decrease with time in the gas content of the steam in the upper part of the reservoir.

If the steam in the upper part of the reservoir is in thermodynamic equilibrium with the liquid water beneath it, how can the steam be super-

heated when it reaches the surface? *Facca and Tonani* [1961, 1962a, 1963] have offered one of perhaps several possible solutions to this problem (section 5 of this chapter). Another solution is suggested by observation of the physical and chemical properties of the thermal fluid produced from the Niland area. Although both liquid and vapor phases are produced simultaneously from the Niland wells, the vapor phase is superheated as much as 9°C, because the vapor is not in equilibrium with pure water but with a concentrated brine. If a concentrated alkali chloride solution, comparable to the Niland brine, existed deep within the thermal systems of The Geysers and the Italian fields, this would account for at least some of the superheat contained in the steam from these systems.

The thermal waters of the Kamchatka-Kurile volcanic zone are classified according to their chemical composition by *Averiev et al.* [1960, 1963].

Isotopic compositions of thermal water in the United States and elsewhere in the world are discussed by *Craig et al.* [1956]. In all the thermal areas examined by these authors, they found that the hot spring waters have about the same deuterium concentration as the local surface water, but are slightly higher in O<sup>18</sup>. They conclude that probably 95% of the water discharged from a thermal area is principally deep circulating meteoric water which has undergone variable amounts of oxygen isotope exchange with local rocks.

*Hulston* [1961] describes studies of the natural variation of the stable isotopes of carbon and sulfur found in the Wairakei thermal fluid. These studies have led to the use of isotope equilibria to determine temperatures of the thermal fluid at depth, and the use of the natural radioactive isotopes of carbon 14 and tritium for estimating the length of time the thermal fluid has been underground. The measured tritium activity indicates the fluid has been underground less than fifty years, if there has been a single circulation path.

*Nencetti* [1961a] concludes from isotopic data that the Larderello thermal fluid is mainly meteoric in origin and has been in underground circulation for longer than 40 years.

By study of the C<sup>12</sup>, C<sup>13</sup>, and C<sup>14</sup> isotopes in the thermal system at Steamboat Springs, Nevada, it has been concluded that the descending

meteoric water spends at least 30,000 to 300,000 years underground, depending on the type of circulation [*Craig*, 1962].

#### 7. PROBLEMS OF EXPLORATION, DEVELOPMENT, AND MANAGEMENT

In any new field of endeavor, it is inevitable that problems will arise that cannot be immediately resolved by appealing to past experience. Three such problems which seem to be particularly acute in the field of geothermal power development are: (1) proper location of production wells; (2) blockage of wells by mineral precipitates; and (3) protection of fresh water reservoirs from contamination by steam well effluent.

Problems 2 and 3 are not common to all thermal fields, and suitable solutions must be found for the specific conditions encountered. When blockage of some of the Wairakei wells by mineral precipitates became a problem, slotted well-liners were installed which periodically could be removed and cleaned. At Casa Diablo, it was found that calcite, which was deposited in the wells where thermal water flashed to steam, could be rapidly removed by reaming the flowing well with a cable tool. This procedure restored the original production capacities. Possible solutions to the problem of effluent disposal are related to local geologic and geographic conditions, and will not be discussed here.

In contrast to the problems of well blocking and effluent disposal, the problem of proper well location is common to all the thermal fields now being explored and developed.

In general, the objective in locating production wells is to intersect the productive fissures at an optimum depth, considering both economic and geologic factors. At Wairakei, for example, wells are located about 60 meters from the traces of the known major faults and on the downdropped side, so that the fissure is intersected between depths of 300 and 600 meters where temperatures are reasonably high [*Grindley*, 1961]. Deeper holes are generally avoided because they would necessitate drilling into hard ignimbrite, which would be time consuming and expensive. Extensive development at Wairakei, however, has shown that even if a fissure is not intersected, production can still

be obtained from the porous reservoir rock into which the fluid migrates. This fluid, however, is at a lower temperature than the fluid in the feeding fissures and consequently reaches the surface at lower well head pressures. Because the area over which the fluid migrates is so much larger than the cross-sectional area of the steeply dipping fissures from which it flows, the fluid in the permeable beds is easier to locate and consequently cheaper to produce. It is therefore found more economic to design turbines to utilize the low pressure steam than to expend the time and effort which would have been necessary to produce sufficient quantities of only high pressure steam. In 1961, approximately 40% of the steam used in the turbines at Wairakei was taken directly from the fissures at pressures ranging from about 13.5 to 15.5 kg/cm<sup>2</sup>, and the other 60% was produced from the surrounding permeable formations at pressures ranging from about 4.5 to 7 kg/cm<sup>2</sup> [Armstead, 1961, p. 14].

In those thermal areas where steeply dipping production fissures do not intersect permeable horizons, as at The Geysers, accurate well location becomes more critical. If the steam-bearing fissure is not intersected, there is no 'secondary' production from horizontal permeable horizons. Results of recent development work 1.5 km west of The Geysers indicate that the fissure carrying the thermal fluid dips at approximately 80°. The well spacing in this area averages approximately 100 meters. If two wells were 100 meters apart on a line perpendicular to the fault trace, the well further from the fault would intersect the production fissure approximately 600 meters deeper than the well closer to the fault. Such differences in production depths can greatly affect the quantity and quality of steam produced, as well as the economics of the drilling operation.

Well location becomes extremely difficult in those areas where the fault trace and dip cannot be accurately determined from surface observation. The alignment of hot springs is not always the best guide for locating the fault trace, because the location of springs is controlled by groundwater migration and the surface drainage pattern, as well as by the fault trace itself.

The problem of well location in areas of this nature has been met with some success in New Zealand and Italy by the application of various

geophysical techniques which include gravity, magnetic, temperature, and resistivity surveys. The applicability of any specific geophysical method, as will be demonstrated by the following examples, is principally determined by subsurface geologic conditions.

Positive gravity anomalies are closely related to both the Wairakei and Niland thermal fields. At Wairakei, the anomaly is caused by the horst block of dense basement rock, which protrudes into the less dense material filling the region of subsidence [Beck and Robertson, 1955]. The faults bounding this block are the fissures through which the thermal fluid reaches the Wairakei reservoir (section 3 of this chapter). The cause of the positive gravity anomaly at Niland, which strikingly coincides with a positive magnetic anomaly and the position of the five rhyolite domes, is not known (section 3 of this chapter).

Negative gravity anomalies have been found beneath the Larderello and Mt. Amiata regions [Marchesini *et al.*, 1962] and beneath the Mayacmas uplift. These anomalies range from 10 to 25 mgals, and average 15 by 30 km in extent. It is possible that these anomalies are related to underlying intrusive bodies.

Even though, in most cases, a genetic relationship between gravity anomalies and associated thermal fluids has not been demonstrated, these anomalies may be useful for empirically defining the limits of an area which should be prospected in detail.

Magnetic surveys have been reported for the Wairakei area [Beck and Robertson, 1955; Studt, 1959; Modriniak and Studt, 1959], the Waiotapu area [Studt, 1963], the Kawerau area [Studt, 1958a], the Niland area [Kelley and Soske, 1936], and the Casa Diablo area [Henderson and White *et al.*, 1963]. Where local conditions are favorable, magnetic surveys are useful for distinguishing gravity anomalies due to structural relief from those due to buried volcanic or intrusive rock bodies. Magnetic anomalies are similar to gravity anomalies in that they are generally too large or too poorly defined to be useful for locating individual production wells. Sometimes, however, detailed land magnetic surveys reveal magnetic lows over thermal areas due to hydrothermal alteration of magnetite to pyrite [Studt, 1961, p. 4]. If the land magnetic survey can be interpreted in

the light of subsurface information, including lithology, alteration, and fluid movement, it may be possible to locate areas in which the thermal fluid is being fed into a reservoir [Studt, 1959]. These areas seem to be characterized by more intense alteration of magnetite to pyrite than other parts of the reservoir, and consequently they produce near-surface negative magnetic anomalies.

Temperature surveys are probably the most satisfactory geophysical method used to locate drill holes when the conducting fissures themselves are not directly observable. In New Zealand, temperatures are taken with a thermocouple at 60-meter intervals and 1-meter depth [Thompson *et al.*, 1961]. The size of the area surveyed is determined by the temperature limits of 1°C to 50°C above ambient at 1-meter depth. The potentiometer readings for each station are computed to degrees centigrade, corrected for seasonal change, and contours are drawn at the outer boundary (1°C above local ambient) and on the 20°C and 50°C isotherms. These surveys have shown that measurably hot areas extend well beyond the directly observable surface activity and make it possible to locate prospect holes efficiently.

Electric resistivity surveys, in conjunction with gravity surveys, have been very helpful in locating major faults in the Italian steam fields. The electrically resistant anhydrite and carbonate rocks, which are the steam reservoirs, are overlain by an impermeable, conductive shale. The resistivity method is successful because the thickness of the shale cover is characteristic of each fault block, so that the resistivity survey shows the position of the faults as well as the comparative thickness of the shale, and therefore the depth to the reservoir [Mazzoni and Breusse, 1954; Alfano, 1960; Battini and Menut, 1961].

The electrical resistivity method is useful not only for determining geologic structure; it can also indicate the presence of a geothermally heated zone. It has been found in Italy that ground heated from 17°C to 150°C decreases in resistivity by a factor of 5, and, if heated from 17°C to 280°C, its resistivity decreases by a factor of 9 [Breusse, 1961]. The effect of temperature on resistivity has been successfully used for natural steam exploration at Kawerau, New Zealand [Studt, 1958a, p. 230-235]. In that area, Studt found that at the water table (3-6

meters deep) the resistivity drops abruptly to several hundred ohm-meters in cold country, and to several tens of ohm-meters in hot. Resistivity surveys utilizing this heat effect are best applied in areas having uniform surface geology and uniform depth to the water table.

Electromagnetic surveys generally have not been included among the techniques used in exploring and developing thermal areas. Recently, however, the AFMAG device has been used to study several hot spring systems in the western United States. This instrument, whose operation is described by Ward [1959], is particularly suited to detect steeply dipping conducting bodies, such as fault zones filled with mineralized water. So far, the results of these AFMAG surveys have not been published.

The problem of proper field management is directly related to the problem of locating successful production wells. Those thermal fields in the advanced stages of development invariably show induced mass and heat discharges considerably larger than their original natural flows (section 5 of this chapter). As yet, very little information is available about the effects of large, sustained, induced discharge on either the reservoir itself or on equilibrium conditions deep within the thermal system. The near-surface effects of production, however, have been studied at Wairakei. Studt [1958b] discusses the hydrology of the Wairakei field and demonstrates the influence of production on piezometric surfaces. The configurations of these surfaces indicate areas where hot water is fed into the reservoir. Because there has been a general decline in the 'thermoartesian' pressure in certain parts of the Wairakei field, Studt [1958b] concludes that cold water is encroaching on the field and that the observed heat flow must be coming, at least in part, from heat stored in the rocks and groundwater. This conclusion raises the question of whether it is possible to locate wells in such a manner as to produce the greatest amount of thermal fluid at optimum pressures and for the longest possible time. In order to answer this question, considerable information is needed about the direction and rate of flow for both the thermal fluid and the encroaching cold water. Such data are particularly important if re-injection is to be used to solve the problem of effluent disposal.

## 8. SUMMARY AND CONCLUSIONS

Day's [1939] paper 'The hot spring problem' is a summary of geologic thinking, up to that time, on the question of heat transfer and convective flow in the upper crust. Since that paper was written, the investigations cited in this chapter have greatly contributed to our understanding of hot spring systems, or at least to the upper, near-surface part of these systems. Geologic and geophysical evidence suggests a magmatic heat source, isotopic data all but confirm a meteoric origin of a large percentage of the thermal fluid, and chemical investigations provide information on the history of the fluid and the manner in which it affects, and has been affected by, the rock through which it circulates. The drilling of several thermal areas has disclosed large reservoirs of thermal fluid. These reservoirs are capable of storing considerable amounts of heat, both in the thermal fluid and in the reservoir rock which contains it. Bodvarsson [1962], using a reservoir model based on the physical characteristics of Iceland's high temperature thermal areas, and applying this concept of stored heat, estimates that  $10^{14}$  kilocalories of heat are stored per square kilometer of surface in these high temperature areas. In spite of all this new information made available in the last decade or so, the nature of the heat source and the mechanism by which heat is transferred to the thermal fluid are still perplexing problems.

Banwell [1963] has proposed theoretical models to explain the known characteristics of the Wairakei thermal system. Reflecting various initial assumptions, Banwell offers several modifications of a model which is based on heat being transferred from a convecting magma through a thin conducting roof rock and into a system of deep circulating meteoric water. An alternative model offered by Banwell involves the absorption of meteoric water by magma deep in the system and its release at a higher level where pressure is lower. Banwell estimates the total energy content of the conductive and convective zones of his larger models to be of the order of  $10^6$  to  $10^8$  megawatt years.

It may be possible to test the applicability of these various models by observing to what extent the large heat discharges, which are induced by drilling, can establish new steady-state conditions of flow throughout the entire system. In-

formation about the variation of heat and mass discharge with time may make it possible to estimate the size of reservoirs, the area of conduction surfaces, and, perhaps, even some physical characteristics of the primary heat source.

In the meantime, much more information is needed about the relationships among heat flow, tectonic processes, and magma emplacement. Present information indicates definite spatial and temporal relationships between structure and areas of high heat flow, but the genetic implications of these relationships are not yet understood.

Continued exploration drilling, in conjunction with geologic mapping, as well as geochemical and geophysical surveys, including heat flow measurements, will supply additional insight into the hot spring problem. Researchers may not agree as to the nature and causes of geothermal energy, but they all agree that the vast amount of geothermal resources can be harnessed for the benefit of man. The utilization of geothermal energy requires neither advanced technology, as in the case of atomic energy, nor massive construction, as in the case of hydroelectric power. Furthermore, geothermal resources are almost unlimited, whereas fuels such as petroleum, natural gas, and coal will be exhausted in the near future.

*Acknowledgments.* I wish to thank J. Healy and D. E. White for their thoughtful review and helpful comments on this chapter. I am also grateful to C. J. Banwell, G. Bodvarsson, G. Facca, F. Penta, and F. Tonani for their reviews of the manuscript.

## REFERENCES

- Alfano, L., Geoelectrical explorations for natural steam near 'Monte Amiata,' *Quaderni Geofis. Appl.*, 21, 3-17, 1960.
- Allen, E. T., and A. L. Day, Steam wells and other thermal activity at 'The Geysers,' California, *Carnegie Inst. Wash. Publ.* 378, 106 pp., 1927.
- Armstead, H. C. H., Geothermal power development at Wairakei, N.Z., *U. N. Conf. on New Sources of Energy*, Rome, paper G4, 20 pp., 1961.
- Askelsson, J., G. Bodvarsson, T. Einarsson, G. Kjartansson, and S. Thorarinsson, On the geology and geophysics of Iceland, Guide to Excursion No. A2, *21st Intern. Geol. Congress*, Copenhagen, 1960.
- Averiev, V. V., The technique of testing geothermal wells, *U. N. Conf. on New Sources of Energy*, Rome, paper G74, 25 pp., 1961.

- Averiev, V. V., V. V. Ivanov, and B. I. Piip, Problems of using volcanic thermae of the Kurile-Kamchatka Island arc for power, *Bull. Volcanologique*, 23, 257-263, 1960.
- Averiev, V. V., V. V. Ivanov, and B. I. Piip, reviewed by G. V. Chilingar, Utilization of thermal waters and steam of the Kurile-Kamchatka Island arc for power, *The Compass*, 40, 177-181, 1963.
- Bailey, E. H., Quicksilver deposits of the western Mayacmas district, Sonoma Co., California, *Calif. J. Mines and Geol.*, 42(3), 199-230, 1946.
- Banwell, C. J., Physical investigations, in Geothermal Steam for Power in New Zealand, *New Zealand Dept. Sci. Ind. Res. Bull.* 117, edited by L. I. Grange, pp. 45-74, 1955.
- Banwell, C. J., Geothermal drillholes—Physical investigations, *U. N. Conf. on New Sources of Energy*, Rome, paper G53, 24 pp., 1961.
- Banwell, C. J., Thermal energy from the Earth's crust, Introduction and part 1, Natural hydrothermal systems, *New Zealand J. Geol. Geophys.*, 6, 52-69, 1963.
- Banwell, C. J., E. R. Cooper, G. E. K. Thompson, K. J. McCree, Physics of the New Zealand thermal area, *New Zealand Dept. Sci. Ind. Res. Bull.* 123, 109 pp., 1957.
- Barth, T. F. W., Volcanic geology, hot springs and geysers of Iceland, *Carnegie Inst. Wash. Publ.* 587, 174 pp., 1950.
- Battini, F., and P. Menut, Sur l'étude structurale de la zone de Roccastrada pour recherche de vapeur par les méthodes géophysiques, gravimétrique, et électrique, *U. N. Conf. on New Sources of Energy*, Rome, paper G26, 19 pp., 1961.
- Beck, A. C., and E. I. Robertson, Geology and geophysics, in Geothermal steam for power, *New Zealand Dept. of Sci. and Indus. Res. Bull.* 117, edited by L. I. Grange, pp. 15-19, 1955.
- Benseman, R. F., The calorimetry of steaming ground in thermal areas, *J. Geophys. Res.*, 64, 123-126, 1959a.
- Benseman, R. F., Estimating the total heat output of natural thermal regions, *J. Geophys. Res.*, 64, 1057-1062, 1959b.
- Bodvarsson, G., Drilling for heat in Iceland, *Oil and Gas J.*, 191-199, 1949.
- Bodvarsson, G., Exploration and exploitation of natural heat in Iceland, *Bull. Volcanologique*, 23, 241-250, 1960.
- Bodvarsson, G., Physical characteristics of natural heat resources in Iceland, *U. N. Conf. on New Sources of Energy*, Rome, paper G6, 19 pp., 1961.
- Bodvarsson, G., An appraisal of the potentialities of geothermal resources in Iceland, *6th World Power Conference*, Melbourne, paper 206 III, 6/3, 16 pp., 1962.
- Bodvarsson, G., and G. Palmason, Exploration of subsurface temperature in Iceland, *U. N. Conf. on New Sources of Energy*, Rome, paper G24, 22 pp., 1961.
- Boldizar, T., Terrestrial heat flow in the natural steam field at Larderello, *Geofis. Pura Appl.*, 56, 115-122, 1963.
- Brousse, J. J., Contributions des méthodes géophysiques à la prospection des champs géothermiques, *U. N. Conf. on New Sources of Energy*, Rome, paper G25, 6 pp., 1961.
- Burgassi, R., Prospecting of geothermal fields and exploration necessary for their adequate exploitation, performed in various regions of Italy, *U. N. Conf. on New Sources of Energy*, Rome, paper G65, 30 pp., 1961.
- Burgassi, R., F. Battini, and J. Mouton, Prospection géothermique pour la recherche des forces endogènes, *U. N. Conf. on New Sources of Energy*, Rome, paper G61, 8 pp., 1961.
- Cassinis, R., Application of seismic methods to geothermal energy exploration, *Quaderni Geofis. Appl.*, 21, 18-27, 1960.
- Cataldi, R., G. Stefani, and M. Tongiorgi, Geology of Larderello region (Tuscany): Contribution to the study of the geothermal basins, *Symp. on Nucl. Geol. on Geothermal Areas*, Spoleto, 1963.
- Chierici, A., Planning of a geothermoelectric power plant: Technical and economic principles, *U. N. Conf. on New Sources of Energy*, Rome, paper G62, 27 pp., 1961.
- Craig, H., C<sup>12</sup>, C<sup>18</sup>, and C<sup>14</sup> concentrations in volcanic gases (abstract), *J. Geophys. Res.*, 67(4), 1633, 1962.
- Craig, H., G. Boato, and D. White, Isotope geochemistry of thermal waters, in Nuclear processes in geologic settings, *Natl. Res. Council Nucl. Ser., Rept.* 19, 29-38, 1956.
- Dawson, G. B., The nature and assessment of heat flow from hydrothermal areas, *New Zealand J. Geol. Geophys.*, 7, 155-171, 1964.
- Dawson, G. B., and R. G. Fisher, Diurnal and seasonal ground temperature variations at Wairakei, *New Zealand J. Geol. Geophys.*, 7, 144-154, 1964.
- Day, A. L., The hot-spring problem, *Bull. Geol. Soc. Am.*, 50, 317-336, 1939.
- de Anda, L. F., El Campo de Energia Geotermica en Pathé, Estado de Hidalgo, Mexico, *20th Intern. Geol. Congr.*, Mexico, section 1, tomo 2, *Volcanologia del Cenozoico*, pp. 257-283, 1957.
- de Anda, L. F., J. I. Septien, and J. R. Elizondo, Geothermal energy in Mexico, *U. N. Conf. on New Sources of Energy*, Rome, paper G77, 25 pp., 1961.
- Decius, L. C., Geological environment of hyperthermal areas in continental United States and suggested methods of prospecting them for geothermal power, *U. N. Conf. on New Sources of Energy*, Rome, paper G48, 20 pp., 1961.
- Dench, N. D., Investigations for geothermal power at Waitapu, New Zealand, *U. N. Conf. on New Sources of Energy*, Rome, paper G17, 19 pp., 1961.
- Dibblee, T. W., Geology of the Imperial Valley region, California, *Calif. Div. Mines Bull.* 170, chapter 2, pp. 21-28, 1954.
- Durr, F., Review of geothermal activity in El Sal-

- vador, *U. N. Conf. on New Sources of Energy*, Rome, paper G11, 4 pp., 1961.
- Eiby, G. A., The New Zealand sub-crustal rift, *New Zealand J. Geol. Geophys.*, 7, 109-133, 1964.
- Einarsson, S. S., Proposed 15-megawatt geothermal power station at Hveragerdi, Iceland, *U. N. Conf. on New Sources of Energy*, Rome, paper G9, 19 pp., 1961.
- Elizondo, J. R., General Report on agenda: Prospection of geothermal fields and investigations necessary to evaluate their capacity, *U. N. Conf. on New Sources of Energy*, Rome, paper G13, 79 pp., 1961.
- Ellis, A. J., Geothermal drillholes—chemical investigations, *U. N. Conf. on New Sources of Energy*, Rome, paper G42, 26 pp., 1961.
- Ellis, A. J., Interpretation of gas analyses from the Wairakei hydrothermal area, *New Zealand J. Sci.*, 5(4), 434-452, 1962.
- Ellis, A. J., and D. W. Anderson, The geochemistry of bromine and iodine in New Zealand thermal waters, *New Zealand J. Sci.*, 4(3), 415-430, 1961.
- Ellis, A. J., and J. R. Sewell, Boron in waters and rocks of the New Zealand hydrothermal areas, *New Zealand J. Sci.* 6(4), 589-606, 1963.
- Ellis, A. J., and S. H. Wilson, The geochemistry of alkali metal ions in the Wairakei hydrothermal system, *New Zealand J. Geol. Geophys.*, 3, 593-617, 1960.
- Facca, G., and A. Ten Dam, Geothermal power economics, in *Consiglio Nazionale delle Ricerche*, Commission Geotermica Italiano, Rome, 1963.
- Facca, G., and F. Tonani, Natural steam geology and geochemistry, *U. N. Conf. on New Sources of Energy*, Rome, paper G67, 21 pp., 1961.
- Facca, G., and F. Tonani, Geologia e geochemica del vapore naturale, *L'Industria Mineraria*, Anno 13, Marzo, 121-131, 1962a.
- Facca, G., and F. Tonani, Natural steam exploration in U.S.A., *Boll. Geofis. Teorica Appl.*, 4(14), 155-171, 1962b.
- Facca, G., and F. Tonani, Theory and technology of a geothermal field, *13th Gen. Assembly IUGG*, Berkeley, California, 50 pp., 1963.
- Fenner, C. N., Bore-hole investigations in Yellowstone Park, *J. Geol.*, 44, 225-315, 1936.
- Fisher, R. G., Geothermal heat flow at Wairakei during 1958, *New Zealand J. Geol. Geophys.*, 7, 172-184, 1964.
- Fooks, A. C. L., Preliminary investigation of the Rabaul geothermal area for the production of electric power, *U. N. Conf. on New Sources of Energy*, Rome, paper G12, 10 pp., 1961.
- Gennai, N., Résultat des forages effectués à Bagnore (Monte Amiata, Italie), *Bull. Volcanologique*, 23, 237-239, 1960.
- Goguel, J., Le Régime thermique de l'eau souterraine, *Ann. Mines*, 10, 3-32, 1953.
- Golding, R. M., and M. G. Speer, Alkali ion analysis of thermal waters in New Zealand, *New Zealand J. Sci.*, 4(2), 203-213, 1961.
- Grange, L. I., The geology of the Roturua-Taupo subdivision, *New Zealand Geol. Surv. Bull.* 37, new series, 138 pp., 1937.
- Grange, L. I., editor, Geothermal steam for power in New Zealand, *New Zealand Dept. Sci. Ind. Res. Bull.* 117, 102 pp., 1955.
- Grindley, G. W., Sheet 8-Taupo., Geological map of New Zealand, 1:250,000, New Zealand Dept. Sci. Ind. Res., Wellington, 1960.
- Grindley, G. W., Geology of New Zealand geothermal steam fields, *U. N. Conf. on New Sources of Energy*, Rome, paper G34, 17 pp., 1961.
- Grindley, G. W., Geology and structure of Waiotapu geothermal field, in Waiotapu geothermal field, *New Zealand Dept. Sci. Ind. Res. Bull.* 155, 10-25, 1963.
- Harada, H., and T. Mori, The present position regarding the utilization of geothermal energy and the role of geothermal energy from the viewpoint of energy economy in Japan, *U. N. Conf. on New Sources of Energy*, Rome, paper G57, 9 pp., 1961.
- Hayakawa, M., and K. Mori, Seismic prospecting at Matsukawa geothermal area, Iwate Prefecture (English abstract), *Bull. Geol. Soc. Japan*, 13, 643-648, 1962.
- Healy, J., Geology and geothermal energy in the Taupo volcanic zone, New Zealand, *U. N. Conf. on New Sources of Energy*, Rome, paper G28, 17 pp., 1961.
- Healy, J., Structure and volcanism in the Taupo Volcanic Zone, New Zealand, in Crust of the Pacific basin, *Am. Geophys. Union, Monograph* 6, 151-157, 1962.
- Healy, J., Volcanic mechanisms in the Taupo volcanic zone, *New Zealand J. Geol. Geophys.*, 7, 6-23, 1964a.
- Healy, J., Geothermal energy, *New Zealand Engineering*, 19(2), 55-60, 1964b.
- Henderson, J. R., B. L. White, et al., Aeromagnetic map of Long Valley and northern Owens Valley, California, *U.S. Geol. Surv. Geophys. Invest. Map GP-329*, 1963.
- Hulston, J. R., Isotope geology in the hydrothermal areas of New Zealand, *U. N. Conf. on New Sources of Energy*, Rome, paper G31, 11 pp., 1961.
- Hunt, A. M., The measurement of borehole discharges, downhole temperatures and pressures, and surface heat flows at Wairakei, *U. N. Conf. on New Sources of Energy*, Rome, paper G19 revised, 23 pp., 1961.
- James, R., Alternative methods of determining enthalpy and mass flow, *U. N. Conf. on New Sources of Energy*, Rome, paper G30, 6 pp., 1961.
- Jennings, C. W., and R. G. Strand, Ukiah Sheet, Geologic map of California, 1:250,000, Calif. Div. Mines and Geol., San Francisco, 1960.
- Kaufman, A., Economic appraisal of geothermal power, *Mining Engineering*, 16(9), 62-66, 1964a.
- Kaufman, A., Geothermal power—An economic evaluation, *U. S. Bur. Mines Inform. Circ.* 8230, 1964b.
- Kelley, V. C., and J. L. Soske, Origin of the Salton

- volcanic domes, Salton Sea, California, *J. Geol.*, 44, 496-509, 1936.
- Koenig, J. B., Santa Rosa Sheet, Geologic map of California, 1:250,000, Calif. Div. Mines and Geol., San Francisco, 1963.
- Kovach, L., C. R. Allen, and F. Press, Geophysical investigations in the Colorado Delta region, *J. Geophys. Res.*, 67(7), 2845-2871, 1962.
- Laizure, C. McK., The Geysers; Development of natural steam wells for power purposes at 'The Geysers,' *Calif. Div. Mines, Rept. of State Mineralogist*, 22, 343-353, 1926.
- Lloyd, E. F., The hot springs and hydrothermal eruptions of Waiotapu, *New Zealand J. Geol. Geophys.*, 2, 141-176, 1959.
- Mahon, W. A. J., Sampling of geothermal drillhole discharges, *U. N. Conf. on New Sources of Energy*, Rome, paper G46, 21 pp., 1961.
- Mahon, W. A. J., The carbon dioxide and hydrogen sulphide content of steam from drillholes at Wairakei, New Zealand, *New Zealand J. Sci.*, 5(1), 85-98, 1962a.
- Mahon, W. A. J., A chemical survey of the steam and water discharged from drillholes and hot springs at Kawerau, *New Zealand J. Sci.*, 5(4), 417-433, 1962b.
- Marchesini, E., Photogeology applied to natural steam exploration, *U. N. Conf. on New Sources of Energy*, Rome, paper G69, 12 pp., 1961.
- Marchesini, E., A. Pistolesi, and M. Bolognini, Fracture patterns of the natural steam area of Larderello, Italy, from airphotographs, *Symp. on Photo Interpretation, Delft*, pp. 524-532, 1962.
- Marinelli, G., Les anomalies thermiques et les champs géothermiques dans le cadre des intrusions récentes en Toscane, *U. N. Conf. on New Sources of Energy*, Rome, paper G58, 8 pp., 1961.
- Marinelli, G., L'énergie géothermique en Toscane, *Extrait Ann. Soc. Geol. Belgique*, 85, 1961-1962, Bull. 10, 417-438, 1963.
- Mazzoni, A., *I Soffioni Boraciferi Toscani e Gli Impianti della Larderello*, An. Arti Grafiche, Bologna, 1948 (2nd edition, 1951).
- Mazzoni, A., and J. J. Breusse, Application de la prospection électrique à la tectonique pour la recherche de vapeur naturelle à Larderello (Italie), *19th Intern. Geol. Cong.*, Algiers, section 15, Fascicule 17, 161-168, 1954.
- McCall, G. J. H., Natural steam as a possible source of power in the Rift Valley of Kenya, *20th Intern. Geol. Cong.*, Mexico, section 1, Tomo 1, *Volcanologia del Cenozoico*, pp. 47-54, 1957.
- McNitt, J. R., Geology of the Geysers thermal area, California, *U. N. Conf. on New Sources of Energy*, Rome, paper G31, 18 pp., 1961.
- McNitt, J. R., Exploration and development of geothermal power in California, *Calif. Div. Mines Geol. Spec. Rept.* 75, 45 pp., 1963.
- Merla, G., Geologia dell' Appennino settentrionale, *Boll. Soc. Geol. Ital.*, 70, 95-382, 1951.
- Migliorini, C. I., I cunei composti nell' Orogenesi, *Boll. Soc. Geol. Ital.*, 67, 29-142, 1948.
- Minucci, G., Rotary drilling for geothermal energy, *U. N. Conf. on New Sources of Energy*, Rome, paper G66, 15 pp., 1961.
- Modriniak, N., and F. E. Studdt, Geological structure and volcanism of the Taupo-Tarawera District, *New Zealand J. Geol. Geophys.*, 2, 654-684, 1959.
- Monro, J. N., Geothermal heat shows possible use in the Fiji Islands, *Mining Engineering*, 16(9), 66-67, 1964.
- Nasini, R., I soffioni ed i lagoni della Toscana e l'industria boracifera, Storia e studi, *Associazione Italiana di Chimica*, Italia, Roma, 1930.
- Nekhoroshev, A. S., The problem of the methods for determining the pressure of volcanic vapors at depth, *Bull. Volcanologique*, 23, 271-276, 1960.
- Nencetti, R., Échantillonnage et analyse des caux de sources thermales ou provenant de manifestations vaporifères, *U. N. Conf. on New Sources of Energy*, Rome, paper G73, 26 pp., 1961a.
- Nencetti, R., Méthodes et dispositifs de mesure en tete des puits employés au champ géothermique de Larderello après éruption d'un sondage, *U. N. Conf. on New Sources of Energy*, Rome, paper G75, 28 pp., 1961b.
- Nencetti, R., Échantillonnage et analyse de gas des sources naturelles de vapeur, *U. N. Conf. on New Sources of Energy*, Rome, paper G76, 24 pp., 1961c.
- Pakiser, L. C., Gravity, volcanism, and crustal deformation in Long Valley, California, *U. S. Geol. Surv. Prof. Paper* 424-B, 250-253, 1961.
- Pakiser, L. C., A gravity study of Long Valley, in Geology and mineral deposits of Mount Morrison Quadrangle, Sierra Nevada, California, *U. S. Geol. Surv. Prof. Paper* 385, 85-92, 1964.
- Penta, F., Temperature nel sottosuolo della regione 'Flegrea,' *Ann. Geof.*, 2(3), 328-346, 1949.
- Penta, F., Ricerche e studi su fenomeni esaltativo-idrotermali ed il problema delle 'forze endogene,' *Ann. Geofis.*, 8(3), 1954.
- Penta, F., Caratteristiche e geni delle manifestazioni esaltivo-idrotermali naturali, *Atti della XIV Riunione della Società Italiana per il Progresso della Scienze*, Napoli, 1954, 31 pp., 1955.
- Penta, F., Sulle origini del vapore acqueo naturale e sull'attuale stato delle relative ricerche (ricerche per 'forze endogene'), *Ric. Sci.*, 29(12), 1959.
- Penta, F., Vapori naturali ("forze endogene"): Stato delle ricerche e considerazioni, *Bull. Volcanologique*, 23, 219-235, 1960.
- Penta, F., Sulle caratteristiche idrotermogeologiche dell'isola di Ischia (Napoli), *Accademia Nazionale dei Lincei, Rend. Classe Sci. Fis., Mat. e Nat.*, [8]34(1), 1963.
- Penta, F., and G. Bartolucci, Sullo stato delle 'ricerche' e dell' utilizzazione industriale (termoelettrica) del vapore acqueo sotterraneo nei vari paesi del mondo, *Accademia Nazionale dei Lincei, Rend. Classe Sci. Fis., Mat. e Nat.*, [8]32(4), 1962.
- Piip, B. I., V. V. Ivanov, and V. V. Averiev, The hyperthermal waters of Pauzhetsk, Kamchatka, as a source of geothermal energy, *U. N. Conf.*

- on *New Sources of Energy*, Rome, paper G38, 21 pp., 1961.
- Rinehart, C. D., and D. C. Ross, Geology and mineral deposits of the Mount Morrison quadrangle, Sierra Nevada, California, *U. S. Geol. Surv. Prof. Paper 385*, 106 pp., 1964.
- Ritchie, J. A., Chemical analysis and laboratory requirements: Experience in New Zealand's hydrothermal areas, *U. N. Conf. on New Sources of Energy*, Rome, paper G29, 12 pp., 1961a.
- Ritchie, J. A., Arsenic and antimony in some New Zealand thermal waters, *New Zealand J. Sci.*, 4(2), 218-229, 1961b.
- Robertson, E. I., and G. B. Dawson, Geothermal heat flow through the soil at Wairakei, *New Zealand J. Geol. Geophys.*, 7, 134-143, 1964.
- Rook, S. H., and G. C. Williams, Imperial carbon dioxide gas field: Summary of operations—California Oil Fields, *Calif. Div. Oil and Gas*, 28(2), 12-33, 1942.
- Saito, M., Known geothermal fields of Japan, *U. N. Conf. on New Sources of Energy*, Rome, paper G1, 11 pp., 1961.
- Stearns, N. D., H. G. Stearns, and G. A. Waring, Thermal springs in the U. S., *U. S. Geol. Surv. Water-Supply Paper 679-B*, 59-191, 1935.
- Steiner, A., Hydrothermal rock alteration at Wairakei, New Zealand, *Econ. Geol.*, 48, 1-13, 1953.
- Steiner, A., Hydrothermal rock alteration, in Geothermal steam for power in New Zealand, *New Zealand Dept. Sci. Ind. Res. Bull. 117*, edited by L. I. Grange, pp. 21-26, 1955.
- Steiner, A., The rocks penetrated by drillholes in the Waiotapu thermal area, and their hydrothermal alteration, in Waiotapu geothermal field, *New Zealand Dept. Sci. Ind. Res. Bull. 155*, 26-34, 1963.
- Studt, F. E., Geophysical reconnaissance at Kawerau, New Zealand, *New Zealand J. Geol. Geophys.*, 1, 219-246, 1958a.
- Studt, F. E., The Wairakei hydrothermal field under exploitation, *New Zealand J. Geol. Geophys.*, 1, 703-723, 1958b.
- Studt, F. E., Magnetic survey of the Wairakei hydrothermal field, *New Zealand J. Geol. Geophys.*, 2, 746-754, 1959.
- Studt, F. E., Preliminary survey of the hydrothermal field at Rabaul, New Britain, *New Zealand J. Geol. Geophys.*, 4(3), 274-282, 1961.
- Studt, F. E., Geophysics of Waiotapu area, in Waiotapu geothermal field, *New Zealand Dept. Sci. Ind. Res. Bull. 155*, 35-41, 1963.
- Studt, F. E., and D. Doyle, Electric power generation from geothermal steam at Wairakei, New Zealand, *Bull. Volcanologique*, 23, 277-282, 1960.
- Sviatlovsky, A. E., Thermal underground waters of the Kamchatka and the role of recent tectonics and volcanism in their dynamics, *Bull. Volcanologique*, 23, 265-270, 1960.
- Thompson, B. N., Quaternary volcanism of the Central Volcanic Region, *New Zealand J. Geol. Geophys.*, 7, 45-66, 1964.
- Thompson, G. E. K., C. J. Banwell, G. B. Dawson, and D. J. Dickinson, Prospecting of hydrothermal areas by surface thermal surveys, *U. N. Conf. on New Sources of Energy*, Rome, paper G54, 25 pp., 1961.
- United Nations, New sources of energy and energy development, Rept. on U. N. Conf. on New Sources of Energy, Rome, 1961, *U. N. Paper E/3577/Rev. 1, St/ECA/72*, 1962.
- van Padang, N. M., The steam borings in Kawah Kamodjang, *Bull. Volcanologique*, 23, 251-255, 1960.
- Vecchia, O., Gravimetric exploration for natural steam in Tuscany, *Quaderni Geofis. Appl.*, 21, 18-27, 1960.
- Ward, S. H., AFMAG—Airborne and ground, *Geophysics*, 4, 761-789, 1959.
- White, D. E., Thermal waters of volcanic origin, *Bull. Geol. Soc. Am.*, 68, 1637-1658, 1957.
- White, D. E., Preliminary evaluation of geothermal areas by geochemistry, geology and shallow drilling, *U. N. Conf. on New Sources of Energy*, Rome, paper G2, 12 pp., 1961.
- White, D. E., Geothermal brine well: Mile-deep drill hole may tap ore-bearing magmatic water and rocks undergoing metamorphism, *Science*, 139(3558), 919-922, 1963.
- Wilson, S. H., Chemical prospecting of hot spring areas for utilization of geothermal steam, *U. N. Conf. on New Sources of Energy*, Rome, paper G35, 19 pp., 1961.
- Yates, R. G., and L. S. Hilpert, Quicksilver deposits of eastern Mayacmas district, Lake and Napa Counties, California, *Calif. J. Mines Geol.*, 42(3), 231-286, 1946.

(Manuscript received June 10, 1964; revised September 21, 1964.)

## Name Index

Authors' names of Chapters in this book and the inclusive page numbers of these Chapters are printed in **heavy type**, page numbers of citations in the text are in ordinary type, and those of bibliographical references listed at the ends of the chapters (including joint authors) are in *italics*.

Where the same author is mentioned in more than one chapter, it may be convenient to differentiate by subject between the successive ranges of page numbers by consulting the list of contents at the beginning of the book.

Names associated with known apparatus, equations, laws, principles, etc., are not entered here but in the Subject Index.

- Adams, J. A. S., 193, 209, 210  
 Adams, L. H., 191, 209  
 Agricola, G., 1, 5  
 Ahrens, L. H., 189, 190  
 Akamatsu, H., 190  
 Alexander, H. W., 88, 186  
 Alfano, L., 251, 261, 262  
 Allan, D. W., 191, 210  
 Allen, C. R., 265  
 Allen, E. T., 244, 262  
 Allen, W. F., 216, 237  
 Anderson, D. W., 257, 264  
 Anderson, E. M., 107, 109, 111, 159, 186  
 Andrae, C., 11, 21  
 Anglin, F. M., 35, 44, 48  
 Arago, D. F. J., 2, 5  
 Armstead, H. C. H., 241, 260, 262  
 Askelsson, J., 257, 262  
 Averiev, V. V., 255, 259, 262, 263, 265
- Bailey, E. H., 248, 263  
 Baldwin, A. L., 157  
 Banwell, C. J., 214, 215, 217, 220, 222, 223, 227, 237, 239, 243, 252, 253, 255, 256, 262, 263, 266  
 Barth, T. F. W., 257, 263  
 Bartolucci, G., 241, 265  
 Battini, F., 242, 261, 263  
 Beck, A. C., 263  
**Beck, A. E.**, 9, 19, 20, 21, 24-57, 24, 25, 27, 28, 31, 32, 34, 35, 36, 38, 41, 43, 44, 45, 46, 48, 51, 58, 69, 87, 92, 95, 96, 106, 109, 159, 186, 189  
 Beck, J. M., 25, 31, 32, 34, 48  
 Beers, N. R., 21  
 Benard, M., 233, 237  
 Benfield, A. E., 3, 5, 14, 21, 24, 25, 48, 88, 98, 99, 107, 111, 158, 159, 186, 237  
 Benioff, H., 237  
 Benseman, R. F., 215, 217, 237, 255, 263  
 Berry, F. A., 10, 21  
 Birch, F., 5, 10, 12, 14, 15, 21, 24, 30, 32, 35, 45, 48, 95, 96, 97, 98, 99, 100, 156, 158, 159, 186, 195, 198, 209, 237  
 Birch, F. S., 114, 120, 157, 158, 186  
 Blackwell, J. H., 19, 21, 36, 37, 48, 50, 51  
 Boato, G., 263  
 Bodvarsson, G., 112, 159, 186, 187, 220, 237, 252, 256, 257, 262, 263  
 Boldizar, T., 109, 111, 112, 113, 159, 187, 256, 263  
 Bollay, E., 21  
 Bolognini, M., 265  
 Bossolasco, M., 15, 22  
 Boussinesq, J., 225, 233, 237  
 Boyd, F. R., 195, 209  
 Boyle, R., 1, 2, 4, 5
- Bradner, H., 46, 49  
 Brailsford, A. D., 33, 48  
 Breusse, J. J., 251, 261, 263, 265  
 Brewer, M. C., 17, 22, 44, 49  
 Browne, E., 1, 5  
 Browne, T., 1  
 Brune, J., 238  
**Bullard, E. C.**, 1-6, 3, 4, 5, 8, 12, 15, 17, 18, 21, 24, 25, 30, 34, 44, 45, 48, 49, 58, 59, 60, 66, 70, 74, 76, 84, 85, 86, 88, 93, 94, 95, 109, 111, 114, 115, 120, 127, 130, 134, 138, 158, 159, 187, 197, 209, 211, 237, 238  
 Bullen, K. E., 199, 200, 209, 238  
 Burgassi, R., 218, 238, 242, 243, 251, 256, 258, 263  
 Burns, R. E., 121, 123, 158, 187  
 Butler, D. W., 69  
 Butler, R. A., 49
- Calvert, S. C., 186  
 Carslaw, H. S., 7, 8, 11, 12, 13, 14, 15, 16, 17, 18, 19, 20, 21, 59, 61, 75, 76, 83, 86  
 Carte, A. E., 93, 94, 95, 158, 187  
 Cassinis, R., 242, 263  
 Cataldi, R., 247, 248, 251, 263  
 Chadwick, P., 109, 111, 159, 187  
 Chandrasekhar, S., 232, 234, 238  
 Cheremenski, G. A., 17, 21  
 Chierici, A., 238, 252, 263  
 Chilingar, G. V., 263  
 Clark, H., 30, 32, 35, 48, 95, 97, 99, 158, 186, 198, 209  
 Clark, S. P., Jr., 10, 21, 46, 49, 95, 97, 98, 99, 109, 111, 112, 158, 159, 187, 188, 192, 198, 199, 200, 209, 232, 235, 238  
 Clark, T. H., 189  
 Clarke, M. E., 17, 22  
 Cochran, W. G., 89, 187  
 Cochrane, J. D., 74, 76  
 Compston, W., 190  
 Cooper, E. R., 263  
 Cooper, L. R., 18, 21  
 Corbato, C. E., 186  
 Cormack, A. M., 46, 49  
 Coster, H. P., 12, 14, 21, 101, 102, 159, 187  
 Cox, A., 186  
 Cox, C. S., 86, 186  
 Craig, H., 259, 263  
 Creutzburg, H., 113, 187  
 Crow, E. L., 88, 187
- Darcy, H. P. G., 215, 238  
 Davis, F. A., 187  
 Dawson, G. B., 214, 215, 238, 239, 255, 263, 266  
 Day, A. A., 60, 66, 70, 114, 115, 120, 158, 187  
 Day, A. L., 244, 262, 263

- De Anda, L. F., 247, 263  
 De Senarmont, H., 20, 21  
 De Vries, D. A., 19, 21  
 Decius, L. C., 244, 263  
 Decker, E. R., 156  
 Dench, N. D., 252, 263  
 Dibblee, T. W., 249, 263  
 Dickinson, D. J., 239, 266  
 Diment, W. H., 25, 32, 35, 44, 45, 49, 97, 98, 99, 101, 113, 120, 157, 158, 159, 186, 187  
 Dobrin, M. B., 231, 232, 238  
 Dobrovolsky, A. D., 86  
 Doig, R. P., 42, 49, 189  
 Donaldson, I. G., 15, 21, 220, 227, 238  
 Doyle, D., 243, 252, 266  
 Drake, C. L., 188  
 Durr, F., 247, 263
- Eaton, J. P., 231, 238  
 Eiby, G. A., 231, 238, 249, 264  
 Einarsson, S. S., 252, 257, 264  
 Einarsson, T., 220, 238, 262  
**Elder, J. W.**, 15, 78, 86, 87, 148, 186, 211-239, 211, 214, 216, 220, 225, 238, 241  
 Elizondo, J. R., 241, 263, 264  
 Ellis, A. J., 257, 258, 264  
 Elsasser, W. M., 237  
 Emmons, H. W., 10, 21  
 Engel, A. E., 156, 187, 188  
 England, J. L., 195, 209  
 Evans, R. D., 193, 194, 210  
 Everett, J. D., 3, 5, 25, 49  
 Ewing, J. I., 75, 76  
 Ewing, M., 5, 76, 115, 121, 143, 146, 187, 188, 190, 238
- Facca, G., 240, 254, 259, 262, 264  
 Fatt, I. S., 20  
 Faxen, O. H., 214, 215, 216, 220, 238  
 Fenner, C. N., 243, 264  
 Finsov, F. W., 22, 49, 189  
 Fisher, O., 3, 5  
 Fisher, R. G., 255, 263, 264  
 Fisher, R. L., 146, 187  
 Fleming, R. H., 86  
 Flugge-de Smidt, R. A. H., 46, 49  
 Fooks, A. C. L., 247, 264  
 Forbes, J. D., 25, 49  
 Foster, T. D., 127, 134, 158, 187  
 Fowler, W. A., 190, 193, 209, 210  
 Frank, F. C., 237  
 Fuglister, F. S., 80, 86  
 Fultz, D., 232, 238  
 Futt, H., 76
- Gafner, G., 46, 49  
 Gamutilov, A. E., 79, 82, 86  
 Garland, G. D., 46, 49, 95, 96, 98, 100, 159, 187  
 Gast, P. W., 193, 210  
 Gennai, N., 258, 264  
 Gerard, R., 4, 5, 76, 114, 120, 158, 187  
 Gilbert, M. C., 186  
 Goguel, J., 217, 238, 252, 264  
 Golding, R. M., 257, 264  
 Goldstein, R. J., 239  
 Goode, H. D., 8, 22  
 Goodman, C., 193, 194, 210  
 Gough, D. I., 9, 13, 21, 93, 94, 95, 158, 186, 187  
 Gozon, J., 109, 159, 187  
 Grange, L. I., 221, 238, 249, 252, 263, 264  
 Greene, G. W., 188  
 Griffiths, E., 3
- Griggs, D., 238  
 Grim, P. J., 76, 114, 120, 127, 158, 159, 186, 187, 188  
 Grindley, G. W., 221, 238, 243, 249, 250, 251, 259, 264  
 Guier, W. H., 153, 187  
 Gutenberg, B., 138, 188, 232, 234, 238
- Hall, A. R., 6  
 Hamaguchi, H., 194, 210  
 Hamilton, W., 186  
 Harada, H., 246, 252, 264  
 Harris, D. L., 239  
 Hart, S. R., 157  
 Hayakawa, M., 237, 246, 264  
 Healy, J., 221, 223, 231, 233, 243, 244, 246, 249, 250, 252, 255, 262, 264  
 Heezen, B. C., 115, 121, 143, 146, 188  
 Heier, K. S., 193, 194, 210  
 Heiskanen, W. A., 113, 188, 238  
 Hele-Shaw, H. S. J., 226, 238  
 Henderson, J. R., 250, 260, 264  
 Herrin, E., 95, 97, 99, 158, 188  
 Herschel, A. S., 25, 49  
 Hess, H. H., 146, 156, 187, 188  
 Hill, M. N., 187, 188  
 Hilpert, L. S., 248, 266  
 Hinsley, F. B., 109, 111, 159, 189  
 Holmes, A., 191, 210  
 Holmyard, E. J., 6  
 Hoover, H. C., 1, 5  
 Hoover, L. H., 1, 5  
 Horai, K., 76, 101, 102, 103, 104, 127, 134, 158, 188, 190
- Horton, C. W., 238  
 Hotchkiss, W. O., 12, 21  
 Houtz, R. E., 188  
 Howard, L. E., 10, 21, 24, 46, 49, 104, 105, 106, 108, 109, 159, 188  
 Hoyle, F., 190, 193, 209, 210  
 Hulston, J. R., 259, 264  
 Humboldt, A. von, 2, 5  
 Hunt, A. M., 255, 264
- Ingersoll, A. C., 21  
 Ingersoll, L. R., 7, 12, 15, 20, 21  
 Isaacs, J. D., 46, 49  
 Ishikawa, T., 238  
 Ivanov, V. V., 263, 265  
 Izsak, I. G., 151, 188
- Jacobs, J. A., 191, 210  
**Jaeger, J. C.**, 7-23, 8, 10, 11, 12, 13, 14, 15, 16, 17, 18, 19, 20, 21, 22, 24, 25, 26, 36, 44, 45, 48, 49, 50, 51, 58, 59, 61, 70, 75, 76, 83, 86, 92, 104, 106, 109, 159, 188  
 Jakob, M., 82, 86, 234, 238  
 James, H., 188  
 James, R., 255, 264  
 Jeffery, P. M., 190  
 Jeffreys, H., 3, 11, 14, 22, 81, 86, 231, 238  
 Jennings, C. W., 248, 264  
 Jessop, A. M., 42, 43, 49  
 Johnson, M. W., 86  
 Jones, C., 18, 21  
 Jonsson, V. K., 239  
 Joyner, W. B., 97, 98, 99, 158, 188
- Kanamori, H., 76  
 Kappelmeyer, O., 15, 22  
 Kaufman, A., 240, 241, 264  
 Kaula, W. M., 151, 154, 186, 188  
 Keevil, N. B., 193, 194, 210

- Kelley, V. C., 249, 260, 264  
 Kelvin, W. T., 3, 8, 22, 191  
 Kennedy, G. C., 156, 188  
 Kjartansson, G., 262  
 Knauss, J., 80, 84, 86  
 Knopoff, L., 199, 210, 231, 234, 238  
 Koening, J. B., 248, 265  
 Kovach, L., 249, 265  
 Kraskovski, S. A., 113, 159, 188  
 Krige, L. J., 44, 49  
 Kuenen, P. H., 198, 210  
 Kuno, H., 238  
 Kuo, J., 238  
  
 Lachenbruch, A. H., 12, 17, 22, 44, 45, 49, 99, 101, 133, 158, 159, 186, 188  
 Laizure, C., 243, 265  
 Lamb, H., 226, 238  
**Langseth, M. G.**, 4, 5, 19, 26, 58-77, 58, 69, 76, 78, 79, 80, 83, 86, 87, 88, 89, 94, 95, 104, 113, 114, 120, 121, 123, 127, 130, 132, 134, 158, 159, 186, 187, 188, 190  
 Lapwood, F. R., 15, 22, 220, 226, 227, 238  
 Law, L. K., 156, 188  
 Lebour, G. A., 25, 49  
 Le Marne, A. E., 16, 17, 22, 45, 50, 105, 108, 159, 188, 189  
**Lee, W. H. K.**, 3, 46, 49, 76, 78, 86, 87-190, 87, 88, 114, 115, 120, 121, 136, 138, 150, 151, 154, 158, 189, 192, 195, 210, 211, 230, 235, 238  
 Lees, C. H., 10, 11, 22, 26, 49, 188  
 Leith, T. H., 95, 159, 188  
 Lennox, D. H., 46, 49, 95, 96, 98, 100, 159, 187  
 Lenzi, D., 237  
 Leonard, B., 188  
 Le Pichon, X., 115, 188, 190  
 Lister, C. R. B., 61, 63, 67, 76, 79, 86, 114, 115, 120, 158, 188  
 Lloyd, E. F., 238, 257, 265  
 Logis, Z., 38, 46, 48, 95, 96, 159, 186  
 Lotze, F., 138, 188  
 Lovering, J. F., 194, 210  
 Lovring, T. S., 8, 9, 13, 18, 21, 22, 98, 100, 158, 186, 189  
**Lubimova, E. A.**, 4, 20, 22, 26, 46, 49, 76, 78-86, 78, 86, 112, 113, 114, 159, 187, 189, 200, 210, 212  
 Lusova, L. M., 22, 49, 189  
  
**MacDonald, G. J. F.**, 10, 46, 49, 78, 86, 88, 138, 141, 150, 151, 154, 188, 189, 190, 191-210, 191, 192, 195, 197, 198, 199, 200, 201, 202, 210, 230, 235, 238  
 MacDonald, W. J. P., 237  
 Macelwane, J. B., 238  
 Magnitsky, V. A., 78, 86  
 Mahon, W. A. J., 257, 265  
 Mairan, J. J. D., 25, 49  
 Major, K. G., 33, 48  
 Mak, S., 186  
 Malkus, W. V. R., 231, 234, 238  
 Malurkar, S. L., 239  
 Marchesini, E., 242, 247, 251, 260, 265  
 Marine, I. W., 187  
 Marinelli, G., 248, 265  
 Mario, P., 238  
 Marshall, B. V., 133, 158, 186, 188  
 Maxwell, A. E., 4, 6, 19, 22, 50, 51, 58, 68, 70, 77, 85, 86, 88, 127, 131, 134, 158, 187, 189, 190, 238  
 Mayhew, M. A., 187  
 Mazor, F., 210  
 Mazzoni, A., 251, 258, 261, 265  
  
 McBirney, A. R., 15, 22, 104, 189  
 McCall, G. J. H., 247, 265  
 McCree, K. J., 263  
 McDowell, A. N., 239  
**McNitt, J. R.**, 24, 113, 218, 221, 238, 240-262, 240, 244, 246, 252, 254, 258, 265  
 Menard, H. W., 100, 123, 127, 143, 146, 156, 186, 188, 189  
 Menut, P., 242, 261, 263  
 Merla, G., 247, 265  
 Messmer, J. H., 20, 23, 33, 50  
 Migliorini, C. I., 248, 265  
 Minakami, T., 217, 238  
 Minucci, G., 242, 265  
 Miscner, A. D., 25, 44, 45, 46, 49, 95, 96, 97, 99, 101, 158, 159, 189  
 Modriniak, N., 221, 238, 249, 260, 265  
 Monro, J. N., 247, 265  
 Morgan, J. W., 194, 210  
 Mori, T., 246, 252, 264  
 Morin, J. B., 1, 6  
 Morinus, see Morin, J. B., 1, 2  
 Mossop, S. C., 43, 46, 49  
 Moye, 10  
 Mullins, R., 109, 111, 159, 189  
  
 Nafe, J. E., 76, 188  
 Nagata, T., 231, 232, 239  
 Nasini, R., 258, 265  
 Nason, R. D., 78, 86, 114, 115, 120, 121, 158, 189  
 Neihsel, J., 187  
 Nekhoroshev, A. S., 255, 265  
 Nelson, C. A., 186  
 Nencetti, R., 218, 219, 239, 255, 258, 259, 265  
 Newstead, G. N., 21, 45, 48, 49, 106, 109, 159, 189  
 Niblett, E. R., 15, 21, 45, 46, 49, 109, 111, 112, 159, 187, 198, 209  
 Nockolds, S. R., 193, 210  
 Northrop, J., 189  
 Novichenok, L. N., 19, 20, 22  
  
 Oertel, G., 186  
 Ortiz, O. F., 157  
  
 Pakiser, L. C., 249, 265  
 Palmason, G., 252, 256, 257, 263  
 Parker, T. J., 239  
 Patterson, W. S. B., 188  
 Peck, A. J., 19, 21  
 Pekeris, C. L., 13, 22, 239  
 Penta, F., 218, 239, 241, 242, 258, 262, 265  
 Pettersson, H., 3, 6  
 Phillips, D. W., 3  
 Piip, B. I., 247, 252, 263, 265  
 Pistolesi, E., 265  
 Powell, R. W., 19, 22, 26, 49  
 Press, F., 265  
 Prestwich, J., 2, 3, 6  
 Priestley, C. H. B., 239  
  
 Ragland, P. C., 193, 210  
 Ramadas, L. A., 239  
 Ramberg, H. A., 156, 189  
 Rao, R. U. M., 101, 102, 159, 190  
 Raspet, R., 187  
 Ratcliffe, E. H., 26, 49, 69, 70, 72, 76  
 Rayleigh, Lord, 231, 232, 233, 239  
 Reed, G. W., 193, 194, 210  
 Reid, W. H., 239  
 Reitzel, J. S., 67, 73, 75, 76, 86, 114, 115, 120, 158, 188, 189

- Revelle, R., 4, 6, 58, 86, 88, 127, 134, 158, 187, 189, 238  
 Reynolds, J. H., 210  
 Rhea, K., 127, 131, 134, 158, 189  
 Richardson, J. G., 239  
 Rikitake, T., 13, 22, 229, 239  
 Riley, G. H., 190  
 Rinchart, C. D., 249, 266  
 Ringwood, A. E., 10, 21, 232, 235, 238  
 Ritchie, J. A., 257, 266  
 Robertson, E. C., 25, 35, 44, 45, 49, 97, 98, 99, 158, 187  
 Robertson, E. I., 214, 237, 239, 255, 260, 263, 266  
 Rogers, F. T., 238  
 Rogers, J. J., 193, 194, 210  
 Rook, S. H., 243, 246, 266  
 Ross, D. C., 249, 266  
 Roy, R. F., 16, 22, 46, 49, 95, 96, 98, 99, 100, 156, 158, 189  
 Ruiz, 157  
 Runcorn, S. K., 188, 189, 200, 210, 231, 236, 239  
  
 Sabinin, D. D., 86  
 Saito, M., 246, 252, 266  
 Sakuma, S., 231, 232, 239  
 Sass, J. H., 11, 14, 20, 22, 24, 26, 32, 36, 45, 46, 49, 50, 104, 105, 106, 108, 109, 159, 188, 189  
 Saull, V. A., 49, 97, 99, 159, 189  
 Saunders, E. D., 157  
 Saxon, D., 46, 50  
 Sbrana, F., 15, 22  
 Scheffer, V., 109, 113, 189  
 Schlichting, H., 217, 239  
 Schmucker, U., 100, 189  
 Schneider, K. J., 226, 239  
 Schossler, K., 10, 22, 111, 112, 113, 159, 189  
 Schroder, J., 28, 50  
 Schwarzlose, J., 10, 22, 111, 112, 113, 159, 189  
 Selater, J., 121, 123, 159, 186, 189  
 Senftle, F. E., 193, 194, 210  
 Septien, J. L., 263  
 Sewell, J. R., 257, 264  
 Shushpanov, A. P., 20, 22, 49, 189  
 Shushpanov, P. I., 20, 22  
 Silva, R., 157  
 Silveston, P. L., 234, 239  
 Simmons, G., 20, 22  
 Singer, C., 1, 6  
 Siple, G. E., 187  
 Sisoiev, N. N., 61, 76, 113, 159, 189  
 Slichter, L. B., 13, 15, 21, 22, 138, 189, 191, 209, 210  
 Smith, J. H., 217, 239  
 Snodgrass, J. M., 77  
 Somerton, W. H., 35, 50  
 Soske, J. L., 249, 260, 264  
 Southwell, R. V., 10, 22  
 Sparrow, E. M., 239  
 Speer, M. G., 257, 264  
 Spicer, H. C., 97, 98, 99, 100, 158, 159, 189  
 Starikova, G. N., 22, 49, 189  
 Stearns, H. G., 266  
 Stearns, N. D., 243, 266  
 Stefani, G., 263  
 Steiner, A., 253, 266  
 Steinhart, J. S., 157  
 Stenz, E., 112, 113, 159, 189  
 Stocks, T., 121, 189  
 Strand, R. G., 248, 264  
 Streeter, V. L., 239  
 Studt, F. E., 217, 221, 237, 238, 239, 243, 247, 251, 252, 254, 260, 261, 265, 266  
 Sverdrup, H. U., 79, 86  
 Sviatlovsky, A. E., 250, 266  
 Swartz, J. H., 50, 189  
  
 Talwani, M., 115, 190  
 Tanaoka, I., 190  
 Tareev, B. A., 81, 86  
 Taylor, G. I., 232, 239  
 Taylor, P. T., 123, 186, 190  
 Tek, M. R., 216, 239  
 Ten Dam, A., 240, 264  
 Thompson, B. N., 249, 266  
 Thompson, G. A., 186  
 Thompson, G. E. K., 211, 215, 222, 223, 227, 239, 255, 261, 263, 266  
 Thompson, L. G. D., 189  
 Thompson, W., 25, 50  
 Thorarinsson, S., 262  
 Tilley, C., 195, 209, 210  
 Tilton, G. R., 193, 194, 210  
 Tiry, G. B., 75, 76  
 Tomoda, Y., 76  
 Tonani, F., 248, 254, 259, 262, 264  
 Tongiorgi, M., 263  
 Townsend, A. A., 233, 239  
 Turkevich, A., 210  
 Tye, R. P., 19, 22  
  
**Udintsev, G. B., 78-86, 78, 86**  
 Uffen, R. J., 189  
 Urey, H. C., 193, 210, 236, 239  
**Uyeda, S., 3, 13, 16, 23, 46, 59, 60, 65, 66, 73, 74, 75, 76, 77, 78, 84, 85, 86, 87-190, 87, 101, 102, 103, 104, 127, 130, 134, 148, 158, 186, 188, 190, 192, 210, 211, 239**  
  
 Vacquier, V., 94, 95, 114, 115, 120, 121, 123, 156, 158, 186, 190  
 Van Orstrand, C. E., 8, 11, 22, 46, 50  
 Van Padang, N. M., 247, 266  
 Vecchia, O., 251, 266  
 Vening-Meinesz, F. A., 113, 188, 231, 238, 239  
 Verhoogen, J., 138, 186, 190, 239  
 Verma, R. K., 46, 50, 101, 102, 159, 186, 190  
 Verzhinskaya, A. B., 19, 20, 22  
 Volkmann, G. H., 79, 86  
**Von Herzen, R. P., 13, 16, 19, 22, 23, 50, 51, 59, 63, 65, 68, 70, 71, 73, 74, 75, 76, 77, 78-86, 78, 80, 83, 84, 85, 86, 88, 89, 93, 94, 95, 104, 114, 115, 120, 121, 123, 127, 130, 131, 134, 148, 156, 158, 186, 189, 190, 211, 239**  
 Vos, B. H., 50, 51  
  
 Walker, D., 237  
 Walker, G. P. L., 187  
 Wang, C., 151, 190  
 Ward, S. H., 261, 266  
 Waring, G. A., 266  
 Wasserburg, G. J., 138, 190, 193, 194, 195, 205, 210  
 Watanabe, T., 101, 127, 134, 159, 186, 190  
 Weaver, J. D., 25, 49, 99, 101, 120, 158, 187  
 Weiss, O., 40, 50  
 Werre, R. W., 32, 49, 97, 99, 157, 158, 187  
 White, B. L., 260, 264  
 White, D. E., 223, 239, 248, 258, 262, 263, 266  
 White, J. F., 188  
 Whitfield, J. M., 193, 210  
 Whitham, K., 188  
 Williams, G. C., 243, 246, 266  
 Williams, T. I., 6

- Wilson, A. F., 107, 190  
Wilson, S. H., 257, 258, 264, 266  
Wooding, R. A., 15, 23, 215, 220, 228, 229, 237, 239  
Woodside, W., 20, 23, 33, 50  
Wooster, W. S., 79, 86  
Worzel, J. L., 76  
Yagi, K., 238  
Yasui, M., 101, 127, 134, 158, 159, 186, 190  
Yates, R. G., 248, 266  
Yoder, H. S., 195, 209, 210  
Yokoyama, I., 229, 239  
Yukutake, T., 190  
Zartman, R. E., 195, 210  
Zierp, J., 239  
Zierfuss, H., 19, 20, 23, 26, 50  
Zobel, O. J., 21

## Subject Index

The letters ff after a page number denote that the subject is mentioned again on one or more of the following pages.

- Aden, Gulf of (see Gulf of Aden)
- Adiabatic temperature gradient of deep ocean water, 79ff
- Africa (see also South Africa), 88, 115, 121, 141, 150, 151, 157, 160
  - heat flow, 93ff, 160
- Albatross expedition, 3
- Aleutian, Trench, 131
- Alps, Europe, 107
- Americas (see also North America)
  - heat flow, 95ff, 160ff
- Amphitrite expedition, 80
- Andaman Sea, 123, 187
- Anisotropic thermal conductivity, 20
- Annual temperature variation, 8
- Appalachian system, 98ff, 147
  - heat flow, 99
- Arctic Archipelago, Canada, 156
- Arctic Ocean, 114, 133, 134, 186
  - heat flow, 133ff, 186
- Argon in the atmosphere, 194ff
- Asia, 4, 88, 101, 102, 141, 163, 164
  - heat flow, 101ff, 163ff
- Atlantic Ocean, 4ff, 21, 74ff, 79, 114ff, 121ff, 132ff, 141ff, 150ff, 156ff, 167ff, 186ff, 190, 209
  - basins, heat flow, 115
  - first heat flow measurements, 4
  - heat flow, 114ff, 167ff
  - North American Basin, 120
- Australia, 49, 50, 104, 105, 107, 141, 143, 157, 162, 163, 188, 189
  - general geology, 104-105
  - heat flow, 104ff, 162ff
- Australian shield, 104ff, 147
  - heat flow, 105
  - Snowy Mountains, 10, 106, 109
- Austria, 109, 111, 165
  - heat flow, 109, 165
- Austrian Alps, 49, 109, 187
- Baja California, Mexico, 69, 131, 134, 190
- Baltic Sea, 107
- Baltic Shield, 166
- Beer, freezing of in Moscow, 1
- Bering Sea, 134, 187
- Bikini Atolls, 50
- Birch's treatment of topography combined with uplift or erosion, 14
- Black Sea, 113, 167
  - heat flow, 113, 167
- British Association for the Advancement of Science, 3
- British Coal Commission, 3
- Bullard's method for calculation of heat flow, 7, 9, 45
- Bullard technique (see Bullard temperature gradient probe)
- Bullard temperature gradient probe, 59, 114, 123, 132, 157
- Bullard thermal gradient probe (see Bullard temperature gradient probe)
- California, 98, 99, 131, 186, 193, 241ff
  - Casa Diablo, 243ff
  - heat flow, 95ff, 160ff
  - Imperial Valley, 249, 263
  - Long Valley, 249ff
  - Niland, 243ff
  - Salton Sea, 249, 265
  - San Andreas Fault, 98
  - The Geysers, 243ff
- Cambridge University, 3, 58
  - gradient recorder, 67
- Canada, 44, 95ff, 134, 162, 187
  - Arctic Archipelago, 156, 188
  - heat flow, 95ff, 162
- Canadian Shield, 49, 95ff, 147
  - heat flow, 95
- Capricorn expedition, 4
- Caribbean Sea, 86, 120, 188ff
- Casa Diablo, California, 243ff
- Central Pacific (see also Pacific Ocean), 79, 80, 151, 156
- Chemical investigation, geothermal areas, 257ff
- Climate, effect of past changes on heat flow, 12
- Continents, heat flow, 138ff, 160ff
- Convection, 81ff, 154, 199ff, 211ff
  - penetrative, 231ff
- Convection currents (see Convection)
- Convection in the mantle, inferences about, 230ff
- Colorado, front range, 21, 48, 98, 100, 186, 209
- Cooling of the Earth (see Thermal history of the Earth)
- Cordillera system, 98ff
  - heat flow, 99-101
- Crust, convection of water in, 220ff
- Cylindrical temperature gradient probe (see Bullard temperature gradient probe), 59
- Czechoslovakia, 109ff, 166
  - heat flow, 109ff, 166
- Damped wave equation, 8
- Darcy's law, 262, 225, 236
- Deep ocean water (see also Ocean bottom water)
  - adiabatic temperature gradient, 79ff
  - temperature profile, 80ff
  - thermal stability of, 79ff
- Deposition of sediments (see Sedimentation)
- Diurnal temperature variation, 8
- Drill holes, temperatures, 16, 40ff
- Drilling disturbance on temperature, 17, 44
- Earth, internal temperature distribution, 203ff
  - major geological features, 142ff
  - radioactivity, 192ff
  - thermal history of, 5, 197ff, 236ff
- Earth currents, 5
- Earth's interior, heat loss from, 138
  - heat sources, 138, 192ff
  - thermal conditions of, 5, 197ff, 236ff
- Earthquake Research Institute, gradient recorder, 65
- Earthquake Research Institute of Tokyo University, 58, 101

- East Germany (see also Germany), 111, 166  
 East Pacific Ocean (see Pacific Ocean)  
 East Pacific Rise, 4, 69, 80, 88, 100, 189  
   heat flow, 130  
 Electrical conductivity, 5, 199  
 Energy, geothermal, 240ff  
   supply for volcanism, 235ff  
 Eniwetok Atoll, 50, 186  
 Equation of heat conduction, 13  
   for moving material, 13  
 Equation of steady heat flow, 8  
   for variable conductivity, 9  
 Erosion, effect on heat flow, 13, 75  
 Eruptive discharges, 217ff  
 Europe, 107, 110, 115, 141, 147, 165, 166  
   Alps, 107  
   general geology, 107  
   heat flow, 107ff, 165ff  
   Swiss Alps, 49, 109, 187, 209  
 Ewing technique of temperature gradient measurement, 4, 60ff, 63, 74, 114, 123, 133, 157  
 Ewing thermograd, 63  
 Finland, 107  
 Flashing discharges, 215ff  
 Fourier series, 8  
 Frank's model, 232  
 Fredholm, integral equation of, 10  
 Free convection, in porous medium, 224ff  
 Free thermal convection (see also Convection), 81ff  
 Frictional heat, 59  
 Front range, Colorado, 21, 48, 98, 100, 186, 209  
 Gauss, method of, 150  
 Geographical distribution of heat flow observations, 88  
 Geoid, 151ff  
 Geophysical deductions, from heat flow observations, 191-210  
 Geothermal areas, chemical investigation, 257ff  
   geologic environment, 247ff  
   heat flow, 211, 255ff  
   physical processes, 211-239  
   pressure, 254ff  
   regions of subsidence, 248ff  
   regions of uplift, 247ff  
   temperature, 252ff  
 Geothermal energy, 240ff  
 Geothermal flux (see Heat flow)  
 Geothermal gradient (see Temperature gradient)  
 Geothermal resources, development, 259ff  
   exploration, 259ff  
   management, 259ff  
   review of, 240-266  
 Germany, 5, 113  
   heat flow, 113, 166  
 Geysers, California, 243ff, 246ff, 251ff, 258ff, 265  
 Gravity, comparison with heat flow, 151ff  
 Great Britain, 5, 48, 93, 107, 109, 111, 147, 165, 186, 237  
   heat flow, 107ff, 165  
 Gulf of Aden, 121, 123, 190  
 Gulf of California, 100, 127, 134, 190, 249  
 Gulf of Mexico, 95, 120ff  
 Gulf of Panama, 130, 134  
 Hawaiian Islands, 131, 134, 189, 238, 243  
 Heat, frictional, 59  
   mass transport of (see also Convection), 76  
 Heat conduction, 7ff  
   differential equation of, 7  
   equation for moving material, 13  
 Heat exchange, between ocean floor and near bottom water, 81ff  
 Heat flow  
   Africa, 93ff, 160  
   Americas, 95ff, 160ff  
   Appalachian system, 99  
   Arctic Ocean, 133ff, 186  
   Asia, 101ff, 163ff  
   Atlantic basins, 115  
   Atlantic Ocean, 114ff, 167ff  
   Australia, 104ff, 162ff  
   Australian interior lowlands, 105ff  
   Australian Shield, 105  
   Austria, 109, 165  
   Black Sea, 113, 167  
   Calculation by Bullard's method, 7ff, 45  
   Canada, 95ff, 162  
   Canadian Shield, 95  
   comparison with gravity, 151ff  
   continents, 138ff, 160ff  
   Cordilleran system, 99-101  
   Czechoslovakia, 109ff, 166  
   dependence on radioactivity, 201ff  
   East Australian Highlands, 106  
   East Pacific Rise, 130  
   effect of changes in surface conditions, 12  
   effect of deposition (see Effect of sedimentation)  
   effect of erosion, 13, 75  
   effect of intrusions, 13  
   effect of past climatic changes, 12  
   effect of sediment distribution, 75  
   effect of sedimentation, 13, 75  
   effect of topography, 75  
   effect of uplift, 13  
   effect of variations in thermal conductivity, 12  
   effect of water flow above bottom sediment, 82ff  
   equality of continental and oceanic averages, 4, 139ff, 197  
   equation of steady flow, 8, 24, 87  
   equation of steady flow for variable conductivity, 9  
   Europe, 107ff, 165ff  
   first measurement in Atlantic, 4, 114  
   first measurement in Pacific, 4, 127  
   geographical distribution of observations, 88  
   geophysical deduction from observations, 191-210  
   geothermal areas, 211, 255ff  
   Germany, 113, 166  
   global analysis of data, 148ff  
   global representation, 148ff  
   global review of data, 134ff  
   Great Britain, 107ff, 165  
   Hungary, 109, 165  
   Iceland, 112, 166, 256ff  
   India, 101, 163  
   Indian Ocean, 121ff, 171ff  
   interior lowlands of North America, 95, 99  
   interpretation of continent-ocean averages, 139ff, 197  
   Iran, 101, 163ff  
   Italy, 109, 166, 255ff  
   Japan, 101ff, 164  
   Japan Sea (see Heat flow, Japan)  
   listing of data, 157-186  
   mean value, 45, 138  
   measurement (see Heat flow measurement)  
   measurements in ocean floor, 58  
   measurements in shallow holes, 8  
   mid-Atlantic ridge, 115  
   Mohole project, 58

- Heat flow (*continued*)  
 non-orogenic areas, 143  
 non-shields, 142ff  
 normal areas, 211  
 North America, 95ff, 160ff  
 Nyasaland, 93ff  
 ocean basins, 148  
 ocean ridges, 148  
 oceans, 138ff  
 orogenic areas, 143  
 Pacific Ocean, 123ff, 176ff  
 Poland, 113, 166  
 Puerto Rico, 95, 99, 101, 120  
 refraction at interface, 16  
 relation to topography, 154  
 reliability of data, 89ff  
 review of data, 87-190  
 review of data at sea, 114-134  
 review of data on land, 92-114  
 shields, 142ff  
 South Africa, 93ff, 160  
 South America, 157  
 surface mechanisms, 212ff  
 Switzerland, 109, 165  
 techniques of measuring through ocean floor, 58  
 topographic correction, 10, 24  
 trench, 120, 123, 131, 143, 148  
 United States, 95ff, 160ff  
 USSR, 113, 166  
 variation of adjacent stations, 69, 89ff  
 variation over short distance, 78  
 volcanic areas, 4, 147, 255ff  
 world, 136ff
- Heat flow measurement, preliminary Mohole site, 68  
 shipboard operation, 73  
 station site selection, 71
- Heat flow probe (see also Bullard temperature gradient probe and Ewing technique), 3, 4
- Heat flux (see Heat flow)
- Heat loss, from Earth's interior, 138
- Heat production, 9  
 in ocean sediments, 76
- Heat sources, 2, 5, 138
- Heat transfer, influence by interstitial water in sediments, 84ff  
 measurements, 225ff  
 through ocean floor, 78-86
- Hele-Shaw cell, measurement in, 226ff
- High pressures, melting relations at, 195
- Horizontal layering, reduction of observations, 8
- Hungary, 1, 5, 109, 112, 165, 187  
 heat flow, 109, 165
- Hydrothermal system, elements of, 223ff  
 Taupo, 221ff
- Iceland, 112, 166, 186, 187, 237, 240, 241, 246, 252, 257, 262, 263  
 heat flow, 112, 166, 256ff
- Imperial Valley, California, 249, 263
- In situ measurement of thermal conductivity, 19
- India, 101, 102, 163, 190  
 heat flow, 101, 163
- Indian Ocean, 3, 114, 121, 123ff, 132ff, 141ff, 147ff, 157, 171ff  
 general geology, 121  
 heat flow, 121ff, 171ff
- Indian shield, 147
- Initial temperature distribution, 201
- Interstitial water in sediments, influence on heat transfer, 84ff
- Intrusion of dykes, 4
- Intrusions, effect on heat flow, 13
- Iran, 101ff, 163ff  
 heat flow, 101, 163ff
- Italy, 109, 112ff, 166, 211, 240, 242, 252, 260, 263  
 heat flow, 109ff, 166, 255ff  
 Larderello, 112, 186, 214, 218ff, 238, 242, 247ff, 251ff  
 Mt. Amiata, 242, 247ff, 251, 258, 260  
 Tuscany, 211, 218ff, 242ff, 266
- Japan, 60, 101ff, 131ff, 164, 188, 240ff, 252, 264  
 heat flow, 101ff, 164
- Japan Sea, 101, 104, 134, 148  
 heat flow (see Japan, heat flow)
- Japan Trench, 101
- Java Trench, 123
- Jeffreys-Bullard reduction, for topographic corrections, 11
- Kawerau, New Zealand, 239, 242, 251, 255ff
- Kurile Trench, 101
- Lake Nyasa, 93, 95, 160
- Lake Taupo, 242
- Larderello, Italy, 112, 186, 214, 218ff, 238, 242, 247ff, 251ff
- Listing of heat flow data, 157-186
- Long Valley, California, 249, 264ff
- Magnetic variations, 5
- Mantle convection, 5, 199ff, 233ff
- Marine sediment (see Sediment)
- Mass transport of heat (see also Convection), 76
- Mayaguez, Puerto Rico, 49, 99, 101, 120, 187
- Mediterranean Sea, 86, 120ff, 147, 189
- Melting relations, at high pressures, 195
- Mexico, 77, 86, 190, 240, 247, 263  
 Baja California, 131, 134, 190
- Mid-Atlantic Ridge, 4, 69, 78, 115, 117, 120ff, 156  
 heat flow, 4, 78, 115ff
- Mines, temperature measurements, 17
- Mohole, samples from, 5
- Mohole project, heat flow measurement, 58, 68
- Mohorovicic discontinuity, 104, 107, 141
- Mt. Amiata, Italy, 242, 247ff, 258ff
- Needle probe, for thermal conductivity measurement, 70
- New Zealand, 211, 213ff, 218, 221, 231, 237ff, 249ff, 260ff, 266  
 Kawerau, 239, 242, 251, 255, 257, 260ff, 265ff  
 Taupo, 211, 213, 221, 223, 227ff, 236, 238, 244, 249, 256, 264ff  
 Waiotapu, 222, 242, 251ff, 257ff, 260, 264ff  
 Wairakei, 15, 215ff, 222ff, 228ff, 239, 242ff, 248ff, 252ff, 255ff
- Niland, California, 243ff, 246ff, 252ff, 258ff
- Nomogram relating thermal conductivity to water content, 72
- Non-orogenic areas, heat flow, 143
- Non-shields, heat flow, 142ff
- Normal areas, heat flow, 211
- North America, 95ff, 131, 137, 141  
 general geology, 95ff  
 heat flow, 95ff, 160ff
- North American Basin, Atlantic Ocean, 120
- North Atlantic Ocean (see also Atlantic Ocean), 76, 86, 116ff, 189
- Nyasaland, heat flow, 93ff

- Ocean, heat flow, 114ff, 138ff  
 major geological features, 143ff
- Ocean basins, heat flow, 115ff, 123, 132, 148
- Ocean bottom, temperature gradient measurement, 58  
 thermal conditions of, 74  
 water temperature, 74
- Ocean bottom water (see also Deep ocean water)  
 heat exchange, 81ff  
 temperature, 79ff
- Ocean floor, heat transfer, 78-86  
 techniques of measuring heat flow, 58
- Ocean ridges, heat flow, 115, 123, 130, 148
- Ocean sediment (see Sediment)
- Ocean thermal areas, 229ff
- Ocean trench (see Trench)
- Ocean water (see Deep ocean water, ocean bottom water)
- Oceanic heat flow (see Ocean, heat flow)
- Orogenic areas, heat flow, 143
- Pacific Ocean, 4, 23, 76, 79ff, 82, 85ff, 95, 104, 114ff, 121, 123, 127ff, 132ff, 135ff, 141ff, 145, 147ff, 150ff, 156ff, 176ff, 187, 189, 211, 238ff  
 first heat flow measurements, 4, 127  
 general geology, 127  
 heat flow, 123ff, 176ff
- Penetrative convection, in the upper mantle, 231ff
- Permafrost, temperature gradients, 2
- Persia (see Iran)
- Physical processes, in geothermal areas, 211-239
- Poland, 112ff, 166  
 heat flow, 113, 166
- Porous medium, free convection in, 224ff
- Preliminary Mohole site, heat flow measurement, 68
- Pressure, geothermal areas, 254ff
- Puerto Rico, 95, 99, 115, 161  
 Mayaguez, 49, 99, 101, 120, 187
- Puerto Rico Trench, 120
- Radial distribution of temperature, 5
- Radiation (see Thermal radiation)
- Radioactivity, calculation of heat flow as a function of, 200ff  
 heat flow dependence on, 201ff  
 observational evidence, 192ff  
 of the Earth, 192ff
- Rayleigh number, 81ff, 225ff
- Red Sea, 123
- Refraction, of heat flow at interface, 16
- Regions of subsidence, of geothermal areas, 248ff
- Regions of uplift, of geothermal areas, 247ff
- Reliability of heat flow data, 89ff
- Resources, geothermal, 240-266
- Reversing thermometers, 61
- Rocky Mountains, 98
- Russia (see USSR)
- Salinity convection, 82
- Salinity gradient, 82
- Salton Sea, California, 249, 265
- San Andreas Fault, California, 98
- Scripps Institution of Oceanography, 4, 58  
 gradient recorder, 63
- Sediment (see also Ocean sediment)  
 effect of distribution on oceanic heat flow, 75  
 heat production, 76  
 interstitial water, 76, 84ff  
 thermal conductivity measurement, 68, 79
- Sedimentation, effect on heat flow, 13, 75ff
- Shallow holes, use for heat flow measurements, 8
- Shields, heat flow, 142ff
- Shipboard operation, for heat flow measurement, 73
- Siberia, 2
- Sierra Nevada, 249
- Silicates, thermal conductivity of, 198ff
- Snowy Mountains, Australia, 10, 106, 109
- South Africa, 5, 21, 40, 48, 93ff, 147, 160, 187  
 general geology, 93  
 heat flow, 93ff, 160
- South African Plateau, 93
- South African Shield, 93ff, 147
- South America, 4, 88, 95, 157  
 heat flow, 157
- South Atlantic Ocean (see also Atlantic Ocean), 118ff
- Soviet Union (see USSR)
- Statistics, application in summarizing data, 88ff
- Steady-state thermal conductivity measurement, 69
- Steaming ground, 214
- Surface condition, effect of changes on heat flow, 12
- Surface discharges, classification, 212ff
- Surface heat flow (see also Heat flow), 195ff
- Surface heat flow mechanisms, 212ff
- Sweden, 107, 113
- Swiss Alps, Europe, 49, 109, 187, 209
- Switzerland, 109, 112, 165  
 heat flow, 109, 165
- Tahiti, 69
- Tasmania, Australia, 5, 22, 109, 188ff
- Taupo hydrothermal systems, 221ff
- Taupo, New Zealand, 211, 213, 221, 223, 227ff, 230ff, 236, 238, 244, 249, 256, 264ff
- Temperature, annual variation, 8
- Temperatures, around drill holes, 16
- Temperature, deep ocean water, 74  
 detecting and recording devices, 63ff  
 disturbance (see Temperature disturbance)  
 diurnal variation, 8  
 due to a sinusoidal oscillation, 8  
 extrapolation to depth, 9  
 geothermal areas, 252ff  
 gradient (see Temperature gradient)  
 in mines, first mention of, 1  
 initial distribution, 201  
 internal distribution in Earth, 203ff  
 measurement (see Temperature measurement)  
 measuring elements, 61  
 measuring equipment, 40ff  
 profile (see Temperature profile)  
 radial distribution, 5  
 underground, 1
- Temperature disturbance (due to), borehole casting, 44  
 convection in borehole, 44  
 cylindrical conductor, 18  
 drilling, 17  
 erosion, 24  
 geological structure, 25, 46  
 local heat production, 46  
 mud and water flow during drilling, 44  
 surface temperature variations, 25  
 topography, 24  
 underground water flows, 25, 45  
 uplift, 24
- Temperature gradient, adiabatic, 79ff  
 Bullard probe (see also Bullard temperature gradient probe), 59

- Temperature gradient (*continued*)  
 cylindrical probe (see also Bullard temperature gradient probe), 59  
 effect of variation in thermal conductivity, 15  
 Ewing technique, 4, 60ff, 63, 74, 114, 123, 133, 157  
 geothermal areas, 252ff  
 in permanently frozen ground, 2  
 measurement, 40ff, 58ff, 79ff  
 ocean bottom measurements, 58  
 reversing thermometers, 61  
 super-adiabatic, 79
- Temperature measurements, collection of, 3  
 in mines and tunnels, 17  
 under Irish Sea, 3
- Temperature profile of deep ocean water, 80ff
- Terrestrial heat flow (see Heat flow)
- Thermal conditions, Earth's interior, 197ff  
 ocean floor, 74
- Thermal conductivity, anisotropic, 20  
 average value, 25  
 bulk value, 31  
 computed, 32ff  
 effect of variations on geothermal gradient, 15  
 effect of variations on heat flow, 12  
 in situ measurement, 19  
 line source methods, 20  
 maximum value, 30  
 measurement (see Thermal conductivity measurement)  
 minimum value, 30  
 nomogram relating to water content, 72  
 of oceanic sediments, 79, 114  
 of silicates, 198ff  
 relation to water content, 70  
 sample selection, 25  
 systematic changes of, 25  
 temperature and pressure effects, 35, 69, 198ff  
 value used to obtain heat flow, 44  
 values for rocks, 7  
 weighted mean, 9
- Thermal conductivity measurement, 26ff, 58ff  
 absolute steady-state, method, 28ff  
 collection of, 3  
 comparison steady-state method, 27  
 divided bar method (see Steady-state method)  
 for sediment, 68ff  
 needle probe method, 19, 70  
 specimens, 30ff  
 steady-state method, 26ff, 69ff  
 transient, 18, 26, 36, 70  
 transient method (in situ), 36  
 transient method (laboratory), 26
- Thermal contact resistance, 26, 36
- Thermal convection, 81ff, 154, 199ff, 211ff
- Thermal diffusivity, definition of, 7  
 values for rocks, 7
- Thermal fluid reservoir, 250ff
- Thermal history of the Earth, 5, 197ff, 236ff
- Thermal radiation, 198ff
- Thermal resistance, definition, 8
- Thermal stability of deep ocean water, 79ff
- Thermal state of Earth's interior, 5
- Thermal systems, physical characteristics of, 252ff
- Thermistors, 40, 62
- Thermocouples, 62
- Thermoelastic stresses, 78
- Topographic correction, 10ff, 24  
 Jeffreys-Bullard reduction, 11  
 simple model solutions, 10
- Topography, effect on oceanic heat flow, 75  
 relation to heat flow, 154
- Transient method for measuring thermal conductivity, 18, 26, 36, 70
- Trench, heat flow, 120, 123, 131, 143, 148
- Tunnels, temperature measurements, 17
- Turbulent convection, 82ff
- Tuscan steam zone, 218ff
- Tuscany, Italy, 211, 218, 220, 242ff, 266
- Ukrainian shield, 147, 187, 189
- Underground temperatures, first systematic discussion, 1
- Underground water movement, 14
- United Kingdom, 5
- United States, 4, 22, 49, 95ff, 131, 160ff, 240, 242ff, 245, 247, 252, 259, 261, 263ff, 266  
 heat flow, 95ff, 160ff
- Uplift, effect on heat flow, 13
- Upper mantle, origin of instability, 232ff  
 penetrative convection, 231ff
- USSR, 4, 107, 112ff, 240, 242, 246, 252  
 heat flow, 113, 166
- Volcanic areas, heat flow, 4, 147, 255ff
- Volcanism, energy supply for, 235ff
- Waiotapu, New Zealand, 222, 242, 251ff, 257ff, 260, 264ff
- Wairakei, New Zealand, 15, 215ff, 222ff, 228ff, 239, 242ff, 248ff, 252ff, 255ff
- Water (see also Ocean water)  
 convection in the crust, 220ff  
 interstitial in sediment, 84ff
- Water content, nomogram relating to thermal conductivity, 72  
 relation to thermal conductivity, 70
- Water flow, effect on oceanic heat flow, 82ff
- West Germany (see also Germany), 113, 187
- Western Atlantic Ocean (see Atlantic Ocean)
- Western Pacific Ocean (see Pacific Ocean)
- Woods Hole Oceanographic Institution, 58, 67
- World, heat flow, 136ff